Fish Histology

From Cells to Organs

2nd Edition

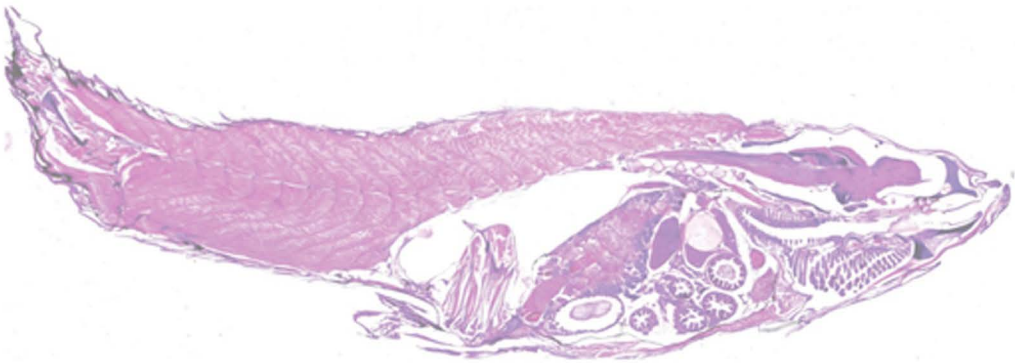

Doaa M. Mokhtar

CRC Press
Taylor & Francis Group
APPLE ACADEMIC PRESS

FISH HISTOLOGY

From Cells to Organs

2nd Edition

FISH HISTOLOGY

From Cells to Organs

2nd Edition

Doaa M. Mokhtar, PhD

APPLE ACADEMIC PRESS

First edition published 2022

Apple Academic Press Inc.
1265 Goldenrod Circle, NE,
Palm Bay, FL 32905 USA

4164 Lakeshore Road, Burlington,
ON, L7L 1A4 Canada

CRC Press
6000 Broken Sound Parkway NW,
Suite 300, Boca Raton, FL 33487-2742 USA

2 Park Square, Milton Park,
Abingdon, Oxon, OX14 4RN UK

Apple Academic Press exclusively co-publishes with CRC Press, an imprint of Taylor & Francis Group, LLC

Library and Archives Canada Cataloguing in Publication

Title: Fish histology : from cells to organs / Doaa M. Mokhtar, PhD.

Names: Mokhtar, Doaa M., author.

Description: 2nd edition. | Includes bibliographical references and index.

Identifiers: Canadiana (print) 20200414836 | Canadiana (ebook) 20200414887 | ISBN 9781771889452 (hardcover) | ISBN 9781003097419 (ebook)

Subjects: LCSH: Fishes—Histology.

Classification: LCC QL639 .M65 2021 | DDC 597—dc23

Library of Congress Cataloging-in-Publication Data

Names: Mokhtar, Doaa M., author.

Title: Fish histology : from cells to organs / Doaa M. Mokhtar, PhD.

Description: Second edition. | Palm Bay, FL : Apple Academic Press, [2021] | Includes bibliographical references and index.

Identifiers: LCCN 2020056017 (print) | LCCN 2020056018 (ebook) | ISBN 9781771889452 (hardcover) | ISBN 9781003097419 (ebook)

Subjects: LCSH: Fishes--Histology.

Classification: LCC QL639 .M64 2021 (print) | LCC QL639 (ebook) | DDC 597--dc23

LC record available at https://lccn.loc.gov/2020056017

LC ebook record available at https://lccn.loc.gov/2020056018

ISBN: 978-1-77188-945-2 (hbk)
ISBN: 978-1-77463-790-6 (pbk)
ISBN: 978-1-00309-741-9 (ebk)

About the Author

Doaa M. Mokhtar, PhD
Professor of Histology, Department of Anatomy and Histology, Faculty of Veterinary Medicine, Assiut University, Assiut, Egypt

Doaa M. Mokhtar, PhD, is a Professor of Histology in the Faculty of Veterinary Medicine at Assiut University in Egypt, where she has been teaching undergraduate and postgraduate courses (cytology, general histology of domestic animals, histology of the body systems, histology of avian, and histology of fish) since 2003. Dr Mokhtar has over 50 publications on fish and related areas to her name. She is also an editor for the *Cytology & Histology International Journal, Journal of Fisheries and Aquaculture Development,* and the *American Journal of Life Science Researches*, and acts as a reviewer for the *International Journal of Molecular Zoology, Journal of Microscopy and Ultrastructure, Anatomia Histologia Embryologia, Anatomical Record,* and *Cell Biology International*. Dr Mokhtar is a member of the Egyptian Society of Histology and Cytology.

Dedication

I dedicate this textbook and atlas to my love and my husband, Dr Ahmed Ibrahim, PhD in Veterinary Surgery, Assiut University, Egypt, for his encouragement and support and for giving me the time to make this work possible.

Contents

Abbreviations

AA	afferent arteriole
AB	Alcian blue
AFs	atretic follicles
AO	acridine orange
AOs	ampullary organs
AP	apoptotic
APs	ampullary pores
AT	arteriolar tract
ATP	adenosine triphosphate
AV	atrioventricular
AVAs	arteriovenous anastomoses
AVT	arginine vasotocin
BAs	branchial arteries
BAT	biliary-arteriolar tracts
BB	brush border
bc	bile canaliculi
BC	blood capillary
BC	buccal cavity
BCs	basal cells
BDs	bile ducts
Bl	basal lamina
BM	bone marrow
BS	blood sinusoids
BT	biliary tracts
BT	bone trabeculae
BV	blood vessels
CCs	club cells
CGs	cardiac glands
CHP	chromium-hematoxylin-phloxine
CNS	central nervous system
CNs	canal neuromasts
CR	cerebellum
CRHC	cell-rich hyaline cartilage

CS	corpuscles of stannius
CT	calcitonin
CT	connective tissue
CTs	collecting tubules
DB	dermal bone
DCs	dendritic cells
DCs	dendritic-like cells
DTs	distal tubules
ECM	extracellular matrix
ECRC	elastic/cell-rich cartilage
ECs	endothelial cells
EDs	efferent ducts
EGCs	eosinophilic granular cells
EP	epidermis
EP	epithelium
FCRC	fibro/cell-rich cartilage
FCs	flask cells
FGs	fundic glands
GA	gill arch
GALT	gut-associated lymphoid tissue
GB	gas bladder
GBM	glomerular basement membrane
GCs	goblet cells
GE	germinal epithelium
GFAP	glial fibrillary acidic protein
GFs	gill filaments
gg	gas gland
GIALT	gill-associated lymphoid tissue
GRs	gill rakers
HCC	hyaline-cell cartilage
HE	hematoxylin and eosin
ICs	interrenal cells
ICs	Ito cells
IgM	immunoglobulin M
IO	infraorbital
IS	intermediate segment
IT	interstitial tissue
IT	isotocin
KCs	Kupffer cells

LCs	lymphocytes
LDs	lipid droplets
LP	lamina propria
LPJ	lower pharyngeal jaw
MALT	mucosal-associated lymphoid tissue
MAs	macrophage aggregates
MC	melanomacrophage cell
mc	monoclonal
MCH	melanin-concentrating hormone
MCs	melanocytes
MCs	mesangial cells
MCs	mucous cells
MFs	mucosal folds
MLF	medial longitudinal fasciculus
MMCs	melanomacrophage centers
MMP	metalloperoxidase
MMPs	matrix metalloproteinases
MMs	melanomacrophages
MO	medulla oblongata
MR	mature reticulocyte
MRCs	mitochondria-rich cells
MRHC	matrix-rich hyaline cartilage
MRs	microRidges
MT	Masson's trichrome
NS	neck segment
OD	oviduct
OL	ovigerous lamellae
ORC	olfactory receptor cells
OT	optic tectum
OT	otic
PAS	periodic acid–Schiff
P-BT	pancreatic–biliary tracts
pc	polyclonal
PCs	principal cells
ph	pharynx
PI	pars intermedia
PNS	peripheral nervous system
PO	preopercular
PSCs	pancreatic stellate cells

PTCs	proximal tubular cells
PTs	proximal tubules
P-VBAT	pancreatic–venous–biliary–arteriolar tracts
P-VBT	pancreatic–venous–biliary tracts
PVCs	pavement cells
RCs	renal corpuscles
RCs	rodlet cells
rER	rough endoplasmic reticulum
RF	reticular formation
RGL	relative gut length
RP	red pulp
RT	room temperature
RTs	renal tubules
SBs	spongy bones
SC	spinal cord
SC	stratum compactum
SCs	supporting cells
SD	space of Disse
SD	sperm duct
SE	serosa
SE	standard error
SEC	stratified epithelial cells
SEM	scanning electron microscopy
sER	smooth endoplasmic reticulum
SG	spermatogonia
SGC	small granule-containing
SGs	secretory granules
SL	secondary lamellae
SL	stratum laxum
SMA	smooth muscle actin
SMCs	smooth muscle cells
SO	supraorbital
STs	seminiferous tubules
SZ	spermatozoa
TA	tunica adventitia
TB	taste bud
TB	toluidine blue
TBs	taste buds
TCs	telocytes

TEM	transmission electron microscopy
TGF	transforming growth factor
ThCs	theca cells
TL	torus longitudinalis
Tps	telopodes
TS	torus semicircularis
TV	tectal ventricle
UB	urinary bladder
UPJ	upper pharyngeal jaw
VAT	venous–arteriolar tracts
VBAT	venous-biliary-arteriolar tracts
VBT	venous-biliary tracts
VC	valvula cerebelli
VD	vas deferens
VS	venous sinus
VT	venous tracts
WCs	wandering cells
WP	white pulp
YG	yolk globule
YR	young reticulocyte
Yvs	yolk vesicles
ZR	zona radiata

Acknowledgments

First of all, thanks forever to ALLAH who is always with me.

For their help, advice, and/or support throughout months of dissections, cutting, staining, photographing, interpreting, writing, editing, and correcting of the present textbook and atlas, I would like to sincerely thank the following persons:

I express my sincere thanks and deep gratitude to Prof Dr A. H. S. Hassan, Prof of Histology, Faculty of Veterinary Medicine, Assiut University, Egypt, for his continuous encouragement, valuable help, constructive criticism, advice during work, and scientific and untiring help that made this work possible.

I am very grateful to Prof Dr Enas A. Abdelhafez, Prof. of Histology, and the head of the Department of Anatomy and Histology, Faculty of Veterinary Medicine, Assiut University, Egypt, for her continuous encouragement and financial assistance.

I offer my sincere thanks to the editorial team at Apple Academic Press, for their guidance, professionalism, collaboration, and unfailing support. In particular, I thank Sandra Sickels, for available by e-mail whenever I needed advice or support.

Preface

Histology is the discipline of biology that involves the microscopic examination of tissue sections in order to study their structure and correlate it with function. Histology can detect signs of disease not easily recognized on gross examination and can, therefore, be of interest in fish health supervision.

The book will provide readers with the most contemporary and useful text possible. The book describes the most important recent developments in the sciences of fish histology. I am also recognizing that the readers are faced with the tasks of learning ever-increasing number of facts in an ever-decreasing period of time. Because of this, every attempt has been made to shorten the text wherever possible and to organize information in a way that will facilitate learning.

Fish constitute nearly 60% of all vertebrate species and are economically of major importance. The reporting of normal histology of fish tissues and organs serves as a foundation upon which to gather and build our ichthyopathology knowledge base.

The aim has been to present a general reference guide providing an extensive set of histological images of fishes. Although several studies treat histological aspects in relation to pathology, no recent synthesis on the normal histology of fish is available. Therefore, I believe that this textbook will be the main contributor to this field. The book is designed to provide students with a foundation in understanding and interpreting histologic and cytologic preparations and normal tissue components.

In this edition, new five chapters were added, including the skeleton of fishes, gas bladder and gas gland, endocrine system, nervous system, and sensory system. Various staining procedures were used in the second edition. As a further aid to learning, many new immunohistochemical and ultrastructural images amplify the text in addition to a particular emphasis on tables to summarize the morphologic and functional features of cells, tissues, and organs.

The text and images for this edition have been updated with the most current information available at the time of publication. The second edition is designed for use by students and researchers, biologists, ichthyologists, fish farmers, veterinarians working in fisheries and, of course, by comparative histologists who want to learn more about the fish world.

All photomicrographs are original. Light microscopy has been illustrated with color photomicrographs. Tissue and organ samples chosen to illustrate this work have been selected from reared food fish, as well as from species in the aquarium and in the wild.

Introduction

It is recognized that a study of fish histology can provide a unifying background to the physiology and pathology. In this textbook and atlas, the structure of tissues and organs of teleosts is described seeming to be helpful for both veterinary medical students and those interested in farm sciences. The information contained in this book emphasizes the relationships and concepts by which cell and tissue structures of fish are inextricably linked with their function. The book also describes the most recent development in the sciences of fish histology.

This second edition covers the normal histology of 10 fish species. It provides original high-quality photomicrographs, tables, updated terminology, and expanded information. Fish Histology Fom Cells to Organs begins with an introduction into the histological techniques for fish sampling followed by an accurate up-to-date description of fish tissues, and finally, I devoted a chapter to each organ and organ systems in fish body.

In this edition, I have expanded many of the beginning chapters that introduce the basic types of tissues to provide the user with a stronger foundation in fish histology. Moreover, I have updated the material for the second edition by adding new five chapters and more than a 100 new photographs.

My aim has been to describe the histologic structure of organs in a variety of fish species. I have used representative examples in instances where tissues and organs from different species share a common structure. Wherever differences exist, I have tried to provide examples that are characteristic of a particular group of fish. The selection of fish species as they have been introduced as ideal models for many experimental studies. Although many studies were done on several fish species, the detailed histology of the skeleton and some organs of these species were not studied before.

It is my hope that students as well as researchers will find this new edition a useful resource.

CHAPTER 1

Introduction to Histotechniques and Fish Gross Anatomy

ABSTRACT

Ten fish species were studied in this book including grass carp or White amur *(Ctenopharyngodon idella),* Nile catfish (*Clarias gariepinus*), Nile tilapia (*Oreochromis niloticus*), red-tail shark (*Epalzeorhynchos bicolor*), guppy (*Poecilia reticulata*), Nile perch (*Lates niloticus*), silver carp (*Hypophthalmichthys molitrix*), Redbelly tilapia (*Coptodon zillii*), Orinoco sailfin catfish (*Pterygoplichthys multiradiatus)*, and molly fish (*Poecilia sphenops*). Immediately after death or euthanasia, the tissue or organ is cut into small pieces and fixed in Bouin's fluid for light microscopical studies. The fixed materials were further processed and sections were obtained at 3 μm and stained with different stains include Harris Hematoxylin and Eosin, trichrome, Verhoff's and Weigert's elastica stains. For histochemical staining, osmic acid reacts with fat, the periodic acid–Schiff reaction and Alcian blue identify varieties of glycosaminoglycans, Grimilus silver impregnation displays some aspects of neuroendocrine cells, Iron HX and bromophenol blue are used to detect the presence of proteins and Best's carmine for detection of glycogen. ATPase, lipase, and phosphatase activity were also investigated. Acridine orange (fluorescent stain) has metachromatic properties that result in the accompanying emission of green and red fluorescence. For the semithin section and electron microscopic studies, tissues were fixed in a mixture of 3% paraformaldehyde–glutaraldehyde fixative. Then, the samples were processed and semithin sections are cut at 1 μm thickness and stained with toluidine blue for light microscopy. Ultrathin sections were cut at 70 nm and were stained with uranyl acetate and lead citrate and examined by JEOL 100CX II transmission electron microscope. For scanning electron microscopy, the tissues are washed in 0.1M cacodylate buffer and transferred to a 1% solution of tannic acid. The samples were processed and mounted on aluminum stubs and

sputter coated with gold/palladium. The specimens were examined with a JEOL and JSM-5400 LV scanning electron microscope. Pictures of the gross anatomy of longitudinal and transverse sections of whole fish were provided. The immunohistochemistry was performed on formalin-fixed, paraffin-embedded, and 4 μm-thick tissue sections.

Ten fish species were studied in this book including grass carp or white amur (*Ctenopharyngodon idella*), Nile catfish *(Clarias gariepinus*), Nile tilapia (*Oreochromis niloticus*), redtail shark (*Epalzeorhynchos bicolor*), guppy (*Poecilia reticulata*), Nile perch (*Lates niloticus*), silver carp (*Hypophthalmichthys molitrix*), Redbelly tilapia (*Coptodon zillii*), Orinoco sailfin catfish (*Pterygoplichthys multiradiatus)*, and molly fish *(Poecilia sphenops*). The referenced fish species have been introduced as ideal models for many experimental studies. Although many studies were done on several fish species, the detailed histology of the skeleton and some organs of these species were not studied before.

Grass carp or white amur (*Ctenopharyngodon idella*) is a large cyprinid fish. They are native in large Asian rivers, such as Amur River Basin in Russia and the West River in China. It is a fast-growing herbivorous fish; it usually feeds on grass or other aquatic vegetation and can be grown together with other fish species.

Nile catfish (*Clarias gariepinus*) is one of the most abundant and widely distributed fish in the Nile River. Catfish has a wide geographical spread, a high growth rate, resistant to handling and stress, and well appreciated in a wide number of African countries. It can be recognized by its long dorsal and anal fins, which gives it a rather eel-like appearance. The catfish is carnivorous in type, where tilapias are its most preferred food items especially the young ones followed by insects, crustaceans, and mollusks, respectively.

Tilapia is a member of the family *Cichlidae*. Nile tilapia (*O. niloticus*) is characterized by strong vertical black bands. This species is naturally distributed in Palestine, the Nile River, as well as most parts of African Rivers and lakes. The *O. niloticus* is gonochoristic, in which each individual possessing a single sexual phenotype. Nile tilapia is characterized by extended spawning seasons, maturity at a small size, and a fast growth rate. It has been termed the aquatic chicken for its extraordinary production capabilities.

The guppy (*P. reticulata*), also known as million fish and rainbow fish, is one of the most popular freshwater aquarium fish species. It is a member of the *Poeciliidae*, whose natural range is in South America and is now found all over the world. The body of guppy is transparent and is

covered with colorless scales and has ornamental dorsal and caudal fins. Guppies are used as a model organism in the field of ecology, evolution, and behavioral studies.

P. sphenops is a species of fish, of the genus *Poecilia*, known under the common name Molly. They inhabit freshwater streams and coastal brackish and marine waters of Mexico. The Molly can produce fertile hybrids with many *Poecilia* species, most importantly the sailfin molly. Mollies rank as one of the most popular feeder fish due to high growth rate, birth size, reproduction, and brood number.

The red-tail shark (*E. bicolor*) is one of the freshwater fish that belongs to the family *Cyprinidae* that originates from the streams and waterways of Thailand. It is characterized by the black body and an orange tail and its skin is covered with transparent scales.

The Nile perch (*L. niloticus*) is one of the biggest freshwater fish. The females exhibit more rapid growth rates than males and attain a bigger size, it reaches 40 kg or more in weight. The species is widespread in Egypt along the Nile River and is of great economic importance as a food fish. However, the Nile perch stocks decrease due to overfishing. Monosex has been evolved as a strategy to direct the fish production toward sex with a higher growth rate.-

The Redbelly tilapia (*C. zillii*) is a species of fish in the cichlid family. It is found widely in Africa but has also been introduced outside its native range. It is an important food fish in Egypt. It was formerly included in the genus Tilapia as *Tilapia zillii*. The length at first maturity is about 10 cm and the spawning season ranged from March to August.

The silver carp (*H. molitrix*) is a species of freshwater cyprinid fish, a variety of Asian carp native to China and Eastern Siberia. This species has a very economic role, it is not only use in aquaculture but also in the enhancement of wild fisheries and water quality control. The silver carp reaches an average length of 60–100 cm (24–39 inches) with a maximum length of 140 cm (55 inches) and a weight of 50 kg.

Orinoco sailfin catfish (*P. multiradiatus*) is one of several tropical fish commonly known as Orinoco sailfin catfish. It belongs to the armored catfish family (Loricariidae). *P. multiradiatus* is mottled brown/black and inhabits freshwater streams and lakes and in weedy, mud-bottomed canals in its native habitat; the Orinoco River basin in Venezuela at the temperature range of 23–27 °C. *P. multiradiatus* browses on a substrate, mainly feeding on benthic algae and aquatic weeds.

1.1 TISSUE PROCESSING FOR LIGHT MICROSCOPY

1.1.1 FIXATION

Immediately after death or euthanasia, the tissue or organ is cut into small pieces (1 × 1 × 0.5 cm) and immediately fixed in Bouin's fluid for 20 h (ideally preserves normal morphology and facilitates further processing).

Three to ten centimeters long fish have the abdomen slit with a scalpel, the intestine detached at the vent, and the internal organs pulled out slightly for optimal fixative penetration. Larger fish (>10 cm) will require an on-site excision of 0.3 cm sections. Do not fix the whole fish. The sample volume should not exceed 1/10th of the volume of fixative.

Some organs require special ways of fixation, such as the liver, gonads, brain, and kidney. The liver fixation was achieved by perfusion via a hepatic portal vein branch. A heparinized isosmotic ringer-like solution was first perfused at a flow rate of ~5.2 mL^{-1} min^{-1} kg body weight. Subsequently, perfusion by fixative was done by 20–40 mL of 3% glutaraldehyde in 0.1M sodium cacodylate buffer (pH 7.3). Both the washout solution and fixative were used at 15 °C. In the case of gonads, brain, and kidney, the heart of the fish should be injected with 10% neutral buffer formalin using an insulin syringe. In addition, these tissues require to be left in the body with the 10% neutral buffer formalin for one to two hours before excision.

The fixed materials should be transferred to 70% ethanol to prevent tissues from overhardening. Then they were dehydrated in graded series of alcohols, cleared in methyl benzoate (solvent). This intermediate step, called clearing, is essential before infiltrating the dehydrated tissue with hot paraffin wax (58–60 °C) because alcohol and paraffin do not mix. During infiltration, hot melted paraffin completely replaces the clearing agent. When infiltration is complete, the specimen is transferred to an embedding mold of fresh paraffin, which is allowed to harden at room temperature (RT) to provide a matrix that can support the tissues during sectioning.

Serial longitudinal and transverse sections were obtained at 3 μm and stained with Harris hematoxylin and eosin (HE). Hematoxylin stains the cell nucleus and other acidic structures (such as RNA-rich portions of the cytoplasm, lysosomes, endoplasmic *reticulum*, ribosomes, etc.) in blue. In contrast, eosin stains the cytoplasmic proteins and a variety of extracellular structures from pink to red. In addition to HE staining procedure, other stain combinations and techniques are available. For example, trichrome procedures (including three dyes), such as Mallory's, Masson's, and Crossmon's,

help to differentiate collagen from muscle cells. In addition, Van Gieson Resorcin Fuchsin identifies collagen and muscle fibers, Gomori's method for reticular fibers, while Verhoff's and Weigert's elastica stains are ideal for elastic fibers

1.2 HISTOCHEMICAL STAINING AND ENZYME HISTOCHEMISTRY

Osmic acid and Sudan black B reacts with fat to give a gray-black color; the periodic acid–Schiff (PAS) reaction and alcian blue (AB) (pH 2.5) reveal different varieties of glycosaminoglycans of proteoglycans and glycoproteins that are present in some tissues and cells. Hematoxylin is the usual counterstain. The PAS-positive sites stain magenta/red; the AB-positive components stain blue. Furthermore, the sections were stained with Safranin O to demonstrate sulfated glycosaminoglycans of the matrix content of the cartilages and the mast cells' granules.

Grimelius silver impregnation displays nerve fibers and some aspects of neuroendocrine cells. Cresyl violet is used to stain the neurons in the brain and spinal cord. Iron HX and Bromophenol blue are used to detect the presence of proteins. The liver sections were stained with Best's Carmine for the detection of glycogen. Long Ziehl–Neelsen for lipofuscins, improved Kupffer's gold chloride method for demonstration of stellate cells, Maldonado's stain for the demonstration of Islets of Langerhans and Perls Prussian blue for the demonstration of iron.

ATPase activity was investigated at pH 4.2, and the activity of alkaline phosphatase was detected by the Gomori calcium method. Acid phosphatase activity is identified with Gomori lead nitrate method and Lipase activity was demonstrated by the Tween method.

1.3 ACRIDINE ORANGE (FLUORESCENT STAIN)

Around 4 μm paraffin sections were dewaxed and rehydrated in ethanol, followed by distal water. Then the sections were fixed in methanol and stained with acridine orange (AO) staining solution (0.01%, pH 3). The sections were examined using a Leitz DM 2500 microscope with the external fluorescent unit Leica EL 6000. AO has metachromatic properties that result in the accompanying emission of green and red fluorescence.

1.4 IMMUNOHISTOCHEMISTRY

The immunohistochemistry was performed on formalin-fixed, paraffin-embedded, and 4 μm-thick tissue sections. The sections were treated with 10 mL Mol Tris buffer and 1 mL Mol ethylenediaminetetra acetic acid (pH 9.0) at 90 °C for 20 min. The endogenous peroxidase was inhibited by immersion of the sections in 3% H_2O_2, then preincubation overnight in 1% bovine serum albumin in PBS at 4 °C. The sections were stained for 30 min at RT, using the following antibodies (Table 1.1): rabbit polyclonal anti-S100 protein for identifying of cells of epithelial, mesodermal, and neuroectodermal origin; rat monoclonal anti-CD117 (c-kit) for demonstration of hematopoietic stem cells, mast cells, telocytes and melanocytes; rabbit monoclonal anti-desmin (the intermediate filament protein); monoclonal mouse antihuman α-smooth muscle actin (SMA) (the typical marker of smooth muscle cells); glial fibrillary acidic protein (GFAP) for demonstration of astrocytes; matrix metalloperoxidase (MMP-9) that is involved in the breakdown of extracellular matrix in normal physiological processes; Caspase 3 (the marker of the apoptosis); and transforming growth factor (TGF-β) that exerts multiple biological functions in proliferation. Sections were counterstained with hematoxylin, examined and photographed under a Leica microscope (Germany).

TABLE 1.1 Identity, Sources, and the Working Dilution of Antibodies Used in this Book

Target	Primary Antibody				
	Supplier	Origin Catalog Number	Dilution	Incubation	Antigen Retrieval
Desmin (Ab1)	Thermo scientific[a]	Rabbit (mc) (MA5-32068)	1:30	1 h at RT	Microwave[b]
S-100 protein	Thermo scientific[a]	Rabbit (pc) (RB-044-A0)	1:200	1 h at RT	Microwave[b]
α-Smooth muscle actin (α-SMA)	Dako[c]	Mouse (mc) (M0851)	1:300	1 h at RT	Microwave[b]
GFAP	Thermo scientific[a]	Rabbit (pc, PA5-16291)	1:50	O/N	Microwave[b]
MMP-9	Abcam[d]	Rabbit (pc) Ab38898	1:100	1 h at RT	Microwave[b]
c-kit (CD 117)	Thermo scientific[a]	Rat (mc) (14-1171-82)	1:100	1 h at RT	Microwave[b]
Caspase-3	Abcam[d]	Rabbit (pc) Ab2302	1:100	1 h at RT	Microwave[b]
TGF-β	Thermo scientific[a]	Mouse (mc) (MA5-16949)	1:100	1 h at RT	Microwave[b]

[a]Thermo Fischer Scientific, UK wit Lab vision corporation; [b]microwave heating in citrate buffer (pH 6.0), 3 × 10 min; [c]Dako, Hamburg, Germany; [d]Abcam, Cambridge, UK.

1.5 SEMITHIN SECTIONS AND ELECTRON MICROSCOPIC STUDIES

Small specimens of tissues were fixed by immersion in 3% glutaraldehyde in 0.1M sodium cacodylate buffer (pH 7.3) for 3 h at 4 °C. The samples were washed in the same buffer for 2 h, postfixed with 1% osmium tetroxide in 0.1M sodium cacodylate buffer at pH 7.2 for 2 h at RT. Next, the samples were dehydrated by ethanol, followed by propylene oxide and embedded in Araldite. Semithin sections were cut at 1μm thickness with Richert Ultracuts (Leica, Germany) and stained with toluidine blue for light microscopy. Ultrathin sections (70 nm) were obtained with Ultrotom-VRV (LKB Bromma, Germany) and stained with lead citrate and uranyl acetate. TEM images were captured with a JEOL-100CX II electron microscope.

For scanning electron microscopy, the tissues are washed in 0.1M cacodylate buffer for 1 h and then transferred to a 1% solution of tannic acid for 2 h at RT. The pieces were washed again in a buffer and postfixed for 2 h in 1% osmium tetroxide. The postfixed materials were washed and dehydrated in a series of increasingly concentrated solutions. They were then mounted on aluminum stubs and sputter coated with gold/palladium for 3 min. The specimens were examined with a JEOL JSM-5400 LV scanning electron microscope.

1.6 DIGITAL COLORED IMAGES

To increase the visual contrast between several structures on the same electron micrograph, digitally colored specific elements (Kupffer cells, Ito cells, telocytes, etc.) were done to make them more visible to the untrained eye. All the elements were carefully hand colored using Adobe Photoshop software version 6.

1.7 MORPHOMETRICAL ANALYSIS

Many measurements were performed using Image-J software on randomly selected images of both paraffin and semithin sections using a 40× objective and 100× objective.

1.8 PICTURES OF GROSS ANATOMY

I have provided gross views of longitudinal and surface sections of whole fish (Figures 1.1–1.10). This allows a better understanding of the location of each organ.

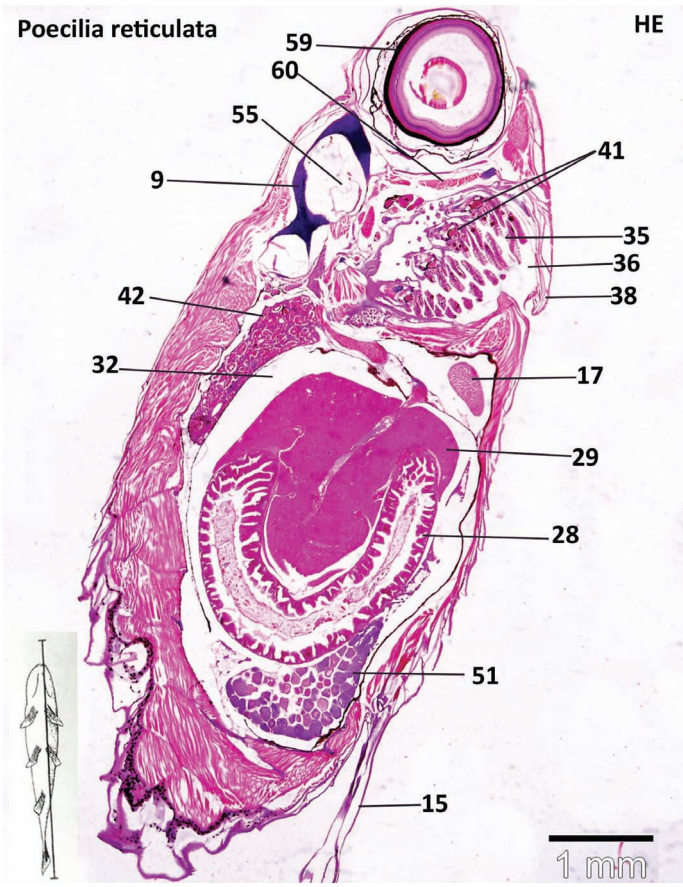

FIGURE 1.1

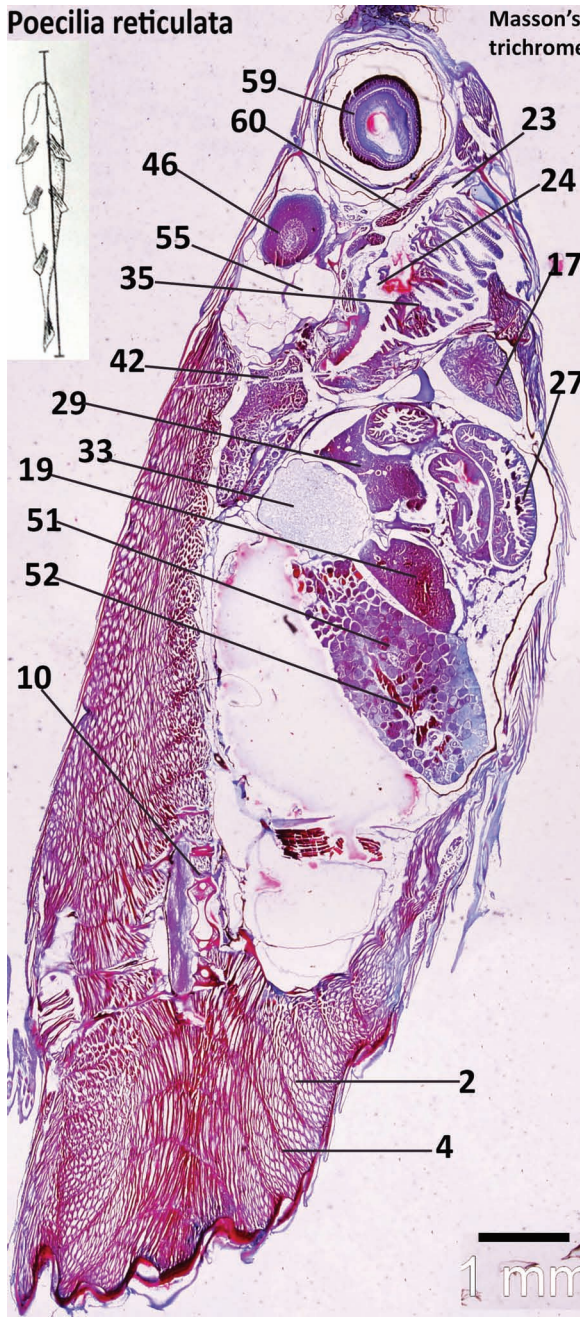

FIGURE 1.2

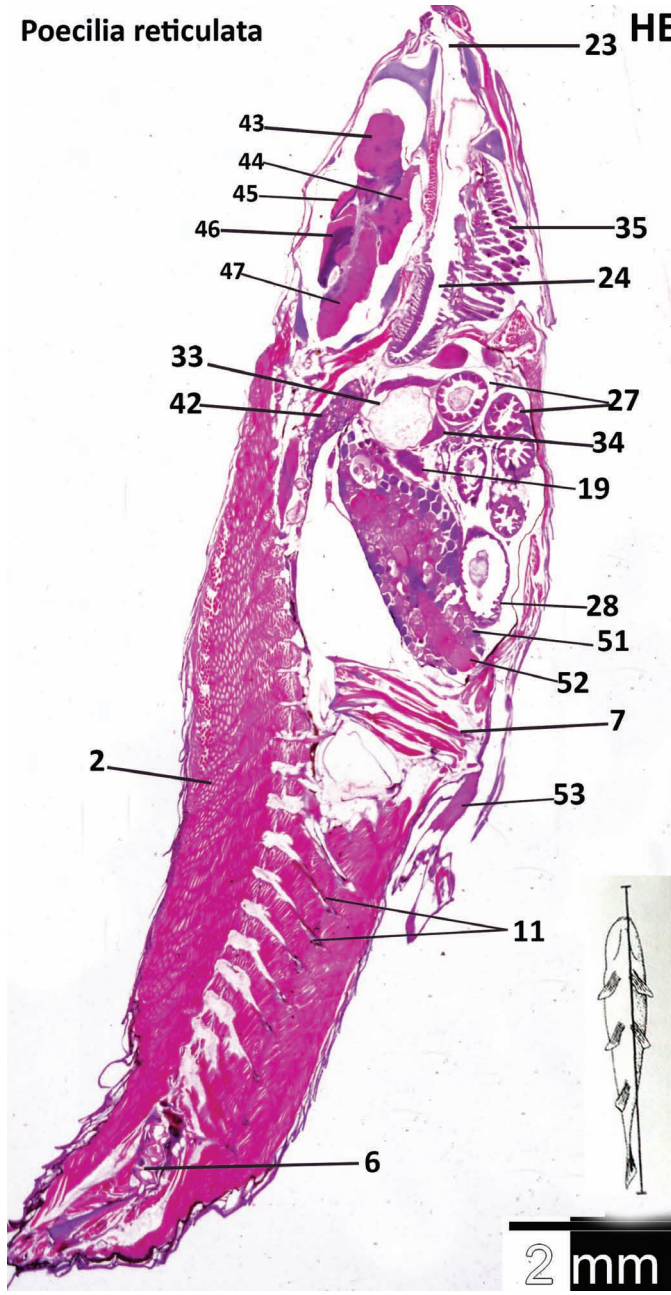

FIGURE 1.3

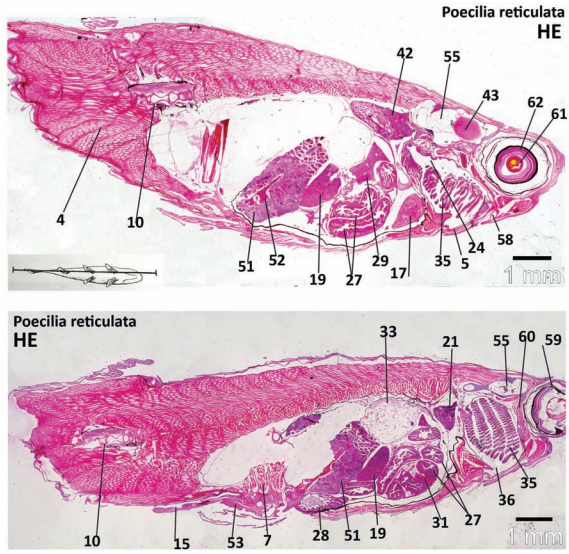

FIGURE 1.4

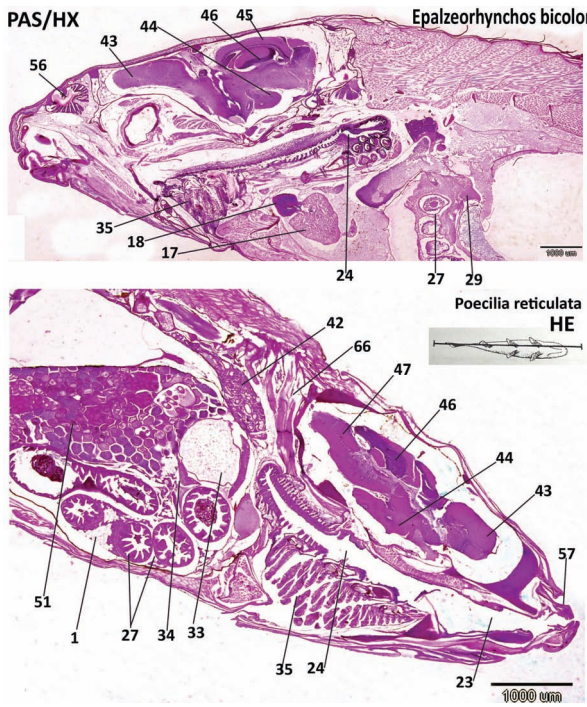

FIGURE 1.5

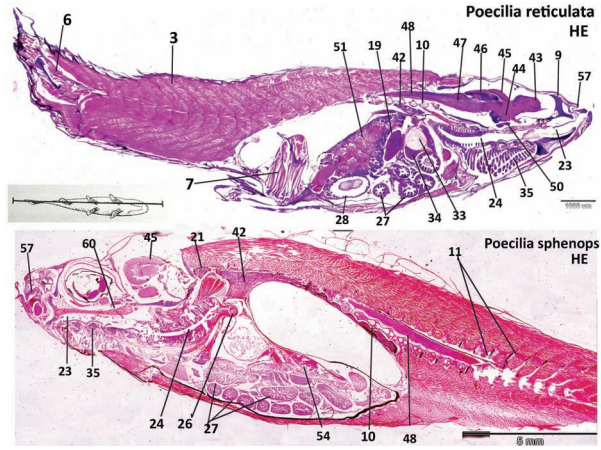

FIGURE 1.6

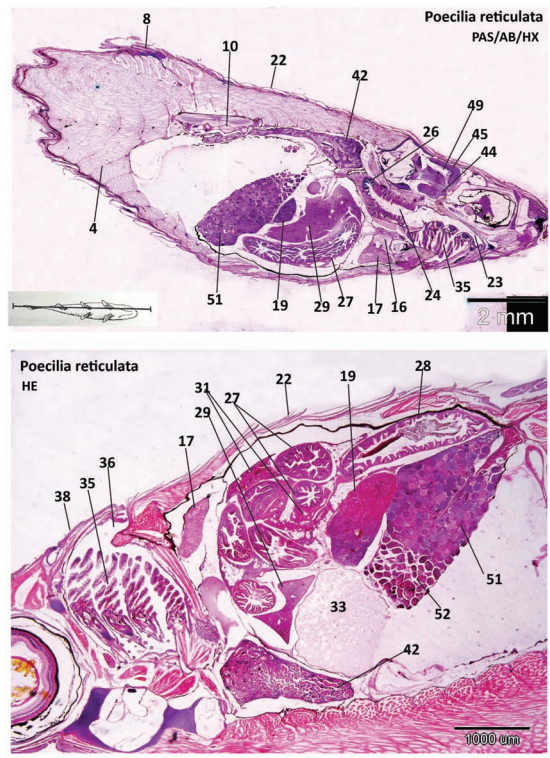

FIGURE 1.7

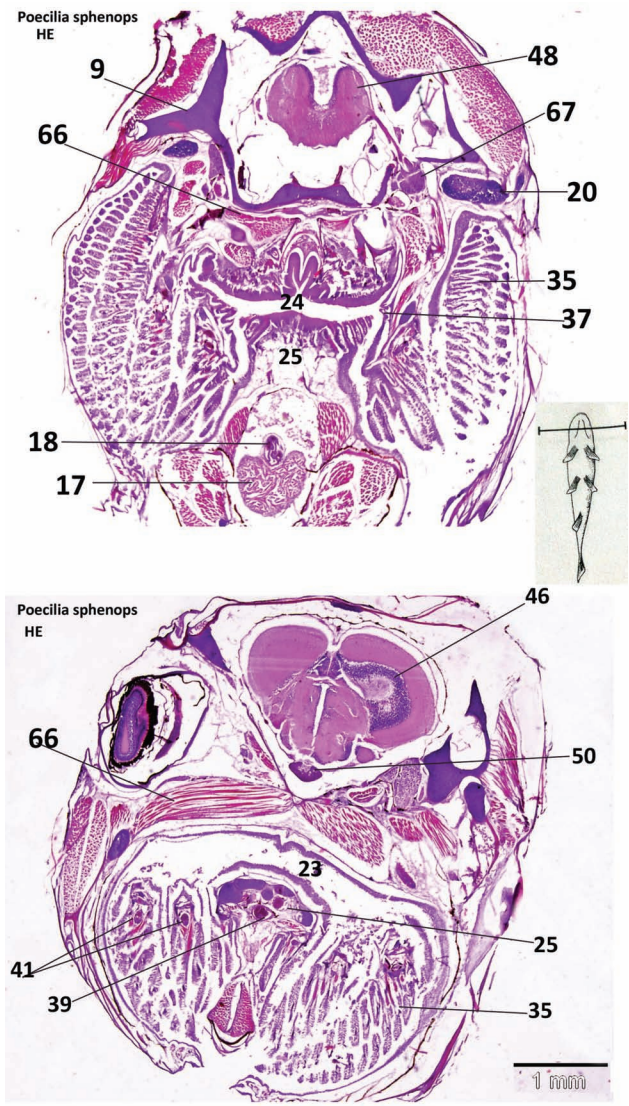

FIGURE 1.8

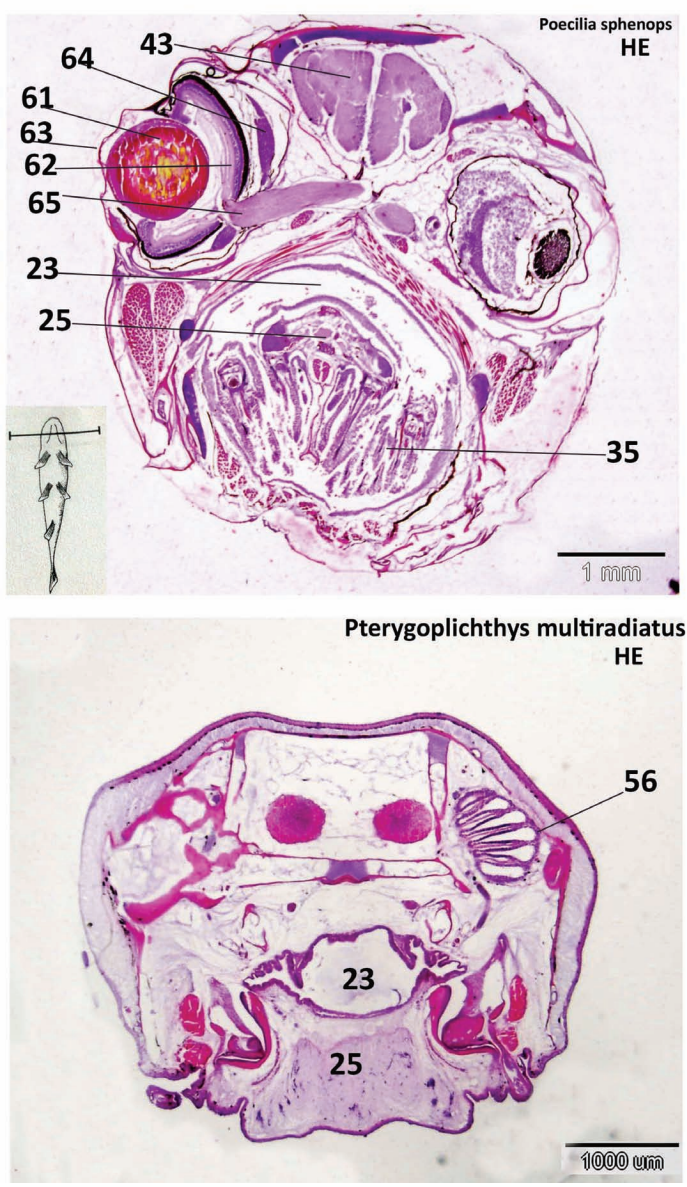

FIGURE 1.9

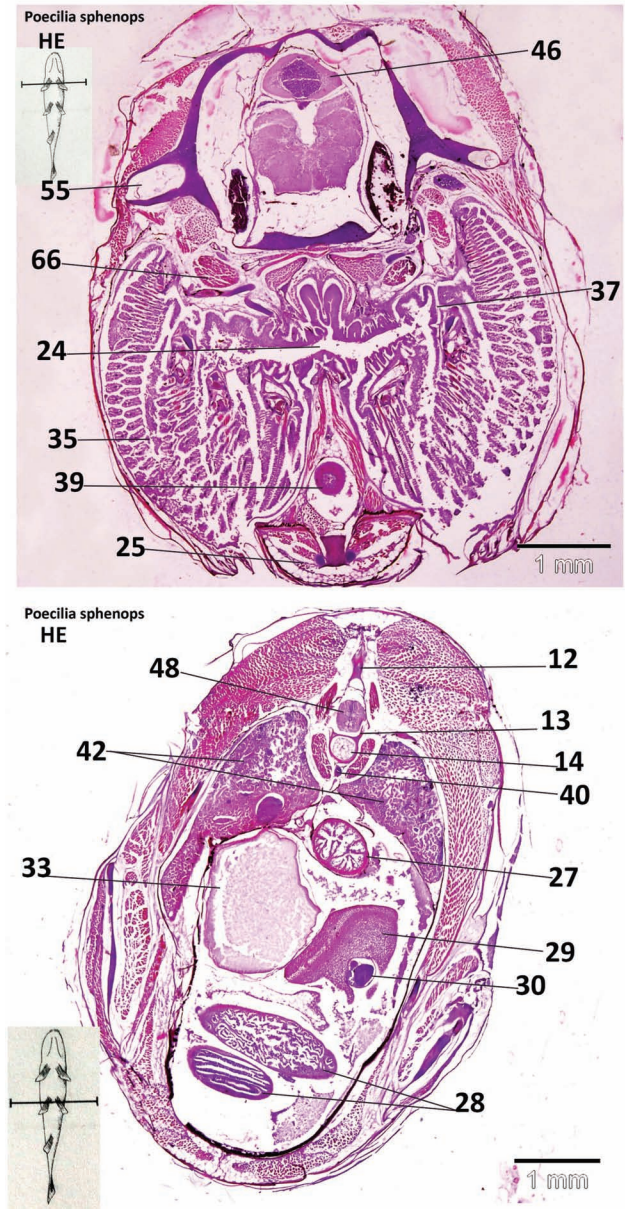

FIGURE 1.10

KEYWORDS

- **guppy**
- **catfish**
- **tilapia**
- ***Poecilia***
- **hematoxylin**

BIBLIOGRAPHY

Amisah, S.; Oteng, M. A.; Ofori, J. K. Growth performance of the African catfish, *Claris gariepinus*, fed varying inclusion levels of *Leucaena leucocephala* leaf meal. *J. Appl. Sci. Environ. Manag.* **2009,** *13*(1), 21–26.

Anne, M. E.; Dawn, P. A. T. Evolutionary implications of large-scale patterns in the ecology of *Trinidadian guppies*, *Poecilia reticulata*. *Biol. J. Linn Soc.* **2001,** *73,* 1–9.

Bancroft, J. D.; Steven, A. *Theory and Practice of Histological Techniques*, 4th ed., Churchill Livingstone: New York, NY, 1996.

Gomori, G. An improved histochemical technique for acid phosphatase. *Stain Technol*. **1950,** *25*, 81.

Gomori, G. Histochemistery of estrases. *Int. Rev. Cytol*. **1952,** *1*, 323.

Guillary, V.; Gasaway, R. D. Zoogeography of the grass carp in the United States. *Trans. Am. Fish. Soc*. **1978,** *107*(1), 105–112.

Hieronimus, H. *Guppies, Mollies, and Platies: Complete Pet Owners Manual Series*, Barron's Educational Series: Hauppauge, NY, 2009.

Maldonado, R.; San-Jose, H. Maldonado's method for pancreatic islet cells. *Stain Technol*. **1967,** *42*, 11–13.

Pearse, A. G. E. *Histochemistry: Theoretical and Applied*, vol. 2, Churchill Livingstone: Edinburgh, 1985.

Popma, T.; Masser, M. *Tilapia Life History and Biology*, Southern Regional Aquaculture Center Publication: Stoneville, MS, 1999, p. 283.

Reynolds, E. S. The use of lead citrate at high pH as an electron-opaque stain in electron microscopy. *J. Cell Biol*. **1963,** *17*, 208–212.

Yang, J. X.; Winterbottom, R. Phylogeny and zoogeography of the cyprinid genus *Epalzeorhynchos bleeker* (Cyprinidae: Ostariophysi). *J. Copeia.* **1998,** *1*, 48–63.

KEY TO THE GROSS ANATOMY FIGURES 1.1 TO 1.10

1 adipose tissue	35 gills
2 epaxial muscles	36 branchial cavity
3 hypaxial muscles	37 gill rakers
4 myosepta	38 operculum
5 hypobranchial musculature	39 ventral aorta
6 caudal fin muscles	40 dorsal aorta
7 gonopodium erector muscles	41 branchial arteries
8 erector muscles of dorsal fin	42 excretory kidney
9 skull skeleton	43 telencephalon
10 vertebra(e)	44 diencephalon
11 ribs	45 mesencephalon (optic lobes)
12 neural arches	46 metencephalon (cerebellum)
13 hemal arches	47 myelencephalon
14 notochord	48 spinal cord
15 pelvic fin	49 brain ventricle
16 heart (atrium)	50 pituitary gland
17 heart (ventricle)	51 testis with cysts
18 heart (bulbus arteriosus)	52 spermatozeugmata in efferent ducts
19 spleen	53 gonopodium
20 thymus	54 ovary
21 hematopoietic kidney	55 inner ear
22 scales	56 olfactory organ
23 buccal cavity	57 nostril
24 pharynx	58 lateral system
25 tongue	59 eye
26 esophagus	60 ocular muscle(s)
27 small intestine	61 lens
28 posterior intestine (rectum)	62 retina
29 liver	63 cornea
30 gall bladder	64 choroid rete
31 pancreatic tissue	65 optic nerve
32 peritoneal cavity	66 striated muscle
33 gas bladder	67 spinal ganglia
34 gas gland	

ALPHABETICAL KEY TO THE FIGURES 1.1 TO 1.10

adipose tissue	1	Figs 1.5
brain ventricle	49	Figs 1.7
branchial arteries	41	Figs 1.8
branchial cavity	36	Figs 1.1, 1.4, 1.7
buccal cavity	23	Figs 1.2, 1.3, 1.5, 1.6, 1.7, 1.8, 1.9
choroid rete	64	Figs 1.9
cornea	63	Fig. 1.9
diencephalon	44	Figs 1.3, 1.5, 1.6, 1.7
dorsal aorta	40	Figs 1.10
dorsal fin muscles	8	Figs 1.7
epaxial muscles	2	Figs 1.2, 1.3
esophagus	26	Figs 1.7
excretory kidney	42	Figs 1.1, 1.2, 1.3, 1.4, 1.5, 1.6, 1.7, 1.10
eye	59	Figs 1.1, 1.2, 1.4
gall bladder	30	Figs 1.10
gas bladder	33	Figs 1.2, 1.3, 1.4, 1.5, 1.6, 1.7, 1.10
gas gland	34	Figs 1.3, 1.5, 1.6
gill rakers	37	Figs 1.8, 1.10
gills	35	Figs 1.1, 1.2, 1.3, 1.4, 1.5, 1.6, 1.7, 1.8, 1.9, 1.10
gonopodium	53	Figs 1.3, 1.4
gonopodium erector muscles	7	Figs 1.3, 1.4, 1.6
heart (atrium)	16	Figs 1.7
heart (bulbus arteriosus)	18	Figs 1.5, 1.8
heart (ventricle)	17	Figs 1.1, 1.2, 1.4, 1.5, 1.7, 1.8
hemal arches	13	Figs 1.10
hematopoietic kidney	21	Figs 1.4
hypaxial muscles	3	Figs 1.6
hypobranchial musculature	5	Figs 1.4
inner ear	55	Figs 1.1, 1.2, 1.4, 1.10
lateral system	58	Figs 1.4
lens	61	Figs 1.4, 1.9
liver	29	Figs 1.1, 1.2, 1.4, 1.5, 1.7, 1.10
mesencephalon (optic lobes)	45	Figs 1.3, 1.5, 1.6, 1.7
metencephalon (cerebellum)	46	Figs 1.2, 1.3, 1.5, 1.6, 1.8, 1.10
myelencephalon	47	Figs 1.3, 1.5, 1.6
myosepta	4	Figs 1.2, 1.4, 1.7
neural arches	12	Figs 1.10
nostril	57	Figs 1.5, 1.6
notochord	14	Figs 1.10
ocular muscles	60	Figs 1.1, 1.2, 1.4, 1.6

CHAPTER 2

Tissues of Fishes

ABSTRACT

Five basic tissues, epithelial tissue, connective tissue, muscular tissue, skeletal tissue, and nervous tissue, are demonstrated in fish. Epithelia are classified into two types according to the number of the layers, first, simple: one cell layer thick, and, second, stratified: many layers of cells. Epithelia are also classified according to the shape of the cells into (1) squamous: flat cells with a flat nucleus; (2) cuboidal: square in shape with a rounded nucleus; (3) columnar: rectangular with oval basally located nucleus; and (4) pseudostratified: two types of cells are demonstrated with nuclei arranged at different levels. Epithelia are further classified by its apical surface specializations into microvilli, microridges, and cilia. Epithelia also form the essential parts of the glands. Taste buds populate in the stratified epithelium of the integument and of the buccopharyngeal to the esophageal cavity. The connective tissue serves as connecting and filling tissues, lying beneath the epithelial tissues of the skin and digestive tract. Each type of connective tissue consists of cells scattered in an extracellular matrix consisting of fibers in an amorphous ground substance. Collagenous, reticular, and elastic fibers occur in connective tissue. The various cell types of connective tissues are divided into two groups: one, the population of fixed cells, which includes fibroblasts and adipose cells, and, another, the population of wandering or free cells whose presence primarily depends on the functional state of the tissue.

As in other vertebrates, five basic tissues, epithelial tissue, connective tissue, skeletal tissue, muscular tissue, and nervous tissue, are demonstrated in fish.

2.1 THE EPITHELIUM

The epithelium is one of the four basic tissues that form the organs. Epithelia generally act as boundaries for transport, protection, segregation, sensation,

and secretion. The epithelium is found covering surfaces and lining cavities. Epithelial cells are supported by a basement membrane that separates them from the underlying connective tissue. The basement membrane is mainly composed of glycosaminoglycans and glycoproteins and may involve in the epithelial differentiation.

Epithelia (Figures 2.1 and 2.2) are classified into two types, according to the thickness and the number of the layers, (1) simple: one cell layer thick, or one cell separates the free (luminal, apical) surface from the underlying basement membrane; (2) stratified: many layers of cells that grow from the basal lamina upward and eventually shed into the lumen or free surface. Epithelia are also classified according to the shape of the cells as follows: (1) squamous: very thin and flat cells with a flat nucleus; (2) cuboidal: square in shape with a rounded nucleus; (3) columnar: rectangular (taller than it is wide) with oval basally located nucleus; and (4) pseudostratified: two types of cells are demonstrated (tall and short) with nuclei arranged at different levels.

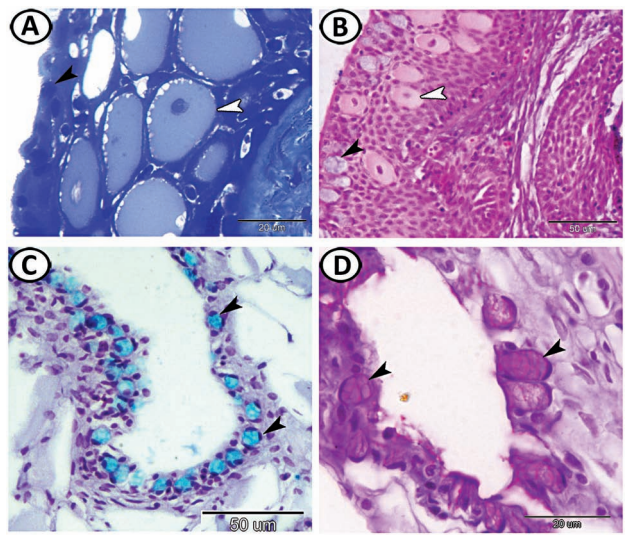

FIGURE 2.1 **(**A**)** Semithin section of the stratified epithelium of the upper lip of the silver carp' skin consists of a variable number of cell layers. In addition to the epithelial cells, many metachromatic mucous cells (black arrowhead) and club cells (white arrowhead) are seen (TB). **(**B**)** The surface of the pharynx of grass carp is lined by a stratified epithelium and many surface mucous cells (black arrowhead) and club cells (white arrowhead). Cells of the bottom-most epithelial layer are usually cuboidal or columnar in shape and in contact with the basement membrane (HE). **(**C**)** Thin stratified epithelium of the head skin of silver carp showing many alcian blue-positive mucous cells (black arrowheads) (AB/HX). **(**D**)** Many PAS-positive mucous cells (unicellular glands—magenta) (black arrowheads) are located on the surface of the skin around the eye of silver carp (PAS-HX).

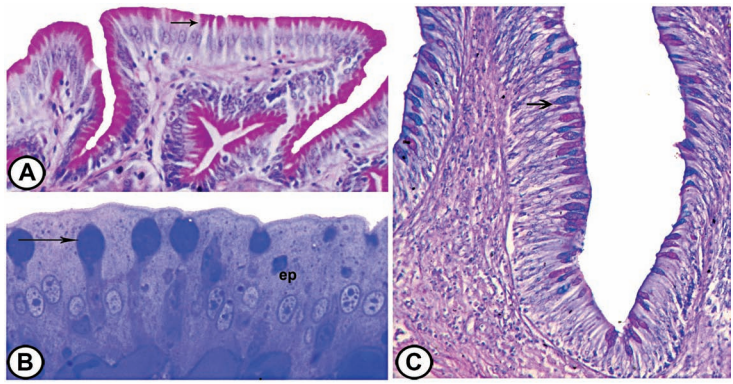

FIGURE 2.2 **(**A**)** The surface of the stomach of Nile catfish is lined with simple columnar epithelium with apical mucopolysaccharides (arrow) (PAS-HX ×400). **(**B**)** In the intestine of grass carp, the mucosal surface is lined with enterocytes [simple columnar epithelium (ep)]. Note the metachromasia of the goblet cells (arrow). **(**C**)** The posterior intestine of grass carp: its surface is lined with enterocytes and PAS (bright pink)—AB (blue)—positive goblet cells (arrow) (PAS-AB-HX ×200).

Epithelia also form the essential parts of the gland, which are masses of cells specialized for the secretion of a given product into the lumen of a duct or a body cavity, or the blood or lymph streams. When the secretion enters a duct or a body cavity, the gland is known as an exocrine gland, such as pancreatic acini (Figure 2.3A). When it enters the blood or lymph to be carried to other parts of the body and affect distant structures, the organ that forms, it is called an endocrine gland, such as the thyroid gland. Most endocrine glands consist of clumps or cords of secretory cells in close opposition to a dense network of small blood vessels. The thyroid gland (Figure 2.3B) is an unusual endocrine gland whose secretory product is stored within spheroidal cavities enclosed by secretory cells; these spheroidal units are called follicles.

Some glands are unicellular, they consist of specialized cells scattered throughout an epithelial lining. In fish, the most common unicellular gland is the mucus-secreting cell (Figures 2.1 and 2.2) found within the skin epithelium or within the digestive tract epithelium. The mucoid substances are released onto the epithelial surface. As this secretory material is synthesized, it fills and expands the apical portion of the cell. The remainder of the cytoplasm and the nucleus are displaced to the narrow basal region of the cell. The mucus plays a role in food coating and lubrication. Taste buds (chemosensory receptors) (Figure 2.3C and D) populate in the stratified epithelium of the integument and of the buccopharyngeal to the esophageal cavity. They

are also located in the fins, gill rakers, and barbels. They function in the perception of smell or taste.

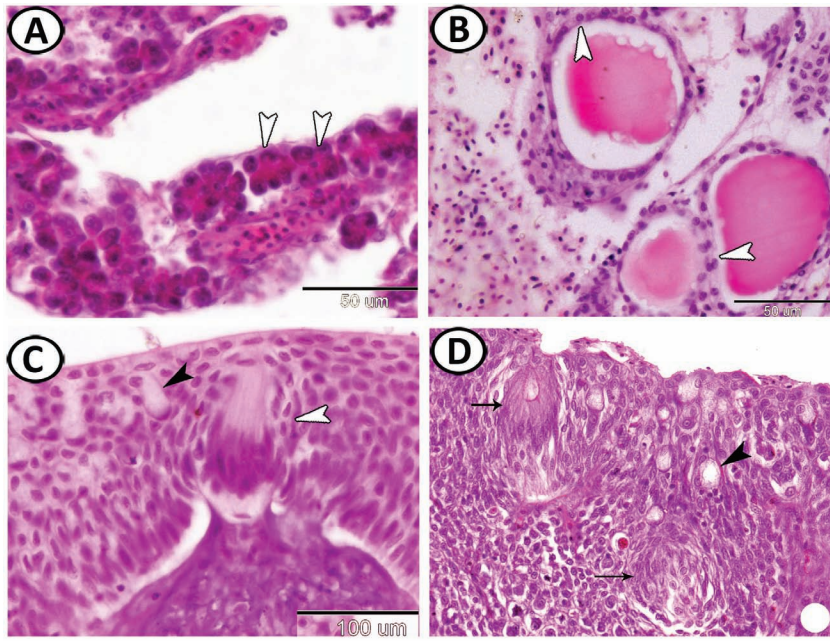

FIGURE 2.3 **(**A**)** The epithelium in the molly fish formed the glands like pancreatic acini (exocrine glandular portion of the pancreas) (arrowheads) (HE). **(**B**)** Cross-sections in the thyroid follicles of grass carp consist of simple cuboidal epithelium (arrowheads). The follicles are filled with glycoprotein bounded to the thyroid hormones (HE). **(**C**)** Stratified epithelium of pharynx of grass carp showing taste bud (white arrowhead) and goblet cells (black arrowhead) (HE). **(**D**)** The covering epithelium of the oesophagus of grass carp contained goblet cells (arrowhead). In addition, intraepithelial taste buds (arrows) are also demonstrated (HE).

Epithelia are further classified by its apical surface specializations into three types (Figure 2.4): (1) microvilli: also known as brush border that increases surface area; (2) cilia: very similar to flagella, function in transport and sensation and characterized by the presence of their basal bodies; (3) microridges: usually display fingerprint-like arrangement as those found on the skin, oesophagus, or olfactory organs.

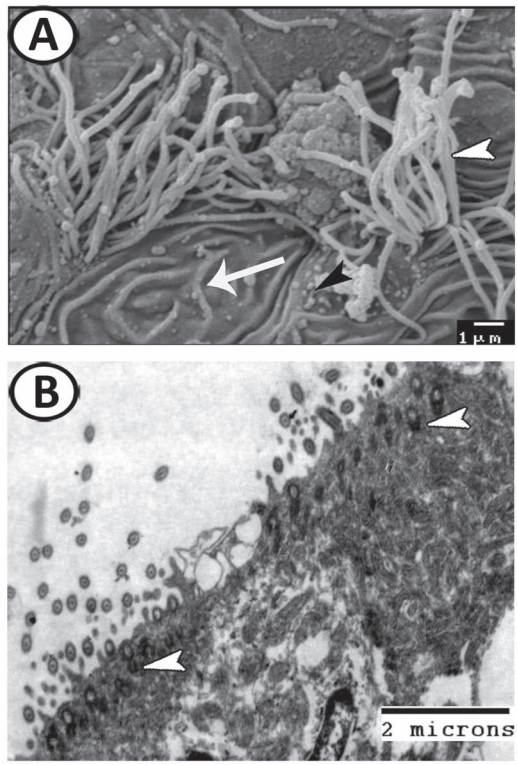

FIGURE 2.4 **(**A**)** SEM of the surface of the olfactory epithelium of red-tail shark showing cilia (white arrowhead), microvilli (black arrowhead), and microridges (arrow). **(**B**)** TEM of the ciliated cells in the olfactory organ of red-tail shark showing basal bodies (arrowheads).

2.2 THE CONNECTIVE TISSUES

The connective tissues (Figures 2.5 and 2.6) serve as connecting and filling tissues, lying beneath the epithelial tissues of the skin, digestive tract, and tubular organs, or between the muscles, between the masses of secreting cells in the glands, and in numerous other locations. Each type of connective tissue consists of cells widely scattered in an abundant extracellular matrix consisting of fibers in an amorphous ground substance. The ground substance, composed largely of glycoproteins and glycosaminoglycans, forms a well-hydrated gel that fills the space between cells, fibers, and blood vessels. Collagenous, reticular, and elastic fibers occur in connective tissue. Ligaments (Figure 2.5F) are composed of dense bands of fibrous connective tissue whose collagen fibers are arranged in a very regular way.

The various cell types of connective tissue are divided into two groups: one, the population of fixed cells, which includes fibroblasts and adipose cells, and, another, the population of wandering or free cells (macrophages, plasma cells, mast cells, etc.) whose presence primarily depends on the functional state of the tissue. The fibroblasts are responsible for the formation of both fibers and ground substance. Inactive fibroblasts, also called fibrocytes, are smaller and spindle-shaped. In loose connective tissue (Figure 2.6A), the ground substance predominates, in addition to the presence of elastic, reticular fibers, and many kinds of connective tissue cells. Telocytes (TCs) (Figure 2.6A) are interstitial (stromal) cell type described in many tissues and organs of vertebrates including fish. TCs are recognized by their spindle-shaped cell body and long cell processes (telopodes). Telopodes are hundreds of micrometers long and extremely thin (0.05–0.2 m), making up a succession of thin, fibrillary segments (podomers) and dilated, cistern-like regions (podoms). These cells are interconnected by homo-and heterocellular junctions to form three-dimensional networks within the interstitial tissue. TCs are involved in structural support, tissue hemostasis, signaling communication, neurotransmission, and regeneration.

In dense connective tissue, the collagenous fibers arranged parallel bundles as that in the dermis of the skin (Figure 2.5A–C) or form a compact meshwork that usually supports the epithelial cells of hollow organs (Figure 2.6B).

The adipose tissue (Figure 2.6C and D) has long been considered a type of connective tissue and can be described as a loose association of lipid-filled cells known as adipocytes associated with stromal-vascular cells, held in a matrix of collagen fibers. The adipocytes are characterized by one large lipid inclusion giving the cell a signet-ring shape that results from distension of the cytoplasm and the apposition of the nucleus to the cell membrane. In sections, individual adipose cells appear as empty elements because the fat was dissolved by the hydrophobic solvents used during the routine histologic preparation of the tissue. Fat cells are fully differentiated cells and are incapable of mitotic division. Therefore, new fat cells that may develop at any time within connective tissue arise as a result of the differentiation of more primitive cells. Although fat cells, before they store fat, resemble fibroblasts, it is likely, that they arise directly from undifferentiated mesenchyme cells present within the body. Initially, small droplets of fat make their appearance within the cytoplasm. The droplets increase in size and finally coalesce to form a single large droplet, and the cytoplasm is reduced to a thin encompassing layer. The nucleus is compressed and flattened.

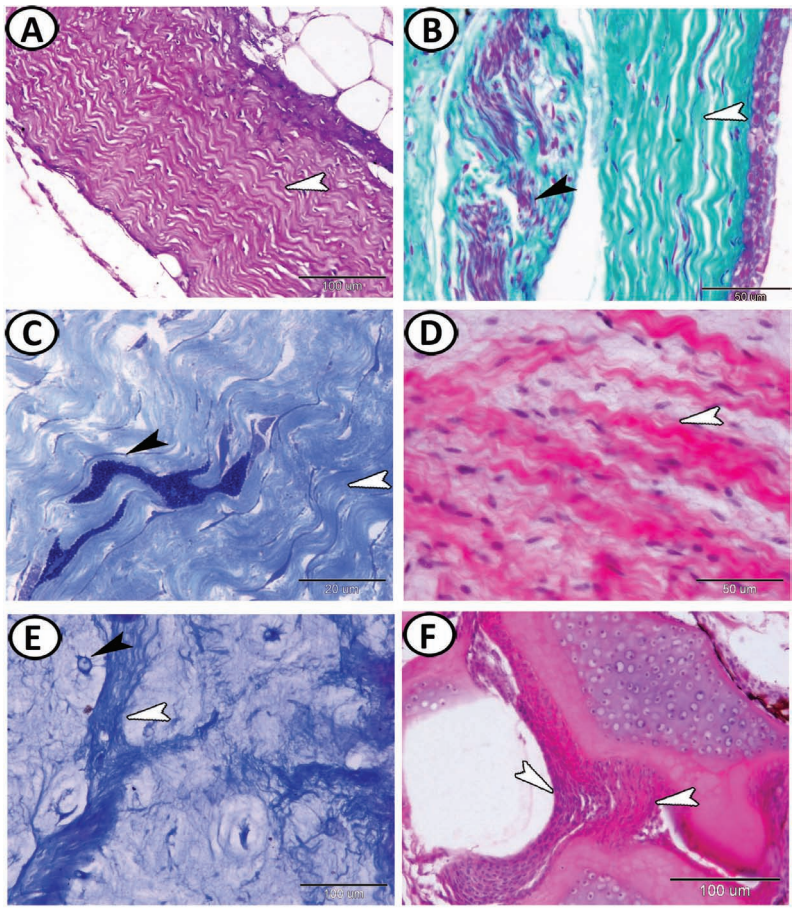

FIGURE 2.5 **(**A**)** Dense regular connective tissues in the pharynx of grass carp showing parallel arranged collagenous fibers (arrowhead) (HE). **(**B**)** Collagenous tissue (green, white arrowhead) in the skin dermis of the operculum of silver carp. Note the presence of nerve bundles (black arrowhead) in the dermis (Crossmon's trichrome). **(**C**)** Semithin section of the dermis of the nostrils of silver carp showing parallel arranged collagenous fibers (white arrowhead). Note the presence of branched melanocyte filled with melanin pigments (black arrowhead) (TB). **(**D**)** Connective tissues of the tongue of grass carp showing thick elastic membranes (arrowhead) (HE). (E) Connective tissues of the submucosa of the tongue of grass carp showing irregular arranged collagenous fibers (white arrowhead). Note the presence of the dispersed arrangement of osteocytes (black arrowhead) (Masson's trichrome). (F) Collagenous fibers (arrowheads) between the cartilages of the fin of guppy (HE).

Skeletal tissues (cartilage and bone), muscular tissues, and nervous tissues of fishes will be the subject of separate chapters.

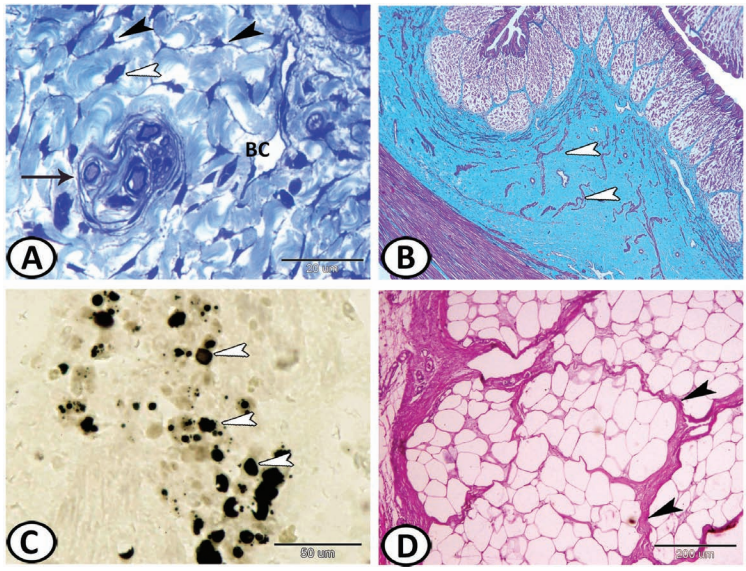

FIGURE 2.6 **(**A**)** Semithin section shows the loose connective tissue in the skin dermis of silver carp contains blood capillary BCs and nerve fibers (arrow) and shows TCs (black arrowheads) and fibroblasts (white arrowhead) between collagen fibers (TB). **(**B**)** Collagenous connective tissue (green) constitutes the submucosa and lamina propria of the fundic region of the stomach of Nile catfish. Note the distribution of smooth muscle fibers (arrowheads) between the collagen fibers (Crossmon's trichrome). **(**C**)** Fat cells (arrowheads) in the ovary of Redbelly tilapia stained by Sudan black B. **(**D**)** In the adipose tissue of the pharynx of grass carp, adipocytes are huge fat-storing cells, which found in lobules and separated by connective tissue septa (arrowheads) (HE).

KEYWORDS

- **adipocyte**
- **epithelial cells**
- **connective tissue**

BIBLIOGRAPHY

Ferguson, H. W. *Systemic Pathology of Fish. A Text and Atlas of Normal Tissues in Teleosts and Their Responses in Disease*; 2nd ed.; Scotian Press: London, 2006.

Martin, C. I.; Johnston, I. A. Endurance exercise training in common carp *Cyprinus Carpio* L. Induces proliferation of myonuclei in fast muscle fibers and slow muscle fiber hypertrophy. *J. Fish Biol.* **2006,** *69*, 1221–1227.

Roberts, R. J. *Fish Pathology*; 3rd ed.; W.B. Saunders: Edinburgh, 2003.

Yasutake, T. W; Wales, J. H. *Microscopic Anatomy of Salmonids: An Atlas*; USFWS: Washington, DC, 1983.

CHAPTER 3

The Muscular Tissues

ABSTRACT

Three types of muscle cells are present in the muscular tissue of fishes: skeletal, cardiac musculature, and smooth musculatures. Skeletal muscle fibers are multinucleated syncytia that originate and insert on the bones of the skeleton. The fish contains two types of skeletal muscle types: red and white that have different degrees of vascularization and myoglobin content. These two kinds of muscles are involved in two kinds of swimming activity. Cardiac muscle fibers consist of anastomosing and branching cardiomyocytes. At sites of end-to-end contact are the intercalated discs. The specially modified conduction pathways (Purkinje fibers) seem to be lacking in fish hearts. Smooth muscle fibers usually form the contractile portion of the walls of most viscera and the tunica media of the arteries and veins. The cells (leiomyocytes) of smooth muscle are spindle-shaped structures without striations. The leiomyocytes are placed close together, forming layers or sheets, although single cells may be formed. The cell contains delicate contractile myofilaments.

The muscular tissue is composed of cells that specialize in mechanical work. Three types of muscle cells are present in the muscular tissue of fishes: (1) the skeletal musculature, consisting of striated, unbranched, and voluntary fibers; (2) the cardiac musculature, consisting of striated and branching involuntary fibers; and (3) the smooth unstriated, involuntary musculature.

3.1 SKELETAL MUSCLE FIBERS

Skeletal muscle fibers (rhabdomyocytes) (Figures 3.1–3.3) are multinucleated syncytia that originate and insert on the bones of the skeleton. The nuclei lie just beneath the membranous sarcolemma that sheathes the cell. Each cell contains several longitudinal thread-like myofibrils that run parallel to each other for the whole length of the fiber. Each myofibril comprises several

myofilaments. The myofibrils can be seen by light microscopy, but myofilaments are visible only by electron microscopy.

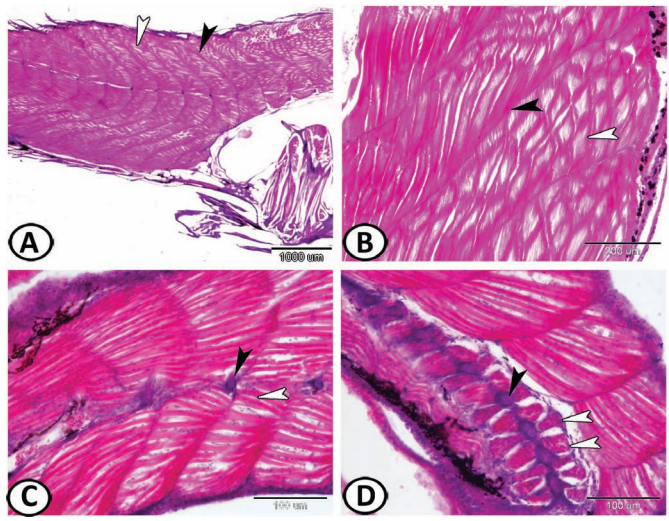

FIGURE 3.1 (A, B) Longitudinal section through the axial trunk musculature of guppy that is divided into a series of myomers that are V-shaped (white arrowheads) separated by collagenous sheath or called myosepta (black arrowheads) (HE). (C, D) The tail region of guppy showing the last vertebrae (black arrowheads) supported by well-developed skeletal muscles (white arrowheads) (HE).

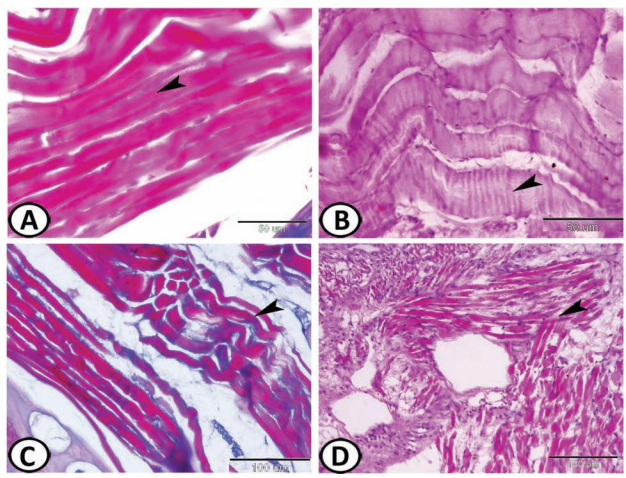

FIGURE 3.2 (A) Trunk muscle (arrowhead) of Molly (Masson's trichrome). (B) Muscles of the pharynx (arrowhead) of grass carp (PAS/HX). (C) Spiracular muscles of the pharynx (arrowhead) of guppy (Masson's trichrome). (D) Skeletal muscles (arrowhead) in the pharynx submucosa of grass carp (HE).

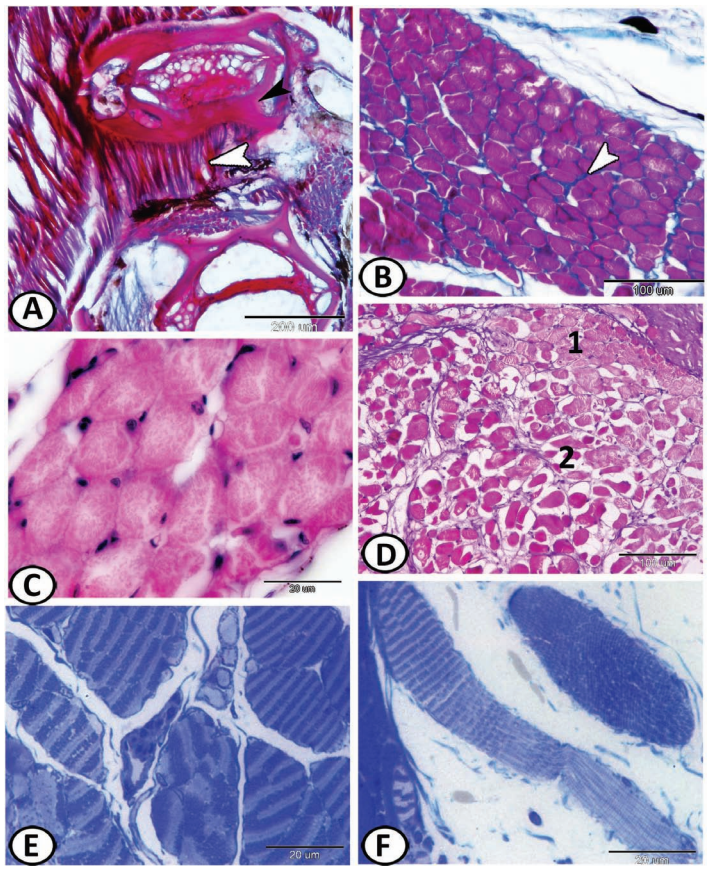

FIGURE 3.3 (A) Skeletal muscles (white arrowhead) support the vertebrae (black arrowhead) of guppy (Masson's trichrome). (B) Transverse section of skeletal muscles under the dermis of the skin of red-tail shark shows the endomysium (arrowhead) of connective tissue between the polyhedral cells (rhabdomyocytes) (Mallory's trichrome). (C) The typical appearance of the skeletal muscle of Nile tilapia is cut in the transverse section and shows the peripheral location of the nuclei. The rhabdomyocytes appear speckled with many dots. These are the myofibrils (actin and myosin myofilaments) (HE). (D) Transverse section of axial myomeres in the lateral line region of grass carp. The rhabdomyocytes that constitute the myotomal mass are composed of superficial small diameters red fibers (1) and inner large diameters white fibers (2). Most muscles are of the intermediate type containing red and white mixed muscles. (E, F) Semithin sections stained by toluidine blue show the ocular muscles of Molly fish that present cross-striations.

The body musculature of fish is arranged into segmental myotomes that have a complex three-dimensional structure. The myotomes form stacked cones in which the muscle fibers follow complex helical trajectories from

one myotome to the next along with the fish. This complex arrangement enabled all fibers across the body section to undergo similar strains during body bending: the arrangement could, therefore, be seen as a gearing system.

The rhabdomyocytes that are sectioned transversally show a polyhedral appearance and peripheral nuclei. The spaces between individual myocytes are filled with loose connective tissue containing capillaries. When viewed in a longitudinal section, rhabdomyocytes show transverse striations of alternating light (I) and dark (A) bands, with an amazing degree of evenness and regularity. Each "I" band is bisected by a dark transverse line, the Z line. Each myofibril is made up of repeating structural units called sarcomeres (between two Z bands). Since the sarcomeres of all myofibrils in a single cell are in register, the result is a typical cross-striation. The muscle fibers are grouped together into bundles (fasciculi) surrounded by loose collagenous tissue (perimysium).

The term myomere is commonly used in fish anatomy and refers to a separate muscle bundle, with parallel fibers running along the long axis of the body. Myomeres are connected by delicate connective tissue septa (myosepta, Figure 3.1A and B). There is an epaxial and a hypaxial myomere for each vertebra in most fishes.

Fish have other small voluntary muscles like extraocular, fin muscles, or the spiracular muscle. Opening/closing movements of the spiracle are controlled by the first dorsal constrictor muscle that regulates water entry into the pharynx (Figure 3.2B and D). Whereas the number of muscle fibers is fixed around the time of birth in mammals, in many species of fish, muscle fiber numbers increase throughout a large part of their life.

The two most distinctly different skeletal muscle types—red and white—have different degrees of vascularization and myoglobin content, which account for their color. These two kinds of muscles are involved in two kinds of swimming activity.

The red fibers are related to sustained activity, while the white fibers are too short, strong bursts of motion. The layer of red muscle lying as a wedge along the lateral line, just beneath the skin and underlying the fins, has a higher lipid content than the white tissue, and a larger number of mitochondria per cell and higher respiratory activity. The red fibers are aerobic, slow-contracting, and fibers. The red muscle is also generously supplied with blood, potentially providing a good site for the injection of drugs. Red muscle cells are usually most prominent in the areas underlying the fins of major propulsion. In salmonids, this is under the lateral line in a configuration to

move the tail. In perch and other species that utilize their pectoral fins for locomotion, red muscle cells are abundant in the areas under these fins.

The white (fast) fibers constitute the bulk of the muscle mass, making up the deep skeletal muscles in the epaxial (dorsal) and hypaxial (ventral) myomeres. These muscles are characterized by low numbers of mitochondria and low respiratory activity. The white fibers are anaerobic and fast contracting but are considered useful in short, strong bursts of swimming during, which they fatigue rapidly.

3.2 CARDIAC MUSCLE FIBERS

The striated muscle fibers of the heart (Figure 3.4) are unlike those of the body musculature in that they consist of a great syncytium of anastomosing and branching fibers (cardiomyocytes). They do not lie parallel to one another, and several planes may be seen when the heart muscle is sectioned for microscopical study. Another important difference is that each cardiac muscle possesses one nucleus. These nuclei are located at regular intervals near the center of the cell, rather than just beneath the sarcolemma (the plasma membrane of a muscle fiber). At sites of end-to-end contact are the intercalated discs (junctional complexes), structures found only in cardiac muscle.

Mature cardiomyocytes exhibit a cross-striated binding pattern identical to that of skeletal muscle. Surrounding the cells is a delicate sheath of endomysial connective tissue containing a rich capillary network. Working cardiomyocytes from fish hearts are smaller than their mammalian counterparts. The sarcoplasmic reticulum is frequently reduced, sometimes to nothing more than peripheral caveolae, T tubules are also reduced. Cardiomyocytes are capable of regeneration, even in older individuals. They show both hyperplastic and hypertrophic growth in contrast to postembryonic mammals where the growth is hypertrophic only.

The specially modified conduction pathways (Purkinje fibers) found in higher vertebrates seem to be lacking in fish hearts. However, rare cardiac pacemaker cells, sometimes seen in histological sections, near the sinoatrial ostium (usually) or elsewhere in the sinus initiate the heartbeat. This signal is then conducted into the atrium and produces the atrial contraction. Heart rate is mainly influenced by vagal inhibition and temperature.

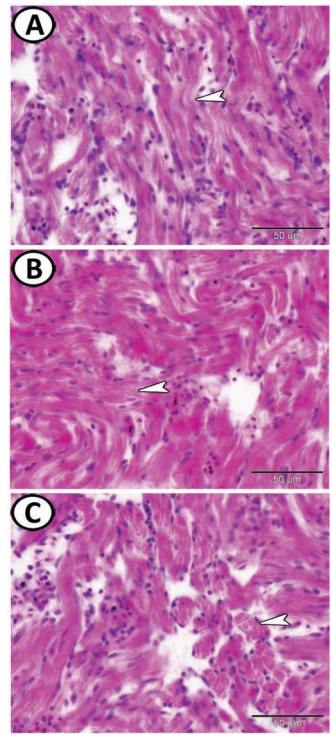

FIGURE 3.4 Cardiac muscle fibers (A, B) longitudinal section of ventricular cardiomyocytes of guppy. This micrograph shows branching of the myofibers (arrowheads) whose ends are in contact with adjacent cells (HE). (C) The cardiac ventricle of guppy. Transverse (arrowhead) and oblique sections in ventricular cardiomyocytes. Cardiac muscle fibers are cylindrical cells with one or rarely two central nuclei.

3.3 SMOOTH MUSCLE FIBERS

Smooth muscle fibers usually form the contractile portion of the walls of most viscera, the tunica media of the arteries and veins, the walls of ducts of various glands, and are found in a variety of other locations. The cells (or fibers or leiomyocytes) of smooth muscle are elongated, spindle-shaped structures with tapering ends, each with a centrally located nucleus (Figure 3.5). They are enclosed by a basal lamina and a network of reticular fibers. They are without striations and thus are said to be smooth. The leiomyocytes are placed close together, forming layers or sheets, although single cells may be formed. The cell contains delicate contractile myofilaments, hard to see with the light microscope.

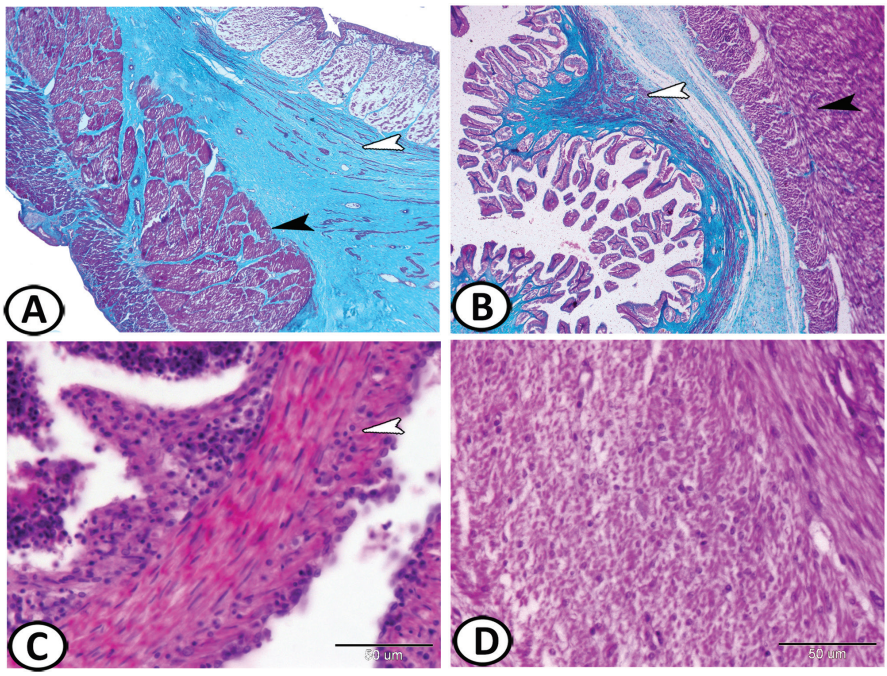

FIGURE 3.5 Smooth muscle fibers (A) transverse section of the wall of the fundic stomach of Nile catfish showing dispersed smooth muscle fibers in the submucosa (white arrowhead) and tunica muscularis (black arrowhead) that consist of inner and outer layers (Crossmon's trichrome). (B) Transverse section of the wall of the pyloric stomach of Nile catfish showing muscularis mucosa (white arrowhead) and tunica muscularis (black arrowhead) (Crossmon's trichrome). (C) Transverse section of the wall of the intestine of guppy showing smooth muscle fibers (leiomyocytes) is mostly arranged in two adjacent perpendicular layers (arrowhead): the outer longitudinal layer and the inner circular one. This arrangement permits peristalsis, that is, the forward propelling of the content of the tube (HE). (D) Cross-sections in smooth muscle fibers of the pharynx of grass carp (HE).

In many tubular visceral structures, such as the gastrointestinal tract, smooth muscle fibers are disposed in many layers with the cells of one layer arranged at right angles to those of the adjacent layer. This arrangement permits a wave of contraction to pass down the tube, propelling the contents forward; this action is called peristalsis. When cut in the transverse section, the central nuclei may appear absent in several sections due to the sectional angle. The contraction process of smooth muscle is slow and not subject to voluntary control.

KEYWORDS

- **myofibrils**
- **epiaxial muscles**
- **cardiac muscles**
- **smooth muscles**

BIBLIOGRAPHY

Altringham J.D., Ellerby D.J. Fish swimming: patterns in muscle function. *J. Exp. Biol.*, **1999,** *202*, 3397–3403.

Johnston I.A. Structure and function of fish muscles. *Symp. Zaal. Sac. Land*., **1981,** *48*, 71–113.

Martin C.I.; Johnston I.A. Endurance exercise training in common carp *Cyprinus carpio* L. induces proliferation of myonuclei in fast muscle fibers and slow muscle fiber hypertrophy. *J. Fish Biol.*, **2006,** *69,* 1221–1227.

CHAPTER 4

The Skeleton of Fish

ABSTRACT

The skeleton is composed primarily of the skull, the vertebral column, and the notochord. Fishes have no sternum. The appendicular part of the skeleton includes pectoral and pelvic girdles with their related fin skeleton. Cartilage is a firm, resistant tissue found in all classes of vertebrates. The chondrocyte is the main constituent cell of cartilage that is isolated within a voluminous extracellular matrix. Covering most elements of cartilage is the perichondrium, which comprises chondroblasts that are capable of forming a new cartilage matrix. There are six main types of cartilages: hyaline-cell cartilage, elastic-cell rich cartilage, fibro-cell cartilage, matrix-rich hyaline cartilage, cell-rich hyaline cartilage, and scleral cartilages. Hyaline-cell cartilage is the most common. Bone is formed in all vertebrates except living agnathans and Chondrichthyes. The bone is composed of osteocytes embedded in a secreted acellular matrix. Bone is not only confined to the internal skeleton but also found as hard plates or scales in the integument. Unlike mammals, fishes do not have any hematopoietic elements within the bone. Macroscopically, three bone types are distinguishable: compact bones, spongy bones, and chondroid bones. There are two types of fish compact bones: cellular and acellular. Cellular bone contains osteocytes and is found in lower orders. Fishes of higher orders usually have acellular bones that are characterized by a lack of osteocytes. In addition to osteocytes, two other bone cells can be observed: osteoblasts and osteoclasts. Two types of ossification could be identified in fish: intramembranous and endochondral ossification. The vertebra bears processes above and below the centrum (a vertebral body), which encloses remains of the notochord. These processes are the neural and hemal arches, which protect the spinal cord. The notochord consists of inner vacuolated cells surrounded by an epithelial-like sheath of cells. It contains very tumescent cells lying closely pressed together. The notochord cells are thick walled and their cytoplasm is filled with a homogeneous, semifluid

content. The dorsal fin consisted of a series of longitudinally arranged bones (pterygiophores) embedded in the dorsal musculature that articulated with the fin rays. The caudal fins were supported by a series of flattened hypural bones that contained hyaline cartilage surrounded by perichondral bone. The teleost scale comprises an outer osseous part and an inner layer that consists of parallel collagen fibers embedded in an organic matrix.

The histological diversity of the skeletal tissues of fishes is impressive compared with that of other vertebrate groups. The skeleton is composed primarily of the skull, the vertebral column, and the notochord, incomplete in most fishes. Fishes have no sternum. The appendicular part of the skeleton includes pectoral and pelvic girdles with their related fin skeleton.

4.1 CARTILAGE

Cartilage and bone are connective tissues with a firm extracellular matrix specialized for support of the body as a whole. Cartilage (Figures 4.1–4.5) is a firm, resistant tissue found in all classes of vertebrates. The chondrocyte is the main constituent cell of cartilage. It is isolated within a voluminous extracellular matrix, which is neither vascularized nor innervated.

Chondrocytes, dispersed in cavities (lacunae), are metabolically active cells that have to synthesize and turn over a large matrix volume comprising collagens, glycoproteins, proteoglycans, and hyaluronan. Cartilage cells at the periphery of the piece are flattened in a plane parallel to the surface. Covering most elements of cartilage is a fibrous layer, the perichondrium, which comprises cells known as chondroblasts that can form a new cartilage matrix.

Cartilage forms the structural elements of the skeleton in embryonic and very young trout, and can almost disappear in older fishes. Initially, an aggregation of mesenchyme cells becomes specialized as chondrocytes. These early chondroblasts multiply to form a compact mass of cartilaginous tissue. Eventually, as the basophilic matrix accumulates around the chondrocytes, these cells become isolated in lacunae, which appear in sections as clear, more, or less spherical spaces. Surrounding the cartilaginous elements is a perichondrial sheath composed of fibroblasts and collagenous fibers. Fishes have a variety of specialized cartilages that are somewhat different from those found in higher vertebrates.

There are six main types of cartilages: hyaline-cell cartilage, elastic-cell rich cartilage, fibro-cell cartilage, matrix-rich hyaline cartilage (MRHC),

cell-rich hyaline cartilage (CRHC), and scleral cartilages. Hyaline-cell cartilage is the most common.

4.1.1 HYALINE-CELL CARTILAGE

Hyaline-cell cartilage (HCC) (Figure 4.1) is typically an avascular tissue that consists of closely packed cells with abundant hyaline cytoplasm and little matrix contains collagenous fibers. Its cellularity approaches to the epithelium (EP). There is an enormous variation in cell size even within the same piece of tissue. The greatest dimension of cells ranges from 10 to 36 µm. There is no pericellular capsule and the matrix closely fills the gaps between cells. The matrix has only a mild affinity for alcian blue and the cells are not shrunken within lacunae.

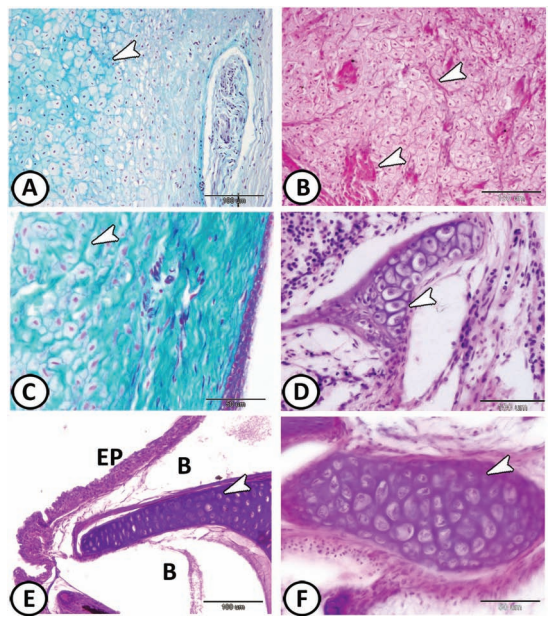

FIGURE 4.1 Hyaline-cell cartilage: (A**)** tightly packed chondrocytes with abundant cytoplasm (arrowhead) in the operculum of silver carp (AB/HX). (B, C) Fibrohyaline-cell cartilage in submaxillary meniscus of silver carp. Note the admixture of hyaline cells with collagenous fibers (arrowheads) (PAS/HX and Crossmon's trichrome, respectively). (D) Chondrocytes are shrunken in the lacuna (arrowhead) in the pharynx of grass carp (HE). (E) A periosteal pad in the premaxilla of Guppy. The pad (arrowhead) is separated from the epithelial tissue (EP) by a bursa (B). The chondrocytes are small at the peripherally of the pad (HE). (F) Hyaline-cell cartilage (arrowhead) in the gill arch of molly fish resembles that of mammals (HE).

Two subtypes of the HCC are described: fibrohyaline-cell cartilage (chondroid) where collagen fibers are prominent in the matrix, and lipohyaline-cell cartilage where fat and hyaline cells are intermingled (rare). The cells of HCC (Figure 4.2) may arrange in rows, form concentric arrays, or no describable patterns. The nuclei may be oval, round, deeply indented (in large cells), or highly irregular. Larger cells have a very low nuclear to cytoplasmic ratio that usually binucleate. The alcian blue and safranin O stain the sulfated glycosaminoglycans contents of the matrix. Hyaline cell cartilage can gradually merge with bone tissues where it participates in chondroidal osteogenesis. HCC usually attach by collagenous fibers in the articular surface or found in association with skeletal muscle fibers (Figure 4.3).

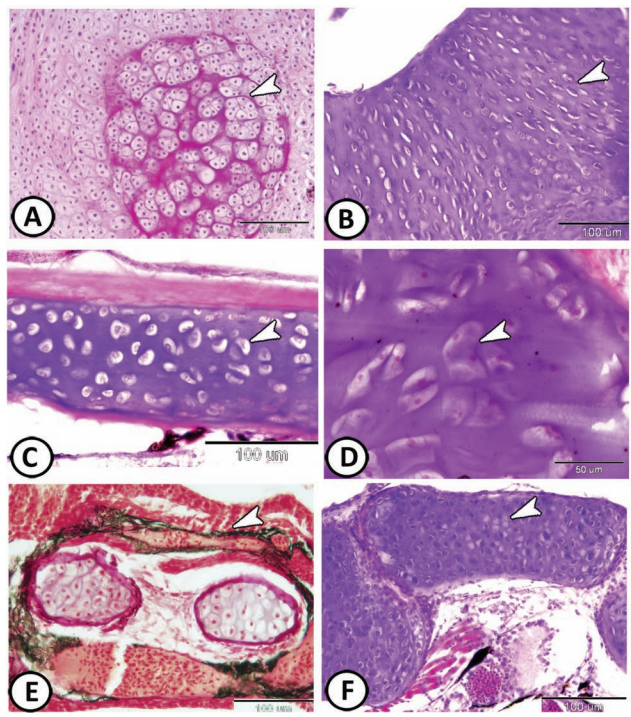

FIGURE 4.2 (A) Hyaline-cell cartilages in the tongue of grass carp arrange in a concentric manner (arrowhead) (PAS/HX). (B) Hyaline-cell cartilages arrange in rows (arrowhead) around the olfactory region of molly (HE). (C) Sagittal section stained by HE showing no describable arrangement of hyaline cell cartilages (arrowhead) in the pectoral girdle of molly. Note the homogenous basophilic matrix. (D) Higher magnification in the hyaline cells (arrowhead) in the pharynx of grass carp (HE). (E) HCC is surrounded by elastic fibers (arrowhead) in the gills of Guppy (Wiegert's Elastica). (F) A transverse section in lipohyaline-cell cartilage (arrowhead) in the tongue of molly fish (HE).

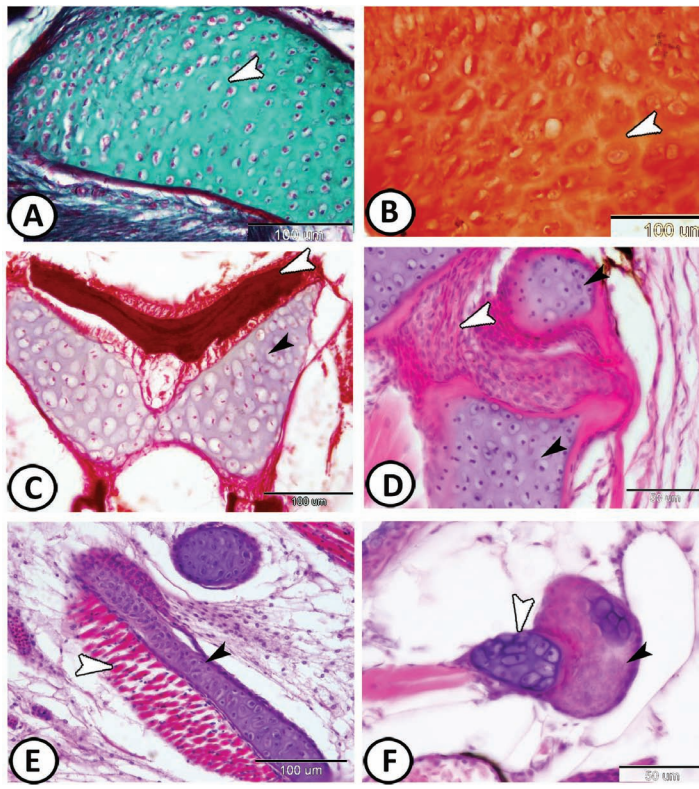

FIGURE 4.3 (A) Hyaline-cell cartilage beneath the nostrils of molly fish is a semirigid form of skeletal tissue, which contains neither blood vessels nor nerves. Chondrocytes (whitish with red nuclei) are mature cells scattered in an abundant extracellular matrix that appears green in color (arrowhead) by Crossmon's trichrome. (B) Higher magnification shows the safranin-positive matrix (arrowhead) in the cartilage around the inner ear of molly fish. (C) HCC (black arrowhead) is attached to the bone (white arrowhead) of the head around the brain of red-tail shark (Weigerts elastica). (D) HCC (black arrowheads) attached to collagenous fibers (white arrowhead) in the dorsal fin of Guppy (HE). (E) HCC (black arrowhead) is attached to skeletal muscle fibers (white arrowhead) in the buccal cavity of molly fish. (F) HCC (black arrowhead) differentiate into hyaline cartilage (white arrowhead) in the submaxillary meniscus of Guppy.

Hyaline-cell cartilage is distributed in the head of teleosts (Figure 4.4). HCC occurs in lips and rostral folds, in prepalatine and submaxillary menisci, in ligaments, at the anterior end of the basihyal, in the pectoral girdle, in adhesive disks, in gill arches, beneath the basioccipital chewing pad, in barbels, next to the facial nerve, around the olfactory region, and in the core of the nasal skin flaps. It is a particularly important tissue in cyprinids and related

fish, and enormous masses of it are present in red-tail shark, and Orinoco sailfin catfish. It acts as a damper against the contractions of the heart or the pressure of occluding pharyngeal teeth, and it provides the mouth region of bottom-dwelling, algal eaters with flexible support. Hyaline-cell cartilages are also present in suckermouth of Orinoco sailfin catfish.

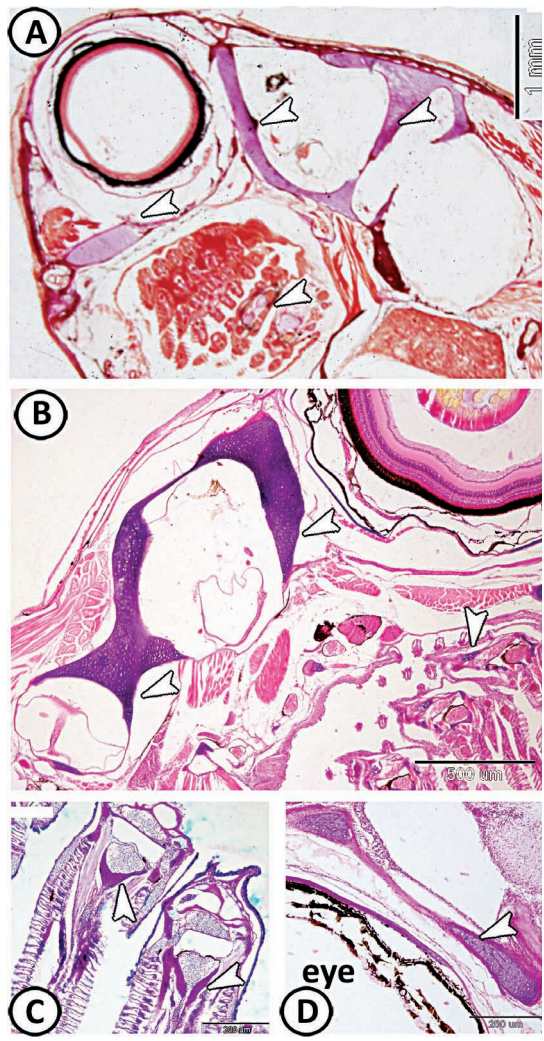

FIGURE 4.4 **(A, B)** Distribution of hyaline cartilages (arrowheads) in the head of molly and Guppy, respectively (Van Gieson/Wigert's Elastica and HE, respectively). (C) Hyaline cartilage (arrowheads) in the gill arches of molly (AB/PAS/HX). (D) Hyaline cartilages (arrowhead) around the eye (HE).

4.1.2 FIBRO/CELL-RICH CARTILAGE

Fibro/cell-rich cartilage (FCRC) (Figure 4.5A–C) is highly cellular fibrocartilage, in which the matrix contains much collagen and the cells are not hyaline. The cells are generally shrunken within lacunae. The cells have a higher nuclear: cytoplasmic ratio. FCRC lacks a discrete perichondrium (i.e., a surrounding envelope of dense fibrous connective tissue, with or without a chondrogenic layer, that is distinct from the cartilage itself) and is never surrounded by perichondral bone. FCRC is a common articular tissue. It is present, alone or with other tissues, in both the submaxillary meniscus and that between the maxilla and premaxilla of many teleosts. Although most of the cells are fibroblasts, a few are chondrocytic and closely packed.

4.1.3 ELASTIC/CELL-RICH CARTILAGE

Elastic/cell-rich cartilage (ECRC) (Figure 4.5D) is highly cellular cartilage in which the matrix is rich in elastic fibers and the cells are not hyaline. The cells can be shrunken within lacunae. ECRC can only be distinguished by the use of elastic stains (orcein, Weigert's elastic, or Van Gieson's). It is frequently distributed in lips, gill filaments, and barbels to give flexible support and they are surrounded by a thick fibrous perichondrium.

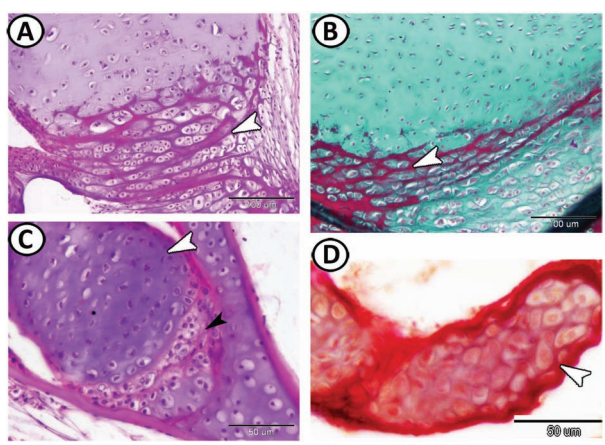

FIGURE 4.5 (A, B) FCRC (arrowhead) in the tongue of grass carp (HE and Crossmon's trichrome, respectively). (C) FCRC (black arrowhead) and hyaline cartilage (white arrowhead) in the maxillary meniscus of Guppy. The FCRC is articular (HE). (D) ECRC (arrowhead) in the lower lip of red-tail shark (Van Gieson Resorcin Fuchsin).

4.1.4 CELL-RICH HYALINE CARTILAGE

It is hyaline cartilage in which >50% of the tissue volume is occupied by cells or lacunae (Figure 4.6A–D). There can be great variation in cell size and shape—even in the same piece of cartilage (e.g., in the gill arches where the cells range from 5 to 15 μm in diameter). In the occipital region, some nuclei in CRHC are sickle-shaped. CRHC frequently forms epiphyseal cartilages (e.g., in the epiphysis of the tongue of grass carp). Many excellent examples of the erosion of chondrocytes during endochondral ossification are provided by CRHC in the tongue. In Figure 4.6D, the hypertrophic cells are being removed by the destructive action of cells in the adjacent bone marrow (BM).

4.1.5 MATRIX-RICH HYALINE CARTILAGE

This is the typical or hyaline cartilage of standard mammalian texts. In routinely processed material, the chondrocytes are shrunken in lacunae and separated from each other (except in regions of cell nests) by considerable quantities of the matrix (Figure 4.6E). MRHC is frequently found in gill arches. MRHC may be permeated by cartilage canals or channels conveying skeletal muscle fibers. Like CRHC it, too, can be calcified.

4.1.6 SCLERAL CARTILAGE—A SPECIAL CASE

The sclera can contain or consist of cartilage, dense fibrous connective tissue or bone. Where cartilage is found, it generally forms, or contributes to, a curved plate that surrounds the outer part of the eye (Figure 4.6F). The thickness of the cartilage plate is fairly constant between species (16–19 μm). Scleral cartilage is difficult to classify, for there is often a central zone of one or two rows of closely packed cells (making the cartilage CRHC), but these are flanked by peripheral zones of the matrix (making the cartilage MRHC). This type of cartilage may rarely be very prominent all around the eye (particularly in certain fish with protruding eyes) but more commonly there are separate pieces of cartilage above and below the eye and frequently is limited to the lower half of the orbit.

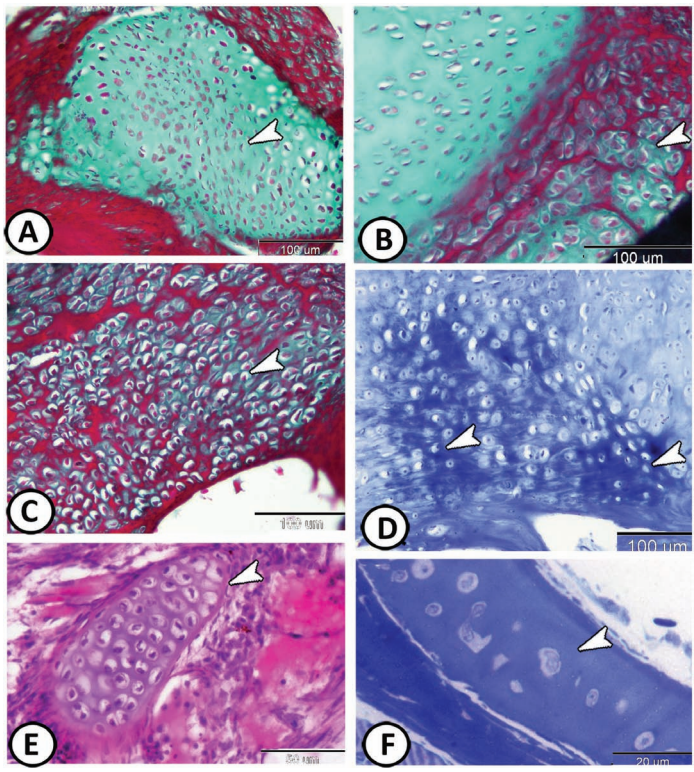

FIGURE 4.6 (A, B) Cell rich hyaline cartilage (arrowheads) in the tongue of grass carp (Crossmon's trichrome). (C) Calcified CRHC (arrowhead) in the tongue of grass carp (Crossmon's trichrome). (D) Calcified CRHC (arrowheads) in the lower lip of silver carp (bromophenol blue). (E) Matrix-rich cartilage (arrowhead) in the gills of Guppy (HE). (F) Scleral cartilage (arrowhead) in red-tail shark (TB).

4.2 BONE

Bone (Figures 4.7–4.10) is formed in all vertebrates except living agnathans (lampreys) and Chondrichthyes (sharks). It is a rigid calcified tissue of limited elasticity. Like cartilage, it is composed of a parenchymal cell, the osteocyte, embedded in a secreted acellular matrix. The osteocytes are present in lacunae in the matrix from which minute canaliculi radiate to form a complicated network connecting all the lacunae into a system of cavities. Bone is not only confined to the internal skeleton but also found as hard plates or scales in the integument.

Histologically, fish bones are like those of higher vertebrates. Unlike mammals, fishes do not have any hematopoietic elements within the bone. Bone is categorized according to the existence of cellular components into cellular and acellular bones. The cellular bone harbors a typical organization of the osteocytic network. The acellular bone is devoid of osteocytes. Cellular bone is found in lower orders, such as the salmoniformes, but their concentration is decidedly lower than that found in mammals. Fishes of higher orders such as perciformes (perch-like) usually have the acellular bone.

In addition to osteocytes (Figure 4.7), two other bone cells can be observed: osteoblasts and osteoclasts. It is accepted that osteocytes derive from osteoblasts that have secreted the bone matrix around themselves. Osteoclasts are large multinucleated cells (mononucleated in juveniles) with phagocytic properties. They dissolve the matrix by releasing lysosomal enzymes. During bone remodeling, many osteocytes are released from their lacunae as osteoclasts actively reabsorb the bone. The relationships between bone, connective tissue, and cartilage are more complex than those in higher vertebrates.

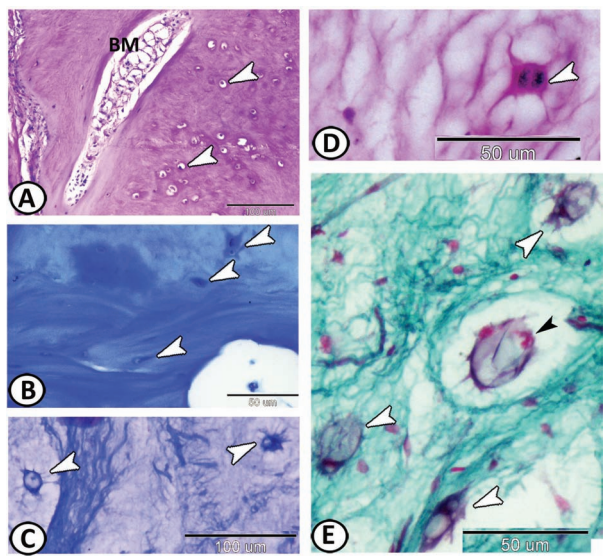

FIGURE 4.7 (A) Section in the cellular bone in the upper lip of silver carp showing osteocytes (arrowheads) and bone marrow (BM) (PAS/HX). (B) Section in the cellular bone in the upper lip of silver carp showing the positive-bromophenol blue matrix around the osteocytes (arrowheads). (C,D) Higher magnification in bony tissue in the tongue of grass carp stained by Masson's trichrome and HE, respectively, showing the osteocytes with well-defined processes (arrowheads). (E) Bony tissues in the tongue of grass carp stained by Crossmon's trichrome showing osteocytes (white arrowheads) and multinucleated large osteoclasts (black arrowhead).

4.2.1 THE BONE OSSIFICATION

Two modes of cartilage-dependent bone growth have been specified for fish, endochondral, and intramembranous ossification.

4.2.1.1 ENDOCHONDRAL OSSIFICATION

It depends on the formation of a transient cartilage template, which is gradually replaced by bone tissue (Figure 4.8A–D). The cartilage template exhibits a specific zonal arrangement where the cartilage grows through a progressive proliferation of chondrocytes. Proceeding the proliferating stage, the resting stage retains the self-renewal capacity. Proliferating chondrocytes exit the cell cycle and undergo hypertrophy. Hypertrophied chondrocytes prepare the extracellular matrix for the deposition of bone tissue. In normal SBs, this zone is followed by a zone of calcification, in which the cartilage matrix becomes ossified and is followed by a degradation zone with chondroclasts and osteoblasts. Laterally, the epiphyseal growth plate is covered by bony tissue. At the edges of these bones, osteoblast clusters are detectable. From these clusters, osteoblast-like cells arise. These osteoblast-like cells cover the outside of the endochondral bones in a monolayered perichondrium. Endochondral bone formation archives bone growth as chondrocytes capable to replicate and produce an extracellular matrix that adopts the bone formation. Chondrocytes are organized in the resting, proliferating, and hypertrophic zones. Cartilage matrix subjects to extensive degradation and erosion particularly by Chondroclasts.

4.2.1.2 INTRAMEMBRANOUS OSSIFICATION

This type of ossification depends on the differentiation of osteoblasts when a bone is formed directly from mesenchyme (Figure 4.8E and F). Osteoblast clusters are large clusters (composed of more than 25 cells) situated at the edges of outgrowing flat bones. Examples include the dentary, the maxillary, and the frontal bone in the metopic suture. The osteoblasts have a large oval, round, or irregularly shaped nuclei. Lateral to these osteoblasts is a zone of differentiating osteoblasts. Within this zone, the cell size and nuclei are smaller and the cells become more elongated. It appears as if the osteoblast clusters differentiate into the typical spindle-shaped osteoblast-like cells of the perichondrium. These spindle-shaped osteoblast-like cells are a single

(mono-) or double (bi-) layer unlike that of the perichondrium of mammals, which is typically multilayered.

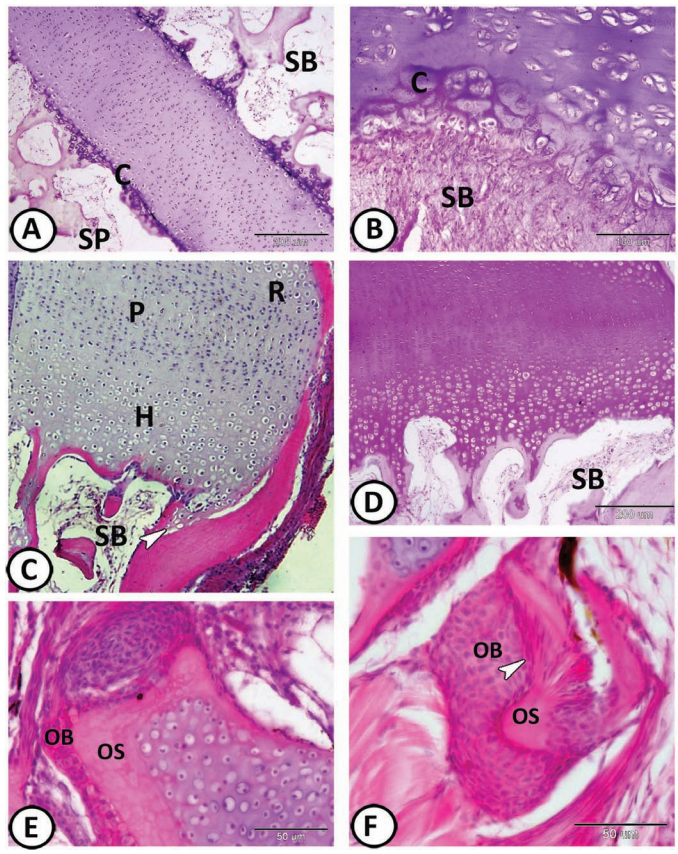

FIGURE 4.8 (A, B) Endochondral ossification in the pharynx of grass carp (HE). Note the zone of calcification (C) and spongy bone (SB). (C, D) Endochondral ossification in the tongue of grass carp (HE, PAS/HX, respectively). Note resting cartilage (R), the zone of proliferation (P), the zone of hypertrophy (H), and SB. Laterally, the epiphyseal growth plate is covered by bony tissue. At the edges of these bones, osteoblast clusters are detectable (arrowhead). (E, F) Intramembranous ossification in dorsal fins of Guppy (HE). Osteoblast clusters (OB) differentiate to osseous bone (OS). Note within this zone, the cells become more elongated (arrowhead).

4.2.2 BONE TYPES

Macroscopically, three bone types are distinguishable: compact bones, SBs, and chondroid bones.

4.2.2.1 COMPACT BONES

Both cellular and acellular bones are covered by spindle-shaped osteoblast-like cells with elongated nuclei (Figure 4.9).

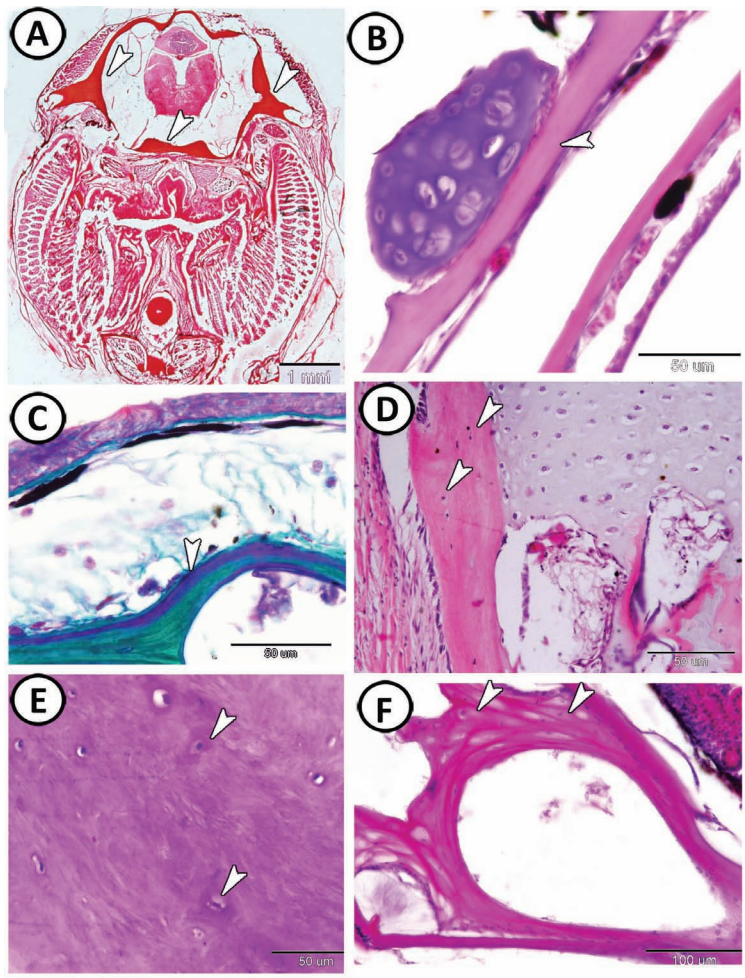

FIGURE 4.9 (A) The distribution of bones (arrowheads) in the skull of molly (safranin O). (B) Acellular bone (arrowhead) around the brain of Guppy (HE). (C) Acellular bone (arrowhead) beneath the dermis of the skin of the head. The osseous endoskeleton of Guppy is devoid of osteocytes (Crossmon's trichrome). (D) Cellular bone in the tongue of grass carp (HE). Note the osteocytes are shown by arrowheads. (E) Cellular bone is seen in silver carp under the dermis of the skin of the upper lip. Some small osteocytes are identified (arrowheads). (PAS/HX). (F) Cellular bone of vertebrae (arrowheads) of molly (HE).

4.2.2.1.1 Cellular Bones

The majority of the skull bones are composed of cellular bones with cells that are entrapped in the bone matrix as osteocytes. The osteocyte is round with oval, round, or atypical nuclei. Moreover, these cells typically have two cytoplasmic processes. This osteocyte type originates from the osteoblast-like cells that line the bony tissue. Cellular compact bone is also found in the lepidotrichia (bony segment) of the fins.

4.2.2.1.2 Acellular Bones

In addition to the cellular bones, the fish skeleton is also composed of several acellular bones with no entrapped osteocytes. These include the lateral ethmoid, the nasal bone, orbitosphenoid, the frontal bone, the supraorbital bone, the parietal bone, pterotic bone, the supratemporal bone, and basioccipital bone. Moreover, some bones have cellular and acellular parts, such as the branchiostegal rays.

4.2.2.2 SPONGY BONES

SBs are present throughout the bony trabeculae network and arise from the process of endochondral ossification (Figure 4.10A–C). The interspace in between the trabeculae is filled with adipocytes, but the hematopoietic connective tissue is absent; this is in contrast to mammals. The inner- and outer-bony surfaces are covered with the osteoblast-like cells. In the inner part, osteoblast clusters, as well as osteoclasts, are observable. They are detected in the pectoral girdle, the pterosphenoid, the lower quadrate bone, the ceratohyal, and the anguloarticular. Some bones of the cranium and gill arches contain SB but, unlike mammals, this is not a site of hematopoiesis. SB is laminated with spaces that give it a sponge-like appearance.

4.2.2.3 CHONDROID BONES

Chondroid bones are mineralized cartilages that are integrated into bones (Figure 4.10D–F). They are observed at the following bone articulation sites: quadro-articular, ethmoid-premaxilla, hyomandibular-prootic, and hyomandibular-opercle. In these intramembranous bones, chondroid bony tissues make up the cartilaginous socket of the joint. Besides these joints, this bone type is also detected within the scleral ossicles of the eye.

Histologically, two types of chondroid bone are distinguishable. In the first, the chondrocytes are surrounded by a calcified matrix, which is directly embedded and not distinguishable from the underlying normal bone tissue (Figure 4.10E). In contrast, in the second type, underlying the calcified chondrocytes, a collagen-rich layer is observed, connecting the chondroid bone to the bony tissue (Figure 4.10F). However, no osteoblasts or osteoblast-like cells are observed in either type. Osteoblasts of type II are only present at the edges of the chondroid bones (Figure 4.10D) where they are differentiating into the osteoblast-like cells. This result suggests that the chondrocytes, rather than the osteoblast-like cells, may be directly responsible for the mineralization of this bone type. Chondroid bone in teleosts is associated with sites that experience mechanical stress, such as beneath articular surfaces. This tissue is considered to meet the support, resistance, and movement demands to which articular bones are subjected. Another property of chondroid bone is that it has the ability to grow rapidly.

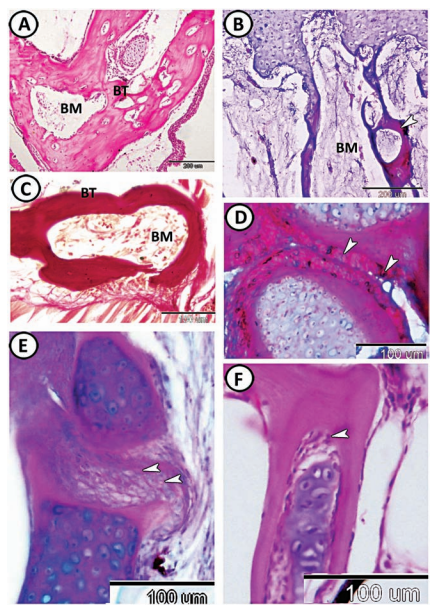

FIGURE 4.10 (A) Spongy bone in the pectoral girdle of Red-tail shark. Note the bone trabeculae (BT) and bone marrow (BM) (HE). (B) SB in the zone of ossification in the tongue of grass carp (Masson's trichrome). Note the BT (arrowhead) and BM. (C) SB in the operculum of Guppy (Weigert's elastica). Note the BT and BM. (D) Chondroid bone (arrowheads) in the articular surfaces of the fins of Guppy (Masson's trichrome). (E) Chondroid bone in molly. Bone (arrowheads) forms in the connective tissue in the proximity of a cartilaginous piece (blue) harboring numerous chondrocytes that will be gradually invaded by BT (PAS-AB-HX). (F) Chondroid bone (arrowhead) around the eye of Guppy (HE).

4.3 VERTEBRAE

Fish are vertebrates. The trunk region showing the vertebral column lying between the spinal cord (SC) and the dorsal aorta. The vertebrae are intermetameric and connected by intervertebral elastic ligaments. The vertebra (Figure 4.11) bears processes above and below the centrum (a vertebral body), which encloses remains of the notochord. These processes are the neural and hemal arches, which protect the SC. Typically, the SC is surrounded by the neural arches. The hemal processes are present only in the caudal region. The centrum of a fish is usually concave at each end, which limits the motion of the fish. This can be contrasted with the cternum of a mammal, which is flat at each end. Dermic fish bones whether or not attached to the vertebrae are found in the intermuscular connective tissue.

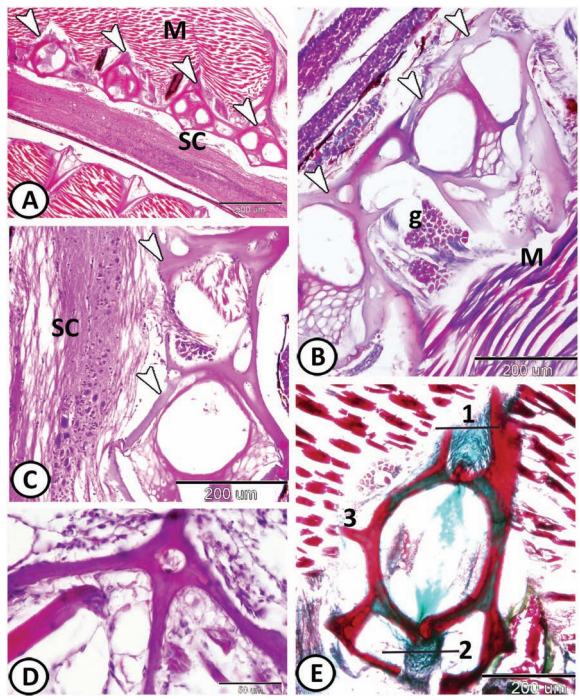

FIGURE 4.11 (A) The trunk region of Molly showing the vertebral column (arrowheads) laying between spinal cord (SC) and muscles (M) (HE). (B) Guppy vertebrae (arrowheads). Note spinal ganglia (g) and trunk muscles (M) (Masson's trichrome). (C) Guppy vertebrae (HE). The vertebra (arrowheads) bears processes, which encloses remains of the notochord. These processes protect the SC. (D) Molly vertebrae (HE). (E) A transverse section in the caudal region of Molly fish (Crossmon's trichrome). This micrograph shows different parts of a vertebra. (1) Neural arches; (2) hemal arches; and (3) transverse processes.

4.4 NOTOCHORD

The most primitive type of supporting tissue in chordates is that of the notochord (Figures 4.12 and 4.13). During development, the notochord sheath or perichondral tube becomes completely invaded by bone and is built into a complex joined rod, which allows for rigidity and flexibility. The notochord, of mesodermic origin, is normally surrounded by a thick inner fibrous sheath and a thin outer elastic one. The notochord is persistent in some adult fish (chondrichtyans, dipnoi, and chondrostei). However, in the majority of the species, it disappears partly, generally being strangled by the development of the vertebrae. Relics of notochord often persist and are ensheathed by vertebral bone in the adult.

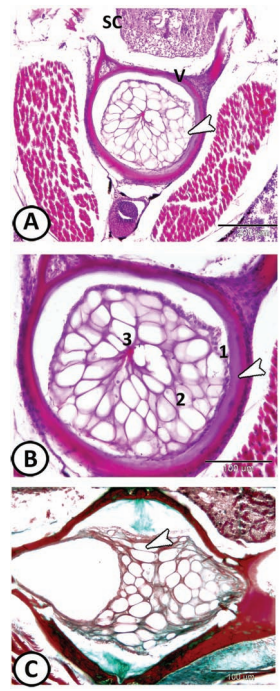

FIGURE 4.12 Notochord of Molly fish. (A) A transverse section through the anterior trunk region shows the position of the spinal cord (SC) and a vertebra (V) whose center surrounds the notochord (arrowhead). The notochord is a rather flexible rod partially persisting throughout life in lower vertebrates (HE). (B) Higher magnification through the notochord showing the notochord sheath (arrowhead) is composed of fibrous tissue. Under the sheath, three areas are found: a simple squamous or cuboidal layer (1), several layers of large vacuolated cells (2), and in the center, cells (3) surrounding lacunae (HE). (C) Notochord cells (arrowhead) lie closely pressed together and the tissue resembles that of plants (Crossmon's trichrome).

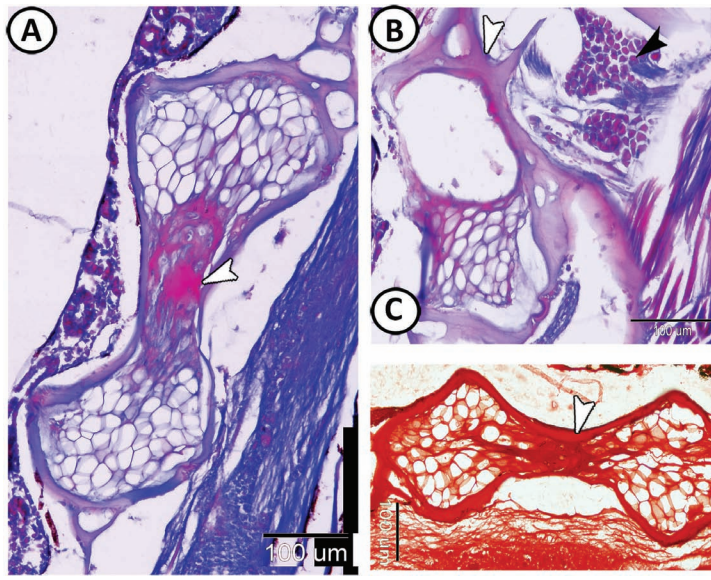

FIGURE 4.13 Notochord of Guppy fish: (A, B) transverse section through the notochord showing very tumescent cells and surrounded by the body of the vertebra (centrum—white arrowhead) with several bony processes. Note the SC, kidney (K), and the dorsal ganglia (black arrowhead) (Masson's trichrome). (C) Notochord cells are thick walled. Note safranin O-positive vertebral body (arrowhead).

The tissue of the notochord differs greatly from that of cartilage in histological appearance. The notochord consists of inner vacuolated cells surrounded by an epithelial-like sheath of cells. It contains very tumescent cells lying closely pressed together. They resemble plant cells more than do most animal tissues. The notochord cells are thick-walled and their cytoplasm is filled with homogeneous, semifluid content. It has been suggested that these vacuoles are lysosome-related organelles originating through H^+ATPase-dependent acidification. Around these cells, a perinotochordal basement membrane is present. This extracellular sheath is composed of three parts: the inner basal lamina in close proximity to the plasma membrane mainly contains laminins, surrounded by a medial layer of collagen fibrils that run parallel to the notochord, and an outer granular layer of loosely organized matrix that is mostly oriented in a perpendicular manner to the notochord. The perinotochordal sheath counteracts the pressure generated from vacuoles, providing the rigidity and the correct stiffness of this structure.

Besides its primary structural function, the notochord is also a source of developmental signals that pattern surrounding tissues. Among the signals

secreted by the notochord, Hedgehog proteins play key roles during embryogenesis. The vertebrate notochord plays a critical role in spine morphogenesis and bone ossification during late developmental stages.

4.5 FINS

The fins (Figure 4.14) are folds of skin supported by skeletal rays. Lepidotrichia are bony segments of dermal (scale) origin located at the distal margin of osteichthyan fins. They originate from the base and extend distally, dichotomously branching toward the margin of the fin.

The dorsal fin (Figure 4.14A and B) consisted of a series of longitudinally arranged bones (pterygiophores) embedded in the dorsal musculature that articulated with the fin rays. The fin rays usually bifurcate proximally and articulate either side of the pterygiophores. In the dorsal fin, FCRC forms an articulating surface between pterygiophores and the fin rays in all species. The only other site in which HCC is seen is on the deep surface of a ligament, which runs between the bifurcations of each fin ray near their articulation with the pterygiophores. Chondroid bone is found in the dorsal fin supports of cypriniforms and perciform. It is found in small quantities beneath the articular surfaces of both the pterygiophores and fin rays.

A cross-section of the dorsal fin (Figure 4.14C) shows that each lepidotrichium comprises a series of opposing concave hemisegment pairs enclosing space for nerve bundles, loose connective tissue, and blood vessels. In the medial layer of hemisegments, collagen is arranged dorsoventrally, while the collagen in the lateral layer of hemisegments is oriented from the base of the fin distally, in a craniocaudal direction. Each hemisegment is usually limited by an envelope of flattened cells that separates it from the surrounding tissues. It is either composed of an acellular matrix or possesses very few cells. Longitudinal sections show that the lepidotrichia consists of a number of segments, which are linked one to another by dense fibrous connective tissue (Figure 4.14D). Fin rays of cartilaginous fishes are slender, unsegmented, and horny, and are called actinotrichia (often erroneously called ceratotrichia).

In the caudal fins, the principal fin rays are supported by a series of flattened hypural bones that contain hyaline cartilage surrounded by perichondral bone. In Guppy (Figure 4.14E), HCC forms a series of rods of tissues (expansions of the periosteum) that connect to each other by fibrous tissue and attached to the hypurals. The fin rays lay in the grooves between the rods.

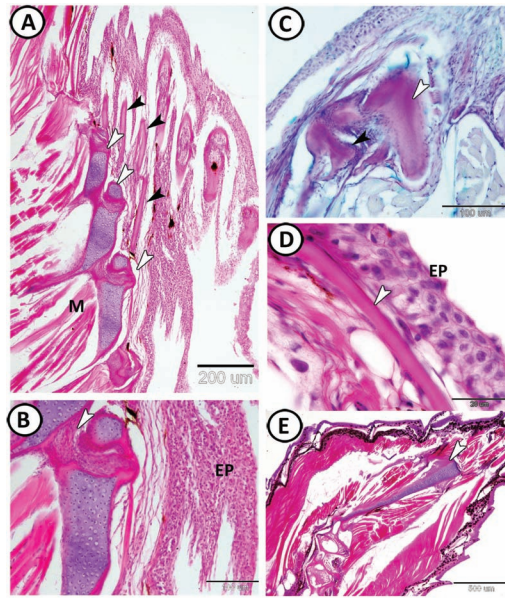

FIGURE 4.14 FINS of Guppy: (A) dorsal fin stained by HE consisted of a series of longitudinally arranged bones (pterygiophores) (black arrowheads) embedded in the dorsal musculature (M), that articulated with the fin rays (white arrowheads). (B) Higher magnification of the dorsal fin showing the stratified squamous EP and the fin rays attached by dense connective tissues (arrowhead). (C) A cross-section of the dorsal fin stained by AB/PAS/HX shows that each lepidotrichium comprises a series of opposing concave hemisegment pairs (white arrowhead). Each hemisegment is usually limited by an envelope of flattened cells (black arrowhead). (D) Longitudinal section of the dorsal fin shows the EP and lepidotrichia (arrowhead) that consists of a number of segments, which are linked one to another by dense fibrous connective tissue (HE). (E) Caudal fin rays are supported by a series of flattened hypural bones that contained hyaline cartilage (arrowhead) (HE).

4.6 SCALES

A fish scale is a small rigid plate that grows out of the skin of a fish. The shin of most fish is covered with these protective scales, which can also provide effective camouflage through the use of reflection and coloration, as well as possible hydrodynamic advantages.

Scales, of dermal origin, are a major feature of most species of teleosts. The scales vary enormously in size, shape, structure, and extent ranging from strong and rigid to microscopic or absent in some fish, such as eels and anglerfishes. The scales present below the dorsal fin and above the lateral line are found to be the largest. The scales in the other parts of the body are relatively smaller in

size. They are of several types. The placoid scale is found in the skin of elasmobranchs and consists of a spine and a basal plate; it contains a pulp cavity and is composed of a layer of dentine covered by enamel. Polypteridae and Lepisosteidae are the only fish, which possess ganoid scales, often rhomboidal in shape, with a thick outer ganoine layer (enamel-like substance). Cosmoid scales are scales with four layers and are characteristic of Sarcopterygii.

The teleost scale (Figure 4.15) comprises an outer osseous part and an inner layer that consists of parallel collagen fibers embedded in an organic matrix. They originate in scale-pockets in the dermis and extend toward the exterior of the animal in an overlapping way and are covered by the epidermis. Teleosts have ctenoid scales (with small spines on the posterior edge, such as those in perch) or cycloid scale (round or oval scale composed of acellular dermal bone without spines such as those in salmon and carp). Scanning electron microscopy (SEM) of the surface of the scales (Figure 4.15D) shows that they consist of many distinct circuli (lines or ridges of growth). Between the circuli, they are spaces, called intercircular spaces. The thickness, arrangement, and relative spacing of circuli of the scale are known to be important in fish taxonomy.

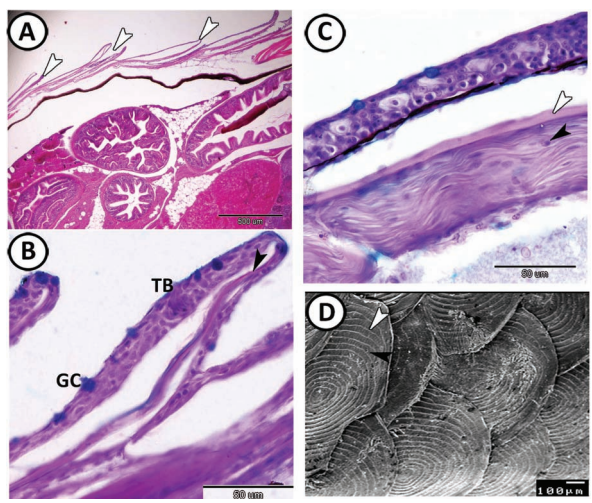

FIGURE 4.15 (A, B) General view of a skin sample taken from mid-dorsal region of the trunk of Guppy. Scales (white arrowheads) comprise an outer osseous part (black arrowhead) and the covering epidermis contained taste bud (TB) and goblet cell (GC) (HE and AB/PAS/HX, respectively). (C) Scales of red-tail shark consist of bone tissue (white arrowhead) and parallel collagen fibers (black arrowhead) (AB/PAS/HX). (D) SEM of the surface of the scales of Guppy shows that they consist of many circuli (white arrowhead) separated by intercircular spaces (black arrowhead).

KEYWORDS

- **cartilage matrix**
- **chondrocytes**
- **hematopoietic elements**
- **bone**
- **notochord**
- **osteocytes**

BIBLIOGRAPHY

Benjamin, M. Hyaline-cell cartilage (chondroid) in the heads of teleosts. *Anat. Embryol*. **1989,** *179,* 285–303.

Benjamin, M. The cranial cartilage of teleosts. *J. Anat.* **1990,** *169,* 153–172.

Bone, Q.; Moore, R. H. *Biology of Fishes*; 3rd ed. Taylor & Francis: New York, NY and Abingdon, 2008.

Dean, M. N.; Summers, A. P. Mineralized cartilage in the skeleton of chondrichthyan fishes. *Zoology.* **2006,** *109,* 164–168.

Corallo, D.; Trapani, V.; Bonaldo, P. The notochord: structure and functions. *Cell. Mol. Life Sci.* **2015,** *72,* 2989–3008.

Munshi, J. S. D.; Dutta, H. M. *Fish Morphology: Horizon of New Research*; Science Publishers, Inc.: Lebanon, NH, 1996.

Sire, J. Y.; Huysseune, A.; Meunier, F. J. Osteoclasts in teleost fish: light- and electron-microscopical observations. *Cell Tissue Res.* **1990,** *260,* 85–94.

Soliman, A. S. The growth cartilage and beyond: absence of medullary bone in silver carp ribs. *Mathews J. Cytol. Histol.* **2018,** *2*(1), 2577–4158.

Weigele, J.; Franz-Odendaal, T. A. Functional bone histology of zebrafish reveals two types of endochondral ossification, different types of osteoblast clusters and a new bone type. *J. Anat.* **2016,** *229,* 92–103.

CHAPTER 5

Cardiovascular System and Blood

ABSTRACT

The fish heart consists of four chambers: the sinus venosus, atrium, ventricle, and bulbus arteriosus. The sinus venosus is a thin-walled chamber whose composition varies between species. An important characteristic of the sinus is that it contains the heart pacemaker. The teleost atrium is a single chamber that shows considerable variability in size and shape between species. It is formed of an external rim of the myocardium with thin trabeculae. The ventricle is characterized by an abundant spongy myocardium that leaves in the lumen some lacunae in which blood circulates. The external ventricular shape has been grouped into three main categories: tubular, sac-like, and pyramidal, this division has several functional implications. The bulbus arteriosus opens in the ventral aorta and contains connective tissue and elastic fibers. Elastic arteries (ventral aorta or gill arteries) are found near the heart, and their media is rich in elastin. Veins are structurally similar to those in mammals but have thinner walls and less abundant smooth muscle. Special types of blood vessels are also recorded. Blood capillaries are histologically like those found in mammals, but they are much more permeable. The main blood cells in fishes are erythrocytes, neutrophils, eosinophils, basophils, heterophils, monocytes, lymphocytes, and thrombocytes.

5.1 HEART

The fish heart (Figure 5.1) typically consists of four chambers coupled in series and located caudo-ventrally to the gill cavity. In teleosts, the four chambers are (in sequence) as follows: the sinus venosus, the atrium, the ventricle, and the highly elastic bulbus arteriosus (or a contractile conus arteriosus in elasmobranchs, chondrostei, and holostei).

The heart of fishes consists of three layers of tissue: the epicardium, myocardium, and endocardium. The external epicardium consists of

a single layer of flattened epithelial cells, the mesothelium, on a thin connective tissue layer, that merges with the pericardial cavity lining. The myocardium varies in thickness in different parts of the heart. It is thin in the sinus venosus but it is contractile. Unlike the mammalian heart, the teleost myocardium is capable of regeneration. The endocardium, homologous to the tunica intima of blood vessels, consists of a one-cell thick layer (endothelium) that may be highly phagocytic in some species (Atlantic cod, plaice). All the cardiac chambers of the fish heart are enclosed in a pericardium of fibrous tissue variably adhering to surrounding tissues, making a rigid space around the heart. The pericardial space is filled with a fluid, an ultrafiltrate from plasma.

The sinus venosus is a thin-walled chamber whose composition varies between species. The volume of the sinus venosus (Figure 5.1) is equivalent to that of the atrium. It is generally described as being formed by muscle and connective tissue. However, the proportion of the two components appears to vary widely. The sinus venosus wall may be mostly made up of connective tissue (as in *Danio rerio*), of connective tissue with sparse myocardial bundles (as in *Pleuronectes platessa*), or mostly of myocardium (as in *Anguilla anguilla*). To add more variation, the myocardium may be replaced by smooth muscle cells in other species, such as *Cyprinus carpio*. The sinus venosus conveys the blood into the atrium from which it is separated by the sinus valve. An important characteristic of the sinus is that it contains the heart pacemaker. In most teleosts, the presence of a specialized ring of tissue located in the sinoatrial region has been identified as the primary pacemaker region. This area is also densely innervated. Other components of the cardiac conduction system, similar to those present in mammals, have not been identified in the teleost heart.

The teleost atrium is a single chamber that shows considerable variability in size and shape between species. It is formed of an external rim of the myocardium with a complex network of thin trabeculae (pectinate muscles) (Figure 5.2). The pectinate muscle layer in the cardiac atrium is radiated from the roof of the atrium forming a star-burst muscular net. The atrial myocardium is surrounded by a subepicardial, thick layer of collagen. Collagen also encircles the atrial trabeculae. In general, the trabecular collagen is more abundant in the atrium than in the ventricle. It probably helps to support the atrial architecture.

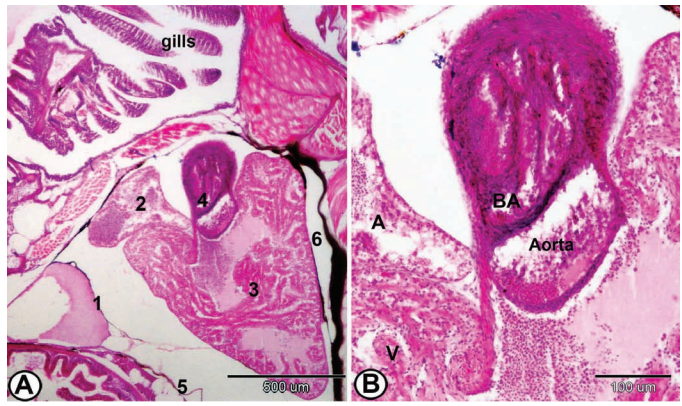

FIGURE 5.1 Histological structure of the heart of guppy stained with HE. (A) The heart is a four-chambered pump. The four chambers are (in sequence) as follows: the sinus venosus (1), the atrium (2), the ventricle (3), and the highly elastic bulbus arteriosus (4). The pericardium (5) and the pericardial cavity (6) are also demonstrated (HE). (B) Magnified view in bulbous arteriosus (BA), which is highly elastic structure, opens in the ventral aorta. Note the presence of atrium (A) and cardiac muscles of the ventricle (V) (HE).

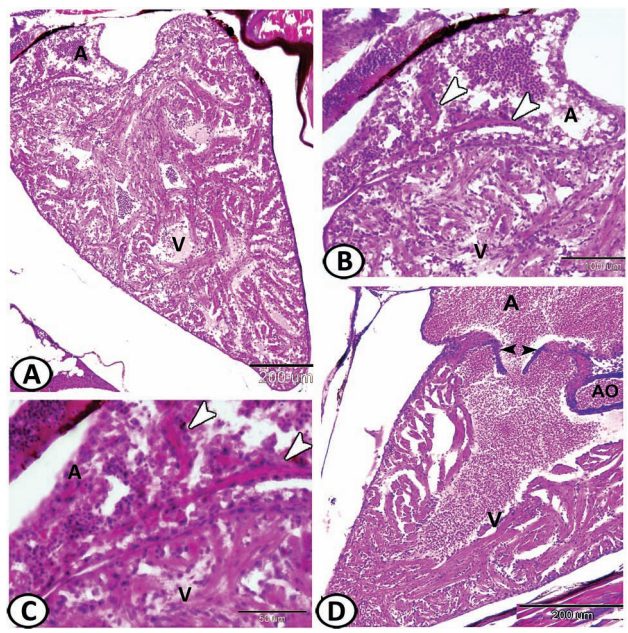

FIGURE 5.2 Histological structure of the atrium of guppy stained with HE. (A–C) The atrium (A) shows numerous spaces filled with erythrocytes and delimited on all sides by muscular strands running in various directions (arrowheads). Note the cardiac muscles in the ventricle (V). (D) AV valves (arrowheads) are located between atrium (A) and ventricle (V). Note the presence of a branch of the ventral aorta (AO).

The ventricle (Figure 5.3) is a highly muscular chamber that has the thickest layer of cardiomyocytes. Its wall, whose thickness is variable according to sex and age, can contain several layers of muscular fibers. It is also characterized by an abundant spongy myocardium that leaves in the lumen some lacunae in which blood circulates. Blood is drawn from the atrium via the atrioventricular (AV) valves into the ventricle as it is dilated (Figure 5.2D). The ventricle generates a high blood pressure.

The external ventricular shape has been grouped into three main categories: tubular, sac-like, and pyramidal. This division has several functional implications. For instance, pyramidal ventricles have been related to an active lifestyle, a robust ventricular wall, and a high output work. The salmonid and scombrid families present this type of ventricle. The very active tuna and molly fish also show a pyramidal ventricle. Furthermore, the relation between the external ventricular shape and the inner architecture is not constant. Sac-like ventricles are observed in many marine teleosts, and tubular ventricles are frequently observed in fishes like the eel, present an elongated body shape.

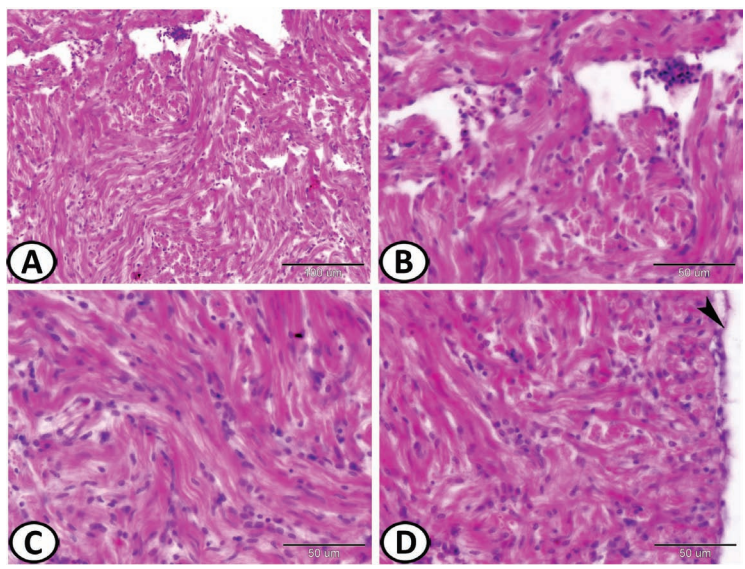

FIGURE 5.3 (A–D) Ventricular cardiomyocytes of guppy. The ventricle is a highly muscular chamber with a narrow lumen. The bundles of cardiomyocytes are mainly longitudinally arranged. Some cardiomyocytes are illustrated with thin elongated nuclei centrally located. The epicardium (black arrowhead) in (D), the outermost layer of the heart, is also demonstrated (HE).

Another heart classification relies on whether the ventricle presents a compact layer, on the relative thickness of the compacta, and the extent of myocardial vascularization. Type-I hearts show entirely trabeculated ventricles and lack a compacta. The ventricles of the rest of the heart types present both an external compacta and an inner spongiosa. Type-II hearts show vessels in the compacta but not in the spongiosa, and type-III hearts have vessels in both the compacta and the spongiosa. Type-IV hearts are different from type-III hearts in that a large proportion of their ventricular mass is formed by a compacta. Most teleost ventricles are entirely trabeculated and, thus, belong to type-I hearts. The trabecular network has been described as a highly organized system of small lumina and trabecular sheets which radiate outward from a central lumen (Figure 5.2A and D). The trabecular sheets would produce enough contractile force, and the communication between the different lumina would facilitate blood squeezing.

The conus is of variable length and contains up to two-valve rows, with a total of four to six valves. These conus valves regulate the ventricular flow dynamics. It is formed by compact myocardium (very evident in completely trabeculated ventricles) and contains more collagen, elastin, and laminin than the ventricular muscle.

The bulbus arteriosus opens in the ventral aorta (Figure 5.1B), the main vessel leaving the heart and leading the deoxygenated blood into the gills. The bulbus is an elastic chamber, which acts as a "shock absorber" when the blood is pumped by the ventricle. It expands during ventricular ejection to store a large part of the cardiac stroke volume. The gradual elastic recovery allows a steady flow of blood toward the gills, preventing damage of the delicate gill vasculature. The wall of the bulbus (Figure 5.4) is endowed with high amounts of elastin material and an external (subepicardial) collagen layer, which probably controls bulbus compliance by limiting circumferential deformation.

From the morphological point of view, the external shape of most bulbus ranges from pear-shaped, to elongated, to thick, and robust. The inner surface of the bulbus is characterized by the presence of ridges. These are longitudinal columns that occupy the full length of the bulbus. On the whole, they are thicker at the base of the bulbus and attenuate toward the ventral aorta. Depending on the species, the ridges may be very prominent or much more discrete. The inner surface of the ridges is covered by endocardium. The ridge endocardium shows histological differences across species, ranging from squamous to columnar. In addition, endocardial cells in many species contain moderately dense bodies. The presence of the dense bodies indicates

a secretory function. The middle layer of the bulbus contains smooth muscle cells and variable amounts of elastin. It may also contain, as in the common eel, a few collagen layers interspersed with the elastin material, or, as in tuna, collagen bundles, blood vessels, and nerves. However, it may lack elastin, as in the Antarctic teleosts. In these species, the elastin material is replaced by a fibrillar network, which is probably made up of glycosaminoglycans. The subepicardium is a thin layer rich in collagen and elastin, fibroblasts, vessels, and nerves.

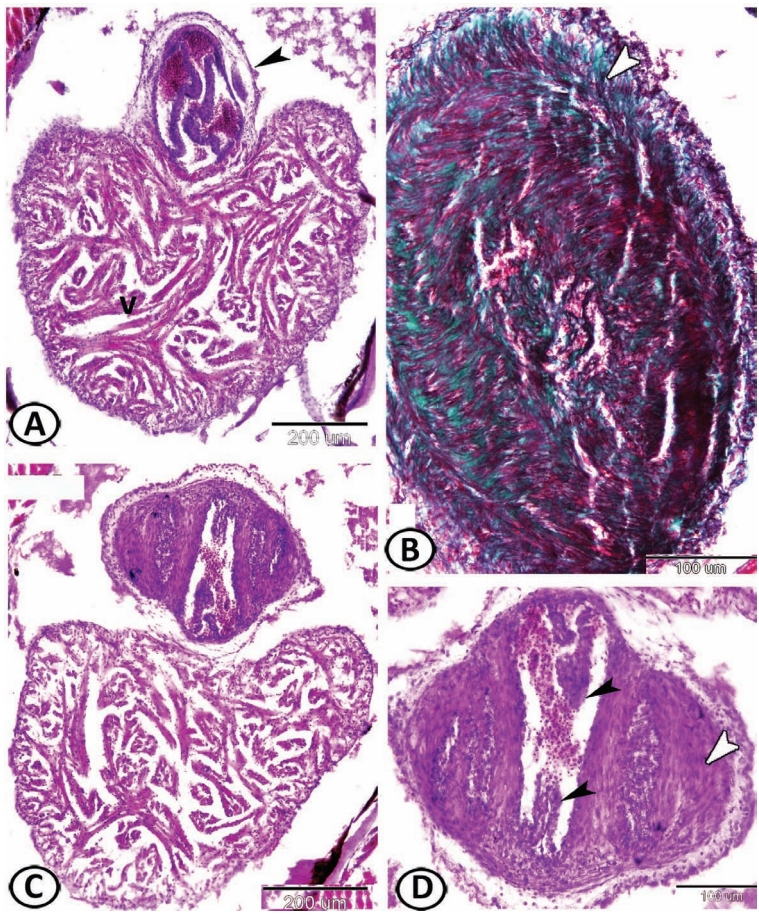

FIGURE 5.4 Histological structure of the heart of molly fish. (A, B) Bulbus arteriosus (black arrowhead) attached to the ventricle (V). The bulbus contains abundant collagen fibers (white arrowhead) (HE and Crossmon's trichrome respectively). (C, D) The conus arteriosus is present and immediately precedes the bulbus. The former is lined by a thin muscular ring of cardiomyocytes (white arrowhead) with two valves (black arrowheads) (HE).

The AV region is formed by a ring of cardiac tissue, which supports the AV valves. When the heart of teleosts with completely trabeculated ventricles is examined, the AV region appears formed by a distinct ring of the myocardium (Figure 5.2C and D). This myocardium is compacted, shows vascular profiles in most of the species, and contains variable amounts of collagen and elastin. A ring of connective tissue contributes to delineating the AV muscle from that of atrium and ventricle. The AV valves are generally formed by two leaflets that contain numerous cells grouped into a dense core and large amounts of connective tissue.

5.2 BLOOD VESSELS

The wall of arteries and veins is distinguished into three layers: an inner coat, tunica intima; an intermediate coat, tunica media; and an outer coat, tunica adventitia (TA). The tunica intima is composed of endothelial cells followed by connective tissue. This connective tissue contains collagenous and elastic fibers. The tunica media is composed of circular smooth muscle that constitutes the thickest layer of the wall. The TA is composed of connective tissue, which consists mostly of collagen fibers.

Elastic arteries (ventral aorta or gill arteries) (Figure 5.5) are found near the heart, and their media is rich in elastin. In general, the smooth muscle in fish arteries has less fibrillar material than in its mammalian counterparts, probably a reflection of the lower blood pressure found in this group. The muscular arteries (Figure 5.5C and D) possess a basic structure (tunica intima, media, and adventitia) like that found in higher vertebrates. The tunica intima comprises a one-cell thick endothelium lying on a subendothelial connective tissue layer. The tunica media is characterized by a more or less thick layer of smooth muscle fibers and the TA consists of loose connective tissue. Small artery is composed of the endothelial layer of tunica intima, single layer of smooth muscle fibers, and fibrous TA.

Veins (Figure 5.6) are structurally similar to those in mammals but have thinner walls and less abundant smooth muscle. Veins are similar in structure to arteries. However, the tunica media, that is, the muscle layer, of the vein is less developed and thinner than that of the artery of the same size, and sometimes is absent. However, the TA of veins is thicker than that of arteries.

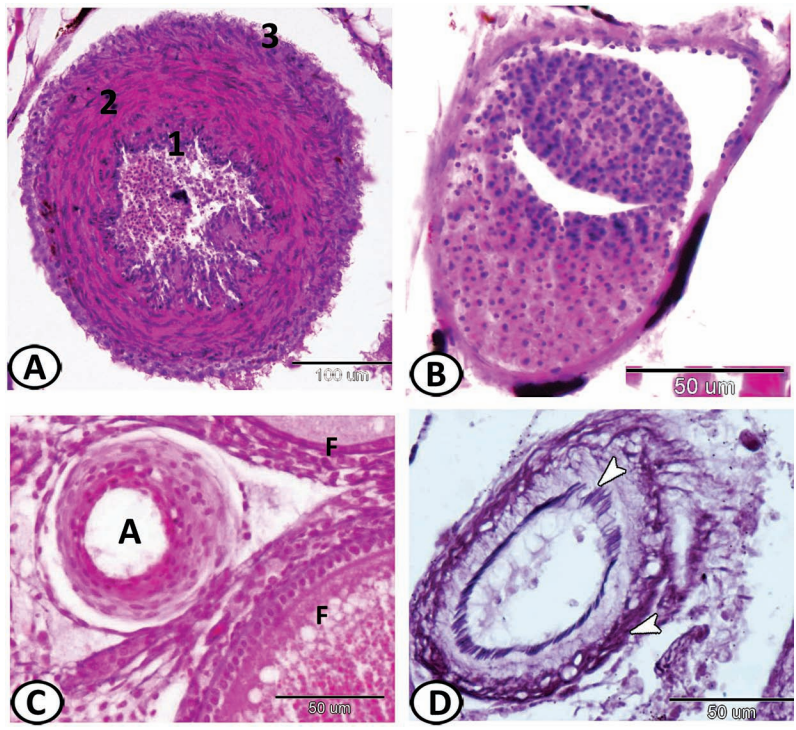

FIGURE 5.5 Histological structure of the arteries. (A, B) Transverse section through the ventral aorta of molly fish stained with HE shows three main layers: an inner layer or intima (1), which consists of an endothelium and varying amount of connective tissue; a media (2) consisting of smooth muscle and some connective tissue; and an adventitia (3) forming the outermost coat and consisting of collagenous and elastic fibers. (C) Medium-sized artery (A) between the ovarian follicles (F) of the redbelly tilapia. The tunica intima is consisted of flattened endothelial cells. The tunica media consists of about 10 layers of smooth muscle fibers. The adventitia merges imperceptibly with the surrounding supporting tissue (HE). (D) Medium-sized artery in the ovarian stroma of the redbelly tilapia showing internal and external elastic lamina (arrowheads) (Weigert's elastica).

Blood capillaries (Figure 5.7C and D) are histologically like those found in mammals, but they are much more permeable. They are composed of endothelial cells, basement membrane, and pericytes. The capillaries are classified into several types depending on the form and position of the endothelial cells and pericytes. There are two types of capillaries: continuous capillaries and fenestrated capillaries. The capillaries of the muscle and retina belong to the former type, while those of glomeruli and pancreas to the latter.

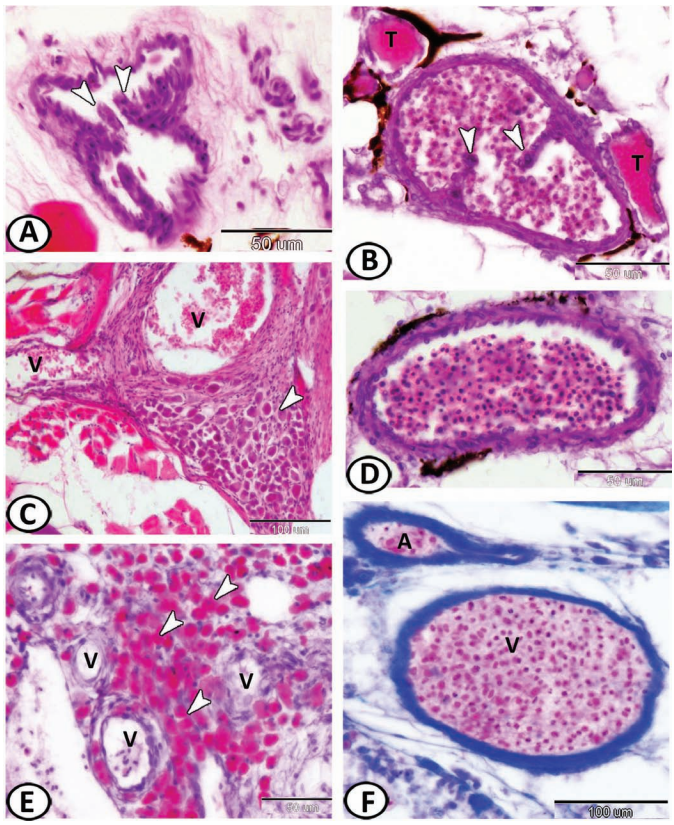

FIGURE 5.6 Histological structure of the veins. (A) A vein in the skin dermis of the eye region of silver carp contains a valve (arrowheads) (HE). (B) A valve in the vein between the thyroid follicles (T) of molly fish. The valve consists of two projections (arrowheads) of the tunica intima of the vein wall. The projections are composed of fibro-elastic tissue covered by endothelium (HE). (C) Veins (V) are surrounded by a sympathetic ganglia (arrowhead) in the ear region of guppy (HE). (D) The vein wall in the buccal cavity of molly is thin. The lumen is filled with erythrocytes. Collagen is stained green (HE)**.** (E) Veins (V) are surrounded by many eosinophils in the abdomen of guppy (arrowheads) (HE). (F) A medium-sized vein (V) and a small artery (A) in red-tail shark are filled with erythrocytes. Note, the artery has a thicker wall as compared to the vein (Mallory trichrome).

The blood vessels of the ovary showed a series of histological changes, which arise as a result of reproductive activity. The ovarian stroma of redbelly tilapia contains many special vascular and cellular elements. The ovary of teleosts is supplied with blood from several arteries that branch off the dorsal aorta, entering the dorsal side of the ovary through the mesovarium. The histological investigation of the ovarian vasculature in redbelly tilapia reveals

several blood vessels bearing special regulatory devices that are frequently scattered around the vitellogenic ovarian follicles in the breeding (spawning) season. It is possible that the distribution of special types of blood vessels may be related to ovarian development, which may supply the endocrine activities including vitellogenin uptake and estrogenic control.

Some veins represent several layers of longitudinally oriented smooth muscle fibers in the tunica media followed by a thick collagenous TA (Figure 5.8A). While some veins show regressive changes in form of thickening of the wall with an increase in collagenous fibrous tissue content (Figure 5.8B). Other veins show double internal elastic lamina followed by tunica media made up of longitudinally oriented smooth muscle fibers intermingled with elastic fibers (Figure 5.8C). The observed regressive changes that occur in the veins are supposed to be developed as the result of increased circulatory demands or due to strain on the dynamics of the peripheral circulation. However, these modifications in blood vessels are considered as physiological processes as they are not uniform in nature, intensity, and distribution.

Arteries with double tunica media contain outer longitudinal and inner circular smooth muscle fibers and clear tunica elastic interna are demonstrated (Figure 5.8D). Throttle artery is provided with longitudinal muscular intimal bolsters that are made up of longitudinally directed smooth muscle cells and few glomus cells. The bolsters form a continuous layer surrounding the lumen and demarcate from the glomus cell media by a distinct fibrous membrane (Figure 5.8E). These muscular pads are capable of constructing or even occluding the lumen of the vessel. The latter devices seem to have an active dynamic function in regulating the blood flow and pressure through the throttling or occlusion mechanism. This type of special regulatory device is observed in many forms. Spirally oriented arterioles are present within the ovarian stroma with extreme thickening of their walls (Figure 5.8F). They may occur as a result of repeated functional activity of the ovary.

The arteriovenous anastomoses are evident in the ovarian stroma and include simple bridge-like arteriovenous anastomoses and glomus organ. In bridge anastomoses, the thick-walled artery connects directly with a thin-walled vein and they are surrounded by one TA, and the origin of the anastomosis is supported by a ring or roll of smooth muscle cells. This transition shows a sharp and abrupt change in the thickness of the tunica media from the artery to the vein (Figure 5.8G). Glomus is frequently observed near the vitellogenic follicles that may be related to maturation or rupture of follicles.

It composes mainly of glomus cell layers and few smooth muscle cells. The glomus cells are mostly rounded or polygonal with a large vesicular nucleus. They are surrounded by layers of loose connective tissue rich in blood capillaries (Figure 5.8H). Haemodynamic, humeral, and thermoregulatory functions are the main roles of the glomus.

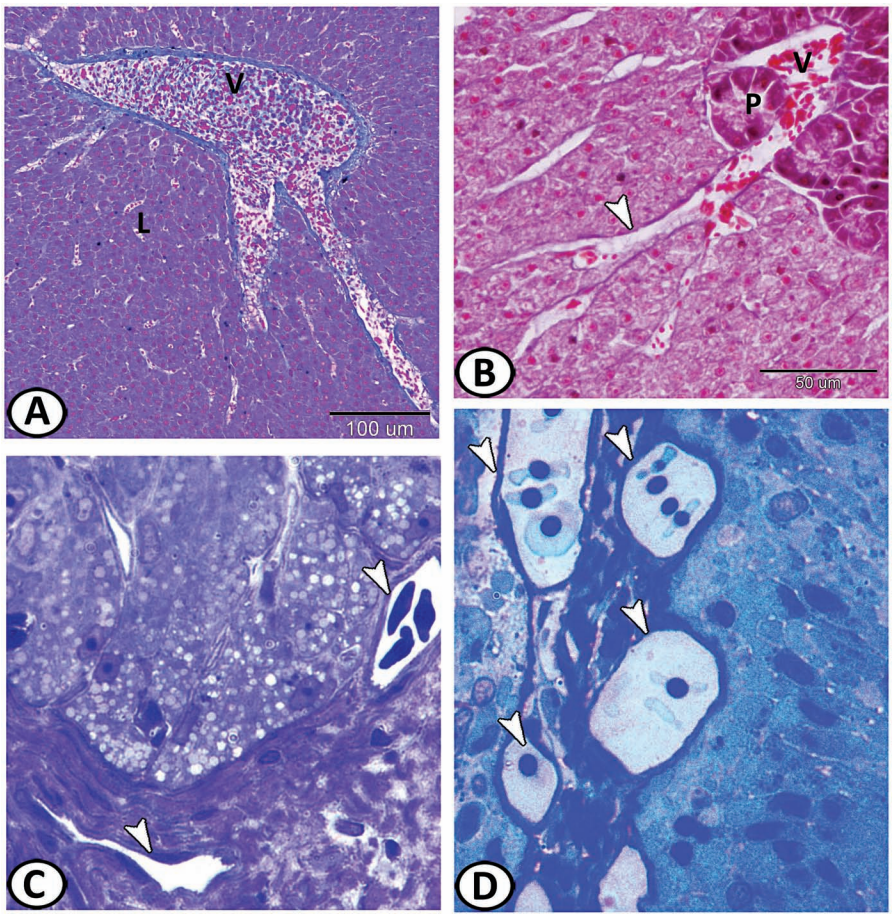

FIGURE 5.7 (A) Vein (V) in the liver (L) of grass carp stained by Maldonado's stain. (B) The hepatopancreatic acini (P) encircles a vein (V) that ramifies up smaller branches (arrowhead), finally communicating with the network of hepatic sinusoids in the hepatopancreas of grass carp (Mallory's trichrome)**.** (C, D) Semithin sections through the blood capillaries (arrowheads) in fundic stomach of Nile catfish and intestinal bulb of grass carp, respectively, stained with toluidine blue (TB) showing very thin wall blood capillaries (arrowheads).

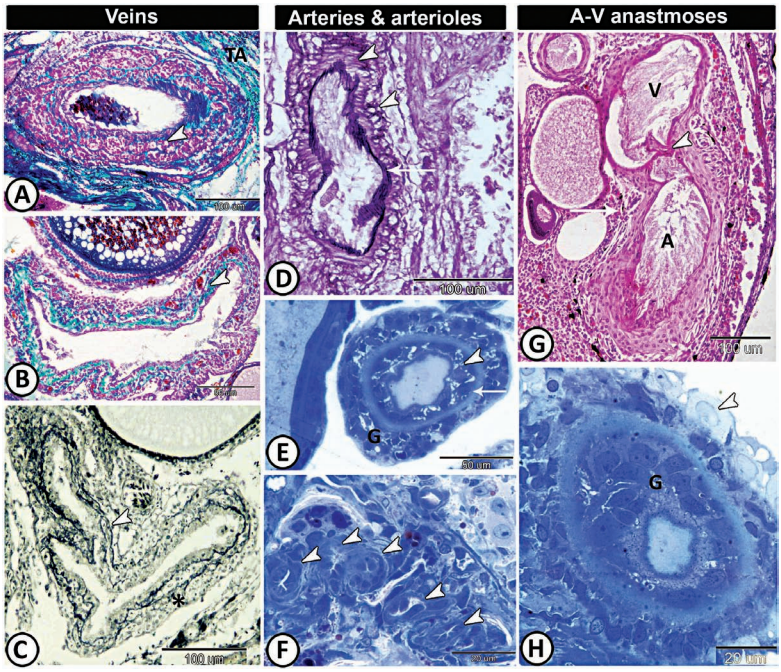

FIGURE 5.8 Light microscopy of special types of blood vessels in the ovary of redbelly tilapia. (A) Special vein stained with Crossmon's trichrome shows longitudinally arranged smooth muscle fibers in the tunica media (arrowhead) followed by thick tunica adventitia (TA). (B) A vein stained with Crossmon's trichrome shows regressive changes (arrowhead). (C) A vein stained with Verhoeff's stain shows double internal elastic lamina (arrowhead) followed by longitudinally oriented smooth muscle fibers intermingled with elastic fibers (asterisk). (D) An artery with double tunica media (arrowheads) and elastic interna (arrow) stained by Weigert's elastica. (E) Throttle artery stained with TB shows longitudinal muscular intimal bolsters (arrowhead), demarcated from the glomus cell media (G) by a fibrous membrane (arrow). **(F)** Spirally oriented arterioles stained with TB showing extreme thickening of their walls (arrowheads). (G) In bridge anastomoses, the artery (A) is connected with the vein (V) and surrounded by one tunica adventitia (TA) (arrow). Note a ring of smooth muscle cells (arrowhead) at the origin of the anastomosis, HE stain. (H) Glomus stained with TB showed glomus cell layers (G) surrounded by connective tissue rich in blood capillaries (arrowhead).

Moreover, these special types of blood vessels exhibit variation in activity for both ATPase and acid phosphatase (Figure 5.9). The glomus cells in glomus vessels show activity for ATPase (Figure 5.9A), while endothelium and tunica media of arteriovenous anastomoses show high ATPase activity (Figure 5.9B), the endothelium and tunica media of arteries display a similar fashion of activity (Figure 5.9C). In addition, special spiral arterioles exhibit a strong reaction to ATPase (Figure 5.9D). The ATPase activity across special

types of blood vessels has been involved in the passage of substances across the wall or related to calcium transport in a fundamental way. Special types of veins and arteries show activity for acid phosphatase in their tunica media (Figure 5.9E and F).

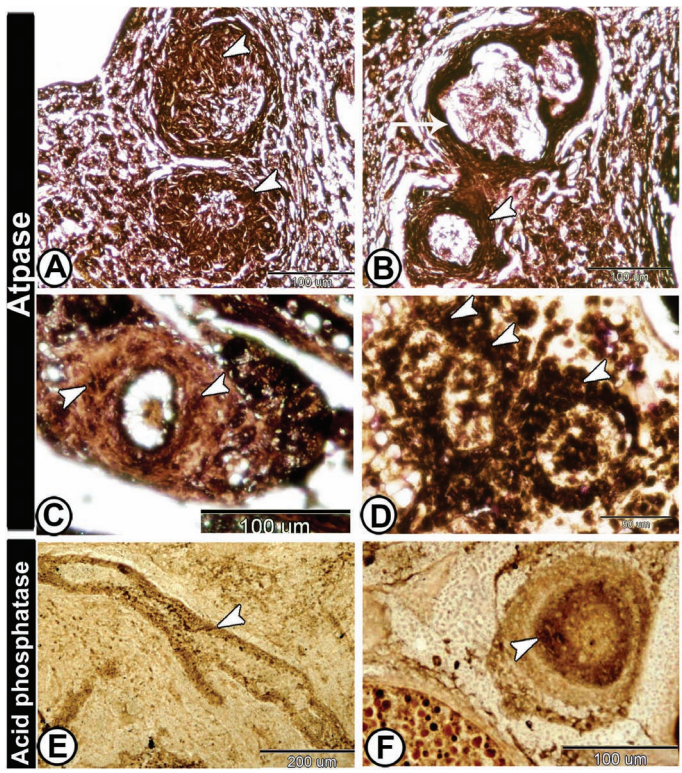

FIGURE 5.9 Enzymatic activity of special blood vessels in the ovary of redbelly tilapia**.** (A) The glomus cells (arrowheads) in glomus vessels show activity for ATPase. (B) The endothelium (arrow) and tunica media (arrowhead) of arteriovenous anastomoses show high ATPase activity. (C) The endothelium and tunica media (arrowheads) of arteries show a strong reaction to the same enzyme. (D) Special spiral arterioles exhibit a strong reaction to ATPase (arrowheads). (E, F) Special types of veins and arteries, respectively, show activity for acid phosphatase in their tunica media (arrowheads).

Immunohistochemical analysis reveals that the endothelium of the blood vessels expresses S-100 protein and the tunica media express desmin. Moreover, the glomus cells show immunoreactivity for S-100 protein (Figure 5.10).

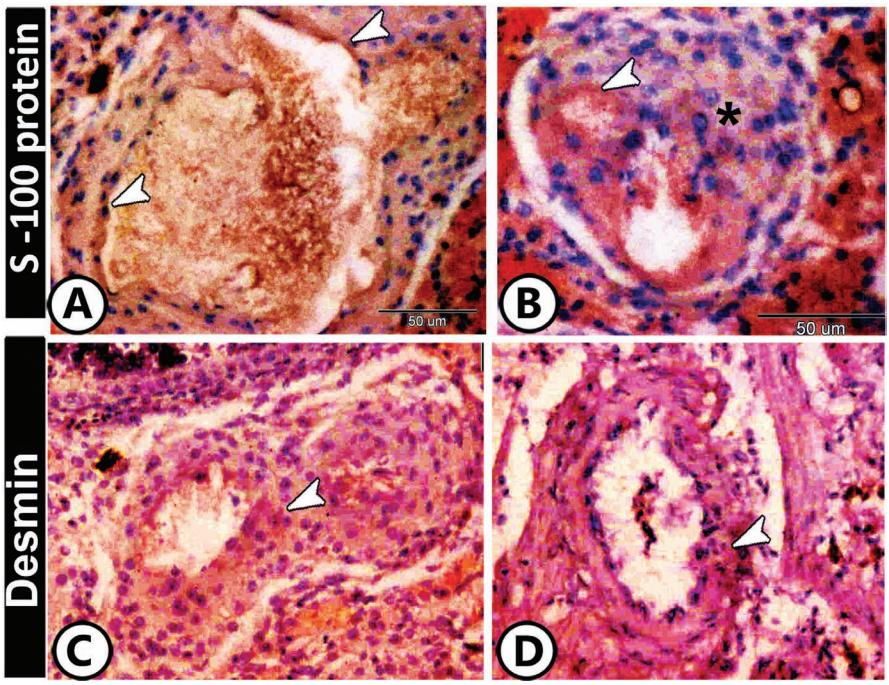

FIGURE 5.10 Immunohistochemical expression of S-100 protein and desmin in the blood vessels in the ovary of redbelly tilapia. (A, B) The endothelium (arrowheads) and glomus cells (asterisk) express S-100 protein. (C, D) The endothelium and the tunica media (arrowheads) express desmin.

By electron microscopy, in special arteriole, the endothelial cells extend long prolongation to the lumen of the vessel. These endothelial cells are of a fenestrated type and contain euchromatic elongated nucleus, mitochondria, numerous micropinocytotic pits, and vesicles. These pits and vesicles indicate an active transcytosis process during the spawning period. The endothelial cells are connected with each other by tight junctions and desmosomes. They are surrounded by smooth muscle fibers and other stromal cells (Figure 5.11A and B).

The wall of the glomus consists of endothelium followed by thin subendothelial connective tissue, tunica media is consisted of clusters of large glomus cells that characterized by electron-lucent cytoplasm rich by dense vesicles and few granules. The nucleus of these cells is large and contains peripherally arranged heterochromatin. Desmosomes-like

junction between the adjacent cells is frequently demonstrated. The presence of this junction indicates communication between them. Since the glomus cells are usually arranged in clusters, excitation of one glomus cell may electronically spread to other cells in the cluster. Consequently, a cluster may behave as a functional unit. Few supporting cells (SCs) are distributed between the glomus cells and their cytoplasm extends long processes and contains mitochondria. Intimate apposition of some parts of glomus cells and intervascular smooth muscle cells are demonstrated. This connection includes the tongue-like projection of smooth muscle with mitochondria and free surface of glomus cells. The electron-dense vesicles of glomus cells show aggregations near this connection (Figure 5.11C) that supposed exocytosis of the contents of vesicles to the connection. The glomus-smooth muscle connection is presumed to participate in vascular regulation.

While in the glomus vessel, its lumen consists of the protruded expansion of glomus cells that incompletely invested by SCs. The glomus cells are characterized by electron-lucent cytoplasm rich by mitochondria, dense-cored vesicles, few granules, and rough endoplasmic reticulum. The nucleus of these cells is large and contained peripherally arranged heterochromatin. Moreover, glomus cells act as local secretory cells affecting smooth muscle. The SCs extend long processes like an octopus that partially enveloped glomus cells. These cells are in close proximity to blood in vessels and contain a large nucleus and thin cytoplasm. The cytoplasm contains vesicles and mitochondria (Figure 5.11D).

5.3 BLOOD

The blood of fishes is a specialized circulating tissue composed of cells suspended in a fluid intercellular substance (plasma). Blood volumes of teleosts are small, being about 5% of body weight. The main lines of blood cells in fishes are red blood cells (erythrocytes), white blood cells (leucocytes), and thrombocytes.

Eight cell types were identified: (1) nucleated erythrocytes, (2) neutrophils (3) eosinophils, (4) basophils, (5) heterophils (6) monocytes, (7) lymphocytes, and (8) thrombocytes.

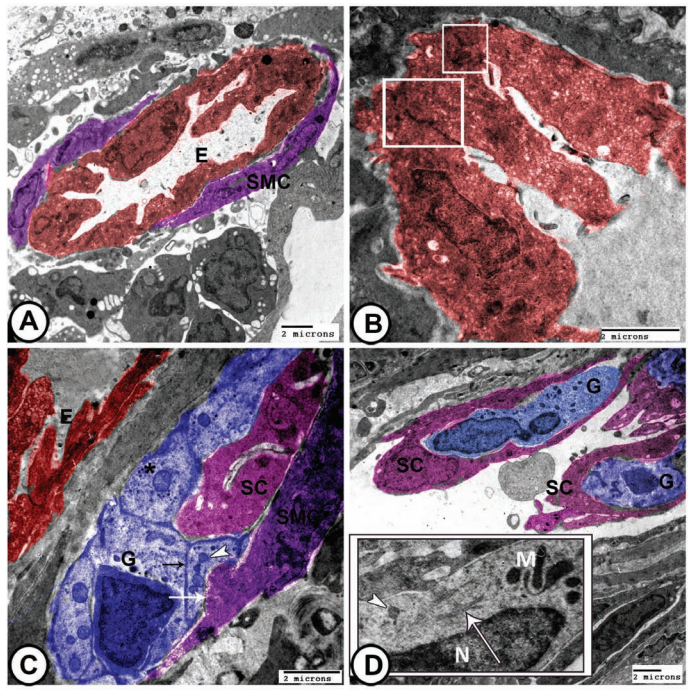

FIGURE 5.11 Digital colored transmission electron microscopy images of the special blood vessels in the ovary of redbelly tilapia. (A) The endothelial cells (E, red) of special arteriole contain mitochondria, numerous micropinocytotic pits, and vesicles and are surrounded by smooth muscle fibers (SMC, violet). (B) The endothelial cells are connected with each other by tight junctions and desmosomes (boxed areas). (C) The wall of the glomus consists of endothelium (E, red), tunica media that consists of glomus cells (G, blue) that are rich by dense vesicles (arrowhead), and few granules (asterisk). Note desmosomes-like membrane thickening between the adjacent cells (black arrow). Few supporting cells (SCs) (pink) extend long processes between glomus cells. Tongue-like projection (white arrow) extends from smooth muscle (SMC, violet) to glomus cells. The electron-dense vesicles of glomus cells showed aggregations near this connection (arrowhead). (D) The lumen of glomus vessel shows protruded expansion of glomus cells (G, blue) that are incompletely invested by supporting cells (SCs) (pink). The glomus cells (inserted boxes) contain a nucleus (N), mitochondria (M), dense-cored vesicles (arrowhead), and rough endoplasmic reticulum (arrow).

5.3.1 CELLULAR COMPONENTS OF THE BLOOD

5.3.1.1 ERYTHROCYTES

In fish, like in other nonmammalian vertebrates, erythrocytes are ovoid in shape with centrally located nucleus (Figure 5.12). The cytoplasm is

saturated with hemoglobin. The number of erythrocytes varies according to the species as well as the age of the individual, season, and environmental conditions. The number ranges 1.05–3.0 × 10^6/mm^3. Remarkably, in several Antarctic notothenioid fish hemoglobin can be much reduced or completely absent, and there are no erythrocytes. The electron microscopy (Figure 5.13) shows that the erythrocytes contain heterochromatic nucleus. The cytoplasm may contain inclusions or vacuoles. These inclusions are identified as degenerating organelles. Although the erythrocytes of males compared with females are generally larger in size.

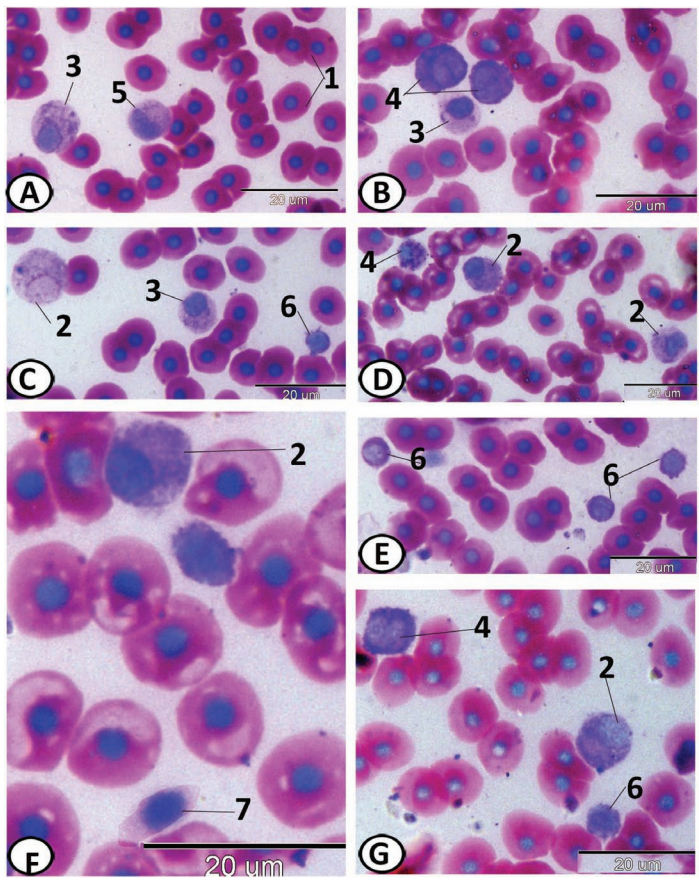

FIGURE 5.12 The blood smear with Giemsa's stain. (A–E) The blood of Nile tilapia. (F, G) The blood of Nile perch. The main blood cells in fishes are (1) erythrocytes are oval in shape and always contain a central, (2) neutrophils, (3) eosinophils, (4) basophils, (5) monocytes, (6) lymphocytes, and (7) thrombocytes.

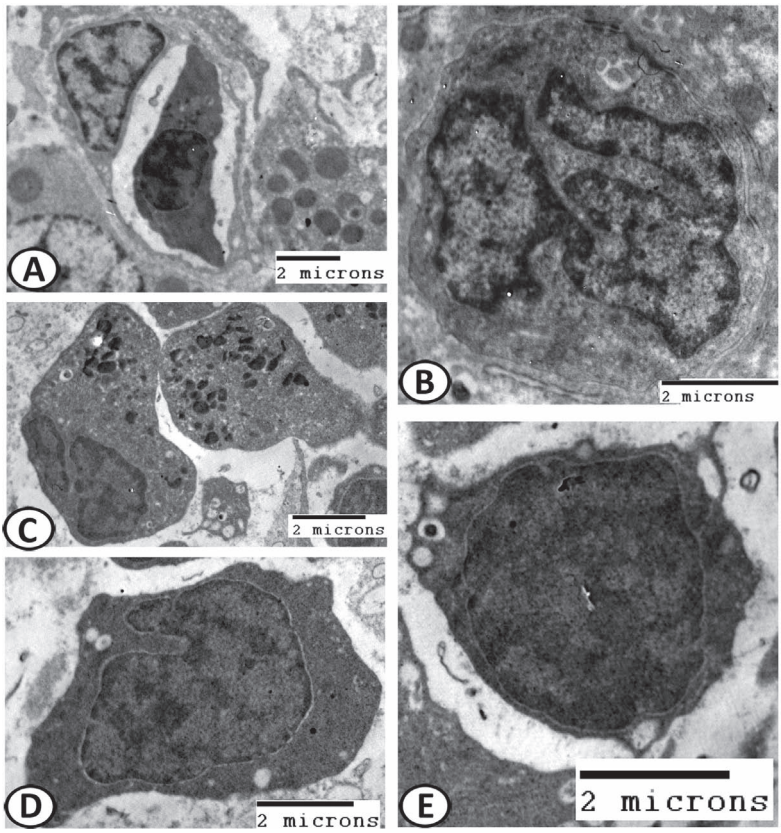

FIGURE 5.13 Electron microscopical characterization of blood cells in the grass carp. (A) Erythrocyte in the blood capillary of interrenal tissues shows a centrally heterochromatic nucleus. The cytoplasm contains inclusions. (B) Neutrophil is characterized by the presence of three-lobed nuclei. (C) Heterophils are characterized by large and fusiform electron-dense cytoplasmic granules. The nucleus is segmented and frequently displaced toward the edge of the cell and contains moderate amounts of heterochromatin. (D) Monocye shows a large kidney-shaped nucleus with a dense chromatin pattern near the membrane. (E) The lymphocyte is round cells and the nucleus occupies virtually the whole of the cell leaving only a narrow rim of cytoplasm.

5.3.1.2 LEUKOCYTES

Like leucocytes in higher vertebrates, the fish leucocytes in peripheral blood are agranulocytes and granulocytes. The agranulocytes have no granules (lysosomes) in the cytoplasm and their nucleus is unlobed.

Among the granulocytes, neutrophils are the most plentiful. The numbers of circulating neutrophils reported in fishes vary over a considerable range (1%–25% of leucocytes). The teleost neutrophil has a grayish granular cytoplasm (Romanowsky dye). In blood smears, neutrophils are round or oval in shape and are usually larger than erythrocytes. In immature cells, the nucleus is eccentric and exhibits the human kidney shaped, but in mature cells, two- or three-lobed nuclei may be recognized. Neutrophils show peroxides and Sudan black-positive reaction.

Eosinophils in the blood of teleosts have been variably reported. They were observed in the blood of various species of salmon (Salmo, Oncorhynchus) but were reported rare or absent from the blood of rainbow trout. Several workers agree that eosinophils are present in the blood of carassius. Eosinophils presented a homogeneous round shape with a round or oval nucleus. The nucleus contains coarse, clumped chromatin, and strongly stained blue. Typically, these cells have been identified by the presence of large rounded cytoplasmic granules, which stain bright red with Romanowsky's stain or eosin and measuring approximately 1.15 ± 0.035 μm. Some eosinophils contain numerous clear vacuoles or a big cytoplasmic vacuole. Mitochondria, endoplasmic reticulum, and Golgi complexes are easily identified. Eosinophils represent activated cells that contain degranulated or coalescent granular material in response to a parasitic infection or other inflammatory stimulus. They are the smallest among the granulocytes, ranging between 13.5 ± 5.67 and 12.6 ± 1.3 μm for males and females, respectively. It is round to oval, single or bilobed, and eccentrically placed near the membrane. Males have a significantly ($P < 0.01$) higher number of eosinophils (20.2 ± 1.2) than females (17.5 ± 1.09).

5.3.1.3 BASOPHILS

As with eosinophils, reports on the presence of basophils in the blood of fishes vary. When present (goldfish, salmonids, and carp), they are easily identified by their deeply stained cytoplasm filled with very dense, dark purple granules. Their large nuclei (7.09 ± 0.25) are round and centrically placed with homogenous chromatin. Many factors can affect the number of basophils and the leukocytic formula, such as age, health status, ecological factors, and the seasons. Mast cells in fishes are identified on the bases of their similarity to those of mammals (connective tissue habitat and metachromatic cytoplasmic granules).

The heterophils contain large, eosinophilic, and fusiform cytoplasmic granules. The cytoplasm, which can be difficult to visualize, is light blue or clear. The nucleus is segmented and frequently displaced toward the edge of the cell and appears basophilic with moderate amounts of heterochromatin. Few mitochondria and endoplasmic reticulum are demonstrated around the electron-dense granules. No significant differences are found between males and females for size; the diameter ranges from 13.9 ± 6.71 in males to 13.3 ± 1.27 in females, and the frequency is 15.4 ± 0.8% in males and 15.7 ± 1.2% in females.

Agranulocytes come in two varieties: lymphocytes and monocytes. Lymphocytes are the most numerous types of leukocytes, constituting 70%–90% of total leukocytes. In teleosts, the average diameter of small lymphocytes varies between 5 and 8 μm (up to 12 μm in large lymphocytes). The lymphocytes are round cells and the nucleus occupies virtually the whole of the cell leaving only a narrow rim of basophilic cytoplasm. The scant cytoplasm contains few mitochondria, polyribosomes, endoplasmic reticulum, and small electron-dense granules.

The monocytes are not numerous (0.1%–0.5% of the leucocytes population). They resemble mammalian monocytes histochemically, possessing a few fine and scattered granules, which stain positively with periodic acid–Schiff and acid phosphatase. The cytoplasm is thrown into pseudopodia. The monocyte contains a large amount of light blue-gray, finely granular or vacuolated cytoplasm, and an oval or kidney-shaped nucleus with a dense chromatin pattern near the membrane. The mean diameter of monocytes is 12 μm and does not differ significantly between males and females. The cytoplasm has mitochondria, a large Golgi complex, endoplasmic reticulum, and some small dense granules. Under appropriate circumstances, they develop into mature cells of the mononuclear phagocyte system (macrophages).

The thrombocytes are predominantly fusiform with a central, ellipsoidal, and deeply stained nucleus. The nucleus contains peripherally located moderate heterochromatin. The cell edges presented some finger-like projections. The cytoplasm is hyaline when stained with a Romanowsky-type dye. Thrombocytes clearly differ from all other leucocyte populations in possessing clear canalicular structures and small variably dense granules in their cytoplasm. Glycogen granules are also found. By Giemsa stained preparations, the chromatin-rich nucleus exhibits a dark blue or dark violet color. The cytoplasm is extremely scant and usually has a light blue area adjacent to one of the poles of the nucleus. In addition to taking part in blood clotting, it has been reported that the piscine thrombocytes are blood

macrophages that form one of the protective barriers against foreign agents and might be considered true digestive cells because they may remove circulating cell fragments directly by phagocytosis. In addition, it is believed that fish thrombocytes are functionally homologous to the platelets of higher vertebrates. The total number of thrombocytes ranges from 60,000 to 70,000/ mm^3.

KEYWORDS

- **teleost atrium**
- **bulbus arteriosus**
- **atrioventricular valves**
- **blood vessels**
- **fish leucocytes**

BIBLIOGRAPHY

Arizza, V.; Russo, D.; Marrone, F.; Sacco, F.; Arculeo, M. Morphological characterization of the blood cells in the endangered Sicilian endemic pond turtle, Emys trinacris (Testudines: Emydidae). *Ital. J. Zool.* **2014,** *81*(3), 344–353.

Fange, R. Fish blood cells. In *Fish Physiology*; Hoar, W. S., Randall, D. J., Farrell, A. P., Eds.; Academic Press Inc.: San Diego, CA, **1992,** 12B, 1–54.

Greer-Walker, M.; Santer, M.; Benjamin, M.; Norman, D. Heart structure of some deep sea fish (Teleostei: Macrouridae). *J. Zool.* **1985,** *205,* 75–89.

Hine, P. M.; Wain, J. M.; Boustead, N. C. The leucocyte enzyme cytochemistry of fish. *New Zeal. Rese. Bull.* **1987,** *28,* 5–75.

Hrubec, T. C.; Smith, S. A. Hematology of fish. In *Schalm's Veterinary Hematology*; 5th ed.; Feldman, B. F., Zinkl, J. G., Jain, M. C., Eds.; Lippincott Williams & Wilkins: Philadelphia, PA, **2000**, 1120–1125.

Icardo, J. M.; Colvee, E.; Cerra, M. C.; Tota, B. The structure of the conus arteriosus of the sturgeon (Acipenser naccarii) heart: II. The myocardium, the subepicardium, and the conus-aorta transition. *J. Anat. Rec.* **2002,** *268,* 388–398.

Old, J. M.; Huveneers, C. Morphology of the blood cells from three species of wobbegong sharks (*Orectolobus sp*.) on the east coast of new south wales. *J. Zool. Biol.* **2006,** *25,* 73–82.

Pavlidis, M.; Futter, W. C.; Katharios, P.; Divanch, P. Blood cell profile of six mediterranean mariculture fish species. *J. Appl. Ichthyol.* **2007,** *23,* 70–73.

CHAPTER 6

Immune System

ABSTRACT

The spleen, thymus, and kidney are regarded as being the major immune organs in fishes, albeit with slightly various roles between species. The spleen is the main erythropoietic tissue in elasmobranchs, holocephalans, and a few teleosts. The teleosts lack lymph nodes and the spleen with the kidney form the two major filtering organs removing foreign agents. The spleen is composed of blood vessels, red and white pulps, and ellipsoids. The head kidney is a unique, important hemobiotic organ in fish. It contains more lymphocytes than the spleen and has been involved in antibody production. The kidney in teleost fish is the equivalent of the bone marrow in vertebrates and is the largest site of hematopoiesis until adulthood. The fish thymus is a paired lymphoid organ situated in the dorsal region of each branchial cavity. The parenchyma of the thymus is composed of several cell types, such as T lymphocytes, undifferentiated cells (lymphoblasts), melanomacrophages, nurse-like cells, immunoglobulin positive (Ig+) cells, mucous cells, rodlet cells, and neuroendocrine cells. The thymus acts as a site of production and differentiation of T lymphocytes (thymocytes) that are involved in cell-mediated immunity. Other studies described the appearance of focal epithelial nests, known as Hassal's corpuscles.

The immune system of fish is physiologically similar to that of higher vertebrates, despite certain differences. In contrast to higher vertebrates, fish are free-living organisms from the early embryonic stages of life and depend on their innate immune system for survival. Nonspecific immunity is a fundamental defense mechanism in fish. In addition, it plays a key role in the acquired immune response and homeostasis through a system of receptor proteins.

The spleen, thymus, and kidney are regarded as being the major immune organs in fishes, albeit with slightly various roles between species. The spleen is the main erythropoietic tissue in elasmobranchs (sharks, rays),

holocephalans (rabbitfish: Chimaera), and a few teleosts (Perca, Scorpaena). In most teleosts, in chondrosteans (sturgeon, paddlefish) and holosteans (gars, bowfin), erythrocytes are produced within the kidney. An extensive network exists for the trapping of blood-borne substances mainly in the kidney and spleen but in some species, other tissues such as the heart and liver are also involved. In the kidney and spleen, populations of lymphocytes and macrophages capable of mounting an immune response are situated close to sites of antigen trapping and often associated with accumulations of melanomacrophages (MMs). However, a primitive gut-associated lymphoid tissue represented by diffuse subepithelial lymphoid aggregates can be found. Species variation in the morphology of the immune system is to be expected, given the large number and diversity of species within the teleost fishes.

6.1 SPLEEN

The teleosts lack lymph nodes and the spleen with the kidney form the two major filtering organs removing foreign agents and effete blood cells from the vascular system. The spleen (Figures 6.1 and 6.2) is usually a solitary dark red organ in the peritoneal cavity adjacent to the gut wall. The same basic elements as in higher vertebrates are typically present: blood vessels (BVs), red and white pulps (WP), and ellipsoids. The spleen is covered by a thin, fibrous capsule (Figure 6.1C) with little evidence of contractile ability. A part of this capsule extends inward forming a net-like trabecula.

The red pulp (RP) is an extensive, interconnecting system of splenic cords and sinusoid capillaries (open capillaries), consisting mainly of erythroid cells and thrombocytes, and usually comprises the majority of the splenic parenchyma. Splenic cords are a mesh of fibroblast-like cells with foci of various blood cells. The WP, consists mainly of lymphoid cells, typically surrounds arterial vessels, melanomacrophage centers (MMCs), and ellipsoids, or forms small clusters in the parenchyma.

The MM (Figure 6.2A and B) is a characteristic immune cell type of teleosts and is prevalent in the spleen. The MM is a phagocyte containing varying amounts of pigment, including melanin (black-brown), hemosiderin, ceroid, or lipofuscin (yellow-pink to golden brown) localized in vacuoles. The MMs are also found in the kidney and liver. The MMCs are thought to be a scavenger structure but their role in the immune system is ambiguous. Chronically stressed fishes, including those that are unhealthy, tend to have

more and larger MMCs. The size and number of MMC also increase with fish age.

The ellipsoids (Figure 6.2C and D) are thick-walled capillaries with a narrow lumen that opens in the pulp and result from the division of the splenic arterioles. They run through a sheath of collagen, reticular fibers, reticular cells, and macrophages. A few species do not have ellipsoids. Ellipsoids appear to have a specialized function in plasma filtration. Moreover, foreign bodies, such as bacterial cells, are trapped by the ellipsoids and may be seen within the reticular meshwork or intracellularly within macrophages of the sheaths.

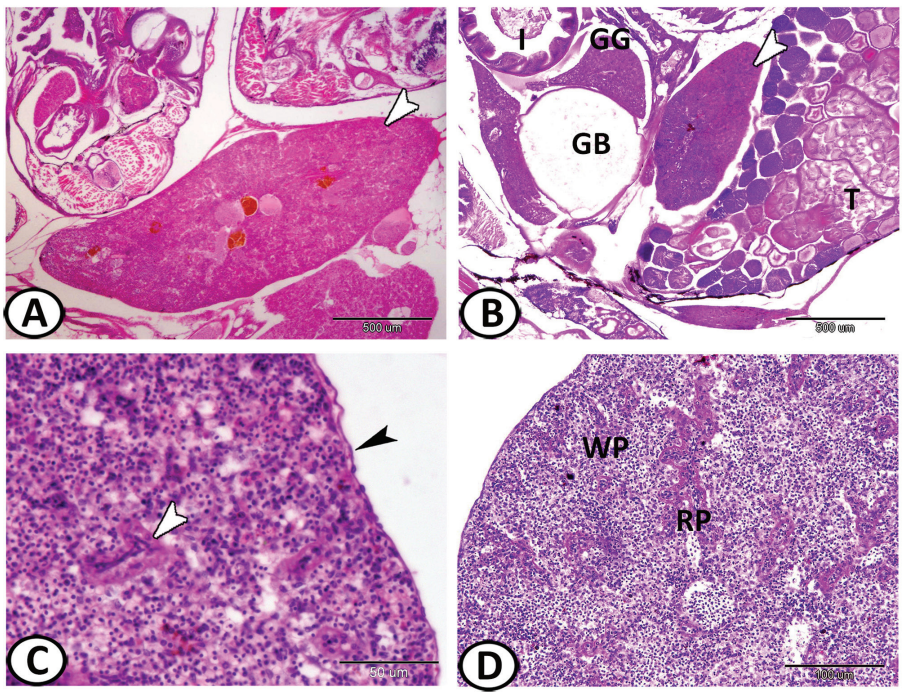

FIGURE 6.1 (A) General view of the spleen (arrowhead) of molly fish that found adjacent to the pregnant uterus containing embryos and showing the distribution of MM centers (orange color) (HE). (B) The spleen of the guppy (arrowhead) is located adjacent to the testis (T), gas bladder (GB), gas gland (GG), and intestine (I) (HE). (C) The spleen of guppy is covered by a fibrous capsule (black arrowhead). Note the presence of ellipsoids (white arrowhead) (HE). (D) The parenchyma of the spleen of molly fish consists of white pulp (WP) and red pulp (RP) (PAS/HX).

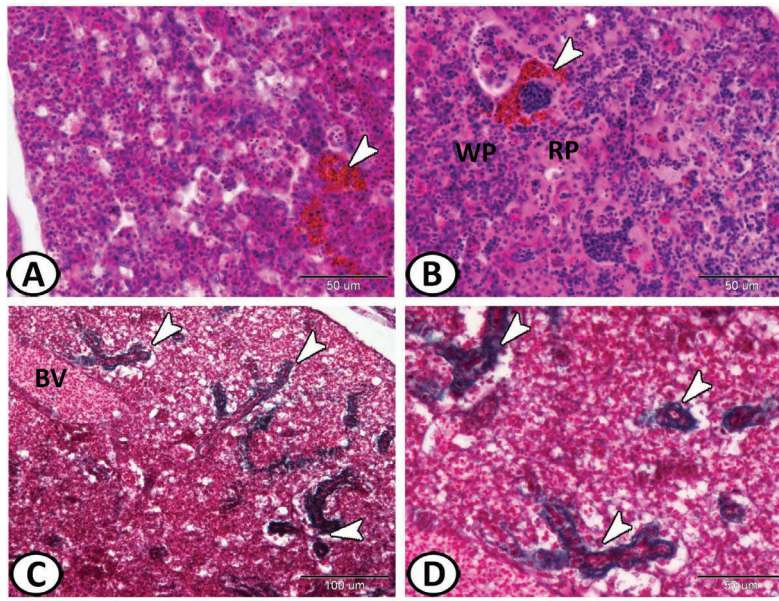

FIGURE 6.2 (A, B) The spleen of guppy fish illustrating components of the parenchyma, red pulp (RP), and white pulp (WP). Note the MM centers (arrowheads) (HE). (C, D) Ellipsoids (arrowheads) of molly fish are termination of splenic arterioles that open to blood vessels (BVs) (Crossmon's trichrome).

6.2 THE HEAD KIDNEY

The anterior part of the kidney (head kidney or pronephros) is a unique, important hematopoietic organ in fish. The pronephros is a basic organ forming the blood elements, and it is also the reservoir of blood cells. The head kidney acts as an important endocrine organ, homologous to mammalian adrenal glands, releasing catecholamines, corticosteroids, and other hormones. Thus, the pronephros is an important organ with key regulatory functions and the central organ for immune-endocrine interactions and even neuroimmunoendocrine connections. It contains more lymphocytes than the spleen and has been shown to be actively involved in antibody production. The head kidney is considered to be the principal lymphoid organ in teleosts for the proliferation and differentiation of B lymphocytes, for the production of macrophages, as the site for capturing and processing the foreign substances and particles.

The kidney in teleost fish is the equivalent of the bone marrow in vertebrates and is the largest site of hematopoiesis until adulthood. In rainbow

trout, the kidney becomes well developed after hatching, when it mainly produces red blood cells and granulocytes. Studies suggest the presence of lymphoid cells that release immunoglobulin M (IgM) between 12 and 14 days of postfertilization and have also shown two variants of IgM by enzyme-linked immunosorbent assay in embryos 8 days before the end of the incubation period. This finding suggests that a source of B cells exists before the end of the incubation period in the kidney or in other hematopoietic sites.

In teleosts, the head kidney is transformed into complex lymphomyeloid or hemopoietic tissues. The lymphomyeloid tissues in fish consist of a mixture of lymphoid and myeloid compartments. However, they are regarded as being less specialized in their structure and function than the corresponding mammalian tissues. Basic hematopoietic structures and mechanisms in fishes are similar to those operating in other vertebrates, and all hematopoietic cell types are very similar to those of mammals. Hematopoiesis is a complex process in which hematopoietic stem cells, the most immature elements of the hematopoietic hierarchy, proliferate and differentiate into various classes of hematopoietic progenitor cells. These progenitor cells further have been shown to be able to differentiate into mature blood cells: erythrocytes, lymphocytes, thrombocytes, granulocytes, and monocytes.

Structurally (Figures 6.3–6.5), the anterior kidney is composed of a network of reticular fibers that provide support for lymph tissue and are found scattered among the hematopoietic cells that line the sinusoid reticulo-epithelium. The main cells found in the anterior kidney are macrophages, which aggregate into structures called MMCs, and lymphoid cells, which are found at all developmental stages and exist mostly as Ig+ cells (B cells). Reticular cells play an important role in supplying the interactions necessary for the function of lymphoid cells and endothelial cells of blood vessels. The latter system is the main component for blood filtering due to its ability to perform endocytosis.

The leucocytic cells observed in hemopoietic tissues are lymphocyte, neutrophil, and macrophage. Lymphocyte (Figures 6.3A and 6.5D) is the smallest cell of leukocytes having a large nucleus surrounded by a thin rim of cytoplasm. The plasma membrane is plicate and occasionally having small pseudopodia. The heterochromatic nucleus is often indented. Small cytoplasmic vesicles are present.

Neutrophils (Figures 6.3C and 6.5A) are the most abundant leukocytes with an irregular and occasionally bilobed nucleus. The nuclear chromatin material is dense and patchy in distribution. The cytoplasm is characterized by the presence of numerous granules scattered in the cytoplasm. Two types

of granules can be identified based on their shape and size. Type I granules are membrane-bound, oval, large, and predominant in the cytoplasm. Type II granules are rod like. The neutrophils containing both types of granules are fewer in number than neutrophils, having the only Type I granules. Both types of granules are observed in the differentiated cells.

The young progranulocyte has a foamy basophilic cytoplasm with scarce fine basophilic granulation. The eccentric nucleus of the basophilic progranulocyte occupies <50% of the cell and has more condensed chromatin than the myelocyte. The basophilic metagranulocyte has a more elongated nucleus and darker foamy cytoplasm with more abundant granulation. The metamyelocyte nucleus is mostly eccentric, sometimes oval, and occupied <50% of the cell volume. Small parts of the cytoplasm near the nucleus are sometimes still faintly bluish but the rest is loaded with specific granulation (Figure 6.3B).

Young basophils (Figure 6.4A) are characterized by the appearance of dense coarse basophilic granules. Granulation occupies the whole cytoplasm in the mature basophil (Figure 6.4C). Young basophils (young progranulocyte and basophilic metagranulocyte) are more abundant than older stages (young basophil and mature basophil). Mature eosinophils (Figure 6.5B) are larger than neutrophils. The eccentrically located elliptical or lobed nucleus is small. The light blue to colorless cytoplasm presented relatively large rosy-red granules.

The thrombocytes (Figure 6.3A) are elongated, fusiform cells with an indentation in the plasma membrane. They are predominantly smaller than the lymphocytes, with a central compact nucleus. The nucleus shows deep heterochromatic sulci and the cytoplasm characterized by the presence of numerous coated vesicles of different shapes and sizes. The thrombocytes of fish should not be considered as the platelets of the higher vertebrates because they are true cells. Thrombocytes have been described in goldfish as cells with dense chromatin and morphologically similar to lymphocytes. The thrombocytes are clearly differentiated from lymphocytes by their spindle shape, clear vacuoles, marginal microtubules, and the electron-dense granules in the cytoplasm

Young reticulocyte (YR) is an oval to a rounded cell with a large oval or round nucleus and irregular-shaped nucleolus (Figure 6.3A). Mature reticulocyte (MR) shows an ellipsoidal profile with slight tapering toward the end of the long axis. The nucleus is diminished in volume compared to YR (Figure 6.4A).

Monocytes (Figure 6.4B) are irregular in shape with a large nucleus. The nucleus is relatively electron-lucent apart from a narrow peripheral band of chromatin and apparent large nucleolus. The cytoplasm contains vesicles of varying size and electron density. Some monocytes are of different sizes and contained many vacuoles in the cytoplasm.

Macrophages are irregular in shape and characterized by the indented nucleus (Figure 6.3D). The plasma membrane shows long processes of pseudopodia. Actively phagocytosing macrophages are seen within the head kidney. The cell cytoplasm is replete with lysosomes, mitochondria, pigments, and other particles. Immunopositivity for the antigen CD45RO in sections of the head kidney, which identifies membrane receptors on T cells, is revealed in the population of T lymphocytes that constitute the lymphoid aggregates, concentrated around BVs and MMCs. Also, macrophages, monocytes, and their precursors show strong immunopositivity for CD68, and also the cells of the granulocytic lineage in various phases of maturation are positive for lysozyme.

The spherical aggregates of MMs (Figure 6.3D) with pigments containing vesicles are found throughout the hemopoietic kidney. Distinct MMCs are seen in the head kidney and are suggestive of analogy with the germinal centers of higher vertebrates. Such a macrophage center with a high level of pigmentation is significant in grass carp because it needs high levels of unsaturated fats in their tissues to maintain the membrane fluidity essential for normal metabolic processes even at low temperatures. These unsaturated fats are particularly prone to peroxidation with the possible formation of pigments that concentrate in macrophage centers. MM centers act as focal depositories for resistant intracellular bacteria. In addition to the primary function of iron capture and storage in hemolytic diseases, other functions include antigen trapping and presentation to lymphocytes. Sequestration of products of cellular degradation and potentially toxic tissue materials are among the other functions.

Barrier cells are among the cells found in the head kidney. They are few with electron-dense, elongated, and branched appearance (Figures 6.4D and 6.5D). Numerous ribosomes, well-developed secretory organelles, and electron-lucent vesicles characterized the cells. Large granules and microfilaments are also present. Dense reticular-like cells recognized as barrier cells in the head kidney of grass carp appear as pericytes or lining the blood vessels (BV) resembling those described in the spleen and bone marrow of mammals. The processes of the barrier cells extending among the extracellular matrix may increase the filtration capacity and clearance

of blood. Furthermore, barrier cells are observed closely associated with clusters of hemopoietic and lymphopoietic cells. It thus forms part of the hemopoietic microenvironment, with the function of isolating putative stem cells, concentrating hemopoietic factors, and regulating the migration of blood cells in circulation. As such, the presence of the barrier cells in the fish head kidney reinforces the proposed homologies between this organ and the mammalian bone marrow.

Mature erythrocytes (Figure 6.5D) are elliptical with an irregular nucleus. The chromatin is highly condensed into large electron opaque blocks. The nucleolus is no longer identifiable.

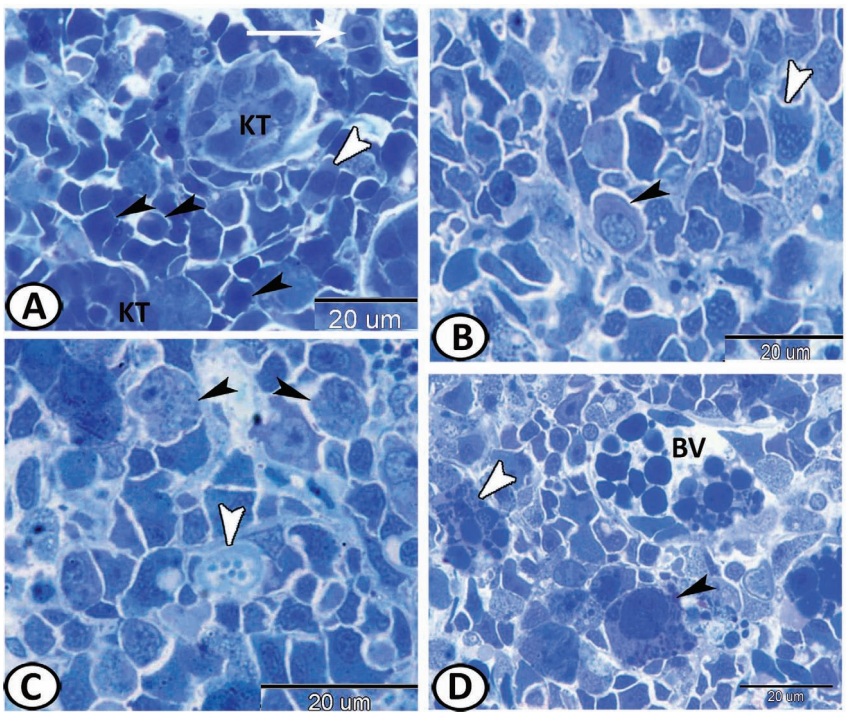

FIGURE 6.3 Semithin sections through the head kidney of grass carp stained by TB. (A) The head kidney consists of lymphoid tissues between the kidney tubules (KTs). The lymphoid tissues are mainly lymphocytes (black arrowheads), young reticulocytes (YRs) (arrow), and thrombocytes (white arrowhead). (B) Metamyelocytes (black arrowhead), immature neutrophil (white arrowhead). (C) The head kidney also contains rodlet cells (RCs) (white arrowhead) and neutrophils (black arrowheads). (D) Typical macrophage (black arrowhead) containing digested materials are observed in the head kidney of grass carp. Note the presence of MM centers (white arrowhead) in neighboring to the blood vessel (BV).

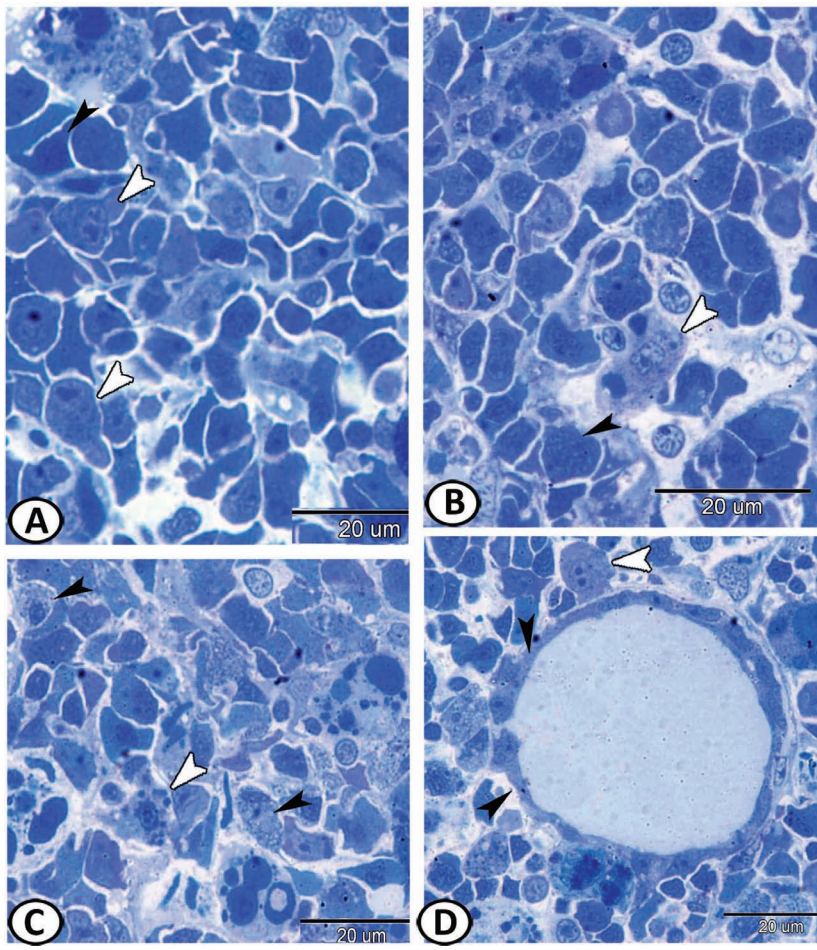

FIGURE 6.4 Semithin sections through the head kidney of grass carp. (A) Young basophils (white arrowheads) and mature reticulocytes (MRs) (black arrowhead). (B) Monocyte (black arrowhead) and macrophage (white arrowhead). (C) Mature basophils (white arrowhead) and basophilic metagranulocytes (black arrowheads). (D) Barrier cells (black arrowheads) and stem hemopoietic cells (white arrowhead).

6.3 THYMUS

The fish thymus (Figure 6.6) is a paired lymphoid organ situated in the dorsal region of each branchial cavity. The thymus acts as a site of production and differentiation of T lymphocytes (thymocytes) involved in cell-mediated immunity, prior to their migration to peripheral lymphoid tissues. It is usually

covered by a thin capsule. The structure that characterizes the thymus of fish is a capsule that surrounds the lymphoid dark tissue. The differentiation of the thymic structure is highly variable in teleosts, and in many species, it is not possible to observe a clear differentiation between the cortex and medulla that is found in higher vertebrates.

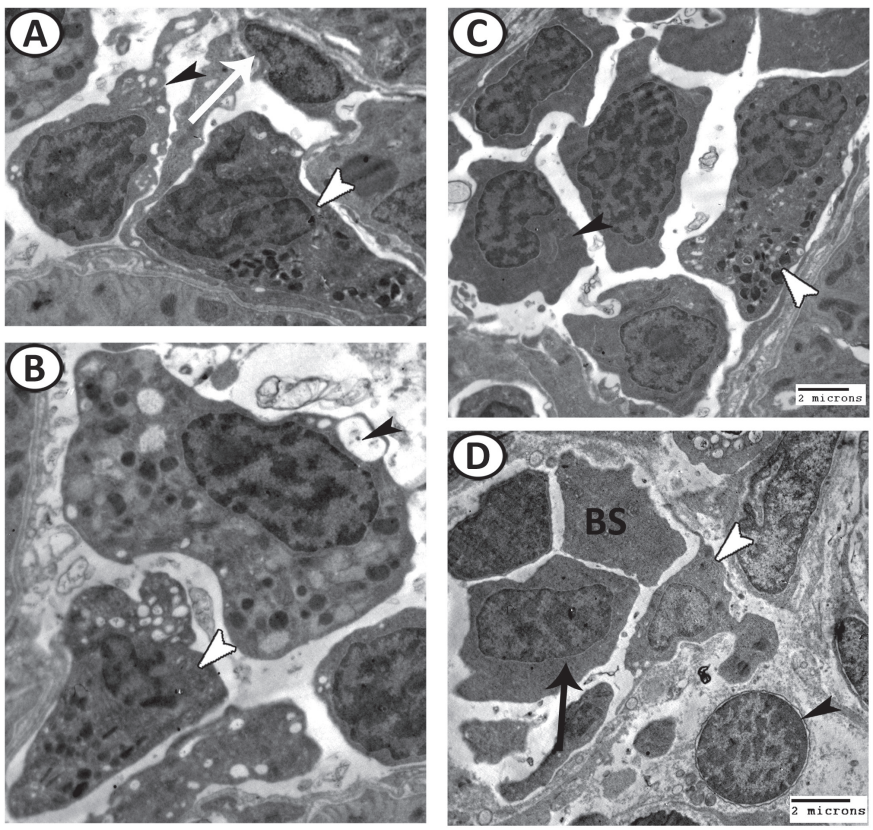

FIGURE 6.5 Transmission electron microscopy of the cellular elements in the head kidney of grass carp. (A) Neutrophil (white arrowhead) with characteristic electron-dense granules, inactive dendritic cell (arrow) characterized by high nuclear to cytoplasmic ratio, and active dendritic cells (black arrowhead) that showed pseudopodia, indented heterochromatic nucleus and the cytoplasm has vacuoles are demonstrated. (B) Immature erythrocytes (black arrowhead) and mature basophil (white arrowhead). (C) Eosinophils (black arrowhead) show rounded electron-dense granules and heterophils (white arrowhead) can be identified by the presence of many vacuoles and rod-like granules. (D) Barrier cells (white arrowhead) extend their processes around the blood vessel (BS). Note the presence of mature erythrocyte (arrow) and lymphocyte (black arrowhead).

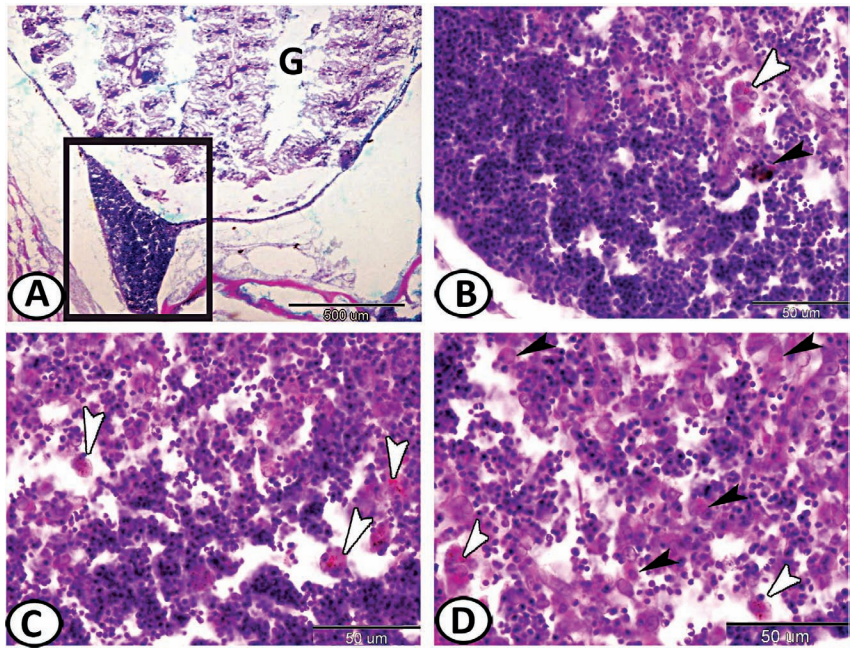

FIGURE 6.6 (A) Thymus of molly fish (square) is a lymphoid organ located dorsally to the gill chamber (G) (PAS-AB-HX). (B) The thymus of guppy consists of the outer zone containing T lymphocytes and the inner zone contains macrophage (black arrowhead) and nurse-like cell (white arrowhead). (C, D) The inner zone of the thymus of guppy showing eosinophilic granular cells (white arrowheads) and rodlet cells (RCs) (black arrowheads).

The parenchyma of the thymus is composed of several cell types, such as T lymphocytes/thymocytes, undifferentiated cells (lymphoblasts), MMs and to a lesser extent by nurse-like cells, immunoglobulin positive (Ig+) cells, mucous cells, RCs, and neuroendocrine cells. Lymphocytes are the most abundant cell type particularly in the outer zone of the organ. They presented a rounded nucleus with one or two well-defined nucleoli and scant cytoplasm. The anti-CD3ε antibody identifies most of the lymphocytes localized in the outer zone and, to a lesser extent, those located in the inner zone of the thymus. The undifferentiated cells that exhibit the morphological features of lymphoblasts are mainly located in the inner zone of the thymus. They are rounded cells with a centrally located circular euchromatic nucleus and are larger than lymphocytes/thymocytes, with a smaller nucleo-cytoplasm ratio.

MMs are forming well-defined centers randomly distributed throughout the thymic parenchyma. Nurse-like cells are infrequently visualized in the inner zone. This cell type displays a polygonal shape with a mean diameter

of 12 μm and a euchromatic nucleus with a prominent nucleolus. The most remarkable feature of the nurse-like cells is a variable number of thymocytes (up to 6) localized within its abundant cytoplasm. Ig+ cells are observed in the inner zone of the thymus, they are rounded and shows a strong cytoplasmic immunoreaction to IgM antibody. Mucous cells are also scattered in the thymus parenchyma. By means of the PAS-Alcian Blue technique, both neutral and acid mucins-containing mucous cells are identified.

RCs are randomly distributed in the thymic parenchyma. RCs show their typical morphology, that is, a thick fibrous layer and several elongated granules in the cytoplasm. Neuroendocrine cells immunoreactive to anti-NPY and -VIP antibodies are located in the inner zone of the thymus. They are large polyhedral cells with abundant cytoplasm and some cellular projections. The euchromatic nucleus is round and exhibits a conspicuous nucleolus. Furthermore, myeloid cells and eosinophilic granular cells can be found in this organ. Other studies described the appearance of focal epithelial nests, known as Hassal's corpuscles.

6.4 CELLS INVOLVED IN IMMUNE RESPONSE

Fish possess lymphocyte populations that are analogous to T cells, B cells, cytotoxic cells (similar to natural killer cells), macrophages, and polymorphonuclear leukocytes. The immune system of teleosts has subpopulations of T lymphocytes that exhibit differential responses to mitogens, B cell acute allograft reactions, mixed leukocyte reactions, and cooperative interactions between T cells, B cells, and macrophages that are essential for the production of antibodies.

In general, the system of phagocytic cells is widely dispersed throughout the body. It is responsible for the removal of spent cells, particles, or macromolecular aggregates from its surroundings. The main cells involved in phagocytosis in fish are neutrophils, the promonocytes of the hemopoietic organs, the monocytes of the blood and lymph, the macrophages of loose connective tissue, the free and fixed macrophages of the spleen and kidney, and in many species, the fixed macrophages of the atrial lining of the heart. These cells remove bacteria mainly by the production of reactive oxygen species during a respiratory burst. In addition, neutrophils possess myeloperoxidase in their cytoplasmic granules, which in the presence of halide and hydrogen peroxide kills bacteria by halogenation of the bacterial cell wall.

Moreover, these cells have lysozymes and other hydrolytic enzymes in their lysosomes. Similarly, macrophages can produce nitric oxide in mammals and can be as potent as antibacterial agents, peroxynitrites, and hydroxyl groups.

An interesting feature of the teleost macrophages is their capacity to form aggregates once they are replete. Usually, these aggregates are in the areas of the MMC in the hemopoietic tissues but such aggregates are also found, frequently pigmented, within or around chronic inflammatory lesions. These pigments, melanin and related pigments, are considered to play a defensive role in many organisms, in their capacity for generating hydrogen peroxide. These centers play an important role in the storage of iron resulting from the breakdown of erythrocytes, breaking down the destroyed tissue, catching the free radical in an immune response, and blood purification from suspended harmful substances. The MMs are characterized by the presence of eccentric nucleoli and cytoplasm with heterogeneous populations (lysosomes, phagosomes, myelin figures, senile RBCs, or plenty of melanin granules of variable size and electron density, Figure 6.7A and B).

RCs (Figure 6.7C) have been found in a large variety of fish organs and tissues, including the kidney, gill, gut, gall bladder, heart, skin, and BV endothelium. These cells were initially described as intracellular parasites and named Rhabdospora thelohani. In contrast, several studies have suggested that these cells are part of a normal population associated with the defense system of fishes.

Ultrastructurally (Figure 6.7D), each RC consists of a plasmalemma in close contact with a thick-layered capsule. The capsules consist of a dense, compact network of microfibrils that form a continuous structure in close contact with the internal portion of the cell. The inner cytoplasm of RCs is occupied by several (up to 15) longitudinal rodlets (club-shaped sacs) surrounded by several light vesicles and vacuoles. Each rodlet comprises of a peripheral cortex and a central dense core (rod). The cortex forms a club-shaped sac with a fine, granular inner zone, and a coarse outer zone. Other cytoplasmic organelles such as the Golgi apparatus, rough endoplasmic reticulum, and free ribosomes are observed. The irregularly shaped nucleus generally occupies a lateral or basal position in RCs in contact with the capsule. The heterochromatin is distributed irregularly in the nucleoplasm.

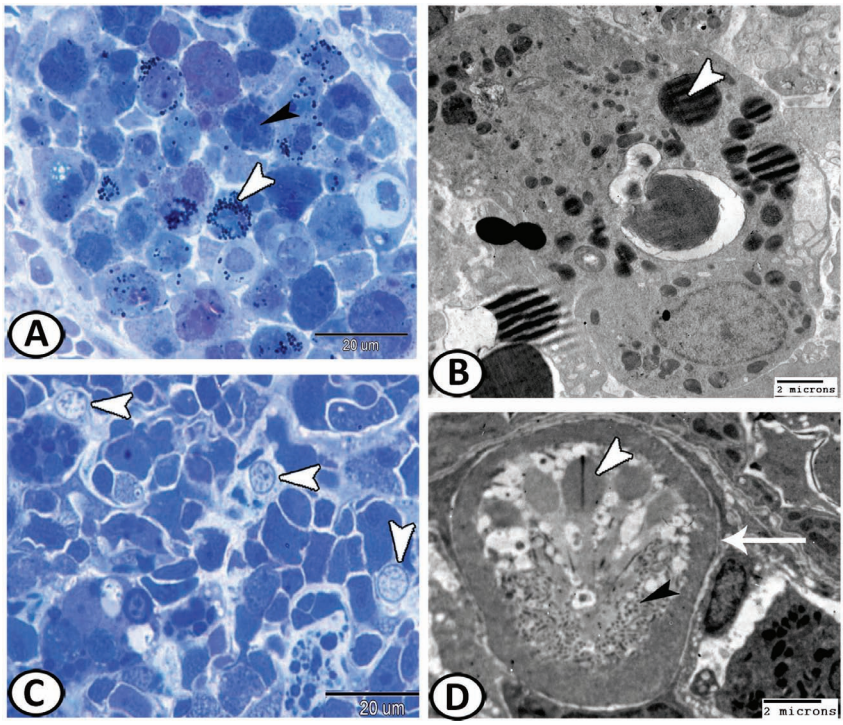

FIGURE 6.7. (A) Semithin section of MM center in the kidney of grass carp showing melanin pigments (white arrowhead) and digested particles (black arrowhead). (B) TEM of MM center in the ovary of Redbelly tilapia showing eccentric nucleus and variable size, digested particles (white arrowhead). (C) Semithin section in the kidney of grass carp showing many RCs (arrowheads). (D) TEM of RC showing thick fibrillary capsule (arrow), rodlet granules (white arrowhead), and polyribosomes (black arrowhead).

6.5 PHYSICAL BARRIERS

Flakes, skin mucus, and gills act as the first barrier to infection. The mucus of fish contains lectins, pentraxins, lysozymes, complement proteins, antibacterial peptides, and IgM, which have an important role in inhibiting the entry of pathogens. In addition, the epidermis is able to react to different attacks (thickening and cellular hyperplasia) and its integrity is essential for osmotic balance and to prevent the entry of foreign agents. On the other hand, defending cells are present, such as lymphocytes, macrophages, and eosinophilic granular cells.

KEYWORDS

- **head kidney**
- **spleen**
- **melanomacrophage**
- **thymus**
- **phagocytic cells**

BIBLIOGRAPHY

Agius, C.; Roberts, R. J. Melano-macrophage centres and their role in fish pathology. *J. Fish Dis*. **2003**, *26*(9), 499–509.

Espenes, A.; Press, C. Mc L.; Dannevig, B. H.; Landsverk T. Investigation of the structural and functional features of splenic ellipsoids in rainbow trout (*Oncorhynchus mykiss*). *Cell Tissue Res*. **1995**, *279*(3), 469–474.

Fänge, R.; Nilsson, S. The fish spleen: structure and function. *Experientia*. **1985**, *41*(2), 152–158.

Kondera E. Cell composition of the head kidney of European chub (*Squalius cephalus* L.). *Arch. Pol. Fish*. **2014**, *22*, 271–280.

Nielsen, M. E.; Esteve-Gassent, M. D. The eel immune system: present knowledge and the need for research. *J. Fish Dis*. **2006**, *29*, 65–78. Romano, N.; Ceccariglia, S.; Mastroliad, L.; Mazzini, M. Cytology of lymphomyeloid head kidney of antarctic fishes *Trematomus bernacchii* (Nototheniidae) and Chionodraco hamatus (Channicthyidae). *Tissue Cell* **2002**, *34*, 63–72.

Uribe, C.; Folch, H.; Enriquez, R.; Moran, G. Innate and adaptive immunity in teleost fish: a review. *Vet. Med*. **2011**, 56(10), 486–503.

CHAPTER 7

Skin and Associated Sense Structures

ABSTRACT

The skin of a fish is a multifunctional organ and may serve important roles in communication, sensory perception, locomotion, respiration, excretion, osmoregulation, and thermal regulation. The skin is a self-active secretory organ that their cellular components provide many useful products. Goblet cells secrete mucus that keeps the body surfaces moist and protects it from stressors, while the club cells produce the alarm substances that initiate the alarm reaction. The dermal chromatophore units provide patterns of coloration and absorb or reflect radiations. They include melanophores, xanthophores, erythrophores, and iridophores. The skin of fish shows various inter-species differences, as some species have scales and others have special cells, such as sacciform cells, eosinophilic granular cells, and rodlet cells. The skin is also a vehicle for cutaneous sense organs that allowed the fish for the detection of predators and foods. Among them are taste buds and the lateral line system. The lateral line is a sensory system that allows fish to sense objects and motion in their surrounding aquatic environment. The lateral line system is categorized into two subsystems: mechanoreceptive neuromasts and electroreceptive ampullary and tuberous organs. Two types of neuromasts occurred in fish species: superficial and canal neuromasts (CNs). The tuberous organ is more frequently occurring in the head region and contains four to five sensory receptor cells that play a significant role in the sensation of weak electrical stimuli. CNs are embedded in the dermis in the form of tunnel-like canals. A large number of superficial neuromasts are located at the lower lips and the head of a red-tail shark. The ampullary organ (AO) is localized in the head region behind the eye and is formed of specialized receptors that play important roles in detecting the electromagnetic fields, as well as temperature gradients. AOs have been classified into two different types based on the size and the length of the canals.

Skin is the structure that covers the body and protects it not only from the entry of pathogens or allergens but also from the leakage of water, solutes, or nutrients. These outside-in and inside-out barrier functions are dependent on the epidermis. The skin of a fish is a multifunctional organ and may serve important roles in communication, sensory perception, locomotion, respiration, excretion, osmoregulation, and thermal regulation. Teleost skin, in particular, is unique and histologically diverse. It is very different from that of mammals because it secretes mucus, which is involved in immune functions. Its structure and function reflect the adaptation of the organism to the physical, chemical, and biological properties of the aquatic environment and the natural history of the organism. The aquatic environment is rich in pathogenic organisms; hence, the skin of aquatic vertebrates is extremely important as the first line of defense against the invasion of environmental pathogens.

The skin is a self-active secretory organ that their cellular components provide many useful products. Goblet cells secrete mucus that keeps the body surfaces moist and protect it from stressors, club cells (CCs) produce the alarm substances that initiate the alarm reaction and melanocytes (MCs) produce pigments to provide the fish with specific colorations. The skin is also a vehicle for cutaneous sense organs allowed the fish for the detection of predators and foods. Among them are taste buds (TBs) and lateral line systems that include neuromasts and electroreceptive organs. The skin of fish shows various interspecies differences, as some species have scales and others have special cells. The skin was composed of the epidermis of nonkeratinized stratified squamous epithelium, followed by dermis of dense regular connective tissue.

7.1 EPIDERMIS

The epidermal cells (ECs), also known as filament containing cells, are the smallest and most numerous cells, being the major epithelium covering cells, and are found all over the epidermis, from basal to superficial layers. The thickness of the epidermis is depending mainly on the number and size of the layers of the cells that constitute the epidermis at different body regions. Frequently, the lips and tail of many fish species have the highest epidermal thickness.

The epidermis of the lower lip consists of stratified squamous epithelium non-cornified that formed of a basal columnar cell layer lies on a wavy

thick basement membrane. On top of this basal layer are several layers of eosinophilic CCs followed by simple squamous cell layers. Pear-shaped TBs are observed at the top of the epidermis (Figure 7.1A). Large numbers of periodic acid–Schiff-alcian blue (PAS-AB)-positive mucous goblet cells are distributed at the superficial layers. CCs are large cells that vary from spherical to saccular in shape and are negative to this stain. The combined PAS-AB reaction imparts a purple-bluish color of varying intensities in accordance with the neutral and acid mucin content of the various mucous cells in the lip (Figure 7.1B). Many eosinophilic granular cells (EGCs) are observed in the basal portion of the epidermis of the lower lip that appears at variable shapes and sizes and fill with alcian blue-positive granules (Figure 7.1C).

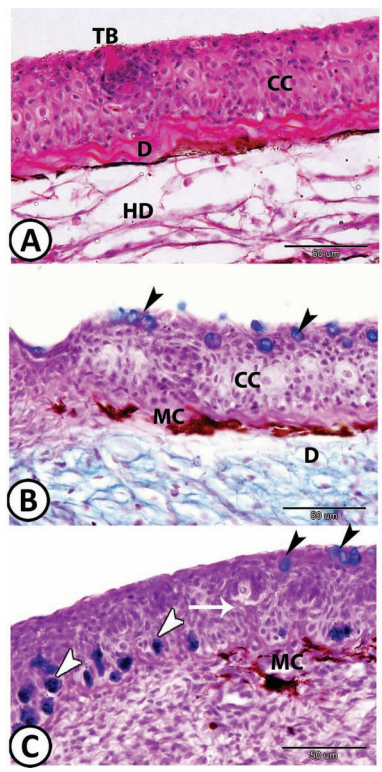

FIGURE 7.1 Organization of the skin of red-tail shark at the lower lips. (A) The skin of the lower lip stained by HE showing taste bud (TB) and club cells (CCs). Note, the dermis (D) is followed by hypodermis (HD). (B, C) The skin of the lower lip stained by PAS-AB-HX showing neuromast (arrow), mucous cells (black arrowheads), EGCs (white arrowheads), and melanocytes (MCs) at the dermis (D). Note, the CCs are negative to the stain.

The epidermis of the upper lip contains a higher number of CCs than those in the lower lip. These CCs show a positive reaction to Crossmon's trichrome (Figure 7.2A). Rodlet cells with their specific rodlet granules are seen in the apical portion of the epidermis (Figure 7.2B). The number of TBs is greater than those in the lower one and in general, they occurred more frequently in the anterior parts of the body than posteriorly (Figure 7.2C). Mucous goblet cells occupy the superficial layers of epidermis that open directly to the surface and stain positive with combined AB (Figure 7.2D). Tuberous organs are frequently occurred in the upper lip and appear as spherical structures of sensory cells surrounded by a cellular capsule (Figure 7.2D and E).

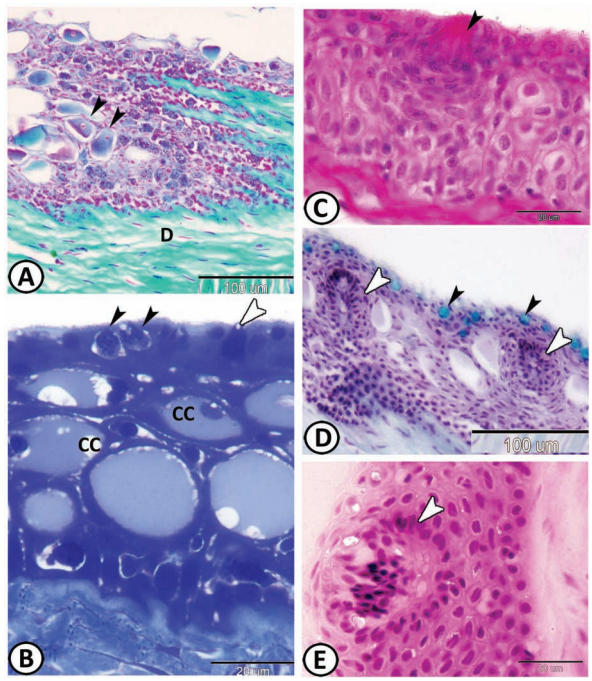

FIGURE 7.2 Organization of skin at the upper lips. (A) Numerous CCs (arrowheads) in silver carp are positive to light green. Note, the dermis (D) is composed of collagenous fibers (Crossmon's trichrome). (B) Semithin section in the upper lip of silver carp stained by TB shows rodlet cells (black arrowheads) in the apical portion of the epidermis in neighboring to the metachromatic goblet cells (white arrowhead). Note the presence of huge CCs. (C) The epidermis of the red-tail shark stained by HE showing TB (arrowhead). (D) The skin of the upper lip of silver carp stained by AB-HX showing mucous cells (black arrowheads), and tuberous organs (white arrowheads). (E) Higher magnification of the tuberous organ (arrowhead) showing many sensory cells surrounded by covering and supporting cells (HE).

The epidermis of the nostrils is characterized by the presence of many basal EGCs that show a metachromatic reaction with toluidine blue. Moreover, rodlet cells are observed in-between the CCs (Figure 7.3A). In the epidermis of the operculum, the mucous goblet cells are restricted on the superficial layer and are positive to PAS-AB stain. TBs are observed as pale staining, pear-shaped structures consisting of columnar sustentacular cells with dark nuclei alternated with fusiform sensory cells with lightly stained nuclei, and associated with small pyramidal basal cells and surrounded by marginal cells (Figure 7.3B). In addition, tuberous organs could be identified in the epidermis of the operculum (Figure 7.3C and D). The tuberous organ lack canal and are formed by epithelial masses that protrude into the dermis. The organ has a few numbers of large sensory cells each enclosed in its own cavity. Tuberous organs play a major role in electrocommunication (detection of conspecific electric signals) and are used for the detection of high-frequency signals.

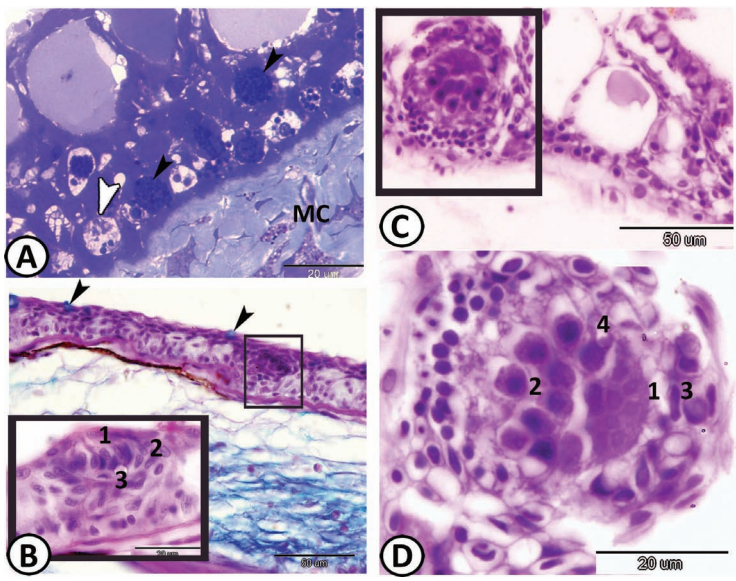

FIGURE 7.3 Organization of skin at the nostrils and operculum. (A) Semithin section stained by TB in the skin of the nostrils of silver carp showing RCs (white arrowhead) and EGCs (black arrowheads). Note the presence of MCs with specific melanin pigments in the dermis. (B) The skin of the operculum of red-tail shark stained by PAS-AB-HX showing mucous cells (arrowheads), TB (square, inserted figure) that consisted of sensory cells (1), supporting cells (2), and basal cells (3). (C, D) The operculum of silver carp stained by HE shows a tuberous organ (square) that consists of electroreceptor cells (1), sensory neurons (2), covering cells (3), and supporting cells (4).

The epidermis of the snout is characterized by the presence of a large number of CCs in a midepidermal level and numerous PAS-positive mucous goblet cells (Figure 7.4A and B). Tuberous receptor organ is distributed in this region and consists mainly of groups of sensory cells (Figure 7.4C). The skin of the orbital region contains many TBs, tuberous organs, and mucous cells. The mucous cells show a positive reaction to both PAS and AB (Figure 7.5).

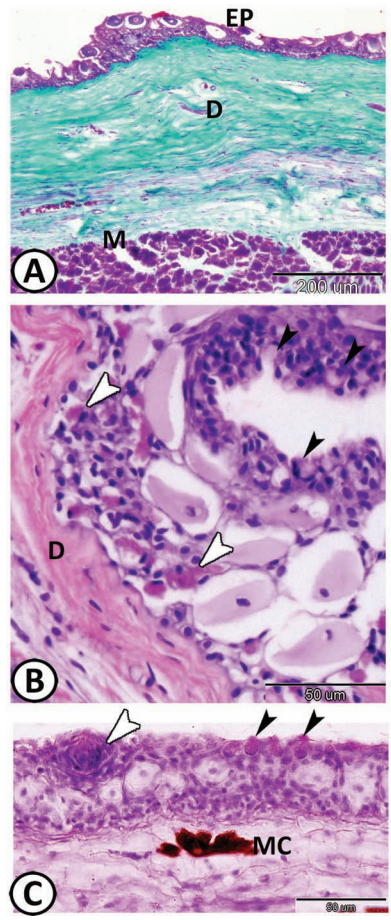

FIGURE 7.4 Organization of the skin at the snout. (A, B) The skin of the snout of silver carp consists of the epidermis (EP), dermis (D) followed by muscle layers (M). The epidermis contains goblet cells (black arrowheads) and EGCs (white arrowheads) (Crossmon's trichrome and HE, respectively). (C) The skin of the snout of red-tail shark stained by PAS-AB-HX showing PAS-positive mucous cells (black arrowheads), tuberous organ (white arrowhead), and MCs.

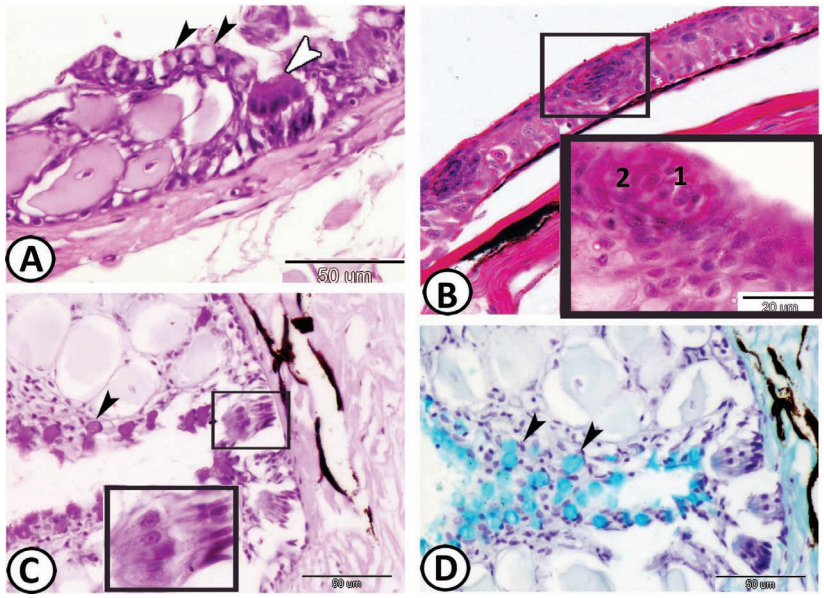

FIGURE 7.5 Organization of the skin in the orbital region. (A) The epidermis of silver carp contains TB (white arrowhead) and mucous cells (black arrowheads) (HE). (B) Tuberous organ in guppy fish consists of electroreceptor cells (1) and supporting cells (2) (HE). (C, D) TBs (boxed areas) and mucous cells (arrowheads) in silver carp are positive to PAS and AB, respectively.

The epidermis of the dorsal portion of the head of red-tail shark has a mean thickness of 38 μm and the density of mucous cells is 8/100 μm (Table 7.1). Many rodlet cells (RCs) are observed at the superficial layers as ovoid cells with a basal nucleus and numerous cytoplasmic inclusions (rodlets). TBs are observed at the superficial epidermal layer (Figure 7.6A and B).

The epidermis of the trunk region of many teleosts as red-tail shark, tilapia, carp, and guppy is covered with scales that originated from dermal scale pockets and protrude posteriorly where they are covered by the epidermis. The epidermis is thinner (11–18 μm) (Table 7.1) above the free portion of the scales. A bulb-shaped TB is demonstrated in the superficial region. Few small spherical PAS-AB-positive mucous goblet cells are observed (Figure 7.6C and D).

The epidermis of the tail region is thick (about 40 μm) but the density of mucous cells is differed according to species that ranged from 2/100 μm in red-tail shark to 14/100 μm in the Guppy (Table 7.1). Highly branched MCs are distributed randomly throughout the deeper layers of the epidermis and in the dermis. These cells are filled with dark brown to black coarse granules (Figure 7.6E and F).

TABLE 7.1 The Mean Thickness of Epidermis (μm) at Different Body Region and the Density of Mucous Cells/100 μm of the Epidermis in Two Fish Species

Body Regions	*Epalzeorhynchos Bicolor*		*Poecilia Reticulata*	
	Thickness of the Epidermis (μm)	Density of Mucous Cells/100 μm	Thickness of the Epidermis (μm)	Density of Mucous Cells/100 μm
Lower lip	51.3 ± 4.1	12.2 ± 2.4	36.1 ± 2.3	14.8 ± 2.3
Upper lip	65.2 ± 5.0	10.5 ± 2.7	58.2 ± 3.6	12.0 ± 2.3
Snout	44.5 ± 3.9	8.1 ± 2.8	38.6 ± 3.0	8.6 ± 1.9
Operculum	42.2 ± 2.8	8.9 ± 2.6	30.8 ± 1.9	8.5 ± 2.8
Dorsum of head	38.6 ± 3.6	8.3 ± 1.4	36.5 ± 2.8	10 ± 1.8
Trunk	18.0 ± 2.2	4.5 ± 1.0	11.6 ± 2.4	6.3 ± 1.3
Tail	40.5 ± 3.7	2.2 ± 1.5	39.4 ± 4.4	14.7 ± 3.7

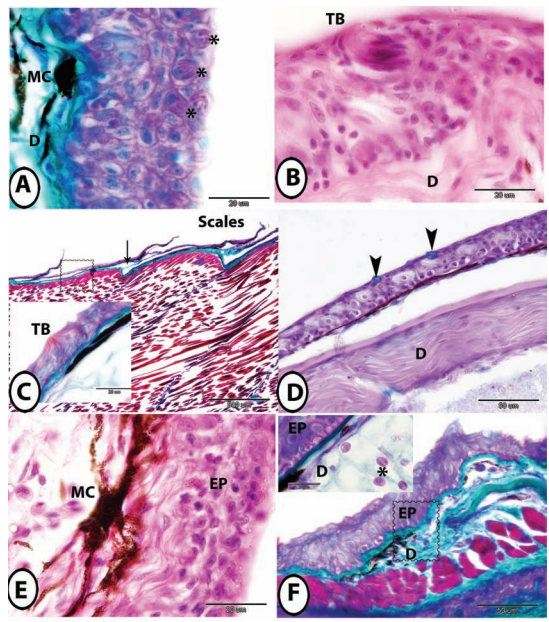

FIGURE 7.6 Organization of the skin of red-tail shark at the head, trunk, and tail. (A, B) The skin of the dorsum of the head stained by Crossmon's trichrome and HE, respectively, showing RCs (asterisks), TB, and MCs on the dermis (D) made up of collagenous fibers. (C) The skin of the trunk stained by Crossmon's trichrome showing scale pockets (arrow), taste bud (square, TB, inserted figure). (D) Higher magnification of the square in (C) showing the skin of the trunk stained by PAS-AB-HX indicates positive stained mucous cells (arrowheads). Note the parallel bundles of collagenous fibers in the dermis (D). (E, F) The skin of the tail stained by HE and Crossmon's trichrome, respectively, showing MCs in the deeper layers of the epidermis (EP). The dermis (D, inserted figure) contained many RCs (asterisk).

The fine structure of the epidermis revealed that the cytoplasm of the epidermal layers appears electron-dense except for the superficial layer. The cytoplasm superficial ECs are electron-lucent and contain many vacuoles and few profiles of rough endoplasmic reticulum (rER). These cells contain an ovoid euchromatic nucleus and are provided by apical microridges (MRs) (Figure 7.7A and B). The mucous cells are distributed on the superficial layer among the ECs. The mucous cells are filled with electron-lucent mucus granules (Figure 7.7A).

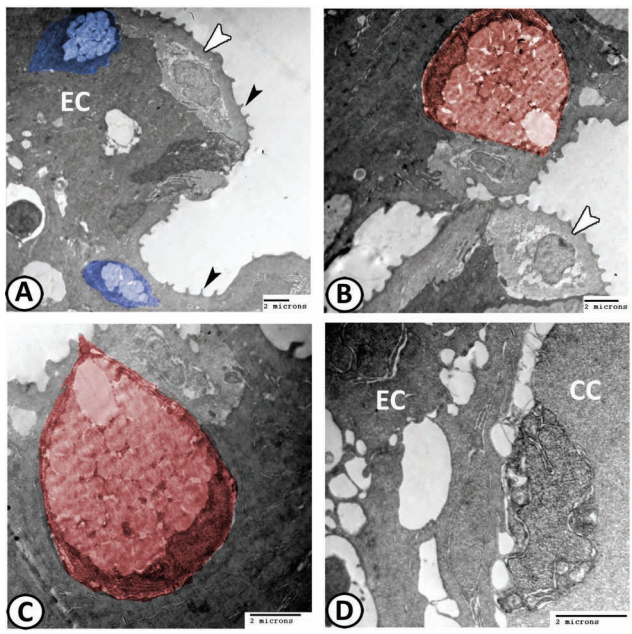

FIGURE 7.7 Digital colored TEM of the superficial ECs of the upper lip of silver carp. (A) The cytoplasm of the ECs is electron dense while the superficial cells (white arrowhead) are electron-lucent. Note the mucous cells (blue) and the apical microridges (black arrowheads). (B, C) The RCs (red) are located among the superficial cells (arrowhead). (D) The CCs are demonstrated in-between the ECs.

7.1.1 MUCOUS CELLS

Besides normal epithelial cells, the fish epidermis contains various types of unicellular glands. Most studied are the goblet (mucous) cells, which are responsible for the production of the mucus layer. Due to this main function of secreting mucus, mucous cell densities in the skin seem to act as a sensitive

first line of immune defense parameter in fishes. The number of mucous cells of fishes is affected by many stressors, and there is now evidence that the enumeration of the skin mucous cells of fishes can be used to monitor stress in them. Both the number of goblet cells and the composition of the mucus, which they produce, may vary depending on their location.

The fish skin mucus acts as a natural, physical, biochemical, dynamic, and semipermeable barrier that enables the exchange of nutrients, water, gases, odorants, hormones, and gametes. The primary function of the epidermis is protection against environmental hazards. In fish, mucogenic cells generally perform this function by secreting their contents on the surface. The distribution of the mucous cells in the epidermis varied greatly from species to species. In red-tail shark, they are condensed at anterior body regions, reduced in the trunk region, and decreased in the tail. However, in the guppy, the mucous cells are condensed in the anterior region and tail and decreased in the trunk. The condensation of mucoid cells in the anterior body regions is very important in lubrication and protection of fish against abrasive injuries during searching for the foods from the bottom.

Furthermore, the mucous cells of most teleosts are PAS-AB positive as the sulfate groups provide acidification of glycoproteins, which is effective to prevent the bacterial and viral invasion. Skin mucus has evolved to have robust mechanisms that can trap and immobilize pathogens before they can contact epithelial surfaces. This occurs because, in this mucus layer, particles, bacteria, or viruses are entrapped and removed from the mucosa by the water current. Furthermore, mucus in most fishes is continuously secreted and replaced, which prevents the stable colonization of potentially infectious microorganisms as well as invasion of metazoan parasites.

Mucus is a complex fluid, and its composition varies throughout the epithelial surface. Mucus is also used by small fishes to collect nutrients suspended in water. Toxic and irritating substances can greatly stimulate mucus secretion. The composition and characteristics of skin mucus are very important for the maintenance of its immune functions. Mucus composition varies among fish species. Furthermore, mucous cells and the compositions of the mucus they produce are influenced by endogenous factors (e.g., sex, developmental stage) and exogenous factors (such as stress, acid, and infections). On some occasions, especially when fish specimens are frightened or injured a high amount of proteins are present on mucus.

Mucins, the most abundant components of the mucus layer, are high molecular weight, filamentous, highly glycosylated glycoproteins (50% of their dry weight consist of carbohydrate chains). They are strongly adhesive,

play a major role in the defense of the mucosa, and impart viscoelastic and rheological properties to the mucosal layer. The recent studies confirm that mucous goblet cells contain a considerable amount of glycoconjugates in all locations of the skin, whereas the other unicellular gland types, the CCs, lacked these glycoconjugates.

The different functions that have been suggested for fish mucus and its role as a clue component of fish immunity have been considered. The skin mucus provides a medium in which the antibacterial mechanisms may act. Fish skin mucus, thus, serves as a repository of a variety of biologically active substances as well as numerous defensive molecules of both the innate and acquired immune system. Mucus performs a variety of functions (besides inhibition of the invasion and proliferation of pathogenic microorganisms) including ion regulation, osmoregulation, lubrication, and parenteral care behavior.

The skin mucus of fishes contains many kinds of biologically active (including defensive) molecules. Many substances with biostatic and biocidal activity (e.g., complement, C-reactive proteins, proteases, lectins, lysozyme, hemolysins, agglutinin, proteolytic enzymes, antimicrobial peptides, antibodies, and immunoglobulins) are present and have been identified in the fish epidermis and/or skin mucus. Although the protective role of the epidermal mucus of fishes has been known for many years, of great interest at the present is to see the skin mucus as a source for isolation of new and potent antimicrobial components.

The most studied enzyme presents in fish mucus is lysozyme. Lysozyme (*N*-acetylmuramide glucanohydrolase or muramidase) is a ubiquitous bactericidal enzyme identified in a wide range of organisms including fishes. Lysozyme is present in mucus, lymphoid tissue, and serum of most fish species but not in others (such as cod and wolfish). The bacteriolytic activity of lysozyme in fish skin mucus and other tissues contributes to its host defense mechanism against bacterial infection.

7.1.2 RODLET CELLS

RCs are unique cells found exclusively in teleosts that are considered a part of a generalized host response not only to a variety of stressors, especially parasitic infection, but also to toxins, neoplasia, and general tissue damage. RCs are encountered in the epidermis of the head region and dermis of red-tail shark and silver carp. RCs are reacted positively to bromophenol blue. They

consist of the capsule that enclosed rodlets or granules. The capsule reacted positively to PAS, while the rodlets reacted negatively to PAS (Figure 7.8C and D). These cells are also commonly observed in organs of fish include kidney, gills, heart, pancreas, and gut. The accurate function of these cells is unknown. They may be involved in water or electrolyte transport or have functions like those of mucous cells, for example, pH control, lubrication, and antibiotic effects. They may be modified goblet cells or may have a regulatory role of these cells in ion transportation and osmoregulation. These may also have considered nonspecific immune cells, involved in immunity as their number is increased in parasitic infection. Recent studies supposed a secretory function to these cells with a holocrine mode of secretion. The location of RCs is probably linked to their potential role as host response cells and the need to secrete into extracellular spaces, usually the external environment or passages leading to the external environment.

The fine structure of these cells (Figure 7.7B and C) revealed that they have a fibrous capsule measuring 0.6–0.8 μm in thickness and contained a single round to ovoid, heterochromatic nucleus at one end of the cell. The cytoplasm is filled with conspicuous club-like structures called rodlets. The apex of the cell harbors an abundance of mitochondria where all the rodlets are oriented. The number of rodlets increases with the growth of the cell, and the rodlets gradually change from round to elongate. In parallel, their sacs inflate, elongating to match the rodlet form, and becoming less opaque. Concomitantly, the RCs' nuclei change from oval to irregular. Rodlets can be forcefully ejected into extracellular spaces or the external environment. The rodlets themselves appear to be passive, stable elements, but their ejection has been suggested to play a role in reducing parasitic infection.

7.1.3 CLUB CELLS

In some teleosts as the guppy, the mucous cells are numerous and well-developed, while CCs are either rare or absent. On the other hand, in other species as red-tail shark, the mucous cells are smaller in number and the CCs are numerous and well-developed. It is suggested that the low density of mucous cells is compensated by the high density of CCs as an effective defense mechanism.

The cytoplasm of CCs is rather poor in organelles and rich in nonvesicle secretion. The few observed organelles (endoplasmic reticulum, Golgi complexes, polyribosomes, and mitochondria) are located in the perinuclear region, while the rest of the cytoplasm is filled with a filamentous substance.

Therefore, the cytoplasmic content can be separated into two regions: one light and electron-lucent around the nucleus and other abundant and electron dense, which occupies nearly the entire cytoplasmic volume. Large vacuoles are occasionally displayed in the peripheral cytoplasm. The plasma membrane shows invaginations throughout its length, making the cell surface irregular and slightly interdigitated with the ECs (Figure 7.7D).

The CCs cytoplasm shows the absence of glycoproteins content, as determined by the negative reaction to the PAS technique. The CCs of many Cyprinidae as red-tail shark secret proteinous substances as they stained positive with bromophenol blue (Figures 7.8A, B and 7.9C).

The CCs are related to the production, storage, and release of the alarm substance, leading to an alarm reaction in phylogenetically close species. The alarm reaction is triggered when the fish are threatened or preyed upon its injured epidermis. This event causes disruption of the plasma membrane of the CCs, resulting in exposition and releasing of cytoplasmic content into the water. Antipathogenic and phagocytic functions for these cells are also suggested. Chondroitin and keratin were also found in the cytoplasm of CCs of some fish, suggesting a healing function, thus helping on the repair of damaged tissue. Serotonin is also demonstrated in these cells supposed a pheromonal function.

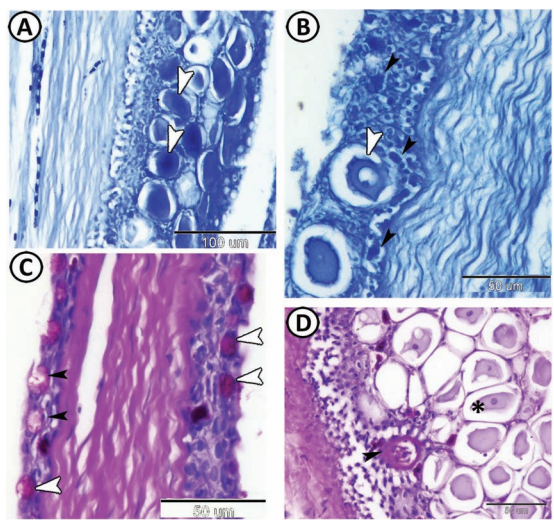

FIGURE 7.8 The skin of silver carp. (A, B) Positive-reacted CCs (white arrowheads) and EGCs (black arrowheads) in the epidermis of the upper lip and snout, respectively, stained with bromophenol blue. (C, D) Positive-reacted mucous cells (white arrowheads), negatively reacted RCs (black arrowheads), and CCs (asterisk) in the epidermis of the upper lip stained by PAS/HX.

7.1.4 PROTEIN SECRETING CELLS

Sacciform cells (serous goblet cells or protein secreting cells) are encountered in red-tail shark. These cells resemble the ordinary mucous goblet cells and are widely distributed in the head and snout. They are pear-shaped cells and their cytoplasm stained deep red with Mallory triple stain, while the mucous goblet cells appeared blue with the same stain (Figure 7.9A and B). Also, sacciform cells stain blue with bromophenol blue (Figure 7.9C) and deep blue with performic acid-methylene blue, and the cell membranes show an intensive reaction (Figure 7.9D). Moreover, these cells are also positive to Weigert's elastica and iron HX stain (Figure 7.9E and F).

Sacciform and CCs have been interoperated recently as a storehouse of biologically active substances and have also been associated with specific functions. The high protein contents secreted by sacciform cells at the surface of the skin may have defensive roles and acts synergistically with mucus glycoproteins to inhibit the adherence and proliferation of microorganisms.

Many studies revealed the presence of tryptophan in serous goblet cells that may be converted into serotonin, a vasoconstrictor amine, facilitating antibody transfer across the epithelium, and play an important role in the local defense mechanism. Additionally, serotonin may also be considered to prevent epithelial injury through an antioxidant effect. Further, serotonin is also reported to be involved in various other functions such as muscle contraction, regulation of ion selection and permeability in the epithelium, prevention of acid secretion, and stimulation of mucus production and secretion. Moreover, the proteinaceous secretions of these cells are rich in various amino acids like tyrosine, lysine, and cysteine. Furthermore, in addition to their role as substrates for protein synthesis, these amino acids may also play a vital role in neurotransmission, osmoregulation, stress response, and antioxidative defense.

The apparent specific response of the serous goblet cells to Verhoeff's elastin stain indicates the presence of elastin-like secretions. The elastin-like secretions may result in the great elasticity of the viscous water-insoluble lipid–mucus–protein complex forming a covering at the surface of the fish. This may provide protection to the fish from various environmental stresses. It has also been suggested that elastin may alter the physical properties of the mucus layer by increasing its viscosity, thereby protecting the fish more effectively against chemical damage.

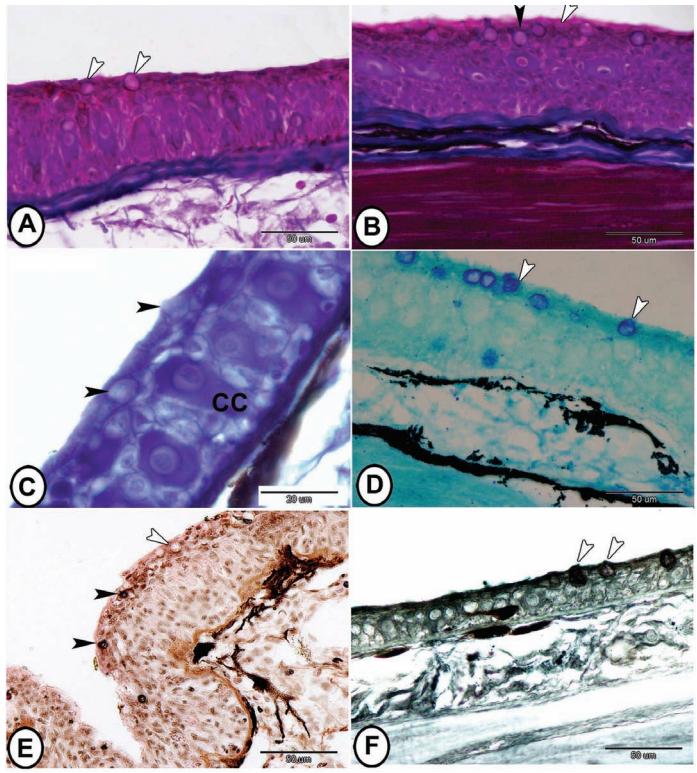

FIGURE 7.9 Histochemistry of the protein secreting cells in red-tail shark. (A, B) The skin stained with Mallory triple stain showing red serous goblet cells (white arrowheads) and blue mucous goblet cells (black arrowhead). (C) The skin was stained with bromophenol blue showing serous goblet cells (arrowheads) and positive stained CCs. (D) The skin was stained with performic acid-methylene blue showing positive stained serous goblet cells (arrowheads). (E) Sacciform cells are positive with Weigert's elastica stain (black arrowheads). Note the negative-stained mucous goblet cells (white arrowhead). (F) Sacciform cells (arrowheads) are positive with iron HX stain.

7.1.5 EOSINOPHILIC GRANULAR CELLS

Skin is considered the largest immunologically active organ. EGCs are spherical cells that occurred in the epidermis of the upper lip, snout, and nostrils. Their nuclei are eccentrically placed and their cytoplasm contains rounded granules stain bright red by hematoxylin and eosin (HE) due to the presence of basic proteins. In addition, EGC granules are stain deep magenta with PAS and alcian blue, indicating their content of sulfated and neutral glycosaminoglycans. They react positively with bromophenol blue (Figure

7.8B) that indicates their contents of protein as well as they show metachromatic reaction with toluidine blue (Figure 7.10). These cells are encountered in many species including salmonids and cyprinids. EGCs are commonly found in the intestinal mucosa, gills, connective tissue surrounds the spinal cord, and in the epidermis of the skin. EGCs are commonly distributed immune cells in the skin of fish (Figure 7.11A and B).

The marked histological and biochemical similarity between fish eosinophils and mammalian mast cells has been noted by many authors and suggested that they release toxic proteins and oxygen radicals onto the body surface of multicellular parasites in areas of inflammation. Acute tissue damage is causing EGC degranulation and release of mediators of inflammation, whereas an increase in the number of these cells is often found in chronically inflamed tissues.

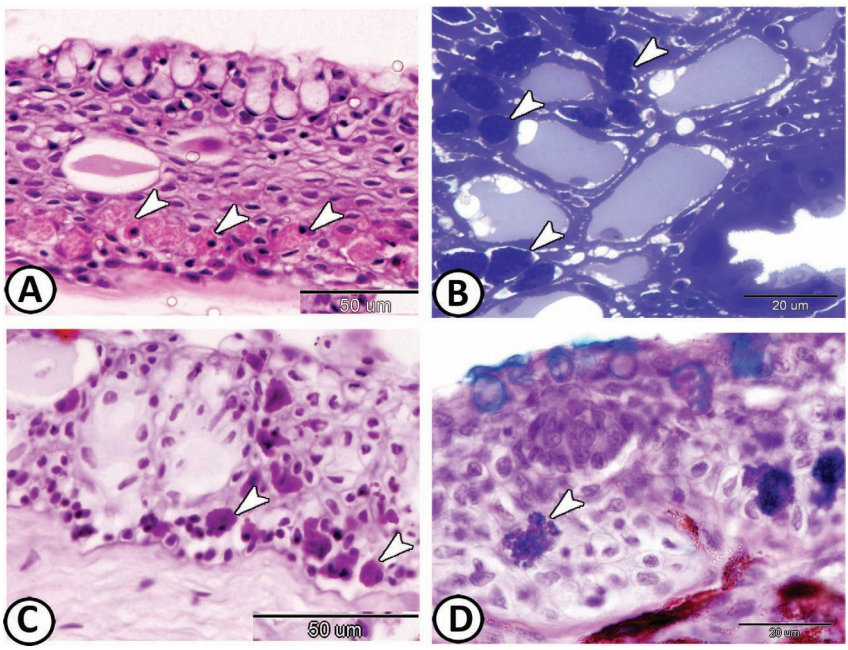

FIGURE 7.10 Eosinophilic granular cells. (A) EGC granules (arrowheads) stained red with HE in the upper lip of silver carp. (B) EGC granules (arrowheads) show a metachromatic reaction with TB in the upper lip of silver carp. (C) EGC granules (arrowheads) are positive to PAS in the snout of silver carp. (D) EGC granules (arrowhead) show staining affinity for combined PAS-AB stain in the lip of red-tail shark.

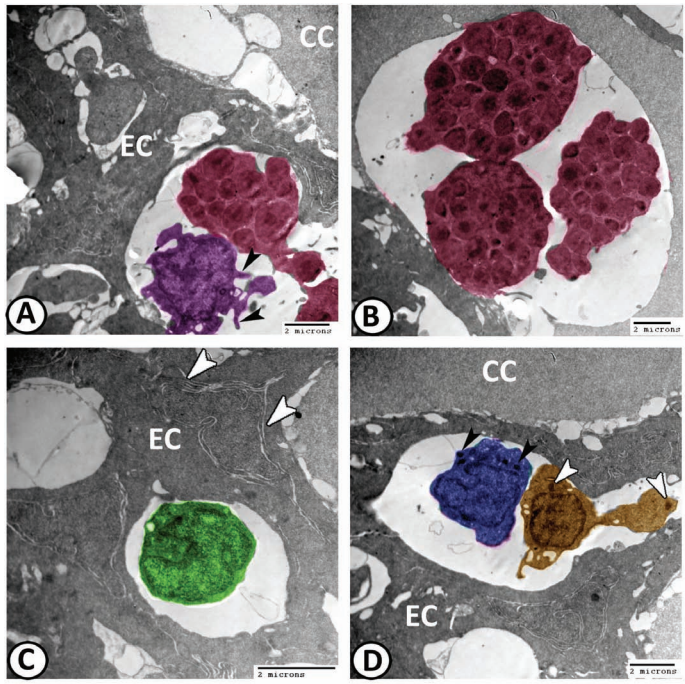

FIGURE 7.11 Digital colored TEM of the distribution of the immune cells in the upper lip skin of silver carp. (A, B) EGCs with their rounded granules (red) could be identified between the ECs and CCs. The dendritic cells (violet) were characterized by short-cell processes (arrowheads), as well as high nuclear to cytoplasmic ratio and small vesicles. (C) Lymphocytes (green) are recorded in the epidermis as small cells with a large nucleus and a thin rim of cytoplasm. Note the interdigitations (arrowheads) of the plasma membrane of the ECs. (D) Basophils (blue) and macrophage (orange) are seen in-between ECs and CCs. The basophils showed irregular shaped-nucleus and electron-dense cytoplasmic granules (black arrowheads). The macrophages are characterized by cell processes and the presence of lysosomes (white arrowheads).

7.1.6 IMMUNE CELLS

The fish's immune system can be subdivided according to the anatomical location. The mucosal-associated lymphoid tissue (MALT) in teleost fish is subdivided into gut-associated lymphoid tissue, gill-associated lymphoid tissue, and skin-associated lymphoid tissue. MALTs contain a variety of leukocytes, including but not limited to lymphocytes (T and B cells), plasma cells, macrophages, and granulocytes. It is well-known that leucocytes are migrating cells that can migrate to the connective tissue. Also, leukocytes and

probably other ameboid cells can migrate through normal mucus secretions. They are characterized by amoeboid-like cell processes, large euchromatic nucleus and the cytoplasm contain mitochondria and vacuoles (Figure 7.12A and B). Neutrophils were also demonstrated as important immune cells in the epidermis of the upper lip (Figure 7.12C). They showed a segmented nucleus, and abundant cytoplasm contained lysosomes and phagocytosed materials.

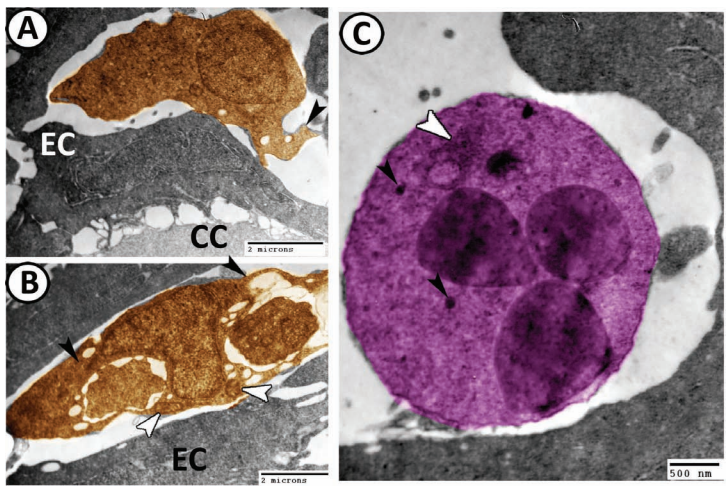

FIGURE 7.12 Digital colored TEM of the leukocytes in the upper lip skin of silver carp. (A, B) Leucocytes (orange) showed amoeboid-like cell processes (black arrowheads) and many cytoplasmic mitochondria (white arrowheads). Note the connections between the CCs and the ECs. (C) Neutrophil is characterized by a segmented nucleus, lysosomes (black arrowheads), and phagocytosed materials in the cytoplasm (white arrowhead).

Lymphocytes are frequently distributed in the intercellular spaces of the deeper epidermal layers of the lips and snout region and stained deep blue with HE and TB. These cells are encountered in immunity. Lymphocytes were recorded in the epidermis as small cells with a large nucleus and a thin rim of cytoplasm that contained rare organelles (Figure 7.11C). Basophils were seen with macrophage in the epidermal layer of the upper lip. The basophils showed irregular-shaped nucleus and electron-dense cytoplasmic granules. The macrophages are characterized by cell processes and the presence of lysosomes (Figure 7.11D).

Recently, dendritic-like cells (DCs), with T cell stimulatory capacities that revealed the properties of mature mammalian DCs have been identified in zebrafish (*Danio rerio*). Furthermore, functional cells with dendritic

morphology, motility, phagocytic ability, and strong T cell stimulatory properties have been identified in several other teleost fish species, such as rainbow trout (*Oncorhynchus mykiss*) and medaka (*Oryzias latipes*). ATPase-positive dendritic cells and IgM-positive lymphocytes are seen in the epidermis. The EGCs may be associated with the dendritic cells (Figure 7.11A). The dendritic cells are characterized by short cell processes as well as high nuclear to cytoplasmic ratio and small vesicles.

7.1.7 PIGMENT CELLS

Chromatophores are pigment-containing and light-reflecting cells, or groups of cells, found in a wide range of animals including fish. The dermal chromatophore units provide patterns of coloration and may also function to absorb or reflect radiations (thereby contributing to the regulation of body temperature). Their roles in coloration have been attributed to the presence of large numbers of a variety of pigment cells' types (chromatophores) that are present at different levels within the dermis, which include melanophores (black/brown), xanthophores (yellow), erythrophores (red), and iridophores (reflective/iridescent).

In fish, skin coloration depends on the distribution of epidermal MCs and dermal melanophores, xanthophores, erythrophores, and iridophores. The coloration in fishes performs adaptive functions and is useful to the animal in a variety of ways, such as camouflage, aggressive purpose, and courting patterns. Many pigments can also have other adaptive functions, such as photoprotection, structural support, microbial resistance, and thermoregulation, while variation in pigment patterns is considered as one of the driving forces of speciation.

MCs and melanophores are dark, melanin-containing cells. MCs showed well-developed, highly branched, and are distributed randomly throughout the deeper layers of the epidermis and in the dermis. These cells are most evident as an almost continuous layer just beneath the basement membrane. The pigment cells are filled with dark brown or black coarse granules (Figure 7.13). MCs are increased in number in the tail, lips, and dorsum of the head in most species.

Melanophores are the most common class of fish pigment cells. The pigmented material of melanophores is called eumelanin, a type of melanin that appears deep brown. It is packaged in vesicles called melanosomes and distributed throughout the cell. Eumelanin is generated from tyrosine in

a series of catalyzed chemical reactions. The melanophores are often star shaped of neuroectodermal origin. Many species are able to translocate the pigment inside their chromatophores, resulting in an apparent change in body color. This process is often used as a type of camouflage or known as physiological color change or metachrosis is most widely studied in melanophores since melanin is the darkest and most visible pigment. In most species with a relatively thin dermis, the dermal melanophores tend to be flat and cover a large surface area.

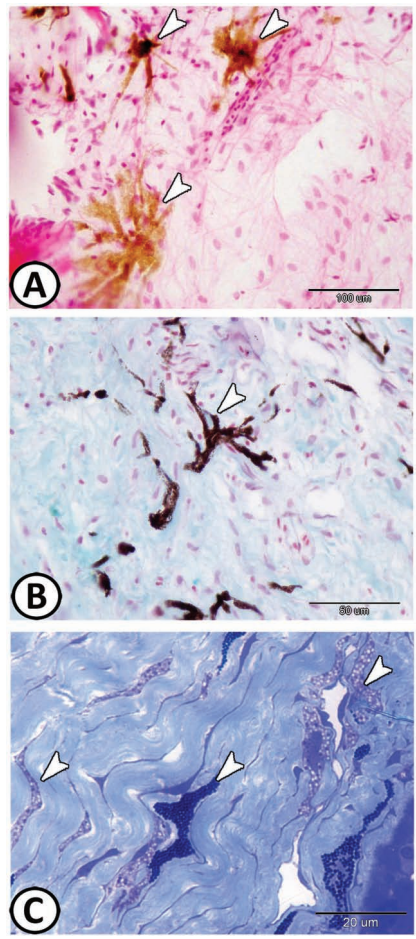

FIGURE 7.13 The MCs (A) melanocytes (arrowheads) are star-shaped dark brown cells that are distributed in the epidermis of the tail region of guppy fish (HE). (B) MCs (arrowheads) in the dermis of the snout of silver carp (AB/HX). (C) MCs (arrowheads) in the dermis of the nostrils of silver carp (TB).

Iridophores, sometimes also called guanophores, are light-reflecting pigment cells that contain light-reflecting platelets made of crystalline guanine inclusions. Those with mainly red/orange carotenoids are termed erythrophores. Xanthophores are yellow pigment cells that contain pterinosomes filled with pteridines or carotenoid vesicles filled with carotenoids. Xanthophore is localized just under the basal lamina of the epidermis. A little bit deeper an iridophore is found and just beneath it, a melanophore extends processes upward around the iridophores and xanthophores.

7.1.8 STEM CELLS

The basal ECs are characterized by electron-dense cytoplasm and heterochromatic nucleus (Figure 7.14A–C). Stem cells could be identified between the basal cells and characterized by high nuclear to cytoplasmic ratio, dividing nuclei, many mitochondria, rER, ribosomes, and many vacuoles (Figure 7.14A and B). These stem cells are involved in tissue maintenance and skin regeneration.

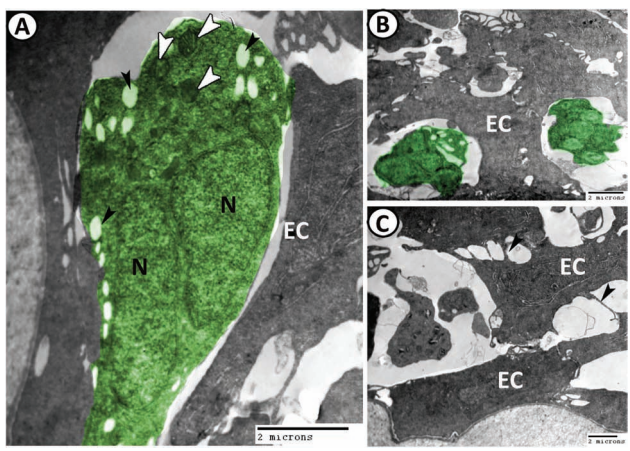

FIGURE 7.14 Digital colored TEM of the basal ECs of the upper lip of silver carp. (A, B) Stem cells (green) between the ECs. Their cytoplasm contains dividing nuclei (N), many mitochondria (white arrowheads), and many vacuoles (black arrowheads). (C) The basal ECs showed many kinds of connections (arrowheads).

7.1.9 TASTE BUD

In fish, the chemical senses, olfaction, and taste are highly developed and very important for a wide range of activities like feeding, orientation, and

social behavior. TBs occur in all taxa of vertebrates and are pear-shaped intraepithelial organs of about 80 μm height and 50 μm width. TBs are intraepithelial chemoreceptive organs that represent the characteristic feature of fish skin. The TBs assist the fish in the recognition and location of food by detecting distinct chemical substances on a short distance and also provide the fish with different information about the environment. Cyprinids and Siluroids are abundantly endowed with TBs.

Fishes are characterized by the presence of widely distributed TBs over various parts of the body include snout, lips, barbels, skin, gill rakers, oropharyngeal cavity, and esophagus of many fish species. TBs differ in size, shape, position, and cellular composition from species to species. In the fish epidermis, they are frequently observed in lips, operculum, head, and trunk region. Typically, TBs are bulb-shaped structures comprising sensory, basal, sustentacular, and marginal cells. They emanate from the basement membrane, often protruding above the epithelial surface.

TBs consist of modified epithelial cells of different types. Vertically oriented, elongate cells include dark cells with many small microvilli, and light cells with one large microvillus are the main constituents. Between the dark and light cells and the basal lamina, the basal cells stretch horizontally. These cells resemble Merkel cells and are not the stem or regenerative cells described as "basal cells" in mammals, but they have synapses and may serve as mechanoreceptive, or as paracrine, or as neuroendocrine cells. TBs are surrounded by marginal cells that build the interface between the regular cells of the squamous stratified epithelium and the sensory epithelium of the TB. Cutaneous TBs are innervated by the branches of the facial nerve (cranial nerve VII).

Occasionally, other types of cells present in teleostean fish TBs have been noted. In rainbow trout, an intermediate cell with a club-shaped apical receptor villus was described. Recently a cell type with several short, thick microvilli has been found in TBs of *Astyanax* and *Anoptichthys*. These cells are characterized by the presence of numerous dense-cored vesicles.

7.2 DERMIS

The dermis is about 15–20 times as thick as the epidermis. It consists of two distinct layers: the outer stratum laxum (SL) and the inner stratum compactum (SC) (Figure 7.15). The SL is adjacent to the basement membrane and composed of loosely arranged connective tissue fibers, mainly collagen, and richly supplied with fine blood capillaries, nerves, and pigment cells. The osteoderms or strands of osteoid tissues may be

embedded in the SL. These areas are stained light pink with HE, greenish-blue with AB, and purple with AB-PAS. These histochemical reactions indicate that glycoproteins with oxidizable vicinal diols, carboxyl groups, and O-sulfate esters are present in low concentrations. Many RCs are observed in the dermis of the tail region of the red-tail shark. This area is also provided with a well-developed wide lateral canal (CN).

Stratum compactum (Figure 7.15F) is comparatively thin. This tissue consists of bundles of coarse collagen fibers arranged parallel to the skin surface and intermingled with a few fine elastic fiber bundles. Many fibrocytes are scattered among the collagen fibers. Branches from the main blood vessels and nerves in the subcutis run through this layer and supply the capillaries in the SL. In the inner surface of the SC, a layer of small-branched pigment cells is discernible. The staining pattern of this layer is similar to that of the SL.

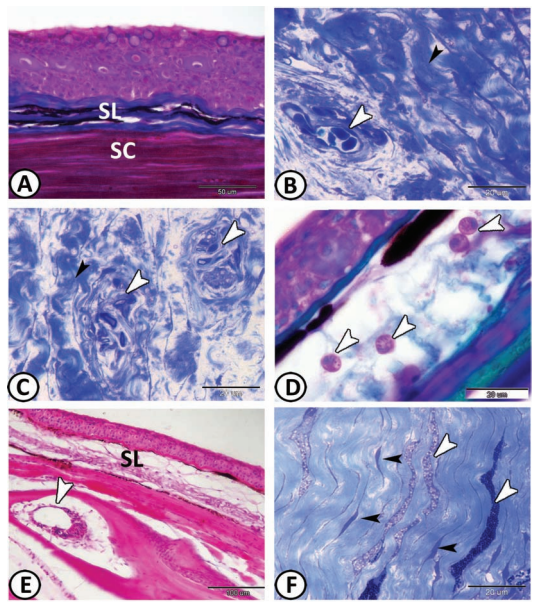

FIGURE 7.15 The dermis layer. (A) SL appeared blue with Mallory trichrome, while SC appeared red. (B) Semithin section through the SL of the lower lip of silver carp showing collagen fibers (black arrowhead) and small blood vessels (white arrowhead) (TB). (C) SL of the lower lip of silver carp showing collagen fibers (black arrowhead) and bundles of nerve fibers (white arrowheads) (TB). (D) Many RCs (arrowheads) were observed in the dermal layer of the tail of red-tail shark stained with Crossmon's trichrome. (E) SL of the dermis layer of red-tail shark appeared light pink with HE stain. Note the presence of osteoderm that surrounds the CN (arrowhead). (F) SC of nostrils of silver carp showing pigment cells (white arrowheads) and TCs (black arrowheads) in-between the collagen fibers.

7.2.1 TELOCYTES

Telocytes (TCs) are interstitial cells that establish relations to various types of cells. TCs have unique morphological characteristics. They are characterized by spindle-shaped cell bodies and multiple cell prolongations called telopodes (Tps). Tps may give rise to dichotomous branches and establish cellular connections to form a complex labyrinthine system. Telopodes are composed of thin segments, podomers and thick ones, podoms, which are rich in calcium release units, mitochondria, endoplasmic reticulum, and caveolae. TCs are reported in gonads, gills, and liver of fish.

In the dermis of silver carp, numerous TCs are observed among the collagen fibers in neighboring fibroblasts (Figure 7.15F). Their cell body contained an oval euchromatic nucleus. The telopodes possessed many secretory vesicles. These TCs established a network in the dermis by their Tps. The Tps are connected to fibroblasts and extended to the ECs (Figure 7.16).

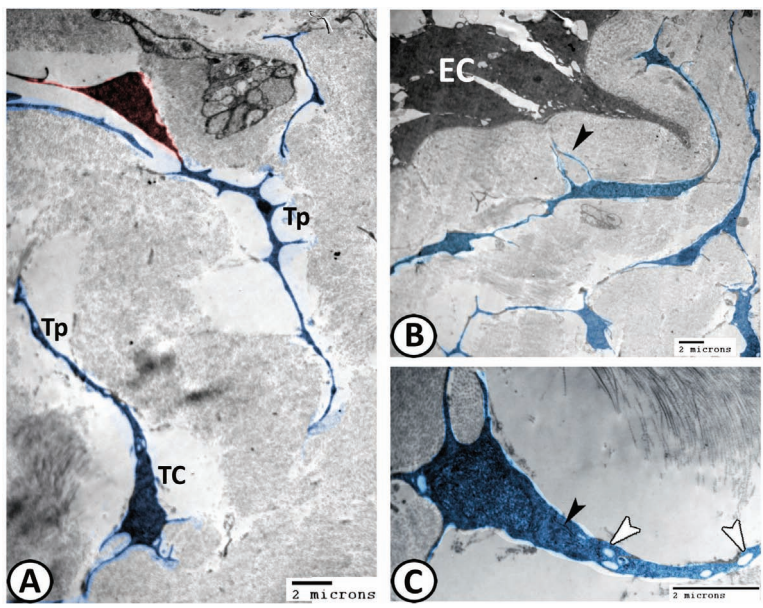

FIGURE 7.16 Digital colored TEM of the distribution of TCs in the upper lip skin of silver carp. (A, B) Numerous TCs (blue) established a network in the dermis by their Tps. Tps are connected to fibroblasts (red) and extended (arrowhead) to the ECs. (C) TCs consist of spindle-shaped cell bodies and Tps that possessed many secretory vesicles (white arrowheads) and rER (black arrowhead).

Telocytes are multifunctional cells, they contribute to the generation and transmission of nerve impulses to involuntary muscles. They serve in mechanoreception and exhibit receptors for excitatory and inhibitory neurotransmitters. They establish contact with immunoreactive cells such as eosinophil, mast cell, and macrophages. TCs play a role in the regeneration of some organs. TCs exert their effect on cells either by establishing cellular contact or through paracrine mode. Two types of cellular contact are documented for TCs: homocellular and heterocellular contact. Homocellular contact is formed between two telopodes or TCs and telopodes or between the cell body of two adjacent TCs. Heterocellular type contact between TCs and stromal cells either fixed or the free cells.

7.3 THE LATERAL LINE SYSTEM

The lateral line is a sensory system that allows fish to sense objects and motion in their surrounding aquatic environment. Fish use their lateral line to detect prey, monitor the movement of conspecifics and predators, and maintain a position in flowing water. The lateral line system is categorized into two subsystems: mechanoreceptive neuromasts and electroreceptive ampullary and tuberous organs.

The functional unit of the lateral line is the neuromast, which can be free-standing on the skin (surface or superficial neuromasts) or in canals that are open to the environments via pores (CNs). Superficial and CNs differ in function and performance but are overlapping in hydrodynamic selectivity. Physiological studies have shown that CNs respond to water movements that are produced by moving objects, such as prey, that is maximized in the direction of the canal axis. CNs typically occur in a distinct line at the base of a canal that runs and extends over the head and flanks. In contrast, superficial neuromasts are located on the surface of the skin and preferentially respond to the velocity of water flow that is not orthogonal to their orientation axis and appear to be best suited to encode flow velocity.

In particular, the number of CN pores displayed large interspecific variation, and an increase in the number of canal pores with fetch/depth ratio was observed, although this relationship is not straight forward among all species. In contrast to CN numbers, superficial neuromast numbers decreased with fetch/depth ratio.

The distribution of neuromasts across the body and head determines the ability of a fish to detect the moving as well as stationary stimuli. These

neuromasts are very diverse in morphology and organization, which are often related to the environment of the fish. Neuromast phenotypes can consequently be used as a diagnostic character for species delimitation.

The lateral line neuromast consists of discrete clusters of sensory hair cells, supporting cells, and mantle cells. At their apical surface, the sensory hair cells carry a ciliary bundle. Each bundle consists of several stereocilia that grow longer from one side of the apical surface to the other. A single true kinocilium occurs in the center of the stereocilia bundle. The stereocilia of superficial hair cells are embedded in a gelatinous matrix called the cupula, and the cupula is drag coupled to the surrounding water. The motion of the hair cell bundles in the neuromast generates electrical potentials that are transduced into action potentials in afferent neurons. The relationship between cupula displacement and the amplitude of the receptor potential is linear and can reach saturation. These signals provide the central nervous system with information about water flow around the body.

There are several types of lateral line canals in various fish species, including reduced canal systems. In herring, *Clupea harengus* (Clupeiformes), the trunk lateral line canals is absent. In the faltfish, *Solea* (Pleuronectiformes), the infraorbital (IO) canals are reduced. In the deep-sea fish, *Anoplogaster cornuta* (Beryciformes), the canals are reduced to shallow chambers and *Phrynichthys wedli* (Lophiiformes) even lacks canal organs. In the black goby, *Gobius niger* (Perciformes), only part of the preoperculomandibular canal is found. Differences in lateral line canal morphology occur in many orders of Neopterygii fish including tetraodontiformes. The tetraodontiformes lack lateral line canals, in these fish all neuromasts are located in lateral line grooves.

Electroreceptor organs in fish form part of the lateral line system that comprises mechanoreceptive sensory systems for hearing, the maintenance of equilibrium, the detection of gravity and rotation, and water currents along the body; it is innervated by cranial sensory nerves. Electroreceptive sensory cells are similar to mechanoreceptive sensory cells of vertebrates.

Ampullary organs (AOs) (or called electroreceptors) (formerly considered as neuromast) are also found in some fish and represent a morphologically and physiologically heterogeneous group of lateral line tonic receptors specialized in detecting the electromagnetic fields as well as temperature gradients. Several different biological functions of the ampullary Electrosense have been proposed, including prey detection, detection of predators, social communication, and detection of mates. AOs have been classified into two different types based on the size and the length of the canals. Wobbegong

sharks possess "macroampullae," which are characterized by large, visible pores, and long canals of up to several centimeters in length that are common in the marine environment. Whereas the "miniampullae" of freshwater rays, with their microscopic size and short canals, is thought to be an adaptation to low conductivity within the freshwater environment.

Ampullary electroreceptors are exceedingly sensitive to weak electric field gradients: about 5 μV/cm in marine fishes, 1–5 μV/cm in freshwater fishes. Teleost ampullary receptor cells, however, bear microvilli but no kinocilium. Ampullary electroreceptor cells and their supporting cells form the sensory epithelium lining an ampulla found at the end of a transepidermal canal, which is open to the outside. Marine fishes usually have long canals, while freshwater fishes have short canals, with the receptor opening directly above the ampulla. The canal is filled with jelly of a low resistivity similar to that of seawater. The AOs of elasmobranchs have long been known as "ampullae of Lorenzini." The ampullary canal is lined with several layers of flattened cells of high resistance connected by tight junctions. Ampullary receptor cells are voltage-to-chemical transducers, in catfish probably operating through nonvoltage-sensitive or nonspecific cation channels.

Tuberous organs consist of 1–35 receptor cells rest on a hillock of supporting cells, exposing 90% of their apical surface into individual perisensory spaces. The luminal surface is well endowed with sensory cells that are richly decorated with microvilli. Only one (branching) nerve fiber contacts all sensory cells at their basal parts. The sensory cells are capable of generating action potentials; transmission to the postsynaptic afferent fiber is thought to be by electrical, fast synapses. The tuberous receptors are usually tuned to much higher frequencies than ampullary receptors. The functions of tuberous receptors are: (1) active object detection (electrolocation), (2) probably to support the location strategy by which other electric fishes may be found from a distance, (3) the transmission (encoding) of electric organ discharge displays.

Mormyromasts are the most complex electroreceptors. They possess two types of sensory cells, which are innervated separately; their apical membranes contact two different chambers of perisensory space, an inner and outer one, which are connected by a short canal and filled with a conducting, mucoid material. The five to seven outer sensory cells differ from all other known electroreceptor cells by not having any apical specialization, neither microvilli nor kinocilium. The three to five inner sensory cells expose most of their microvilli-covered surface to their part of the perisensory space, the inner chamber. A mysterious mucoid ball rests on top of the inner sensory cells. The inner sensory cells are contacted by a single, branching nerve fiber, while two or three branching nerve fibers contacting the outer sensory cells.

Although Myxiniformes probably lack electroreception, it is well-developed in Petromyzoniformes and all other nonteleost fishes except Holostei. The density of the electroreceptive organs is higher in the head (approximately 10–20/mm^2) more than the trunk (10–20/mm$^{2.}$). On the trunk, the density is higher along the dorsal edge than on the lateral surface. This is important because the prey detection occurs along the dorsal edge.

7.3.1 LIGHT MICROSCOPY OF THE LATERAL LINE SYSTEM

In red-tail shark, the lateral line system is divided into mechanoreceptive neuromasts and electroreceptive tuberous receptor organs. The tuberous organ is more frequently occurring in the head region. The upper region of tuberous organ is covered by simple squamous epithelial cells to prevent the current from passing to the organ. The tuberous organs contain four to five elongate nonciliated sensory receptor cells within a cellular capsule. A single layer of supporting cells is present between the base of the receptor cells and the base of the capsule. A single nerve fiber innervates each group of organs and conveys the sensory information to the brain (Figure 7.17A and B). Tuberous organ is also encountered in some fish species as gymnotid that plays a significant role in the sensation of weak electrical stimuli.

In addition, red-tail shark has two types of neuromasts: canal (deep) and superficial neuromasts. CNs are embedded in the dermis in the form of tunnel-like canals. Large CNs are observed in the superficial layer of the epidermis of the head and the operculum and are invested by a dense fibrous wall without any cartilaginous support. CN is lined by stratified cuboidal epithelium with mucous cells and opened directly to the surface epithelium by a pore (Figure 7.17C and D).

A large number of superficial neuromasts are located at the lower lips and the head of red-tail shark. Four main cell types are encountered in the superficial neuromast: sensory hair cells, supporting cells, basal cells, and surrounded by crescent-shaped mantle cells. The superficial neuromasts in many cases are covered by the cupula (dome of gelatinous materials) extending into the surface (Figure 7.18). Hair cells are basic transducers for sound, vibration, and in determining position in vertebrates. On the other hand, the support cells encircle the hair cells and secrete a gelatinous-like material or "cupula" that covers the whole neuromast. The cupula enables the organ to communicate with the exterior and it is involved in the perception of the local water movements.

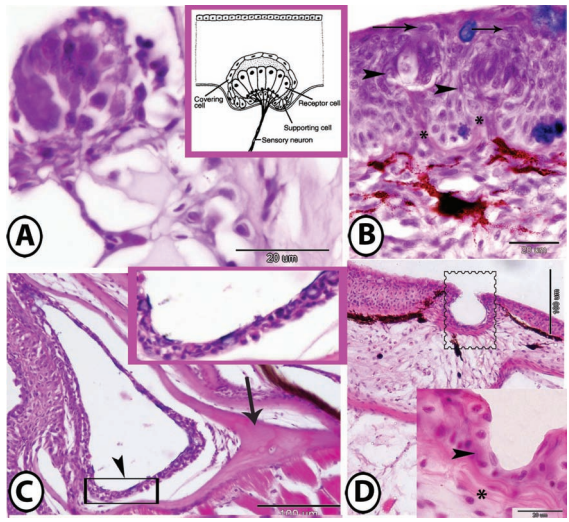

FIGURE 7.17 Lateral line system. (A) Tuberous organ (inserted figure) of silver carp stained by HE. (B) Tuberous organs (arrowheads) of red-tail shark stained by PAS-AB-HX are covered by flattened cells (arrows) and innervated by nerve fibers (asterisks). (C, D) Canal neuromast (arrowhead) of guppy and red-tail shark, respectively, stained by HE surrounded by fibrous tissue (asterisk) or bones (arrow).

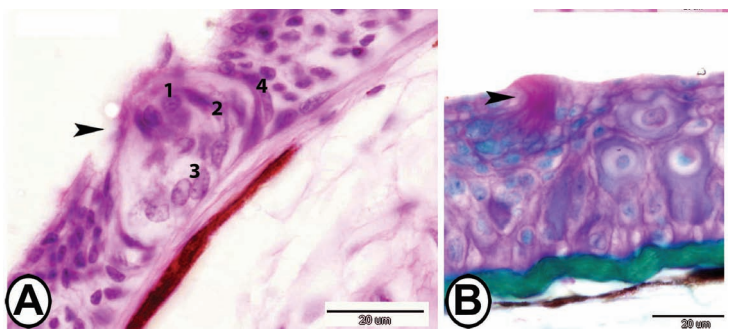

FIGURE 7.18 Superficial neuromast of red-tail shark. (A) Superficial neuromast (arrowhead) stained by HE formed of sensory cells (1), supporting cells (2), basal cells (3), and mantle cells (4). (B) Superficial neuromast stained with Crossmon's trichrome showing attached cupula (arrowhead).

The lateral line system of guppy is divided into two subsystems: AO and neuromasts. The AO is localized in the head region behind the eye; it is ranged in size from 200 to 250 μm in length and from 100 to 125 μm in diameter. The AO is formed of specialized receptors. These receptors are generally ampoule-shaped, and their lumen opened to the surface through

a short channel. The upper part of sensory cells is covered by a mucus-like substance called the cupula. The sensory epithelium is found in a chamber situated in the basal portion of the epidermis or somewhat depressed into the dermis. The sensory epithelium of the organ is formed by eight sensory cells. The sensory cells are pyriform in shape with dark cytoplasm with a large rounded centrally located nucleus and had microvilli on their apical surface with axon nerve endings in their basal part that arise from the underlying conjunctive tissue. Supporting cells are tall and narrow cells that completely enveloping the sensory cells with a basally located nucleus (Figure 7.19A and B).

The canal of the AO of guppy contains mucous cells that stained slight violet with PAS-AB stain, also the apical border of support cells was AB-positive (Figure 7.19B). The presence of the neutral mucosubstances that fill the ampulla along with the acid mucosubstances secreted by abundant mucous cells of the epidermis suggests that it may modulate the intensity of signals from receptor cells and/or give some protection and these materials have excellent electric conductivity. The ampullary pores (APs) are distributed throughout the head and lined with a single layer of squamous cells (Figure 7.19C). The transverse-section through the AO shows that it composes of a sac of fusiform receptor cells that lie below the AP (Figure 7.19D).

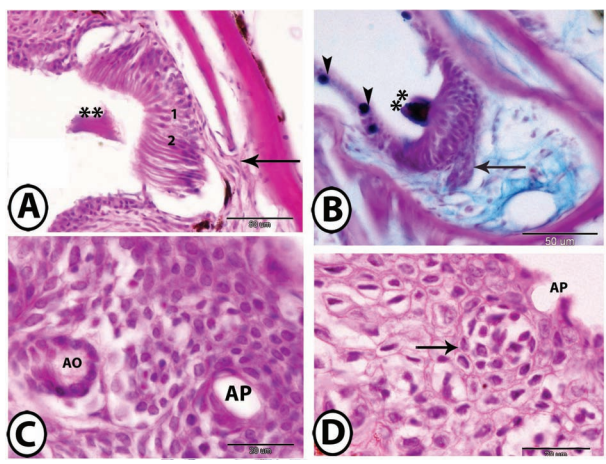

FIGURE 7.19 The lateral line system of Guppy. (A, B) The AO is formed of sensory cells (1), supporting cells (2), and covered by cupula (asterisks) and provided with a basal bundle of nerve fibers (arrow). Note that the ampullary channel contains PAS-AB positive mucous cells (arrowheads) (HE and PAS-AB-HX, respectively). (C) A transverse skin section of the epidermis is stained by HE showing an ampullary pore (AP) in close proximity to an AO. (D) A skin section stained with HE showing cross section of the AO (arrow) under an AP.

The superficial and deep (canal) neuromasts of guppy differ from those present in red-tail shark. The canals neuromast is widely distributed in the head and operculum and open at intervals to the exterior and surrounded by dermal bone (DB). The CN is lined by two layers of sensory cells with apical microvilli and the opposite side of the canal is lined with a simple squamous epithelium containing AB-positive mucous cells as these canals are filled with fluid (water and mucous secretion), which allow transmission of vibrations to the neuromasts through the skin pores. A bundle of nerve fibers lied below the canal and passed between the DBs (Figure 7.20A). The CN of guppies is surrounded by an osseous coat, while that of red-tail shark is supported by a fibrous coat and this may be an adaptive means against squeezing the contents of the canal by high water pressures in the bottom.

The superficial neuromast of guppy is concentrated in lips and the head. They rise above the surface epithelium and lined with sensory, supporting, basal cells, and surrounded by mantle cells. Some mucous cells are present in the epithelium adjacent to the neuromast (Figure 7.20B).

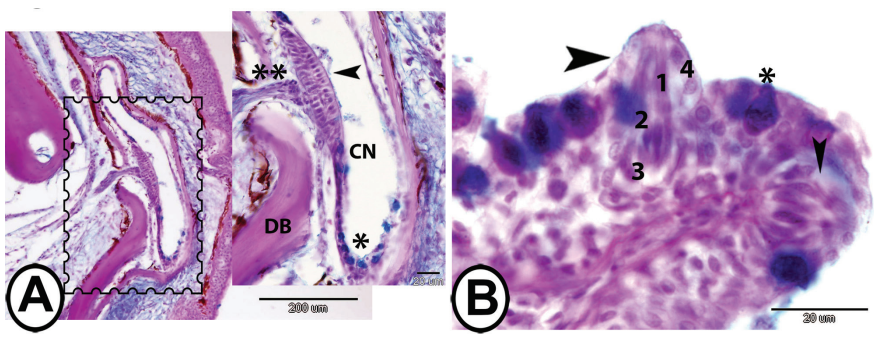

FIGURE 7.20 Neuromast of guppy. (A) Canal neuromast (square, inserted figure) stained with PAS-AB-HX showing the dermal bone that surrounded the CN, which lined by sensory cells (arrowhead), AB-positive mucous cells (asterisk). Note the presence of nerve fibers (two asterisks) below the neuromast. (B) Superficial neuromasts (arrowheads) stained by PAS-AB-HX is formed of sensory cells (1), supporting cells (2), basal cells (3), and surrounded by mantle cells (4). Note the presence of mucous cells (asterisk) near neuromasts.

7.3.2 SCANNING ELECTRON MICROSCOPY OF THE LATERAL LINE SYSTEM

The lateral line system and their associated pores based on their position around the head of red-tail shark are categorized into infraorbital (IO), supraorbital (SO), and otic (OT) lines (Figure 7.21). Each CN opened as a pore in the skin

of the head region (Figure 7.22A and B). The tuberous receptor organ is formed of a group of sensory cells found in pits but is not covered by the epidermis (Figure 7.22C). Microvilli projecting from the surfaces of the receptor cells are observed (Figure 7.22D). Each electroreceptor cell consists of a small pit in the skin with a cluster of sensory cells at the bottom of the pit (Figure 7.23A and B). The receptor cells act like miniatures voltmeters and monitor of the voltage drop across the skin (the so-called transdermal potential).

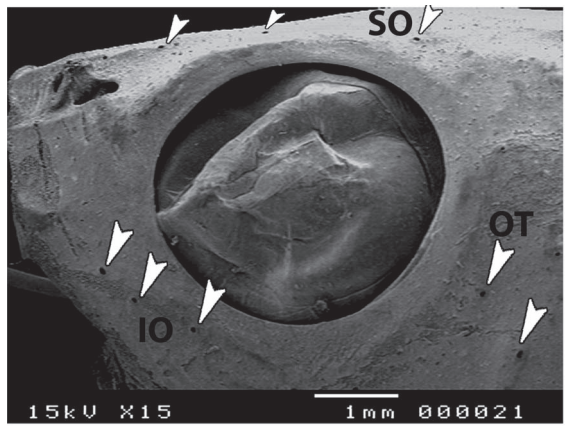

FIGURE 7.21 SEM of the lateral line (arrowheads) of red-tail shark that branch in the head into SO, IO, and OT.

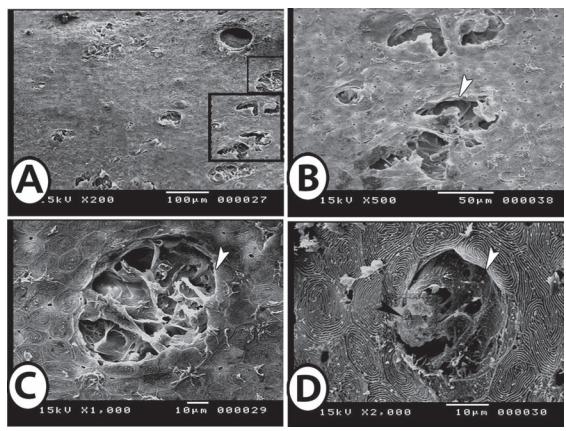

FIGURE 7.22 SEM of the lateral line system of red-tail shark. (A) Pores of lateral lines (large square). (B) Magnified view of a large square in (A) showing details of the pores (arrowhead). (C) Higher magnification of the small square in (B) showing the tuberous receptor organ (arrowhead). (D) Tuberous receptor organ (white arrowhead) showing microvilli (black arrowhead) projecting from the receptor cells.

Superficial neuromast is noticed in the upper lips and dorsum of the head localized mainly within the anteorbital area (Figure 7.23C and D) and may present as isolated elements or found in rows (Figure 7.24A). Each neuromast is sitting on an epidermal protrusion (Figure 7.24B). The epidermal protrusion is encircled with an epithelial ring that shows shallow depression or invaginations to form a characteristic ring-like pattern. The top of the protrusion possesses hair bundles (Figure 7.24C and D). Neuromast with an attached cupula was observed (Figure 7.24E) and a neuromast that highly elevated over the epidermal surface was also recorded (Figure 7.24F).

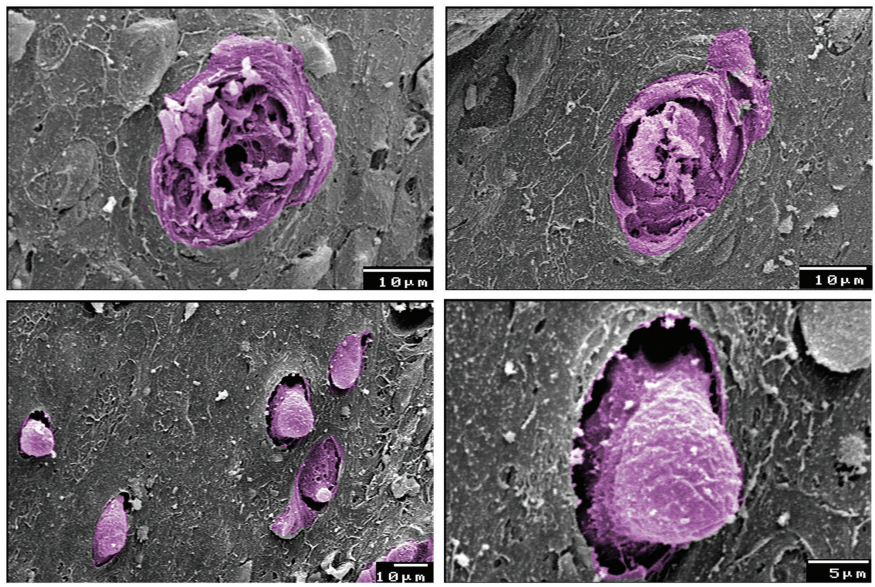

FIGURE 7.23 Digital colored SEM of the lateral line system of silver carp (A, B) Tuberous organ (pink). (C, D) Superficial neuromasts (pink) are widely distributed on the skin of the orbital region.

Groups of elevations are demonstrated in the dorsal surface of the head of red-tail shark and appeared conical in shape (Figure 7.25A). The apex of each elevation is characterized by the presence of TBs that protruded above the epithelial surface. At the summit of this elevation, numerous closely packed microvilli are originated and short cilia are observed in the center (Figure 7.25B).

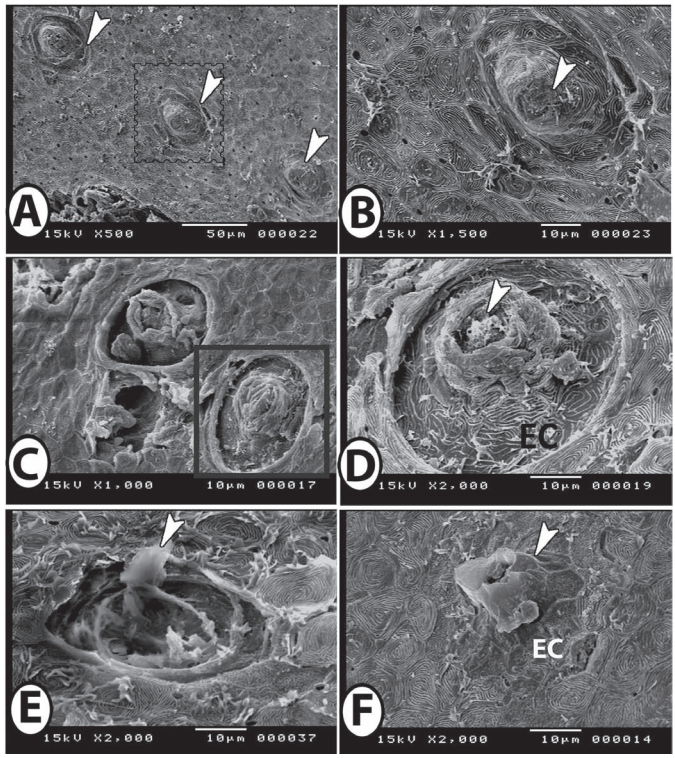

FIGURE 7.24 SEM of the neuromasts of red-tail shark. (A) Superficial neuromasts are arranged in rows (arrowheads). (B) Higher magnification of the square in (A) showing superficial neuromast (arrowhead). (C, D) The ring-like pattern of neuromast (square) formed of ECs. Note the hairs from sensory cells at its apex (arrowhead). (E) Superficial neuromast with attached cupula (arrowhead). (F) Neuromast (arrowhead) is elevated above the ECs.

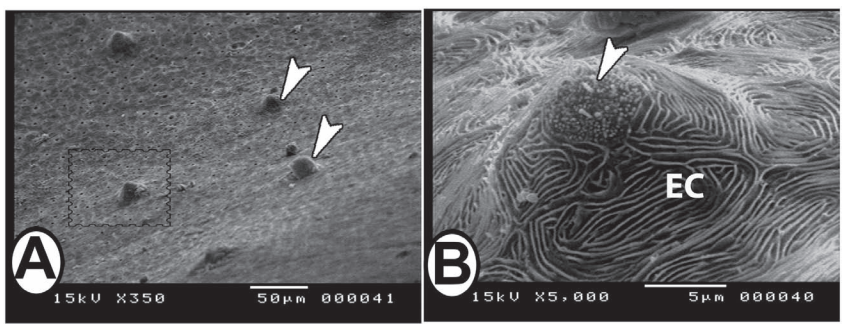

FIGURE 7.25 TBs of red-tail shark. (A) The TBs appear as epidermal elevations (arrowheads, square). (B) Higher magnification of the square in (A) showing the conical nonkeratinized protuberance of ECs with a TB at a summit (arrowhead).

The surface of the ECs is appeared polyhedral in shape bearing well-organized fingerprint-like MRs and interspersed by openings of mucous cells and MCs (Figure 7.26A). The broken surface of the epidermis indicated the presence of large CCs and MCs with cytoplasmic processes (Figure 7.26B). The fingerprint-like MRs on the surface of ECs may provide structural integrity to the epithelium and increase the surface area, as well as providing mechanical flexibility to the wall during distortion or stretching, retaining the mucus, facilitate the movement of materials over the surfaces, and prevent physical abrasions.

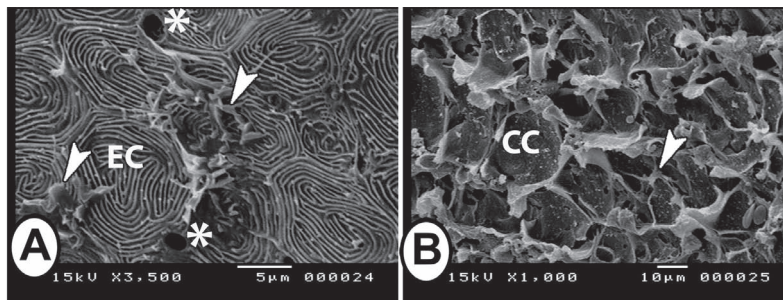

FIGURE 7.26 Epidermal surface of red-tail shark. (A) The surface of the epidermis showing ECs with MRs, interspersed by the openings of mucous cells (asterisks) and MCs (arrowheads). (B) Broken surface of the epidermis showing CCs and MC (arrowhead).

Contrariwise, the lateral line system and their associated pores of guppies based on their position around the head are categorized into SO, OT, and preopercular (PO) lines (Figure 7.27A). The AO is localized within grooves or minute pores in the head region behind the eye, beside the lateral line channels (Figure 7.27B).

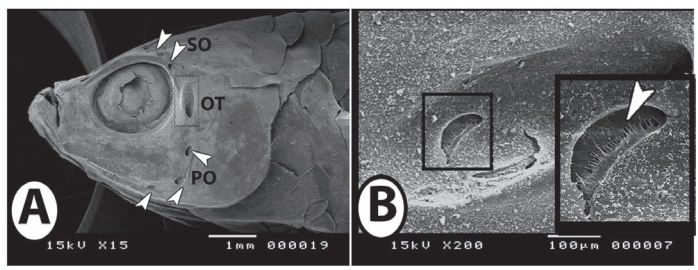

FIGURE 7.27 SEM of the lateral line system of guppy. (A) The lateral line (arrowheads) branch in the head into SO, OT (square), and PO. (B) Higher magnification of the square in (A) showing AO (square, inserted figure) in a pit in the skin of the head formed of receptor cells (arrowhead).

Moreover, many morphological studies have assessed the light microscopy of the AO, while the use of scanning electron microscopy has been used very little. From the surface view, the AO appears spherical with the attached cupula (Figure 7.28A). In the lateral view, it appeared spherical with an alveoli-like appearance (Figure 7.28B). Within the different ampullary groups, variations in alveolar morphology exist and have been classified into five types based on the alveolar arrangement: single-alveolate, multialveolate, branched alveolate, centrum cap, and club-shaped. AOs differ in structures from species to species and this difference resulted from different environmental conductivity. The morphological analysis and a comparison of the different distribution patterns are used to infer how electroreception may participate in natural feeding behavior, as well as possible adaptations of electroreception to the respective habitat types of each species.

AP distribution patterns are relatively unique, with the majority of pores occurring on the dorsal region of the head, which are analogous in location to the AOs. The diameter of the APs ranges from 5 to 10 μm. Superficial neuromasts with attached cupula are observed along the line of the AO. The surface of the epidermis is composed of polyhedral epithelial cells that are covered by fingerprint-like pattern MRs. The boundaries between cells are clearly defined (Figure 7.28C and D).

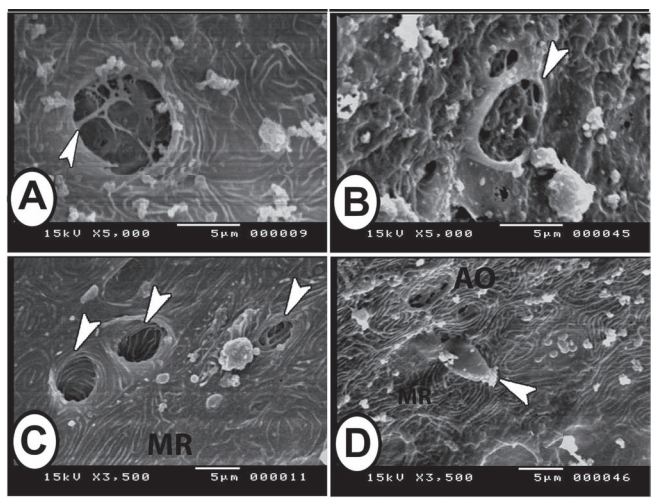

FIGURE 7.28 SEM of the AO and neuromast of guppy. (A) Surface view of the AO with the attached cupula (arrowhead). (B) Lateral view of the AO (arrowhead) with the alveolar-like appearance of the organ. (C) Different sizes and shapes of ampullary pores (arrowheads). Note the presence of fingerprint-like microridges (MRs) of the surrounding ECs. (D) Superficial neuromast with attached cupula (arrowhead) that occurs near AO among MRs of ECs.

KEYWORDS

- **epidermis**
- **rodlet cells**
- **mucous cells**
- **lateral line**
- **club cells**
- **melanocytes**

BIBLIOGRAPHY

Abd-Elhafeez, H. H.; Mokhtar, D. M. Comparative morphological study of lips and associated structures of two algal grazer fish. *J. Advan. Microsc. Res.* **2014,** *9,* 1–10.

Cernuda-Cernuda, R.; Garcia-Fernandez, J. M. Structural diversity of the ordinary and specialized lateral line organs. *Microsc. Res. Tech.* **1996,** *34,* 302–312.

Damasceno, E. M.; Monteiro, J. C.; Duboc, L. F.; Dolder, H.; Mancini, K. Morphology of the epidermis of the neotropical catfish *Pimelodella lateristriga* (Lichtenstein, 1823) with emphasis in club cells. *PLoS One.* **2012,** *7*(11), 1–7.

Harvey, R.; Batty, R. S. Cutaneous taste buds in cod. *J. Fish Biol.* **1998,** *53,* 138–149.

Kottler, V. A.; Koch, I.; Flötenmeyer, M.; Hashimoto, H.; Weigel, D. Multiple pigment cell types contribute to the black, blue, and orange ornaments of male guppies (*Poecilia reticulata). PLoS One.* **2014,** *9*(1), 85647.

Manera, M.; Dezfuli, B. S. Rodlet cells in teleosts: a new insight into their nature and functions. *J. Fish Biol.* **2004,** *65,* 597–619.

Mittal, A. K.; Ueda, T.; Fujimori, O.; Yamada, K. Histochemical analysis of glycoproteins in the unicellular glands in the epidermis of an Indian fresh water fish *Mastacembelus panculus* (Hamilton). *Histochem. J.* **1994,** *26,* 666–677.

Mokhtar, D. M.; Abd-Elhafeez, H. Light- and electron-microscopic studies of olfactory organ of red-tail shark, *Epalzeorhynchos bicolor* (Teleostei: Cyprinidae). *J. Microsc. Ultrastruct.* **2014,** *2*(3), 182–195.

Powell, M. D.; Wright, G. M.; Burka, J. F. Morphological and distributional changes in the eosinophilic granular cells (EGC) population of the rainbow trout (*Oncorhynchus mykiss Walbaum*) intestine following systemic administration of capsacin and substance P. *J. Exp. Zool.* **1993,** *266,* 19–30.

Reite, O. B. The rodlet cells of teleostean fish: their potential role in host defense in relation to the mast cells/eosinophilic granule cells. *Fish Shellfish Immunol.* **2005,** *19,* 253–67.

Takeuchi, I. K. Electron microscopy of two types of reflecting chromatophores (iridophores and leucophores) in the guppy, *Lebistes reticulatus* peters. *Cell Tissue Res.* **1967,** *173*(1), 17–27.

Wark, A. R.; Peiche, C. L. Lateral line diversity among ecologically divergent three spine stickleback populations. *J. Exp. Biol.* **2010,** *213,* 108–117.

Whitehead, D. L.; Tibbetts, I. R.; Daddow, L. Y. M. Microampullary organs of a freshwater eel-tailed catfish, *Plotosus (tandanus) tandanus*. *J. Morphol.* **2003,** *255,* 253–260.
Yashpal, M.; Mittal, A. K. Serous goblet cells: the protein secreting cells in the oral cavity of a catfish, *Rita* (Hamilton, 1822) (Bagridae, Siluriformes). *Tissue Cell* **2014,** *46,* 9–14.

CHAPTER 8

The Digestive System

ABSTRACT

The gastrointestinal tract consists of the pharynx, esophagus, stomach, and intestine that ends at the anus. The differences in the structures among fish gastrointestinal tracts are related to feeding habits, food, age, body shape, and weight. The esophagus of many teleosts is divided into anterior and posterior parts However, taste buds are present in the esophagus of some species. The stomach of fish possesses different configurations according to the feeding habits, while juveniles and adults of a variety of fishes are stomachless. The stomach of catfish is divided into three regions according to structure: cardiac, fundic, and pyloric regions. The cardiac mucosa is characterized by a large number of well-defined long folds, occupy by closely packed simple branched tubular gastric glands. The fundic region is characterized by a great number of simple branched tubular gastric glands composed of oxyntico-peptic cells that contain a tubulovesicular network. The pyloric region is characterized by the absence of gastric glands. The absence of the true stomach in carp is replaced by a simple dilatation at the anterior part of the intestine called the intestinal bulb. The mucosa of the bulb shows numerous folds, arranged in zigzagging-like patterns. The surface epithelium consists of simple columnar, enteroendocrine, and goblet cells (GCs). No multicellular glands of gastric or intestinal-type are found in their lamina propria. The intestine of fish is divided into three portions according to the thickness of the wall, length of mucosal folds, and thickness of muscularis; anterior, middle (posterior), and rectum. The surface epithelium of the three regions consists of enterocytes covered with microvilli with numerous GCs.

The gastrointestinal tract consists of the pharynx (ph), esophagus, stomach, and intestine that ends at the anus. Food enters a short, often greatly distensible esophagus leading to a thick-walled stomach. The histological structure of the gastrointestinal tract of numerous fish species generally consists of tunica mucosa, submucosa, muscularis,

and serosa (SE). The differences in histological structures among fish gastrointestinal tracts are related to feeding habits, food, age, body shape, and weight.

The gastrointestinal tract of carnivorous fish as *Nile catfish* occupies a small part of the abdominal cavity, and it consists of the oesophagus, stomach, and intestine. Its mean length is 38.20 ± 3.90 cm. While the gastrointestinal tract of herbivorous fish, such as *grass carp* is coiling repeatedly and occupies a greater part of the abdominal cavity, and it consists of the oesophagus, intestinal bulb, and intestine. The gastrointestinal tract of *grass carp* shows a highly significant increase in length compared with that of catfish and its mean length is 71.50 ± 4.80 cm. The relative gut length (RGL) (%) that represents the length of the digestive tract to standard body length is short in catfish, approximately 1.07%, while that of grass carp is 1.92% (Figures 8.1 and 8.2).

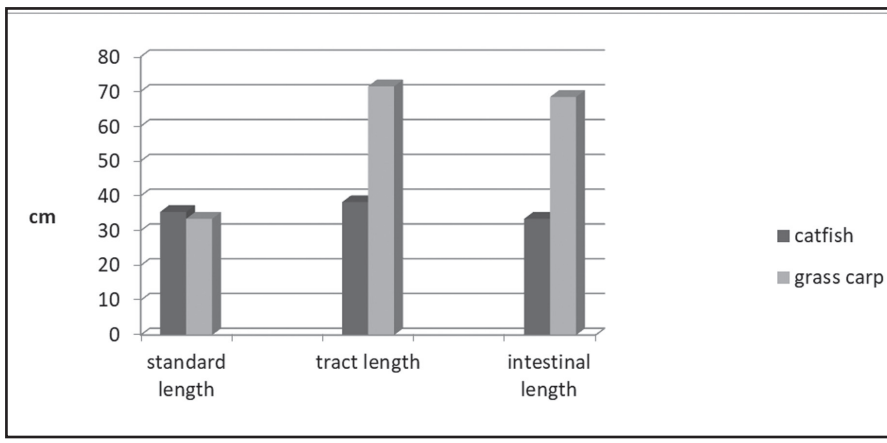

FIGURE 8.1 The mean standard length of fish, gastrointestinal tract length, and intestinal length of catfish and grass carp in centimeters.

8.1 LIPS

Lips are specialized structures that covered the jawbones. The morphological features of these structures act as a key for the understanding of different feeding habits of fish species as well as physiological adaptation and modification in relation to various environments. The lip is a multifunctional organ

that varies in structure in relation to physiological functions, nutrition, and feeding behavior (sensory, prehensile, or adhesive).

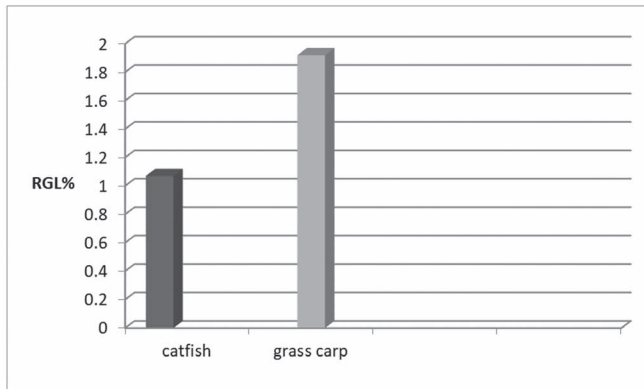

FIGURE 8.2 The mean values of RGL % of both catfish and grass carp.

The surface of the upper lip of Orinoco sailfin catfish (*Pterygoplichthys multiradiatus)* is covered by a raw of long slender dagger-like teeth with a bisected crown. However, the surface of the lower lip possesses a raw of long slender dagger-like teeth (Figure 8.3A). The epithelium of the lower lip is keratinized and is provided with well-organized large fungi-form papillae (8–10 per unit area) of 140–160 μm in length (Figure 8.3B). The apex of these papillae bears taste buds (TBs) as well as straight and slender teeth-like projections called uniculi, which direct backwardly and range from 30 to 35 per papilla, and their length reaches 7–10 μm (Figure 8.3B and C). Some of the uniculi are shedding from the surface and new growing ones are observed (Figure 8.3C). These uniculi have multifunctional roles, involved scraping off the substrate, protection, and adhesion.

The surface of the papillae of the lower lip is covered by epithelial cells bearing numerous microvilli and is characterized by the presence of TBs (Figure 8.3D). TBs are characterized by sunken taste pore below the level of the epithelium with prominent taste hairs. These TBs may enhance the efficiency in perception and sorting of food types as well as in assessing the quality and palatability of food items. The surfaces of the depressions between the papillae are covered with compactly arranged epithelial cells (6–8 μm in diameter), bearing interwoven microridges (MRs) that forming a web-like pattern (Figure 8.3E).

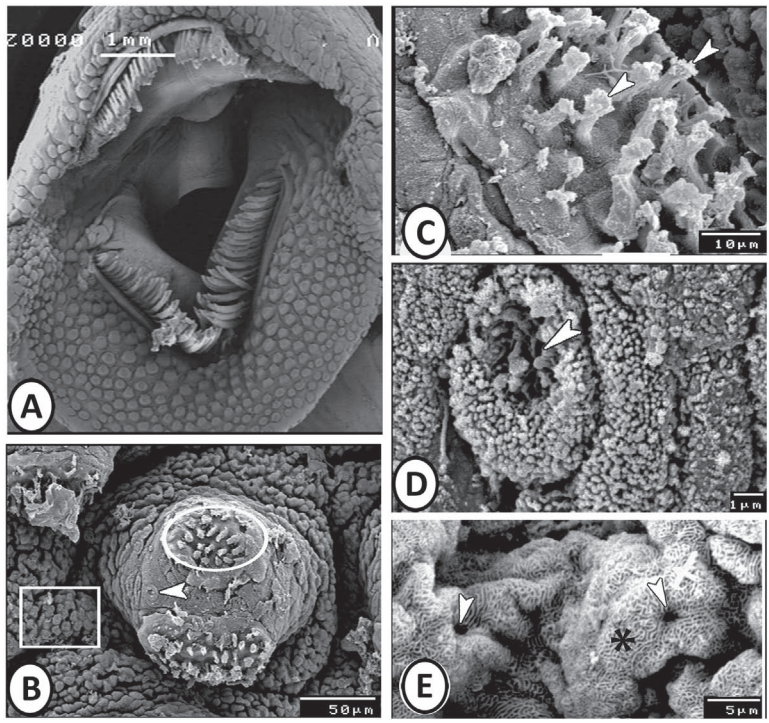

FIGURE 8.3 SEM of the lips of Orinoco sailfin catfish. (A) General view of the upper and lower lip. Note the dagger-like teeth. (B) Fungi-form papillae in the lower lip with TBs (arrowhead) and uniculi (circle). (C) Higher magnification in the uniculi of the papillae (arrowheads). (D) TB (arrowhead) is characterized by a sunken taste pore that is surrounded by epithelial cells bearing microvilli. (E) Magnified square in (B) showing that the epithelium between the papillae displays a web-like pattern of MRs (asterisk) interspersed with mucous cell openings (arrowheads).

8.2 ORAL CAVITY AND PHARYNX

The buccal (oral) cavity of fish (Figure 8.4) plays an important role in the seizure and selection of food and rejection of undesirable items ingested by fish. TBs in fish are distributed on the tongue, the surface of the ph, lips, and the barbels around the mouth. The lining of the roof of the buccal cavity (BC) is made up of mucosa, submucosa, and muscularis. The mucosa comprises many layers of stratified polygonal epithelial cells. TBs and a large number of mucous cells are present in between the epithelial cells.

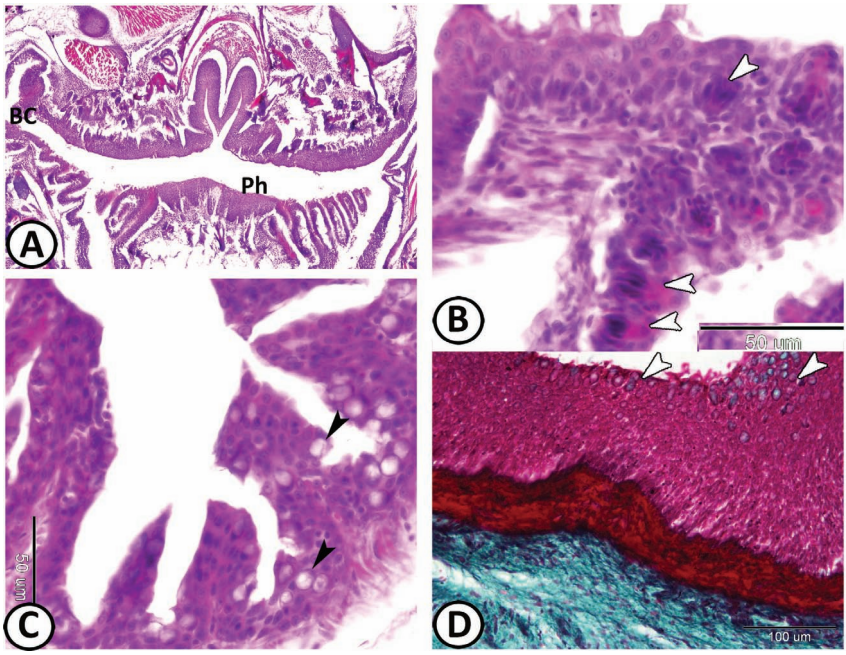

FIGURE 8.4 (A) The buccal cavity (BC) extends to the pharynx (Ph) of molly fish (HE). (B, C) The epithelium of the BC of guppy stained by HE showing TBs (white arrowheads) and GCs (black arrowheads). (D) The wall of the BC of grass carp stained by Crossmon's trichrome showing the epithelium with many mucous cells (arrowheads) and a thick collagenous connective tissues below.

The pharynx (Figures 8.5 and 8.6) is divided into anterior and posterior parts. The anterior portion is characterized by the presence of stratified epithelium with TBs and mucous cells, as well as the presence of pharyngeal teeth and jawbones. In a few species, the pharynx epithelium is lined by a horny layer. Numerous lymphocytes are distributed in the basal region of the epithelium. Club cells (CCs) are found in the epithelium of pharynx in some species as *grass carp* (Figure 8.6A and B). The posterior part of the pharynx is lined by simple epithelium and has an abundance of alcian blue-positive mucous-secreting cells. These cells keeping moist of these areas that are subjected to mechanical abrasions. The pharynx is supported by a thick fibromuscular layer that consists of bundles of skeletal muscles and collagen fibers. These structures may help to swallow the food by squeezing it to extract a maximum of water.

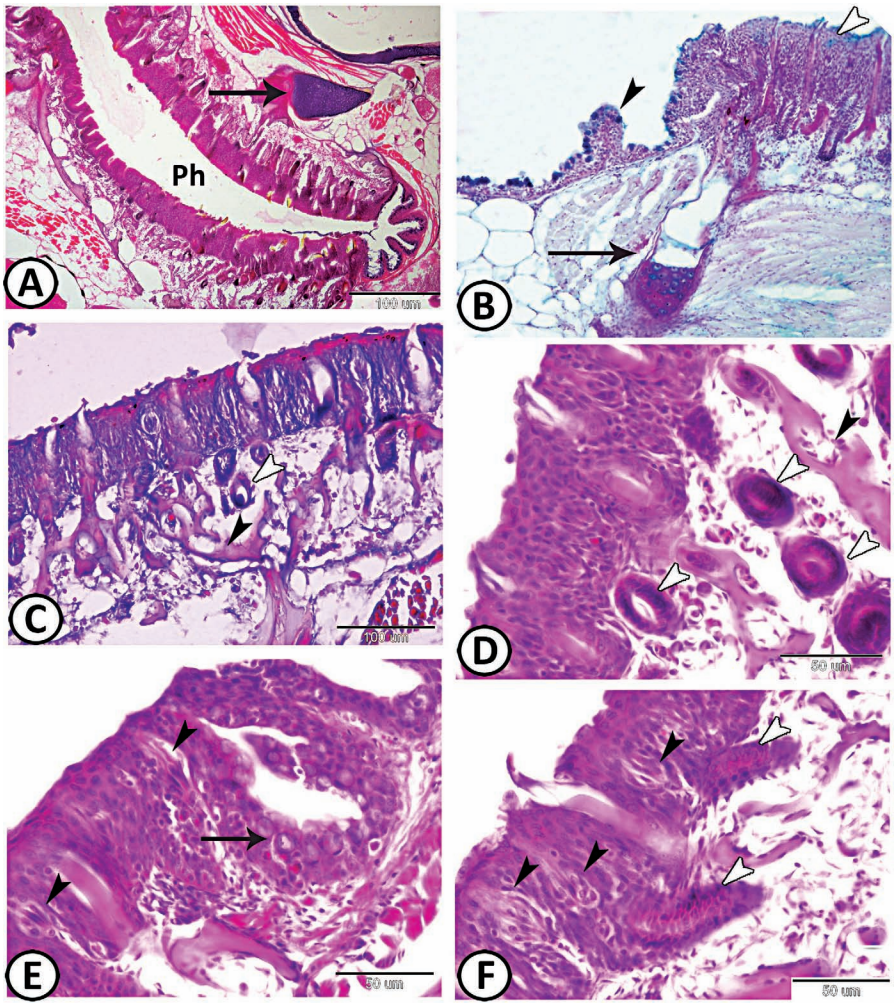

FIGURE 8.5 (A, B) General view of the pharynx (Ph) of guppy. The anterior portion (white arrowhead) is lined by stratified epithelium, while the caudal portion is lined by simple columnar epithelium with GCs (black arrowhead). Note the neighboring cartilage of the operculum (arrow) (HE and PAS-AB/HX, respectively). (C, D) The wall of the anterior portion of the pharynx of guppy contains teeth (white arrowheads) and jawbones (black arrowheads) (Masson's trichrome and HE, respectively). (E, F) The epithelium of the pharynx of the anterior portion of guppy is penetrated by teeth (white arrowheads), mucous cells (arrow), and TBs (black arrowheads) (HE).

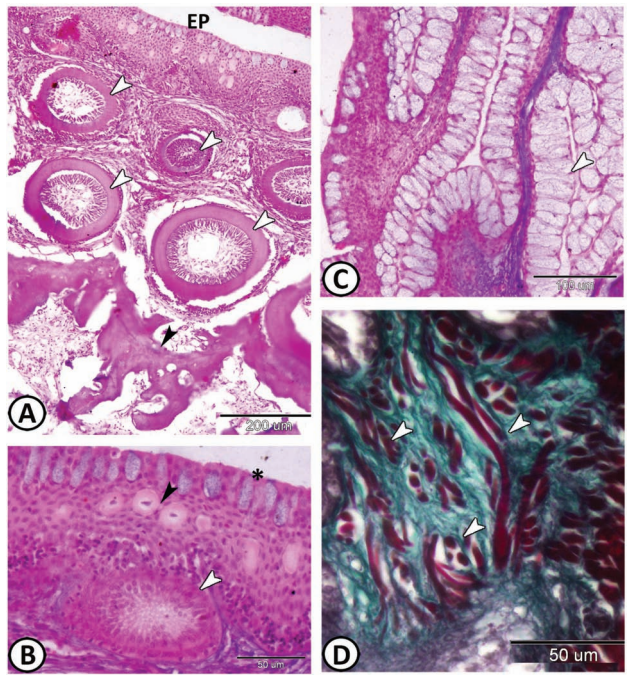

FIGURE 8.6 (A) The anterior portion of pharynx of grass carp consists of stratified epithelium (EP), loose connective tissue contained teeth (white arrowheads) and jawbones (black arrowhead) (HE). (B) Higher magnification showing the epithelium consists of the stratified epithelium with GCs (asterisk) and CCs (black arrowhead). Note the teeth contained pulp cavity (white arrowhead) (HE). (C) The epithelium of the caudal region of grass carp contains abundant mucous cells (arrowhead) (HE). (D) The fibromuscular layer of the pharynx of molly contains collagen fibers (green) and skeletal muscle fibers (arrowheads) (Crossmon's trichrome).

In fish, the pharyngeal jaw apparatus, a food processing structure, is located at the anterior region of the pharynx. It constitutes a highly complex functional system and consists of an upper pharyngeal jaw (UPJ) and a lower pharyngeal jaw (LPJ). The UPJ is attached to the neurocranium on the roof of the pharynx. The LPJ is located opposite the UPJ, on the floor of the pharynx. Both the UPJ and LPJ work against each other to manipulate, winnow, macerate, transport, and crush food items ingested by the fish. The UPJ is represented by a pad-like structure, named variously by different authors: dorsal cornified or horny pad, callous pad, and chewing pad. The chewing pad is roughly heart-shaped and its epithelium covering is mainly composed of the epithelial cells. The mucous goblet cells (GCs), the eosinophilic granular cells, the lymphocytes, and the TBs are absent

Four pairs of teeth (pharyngeal teeth) on their inferior pharyngeal bones are found in *grass carp*. Food is triturated between these teeth and the horny epithelium. Teeth (Figure 8.7) are generally homodont (all teeth with similar morphology) but many cases of heterodonty (dentition with different kinds of teeth) occur as in *Characidae*, *Sparidae*, *Blenniidae*, etc. Most species have teeth that may be divided into three types, according to their position in the oral cavity. The jaw teeth are borne on the premaxilla and the maxilla bones above and the dentary below. Oral teeth are borne by the vomer, palatine, and ectopterygoid bones and sometimes by the tongue. The pharyngeal teeth represent the third type and develop from various sources; they are common in herbivores and molluscivores.

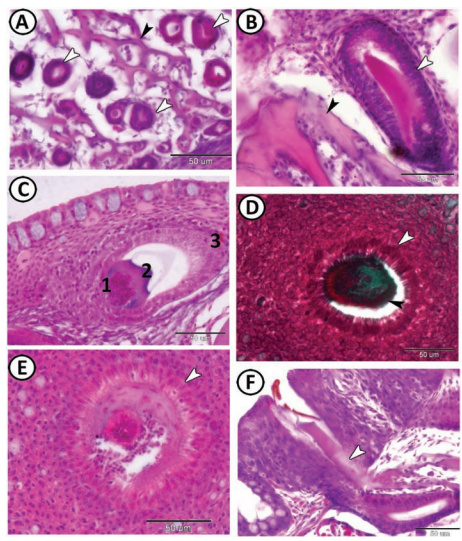

FIGURE 8.7 (A, B) Immature teeth (white arrowheads) are supported by jawbones (black arrowheads) in the guppy (HE). (C) The mature tooth in grass carp can be recognized by the pulp core (1), the dentine (2), and the enamel cap (3) (HE). (D) Mature teeth of grass carp showing pulp core (red), dentine (black arrowhead), and inner epithelium (white arrowhead) (Crossmon's trichrome). (E) Higher magnification of the mature teeth (arrowhead) of grass carp (HE). (F) Mature teeth (arrowhead) of the guppy (HE).

The general form of the teeth varies according to the fish feeding habits. They may be pointed, spherical, curved, dagger-shaped, canine, or molariform in shape. A typical tooth has a broad base and a pointed apex, which is characteristic of this carnivorous cichlid. A few species of fishes are naturally toothless, for example, the sturgeons, seahorses, and pipefishes. The tooth consists of a pulp core, a dentine layer-secreted by odontoblasts, and the inner epithelium with ameloblasts secreting the enamel cap. The structure of

the enamel is very complex. Ground sections of the teeth exhibit fiber-like striations extending from the dentinal tubules, which are arranged radially from the superficial layer to the intermediate layer. The teeth are more or less movable as it is testified by the presence of basal ligaments.

8.3 THE TONGUE

The tongue of fish consists of tunica mucosa, tunica submucosa, and osteocartilaginous skeleton (Figures 8.8 and 8.9). The tunica mucosa is lined with stratified epithelium interrupted by numerous GCs that are intensively positive reacted to PAS and AB techniques. Scattered pear-shaped TBs are seen on the mucosal surface. The thick lamina propria (LP) is composed of loose and dense connective tissue, which continues laterally and ventrally extending up to the ventral jaw muscles. In most fishes, the tongue is poorly developed and reveals the absence of specific muscles. Cartilage is sometimes found particularly in Chondrichthyes.

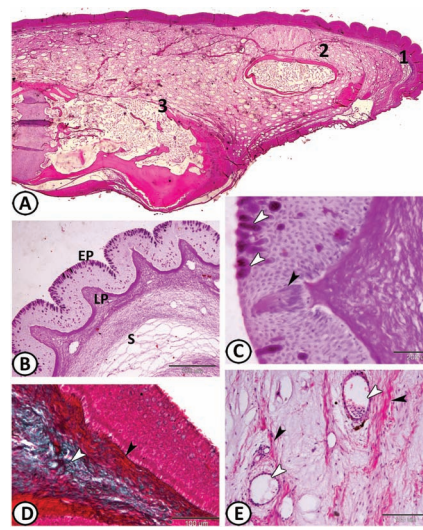

FIGURE 8.8 The tongue of grass carp. (A) General view of tongue stained by HE. The wall consists of mucosa (1), submucosa (2), and osteocartilaginous skeleton (3). (B) Longitudinal section of the tongue stained by PAS/HX showing the epithelium (EP) that form dermal papillae in the LP, followed by submucosa (S). (C) Higher magnification of the epithelium showing numerous PAS-positive mucous cells (white arrowheads) and TB (black arrowhead). (D) By Crossmon's trichrome, the LP is dense (black arrowhead) and the submucosa is loose connective tissue (white arrowhead). (E) The submucosa contains BV (white arrowheads) and collagen fibers (black arrowheads) (HE).

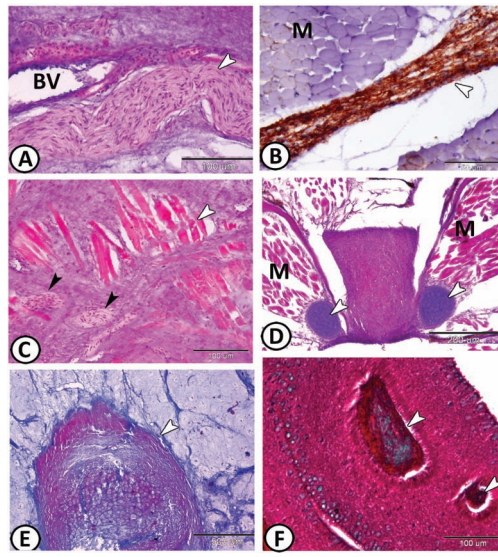

FIGURE 8.9 (A) Bundles of nerve fibers (arrowhead) are distributed in the submucosa of the tongue of grass carp. Note the presence of BV (HE). (B) These nerve fibers (arrowhead) are immunoreactive to GFAP and distributed around the muscles (M) of molly fish. (C) Bundles of skeletal muscles (white arrowhead) and nerve fibers (black arrowheads) are found in the tongue of grass carp (HE). (D, E) The tongue of guppy contains hyaline cartilages (arrowheads) that are surrounded by muscle bundles (M) (HE and Masson's trichrome, respectively). (F) Mature teeth (arrowheads) could be seen among the surface epithelial cells of the tongue of grass carp (Crossmon's trichrome).

The submucosa layer of the tongue contains loose connective tissue. This layer is also remarkable with blood vessels (BV), nerve fibers, and pigment cells. Additionally, several teeth in an elongated shape are found but only centrally at the anterior tip of the tongue and among the dermal papilla of the tongue. The teeth of grass carp could be classified into two stages based on the histological characterizations: immature and mature teeth. Mature teeth are formed from dentine-like material and consist of a dentine layer, which is surrounded by (1) enamel cap (enamel coating), (2) dentine pulp, and (3) pulp core among the spongy bones. Each tooth is clearly separated by oral stratified epithelium, which contained numerous mucous cells. These cells are positively stained with AB reactions. Immature teeth consist of three parts: (1) scleroblast, which is seen in the basal layer, (2) odontoblast, which secreted to its predentine, and (3) enamel organ, which contains an outer enamel epithelium and enameloid. Overall the tongue structure is also

supported by hyaline cartilage, which is oriented from the posterior to the near the tip of the tongue.

Chondrichthyes lack a truly flexible and muscular tongue and for processing the prey, they use a diversity of jaw muscles. They possess only a mucosal thickening at the anterior part of the floor of the buccopharyngeal cavity. The mucosa is thick and resembles that of the pharynx. Mucous cells are particularly abundant and nearly as numerous as the ordinary epithelial cells. The stratum compactum of the supporting connective tissue is well-developed and contains various BV. This tongue-like structure is also supported by a centrally located piece of hyaline cartilage.

8.4 THE MORPHOLOGICAL STRUCTURE OF THE GASTROINTESTINAL TRACT

The esophagus runs from the posterior end of the pharynx anteriorly to the anterior part of the cardiac region of the stomach caudally; being ventrally overlapped by the liver, its anterior region is wide and funnel-shaped, and its posterior region is tubular in shape. Its mean length in catfish is 0.78 ± 0.20 cm. The oesophagus of catfish is divided into two parts: according to diameter and shape. The mean diameter of the anterior part is 0.65 ± 0.11 cm and that of the posterior part is 0.48 ± 0.09 cm. The esophagus of grass carp runs from the posterior end of the pharynx anteriorly to the intestinal bulb caudally, being ventrally overlapped by the liver and its shape is cylindrical, and straight along its entire length. The esophagus of grass carp is not divided, as its diameter is the same along its entire length, its mean diameter is 0.51 ± 0.10 cm (Table 8.1).

TABLE 8.1 Statistical Analysis of Various Measurements of Nile Catfish and Grass Carp

Measurements	Nile Catfish	Grass Carp
Body weight (g)	406.4 ± 9.60	421.60 ± 8.70N.S.
Total length of fish (cm)	38.6 ± 5.60	40.60 ± 6.21N.S.
Standard length of fish (cm)	35.4 ± 3.01	37.20 ± 4.0N.S.
Total length of gastrointestinal tract (cm)	38.2 ± 3.90	71.50 ± 4.80**
Length of esophagus (cm)	0.78 ± 0.20	1.16 ± 0.23N.S.
Diameter of esophagus (cm)	0.65 ± 0.11 (anterior part) 0.48 ± 0.09 (posterior part)	0.51 ± 0.10

TABLE 8.1 *(Continued)*

Measurements	Nile Catfish	Grass Carp
Length of stomach (cm)	3.2 ± 0.61	–
Length of intestinal bulb (cm)	–	1.82 ± 0.57
Diameter of intestinal bulb (cm)	–	1.15 ± 0.41
Length of intestine (cm)	33.4 ± 2.90	68.44 ± 3.40**
Diameter of intestine (cm)	0.42 ± 0.10 (anterior part)	0.77 ± 0.13 (anterior part)*
	0.30 ± 0.07 (posterior part)	0.56 ± 0.09(posterior part)*
	0.33 ± 0.11(rectum)	0.63 ± 0.10 (rectum)*
RGL(%)	1.07	1.92

The values are represented by mean ± standard error. Differences reconsidered as: (N.S.): not significant if $P > 0.05$; *Significant if $P < 0.05$; **Highly significant if $P < 0.01$.

It appeared from the previous table that the wide species variations in the length of the tract resulted chiefly from variations in length of intestine, so there is a positive correlation between the length of intestine and RGL.

The stomach appears as a curved muscular sac, located in the dorso-cranial region of the peritoneal cavity behind the liver. It extends from the esophagus to the intestine. The mean length is 3.2 ± 0.61 cm. The stomach of catfish is J-shaped with the ascending limb ended at the end of the pyloric region. It attains its greatest diameter about the middle of its length, posterior to which it becomes more slender especially near the pyloric end. The stomach is Y-shaped in *Oreochromis niloticus*, true cods and ocean perch and U-shaped in Salmo, and *Loricariidae*. Any of these configurations must be convenient for containing the ingested food. The stomach of fish is absent in early developmental stages, but the lack of the stomach is not restricted to the larval fish. Juveniles and adults of a variety of fishes are stomachless, such as cyprinids (carp, goldfish), beloniforms (needlefish), and scarids.

The stomach of catfish is divided into three regions: cardiac, fundic, and pyloric regions. The cardiac region is an initial region that is close to the entry point of the esophagus. The cardiac region appears shorter than fundic but longer than pyloric region. The fundic region is the large sac-shaped blind middle region, which communicates with the other two regions of the stomach. The pyloric region is the terminal small region. The end of the pyloric region extends toward the beginning of the intestinal tube.

In grass carp, the stomach is absent and replaced by dilatation in the anterior part of intestine called the intestinal bulb. The intestinal bulb is located below the liver, as the liver lobes covered the intestinal bulb and the gall bladder is found in juxtaposition to the anterior portion of the bulb. The coils of the intestine surround the bulb. The intestinal bulb extends from the esophagus anteriorly to the anterior intestine caudally. The mean length is 1.82 ± 0.57 cm. The diameter of the intestinal bulb depends upon the feeding conditions, but at its widest point, it is wider two to three times than the remainder of the intestine. After feeding, a 10 folds increase in the diameter is possible. The mean diameter of the bulb is 1.15 ± 0.41 cm. The intestinal bulb is a straight tube that is larger at its anterior end and narrowed gradually until it merged into the anterior intestine.

The intestine of catfish is a convoluted tube, run from the end of the pyloric region of the stomach posteriorly toward the anal opening, along the ventral side of the peritoneal cavity. The intestine of catfish shows few convolutions and is divided into: (1) the pyloric (anterior) intestine: the initial wide part that narrowed to form, (2) the middle (posterior) intestine: this is the most coiled part of the intestine. The middle intestine accounted for 80% of the total length of the intestine and then thickens to form, and (3) the rectal intestine, which is the terminal straight part. The rectal intestine is very short. It ends at the anus that is situated in front of the anal fin. There is no true large intestine and little morphologic differentiation into regions is present. The intestine of catfish is short; its mean length is 33.4 ± 2.90 cm. The mean diameter of the anterior intestine is 0.42 ± 0.10 cm, the posterior intestine is 0.30 ± 0.07 cm, and the rectum is 0.33 ± 0.11 cm.

The intestine of grass carp is entirely separated from the air bladder and occupied the ventral position of the body cavity. The intestine of grass carp is a simple coiled tube that shows many convolutions and is divided into the anterior, middle, and rectal intestine as in Nile catfish. The rectum is distinguished from the rest of the intestine by its straight course to the anus and its darkness with fecal matters. The intestine of grass carp is long and shows a highly significant increase compared with that of catfish, the mean length is 68.44 ± 3.40 cm. Also, the diameter of the intestine of this species is increased significantly compared with that in catfish. The mean diameter of the anterior intestine is 0.77 ± 0.13 cm, the posterior intestine is 0.56 ± 0.09 cm, and the rectum is 0.63 ± 0.10 cm.

8.5 ESOPHAGUS

The esophagus of many teleosts as Nile catfish is divided into two parts: anterior and posterior parts based on the type and thickness of the epithelium and tunica muscularis.

8.5.1 THE ANTERIOR PART OF ESOPHAGUS OF NILE CATFISH

The mean diameter of the anterior part of esophagus is 5186.67 ± 42.87 µm and the mean thickness of its wall is 2461.15 ± 48.11 µm. The wall of the esophagus is formed of four distinct layers: tunica mucosa, tunica submucosa, tunica muscularis, and tunica adventitia. The mean thickness of the tunica mucosa is 1397.33 ± 59.49 µm. The mucosa consists of approximately 36 parallel complex and elongated leaf-like folds that are referred to as primary, secondary, and tertiary folds. These folds arrange longitudinally that occlude the lumen, which has a very complex folded appearance in the histological cross sections. This folded appearance may allow maximal distension for prey and breaking down food. Some wider channels of the lumen are present; their mean diameter is 264.37 ± 18.43 µm. The mean height of mucosal folds (MFs) is 1190.80 ± 32.58 µm and their mean width is 172.48 ± 5.88 µm (Table 8.2 and Figure 8.10).

TABLE 8.2 Statistical Analysis of Various Measurements of Nile Catfish and Grass Carp

Measurements	Nile Catfish		Grass Carp
	Anterior Part of Esophagus	Posterior Part of Esophagus	Esophagus
Diameter of the organ (µm)	5186.67 ± 42.87	4342.81 ± 34.45	4693.39 ± 40.32
Thickness of the wall (µm)	2641.15 ± 48.11	1504.61 ± 12.77	1998.27 ± 43.37
Diameter of the lumen (µm)	264.37 ± 18.43	1333.59 ± 82.76	696.85 ± 56.19
Thickness of the mucosa (µm)	1397.33 ± 59.49	299.68 ± 10.23	916.0 ± 14.70
Number of MFs/cross section	36.20 ± 5.0	26.41 ± 7.10	20.0 ± 3.90
Height of MFs (µm)	1190.80 ± 32.58	263.36 ± 7.03	655.56 ± 14.38
Width of MFs (µm)	172.48 ± 5.88	104.55 ± 1.8	163.40 ± 9.46
Height of the epithelium (µm)	112.49 ± 2.74	28.60 ± 1.37	65.33 ± 2.18
Thickness of submucosa (µm)	460.72 ± 16.2	216.69 ± 7.50	310.7 ± 16.08
Thickness of muscularis (µm)	800.10 ± 32.77	1070.54 ± 6.32	861.07 ± 72.78

The values are represented by mean ± standard error. Differences were considered as not significant if $P > 0.05$; (N.S.), significant if $P < 0.05$, and highly significant if $P < 0.01$.

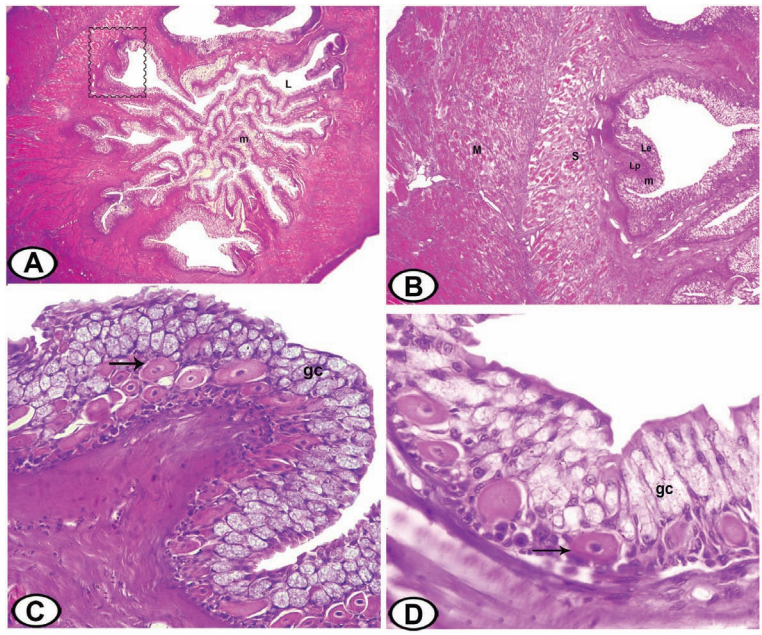

FIGURE 8.10 Histology of the anterior part of the esophagus of Nile catfish stained by HE. (A) The general view of the anterior part showing the highly folded mucosa (m) and wide channels of the lumen (L) present between the folds. The square indicated one MF (×25). (B) The wall of the anterior part consists of mucosa (m), submucosa (S), and muscularis (M). Notice the MF consisted of lamina epithelialis (Le) and LP (×40). (C) Higher magnification of one MF showing the mucosal epithelium consisting of stratified epithelium, contained goblet cells (GCs) and CCs (arrow) (×250). (D) The stratified cuboidal epithelium of the anterior part of the esophagus contains GCs and CCs (arrow) (×400).

The mean height of the epithelium is 112.49 ± 2.74 μm. The epithelium is stratified cuboidal in type; the deeper layer is columnar, the middle layer contains a large number of the goblet and CCs, while the superficial cells are cuboidal. This stratified epithelium has ill-distinct cell boundaries, homogeneous acidophilic cytoplasm with rounded darkly stained nuclei. Occasional leucocytes are found between the epithelial layers, especially in the basal part (Figure 8.10). The epithelium of the anterior part of the esophagus of carnivorous fish acts as a constitutive adaptation that protects the esophagus against live prey damages.

The epithelium of the esophagus of Nile catfish also contains a high density of club (alarm) cells. The CCs are large polyhedral cells with homogeneous acidophilic cytoplasm with one to two central rounded nuclei. These cells are located at different levels of the epithelial strata, but especially in the basal region of the epithelium (Figure 8.10). They are periodic-acid Schiff (PAS)- and alcian blue-negative (Figure 8.11). By transmission electron microscopy, the CCs appear as large, polyhedral electron-lucent, and binucleated cells. Their nuclei are polymorphic and euchromatic and contain distinct nucleoli. Their cytoplasm contains many large elongated mitochondria and rough endoplasmic reticulum (rER), which are arranged mainly around the nucleus. In addition, free ribosomes and many vesicles of different sizes are scattered all over the cytoplasm, which contains moderate electron-dense secretory materials (Figure 8.12).

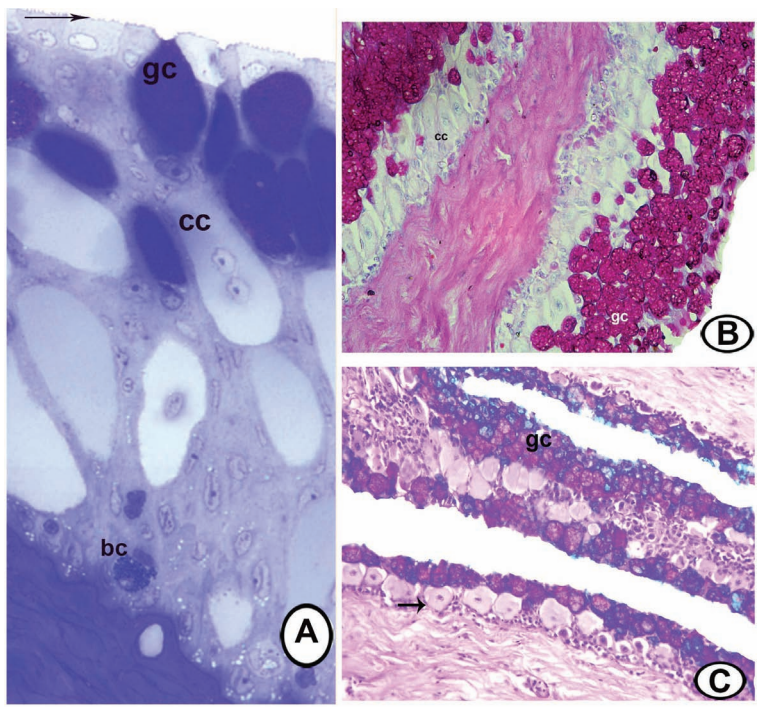

FIGURE 8.11 Histochemical analysis of the anterior part of the esophagus of Nile catfish. (A) Semithin section through the stratified mucosal epithelium of the anterior part of the esophagus showing the apical microridges (MRs) (arrow) and contains CCs, GCs, and BCs (toluidine blue, ×1000). (B) PAS-positive GCs. Notice the negative reaction of CCs (PAS/HX, ×400). (C) Alcian blue- and PAS-positive GCs. Notice the negative reaction of CCs (arrow) (combined AB and PAS, ×200).

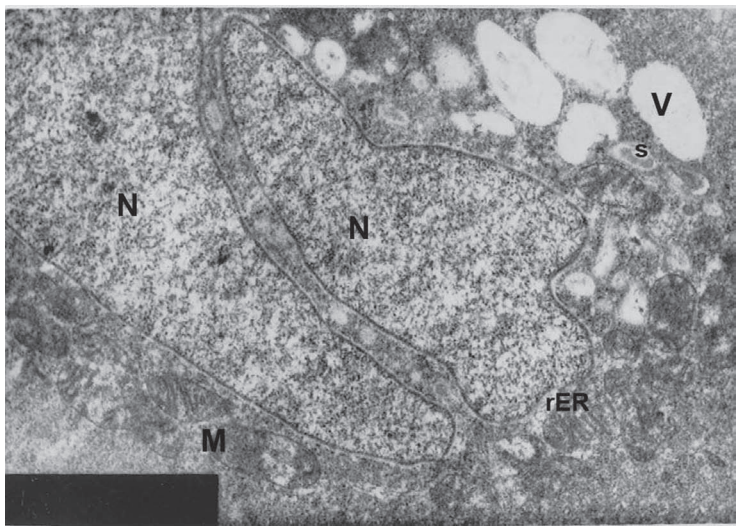

FIGURE 8.12 Transmission electron micrograph of the CCs of the anterior part of esophagus of Nile catfish showing two nuclei (N), many vesicles (V) contain moderate dense secretory materials (s) and mitochondria (M) (×10,000).

Several names have been given to CCs, such as "clavate," "giant," and "alarm substance cells." The CCs are demonstrated in the skin and lips of many fish species that might be responsible for the induction of the fright reaction to other fish. These cells exude a proteinaceous secretion. When these secretions mixed in water are sensed by introducers through the olfaction. Therefore, the main function of these cells is to induce defensive behavior in fish. The defensive behavior of these cells is evident through the production of toxic or antipathogenic agents, substances that deter predators. In addition, the CCs are shown to have phagocytic action by the ingestion of wandering cells (WCs). However, CCs must be damaged or broken before the alarm substances are released. Moreover, the structure of these cells in skin and lip differed from that in the esophagus; in lip and skin, they have cytoplasmic processes, and their cytoplasm contains fine coiled filaments. On the other hand, these cells are absent in the oesophagus of other fish species.

Numerous rounded to oval GCs of different sizes are present in the superficial half of the epithelium. These cells appear large with foamy cytoplasm and are consisted of rounded mucous globules that are intensively stained with alcian blue and PAS. Semithin sections show that the mucosal epithelial cells are stratified in type and their superficial cells bear MRs, in addition to

the presence of metachromatic GCs. The CCs appear as giant polyhedral cells with pale staining cytoplasm. They are mononucleated or binucleated cells, where the two nuclei are situated very close to each other. Undifferentiated or basal cells (BCs) are located at the base of the epithelium (Figure 8.11). These cells undergo cytoplasmic changes and eventually become epithelial cells or GCs and also the CCs arise from it. The LP is composed of dense connective tissue, mainly compactly arranged collagenous fibers, which are extended to fill the core of the MFs (Figure 8.13).

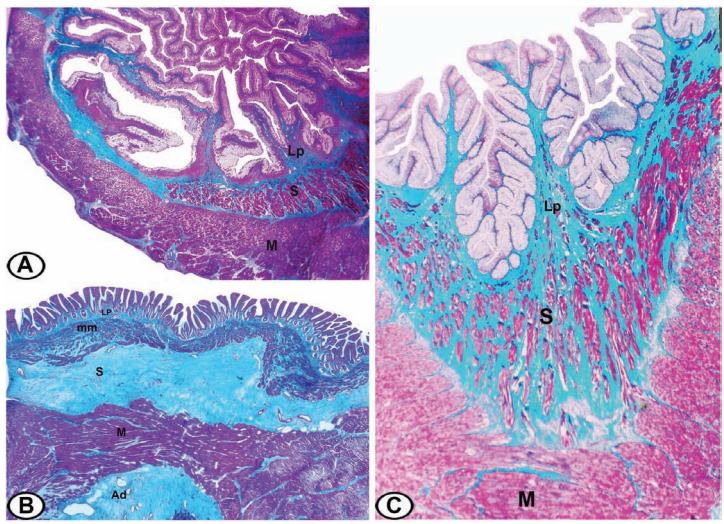

FIGURE 8.13 General structure of the esophagus of Nile catfish and grass carp stained by Crossmon's trichrome. (A) The anterior part of esophagus of catfish showing the connective tissue of the LP and submucosa (S) stained green and the muscles (M) stained red (×5). (B) The posterior part of the esophagus of catfish showing LP, submucosa (S), and adventitia (ad) stained green, and the muscularis mucosa (mm) and tunica muscularis (M) are stained red (×25). (C) The wall of the esophagus of grass carp showing LP, submucosa (S) stained green, while tunica muscularis (M) and the muscles in submucosa stained red (×25).

Scanning electron microscopic observations of the mucosa of the anterior part of the esophagus reveal numerous primary, secondary, and tertiary longitudinal folds. The surface layer of the epithelium is polyhedral in shape and exhibits prominent microvilli and fingerprint-like MRs (Figure 8.14). The presence of these prominent microvilli indicates an adaptation to rapid ion absorption. The fingerprint-like MRs may represent a mechanical adaptation that would withstand the trauma resulting from ingesting bulky materials.

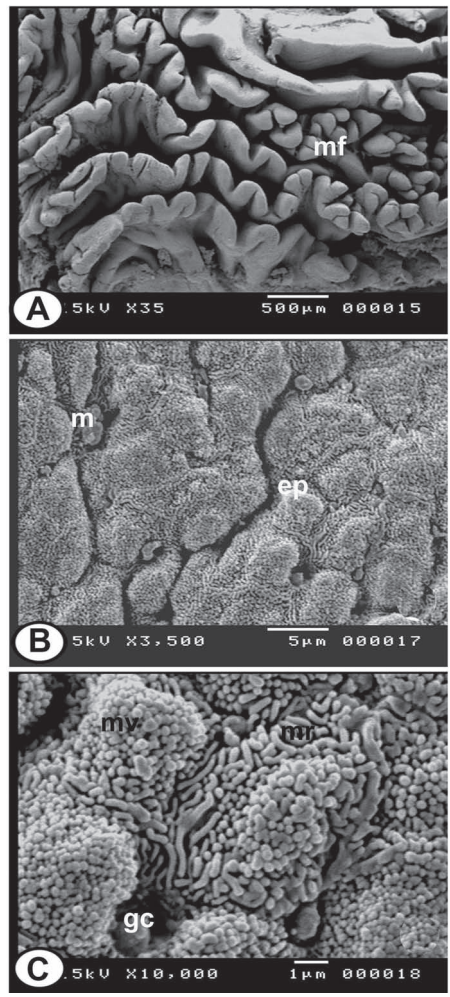

FIGURE 8.14 Scanning electron micrograph of the anterior part of the esophagus of Nile catfish. (A) The mucosa is thrown into a large number of MFs (×35). (B) The surface epithelium displays polyhedral-shaped superficial epithelial cells (ep). Notice the presence of mucous cells (m) between the epithelium (×3500). (C) The epithelium of the anterior part showing microvilli (mv) and microridges (mr). Notice the presence of GCs (×10,000).

The mean thickness of the tunica submucosa of the anterior part of the esophagus of catfish is 460.72 ± 16.72 µm. It is formed mainly of collagenous fibers. Bundles of striated longitudinal muscles are also observed in this layer. The tunica muscularis is composed of a thick outer circular layer and a thin inner longitudinal layer of striated muscles. Its mean thickness is

800.10 ± 32.77 µm. The anterior part of the esophagus of catfish is covered externally by tunica adventitia. It is formed of loose connective tissue, which contains small BV and elastic fibers (Table 8.2 and Figure 8.13).

8.5.2 THE POSTERIOR PART OF ESOPHAGUS OF NILE CATFISH

The mean diameter of the posterior part of the esophagus of catfish is 4342.81 ± 34.45 µm and the mean thickness of its wall is 1504.61 ± 12.77 µm. As in the anterior part of the esophagus, the wall of the posterior part is formed of four distinct layers: tunica mucosa, tunica submucosa, tunica muscularis, and tunica adventitia. Tunica mucosa is a thin layer; its mean thickness is 299.68 ± 10.23 µm. The mucosa contains approximately 26 short narrow and blunt folds. The esophageal lumen becomes wider and less irregular than that of the anterior part; its mean diameter is 1333.59 ± 82.76 µm. The mean height of the MFs is 263.36 ± 7.03 µm. The MFs are narrower than the anterior part; its mean width is 104.55 ± 1.80 µm (Table 8.2 and Figure 8.15).

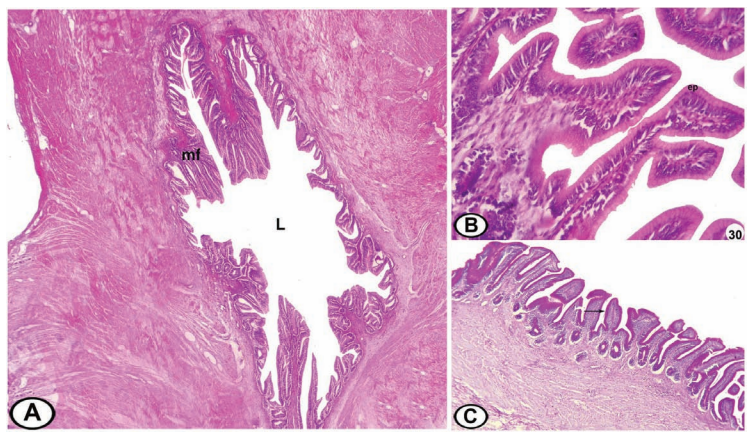

FIGURE 8.15 The posterior part of the esophagus of Nile catfish. (A) The mucosa is thrown into short MFs leaving a wide lumen (L) (HE, ×25). (B) Simple columnar epithelium (EP) (HE, ×400). (C) PAS-positive apical part of the epithelial cells (arrow) (PAS, ×100).

The mucosa is lined with mucous-secreting simple columnar epithelium. The mean thickness of the epithelium is 28.60 ± 1.37 µm. The apical part of the epithelium is reacted positively to PAS (Figure 8.15) that may play a role in pregastric digestion or even absorption. In addition, the posterior

esophageal region acts as a site of selective ionic diffusion, so osmoregulatory functions are proposed for this epithelium, which is associated with wide BV. The semithin sections show that the mucosal epithelium of the posterior part consists of tall columnar cells with a middle oval light nucleus that contains distinct nucleoli. The apical part of these cells contains mucous granules, which reacts positively to toluidine blue. Some basal dark cells of irregular shapes are present in the basal part of the epithelium. Many argyrophilic neuroendocrine cells are present in the esophageal epithelium of the posterior part (Figure 8.16). The LP consists of dense connective tissue, formed mainly of compactly arranged collagenous fibers, which is extended to fill the core of the MFs (Figure 8.13). The muscularis mucosa consists of bundles of smooth muscle fibers, surrounded by numerous collagenous fibers.

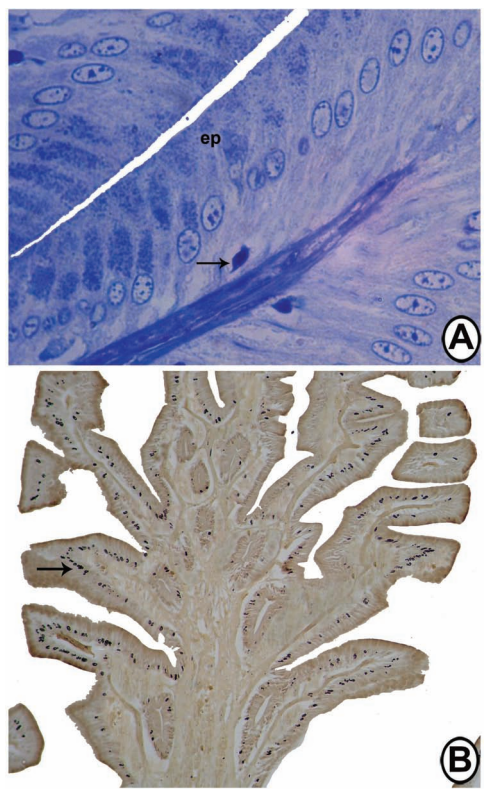

FIGURE 8.16 (A) Semithin section through the mucosa of the posterior part of esophagus of Nile catfish showing a positive-toluidine blue reaction of the apical epithelial cells (EP). Notice the presence of the BCs (arrow) (toluidine blue, ×1000). (B) Argyrophilic enteroendocrine cells (arrow) (Grimelius, ×200).

Scanning electron microscopic observations of the mucosa of the posterior part of the esophagus reveal simple longitudinal MFs. The surfaces of the polygonal epithelial cells exhibit short microvilli and small MRs. Numerous small holes for mucous extrusion in addition to some mucous droplets are present, as shown in Figure 8.17.

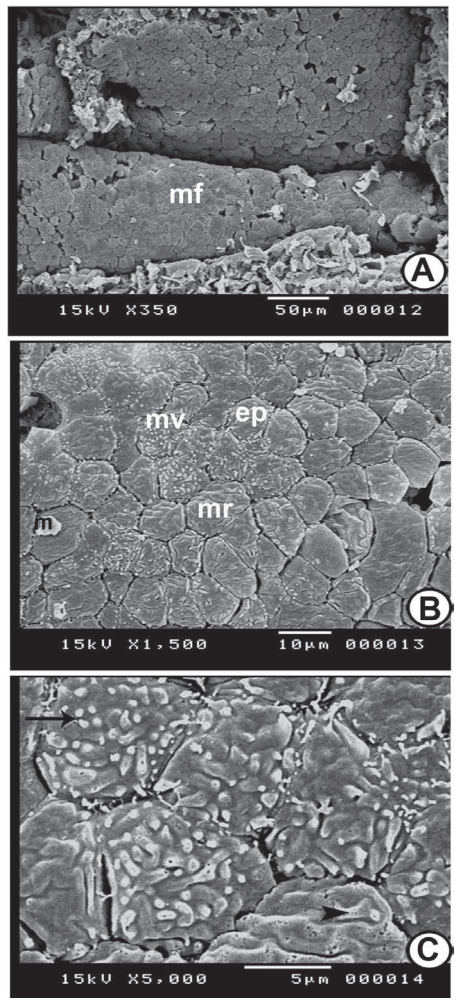

FIGURE 8.17 SEM of the posterior part of the esophagus of Nile catfish. (A) The mucosa is thrown into simple longitudinal MFs (×350). (B) The surface epithelium showing polyhedral-shaped superficial epithelial cells (ep) that covered with microvilli (mv) and microridges (mr). Note the presence of mucus (m) on the epithelial cells (×1500). (C) The epithelial cells of the posterior part of the esophagus of catfish showing microvilli (arrow) and MRs (arrowhead) (×5000).

The mean thickness of the tunica submucosa is 216.69 ± 7.50 µm. It is formed of dense connective tissue and contains numerous collagenous fibers. The striated muscles that are present in the submucosa of the anterior part of the esophagus diminish posteriorly and they are absent in the posterior portion of the esophagus. This tunic is free of glands.

The posterior part of the esophagus has thicker muscularis than that found in the anterior part. It is composed of inner circular and outer longitudinal smooth muscle fibers that are held by connective tissue fibers. Its mean thickness is 1070.54 ± 6.32 µm. The thickness of the tunica muscularis particularly in the posterior part of the esophagus of Nile catfish may represent a powerful tool to strengthen the esophageal wall, protect it from engorged bulky food, facilitate the regurgitation, and also act as a triturating device for the solid ingested materials. The tunica muscularis of posterior part of the esophagus of catfish extends to gastric muscularis and may play a role in increasing the motility, which optimizes stomach digestion in carnivorous fish with irregular intakes of large quantities of food. The tunica adventitia is formed of loose connective tissue that contains collagenous fibers and small BV (Table 8.2 and Figure 8.13).

8.5.3 ESOPHAGUS OF GRASS CARP

The esophagus of grass carp has the same structure and appearance along its entire length. Its mean diameter is 4693.39 ± 40.32 µm and the mean thickness of its wall is 1998.27 ± 43.37 µm. The mean thickness of the tunica mucosa is 916.0 ± 14.70 µm, which constitutes approximately 45.83% of the thickness of the wall. The mucosa is formed of distinct longitudinal folds (about 20). The lumen is star shaped and appeared wider than in the anterior esophageal part of catfish. The folds are generally narrow at the tip but are occasionally broadened in the basal part. The MFs of the esophagus of grass carp are shorter and less tortuous than in catfish. Its mean diameter is 696.85 ± 56.19 µm. The mean height of the folds is 655.56 ± 14.38 µm and its mean width is 163.40 ± 9.46 µm (Table 8.2 and Figure 8.18).

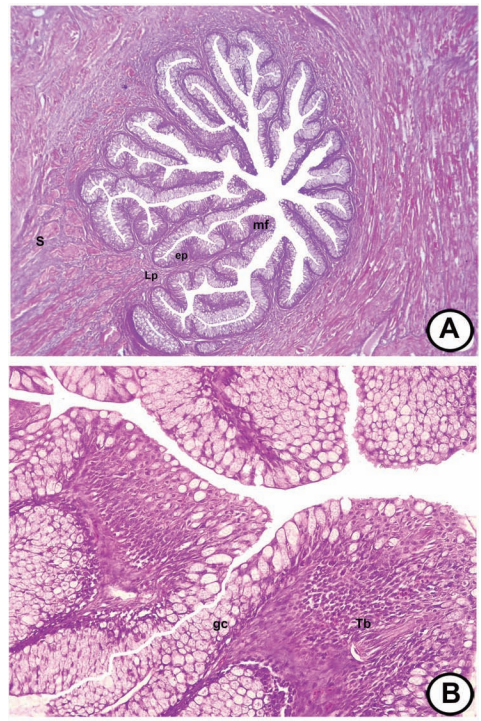

FIGURE 8.18 The esophagus of grass carp stained with HE. (A) The esophageal MFs formed of lamina epithelialis (EP), LP, followed by submucosa (S) (×25). (B) The stratified epithelium showing TBs and GCs (×200).

The mean height of the epithelium is 65.33 ± 2.18 μm. The lining epithelium of the esophagus of grass carp is of a stratified cuboidal type along its entire length, containing GCs, and TBs. Oval and prominent TBs are observed only in the most cranial portion of the esophagus. It occurs between the epithelial cells in the form of fusiform bundles of pale spindle cells with an oval nucleus, which are regarded as gustatory cells. The exposed extremity of the TB is sunk in a pit, which is probably similar to the gustatory pore seen in mammals (Figure 8.18), indicating that the fishes select the type of food intake by either food rejecting or swallowing. The TBs act as chemoreceptors for a specific selection of food before swallowing. However, TBs are present in the esophagus of some species as sea bream, eel, and *O. niloticus*. It is worth to mention that the epithelial lining of the esophagus of grass carp performs various functions, such as gustatory and mucus production to facilitate rapid and efficient swallowing action.

High populations of rounded GCs are found in patches, which are the most prominent and distinctive feature of the esophageal epithelium of grass carp. GCs are more numerous in the epithelium of the esophagus of grass carp than those of catfish and are reacted positively to PAS and alcian blue (Figure 8.19). The GCs secrete both acid and neutral mucopolysaccharides, which play a role in the lubrication of food and protection of mucosa during swallowing. The GCs are arranged in a continuous sheath in the esophagus of grass carp, and this may provide rapid lubrication to the rough age-rich materials in the gut and to capture the excess of water from the food particles during the swallowing.

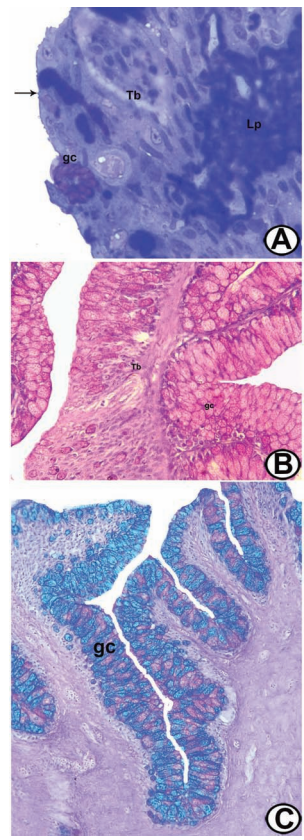

FIGURE 8.19 Histochemistry of the esophagus of grass carp. (A) Semithin section through the stratified epithelium of the esophagus showing MRs (arrow), metachromatic reaction of GCs, and TB. Notice the presence of connective tissue LP (Toluidine blue, ×1000). (B) The epithelium showing TBs and PAS-positive GCs (PAS, ×400). (C) The epithelium of esophagus of grass carp showing alcian blue (numerous cells) and PAS-positive (fewer cells) GCs (combined AB and PAS, ×200).

The increased number of GCs in the esophagus of all fish species, in general, is probably due to the absence of salivary glands, as the mucin excreted in the esophagus and buccal cavity compensates the absence of salivary glands in fish. In addition, the esophageal mucin has a role in the enzymatic digestion of food via its contents of neutral mucosubstances, and it might have an osmotic function through binding and transportation of water, and ions content.

Semithin sections show MRs in the apical part of the superficial epithelial cells of the esophagus of grass carp. Undifferentiated basal cells are located at the base of the epithelium. GCs are not found typically at the surface but usually are lain deeply and characterized by a metachromatic reaction to toluidine blue. TBs appear as a fusiform structure of pale cells with prominent taste pore (Figure 8.19).

Scanning electron microscope observation of the esophageal mucosa reveals numerous folds that leave distinct long concavities in between them. The mucosa exhibits compactly arranged pentagonal or hexagonal surfaces of the superficial cells of the stratified epithelial cells. The luminal plasma membrane of these cells presents complex or linearly arranged MRs in the form of an alveolar pattern. Discrete oval or circular openings of mucous cells are located between the stratified epithelial cells, which are slightly sunken with respect to the surrounding MRs. The network of the alveolar MRs reveals that each cell is clearly limited by boundary MRs, so that the cellular contacts are marked by two parallel MRs (Figure 8.20). Furthermore, the alveolar pattern of MRs can perform other functions, such as retaining and spreading mucus that creates an optimally lubricated surface for the passage of food, in addition to increase the surface area of the epithelium lining the esophagus and allow the surface to stretch. MRs are also observed in the epithelium of the skin, gills, buccal cavity, and pharynx of some fish species.

LP of the esophagus of grass carp is formed of finger-like processes of loose connective tissue. It contains mostly collagenous fibers, numerous flattened fibroblasts, and thick longitudinal smooth muscle fibers. The presence of numerous elastic fibers in the LP and submucosa increases the elasticity for swallowing large items of foods. In addition, the extensive core of LP in the MFs of the esophagus of catfish is probably to maintain the integrity of the wall and prevent rupture of the mucosal lining as it is to be stretched around the prey during the act of swallowing.

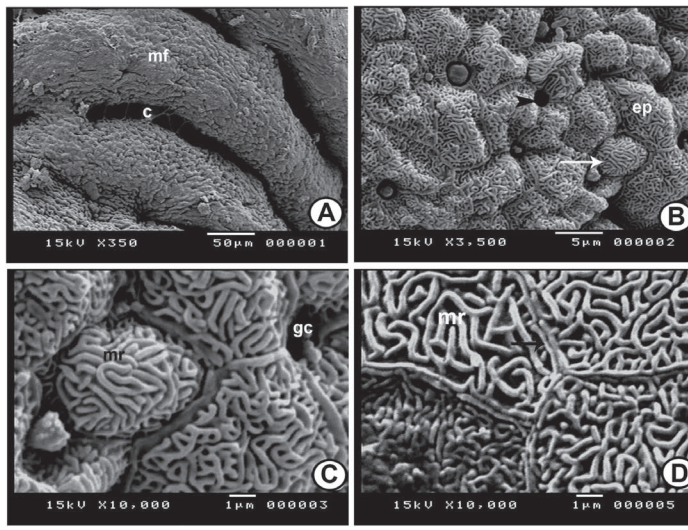

FIGURE 8.20 SEM of the esophagus of grass carp. (A) The esophageal MFs and long concavities (c) between them (×350). (B) Scanning electron micrograph showing the pentagonal shape of superficial epithelial cells (EP) that is covered with MRs (arrow). Notice the presence of mucous pore (arrowhead) between the epithelial cells (×3500). (C) Scanning electron micrograph of the epithelial cells of the esophagus showing the alveolar pattern of MRs. Notice the presence of pore for GCs (×10,000). (D) The surface epithelial cells are covered with MRs. Notice the boundaries between them are formed of two parallel MRs (arrow) (×10,000).

The muscularis mucosa is thick and formed of isolated bundles of smooth muscle fibers located under the LP. The tunica submucosa is formed of dense irregular connective tissue that contains collagenous fibers and numerous striated longitudinal muscle bundles that are sparsely distributed. Its mean thickness is 310.70 ± 16.08 µm. The mean thickness of the tunica muscularis is 861.07 ± 72.78 µm (Table 8.2). It is formed of inner circular and outer longitudinal layers of skeletal muscle fibers (Figure 8.13). These striated muscles might be important for catfish to reject any unpalatable food and provide reinforcement to the esophagus, which is subjected to violent extensions by the ingestion of food. However, these muscles in the submucosa of grass carp may be related to the coordination of the contraction of the esophagus with movements of the pharyngeal teeth to allow expansion of the esophagus for the ingestion of foods. The esophagus of grass carp is covered externally by tunica adventitia, which is formed of loose connective tissue, containing elastic fibers and BV.

8.6 STOMACH

The stomach of catfish is shown to be divided into three regions according to structure: cardiac, fundic, and pyloric regions.

8.6.1 THE CARDIAC REGION OF THE STOMACH

The mean diameter of the cardiac region is 5990.66 ± 41.90 µm, and the mean thickness of the wall is 2130.69 ± 17.33 µm. The tunica mucosa is thick; its mean thickness is 1836.53 ± 9.98 µm. The cardiac mucosa is characterized by a large number of well-defined long folds (about 41 folds). The cardiac region has the highest MFs; its mean height is 1273.47 ± 3.92 µm, and its mean width was 237.32 ± 15.30 µm. The mean diameter of the lumen is 1729.28 ± 58.42 µm (Figure 8.21A and Table 8.3).

TABLE 8.3 The Measurements of Stomach of Nile Catfish

Pyloric Region	Fundic Region	Cardiac Region	Measurements
6682.06 ± 30.25	7467.92 ± 48.39	5990.66 ± 41.90	Diameter of the organ (µm)
2488.41 ± 52.0	2709.0 ± 47.42	2130.69 ± 17.33	Thickness of the wall (µm)
1705.24 ± 67.90	2049.92 ± 71.09	1729.28 ± 58.42	Diameter of the lumen (µm)
1050.95 ± 57.0	1518.0 ± 59.85	1836.53 ± 9.98	Thickness of mucosa (µm)
9.11 ± 2.17	9.50 ± 1.89	41.12 ± 6.05	Number of MFs/cross section
947.37 ± 21.94	1279.25 ± 19.71	1273.47 ± 3.92	Height of MFs (µm)
986.97 ± 59.9	1336.13 ± 66.06	237.32 ± 15.30	Width of MFs (µm)
28.46 ± 1.11	26.6 ± 1.01	30.83 ± 1.77	Height of the epithelium (µm)
–	98.86 ± 3.98	515.97 ± 44.48	Length of gastric pits (µm)
–	17.0 ± 0.78	479.93 ± 11.82	Diameter of gastric glands (µm)
–	7.77 ± 0.36	19.4 ± 0.81	Height of glandular epithelium (µm)
370.24 ± 23.2	350.44 ± 14.44	118.18 ± 5.32	Thickness of submucosa (µm)
1179.97 ± 21.96	786.93 ± 8.31	226.89 ± 6.48	Thickness of muscularis (µm)

The mean height of the epithelium is 30.83 ± 1.77 µm. The surface epithelial cells are simple columnar type. Few GCs are found between the surface epithelium (Figure 8.21B). Semithin sections of the surface epithelium show a positive reaction to toluidine blue. The epithelium is covered with distinct microvilli. The nuclei of these cells are vesicular with distinct

nucleoli and are centrally located. Under the epithelium, there are small and irregular cells that have indistinct outlines and scanty cytoplasm with dense dark nuclei, similar to those found in lymphocytes, these may be migratory cells (Figure 8.22A).

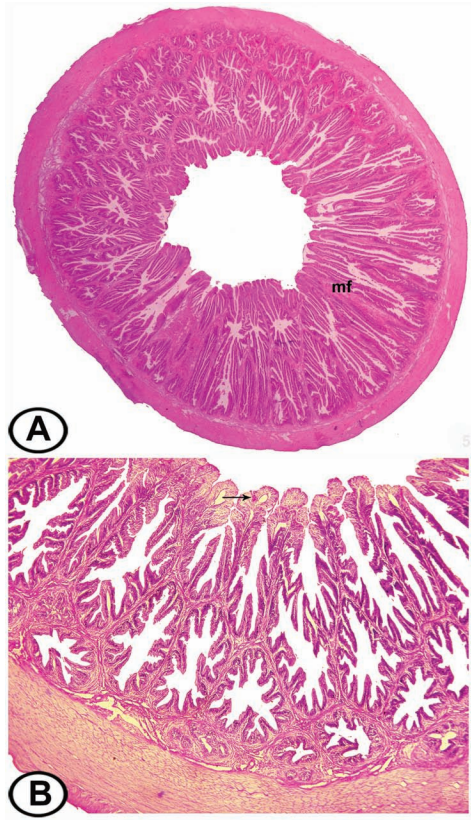

FIGURE 8.21 General view of the cardiac region of the stomach of Nile catfish. (A) The wall has a large number of MFs (HE, ×16). (B) PAS-positive GCs (arrow) on the luminal surface of the epithelial cells (PAS, ×25).

The LP consists of loose connective tissue that is exclusively occupied by closely packed simple branched tubular gastric (cardiac) glands, which fill most the depth of the mucosa and opened into the crypts of the MFs (gastric pits or foveolae). Gastric pits are formed by invaginations of the epithelial layer into the LP. These glands are arranged perpendicular to the gastric mucosal surface (Figure 8.21B). The gastric pits are more distinct than in the other stomach parts, the mean length of gastric pits is 515.97 ± 44.48 µm.

The gastric glands of the cardiac region are arranged in rounded to oval lobules with a wide lumen in the LP and occupy a great part of the thickness of the mucosa. The mean diameter of the gastric glands lobules is 479.93 ± 11.82 µm. These glands are composed of numerous secretory tubules that are lined with a single layer of low-columnar granular cells with deep-stained eosinophilic cytoplasm. The nuclei of these cells are rounded, vesicular with distinct nucleoli, and are centrally located. The mean height of the glandular epithelium is 19.40 ± 0.81 µm (Table 8.3 and Figure 8.22B).

Semithin sections showing that the glandular epithelium is composed of one type of cells, which appears pyramidal with a granular cytoplasm. The nuclei are spherical, vesicular with distinct nucleoli, and located at the basal third of the cells. The cytoplasm contains numerous granules of different sizes and densities that appear in the form of rods and spheres, some of them are stained intensely with toluidine blue (Figure 8.22C).

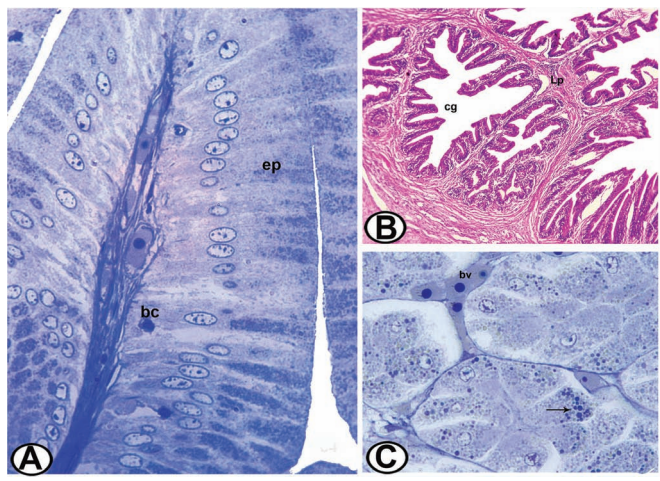

FIGURE 8.22 The surface and glandular epithelium of the cardiac region of Nile catfish. (A) Semithin section through the surface simple columnar epithelium (EP) showing a positive reaction of the GCs. Note the presence of the basal cells (BCs) (toluidine blue, ×1000). (B) The LP of the cardiac region contains cardiac glands (cg) (HE, ×100). (C) Semithin section through the CGs showing granular cytoplasm (arrow). Note the presence of the blood capillaries (bv) containing RBCs (toluidine blue, ×1000).

Scanning electron microscopic observations show that the mucosa of the cardiac region is provided with numerous long primary folds and gastric pits, through which the tubular gastric glands open (Figure 8.23A). The presence of gastric MFs in catfish is to allow the fish to accommodate large variations

in meal size, by permitting a great deal of distention when excess food is present. The distension serves as a powerful stimulus for gastric digestive secretions in teleosts. It is also possible that this pattern of folding may slow down the passage of food in the stomach and divide the ingested bolus into smaller portions for more efficient mixing with the digestive fluid. The luminal surface of epithelial cells of the cardiac region exhibits polygonal borders. Some mucous droplets are deposited on the surface (Figure 8.23B).

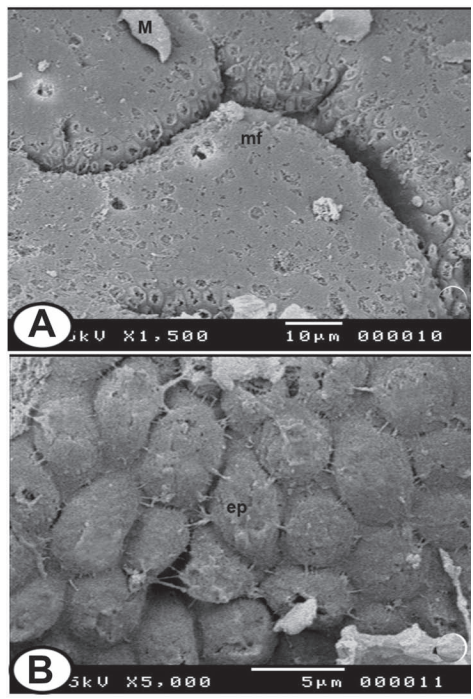

FIGURE 8.23 SEM of the cardiac stomach of Nile catfish. (A) The mucosa is thrown into primary MFs with gastric pits (arrow) in between them. Note the presence of mucous droplets (M) on the surface. (B) The surface polyhedral shaped epithelial cells (EP) of the cardiac region.

The cardiac glands (CGs) by transmission electron microscopy appear to be lined by one type of cells with a granular cytoplasm. The nuclei are rounded, euchromatic, and basally located with prominent nucleoli. The cytoplasm contains numerous granules of different sizes and shapes and well-developed rER located around the nucleus. In addition, a large number of free ribosomes are scattered all over the cytoplasm (Figure 8.24).

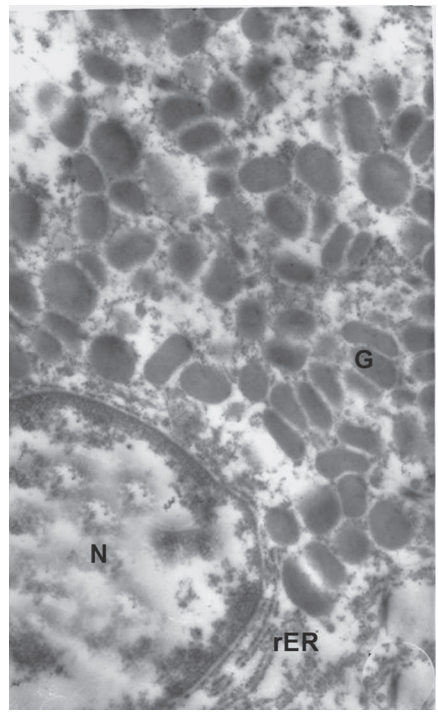

FIGURE 8.24 Transmission electron micrograph of the CGs showing glandular epithelium contained rounded nucleus (N) and a large number of granules (G) and rER (×14,000).

Tunica submucosa of the cardiac region is a thin layer; its mean thickness is 118.18 ± 5.32 μm. It consists of loose connective tissue with many collagenous fibers, fine elastic fibers, and numerous BV. The tunica muscularis is a thin layer; its mean thickness is 226.89 ± 6.48 μm. It is composed of inner thick circular and a thinner outer longitudinal layer of smooth muscle fibers. The tunica SE consists of mesothelium and subjacent connective tissue that contains BV and elastic fibers (Figure 8.21).

8.6.2 FUNDIC REGION OF THE STOMACH

Light microscopic observations reveal that the wall of fundic region of the stomach is composed of tunica mucosa, tunica submucosa, tunica muscularis, and tunica SE. The fundic region is thrown into about nine longitudinally oriented dome-shaped folds of different sizes. These folds are projected into a lumen, which is narrow and stellate in cross section when empty. These

folds include the LP and submucosa, as well as the lining epithelium (Figures 8.25 and 8.26).

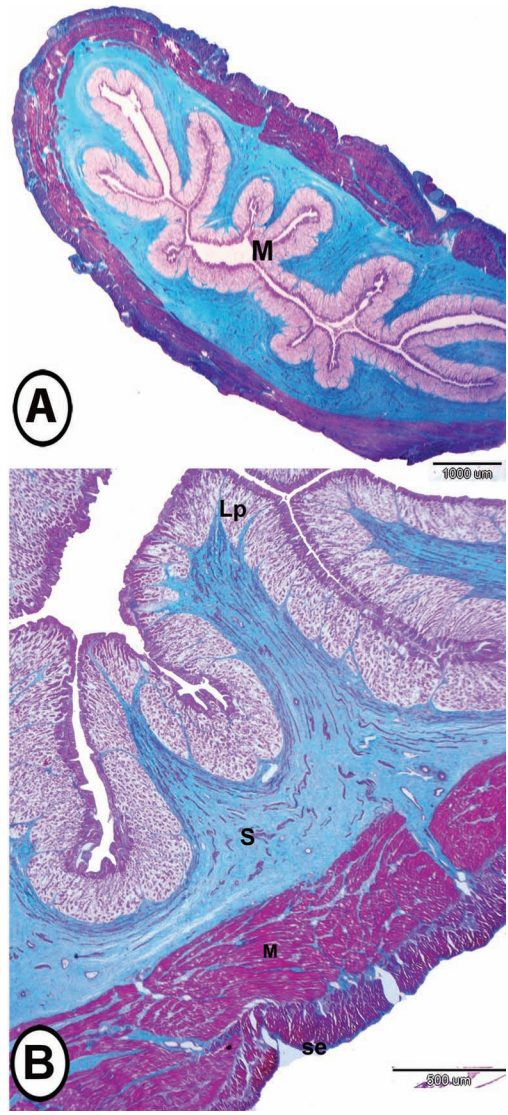

FIGURE 8.25 The histological structure of the fundic region of the stomach of Nile catfish stained with Crossmon's trichrome. (A) The mucosa (M) was thrown into many longitudinal folds. (B) The fundic region showing LP, submucosa (S), and SE stained green, while tunica muscularis (M) stained red.

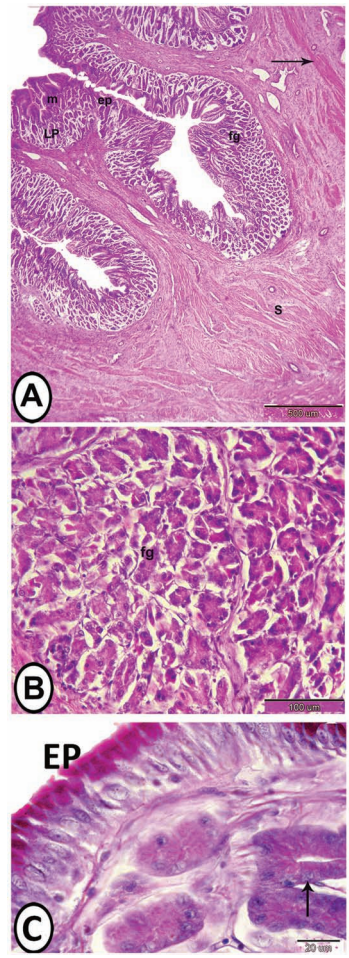

FIGURE 8.26 The wall of the fundic region of the stomach of Nile catfish stained with HE. (A) The folded mucosa (m) of the fundic region includes epithelium (EP) and LP that contains fundic glands (FGs), surrounded with submucosa (S) that contains diffuse smooth muscle bundles (arrow) (hematoxylin and eosin). (B) FGs resemble the pancreatic acini. No parietal or chief cells. (C) The fundic region showing alcian blue-negative and PAS-positive FGs (arrow). Note PAS-positive apical part of the surface simple columnar epithelium (EP).

The surface epithelial cells are high columnar mucosecretory in type with tapering infranuclear region. Migrating cells are seen among the epithelial cells especially in the basal part. No GCs are observed between the epithelial cells of the fundic region. The surface cells show a strong PAS-positive reaction in the apical portion and the brush border made of microvilli. The

epithelial cells are negative to alcian blue by combined alcian blue-PAS stain (Figure 8.26). Strong acid phosphatase activity is observed in the basal parts of the epithelium (Figure 8.27A). Oval- to round-shaped enteroendocrine cells are scattered among the superficial columnar cells (near the basal lamina), which stain positive to Grimelius stain (Figure 8.27B).

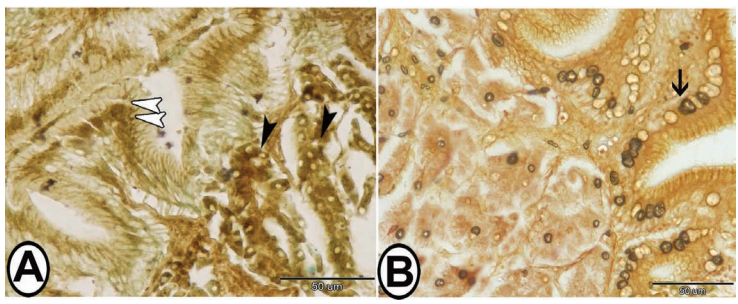

FIGURE 8.27 The histochemical analysis of the surface and glandular epithelium of Nile catfish. (A) The surface epithelium (white arrowheads), as well as the glandular cells (black arrowheads), showed positive reactivity for acid phosphatase (Gomori lead nitrate method). (B) The mucosa of the fundic region showing a positive reaction of enteroendocrine cells on the surface epithelium (arrow) and FGs (Grimelius silver stain).

The surface epithelial cells of the stomach are PAS-positive, which indicated that it contained neutral mucosubstances, which play a role in the digestive activity, such as facilitating the movement of the great-sized particles of food and then emulsifying it into chyme after mixing with several digestive enzymes. These mucosubstances are also related to the absorption of easily digested molecules, such as disaccharide and short-chain fatty acids. On the other hand, the secretion of mucosubstances from the gastric epithelium plays a role in protecting the underlying mucosa from the acid environment and proteolysis, neutralizing the gastric pH and act as a defensive mechanism against bacteria.

The LP is consisted of loose connective tissue and contains a great number of simple branched tubular gastric glands, which occupy most of the depth of the mucosa and open into the bottom of each crypt of the MFs (gastric pits or foveolae). The gastric pits are lined with eosinophilic cylindrical cells that are shorter than columnar surface cells with a basal large oval nucleus (Figure 8.25). The apices of these cells are projected into a small lumen, and their cytoplasm stains intensely with PAS (Figure 8.26). The gastric pits are stained positive with PAS, which indicates the presence of glycoconjugates with sugar residues analogs to those found at the epithelial surface. The

gastric pits provide a maximal amount of the digestive surface and allow free access of the glandular products to the lumen.

The fundic glands (FGs) are arranged in groups, perpendicular to the gastric mucosal surface. Each gland is composed of clusters of polygonal cells called oxyntico-peptic cells that are radially arranged around a very narrow glandular lumen. These cells have basally located spherical vesicular nuclei. The FGs of catfish resemble the mammalian pancreatic acini, in which they have about one-fourth of the cell nearer the base is stained pale blue while the rest is stained red. The cytoplasm of these glandular cells appears densely granular that contained acidophilic secretory granules (SGs). There are no parietal, chief, or mucous neck cells as in mammals (Figure 8.25B).

The glandular cells are positive to PAS and negative to alcian blue (Figure 8.26C). The mean height of the glandular epithelium is 7.77 ± 0.36 μm. The diameter of each gastric gland is approximately the same, which its mean diameter is 17.0 ± 0.78 μm (Table 8.3). Oval- to round-shaped enteroendocrine cells are scattered among the glandular epithelium, which stained positive to Grimelius stain (Figure 8.27B). The glands are surrounded by collagenous fibers and smooth muscle fibers (Figure 8.25A).

The gastric LP observed in cardiac and fundic regions of the stomach of catfish may help to keep the glands in position and it is rich in collagenous fibers that might form a protective, supporting, and strengthing layer in the carnivorous fish. The smooth muscle fibers around the gastric glands of catfish may probably play an important role by their contraction to induce the release of glandular and faveaolar secretion into the gastric lumen and prevent occlusion of foveolae by ingested food. In addition, these muscle fibers may aid in the movement of the folds, which blend the food bolus to facilitate mixing with gastric juice in the stomach.

Semithin sections show that the internal surface of the fundic region of the stomach is composed of folded mucosa that is filled with FGs. The luminal surface of the mucosa is punctuated by shallow depressions of numerous gastric pits (Figure 8.28A). The surface epithelium is composed of tall narrow columnar cells. The apical part of the cytoplasm of epithelial cells showed mucosubstances that are stained intensely with toluidine blue. The basal part of the epithelium contains polymorphic cells with many cytoplasmic processes that stain positive with toluidine blue, which may be undifferentiated basal cells (Figure 8.28B). The glands open in groups of two or three into the gastric ducts. Its ducts are lined by simple squamous flat cells and open in the gastric pits of the MFs. Occasional smooth myocytes, fibroblasts, and minute blood capillaries are observed between the glands

(Figure 8.28C). The glandular cells (oxyntico-peptic cells) are pyramidal in shape and their cytoplasm contains a large number of vesicles of different sizes (Figure 8.28D).

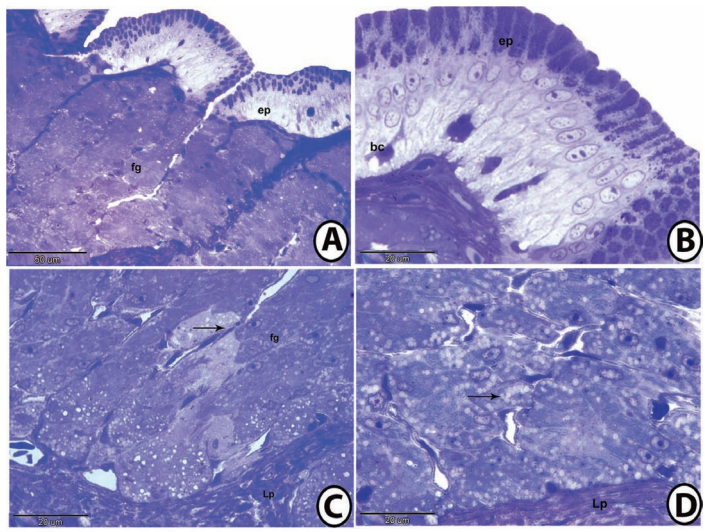

FIGURE 8.28 Semithin section through the fundic mucosa of Nile catfish stained with toluidine blue. (A) The surface epithelium (EP) showing gastric pits that lead to the FGs. Notice the abrupt transition from gastric pits to gastric glands. (B) The surface simple columnar epithelium (EP) showing a positive reaction to TB stain at their apical parts. Note the presence of undifferentiated basal cells (BCs). (C) The LP contains the FGs that opened into ducts lined by simple squamous epithelium (arrow). (D) The LP showing the FGs that consisted of oxyntico-peptic cells that contained many vesicles (arrow).

Scanning electron microscopic observations (Figure 8.29) reveal that the luminal surface of the mucosa of the fundic region has a meshwork appearance of a large number of primary longitudinal folds. The mucosal surface shows deep concavities between the MFs. The most prominent feature of the fundic region is the presence of a large number of gastric pits of different sizes, which punctuated the surface of the mucosa. The hexagonal borders of superficial epithelial cells give the gastric surface a honeycomb-like appearance. These cells are uniformly covered with few and short microvilli, which give it a velvety appearance. Some mucous droplets are deposited on the surface. In Figure 8.29D, the epithelial sheet of the fundic region has been damaged and the individual columnar cells are observed. They are tall and cylindrical with a narrow infranuclear region. The apical borders are covered with many short microvilli.

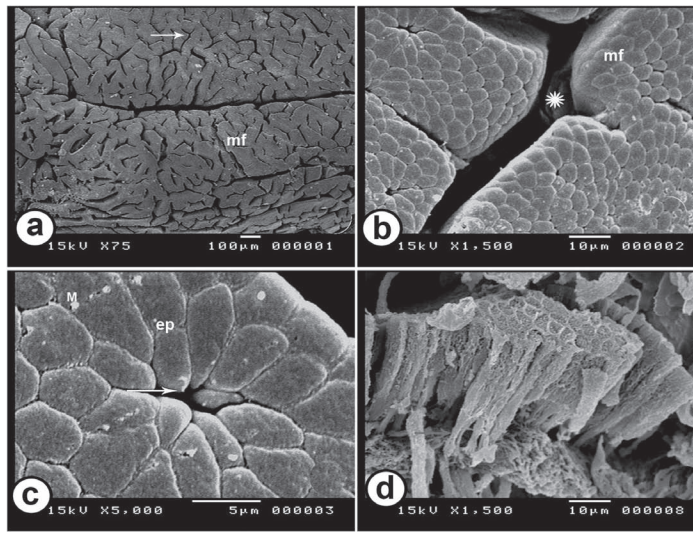

FIGURE 8.29 SEM of the fundic region of Nile catfish. (A) The primary MFs of the fundic region of the stomach showing the presence of a large number of gastric pits (arrow). (B) Scanning electron micrograph of the fundic region showing the presence of large concavities (asterisk) between the MFs. (C) Scanning electron micrograph of the surface polyhedral-shaped epithelial cells (EP) of the fundic region. Note the presence of the gastric pits (arrow) and the deposition of some mucous droplets (M) on the surface. (D) Scanning electron micrograph of a damaged surface in the fundic mucosa showing tall columnar surface epithelium with infranuclear region (arrow).

Transmission electron microscopic observations to the FGs (Figure 8.30) show that they are lined with one type of cells "Oxyntico-peptic cells." These cells are polygonal in shape with the basally located spherical nucleus, with prominent central nucleolus. Spherical-shaped vesicles of different sizes and density, which represent the formation of secretory or zymogen granules are distributed in the cytoplasm. In many images, the granules are found in the apical portions of the cell, suggesting that their contents are about to be released via exocytosis. The luminal surface contains short microvilli, which are projected into the glandular lumen. The supranuclear portion of the cytoplasm contains a tubulovesicular network that is composed of smooth membranous elements. A great number of large mitochondria are located all over the cytoplasm. The rER is located around the nucleus. The well-developed Golgi complexes and lysosomes are arranged around the nucleus. Oxyntico-peptic cells could be involved in the production of gastric juices. The Golgi complex is involved in the formation of secretory or zymogen granules, whose contents are eventually released into the glandular lumen.

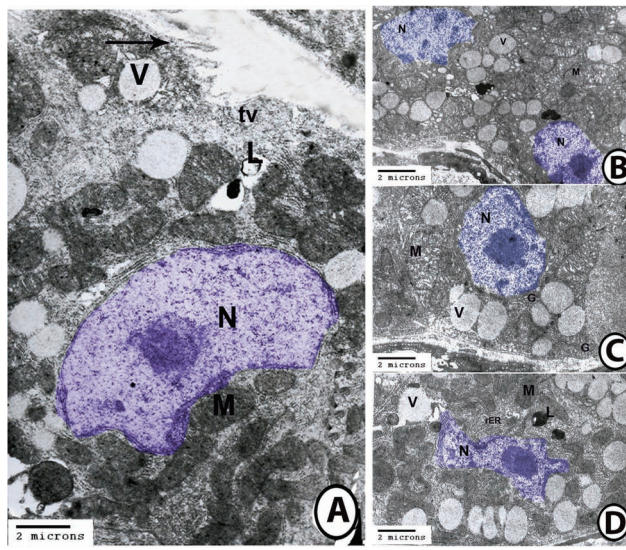

FIGURE 8.30 Transmission electron microscopy of the gastric glands of Nile catfish. (A) The oxyntico-peptic cell of the FGs contained nucleus (N), lysosomes (L), mitochondria (M), and secretory vesicles (V). Notice the presence of short apical microvilli (arrow) and tubulovesicular network (tv). (B) Transmission electron micrograph of the FGs showing two oxyntico-peptic cells contained euchromatic nucleus (N) with large nucleolus and a large number of mitochondria (M) and secretory vesicles (V). (C) The oxyntico-peptic cell of the FGs contained nucleus (N), Golgi complexes (G), mitochondria (M), and secretory vesicles (V). (D) The oxyntico-peptic cell of the FGs contains nucleus (N), lysosomes (L), mitochondria (M), rER, and secretory vesicles (V).

Both the surface and exocrine glandular cells secrete gastric juices containing digestive enzymes, including lipolytic enzymes. Thus, the well-developed gastric glands and the epithelial columnar cells that are rich in neutral mucins implied that the stomach of Nile catfish has strong capabilities of digestion and absorption.

The tunica submucosa of the fundic region increases in thickness toward the pyloric region; its mean thickness is 350.44 ± 14.44 μm. It consists of loose connective tissue with many collagenous, elastic fibers, and numerous BV with a large number of smooth muscle fibers. The tunica muscularis is a thick layer; it is composed of thick inner circular and a thinner outer longitudinal layer of smooth muscle fibers. The smooth muscular layer of the stomach may aid in the final breakdown of the food before entering the intestine. The tunica SE is a thin layer of connective tissue, covered with mesothelium (Figure 8.25B).

8.6.3 THE PYLORIC REGION OF THE STOMACH

The mean diameter of the pyloric region is 6682.06 ± 30.25 µm and it is characterized by a thick wall, which its mean thickness is 2488.41 ± 52.0 µm and the mean diameter of the lumen is 1705.24 ± 67.90 µm (Table 8.3). Light microscopic observations reveal that the wall of the pyloric region of the stomach is composed of tunica mucosa, tunica submucosa, tunica muscularis, and tunica SE.

The mean thickness of the mucosa is 1050.95 ± 57.0 µm. The MFs of the pyloric region are similar to the gastric pits of the fundic region. These folds include the LP as well as the lining epithelium. The pyloric region has about nine MFs, which appear shorter than other parts of the stomach. The mean height of the MFs is 947.37 ± 21.94 µm and its mean width is 986.97 ± 59.9 µm (Table 8.3 and Figure 8.31).

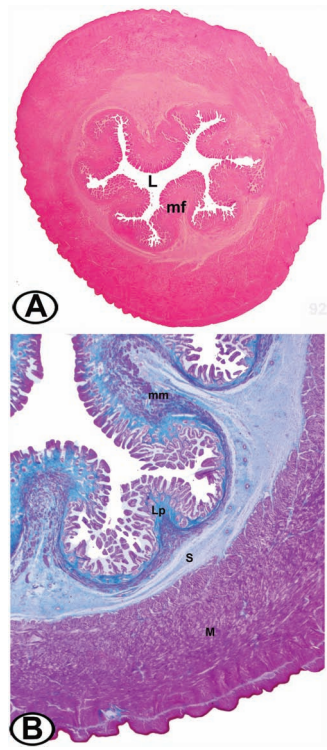

FIGURE 8.31 The histological structure of the pyloric region of Nile catfish. (A) The mucosa is thrown into MFs and irregular shaped lumen (L) (HE, ×8). (B) The wall of the pyloric region is composed of LP, submucosa (S) stained green, while tunica muscularis (M) and muscularis mucosa (mm) stained red (Crossmon's trichrome, ×50).

The mean height of the surface cells is 28.46 ± 1.11 µm. The surface epithelium is formed of a single layer of simple columnar cells with an oval basal nucleus and few GCs. The semithin sections show that the epithelium is formed of columnar cells, covered by short microvilli. It contains moderately basophilic, oval nuclei with one or two nucleoli located at the basal half. Few GCs are present between epithelium that reacted positively to toluidine blue. Some basal or undifferentiated cells appear in the basal part of the epithelium (Figure 8.32).

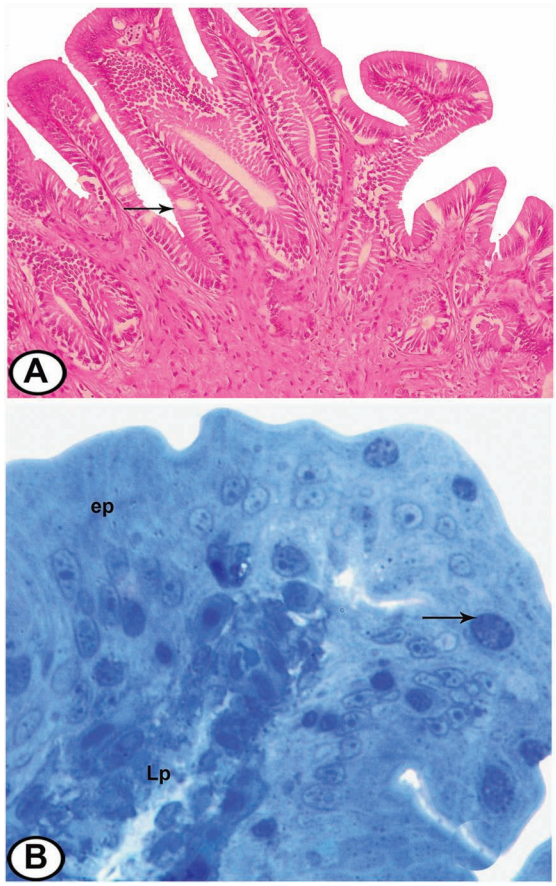

FIGURE 8.32 The surface epithelium of the pyloric region of Nile catfish. (A) The lamina epithelialis is formed of simple columnar epithelium with few GCs (arrow) (HE, ×250). (B) Semithin section of the surface simple columnar epithelium (EP) of the pyloric region showing a positive reaction of the GCs (arrow). Note the presence of connective tissue core of LP (TB, ×1000)

Scanning electron microscopic observations (Figure 8.33) of the mucosa of the pyloric region of the stomach show that it is provided with numerous primary folds. The mucosal surface shows deep concavities and the folds are devoid of gastric pits. Some mucous droplets are deposited on the surface. The hexagonal borders of the surfaces of superficial epithelial cells give the gastric surface a honeycomb-like appearance. These epithelial cells are covered with few and short microvilli.

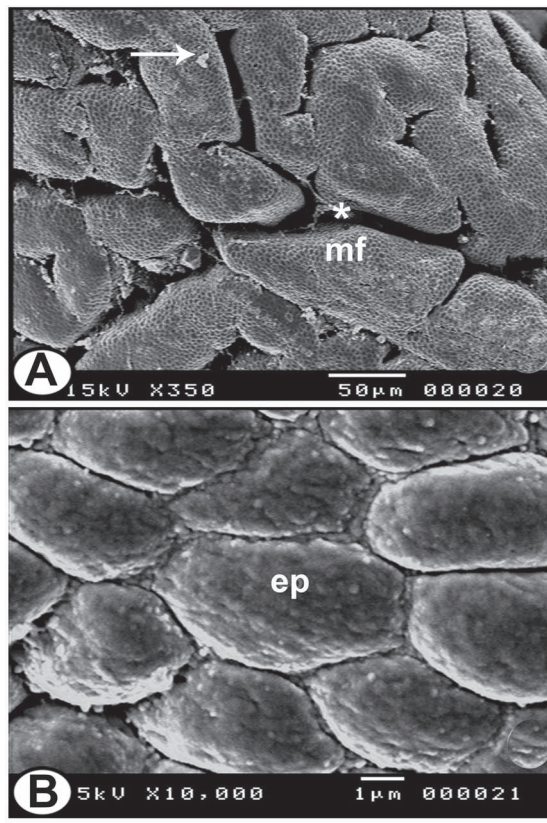

FIGURE 8.33 SEM of the pyloric region of Nile catfish. (A) The primary MFs leave deep concavities (asterisk) between them. Note the presence of some mucous droplets (arrow) on the surface. (B) Scanning electron micrograph of the surface polyhedral-shaped epithelial cells (EP), covered by short few microvilli.

The pyloric region is characterized by the absence of gastric glands. The LP consists of loose connective tissue with abundant collagenous fibers

and elastic fibers. The muscularis mucosa is composed of thick bundles of smooth muscle fibers, which stained red with Crossmon's trichrome (Figure 8.31B).

The tunica submucosa is a wide layer; its mean thickness is 370.24 ± 23.20 µm. It consists of loose connective tissue with many collagenous fibers, few smooth muscle fibers, elastic fibers, and numerous BV. The tunica muscularis is a thick layer; its mean thickness is 1179.97 ± 21.96 µm (Table 8.3). It is composed of an inner circular and a thinner outer longitudinal layer of smooth muscle fibers. The pyloric region contains a third middle oblique layer. The outer layer of the muscles is extensively folded that gives the outer surface of the pyloric a ridged appearance. The smooth muscular layer of the stomach may aid in the final breakdown of the food before entering the intestine. The thick muscular layers in the pyloric region are required for the expulsion of food to the intestine; also, these indicated that the catfish has some degree of voluntary control over the passage of food into the intestine. The tunica serosa consists of mesothelium and subjacent connective tissue (Figure 8.31B).

8.7 THE INTESTINAL BULB

Cyprinid fishes (such as goldfish and carp) have one of the simplest types of gastrointestinal tract among vertebrates. Those fish species do not possess a true stomach, and even in the intestine, there is no differentiation of the intestinal glands or crypts of Lieberkuhn. The absence of the true stomach in grass carp is replaced by a simple dilatation at the anterior part of the intestine called the intestinal bulb.

The mean diameter of the bulb is 5148.65 ± 41.54 µm, and the mean thickness of the wall is 1598.03 ± 31.58 µm. The wall of the intestinal bulb is composed of tunica mucosa, tunica submucosa, tunica muscularis, and tunica SE. The mean thickness of the tunica mucosa is 1109.80 ± 13.85 µm. The mucosa shows numerous (about 52), deep longitudinal folds. A large distinct concavity is noted to be present between the MFs. The folds of the intestinal bulb are higher and more complex than that of the intestine. The mean height of the folds is 1066.98 ± 42.40 µm, and their mean width is 181.38 ± 5.58 µm. The mean diameter of the lumen is 1952.59 ± 42.86 µm (Table 8.4 and Figure 8.34A and B).

TABLE 8.4 The Measurements of the Intestinal Bulb of Grass CARP

Intestinal Bulb	Measurements
5148.65 ± 41.54	Diameter of the organ (μm)
1598.03 ± 31.58	Thickness of the wall (μm)
1952.59 ± 42.86	Diameter of the lumen (μm)
1109.80 ± 13.85	Thickness of mucosa (μm)
52.01 ± 5.02	Number of MFs/cross section
1066.98 ± 42.40	Height of MFs (μm)
181.38 ± 5.58	Width of MFs (μm)
38.80 ± 1.89	Height of the epithelium (μm)
119.98 ± 4.65	Thickness of submucosa (μm)
401.52 ± 11.53	Thickness of muscularis (μm)

The values are represented by mean ± standard error.

The mean height of the epithelium is 38.80 ± 1.89 μm. The epithelium is composed of tall simple columnar cells. Some differences in the height of the columnar cells are present. Nuclei of columnar cells are oval in shape and located at the center or at the basal third of the cell. The GCs are sparsely present. Besides these two types of cells, some migratory cells, such as many lymphoid cells and some apoptotic (AP) cells, are present mostly in the epithelial layer near the basement membrane (Figure 8.34C). The GCs are reacted positively to PAS and alcian blue. The mucin secreted by mucous cells of the bulb keeps it moist and provides lubrication to the food, thus enables easy transport of ingested materials and protects the epithelial cells from mechanical injury. Spindle-shaped enteroendocrine cells could be identified between the absorptive cells that extend to the lumen in a parallel fashion (Figure 8.35). Enteroendocrine cells secrete serotonin, gastrin, and enteroglucagon.

The semithin sections (Figure 8.35C) reveal that the epithelium of the bulb is composed of simple columnar cells covered by microvilli. Their nuclei are vesicular, oval, and located at the basal third of the cells. The cells rest on the folded basal lamina. GCs show a metachromatic reaction to toluidine blue. The epithelium also contains apoptic cells, many secretory granules contained digestive enzymes and large numbers of vacuoles mostly in the basal part, some of these vesicles are also observed inside the blood capillaries underlying the columnar cells.

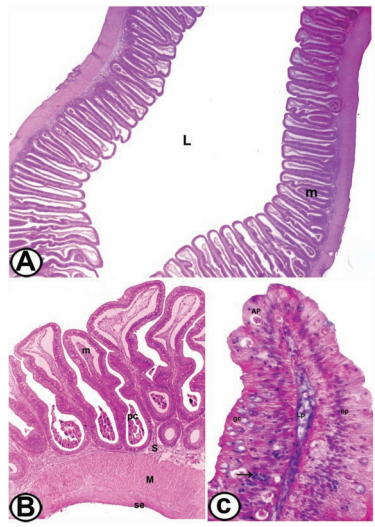

FIGURE 8.34 The histological structure of the intestinal bulb of grass carp stained with HE. (A) The mucosa (m) is folded left wide lumen (L) (×25). (B) The wall of the intestinal bulb showing folded mucosa (m), submucosa (S), muscularis (M), and SE. Note the presence of plant cells (PCs) between the MFs (×100). (C) The MF showing columnar epithelium (EP) with GCs, apoptotic (AP) cells, lymphoid cells (arrow), and LP (×400).

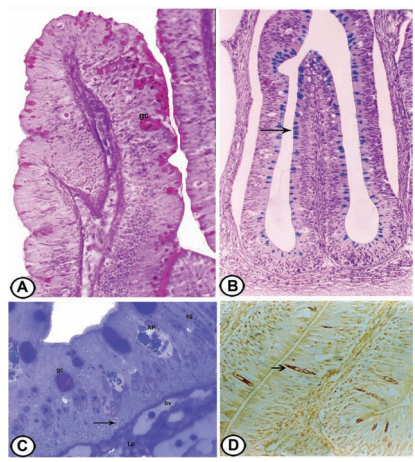

FIGURE 8.35 The histochemistry of the intestinal bulb of grass carp. (A) The epithelium of the intestinal bulb showing PAS-positive GCs (×200). (B) The epithelium showing alcian blue-positive GCs (arrow) (combined AB and PAS, ×100). (C) Semithin section of the surface simple columnar epithelium of the intestinal bulb showing GCs, AP cells, and secretory granules (SGs). Note the presence of vacuoles (arrow) mostly in the basal part and some of them are present in the BV of LP (toluidine blue, ×1000). (D) The epithelium of the intestinal bulb showing argyrophilic enteroendocrine cells (arrow) (Grimelius silver stain, ×400).

The digestive enzymes (usually lipolytic and amylolytic enzymes) are involved in the digestion of food. These enzymes do not produce complete digestion of the food. The intestinal bulb and anterior intestine of grass carp contain lipase and trypsin, and some other enzymes present in the lumen, such as amylase, maltase, and invertase.

The LP is composed of a thin sheet of fibrous connective tissue that extends to fill the core of the MFs. It contains well-developed BV, smooth muscle cells, numerous lymphocytes, and cells from the connective tissue in addition to large lymphatic vessels. No multicellular glands of gastric or intestinal-type are found in this region. This region is also contained parallel collagenous fibers and elastic fibers underneath (Figure 8.36).

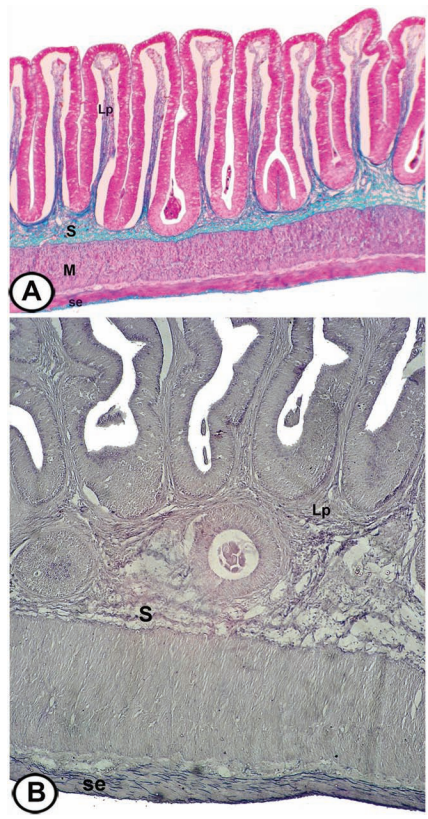

FIGURE 8.36 The wall of the intestinal bulb of grass carp. (A) The LP, submucosa (S), and SE stained green, while tunica muscularis (M) stained red (Crossmon's trichrome, ×50). (B) The intestinal bulb showing the presence of elastic fibers in LP, submucosa (S), and SE (Weigert's Elastica, ×100).

Scanning electron microscopy (SEM) (Figure 8.37) shows that the mucosa of the intestinal bulb is thrown into numerous longitudinal primary folds, which are variable in appearance; most commonly, they are arranged in zigzagging-like patterns, which course along the long axis of the intestinal bulb. Quite distinct concavities are present between the folds. The intestinal bulb in grass carp serves as a temporary storage part for ingested food, which is supported by a large diameter of its lumen that represented 37.92% of the diameter of the bulb. A large number of zigzag-shaped MFs and thick mucosa of the bulb with the resultant increase in the surface area may aid in the mixing of food with the hepatic and pancreatic digestive juices as well as with the mucus secreted by the GCs. The epithelium is composed of closely packed polyhedral-shaped epithelial cells. These cells are covered by a heavy coat of long microvilli. A very little minute pores through which GCs discharged their contents are also demonstrated.

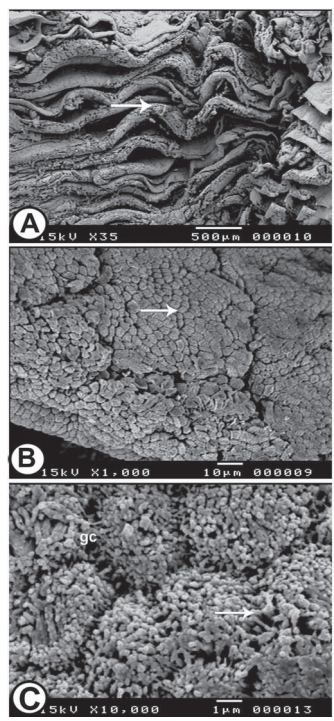

FIGURE 8.37 SEM of the intestinal bulb of grass carp. (A) The bulb showing a zigzag-like arrangement of the MFs (arrow). (B) The surface polyhedral-shaped epithelial cells (arrow) of the intestinal bulb. (C) The surface epithelial cells of the intestinal bulb are covered by numerous long microvilli (arrow). Note the presence of minute pores of GCs.

The tunica submucosa is made up of loose connective tissue containing numerous wavy collagenous fibers, as well as elastic fibers. The mean thickness of the submucosa is 119.98 ± 4.65 μm. Tunica muscularis is composed of thick inner circular and thin outer longitudinal layers of smooth muscle fibers; its mean thickness is 401.52 ± 11.53 μm (Table 8.4). This muscular thickness may help in the breakdown of food. The tunica SE is formed of a layer of mesothelium and the subjacent thick connective tissue layer contained many fine elastic fibers (Figure 8.36).

8.8 THE INTESTINE

The high RGL values are recorded in herbivorous species, whereas intermediate values are associated with omnivorous and low values in carnivorous ones. A functional explanation for the long gastrointestinal tract of herbivorous is that some components of the diet are slow to digest and required both a long time and more extensive exposure to the digestive enzymes. This phenomenon can be supported by the demonstration of a large diameter of the intestine of grass carp (one of the herbivorous fish) required for increasing the storage capacity of the food for longer periods to complete the process of digestion and absorption.

The intestine of fish is divided into three portions according to the thickness of the wall, length of MFs, and thickness of muscularis: anterior, middle (posterior), and rectum.

8.8.1 THE ANTERIOR INTESTINE

The anterior intestine is characterized by a wide diameter that its mean diameter is 6546.22 ± 41.15 μm and in the mean thickness of the wall was 2344.23 ± 6.05 μm. The light microscopic observations reveal that the wall of the anterior intestine of grass carp is composed of tunica mucosa, tunica submucosa, tunica muscularis, and tunica SE. The mean thickness of the tunica mucosa is 1951.42 ± 28.30 μm. The mean diameter of the lumen is 1857.76 ± 37.17 μm. The mean number of MFs is 58 (Table 8.5), as usually the number of MFs depends on the nature of food. There are no intestinal villi in the intestine of grass carp. The MFs appear swollen and bulged toward the lumen in the form of wavy longitudinal, tall folds (Figure 8.38A). The presence of many folds in the anterior intestine can delay the speed

of the intestinal movement, which probably allows for partial retention of semidigested food for effective digestion and absorption.

TABLE 8.5 Morphometrical Analysis of Anterior Intestine of Grass Carp

Measurements	Anterior Intestine of Grass Carp
Diameter of the organ (μm)	6546.22 ± 41.15
Thickness of the wall (μm)	2344.23 ± 6.05
Diameter of the lumen (μm)	1857.76 ± 37.17
Thickness of mucosa (μm)	1951.42 ± 28.30
Number of MFs/cross section	58.85 ± 9.0
Height of MFs (μm)	1901.07 ± 7.06
Width of MFs (μm)	160.84 ± 11.52
Height of the epithelium (μm)	39.16 ± 2.25
Thickness of submucosa (μm)	69.67 ± 2.34
Thickness of muscularis (μm)	356.46 ± 8.22

The values are represented by mean ± standard error.

The mean height of the MFs is 1901.07 ± 7.06 μm. The mean width of MFs is 160.84 ± 11.52 μm. The mean height of epithelium is 39.16 ± 2.25 μm. The high number and height of the MFs may result in an increase in the retention time of food and subsequently increasing the digestion of substances by pancreatic juices and mucosubstances of GCs.

The epithelium is consisted of enterocytes (simple columnar epithelium) and contains numerous isolated GCs. GCs are regularly oval in shape and appear somewhat deeper in position, connect to the surface by the neck and small pores. Wandering cells are more common around the bases of the columnar cells and might migrate to the free border of the cells (Figures 8.38B and 8.39A).

The semithin sections show that the mucosal epithelium is lined by simple columnar cells and GCs. Each columnar cell is long and slender containing a large oval nucleus, which is situated at the basal portion of the cell at variable height. These columnar cells are covered by numerous microvilli that have an absorptive function. The GCs are consisted of: (1) apical expanded portion, which contains positive toluidine blue mucosubstances that connect to the surface by small pores, and (2) narrow portion, which contains a narrow nucleus located at a higher position than the nucleus of enterocytes (Figure 8.39B).

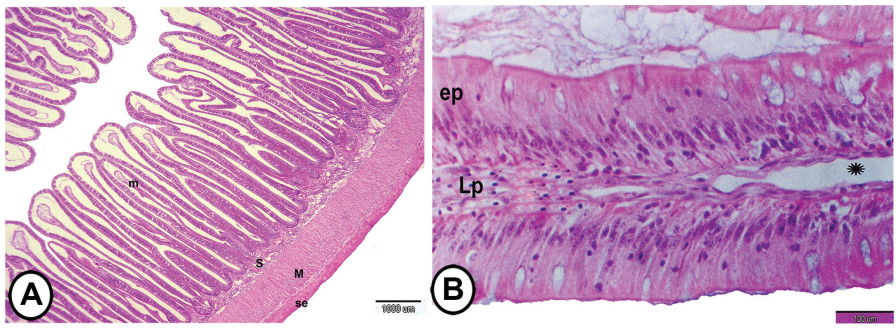

FIGURE 8.38 The histological analysis of the anterior intestine of grass carp stained by HE. (A) The wall of the anterior intestine consists of folded mucosa (m), submucosa (S), muscularis (M), and SE (hematoxylin and eosin). (B) The MF of the anterior intestine showing epithelium (EP) that consisted of simple columnar epithelium with GCs and LP. Note the presence of large lymphatic vessels (asterisk).

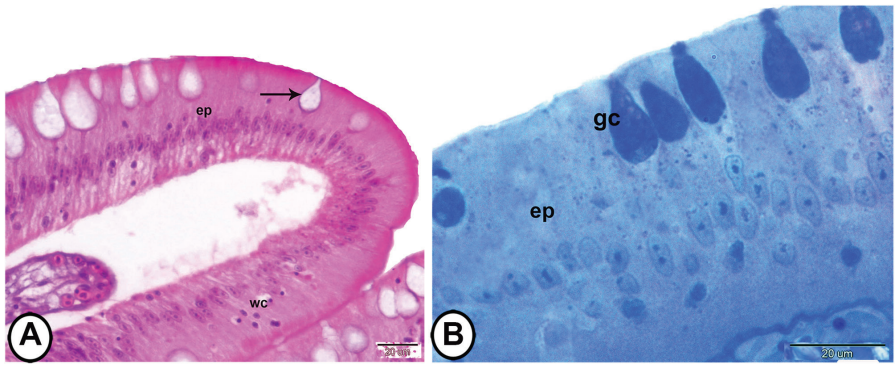

FIGURE 8.39 The surface epithelium of the anterior intestine of grass carp. (A) The simple epithelium (EP) of anterior intestine showing GCs (arrow) and wandering cells (WCs) (HE). (B) Semithin section of the simple columnar epithelium (EP) with GCs (TB).

Histochemical analysis (Figure 8.40) reveals that the GCs are numerous, which constitute a continuous sheet and reacted intensely positive to PAS, alcian blue, and combined PAS–alcian blue. Spindle-shaped enteroendocrine cells were located between the columnar cells and reacted positively to Grimelius stain. Most of these cells reach the lumen that may be an open type. The enterocytes of the anterior segment of the intestine of grass carp are involved in the absorption of fatty acids. Moreover, gastrin, gastric inhibitory peptide, glucagon, pancreatic polypeptide, substance P, vasoactive intestinal polypeptide, and secretin endocrine cells are found in the gut of grass carp, which has an elongated shape. Most of the enteroendocrine

cells are of open type, which indicates that the gut contents may stimulate or inhibit the peptide release from the basal part of the cell, by acting on their apical part.

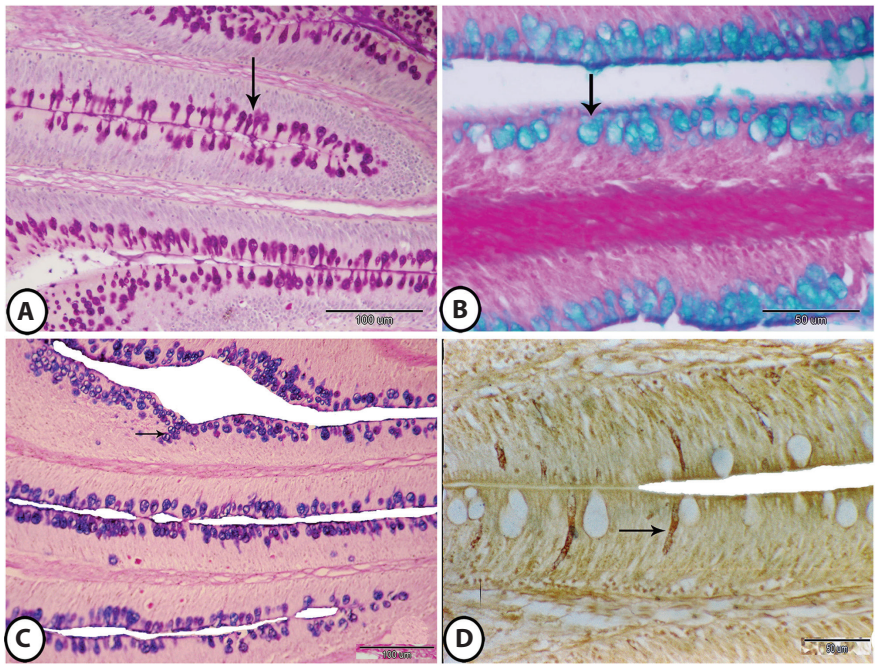

FIGURE 8.40 The histochemical analysis of the anterior intestine of grass carp. (A) A positive reaction of GCs to PAS (arrowhead). (B) A positive reaction of GCs to alcian blue (arrowhead). (C) The epithelium of anterior intestine showing PAS- and alcian blue-positive GCs (arrow) (combined AB and PAS). (D) The epithelium of the anterior intestine showing oval-shaped enteroendocrine cells (arrow) (Grimelius silver stain).

Scanning electron microscopic observations (Figure 8.41) revealed that the mucosal lining of grass carp is supported by densely backed polyhedral columnar cells, intercalated with a large number of GCs. The apices of the epithelial cells are covered with prominent microvilli. In Figure 8.41B, the epithelial sheet had been damaged and the individual enterocytes are clearly observed. The microvillus borders of these cells are clearly discernible as light bands at the tops of enterocytes. Also, the typical GCs are observed between the columnar cells.

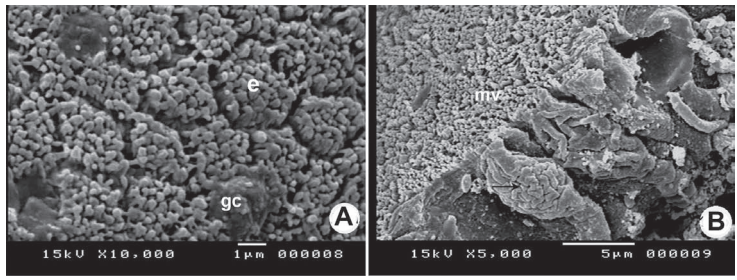

FIGURE 8.41 SEM of the anterior portion of the intestine of grass carp. (A) The surface polyhedral-shaped enterocytes (e) are covered with microvilli. Notice the presence of large pores leading to the GCs. (B) Scanning electron micrograph of the damaged surface epithelium of the anterior intestine that is covered with microvilli (mv). Note the presence of typical GCs (arrow).

Scanning electron microscopic observations show that the mucosa of the anterior intestine of catfish exhibits a large number of complex branched folds, which show reticulum-like arrangement. Deep concavities are present between the folds. The mucosal surface is filled with pores, through which the GCs release their contents. The polyhedral enterocytes are covered with microvilli, which is interrupted by the pores of GCs (Figure 8.42).

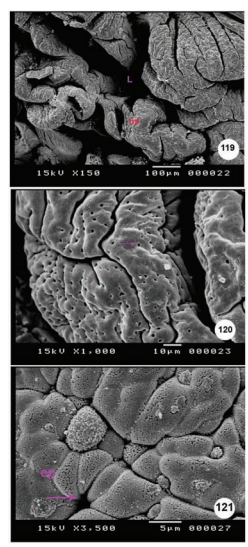

FIGURE 8.42 (A) SEM of the anterior intestine of Nile catfish showing a reticulum-like arrangement of the MFs, leaving wide lumen (L) in between. (B) The mucosa of the anterior intestine of catfish showing many pores of GCs (arrow). (C) The surface polyhedral-shaped epithelial cells (EP) of the anterior intestine are covered with microvilli. Note the presence of pores for GCs (arrow).

The LP is formed of a loose connective tissue layer that extends into the MFs. It contains collagenous fibers, fibroblasts, lymphocytes, and smooth muscle fibers. Large lymphatic vessels are found in the LP and are easily identified as blank spaces under the epithelial layer. There are no traces of multicellular intestinal glands. The tunica submucosa is a thin layer of connective tissue and contains fine elastic fibers found around the blood capillaries. Its mean thickness is 69.67 ± 2.34 μm. The tunica muscularis consists of thick inner circular and thin outer longitudinal smooth muscle fibers followed by thin tunica SE (Figure 8.38A). The mean thickness of muscularis is 356.46 ± 8.22 μm, which constitutes about 15.20% of the thickness of the wall (Table 8.5).

8.8.2 THE POSTERIOR INTESTINE

The mean diameter of the posterior intestine of grass carp is 4291.20 ± 42.10 μm, the mean thickness of the wall is 1320.35 ± 10.29 μm, and the mean diameter of the lumen is 1650.50 ± 42.37 μm. Light microscopic observations revealed that the wall of the posterior intestine of grass carp is composed of tunica mucosa, tunica submucosa, tunica muscularis, and tunica SE. The mean thickness of the mucosa is 925.09 ± 22.63 μm and the number of MFs reached about 24 folds/cross section. The MFs appear slender and slightly wavy (Figure 8.43A). The mean height of the folds is 902.45 ± 5.22 μm, which constitutes about 68.34% of the thickness of the wall, while their mean width is 204.51 ± 10.71 μm (Table 8.6).

TABLE 8.6 Morphometrical Measurements of Posterior Intestine of Grass Carp

Measurements	Posterior Intestine of Grass Carp
Diameter of the organ (μm)	4291.20 ± 42.10
Thickness of the wall (μm)	1320.35 ± 10.29
Diameter of the lumen (μm)	1650.50 ± 42.37
Thickness of mucosa (μm)	925.09 ± 22.63
Number of MFs/cross section	24.17 ± 4.11
Height of MFs (μm)	902.45 ± 5.22
Width of MFs (μm)	204.51 ± 10.71
Height of the epithelium (μm)	46.04 ± 0.77
Thickness of submucosa (μm)	109.35 ± 5.72
Thickness of muscularis (μm)	311.72 ± 2.66

The mean height of the epithelium is 46.04 ± 0.77 μm. It consists of tall simple columnar absorptive cells (enterocytes) with an oval vesicular nucleus situated nearly in the middle region. These columnar cells are provided with microvilli. Small lymphocytes are scattered in the basal part of the epithelium (Figure 8.43B). Leucocytes occur in all parts of the teleosts digestive system, most extensively in the intestine, where lymphocytes, plasma cells, granulocytes, and macrophages are present in and under the epithelium. Although large lymphoid centers are lacking, many lymphoid cells, either scattered or in small groups were reported to be present in the epithelium and LP, so that intraepithelial lymphocytes are necessary for a local or mucosal immune response. Moreover, Immunoglobulin M was demonstrated in gut mucus of some fish species, which indicate the existence of a local immune system in the intestine.

The enterocytes are both absorptive and secretory in function. The brush border contributes >90% to the total intestinal surface area in *Tilapia aurea* and *Tilapia zilli* and forms the critical digestive/absorptive interface, a functional microenvironment where enzymes involved in further food breakdown are located and where absorption and transport will occur. A number of enzymes like alkaline phosphatase, disaccharidases, leucine aminopeptidase, and tri- and di-peptidases are localized to the brush border membrane in vertebrates including fishes. Most of the animal protein is digested and absorbed in the middle part of the intestine of carnivorous fishes (rainbow trout, cichlids, and *Oncorhynchus mykiss*), whereas a constant rate of absorption had been demonstrated for plant protein throughout the whole intestine of the herbivorous fish (cyprinids).

Moreover, the abilities to absorb the protein in the intestine of carnivorous fish are well-developed, but carbohydrate absorption is low compared to omnivorous and herbivorous fishes, while the absorption of protein is less developed in herbivorous fish. However, the activity of pancreatic enzymes was maximal in the anterior intestine and decreased distally. In addition, some fermented bacteria are detected in the posterior part of the intestine of carp, which supported that fermentation of the carbohydrate occurs in the intestine of carp.

The LP is formed of a connective tissue layer that is extended into the MFs. It contained blood capillaries and elastic fibers, collagenous fibers, and smooth muscle cells. Dense collagenous LP may support the intestinal epithelium. Fenestrated blood capillaries in the LP of the intestine may have a role in fluid and nutrients transport. The intestinal glands are absent in the intestine of all fishes except in two carnivorous fish species (Characiformes

and Gadidae), which are consisted of columnar cells and GCs and had mucus secretory activity. Therefore, the origin of digestive enzymes in the fish intestine is not evident as in higher vertebrates, but pinocytotic vesicles and well-developed lysosomal systems could provide the intracellular digestion of foods.

The tunica submucosa is a connective tissue layer that contains thick parallel collagenous fibers and distinct elastic fibers with blood capillaries. The submucosa thickness is 109.35 ± 5.72 μm. The tunica muscularis is a thin layer, consisted of inner circular and outer longitudinal smooth muscle fibers. The mean thickness is 311.72 ± 2.66 μm (Table 8.6). The tunica SE is thick and composed of connective tissue that contains a large number of thin elastic fibers and is covered by mesothelium (Figure 8.43C and D).

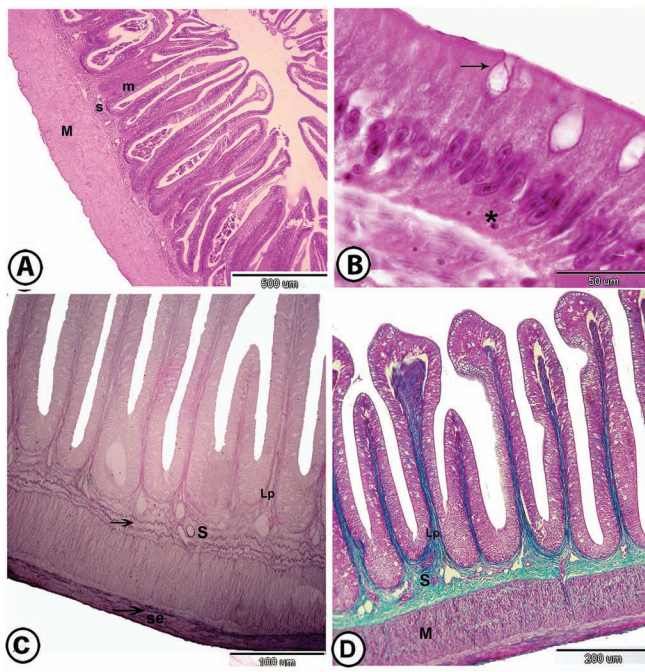

FIGURE 8.43 The histological analysis of the posterior intestine of grass carp. (A) The wall of the posterior intestine showing folded mucosa (m), submucosa (S), and muscularis (M) (HE). (B) Photomicrograph of the simple columnar epithelium of posterior intestine with GCs (arrow). Note the presence of lymphocytes in the basal part of the epithelium (asterisk) (HE). (C) The wall of the posterior intestine showing the presence of elastic fibers (arrows) in LP, submucosa (S), and thick SE (Weigert's Elastica). (D) The LP and submucosa (S) stained green, while tunica muscularis (M) stained red (Crossmon's trichrome).

Histochemical analysis (Figure 8.44A–C) revealed that the GCs are numerous and stained intensely positive with alcian blue and combined alcian blue-PAS. Also, these cells show a positive reaction to neutral mucosubstances by PAS. The presence of fewer mucous cells in the anterior intestine is probably because the need for lubrication of food is minimized in the anterior intestinal region, as it enters this region in semidigested condition. Therefore, it can be suggested that excess of mucus in this region would weaken the digestive juices as well as impair the absorption.

The posterior intestine has a high number of GCs, which play a role in the lubrication of undigested food materials for onward progression into the rectum. Their secretions may protect the delicate microvilli from the mechanical injury and allow easy transport of the ingested food materials. Also, mucopolysaccharides have many functions; it forms a diffusion barrier for various ions and fluids that allow their absorption, representing a physical barrier between the mucosa and enzymatic agents, and also act as cofactors of enzymatic hydrolysis. The presence of a large amount of acid mucin in the posterior intestine of the herbivorous grass carp could facilitate the elimination of food residues. It is well-known that the digestion of plant nutrient food is supposed to produce more residues than that of animal nutrient food does. Acid mucus might be secreted after enzymatic secretions to prevent degradation of glycoprotein; it also amplifies the viscosity and adhesive properties of the mucus, which might assist the adsorption of water-soluble molecules and particulate food materials.

In addition, many ovoid-shaped enteroendocrine cells (Figure 8.44D) are distributed in the epithelium of the posterior intestine among the enterocytes. In semithin section (Figure 8.44E), the enterocytes are tall and narrow, carried microvilli with an oval vesicular nucleus. The cytoplasm of the enterocytes contained a large number of larger vesicles than these in catfish, which might represent the pinocytotic activity to some fluid nutrients. The rounded GCs give a positive reaction to toluidine blue. The intestinal epithelium represents a cell renewal system. Cell proliferation takes place in the basal part of the MFs. The proliferation proceeds in waves through the intestinal mucosa, not simultaneous in all folds, and the old epithelial cells migrated to the top of the folds where they are probably discarded. The renewal time of the intestinal epithelium in grass carp is relatively long (10–15 days).

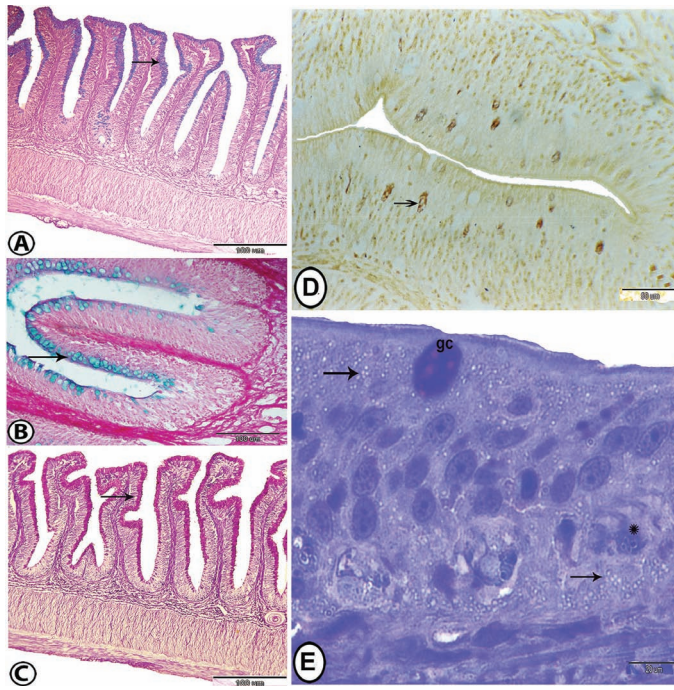

FIGURE 8.44 The histochemical analysis of the GCs of the posterior intestine of grass carp. (A) Numerous alcian blue positive GCs (arrow) (combined AB and PAS). (B) Higher magnification of the GCs (arrow) that reacted positively to alcian blue (alcian blue/Van Gieson). (C) The posterior intestine of grass carp showing numerous PAS-positive GCs (arrow) (PAS). (D) Numerous enteroendocrine cells (arrow) are present among the enterocytes (Grimelius silver stain). (E) Semithin section of the simple columnar epithelium of the posterior intestine showing a metachromatic reaction of GCs. Notice the presence of a large number of vesicles (arrows) and cell proliferation (asterisk) in the basal part of the epithelium (TB).

The presence of pinocytotic vesicles and numerous vacuoles in the posterior intestine of both herbivorous and carnivorous fishes is considered evidence of the uptake of undigested protein-like substances. This process begins with the proteins that are incorporated into pinocytotic vesicles and transported to supranuclear vacuoles where they accumulate. The vacuoles are considered as secondary lysosomes, in which ingested proteins undergo enzymatic degradation, so proteolysis proceeds by intracellular enzymes. Moreover, in species having a stomach, the enterocytic pinocytotic vacuoles may be smaller. However, the formation of large vesicles in agastric species indicated a greater capacity for enodcytosis, perhaps in relation to less effective intraluminal digestion. This type of absorption of macromolecules is

related to the lack of complete extracellular digestion and the peptic secretion did not exist in stomachless fishes. In addition, the pancreatic trypsin which is present in the intestinal lumen does not produce complete hydrolysis of protein.

Glial fibrillary acidic protein (GFAP) is a highly conserved intermediate filament protein expressed in enteric glia, satellite and Schwann cells, chondrocytes, myoepithelial cells of breast glands, human lymphocytes, Kupffer cells in rat liver, mouse bone marrow and spleen, rat endothelial cells, mouse lens epithelial cells, and medial layer cells of ascending aortic walls. GFAP expression is also recorded in the tunica muscularis and telocytes of molly fish (Figure 8.45).

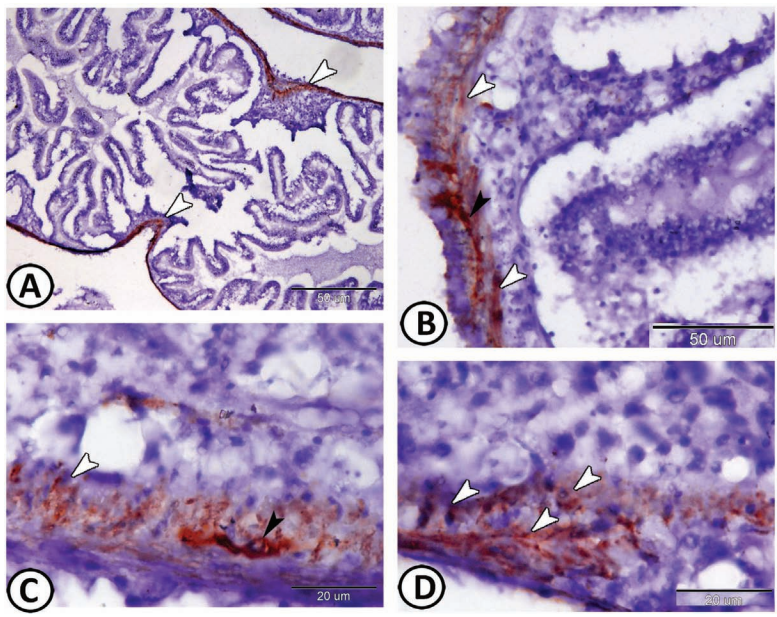

FIGURE 8.45 (A–D) GFAP expression in the tunica muscularis (white arrowheads) of molly fish. Note GFAP-immunoreactive telocytes (black arrowheads).

SEM (Figure 8.46) shows that the mucosa of the posterior intestine of grass carp runs in a direction roughly perpendicular to the long axis of the tube. The concavities between the folds are shallow. The luminal surfaces of the epithelial cells are covered by microvilli and intercalated with large-sized pores leading to mucous cells. At the meeting angels between several cells, large amounts of mucus from underlying mucous cells are extruded.

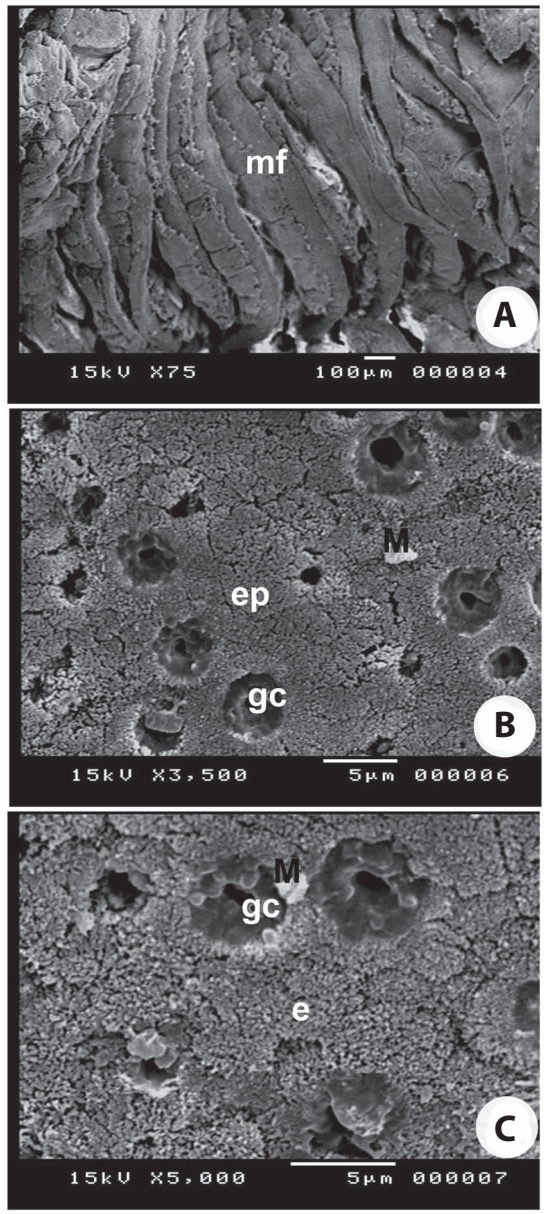

FIGURE 8.46 SEM of the mucosa of the posterior intestine of grass carp. (A) The MFs are separated by concavities. (B) Scanning electron micrograph showing the closely packed epithelial cells (EP) with GCs. Notice the presence of mucous droplets (M) on the surface. (C) The enterocytes (e) of the posterior intestine are covered by microvilli. Note the presence of large GCs and mucous droplets (M).

8.8.3 THE RECTUM

The mean diameter of the rectum is 4302.80 ± 24.45 μm, the mean thickness of the wall is 1542.19 ± 39.04 μm, and the mean diameter of the lumen was 1218.42 ± 45.03 μm. The large diameter of the lumen may relate to a temporary storage of undigested foods. Light microscopic observations reveal that the wall of the rectum of grass carp is composed of tunica mucosa, tunica submucosa, tunica muscularis, and tunica SE. The mean thickness of the mucosa is 594.56 ± 23.13 μm, which constitutes about 38.55% of the thickness of the wall. The mean number of MFs is 16 folds/cross section. The MFs appear short and thick, some of these folds contained smaller secondary folds (Figure 8.47A). The mean height of the folds is 366.15 ± 21.59 μm and their mean width is 125.0 ± 3.73 μm (Table 8.7).

TABLE 8.7 Statistical Analysis of the Measurements of Rectum of Grass Carp[a]

Measurements	Rectum of Grass Carp
Diameter of rectum (μm)	4302.80 ± 24.45**
Thickness of the wall (μm)	1542.19 ± 39.04**
Diameter of the lumen (μm)	1218.42 ± 45.03*
Thickness of mucosa (μm)	594.56 ± 23.13*
Number of mucosal folds/cross section	16.52 ± 2.79 N.S
Height of mucosal folds (μm)	366.15 ± 21.59
Width of mucosal folds (μm)	125.0 ± 3.73
Height of the epithelium (μm)	50.78 ± 1.22*
Thickness of submucosa (μm)	152.72 ± 7.21*
Thickness of muscularis (μm)	791.67 ± 26.35**

Differences reconsidered as: (N.S.): not significant if $P > 0.05$; * Significant if $P < 0.05$; ** Highly significant if $P < 0.01$.

[a]The values are represented by mean ± standard error.

The mean height of the epithelium is 50.78 ± 1.22 μm. The rectal epithelium is formed of a single layer of simple columnar cells with numerous GCs. The columnar cells bear microvilli and taper slightly toward the basal membrane with few intercellular spaces. Free lymphatic cells are present in the basal part of the epithelium (Figure 8.47B).

The LP consists of a connective tissue layer that extends into the MFs and contains collagenous fibers, fibroblasts, and smooth muscle cells. The tunica submucosa consists of connective tissue fibers rich with blood capillaries. Its

mean thickness was 152.72 ± 7.21 µm. The tunica muscularis is composed of a thick layer of smooth muscle fibers, in which the circular layer increased in thickness about three times that of the longitudinal one, followed by a thin serosal membrane (Figure 8.47A). Its mean thickness is 791.67 ± 26.35 µm (Table 8.7). The thick muscularis layer would contribute to the expulsion of fecal materials to the anus. In addition, the change of smooth muscle fibers of the intestine to striated muscles near the anus may aid in the elimination of fecal matter.

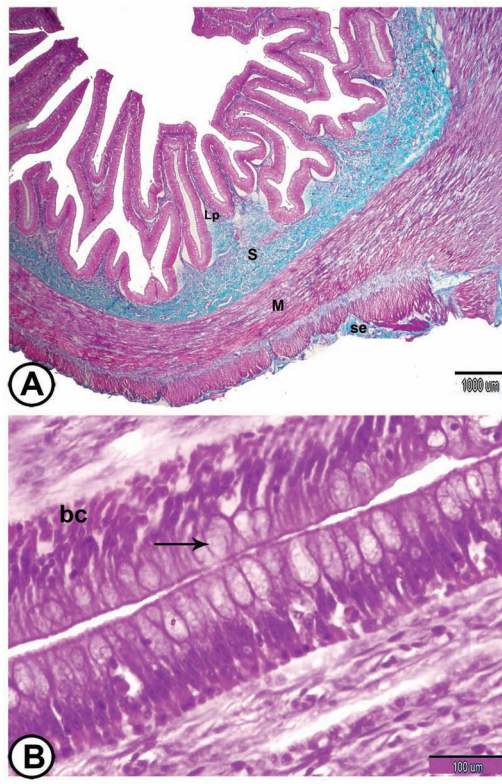

FIGURE 8.47 The histological structure of the rectum of grass carp. (A) The rectum of grass carp showing LP, submucosa (S), and SE stained green, while the tunica muscularis (M) stained red (Crossmon's trichrome). (B) Photomicrograph of the simple columnar epithelium of rectum with numerous GCs (arrow). Note the presence of basal cells (BCs) (HE).

At the anal aperture, the MFs are very few and flattened. The simple columnar epithelium with GCs of the intestine change to the stratified epithelium of the anus and the GCs are completely disappeared (Figure 8.48).

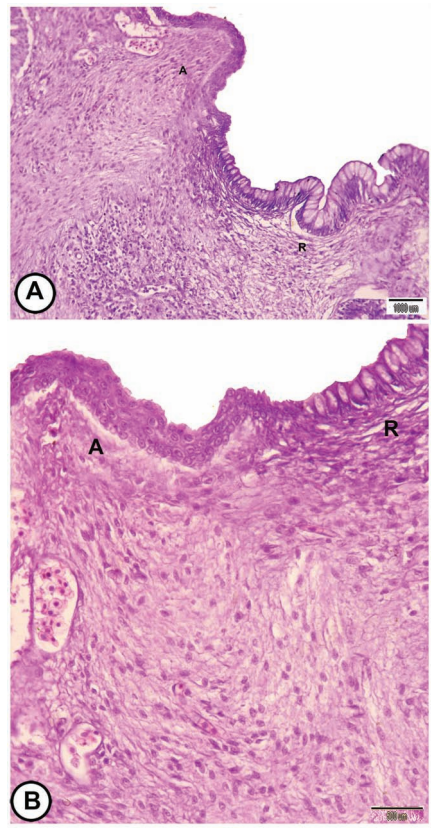

FIGURE 8.48 The junction between the rectum and the anus of grass carp stained with HE. (A) The junction of the rectum (R) to the anus (A) showing a decrease in the number of the MFs and a change of simple epithelium of the rectum to the stratified epithelium of the anus. (B) The junction of the rectum (R) of grass carp to the anus (A) showing a change of simple epithelium of the rectum to the stratified epithelium of the anus.

The histochemical analysis (Figure 8.49) reveals that the epithelium of the rectum is contained numerous GCs that reacted positive to PAS and combined PAS-alcian blue. Semithin sections show that the enterocytes are tall and narrow, carry microvilli with an oval vesicular nucleus. The cytoplasm of these cells contains some small vesicles, which indicated an absorption function to some substances, and this absorptive role is confirmed by the presence of microvilli and the height of the epithelium. The rectum of stomachless herbivorous fish is involved in the absorption of fluid and ions.

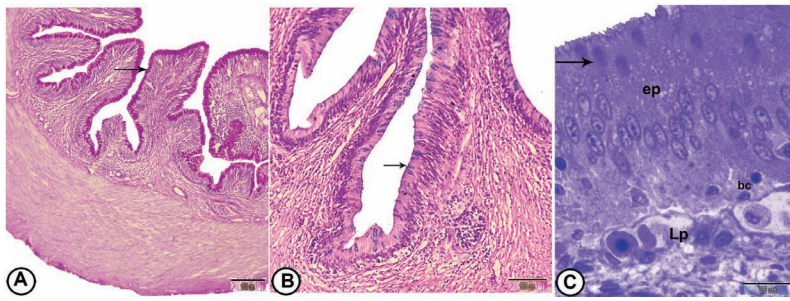

FIGURE 8.49 The histochemical analysis and semithin sections of the rectum of grass carp. (A) The rectum showing PAS-positive GCs (arrow) (PAS/HX). (B) The rectum of grass carp showing few alcian blue-positive GCs (arrow) (combined AB and PAS). (C) Semithin section through the wall of the rectum showing the mucosa composed of the simple epithelium (EP) and connective tissue LP contains many blood capillaries. The epithelium contains metachromatic GCs (arrow). Note the presence of the basal cells (BCs) in the basal portion of the epithelium (toluidine blue).

Also, the semithin sections show the presence of small GCs that give a metachromatic reaction to toluidine blue. Wandering leucocytes are present in the basal part, which might migrate to the apical part. The increasing number of GCs in the rectum may respond to an increased need for lubrication related to the expulsion of feces and protection of mucosa and can be related to the assimilation of ions and fluids. The intestinal mucosa in general acts as a selective barrier to the nutrients and also prevents many toxins and pathogens.

Scanning electron microscopic observations (Figure 8.50) reveal that the rectal mucosa of grass carp is characterized by the presence of wavy folds. The mucosal lining is supported by densely backed pentagonal columnar cell contours. The apices of the epithelial cells are covered with prominent microvilli. Large amounts of mucous are extruded between the enterocytes.

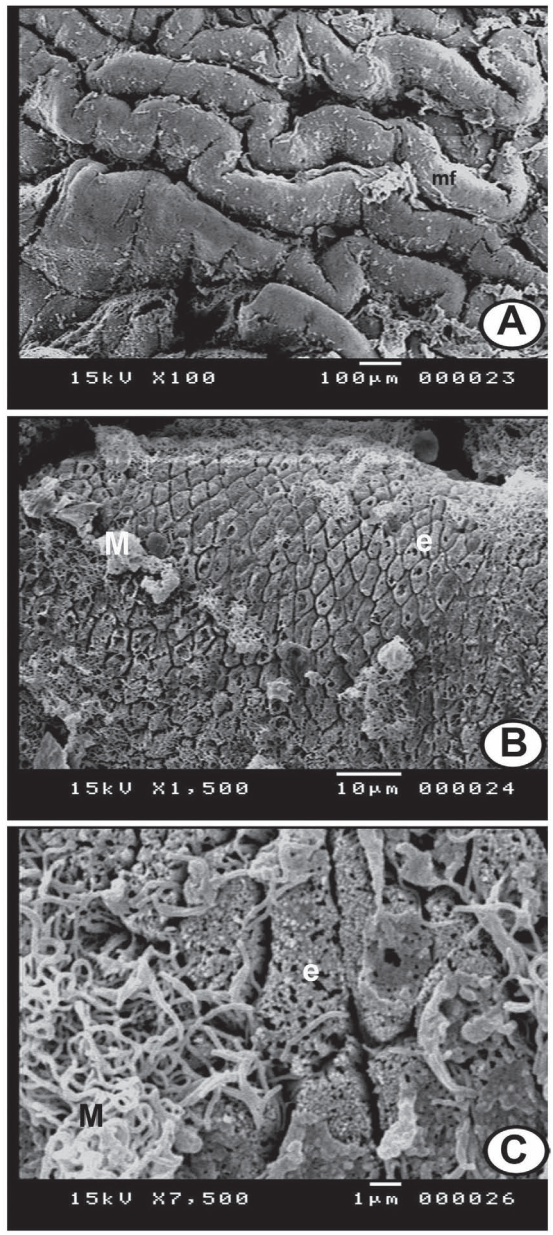

FIGURE 8.50 SEM of the rectum of grass carp. (A) The mucosa showing a wavy arrangement of MFs. (B) Scanning electron micrograph showing the pentagonal contour of the enterocytes. (e) Note the presence of large mucous droplets (M). (C) The enterocytes (e) are covered by microvilli with a large amount of mucous droplets (M) on the surface.

KEYWORDS

- **esophagus**
- **gastrointestinal tract**
- **tunica mucosa**
- **intestinal bulb**
- **gastric glands**

BIBLIOGRAPHY

Abd-Elhafez, E. A.; Mokhtar, D. M.; Abu-Elhamed, A.; Hassan, A. H. S. Comparative histomorphological studies on oesophagus of catfish and grass carp, *J. Histol.* **2013,** *2013*, 10, article ID 858674.

Marchetti, L.; Capacchietti, M.; Sabbieti, M. G.; Accili, D.; Materazzi, G.; Menghi, G. Histology and carbohydrate histochemistry of the alimentary canal in the rainbow trout *Oncorhynchus mykiss, J. Fish Biol.* **2006,** *68,* 1808–1821.

Abbate, F.; Guerrera, M. C.; Montalbano, G.; Carlos, F. D.; Suárez, A. A.; Ciriaco, E.; Germanà, A. Morphology of the European sea bass (*Dicentrarchus labrax*) tongue, *J. Microsc. Res. Tech.* **2012**, 75(5), 643–649.

Mokhtar, D. M.; Abd-Elhafez, E. A.; Hassan, A. H. S. A histological, histochemical and ultrastructural study on the fundic region of the stomach of Nile catfish (*Clarias gariepinus*), *J. Cytol. Histol.* **2015,** *6*(4), 341.

Mokhtar, D. M.; Abd-Elhafez, E. A.; Hassan, A. H. Light and scanning electron microscopic studies on the intestine of grass carp (*Ctenopharyngodon idella*): I-Anterior Intestine*, J. Aquacult. Res. Dev.* **2015,** *6*(11), 374.

Mokhtar, D. M.; Abd-Elhafez, E. A.; Hassan, A. H. Light and scanning electron microscopic studies on the intestine of grass carp (*Ctenopharyngodon idella*): II-Posterior Intestine, *J. Aquacult. Res. Dev.* **2015,** *6*(11), 380.

CHAPTER 9

Glands Associated with the Digestive Tract

ABSTRACT

The liver is a large digestive gland composed of parenchymal cells and lattice fibers. The fish hepatic parenchyma is not arranged into distinct lobules. Three patterns of organization of fish hepatic parenchyma are recognized. The first pattern is composed of hepatocytes that are radially arranged around the central vein. The second arrangement called a tubular pattern, in which the sinusoids form a network around the hepatic tubules. The third arrangement is present in some fresh and marine teleosts, the hepatocytes lie in anastomosing lamina around the central vein. Serial paraffin section of the liver identified different kinds of vascular–biliary structures as follows: first, pancreatic–venous–biliary–arteriolar tracts (P-VBAT); second, venous–biliary–arteriolar tracts (VBAT); third, pancreatic–venous–biliary tracts (P-VBT); fourth, venous–biliary tracts (VBT); fifth, venous–arteriolar tracts; sixth, isolated veins named as venous tracts; seventh, isolated bile ducts (BDs), named as biliary tracts; eighth, biliary–arteriolar tracts; ninth, pancreatic–biliary tracts (P-BT); tenth, pancreatic–venous tracts (P-VT). Macrophages aggregates are frequently associated with VBT and P-BT. The hepatic satellite cells (perisinusoidal cells) are observed in many species. The sinusoids are lined by endothelial and Kupffer cells (in some species). The biliary duct system is constituted of bile canaliculi, ductules, and BDs. Telocytes with their characteristics telopodes are located around the BDs. The pancreas of fish is a lobulated compound acinar gland, divided into exocrine and endocrine portions. Exocrine pancreatic tissues consist of scattered serous acini and is observed in two forms: first, disseminated in the spleen tissue, in mesentery around the intestine and intestinal bulb; and second, intrahepatically, around the branches of the portal vein. Two alveolar cell types are present in pancreatic acini: centroacinar cells and typical pyramidal acinar cells. Pancreatic stellate cells are demonstrated in the perivascular and

the periacinar space of the pancreas. The acini show high lipase and alkaline phosphatase activity and moderate activity for acid phosphatase. The duct system is composed of the intralobular duct, interlobular pancreatic duct, and the main duct. The endocrine parts of the pancreas are organized as lightly staining Langerhan's islets between exocrine acinar cells.

9.1 LIVER

The fish liver is considered a key organ that controls various life functions: metabolism of protein, lipid, and carbohydrates, bile formation, glycogenolysis, and detoxification. In addition, it acts as a center for the storage of many substances, mainly glycogen and lipid. The fish liver is considered an interesting model for studying the interaction between environmental factors and the health of the fish as it reflects the status of the aquatic ecosystem. The liver structure varies between fish species. Moreover, obvious differences exist within the same family, so a definite interest in studying hepatic structure for a particular species. In addition, the liver plays a major role in the process of vitellogenesis and energy production during spawning as hepatocytes show differences according to species, sex, age, spawning season, and nutritional state.

Grossly, the liver of grass carp consists of two lobes. However, the liver is divided into three lobes into many Teleostei species, while lobulation is not found in some Teleostei. The liver of grass carp, guppy, and molly fish (Figure 9.1) had no definite shape or size as it adapted to the space available between the other visceral organs. It consists of two thick and wide lobes (left and right) with a long thin process that extends from the right lobe to the posterior part of the body cavity and encircles the whole digestive tube and occupies a position between the intestinal loops. The gallbladder is located between the liver and the anterior intestine. The color of the liver in carnivores fish is reddish-brown and in herbivores is a lighter brown.

Histologically, the liver is covered by a thick connective tissue capsule (48.23 ± 2.69 μm), made up mainly of collagenous fibers. The outer part of the capsule is covered by a thin peritoneal envelope (Figure 9.2A). Gomori's stain reveals the presence of a network of reticular fibers that encircles the sinusoids between the hepatic lamina and is concentrated around the blood vessels (BVs) (Figure 9.2B). The liver of grass carp is a compound organ in the form of hepatopancreas. The liver is not organized into lobules; their outlines are diffuse in teleosts. Although all the structural components

[hepatocytes, BVs, and bile ducts (BDs)] are present in the liver of fish, they are differently organized in the hepatic parenchyma compared with mammals. The pancreatic tissue in the form of serous cell clusters (exocrine tissue) is penetrated into the liver along with the portal vein. In addition, islands of pancreocytes scattered throughout the liver, without an apparent regular pattern (Figure 9.2C).

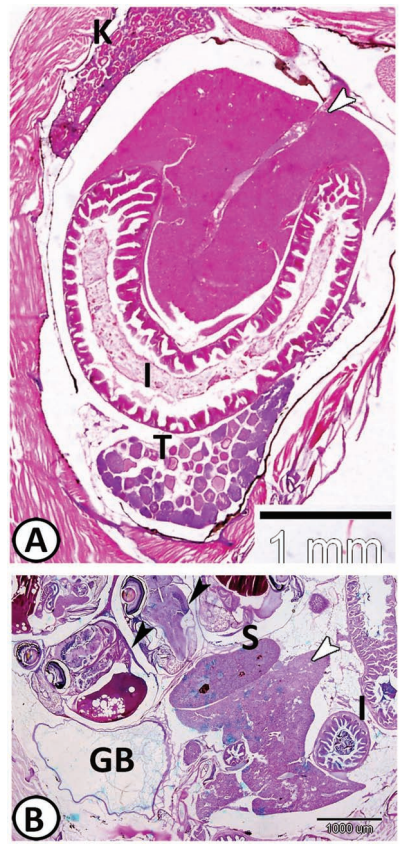

FIGURE 9.1 (A, B) General view of the liver of guppy and molly, respectively. The liver (white arrowheads) is occupied most of the abdominal cavity and is related to the intestine (I), gas bladder (GB), and spleen (S). Note testis (T) in guppy, kidney (K), and embryos in the uterus of molly (black arrowheads) (HE and PAS-AB/HX, respectively).

The hepatopancreatic acini encircle a vein that ramified up smaller. The hepatopancreatic acini encircled a vein that ramified up smaller branches, finally communicating with the network of hepatic sinusoids (Figure 9.2D).

The hepatocytes are organized in a continuous cell mass, interrupted by sinusoids, so when seen at light microscopy they appear as a meshwork of two (or more) hepatocytes-thick plates. Also, the sinusoids were disposed radially of around truly isolated veins (i.e., not coupled to arterioles or BDs) (Figure 9.2E). The sinusoids are lined by endothelial cells (ECs) as well as Kupffer cells (KCs).

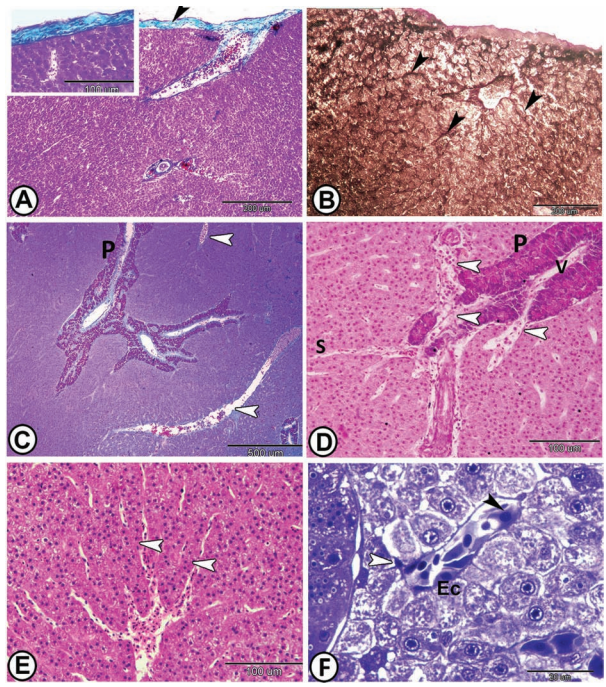

FIGURE 9.2 General structure of the liver of grass carp. (A) The liver is surrounded by collagenous c.t. capsule (arrowhead, inserted figure) (Crossmon's trichrome). (B) Argyrophilic reticular fibers (arrowheads) outline the hepatic sinusoids and large BVs and extend throughout hepatic parenchyma (Gomori's silver stain). (C) The pancreatic tissues (P) were distributed throughout the liver parenchyma in form of hepatopancreas. Note the distribution of many BVs (arrowheads) randomly (Maldonado's stain). (D) The hepatopancreatic acini (P) encircles a vein (V) that ramifies up smaller branches (arrowheads), finally communicating with the network of hepatic sinusoids (S) (HE). (E) The hepatocytes tunnel by sinusoids to form two or more cell-thick plates (arrowheads) (HE). (F) The sinusoids are lined by ECs and large branched KCs (black arrowhead). Note the hepatic stellate cell (white arrowhead) (TB).

The KCs are stellate in shape with a large oval dark nucleus that project into the lumen of sinusoids (Figure 9.2F). KCs are situated in the hepatic sinusoids in grass carp, spotted pimelodus, and Juvenile crocodile. However,

no classical KCs are present in the liver of *Kareius bicoloratus* and *Salmo trutta fario*. KCs play an important role in removing degenerated blood cells, degrading hemoglobin, and eliminating toxic and foreign substances by the presence of many lysosomes in their cytoplasm. In addition, tubulosomes are evident in the cytoplasm of KCs in association with phagosomes. These structures may be specialized lysosomes involved in the breakdown of phagosomal contents.

9.1.1 THE SPATIAL DISTRIBUTION OF VASCULAR–BILIARY COMPONENTS

The input of afferent vessels is not only occurred in the hilum but pierced the liver of grass carp at various points. The vascular elements and biliary channels are randomly distributed throughout the hepatic parenchyma. Serial paraffin sections of the liver identify isolated vessels or BDs and/or associations of two to three kinds of vascular–biliary structures, as follows.

(1) Pancreatic–venous–biliary–arteriolar tracts (P-VBAT) that are characterized by the association of pancreocytes with an afferent vein, plus BDs, and small arteries (Figure 9. 3A and B).
(2) Venous–biliary–arteriolar tracts (VBAT) (rarely observed) (Figure 9.3C).
(3) Pancreatic–venous–biliary tracts (P-VBT) (Figure 9.3D).
(4) Venous–biliary tracts (VBT) (Figure 9.3E);
(5) Venous–arteriolar tracts (VAT) (Figure 9.3F).
(6) Isolated veins named as venous tracts (VT), which were most frequent and most of them being part of the venous efferent system) (Figure 9.3G).
(7) Isolated BDs, named as biliary tracts (BT) (Figure 9.3H). The BT is quite frequent, either seen in longitudinal or in cross sections (in the form of a group of two to three ducts) sharing adventitial connective tissue.
(8) Pancreatic–venous tracts (P-VT) that consisted of an incomplete acinar sleeve, encircled a vein (Figure 9.3I).
(9) A longitudinal section of BD associated with pancreocytes, forming pancreatic– biliary tracts (P-BT) (Figure 9.4A).
(10) Biliary–arteriolar tracts (BAT) (rare) (Figure 9.4B). Isolated arterioles or arteriolar tract (AT) are not observed in grass carp.

The presence of VBAT has only been recorded in the Atlantic croaker, *Micropogon undulatus*, Atlantic salmon, rainbow trout, brown trout, grass carp, and guppy (*Poecilia reticulata*). However, a reduced arterialization of the liver of both guppy fish and grass carp is noticed, as no isolated arterioles and the arterioles, in general, are rare, contrasting with an over predominance of distribution of the venous vascularization. The distribution of the vascular pattern is correlated with environmental/physiological adaptations that may implicate different liver needs as to receiving lower/higher arterialized blood.

Macrophages aggregates are well-distinct, which are associated with VBT and P-BT. Macrophage aggregates have been suggested as reliable biomarkers for water quality as they increase in size or number in a condition of environmental stress. Macrophage aggregates (MAs) are widely distributed in the liver of many fish species. While in some species, they are commonly associated with pancreatic–venous complexes, such as those in Nile tilapia and *Geophagus brasiliensis*. The number and contents of MAs are differed according to species, health status, and age.

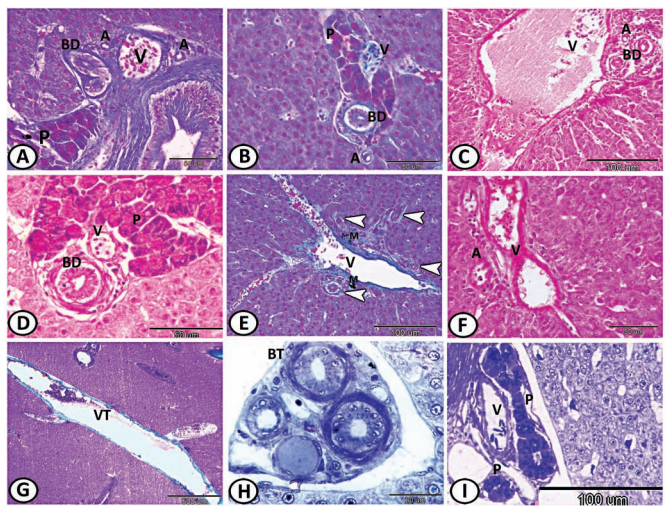

FIGURE 9.3 The spatial distribution of vascular–biliary components of grass carp. (A, B) Pancreatic–venous–biliary–arteriolar tracts (P-VBAT) are composed of pancreocytes (P) with an afferent vein (V), plus biliary ducts (BDs) and small arteries (A) (Maldonado's stain). (C) VBAT is formed of a vein branch (V), an artery branch (A), BDs (HE). (D) P-VBT is characterized by the association of BD and vein (V) with pancreocytes (P) (HE). (E) VBT; four BDs (arrowheads) are associated with vein (V). Note, MM aggregates (M) in the vein adventitia (Maldonado's stain). (F) VAT is a combination of artery (A) and vein (V) (HE). (G) Isolated veins are named as VT (Crossmon's trichrome). (H) Group of isolated BDs, named as BT (TB). (I) P-VT consists of an incomplete sleeve of the pancreas (P) around vein (V) (TB).

The intrahepatic BD is prominent, lined by simple columnar epithelium surrounded by a connective tissue layer mainly of collagen fibers, followed by a thin circularly arranged layer of smooth muscle fibers (Figure 9.4C). The apical surfaces of the ductal cells are covered by PAS-positive brush borders (Figure 9.4D). The BDs are surrounded by telocytes (TCs) that are demonstrated as small branched cells, darkly stained by toluidine blue, and extend their thin processes around the BDs (Figure 9.4E).

Eosinophilic granule cells/mast cells are located around the isolated BD (Figure 9.4F) or in the stromal connective tissue around the BAT (Figure 9.4G). These cells are characterized by rounded cell bodies of various size with an eccentric nucleus and eosinophilic granules with HE, as well as they show metachromatic reaction with toluidine blue. Moreover, these cells are observed in the liver in *Ohrid trout* and *Nile tilapia*. However, no eosinophilic granular cells are observed in some fish species as a guppy. So, their normal presence in the liver is species specific.

The rodlet cells (RCs) are observed in all liver samples. Most RCs (90%) are detected in close contact with the endothelium of large veins (Figure 9.4H) and 10% in peripancreatic connective tissues (Figure 9.4I). They are mostly in the mature stage and characterized by oval to rounded shape with intracytoplasmic rodlets or granules and surrounded by a thick capsule. The location of RCs in the endothelium of BVs supports the suggestion that RCs secrete some enzymatic and proteinous substances to the circulation. Several functions were encountered by these cells. RCs are considered as migrating secretory cells. However, some authors observed an increase in their number in parasitic infestation and considered them as nonspecific immune cells, which involved in immunity. Other authors reported them a type of eosinophilic granulocyte. A regulatory role is also associated with these cells in water or electrolyte balance, ion transportation, and osmoregulation. Moreover, these cells were observed in many organs of fish include heart, kidney, gills, skin, pancreas, and gut. In addition, they were recorded in the liver of brown trout and in some nonsalmonid species.

Hepatocytes are polyhedral cells with large spherical centrally to eccentrically situated nuclei with a prominent dark nucleolus. Several small vacuoles for lipid droplets (LDs) are recorded in their cytoplasm. Different staining affinity of hepatocytes for toluidine blue is observed throughout the parenchyma (Figure 9.5A). The hepatocytes' cytoplasm are strongly PAS-positive (Figure 9.5B). By Best's carmine, the glycogen appears as large deep red deposits identified throughout the parenchyma (Figure 9.5C). The presence of glycogen may indicate the ability of fish to synthesis or breakdown of glycogen according to metabolic needs.

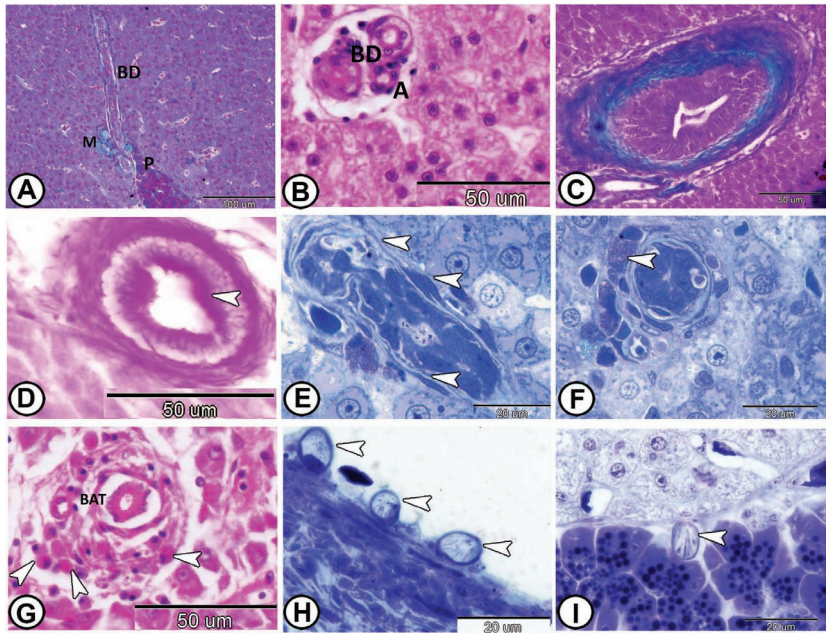

FIGURE 9.4 BD and associated structure of grass carp. (A) A longitudinal section of the BD runs to the pancreatic tissues (P). Note the presence of macrophage aggregates (M) (Maldonado's stain). (B) BAT; arteriole (A) with BDs (HE). (C) Intrahepatic BD is surrounded by collagenous fibers and smooth muscle layers (Crossmon's trichrome). (D) Isolated BD shows PAS-positive apical border (arrowhead) (PAS). (E) The BD is surrounded by TCs (arrowheads) (TB). (F) The BD is surrounded by metachromatic mast cells (arrowhead) (TB). (G) Mast cells (arrowheads) in the stromal tissues around BAT (HE). (H) RCs (arrowheads) are attached to the endothelium of the vein (TB). (I) RC (arrowhead) is located in peripancreatic connective tissue (TB).

Both hepatocytes and sinusoids express strong ATPase-positive reaction in the form of brown deposits (Figure 9.5D). Moreover, the hepatocytes show a strong reaction for acid phosphatase (Figure 9.5E), as well as alkaline phosphatase (Figure 9.5F). Alkaline phosphatase activity in hepatocytes is concerned with the deposition of glycogen and the absorption of glucose. Acid phosphatase is one of the marker enzymes for lysosomes. The occurrence of acid phosphatase activity in the liver may aid in detoxification and other physiological processes. ATPase works in the collaboration of alkaline phosphatase. The ATPase plays a major role in maintaining the functional integrity of the cell membrane and other cellular activities.

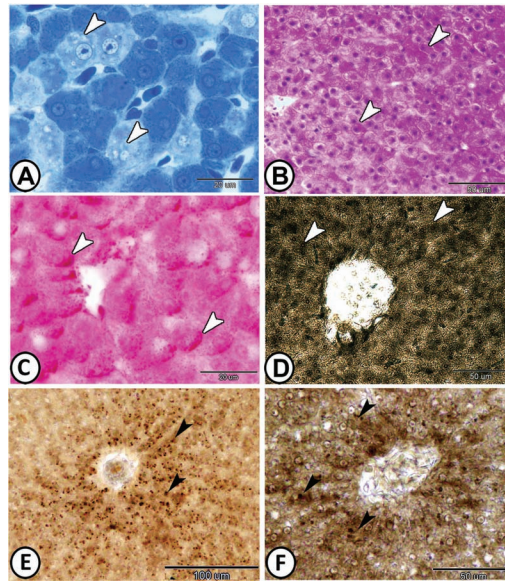

FIGURE 9.5 Hepatocytes histochemistry and enzyme histochemistry in the liver of grass carp. (A) Hepatocytes (arrowheads) with rounded central to eccentric nuclei (TB). (B) Hepatocytes are strongly PAS-positive (arrowheads) (PAS-HX). (C) Large glycogen deposits (arrowheads) are identified throughout the cellular parenchyma (Best's carmine). (D) Strong positive reaction for ATPase (arrowheads) in both hepatocytes and sinusoids. (E) Strong acid phosphatase activity (arrowheads) (Gomori lead method). (F) Strong activity for alkaline phosphatase (arrowheads) (Gomori calcium nitrate).

The aggregates of pigmented macrophages are commonly observed in the liver of grass carp and they concentrated in the adventitial layer of venous vessels (Figure 9.6A), between hepatocytes (Figure 9.6B), and around the BD (Figure 9.6E). The MAs are heterogeneous in composition, containing iron, melanin, lipofuscin, lipid, and glycogen. The MAs show LDs and dark black deposits mostly for melanin pigments (Figure 9.6A and B). They are characterized by golden-brown cytoplasm with HE methods (Figure 9. 6C). In addition, these cells give a positive reaction with PAS (Figure 9.6D). Their lipofuscin contents appeared pink with Long Ziehl-Neelsen (Figure 9.6E). Also, the iron contents of these aggregates appear blue by Perls Prussian blue (Figure 9.6F). Hemosiderin is a waste product of iron metabolism and occurs as yellow to brown intercellular granules, which often phagocytize senescent red blood cells. The clinical studies have shown the association of MAs with a range of highly resistant intracellular bacteria and parasites. Furthermore, these aggregates may be a site of primary melanogenesis rather than melanin storage.

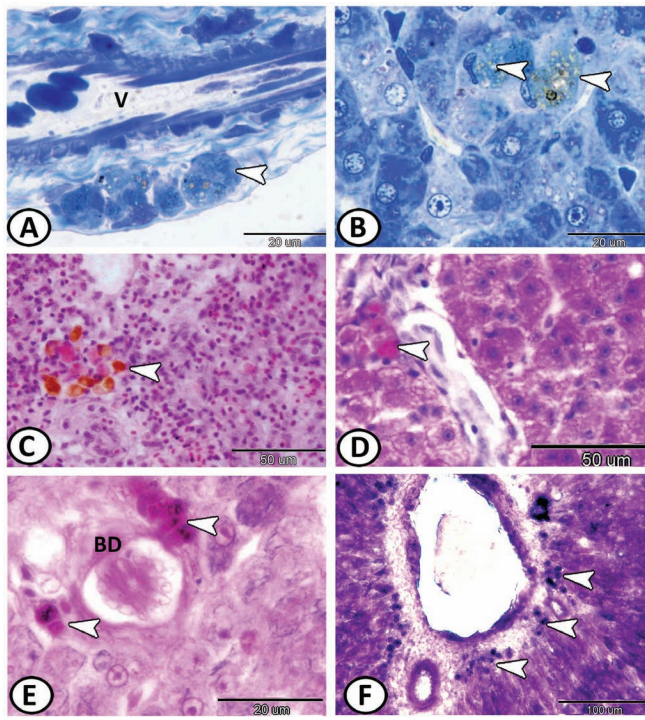

FIGURE 9.6 The MM aggregates in the liver of grass carp. (A) Pigmented macrophages (arrowhead) in the adventitia of large vein (V) (TB). (B) Pigmented macrophages (arrowheads) are between hepatocytes (TB). (C) MAs (arrowhead) are golden brown with HE. (D) MAs (arrowhead) show a PAS-positive reaction (PAS-HX). (E) Positive lipofuscin contents (arrowheads) appear pink with Long Ziehl-Neelsen around a BD. (F) The iron contents of these aggregates (arrowheads) appear blue by Perls Prussian blue.

9.1.2 SCANNING ELECTRON MICROSCOPIC EXAMINATION OF THE LIVER

In grass carp, the hepatic parenchymal cells are arranged in plates, separated by the hepatic sinusoids (Figure 9.7A and B). The ECs of the sinusoids are highly fenestrated. The KCs are observed in the lumen of sinusoids and possessed many filopodia that penetrated the fenestrae (Figure 9.7C– F). The hepatocytes exhibit microvilli toward the perisinusoidal space (Figure 9.7E and F).

The perisinusoidal space [space of Disse (SD)] contains stellate hepatic cells (Ito or perisinusoidal cells). These cells are characterized by elongated

to ovoid cell body and many long, slender dendritic cytoplasmic processes direct and wrap around the sinusoids. Some of these processes extend across the perisinusoidal space and establish contact with neighboring hepatocytes (Figure 9.7G). This vital contact may facilitate the intercellular transport of cytokines and soluble mediators. Desmin in these cells was detected in some fish species, which is an intermediate filament typical of contractile cells. Also, Ito cells (ICs) are included in collagen production that responsible for fibrosis associated with the natural degeneration of biliary tree in brook lamprey. ICs are fat-storing cells and source of Vitamin A in brown trout.

TCs with long cell processes [telopodes (TPs)] are extended between the hepatocytes. RCs are also recorded between the hepatocytes that are characterized by long cytoplasmic rods (Figure 9.7H). A pancreatic tissue encircled a vein is observed in the hepatic parenchyma (Figure 9.7I). The presence of such cells in the adventitia of veins is a guide to accurately identify the portal venous branches in many species. This approach resulted in the notion that the isolated veins observed in the histological section represent efferent veins, collecting blood from the nearby sinusoids.

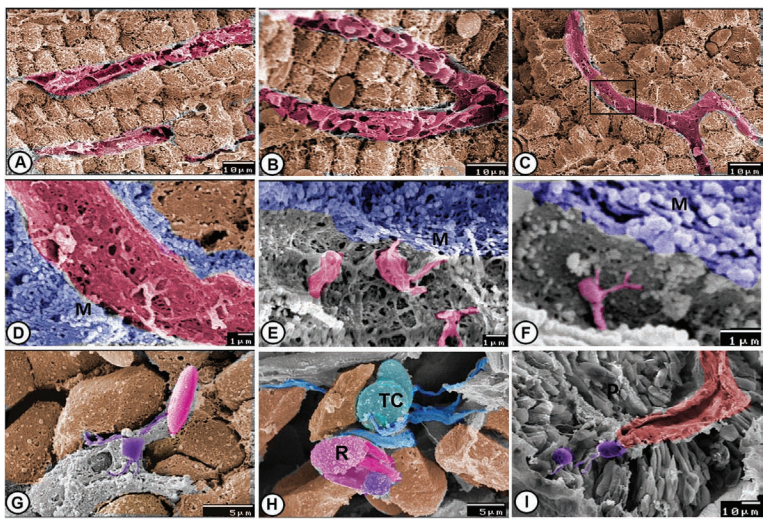

FIGURE 9.7 Scanning electron microscopy of the liver of grass carp. (A, B) The hepatocytes are arranged in plates (orange), separated by the hepatic sinusoids (red). (C, D) The sinusoidal ECs are highly fenestrated (red). (E, F) The KCs (pink) have many filopodia that penetrate the fenestrae of sinusoids. The blue color in (D–F) indicates the microvilli (M) of hepatocytes. (G) The SD contains ICs (violet) that establishes contact with neighboring hepatocytes (orange). Note the red blood cell (pink) in the sinusoidal lumen. (H) TCs with long cell processes (blue) extend between the hepatocytes (orange). RCs (R) are characterized by long cytoplasmic rods (pink). (I) A pancreatic tissue (P) encircles a vein (red). Note PSCs (violet).

9.1.3 TRANSMISSION ELECTRON MICROSCOPY

9.1.3.1 THE HEPATOCYTES

They display a polygonal shape with a single spherical euchromatic nucleus. Their cytoplasm is characterized by a large amount of smooth endoplasmic reticulum, spherical lysosomes, a large number of mitochondria, and different sized LDs (Figure 9.8A). In the hepatic cell/capillary interface, there is a classical SD, with a width of 1.29 + 0.37 μm. The ECs of the sinusoids contain a spindle-shaped nucleus surrounded by thin cytoplasm contained macropinocytotic vesicles. Their attenuated cytoplasmic extensions have fenestrations (Figure 9.8B).

9.1.3.2 THE KUPFFER CELLS

KCs are pleomorphic cells, situated in the hepatic sinusoids (Figure 9.8B–F). They project slightly to the sinusoidal lumen and established close contact with ECs (Figure 9.8B). They possess irregular cell surfaces and contained lysosomes, phagosomes in the form of vacuoles varying widely in diameter, density, and shape as well as few fat droplets (Figure 9.8D and E). Small groups of parallel tubular structures can be observed in their cytoplasm termed tubulosomes that arrange in longitudinal profiles in the vicinity of lysosomes (Figure 9.8F). The nuclei of the KCs are indented and frequently eccentrically located. Clumps of heterochromatin are distributed throughout the nuclei and form distinct rim along with the nuclear envelope (Figure 9.8C–F).

9.1.3.3 THE INTRAHEPATOCYTIC MACROPHAGES AND MELANOMACROPHAGES

The macrophages are characterized by many cytoplasmic processes. Their cytoplasm is characteristically displayed many small dense vesicles (lysosomes), phagocytic vacuoles, and huge dense bodies with heterogeneous content that represented phagososomes (Figure 9.9A). Moreover, melanomacrophages (MMs) are characterized by pseudopodia-like processes, eccentric nucleus, and their cytoplasm contains numerous melanin-like granules (Figure 9.9B).

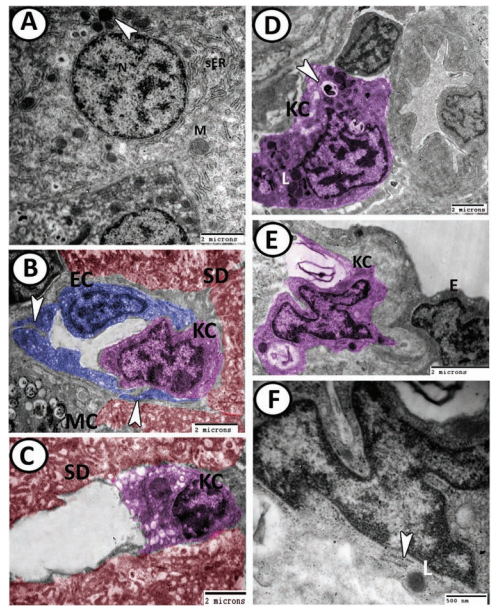

FIGURE 9.8 Digital colored TEM micrographs of the hepatocytes and KCs in the liver of grass carp. (A) Hepatocytes with large round nucleus (N). Their cytoplasm contains mitochondria (M), sER, and lysosomes (arrowhead). (B) Hepatic sinusoids are lined with EC (blue) and KC (violet) and surrounded by space of Disse (SD) and MMs. Note fenestration (arrowheads) in the ECs. (C) KC (violet) with its body connecting the SD that packed with microvilli (red). (D) KCs (violet) contain many lysosomes (L) and phagosomes (arrowhead). (E) KC (violet) exhibits an irregular shape and associated with endothelium (E) in the sinusoidal wall. (F) Higher magnification of (E) showing the cytoplasm of KCs contains tubulosomes (arrowhead) in the vicinity to lysosomes (L).

9.1.3.4 THE DENDRITIC-LIKE CELLS

They are wandering lymphocytes (LCs) located in the sinusoidal lumen and perisinusoidal connective tissue adjacent to ECs and associated with macrophages and LCs. Dendretic cells (DCs) are characterized by irregular shape, obviously high nuclear to cytoplasmic ratio, multiple dendrites-like cytoplasmic processes, heterochromatic nucleus, few cytoplasmic Birbeck-like granules, and vesicles located mainly in their processes. The Birbeck-like granules are electron-dense and exhibit different sizes and shapes (round and tennis-racket) (Figure 9.9C and D). Figure 9.9D may illustrate further phagocytosis of degenerated endothelium. DCs are identified in some teleosts as rainbow trout, salmonids, medaka, zebrafish, and channel catfish in different

tissues, such as kidney, spleen, and gills. They share many functional and morphological features reported in mammals. DCs are one of the antigen-presenting cells with dendritic morphology, motility, phagocytic ability, and strong T cell stimulatory properties.

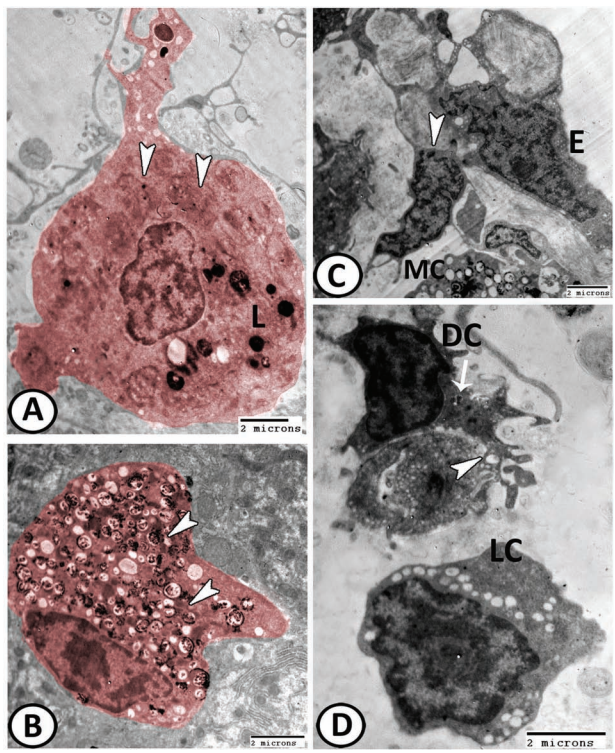

FIGURE 9.9 Digital colored TEM micrographs of the macrophages and dendritic-like cells in the liver of grass carp. (A) Macrophage (orange) with many lysosomes (L) and pahgosomes (arrowheads). (B) MM (orange) contains many melanin pigments (arrowheads). (C) Dendretic-like cell (arrowhead) in perisinusoidal c.t. extends their processes to neighboring endothelium (E) and melanomacrophage cell (MC). (D) DC is in the sinusoidal lumen in the vicinity of lymphocytes (LC). Note the connection of their dendritic processes with degenerated endothelium and the presence of vesicles (arrowhead) in the processes and few granules (arrow) in the cytoplasm.

9.1.3.5 THE ITO CELLS

These cells are characterized by their location near the SD or intercalated between hepatocytes, flattened cytoplasmic processes, the absence of

microvilli, and the eventual presence of many membranes and nonmembrane bound LDs. Their nuclei exhibit irregular nuclear envelope with euchromatin and clumps of heterochromatin (Figure 9.10A and B).

9.1.3.6 THE RODLET CELLS

RCs are characterized by a thick capsule, ovoid-shaped rodlet granules or inclusions, and a basally located nucleus. The rodlet granule consists of a central electron-dense core, surrounded by a less electron-dense matrix (Figure 9.10C).

9.1.3.7 THE MAST CELLS/EOSINOPHILIC GRANULE CELLS

Eosinophilic granule cells are found in the connective tissue stroma around the BD. It is characterized by a centrally located nucleus and many electron-dense cytoplasmic granules (Figure 9.10D).

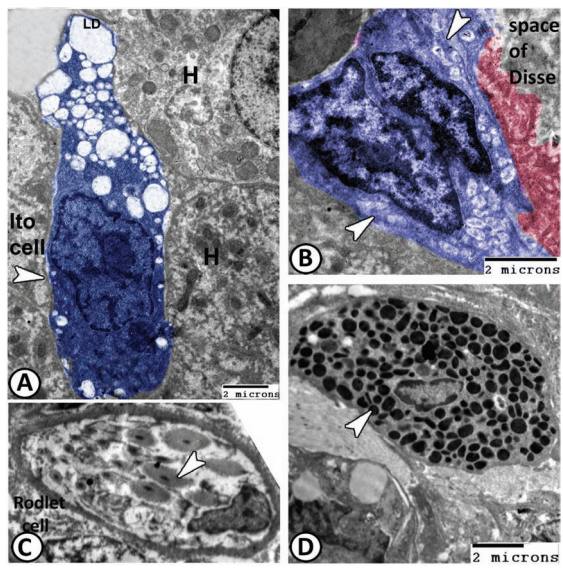

FIGURE 9.10 Digital colored TEM micrograph of Ito, rodlet, and mast cells in the liver of grass carp. (A) IC (blue, arrowhead) is situated between hepatocytes (H). Note the presence of many LDs. (B) Two ICs (blue, arrowheads) with many LDs are adjacent to the SD (red). (C) RC shows rodlet granules (arrowhead). (D) Mast cell with many electron-dense granules (arrowhead).

9.1.3.8 THE TELOCYTES

TC is a characteristic type of interstitial cells that have a wide range of biological functions in different tissues and organs of humans and other mammals.

They are observed in the interstitial connective tissues around the BDs and BVs of grass carp (Figure 9.11A–C). Their characteristic features resemble those of mammals as they appear as elongated cells with spindle cell body and two cytoplasmic processes called TPs. The TPs are subdivided into a dilated segment called podomes and a thin one called podomers. The podomes contain secretory vesicles. Their nuclei are elongated and mainly euchromatic except for a thin rim of heterochromatin attached to the nuclear envelope. The cytoplasm contains mitochondria and caveolae. TPs of different TCs are connected with each other (Figure 9.11B and C) and establish close contact with endothelium and IC (Figure 9.11A).

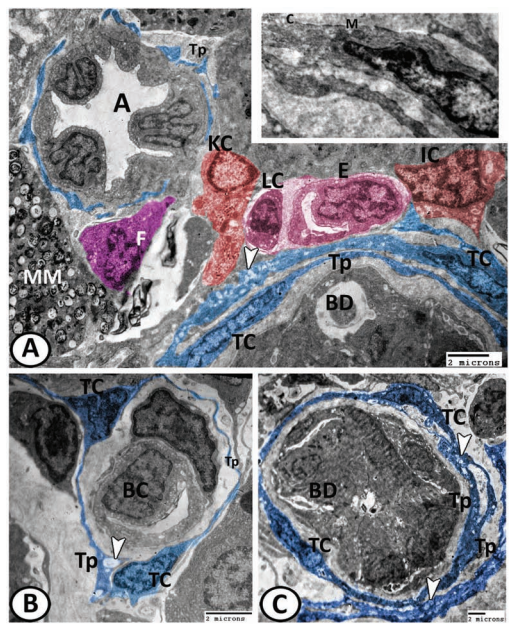

FIGURE 9.11 Digital colored TEM micrograph of TCs in the liver of grass carp. (A) BD is surrounded by TCs (blue) and their TPs. TC contains mitochondria (M in the inserted figure) and caveolae (C). Note the presence of fibrocyte-like cells (F) and MM. Lymphocyte (LC) is situated in a sinusoidal lumen, adjacent to KC. Ito cell (IC) and sinusoidal endothelium (E) establish direct contact with TC. (B) Two TCs surround the blood capillary (BC) and connected with their TPs.(C) TCs with their TPs encircle a BD. Note the presence of many secretory vesicles (arrowheads) in the podoms of TPs in (A–C).

9.1.4 THE BD SYSTEM

The bile canaliculi (bc) (Figure 9.12A) are formed by the opposition of two to three hepatocytes. Adjacent to the lumen, the cells are connected by distinct tight junctions, followed by desmosomes. Numerous microvilli are protruded from the hepatocytes into the lumen of the bc. The wall of the bile ductule (Figure 9.12B) is constituted by two elongated flat biliary epithelial cells, which join together by evident tight junctions, and desmosomes. The BD is constituted by five to six pyramidal cells with basally located nuclei that some of them contained single nucleoli. The most characteristic ultrastructural features of these cells are the presence of basal lamina, distinct microvilli projected into the lumen, and evident tight junctions followed by desmosomes (Figure 9.12C). The cytoplasm of these epithelial cells contains numerous mitochondria. The BDs are surrounded by smooth muscle cells (SMCs) and TCs with their TPs. The perisinusoidal macrophage is associated with BDs and is characterized by an irregular shape, with a thick cytoplasmic process and the cytoplasm is rich in perinuclear phagososome (Figure 9.12D).

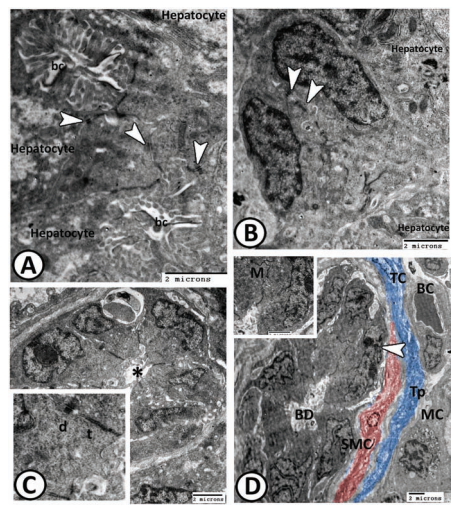

FIGURE 9.12 Digital colored TEM micrograph of BD system in the liver of grass carp. (A) The bile canaliculi (bc) between hepatocytes and adjacent junctional complexes (arrowheads). (B) The bile ductule is formed by two epithelial biliary cells joined by tight junctions and desmosomes (arrowheads). (C) The BD is characterized by the presence of microvilli (asterisk) projected into the narrow lumen. The biliary cells are connected by tight junctions followed by desmosomes (t, d in the inserted figure). (D) BD is surrounded by SMCs, and TC with their TPs. Note the presence of macrophages (MC) and blood capillary (BC) in association with the duct. The arrowhead indicates a magnified inserted figure that showing many mitochondria (M) in the ductal cells.

In the biliary system, toxic substances are neutralized and eliminated in the liver. Many species differ in the composition and structure of the biliary system of the liver. Lamprey (*Petromyzon marinus*) lacked their biliary system and gallbladder in adults but they existed during early development. While the hepatocytes of Atlantic salmon (*Salmo salar*) did not show intracellular bile canaliculi. Crucian (*Carassius carassius*) had the only canaliculus inside each hepatocyte and lacked intercellular BT.

Three patterns of organization of fish hepatic parenchyma are recognized. The first pattern occurs in *large-mouth bass, pike,* and *rainbow trout* and is composed of hepatocytes that are radially arranged around the central vein in two cell thick laminae separated by sinusoids. The second arrangement called tubular pattern occurs in *hagfish,* the hepatocytes lie in the form of tubules, and the sinusoids form a network around the tubules. The third arrangement is present in some fresh and marine teleosts, the hepatocytes lie in anastomosing lamina around the central vein.

9.2 PANCREAS

The pancreas of fish is a lobulated compound acinar gland, divided into two compartments with exocrine and endocrine functions. The pancreas plays an important role in the regulation of energy balance and nutrition through the synthesis and release of protein digestive enzymes and hormones. The pancreas of teleosts fish is classified into disseminated, compact, and intrahepatic types. The disseminated type occurs around the gall bladder and in mesentery; the compact pancreas is located in the splenic mesentery, and acts as a discrete organ, while the intrahepatic pancreas is located inside the liver. Exocrine pancreatic tissues that are found in association with the liver around portal vessels are collectively called hepatopancreas. During ontogenesis, the exocrine pancreatic tissue develops around the portal vein, and then penetrates the parenchyma of the liver, or remains extra-hepatic depending on the species.

Grossly, the pancreas appears as groups of yellowish masses that are distributed in mesenteries around the intestine, spleen, and intestinal bulb. It is also diffusely spread within the hepatic tissue to form hepatopancreas, but the pancreas could not be seen macroscopically within the liver.

9.2.1 HISTOLOGICAL ANALYSIS OF THE PANCREAS

The pancreas is a highly lobulated gland, each lobule is composed of closely packed secretory pancreatic acini separated by thin connective tissue septa (Figures 9.13 and 9.14A). The pancreas is divided into exocrine and endocrine portions. Exocrine pancreatic tissues of the grass carp and guppy are observed in two forms: the first one is disseminated in mesenteries around the intestinal bulb (Figures 9.13 and 9.14B) and the anterior portion of the intestine (Figures 9.13 and 9.14C), as well as embedded in splenic tissue (Figure 9.14D); the second form is intrahepatic, around the branches of the portal vein (Figure 9.15).

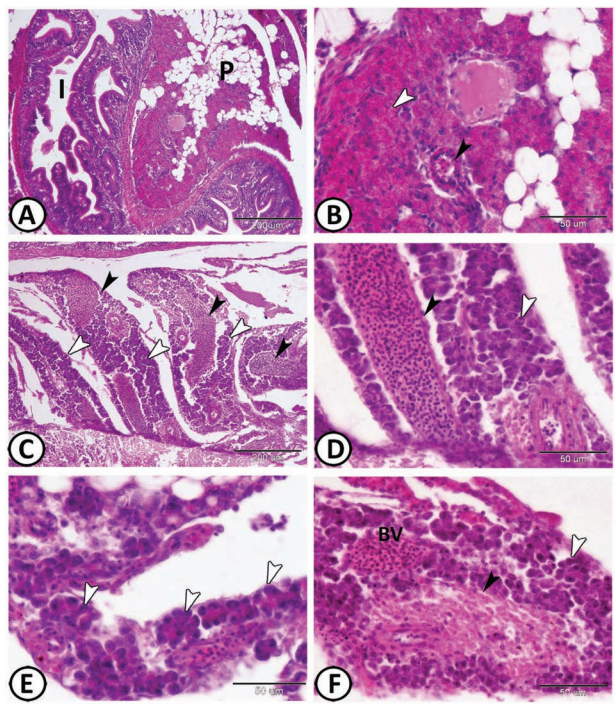

FIGURE 9.13 The distribution of the pancreatic tissues in guppy stained by HE. (A, B) The pancreatic tissues (P, white arrowhead) form large lobules around the intestine (I). Note the presence of a pancreatic duct (black arrowhead). (C, D) The pancreatic tissues (white arrowheads) formed many lobules in the mesenteries around the BVs (black arrowheads). (E) Higher magnification of the pancreatic acinar cells showing the basophilic basal portion and acidophilic apical zymogen granules (arrowheads). (F) Exocrine pancreatic tissues (white arrowheads) encircle the endocrine portion (black arrowhead). Note the BVs in neighboring to the endocrine portion.

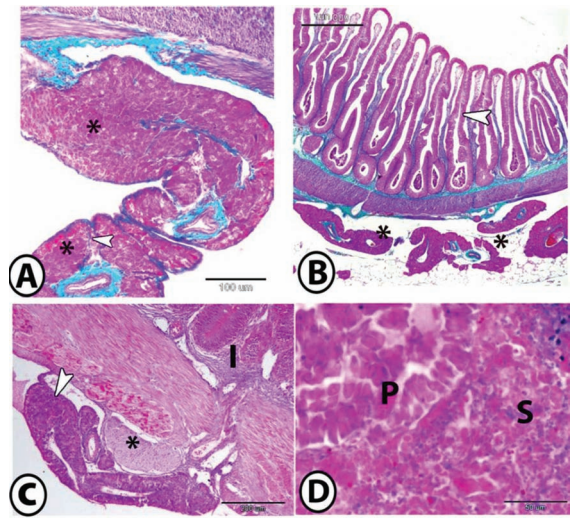

FIGURE 9.14 The distribution of the exocrine portion of the pancreas of grass carp. (A) The pancreas is formed of many lobules (asterisks) separated by connective tissue septa (arrowhead) (Crossmon's Trichrome). (B) Disseminated form of exocrine pancreatic tissues (asterisks) distributed in the mesenteries around the intestinal bulb (arrowhead indicate folds of the intestinal bulb) (Crossmon's Trichrome). (C) Disseminated form of exocrine pancreatic tissues (arrowhead) distributed in the mesenteries around the intestine (I). Note the presence of pale staining islets of Langerhans (asterisk) scattered between the exocrine portion of the pancreas (HE). (D) Disseminated form of exocrine pancreatic tissues (P) distributed in the splenic tissue (S) (HE).

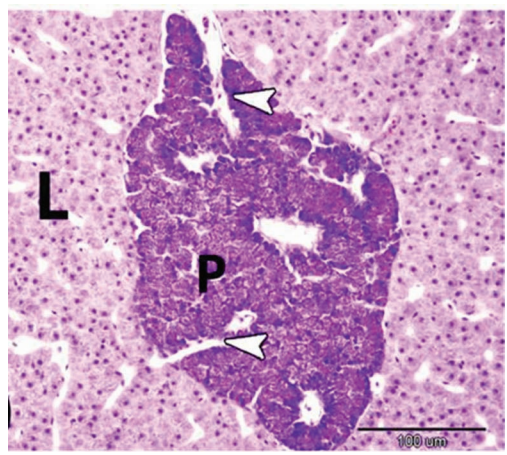

FIGURE 9.15 Intrahepatic form of exocrine portion of the pancreas or hepatopancreas of grass carp formed of clusters of pancreatic acini (P) distributed around branches of the portal vein (arrowheads) of the liver (L) (HE).

Exocrine pancreatic tissue consisted of scattered serous acini. Two alveolar cell types are present in the acini: centroacinar and typical acinar cells. The centroacinar cells are polyhedral cells attached by their basal ends to the portal veins and their apices toward the central lumen and represent the terminal end of the pancreatic duct system. The typical acinar cells are polyhedral in shape, arranged in groups to form the pancreatic acini with a central narrow lumen, where the products of these exocrine cells are secreted. The basal cytoplasm is basophilic, and the apical cytoplasm contained eosinophilic zymogen granules, which varied in density (Figure 9.16A). The nucleus was spherical and basally located with a prominent central nucleolus.

Semithin sections revealed the presence of rounded zymogen granules of variable size and some of them appeared dark in color with toluidine blue and others are observed in a light color (Figure 9.16B). The zymogen granules contain proenzymes responsible for the digestion of protein, carbohydrates, fats, and nucleotides. The acinar cells of the grass carp show differences in the staining activity of zymogen granules by toluidine blue, which indicates the presence of different enzymes within the granules. The presence of these different active enzymes may help in food digestion.

MM centers with heterogenic contents mainly of lipofuscins are observed in hepatopancreas in association with BVs. The number and contents of MM centers differ according to species, health status, and age. They usually concentrate on lipofuscin, melanin, ceroid, or hemosiderin pigments. Pancreatic stellate cells (PSCs) are demonstrated by improved Kupffer's gold chloride and Grimelius silver stain to be small branched cells with many cytoplasmic processes in perivascular and periacinar space (Figure 9.16C). RCs are observed in the external surface of hepatopancreas, as well as between the acinar cells, and were characterized by rounded to oval shape and intracytoplasmic granules or rodlets surrounded by a thick capsule (Figure 9.16D).

9.2.2 HISTOCHEMISTRY AND ENZYME ACTIVITY OF PANCREATIC ACINI

Exocrine pancreatic cells show a PAS-positive reaction. Abundant amounts of glycogen are demonstrated in the pancreatic parenchyma by Best's carmine stain that also revealed a stronger reaction in centroacinar cells. A negative reaction of the pancreatic acini to alcian blue is recorded. The LDs

in the cytoplasm of pancreatic acinar cells stained brown to black by osmium tetraoxide (Figure 9.17). The presence of neutral mucopolysaccharides, glycogen, and lipid indicated high storage activity of these cells.

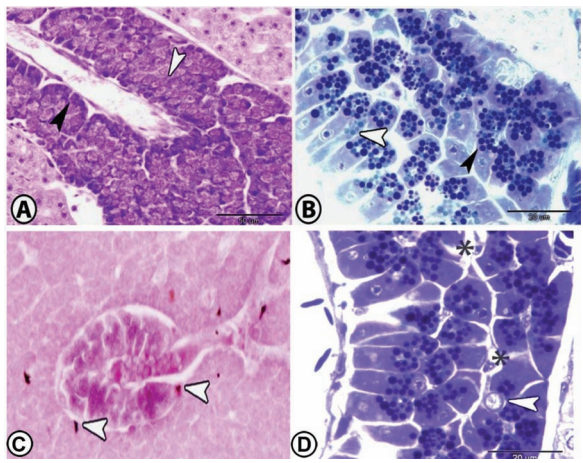

FIGURE 9.16 The structure of the pancreatic acini of grass carp. (A) The pancreatic acini formed from two types of cells: centroacinar (black arrowhead) and typical acinar cells (white arrowhead) (HE). (B) Semithin sections of pancreatic acinar cells showing dark zymogen granules (black arrowhead) and light ones (white arrowhead) (Toluidine blue). (C) PSC (arrowheads) gives a positive reaction to Kupffer's gold chloride staining. (D) Semithin sections of pancreatic acini showing RCs (arrowhead) interspersed between pancreatic acinar cells. Many small PSCs (asterisks) extended between the acinar cells are noticed (Toluidine blue).

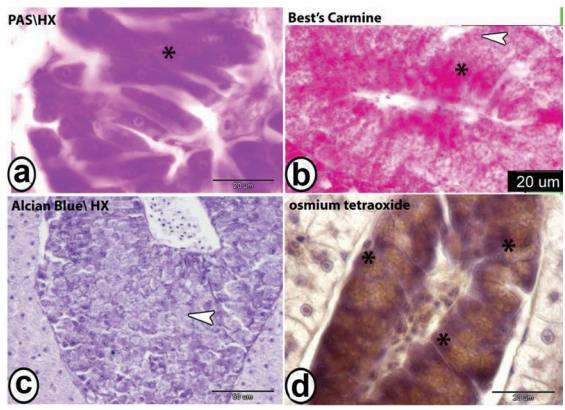

FIGURE 9.17 The histochemistry of the pancreas of grass carp. (A) The pancreatic cells showing a PAS-positive reaction (asterisk). (B) Pancreatic acini showing strong Best's carmine reaction (arrowhead); however, a stronger reaction is demonstrated in centroacinar cells (asterisk). (C) A negative alcian blue reaction of acinar cells (arrowhead) is noted. (D) The exocrine part of the pancreas showing a positive reaction to osmium tetraoxide (asterisks).

The acini show high activity for alkaline phosphatase in the form of blackish granules scattered in the cytoplasm and zymogen granules. Moderate activity for acid phosphatase was determined in the form of homogenous dark granules in the pancreatic acinar cells. The acini also show a high lipase activity in the form of numerous black granules scattered throughout the acinar cells (Figure 9.18).

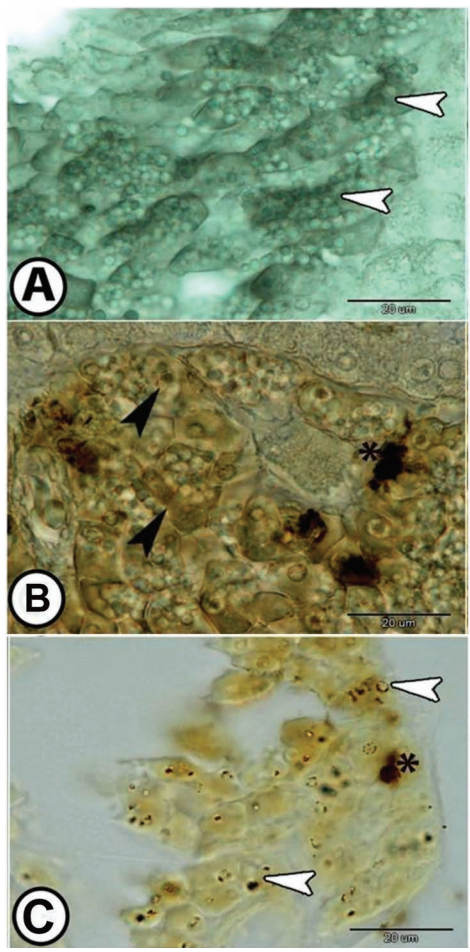

FIGURE 9.18 The enzyme activity of the pancreatic acini of grass carp. (A) A high alkaline phosphatase activity (arrowheads) of pancreatic acini (Gomori calcium method). (B) A moderate acid phosphatase activity (arrowheads) of pancreatic acini. High activity is observed in macrophage centers (asterisk) (Gomori lead nitrate method). (C) High lipase activity (arrowheads) of pancreatic acini. High activity is observed in macrophage centers (asterisk) (tween method).

9.2.3 SCANNING ELECTRON MICROSCOPY OF PANCREATIC ACINI

The pancreatic acinus is formed of 12–22 acinar cells. They are rounded to oval in shape and measured 70–100 μm in diameter. Pancreatic serous acinus is surrounded by a connective tissue capsule. The acinar cells are covered by minute microvilli. The acini are also organized into the form of columnar cords of acinar cells. Oval-shaped PSCs are observed in association with pyramidal pancreatic cells as their dendritic-like processes extended in between them. The lateral surfaces of the acinar cells expose a number of rounded elevations, which probably corresponded to zymogen granules (Figure 9.19).

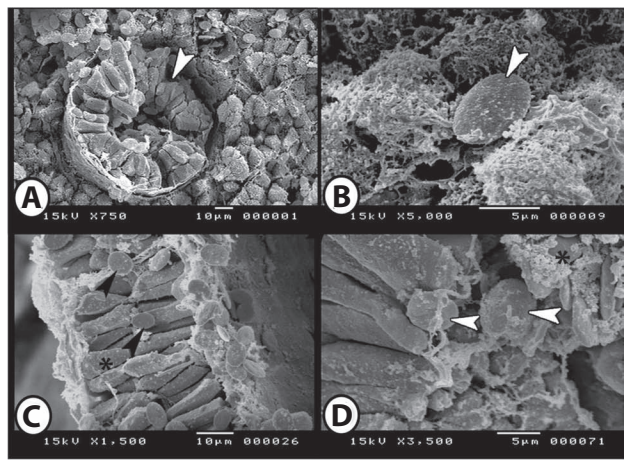

FIGURE 9.19 The surface architecture of the pancreatic acini of grass carp. (A) Serous pancreatic acini surrounded by connective tissue capsule (arrowhead). (B) Pancreatic acinar cells are covered by microvilli (asterisks). PSC (arrowhead) is observed between the acinar cells. (C) PSC (arrowheads) extended their processes among columnar cords of pancreatic acinar cells (asterisk). (D) PSC (arrowheads) extended their processes among the pancreatic cells. Note the presence of elevations of zymogen granules (asterisk).

PSCs comprise 4%–7% of the pancreatic cell mass. They have received several names such as fat-storing cells, lipocytes, pericytes, and parasinusoidal cells. They are detected ultrastructurally by the presence of multiple LDs in their cytoplasm and are found in a wide variety of species, ranging from lampreys (primitive fish) to humans and have been observed in many tissues: including liver, adrenal gland, spleen, ductus efferent, and uterus. These cells express specific filamentous proteins such as desmin and vimentin, and myofibroblast marker α-smooth muscle actin. PSCs are

vitamin A storing cells and during injuries are transformed into an activated form that produces large amounts of fibronectin and laminin (extracellular matrix proteins), resulting in fibrosis. Also, these cells have an immune function since it engulfs the damaged pancreatic parenchymal cells.

9.2.4 ULTRASTRUCTURE OF PANCREATIC ACINI

The acinar cells of the grass carp are pyramidal in shape, and their cytoplasm contained many rounded membrane-bounded secretory zymogen granules of variable size that contained electron-dense materials with a mean diameter of 1.5 μm. The granules are distributed in the cytoplasm but mainly concentrated in the apical portion of the acinar cells. The nuclei of these cells are rounded and basally located with a distinct central nucleolus. The heterochromatin is represented by small dense granular areas attached to the inner side of the nuclear envelope. Abundant well-developed rough endoplasmic reticulum with concentrically distributed dilated cisternae filled the most basal region of the cell, with small amounts also occurring in the apical region among zymogen granules. Many LDs of variable size are observed in the acinar cells. Centroacinar cells are observed adjacent to the typical acinar cells and were characterized by a more electron-lucent cytoplasm with a few organelles mainly free ribosomes and oval euchromatic nucleus (Figure 9.20). Both centroacinar and duct cells apparently secrete bicarbonate and water since carbonic anhydrase, the enzyme responsible for the formation of bicarbonate has been demonstrated in their epithelia.

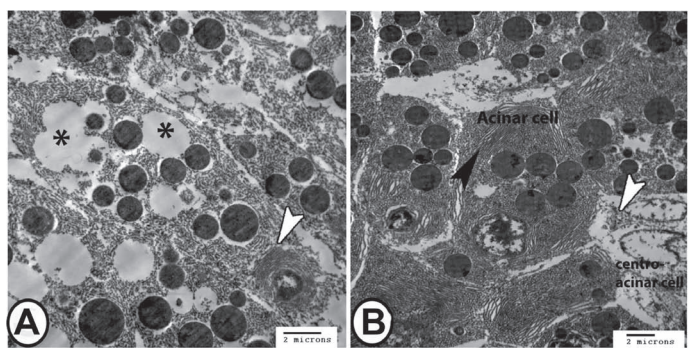

FIGURE 9.20 The ultrastructure of pancreatic acini of grass carp. (A) Acinar cells are filling with zymogen granules that are concentrated apically. Concentrically arranged rough endoplasmic reticulum (rER) (arrowhead) and many LDs (asterisks) are observed. (B) Electron-lucent centroacinar cells with ribosomes (white arrowhead) adjacent to acinar cells with abundant rER (black arrowhead).

9.2.5 THE DUCT SYSTEM OF EXOCRINE PANCREATIC TISSUE (FIGURE 9.21)

A number of BVs with erythrocytes and pancreatic ductules are scattered in the pancreatic tissue. The duct system of the pancreas consists of intralobular, interlobular pancrepancreatic ducts, and main duct. The intralobular pancreatic ducts are small (80–100 μm in diameter), present in the pancreatic lobules, and consisted of a simple cuboidal epithelium surrounded by layers of collagenous and elastic fibers. The interlobular pancreatic ducts are larger (500–750 μm in diameter), present between the pancreatic lobules, and the mucosa was thrown into mucosal folds. The wall of the interlobular duct consisted of simple columnar epithelium with numerous apical LDs, goblet-like cells with a basal nucleus, RCs, and small dark basal cells, and surrounded by layers of collagenous fibers.

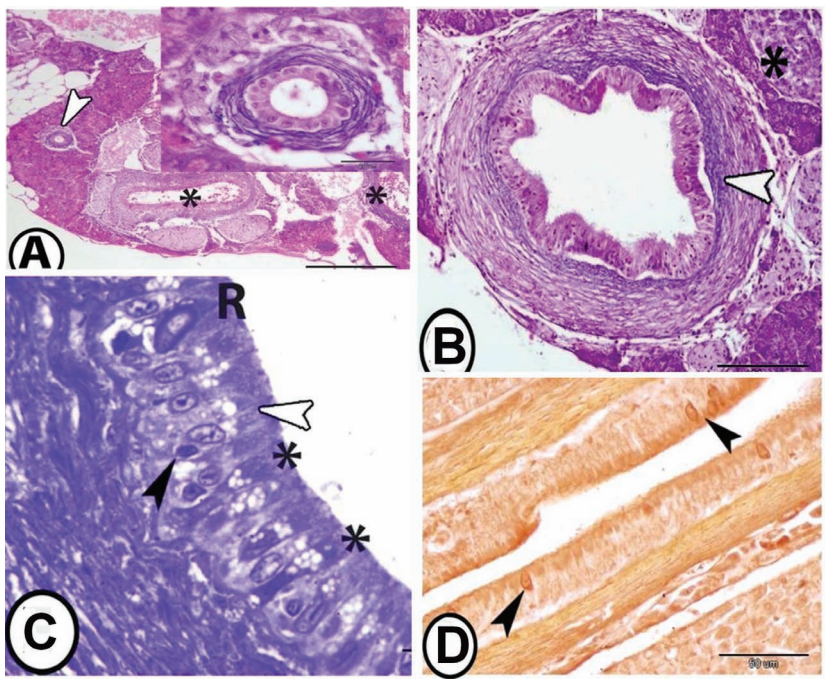

FIGURE 9.21 The duct system of the exocrine pancreatic tissue of grass carp. (A) Intralobular pancreatic duct (arrowhead and inserted figure) is lined by cuboidal cells surrounded by collagenous fibers. Note the presence of many BVs (asterisks) in the pancreatic tissue (HE). (B) Interlobular pancreatic duct (arrowhead) with folded mucosa located between pancreatic lobules (asterisk) (HE). (C) The wall of the interlobular duct stained by toluidine blue indicates its epithelium that lined by simple columnar cells (white arrowhead), goblet-like

cells (asterisks), basal cells (black arrowhead), and RCs (R). (D) Epithelium of the main duct contained argyrophilic cells (arrowheads) stained by the Grimelius silver method.

The presence of goblet-like cells in the wall of the interlobular duct suggests an adaptation for protection against pathogens. The apical brush border of the epithelial cells of the interlobular duct gives a strong alcian blue-positive reaction. The main duct was the larger duct (1100–1400 μm in diameter), opened in the middle portion of the intestinal bulb, and surrounded by collagenous fibers. The main pancreatic duct composes of a simple columnar epithelium with PAS-positive apical portion indicated the presence of neutral mucopolysaccharide materials and may suggest transport of molecules across the cell membrane. The main duct of the grass carp pancreas opens into the intestinal bulb and its wall contained argyrophilic cells that may be somatostatin or glucagon-producing cells.

KEYWORDS

- **acini**
- **Ito cell**
- **hepatocytes**
- **melanomacrophage**
- **bile ducts**

BIBLIOGRAPHY

Bassity, E.; Clark, T. G. Functional identification of dendritic cells in the teleost model, rainbow trout (*Oncorhynchus mykiss*), *PLoS One* **2012,** 7(3), e33196.

Cretoiu, S. M.; Popescu, L. M. Telocytes revisited, *Biomol. Concepts* **2014,** 5, 353–369.

El-Bakary, N. E. R.; El-Gammal, H. L. Comparative histological, histochemical and ultrastructural studies on the liver of flathead grey mullet (*Mugil cephalus*) and sea bream (*Sparus aurata*), *Glob. Vet.* **2010,** 4(6), 548–553.

Figueiredo-Fernandes, A. M.; Fontainhas-Fernandes, A. A.; Monteiro, R. A. F.; Reis-Henriques, M. A.; Rocha, E. Spatial relationships of the intra hepatic vascular-biliary tracts and associated pancreatic acini of Nile tilapia, *Oreochromis niloticus (Teleostei, Cichlidae)*: A Serial Section Study by Light Microscopy, *Ann. Anat.* **2007,** *189*, 17–30.

Jordanova, M.; Miteva, N.; Rocha, E. A quantitative study of the hepatic eosinophilic granule cells and rodlet cells during the breeding cycle of Ohrid trout, Salmo letnica Kar. (Teloestei, Salmonidae), *Fish Shellfish Immunol.* **2007,** 23, 473–478.

Mokhtar, D. M. Histological, histochemical and ultrastructural characterization of the pancreas of the grass carp *(Ctenopharyngodon idella), Eur. J. Anat.* **2015,** *19*(2), 145–153.

Rocha, E.; Monteiro, R. A. F.; Pereira, C. A. The liver of the brown trout, *Salmo trutta fario*: a light and electron microscope study, *J. Anat*. **1994,** 185, 241–249.

Sales, C. F.; Silva, R. F.; Amaral, M. G. C.; Domingos, F. F. T.; Ribeiro, R. I. M. A.; Thomé, R. G.; Santos, H. B. Comparative histology in the liver and spleen of three species of freshwater teleost, *Neotrop. Ichthyol.* **2017,** 15(1), e160041.

Sousa, S.; Rocha, M. J.; Rocha, E. Characterization and spatial relationships of the hepatic vascular–biliary tracts, and their associated pancreocytes and macrophages, in the model fish guppy (*Poecilia reticulata*): a study of serial sections by light microscopy, *Tissue Cell* **2018,** 50, 104–113.

Wilpe, E.; Groenewald, H. B. Kupffer cell structure in the juvenile nile crocodile, *Crocodylus niloticus*, *J. Morphol.* **2014,** 275, 1–8.

CHAPTER 10

Gas Bladder and Gas Glands

ABSTRACT

The swim (gas) bladders come in two kinds: physostomous and physoclistous. The swim bladder consists of three layers: tunica externa, submucosa, and mucosa. Numerous blood vessels penetrate the tunica externa that constitute a widely distributed rete mirabile. The gas gland is separated from the lumen of the swim bladder by an inner epithelial layer and smooth muscles. This close association of smooth muscles with the gas gland tissue may be important for gas secretion. The gas gland originates from the gas bladder (GB) epithelium, which is formed of folded columnar epithelial cells highly vascularized by long loops of densely packed capillaries, a *rete mirabile*. The *rete* in companion with the gas gland permits the gas secretion into the GB. Furthermore, the gas secretion in the bladder is possible by the countercurrent organization of the venous and arterial capillaries of the *rete mirabile*. Despite the fact that the hydrostasis is the main function of the gas-filled organs in most bony fishes, these organs may have a respiratory role.

10.1 THE GAS BLADDER

Embryologically, the gas bladder (GB) originates from the upper digestive tract but has no digestive function. Numerous bony fishes have a GB that appears as a single elongated sac dorsally situated to the digestive tract, located retroperitoneally (Figure 10.1A). The air-bladders exhibit remarkable morphological diversity. In the zebrafish, it is divided into two compartments.

The GBs are classified into two types: physostomous and physoclistous. The physostomous GBs are connected to the esophagus by a duct named "the pneumatic duct." This kind of bladder is distinctive for sturgeons and primitive teleosts, such as *Cyprinidae* and *Anguillidae.* On the other hand, the pneumatic duct is lost during embryonic development in physoclist

fishes. This kind of GB is demonstrated only in advanced teleosts, such as *Gadidae, Percidae, Tetraodontidae*, and *Balistidae*. Typically, the emptying and the filling of the GB are, respectively, performed by a resorbing portion (the oval), and a secretory portion the gas gland but the anatomy of these portions differs from species to species. The oval in cod or perch can be separated from the rest of the organ by muscular layers that are designed to permit the gas resorption. The pneumatic duct in European eel (*Anguilla Anguilla)* develops into the resorbing portion of the GB, which is separated from the secretory part by a sphincter.

The swim bladders are filled with air that enters through the pneumatic duct or with gases (O_2, N_2, CO_2,) secreted into the GB from the blood. As the main function of the GBs is the control of the fish buoyancy, they have often named swim bladders. Sometimes, they may be richly vascularized to take part in supplementary respiration and named respiratory, air, or GBs.

The internal vascular walls of respiratory GBs are subdivided into numerous partitions that increase the surface area for external respiration exchange. The GBs are absent in many fish such as *Blennidae, Thunnidae, Pleuronectidae, Scombridae,* some *Scorpenidae,* and Chondrichthyes, so they are not necessary for life. The GB can be one-, two-, or three-chambered, and its presence or absence may reflect the behavior of the fish.

The swim bladder wall (Figure 10.1B) composes of many layers. The tunica interna is formed of a single layer of columnar, surfactant-producing epithelium. Rodlet cells can be found in the epithelium of many species of teleost. The submucosa, where most blood vessels (BVs) are found, may be occupied with guanine crystals that cause the wall of the swim bladder impermeable to gases. In addition, large amounts of membranous materials are present in some fish, which are typically organized in a bilayer structure. Beneath the submucosa, a layer of smooth muscle cells, termed the muscularis mucosae can be distinguished. The outer layer (tunica externa) consists predominantly of fibromuscular tissue.

10.2 THE GAS GLAND

The gas gland originates from the bladder epithelium, which is formed of folded columnar epithelium highly vascularized by long loops of densely packed capillaries (Figure 10.1C and D). This structure is termed a rete mirabile (Figure 10.2). This rete in association with the gas gland permits the gas secretion into the bladder. However, the production of gas in the bladder is

possible among others by the countercurrent arrangement of the arterial and venous capillaries of the rete mirabile. Despite the fact that the hydrostasis is the main function of the gas-filled organs in most bony fishes, these organs may have a respiratory role.

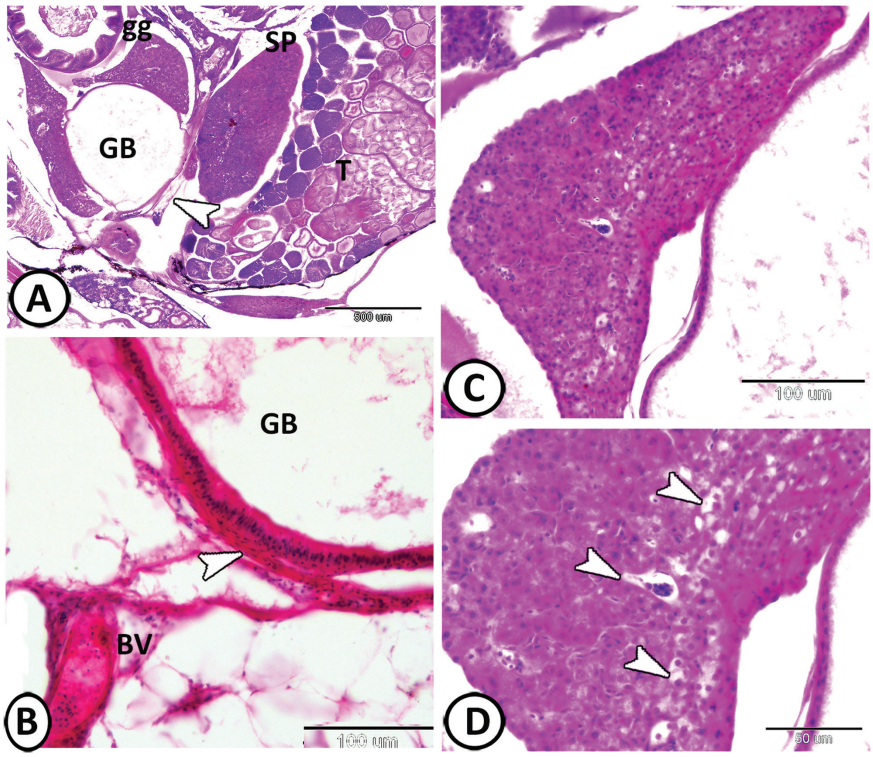

FIGURE 10.1 (A) The GB of guppy appears as a simple saccular dorsal outgrowth extending along the abdominal cavity. In physoclists (Perciformes and others advanced teleosts including the guppy), the GBs are completely closed, separated from the gut through the loss of the pneumatic duct. Note the anteriorly located gas gland (GG) supplied by arterial and venous capillaries (arrowhead). Note the spleen (SP) and a portion of the testis (T) (HE). (B) The wall of the GB is composed of simple columnar epithelium, surrounded by connective tissues and smooth muscle fibers (arrowhead). Note the presence of the BV that supplied the bladder (HE). (C) The gas gland is a modification of the inner lining (tunica interna); it is composed of a highly specialized and vascularized epithelium whose cells produce lactic acid and CO_2. The induced acidification allows gas diffusion from afferent arterial capillaries into the bladder (HE). (D) High magnification shows gas gland cells with capillaries (arrowheads) in between.

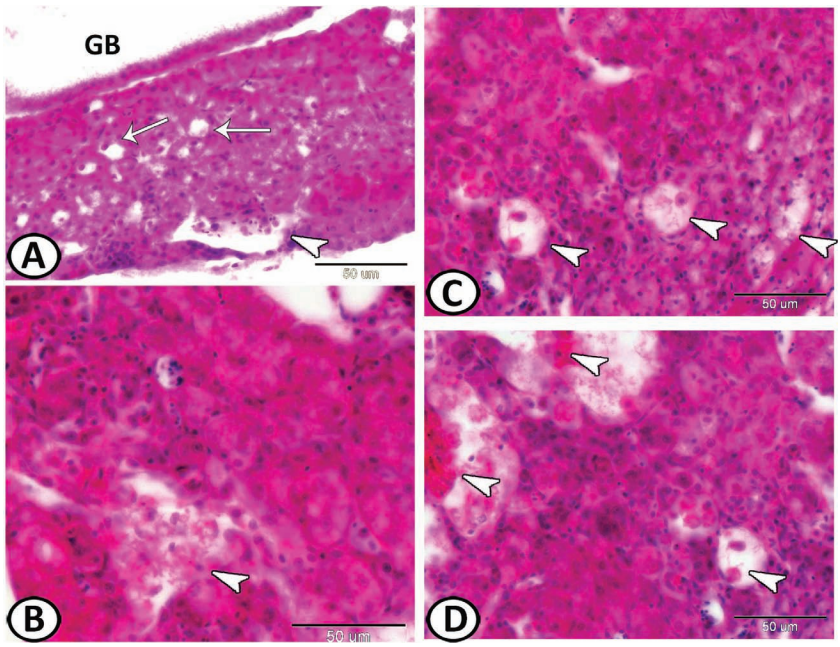

FIGURE 10.2 (A, B) The main BV entering the anterior part of the GB breaks up into smaller branches (arrowheads), which subdivide into a multitude of capillaries (arrows) (HE). (C) The rete mirabile is a dense bundle of parallel arterial and venous capillaries arranged side by side and supplying the gas gland with blood. The rete mirabile is a wonderfully complex structure. It consists of a countercurrent arrangement of arterial and venous capillaries (arrowheads), which do not communicate until they reach the gas gland (HE). (D) The pattern of arrangement of numerous blood capillaries in the rete mirabile and the abundance of blood cells (arrowheads) gives a fascinating appearance (HE).

A phylogenetically diverse group of fishes breathes air through air bladder. Air-breathing with an air bladder is limited to those fishes that have retained a connection between the bladder and the esophagus. This occurs in various primitive teleosts, such as the tarpons *(Megalopidae*), the bony tongue fishes *(Osteoglossoidei*), the gars (*Lepidosteidae*), the aba (*Gymnarchidae*), the bowfin (*Amiidae*), the trahiras (*Erythrinidae*), and the knifefishes (*Notopteridae*).

Functional lungs are demonstrated among relatively primitive fishes that include the lungfishes (Dipnoi) and bichirs *(Polypteridae*) among preteleosts. Most deep-sea species (Myctophiformes, Stomiiformes, and Aulopiformes) and bottom-dwelling teleosts (*Blennidae, Cottidae, and Pleuronectidae*) whose food gathering and protective mechanisms depend on their staying

at the bottom of the sea lack a GB. Moreover, it is greatly reduced or lost in other fishes whose functioning will be disrupted by a large gas bubble. This occurs in most rapidly swimming marine fishes, such as tunas, mackerels (*Scombridae*), and pelagic sharks, as well as freshwater species that live in strong streams. Furthermore, GB performs many other functions. It participates in sound production (*Triglidae, Balistidae, and Batrachoididae*), it also facilitates the auditory reception in many teleosts (*Ostariophysi*) through tiny Weberian ossicles.

KEYWORDS

- **air bladder**
- **gas gland**
- **gas bladder (GB)**
- **rete mirabile**

BIBLOGRAPHY

Blaxter, J. H. S.; Tytler, P. Physiology and function of the swimbladder, *Adv. Comp. Physiol. Biochem.* **1978,** *7*, 311–334.

Jones, F. R. H.; Marshall, N. B. The structure and function of the teleostean swim bladder, *Biol. Rev.* **2008,** 28(1), 16–82.

Icardo, J.; Colvee, E.; Lauriano, E. R.; Capillo, G.; Guerrera, M. C.; Zaccone, G. The structure of the gas bladder of the spotted gar, *Lepisosteus oculatus*, *J. Morphol.* **2015,** 276, 90–101.

Maina, J. N. Functional Morphology of the gas-gland cells of the air-bladder of *Oreochromis alcalicus grahami* (Teleostei: Cichlidae): an ultrastructural study on a fish adapted to a severe, highly alkaline environment, *Tissue Cell* **2000**, 32(2), 117–132

Zaccone, D.; Sengar, M.; Lauriano, E. R.; Pergolizzi, S.; Macri, F.; Salpietro, L.; Favaloro, A.; Satora, L.; Dabrowski, K.; Zaccone, G. Morphology and innervation of the teleost physostome swim bladders and their functional evolution in non-teleostean lineages, *Acta Histochem.* **2012,** 114, 763–772.

CHAPTER 11

Excretory System

ABSTRACT

The kidney of the teleost is a mixed organ comprising hematopoietic, phagocytic, endocrine, and excretory elements. The component structure of the fish nephron varies considerably between marine, euryhaline, and freshwater. A typical freshwater nephron consists of cytologically distinct regions: renal corpuscles (RCs), neck segment, proximal, intermediate, and distal tubules (DTs). The fish RCs consist of a glomerulus and Bowman's capsule. The neck region is continuous with the parietal and visceral epithelia of Bowman's capsule and shows a narrow lumen surrounded by ciliated epithelial cells. The proximal convoluted tubule is lined by eosinophilic-granular columnar cells with a well-developed brush border. The intermediate segment has a narrow lumen surrounded by cuboidal cells that often have cilia. Within the DTs, more water is resorbed and urine concentrated or diluted. Collecting tubules and ducts are located throughout the kidney and are involved in the collection of concentrate for excretion and more water resorption. The ureters, which conduct the urine from the collecting ducts to the urinary papilla, may fuse at any level and may be dilated, after fusion, to form a bladder. The bladder can be only a simple dilation of the ureters or a true saccular organ emptying outside by a urogenital pore.

The fish urinary system is composed of the kidney, extrarenal urinary ducts, and the urinary bladder (UB). The kidney of the teleost is a mixed organ comprising hematopoietic, phagocytic, endocrine, and excretory elements. The kidneys vary greatly between different species of fish, both grossly and histologically, often (partially or totally) fused (Clupeidae, Salmonidae, Anguillidae, Cyprinidae, etc.). The kidney of fish is usually located in a retroperitoneal position up against the ventral aspect of the vertebral column. It is a light or dark brown or black organ normally extending the length of the body cavity. The entire kidney of adult fishes is a mesonephros type. It is usually divided into anterior or head kidney, which is largely composed of hematopoietic elements, which also contains chromaffin and

adrenocortical endocrine elements; few renal tubules (RTs) are observed. The posterior kidney (Figure 11.1A–C) contains more RTs with a lesser amount of interstitial hematopoietic and lymphoid tissues and thus functions as an osmoregulatory organ. The ureters, which conduct urine from the collecting ducts to the urinary papilla, may fuse at any level and may be dilated, after fusion, to form a bladder. The urinary ducts open to the outside posterior to the anus.

11.1 THE EXCRETORY KIDNEY

The primary function of the kidney in fish is the osmotic regulation of water and salts rather than the excretion of nitrogenous wastes as in mammals. In fish, the majority of nitrogenous wastes are excreted by the gills. In freshwater, the kidney must conserve salt and eliminate excess water. This is accomplished by a high glomerular filtration rate, reabsorption of salts in the proximal tubules (PTs), and dilution of urine in the distal convoluted tubule.

11.1.1 THE NEPHRON

The primary task of a freshwater fish kidney is to produce copious dilute urine to counteract the passive influx of water across the gills and integument. By contrast, saltwater fish need to conserve fluid and this is achieved through modifications in the histology of nephrons. So, the component structure of the fish nephron varies considerably between marine, euryhaline, and freshwater forms mirroring the significant differences between their respective functions. Even though this is true, the basic cellular architecture is similar.

The characterization of nephron segments varies among fishes because some species lack some segments, and also the cellular structure can be different within the same portion for different species, especially because the major function of this organ is directly correlated with fish habitat under adaptation to the water of different salinities. Some fish lack renal corpuscles (RCs) altogether and their kidneys are termed aglomerular. This type is predominantly found in marine species and euryhaline fishes in seawater, such as toadfish (family Batracoididae), anglerfish (order Lophiiformes), sea horses (genus *Hippocampus*), and needlefish (family Belonidae). Teleosts, such as eels, salmonids, and ostariophysids (e.g., carps and catfishes) possess a long multisegmental nephron, whereas, in marine teleosts of different orders, such as percids (family Percidae), killifish (order Cyprinodontiformes), flounder

(order Pleuronectiformes), and sticklebacks (family Gasterosteidae), the nephron is shorter because the distal segment is absent.

Each nephron consists of several segments with specific structure and function. A typical freshwater nephron consists of cytologically distinct regions: RCs, neck segment (NS), proximal, intermediate, and distal tubules (DTs). The DTs connect to small collecting tubules (CTs), which join larger collecting ducts that empty into ureters. Fluid loss is limited in saltwater fish by reducing the size and number of glomeruli. Cells with melanin pigment are seen in hematopoietic tissue; these cells are called melanomacrophages (MMs) that are organized in MM centers. These centers are widespread in salmonids. The hematopoietic tissue fills among the nephrons (Figure 11.1D–F).

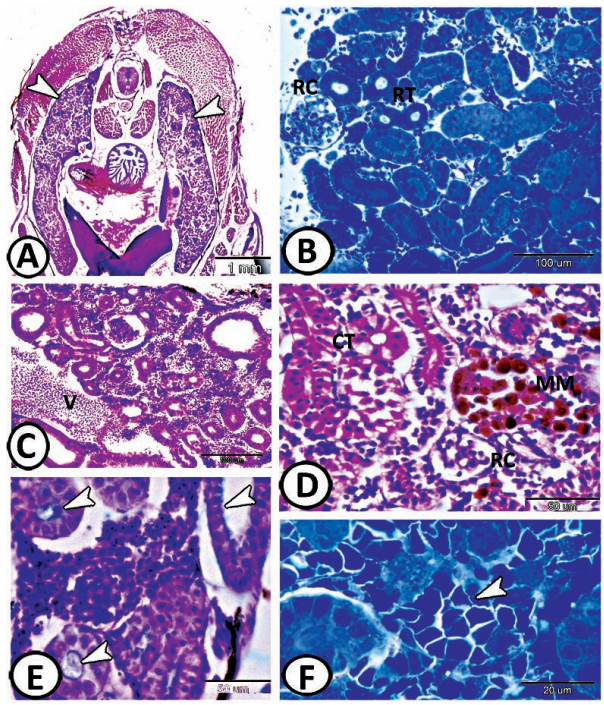

FIGURE 11.1 (A) A transverse section showing the general view of a mesonephric kidneys (arrowheads) in molly fish (HE). (B) Semithin section stained by TB showing the kidney parenchyma of grass carp that has numerous renal tubules (RTs) surrounded the renal corpuscle (RC). (C) Renal arteries from the dorsal aorta supply the kidney of guppy and blood is carried away by posterior cardinal veins (V) (PAS-HX). (D) Grass carp's kidney possesses well-vascularized RCs, collecting tubules (CTs), and MM centers (HE). (E) Transverse and longitudinal sections of PTs can be distinguished from the other tubules by their AB-positive BBs (arrowheads) (AB/HX). (F) Semithin section stained by TB showing the heamopoietic tissues (arrowhead) that were distributed between the RTs of grass carp.

In general, the RCs of marine teleosts are smaller and lower in number than those of freshwater species. The degree of glomerular development has been related to the glomerular filtration rate, which is low in marine, and high in freshwater fishes. The fish RCs (Figure 11.2A and B) with a diameter of 60–90 μm consist of a glomerulus and a glomerular (Bowman's) capsule. The glomerulus is a globular network of densely packed anastomosing capillaries that invaginates Bowman's capsule. The relatively wide diameter afferent arteriole (AA) enters Bowman's capsule at the vascular pole of the RC and then forms the network of glomerular capillaries. The efferent arteriole drains the glomerulus and leaves the capsule at the vascular pole, which is usually situated opposite the entrance to the RT, the urinary pole. Bowman's capsule consists of a single layer of flattened cells in most fish species resting on a basement membrane; it forms the distended, blind end of the RT. Bowman's capsule has two layers: visceral and parietal layers. The internal or visceral layer of the glomerular capsule surrounds the glomerular capillaries with modified epithelial cells called podocyte.

At the vascular pole of the RC, the epithelium of the visceral layer is reflected to form the simple squamous parietal layer of the glomerular capsule. The space between the visceral layer and the parietal layer of the RC is called the capsular (urine) space. There are numerous nuclei in the glomerulus that bare capillary endothelial cells (ECs), mesangial cells (MCs), and podocyte. The development of the diameter and number of glomeruli clusters is strongly age dependent. The RC is an elaborate structure that specializes in the production of the glomerular filtrate and the retention of plasma proteins in the circulation. This filtrate then passes into the RT where it is altered to form urine.

Juxtaglomerular cells are very scarce and are located in a single cell layer around some of the arteries running to clusters of glomeruli. A relationship of MCs with juxtaglomerular cells, which are probably modified smooth muscle cells, was suggested. The juxtaglomerular cells, as well as the MCs and the smooth muscle cells, reacted similarly to mineralocorticoid deficiency. Both the juxtaglomerular cells and the MCs were more numerous in marine specimens. Several functions have been attributed to the mesangium. A role as a pressure receptor controlling the secretion of renin may be a functional link with the juxtaglomerular cells and supporting function for maintaining the structural integrity of the glomerulus. On the basis of this hypothesis, the degree of development of the mesangium may be expected to be proportional to the intensity of the filtration pressure, and accordingly, to the glomerular filtration rate.

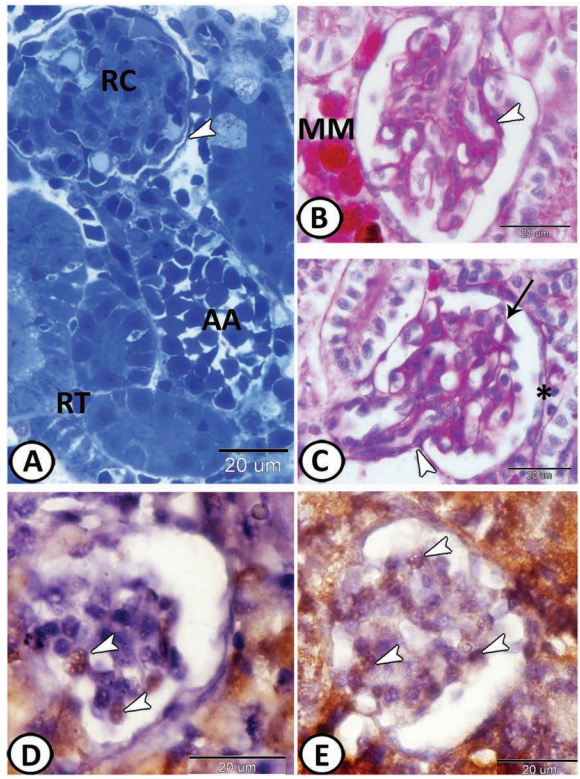

FIGURE 11.2 (A) Semithin section stained by TB showing a wide diameter afferent arteriole (AA) enters Bowman's capsule (arrowhead) at the vascular pole of the RC. The corpuscle is surrounded by RTs of various diameters. (B) A large RC containing a well-developed glomerulus (arrowhead) in grass carp that showing a staining affinity for PAS. Note an intense positive reaction in the MM center surrounding the corpuscle (PAS/HX). (C) The neck region (arrowhead) is continuous with the parietal (asterisk) and visceral epithelia of Bowman's capsule. Glomeruli (arrow) consist of a network of capillaries and the numerous nuclei inside are mainly those of podocytes and capillary ECs (PAS-HX). (D) α-SMA expression in the podocytes of the RC (arrowheads) of grass carp. (E) TGF-β expression in the podocytes (arrowheads) of grass carp.

The podocytes express both α-SMA and the transforming growth factor gene, TGF-β (Figure 11.2D and E). Podocytes are highly differentiated cells with a complex cellular morphology. They are located inside the kidney glomerulus, a twisted globe of capillaries through which the blood is filtered hydrostatically through a high-volume/high-discrimination filtration barrier. The podocytes are characterized by the presence of foot processes containing an elaborate and dynamic actin-based cytoskeleton. This structure maintains the normal architecture of the foot processes, including the proper positioning

of transmembrane proteins and the slit diaphragm. The major molecular components of the cytoskeleton are actin, α-actinin, and synaptopodin. TGF-β is a key regulator of extracellular matrix (ECM) protein synthesis in renal cells. Besides ECM protein synthesis, TGF-β has effects on proliferation, hypertrophy, and apoptosis in the renal cells. Most cells secrete TGF-β. TGF-β is known to stimulate the production of type IV collagen, fibronectin, and laminin in podocytes. The TGF-β pathway controls an array of cellular responses to various forms of chronic glomerular injury, including ECM accumulation, proliferation, hypertrophy, and podocyte apoptosis.

The urinary pole shows an NS that consists of a short tubule of cells connecting the flattened epithelium of Bowman's capsule with the cylindrical cells of the first proximal segment. The neck region (Figure 11.2C) is continuous with the parietal and visceral epithelia of Bowman's capsule and shows a narrow lumen surrounded by ciliated cuboidal/columnar epithelial cells. The cytoplasm of these cells stains slightly basophilic. The transition from the NS to the PT is sharply defined. This transition is defined by a considerable increase in the outer tubular diameter (from 21–27 to 36–47 μm).

The total PT length is 600–766 μm. The proximal convoluted tubule (Figure 11.3A and B) is the longest and most developed segment of the nephrons. This tubule is lined by eosinophilic-granular simple columnar cells with a well-developed brush border (BB). In these cells, the nuclei are mainly spherical and situated in the lower part of the cells. The BBs enhance the reabsorption of fluid and solutes from the lumen through or between the cuboidal epithelial cells into capillaries. Proximal convoluted tubule resorbs 85% of the water and sodium chloride. In addition, glucose, amino acids, proteins, vitamin C, and inorganic elements are also resorbed.

The PT is divided into two portions: the PT segment I (PTI) extending from the end of the neck segment to the start of the second straight portion, and the PT segment II (PTII) corresponds to this latter straight portion. The PT contains, in transverse sections, 8–9 cells at the beginning of the first portion (PTI) and 12–13 cells in the zone of the largest diameter (arcuate portion). The PTI contains a single cell type. These cells show a truncated pyramidal shape (17–22 μm tall) and exhibit a regular BB of microvilli (4–5 μm tall). The PTII is formed by multiciliated and BB cells. Both segments of the PT show a staining affinity to PAS in their cytoplasm and BBs (Figure 11.3D and E). The microvilli react positively for alkaline phosphatases, enzymes known to be involved in transport processes. An indication that glucose reabsorption takes place in these cells is the presence of PAS-positive material in the BB and in the most apical part of the cytoplasm.

The PTs express both a-SMA and the growth factor gene, TGF-β (Figure 11.3F and G). TGF-β seems necessary for epithelial cell homeostasis and optimal structure and function and exerts a broad range of biological activities. It plays pivotal roles during embryonic development where it is involved in the induction of cell differentiation and organogenesis. Furthermore, TGF-β1 has been implicated in the pathogenesis of renal fibrosis. The proximal tubular cells (PTCs) have been considered as a source of interstitial myofibroblasts. *In vitro*, studies also suggest that TGF-β-induced phenotypic alterations of PTC form fibroblastoid morphology. In addition, TGF-β induces expression of a-SMA in the renal PTCs.

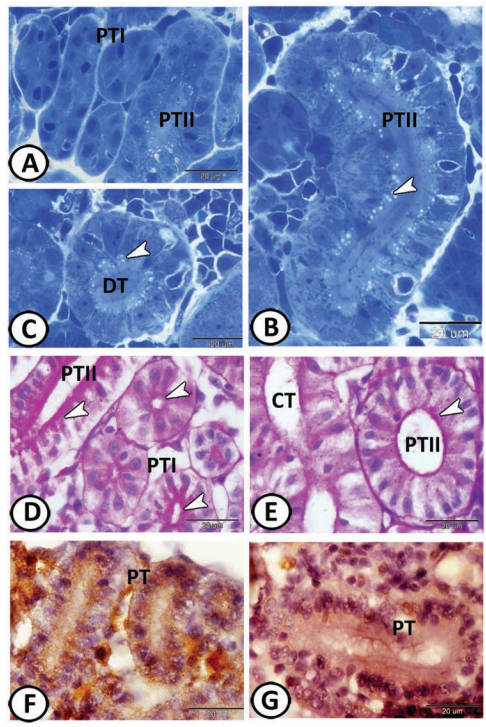

FIGURE 11.3 (A, B) Semithin sections through the proximal tubules (PTs) (PTI, PTII) of the trunk kidney of grass carp stained by TB. PTII is lined with high columnar cells with centrally located nuclei and provided with a brush border and numerous apical vacuoles (arrowhead). Their lumen contents are interpreted as vesicular material. (C) Semithin section through the distal tubules (DTs) of grass carp showing apical small vacuoles (arrowhead) (TB). (D) Four transverse sections of PTI and one longitudinal section of PTII of grass carp showing PAS-positive BBs (arrowheads) PAS/HX. (E) Transverse section of CTs and PTII of grass carp showing apical PAS-positive microvilli (arrowhead) (PAS/HX). (F) TGF-β expression in the PTs of grass carp. (G) α-SMA expression in the PTs of grass carp.

The intermediate segment (IS) appears as the narrowest portion of the nephron (17–21 μm in outer diameter with a length of 200–380 μm). The IS (Figure 11.4A) consisted of cuboidal (13–16 μm tall) multiciliated cells, which aid in the movement of the filtrate along the nephron. There are five to six cells in each cross section and it has a narrow lumen. The transition from the IS to the DT is defined by an abrupt increase in the external tubular diameter (from 17–21 to 30–38 μm).

The DTs' length is 851–986 μm. The DT (Figure 11.3C) contained seven to eight cells in cross section. They are characterized by low columnar cells with oval, basally located nuclei, and no BB, stain less intense than PTs. Within the DTs, more water is resorbed and the urine is concentrated or diluted. In marine fishes, the glomeruli are smaller and the IS is absent. The requirement here is to slow down the movement of fluid so that there is a time for the maximum amount of passive diffusion of water back into the blood. The distal segment is also often absent in many fish species.

The CTs and ducts (Figure 11.4) are located throughout the kidney; usually, the lumen is irregular. The CT is formed by lightly eosinophilic principal cells (PCs) and a high number of flask cells (FCs) with basal nuclei and no BB. The FC central cavity is often occupied by amorphous material that stained intensely with toluidine blue. These cells are important in ion transport and may also have a secretory role. In addition, the CTs are involved in the collection of concentrate for excretion and more water resorption. Large collecting ducts are lined with a mucous pseudostratified epithelium, encircled by connective tissues, and several layers of smooth muscle cells (leiomyocytes). The epithelium is highly folded and the surface outline shows dome-shaped cells with thickened plasma membranes.

11.1.2 ULTRASTRUCTURE OF THE RENAL COMPONENTS

11.1.2.1 THE RENAL CORPUSCLE

The glomerulus consists of capillary loops, lined by ECs and underlined by a glomerular basement membrane (GBM), and MCs irregularly distributed between the endothelium and the basement membrane (Figure 11.5). The endothelium shows numerous open pores 260–720 nm in diameter, closed by a single membrane, the diaphragm. The fenestrated areas are limited in extent when compared with mammalian glomeruli. Secretory granules of high electron density are frequently observed in the cytoplasm of the ECs.

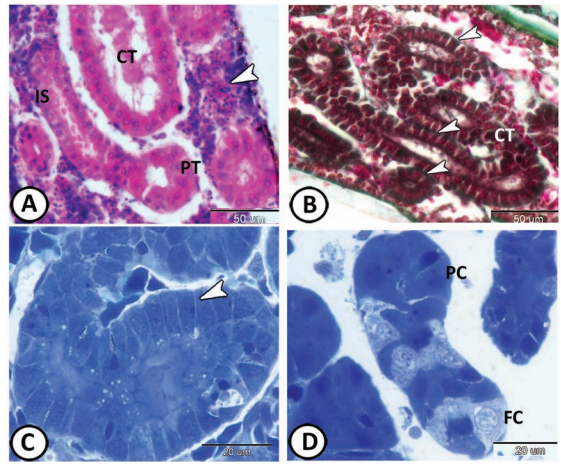

FIGURE 11.4 (A) A transverse section through CTs in the guppy. Note the connection between the PT and the intermediate segment (IS). Nests of hematopoietic tissue are obvious (arrowhead) (HE). (B) CTs of molly fish constructed of tall columnar epithelial cells enclosing wide lumens and surrounded by a thin sheath of connective tissue (arrowheads) (Crossmon's trichrome). (C, D) Semithin section stained by TB showing the CTs (arrowhead) of grass carp formed of principal cells (PCs) and flask cells (FCs).

The GBM is interposed between the podocytes and the capillaries. These three elements are the capillary wall, GBM, and podocytes constitute the filtration barrier. The GBM is formed by three layers: a lamina rara, a lamina densa, and a subendothelial lamina. The lamina rara, which underlay the foot processes, is the thinnest GBM layer (31–37 nm thick). The lamina densa shows a uniform electron density (92–112 nm thick). The subendothelial lamina consisted of two distinct zones. The first apposed to the lamina densa shows a variable thickness (between 266 and 433 nm). It consisted of a loose network of microfibrils, amorphous material, and a few collagen fibers. The second, the subendothelial zone, is located under the endothelial basal surface. It consisted of an electron-lucent space.

SEM of the vascular tuft of the RC looks like a bunch of grapes, and the external surface is dominated by the presence of the podocyte bodies. The body of the podocytes is polyhedral in grass carp. The cell nucleus occupies most of the cell body and is surrounded by a thin rim of cytoplasm. The cytoplasm contains a prominent endoplasmic reticulum and Golgi apparatus, but cytoskeletal elements (such as microtubules and microfilaments) are scarce. The major processes of the podocyte are short that extended over contiguous capillary loops, thus covering a large capillary area. The fish

podocytes when compared to mammalian podocytes, a limited number of cytoplasmic processes (pedicels), interconnected by membranes (filtration-slit-membranes) are demonstrated. These cells show signs of considerable metabolic activity and the indentations in the cell membrane suggest pinocytotic processes. Within a single RC of grass carp, most areas present regular foot processes showing the characteristic interdigitating pattern, with filtration slits and well-developed slit diaphragms.

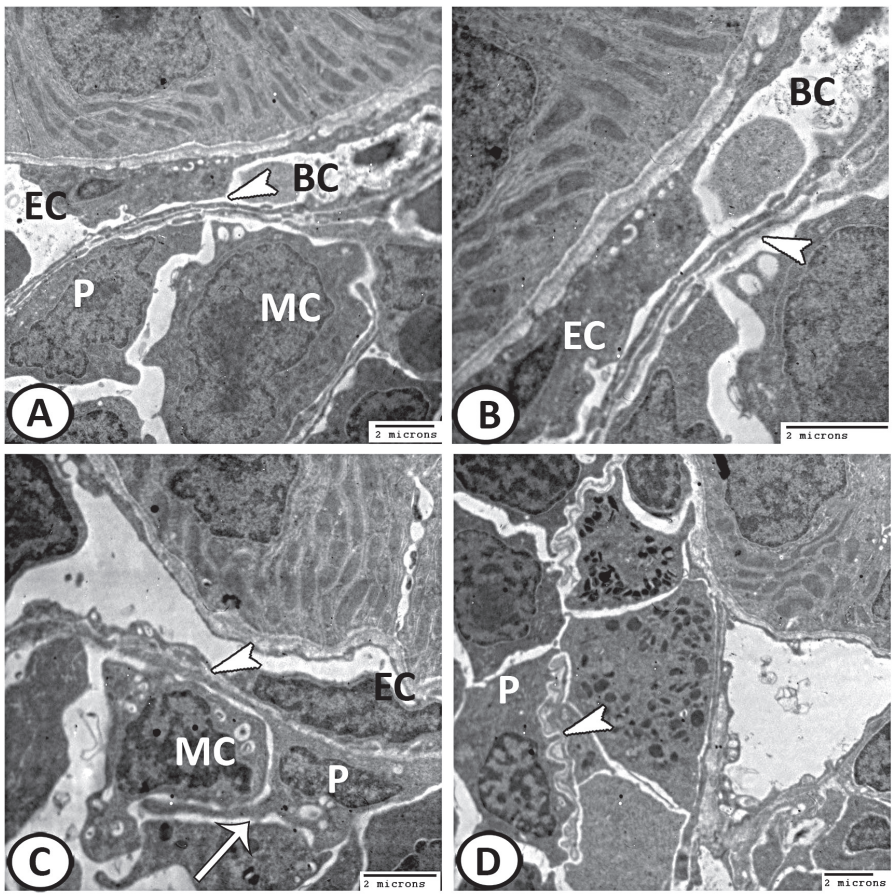

FIGURE 11.5 (A-C) Transmission electron microscopy (TEM) of the renal corpuscle of Grass carp showing a panoramic view of a glomerulus. The podocyte (P) cell body is attached directly to the GBM (arrowheads) that surround the endothelial cells (EC) of the blood capillary (BC), and forming the structure of the filtration barrier. Note, the podocyte processes (arrow) and mesangial cell (MC). (D) A lower magnification showing the well-developed foot processes (arrowhead) of podocytes (P).

The glomerular capillary tuft is formed by three to four capillary loops. The glomerular MCs cover most of the glomerular capillary surface. The MCs appeared to be very scarce in freshwater fish. They occur almost exclusively near the vascular pole. The MCs possess elongated cell bodies and long, thick cytoplasmic processes embedded in the subendothelial lamina. These processes contain longitudinal bundles of actin filaments, mitochondria, and dense bodies. The MCs establish contact with each other and with the ECs by means of the cellular processes. The MCs represent an obstacle to the free passage of molecules through the filtration barrier. The presence of large actin filament bundles suggests that these cells are able to contract. Contraction of MCs in response to functional requirements may quickly modify the structural arrangement of the filtration barrier and, consequently, the filtration rate. Indeed, it has previously been suggested that MCs are the structure responsible for quick adaptation from a freshwater to a saline environment. The small stellate MCs may perform a different functional role. Their morphology is similar to that of dendritic cells, suggesting that they may be involved in the uptake and processing of small particles and macromolecules.

11.1.2.2 THE PROXIMAL TUBULES

The ultrastructural features that characterize PTI (Figure 11.6A) are the epithelia with columnar cells, and the presence of an apical "endocytic apparatus" consisting of apical cytoplasmic invaginations, small vesicles, large vacuoles with fine granular contents, and numerous lysosomes. Long and numerous BBs, owing to the narrowness of the tubular lumen at the PTI level, the microvilli occupied most of the lumen. A large- and smooth-contoured nucleus, with abundant heterochromatin distributed in a "blots-of-ink" pattern, is basally located (most tubular cells along the nephron showed the same heterochromatin pattern). Many profiles of rER and numerous filamentous mitochondria are located in the perinuclear zone, parallel to the cell axis, and basal invaginations of the cell membrane. In the case of PTII (Figure 11.6B), their cells are also columnar but taller than PTI, with central oval nuclei, with small round or elongated vesicles in the apical cytoplasm, and a lower apical vesicular density than seen in PTI. Mitochondria are dispersed throughout the cytoplasm. As in PTI, numerous invaginations exist in the lateral and basal cell membranes (basolateral tubular system).

11.1.2.3 THE DISTAL TUBULES

The DTs ultrastructure (Figure 11.6C), shows low cuboidal epithelial cells, elaborate membrane amplification, high density of mitochondria arranged perpendicular to the basal lamina and parallel to cell membrane infoldings, and few short apical microvilli. The apical cytoplasm contains numerous vacuoles. The nuclei are large with abundant heterochromatin.

11.1.2.4 THE COLLECTING TUBULES

The CTs (Figure 11.6D) consist mainly of the PCs that are prismatic (20–23 μm tall), with a smooth apical surface. Their cytoplasm contains mitochondria, free ribosomes, microfilaments, and glycogen deposits. The nucleus is large and ovoid, basally located, and contains abundant heterochromatin. The FCs display a characteristic pear shape with a large and prominent rounded basal pole. They are more voluminous and taller (25–29 μm) than the PCs. The cytoplasm of these cells showed a clear appearance under the light microscope and on transmission electron microscopy (TEM). Nonetheless, the most prominent feature of the FCs is the presence of a central cavity communicating with the tubular lumen.

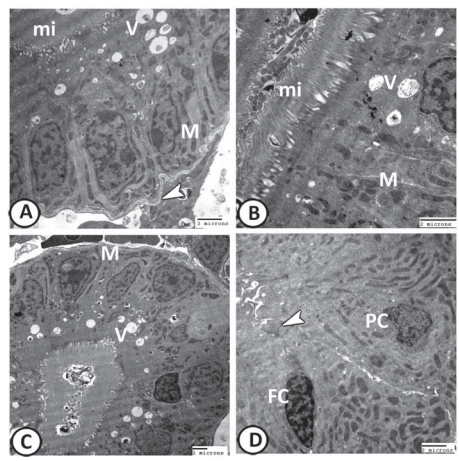

FIGURE 11.6 (A) TEM of PTI of grass carp showing numerous microvilli (mi), apical vesicles (V), and numerous basal mitochondria (M). Note the basal infoldings (arrowhead). (B) TEM of PTII showing microvilli (mi), apical vesicles (V), and mitochondria (M). (C) TEM of the distal convoluted tubule of grass carp showing numerous vesicles (V) and mitochondria (M). (D) TEM of the CTs of grass carp showing PCs and FC. Note the cavity of FCs (arrowhead) that lead to the tubular lumen.

11.2 THE URETER AND URINARY BLADDER

The ureters (Figure 11.7) open directly to the outside by a urinary pore or end into the bladder as in Cyprinidae. The ureter is lined by simple columnar epithelium, followed by smooth muscles and connective tissue.

The bladder can be only a simple dilation of the ureters or a true saccular organ (Barbus, Mystus, etc.). In many bony fishes, an enlargement of the urinary ducts serves as a bladder. An empty bladder exhibits mucosal folds that disappear when the bladder is distended (filled with urine). The lumen of the bladder is lined by a simple columnar nocuous epithelium. The luminal epithelium is characterized by the presence of microvilli. The presence of microvilli indicates that the water and or other materials are being actively reabsorbed. Beneath the epithelium is a thin layer of loose connective tissue lamina propria. A submucosa is lacking. Well-developed smooth muscle layers surrounding the UB can be identified and covered by a mesothelium of the peritoneum. Large blood vessels and nerves are distributed in the connective tissue between the mesothelium and the muscular layers.

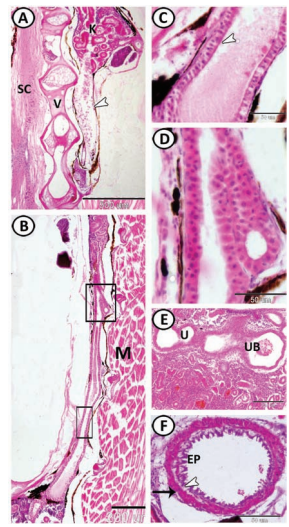

FIGURE 11.7 (A) A longitudinal section of guppy stained by HE showing the kidney (K) lying just beneath the vertebral column (V) and spinal cord (SC). Note the blood is carried away by the posterior cardinal vein (arrowhead). (B) A longitudinal section of guppy stained by HE showing the ureter (boxed areas). Note rhabdomyocytes (M) of the epaxial musculature. (C, D) Magnified images of (B) showing the ureter that lined by simple columnar epithelium covered by microvilli (arrowhead). (E) The ureter (U) of molly fish leads to dilatation for the UB (HE). (F) The UB of guppy lined by pseudostratified epithelium (EP), connective tissues (arrowhead), and smooth muscle fibers (arrow) (HE).

The UB has previously been considered to function solely as a storage chamber for urine. Recently, it has been demonstrated that the UB of starry flounder also plays an important role in osmoregulation by modifying the concentration of the urine. Analysis of the fluid contained in the UB revealed ammonia-N and urea-N. These are among the nitrogen-containing compounds excreted as urine by fishes.

In some fish species, the UB opens independently as the urinary pore as Pacific cod. On the other hand, in some teleosts, the oviduct or spermiduct and the ureter unite posteriorly and form a urogenital pore.

11.3 CHLORIDE CELLS

Key structures in ionic exchange across the gills in teleost fish are the chloride cells (Figure 11.8), which are implicated in pumping salt inwards (Ca^{2+} and Cl^{-}) in freshwater and outwards (Cl^{-}) in seawater. They are located principally at the junction between the primary and secondary lamellae (SL). These cells stain strongly with eosin and are richly endowed with mitochondria intricately laced with a tubular network of the smooth endoplasmic reticulum. Chloride cells are sometimes present at the beginning of the digestive tract.

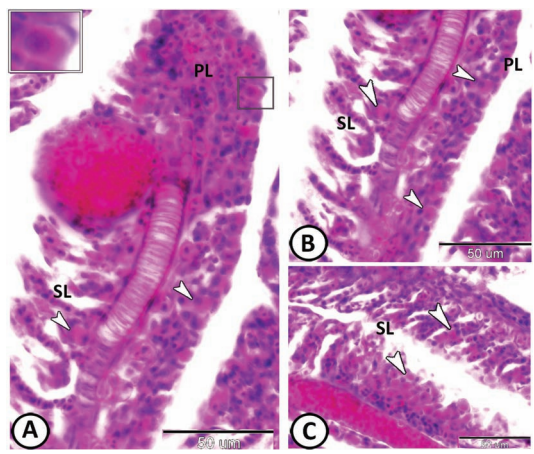

FIGURE 11.8 (A–C) Chloride cells (arrowheads, boxed areas) located within the thick epithelium of a primary lamella (PL) (gill filament) of guppy. The granular appearance and the eosinophilia of the cells are due to the abundance of mitochondria, which are in close relation with the basolateral infoldings of the plasma membrane. Note their presence also in the secondary lamellae (SL) (HE).

In freshwater, the teleosts hyperosmoregulate, their blood osmolality (about 300 mOsm/kg) is higher than that of the surrounding freshwater (about 5–10 mOsm/kg). They are exposed to diffusive ion loss and water invasion along the osmotic gradient. These teleosts pump sodium and chloride from the medium across the gill epithelium. The primary osmoregulatory function of the urinary system is then to excrete excess water and to retain most of the filtered solutes including ions, through active reabsorption, resulting in the formation of large quantities of dilute, hypotonic urine. In marine fish, the teleosts hyposmoregulate. Their blood osmolality (about 350 mOsm/kg) is lower than that of the surrounding seawater (about 1000 mOsm/kg). They are exposed to salt loading and dehydration. To compensate for water loss, marine teleosts drink seawater and actively absorb ions through the gut, a process that induces passive water absorption along the osmotic gradient. Excess ions are excreted by the gills (mainly Na^+ and Cl^-) and the kidney (mainly Mg^{2+} and $(SO_4)_2$).

The osmoregulatory function in fish is based on the presence of ionocytes or mitochondria-rich chloride cells in which the ion-transporting enzyme Na^+/K^+-ATPase is localized on the basolateral membrane. The abundance of ionocytes and Na^+/K^+-ATPase affects the osmoregulatory capacity, which controls the ability of fish to tolerate salinity and its fluctuations. Therefore, the chloride cells of the freshwater and marine species seem to be of a different nature.

KEYWORDS

- **kidney**
- **ultrastructure**
- **nephron**
- **ureter**
- **podocyte**

BIBLIOGRAPHY

Kurtovic, B.; Teskeredzic, E.; Teskeredzic, Z. Histological comparison of spleen and kidney tissue from farmed and wild European sea bass (*Dicentrarchus labrax*), *Acta Adriat.* **2008,** *49*(2), 147–154.

Mobjer, N.; Jespersen, Å.; Wilkinson, M. Morphology of the kidney in the West African Caecilian, *Geotrypetes seraphini* (Amphibia, Gymnophiona, Caeciliidae), *J. Morphol*. **2004,** 262, 583–607.

Morovvati, H.; Mahabady, M. K.; Shahbazi, S. Histomorphological and anatomical study of kidney in berzem (*Barbus pectoralis)*, *Int. J. Fish Aquac.* **2012,** *4*(11), 221–227.

Morovvati, H.; Erfanimajd, N.; Peyghan, R.; Mobaraki, G. H. Histological study of excretory portion of kidney in grass carp *(Ctenopharygodon idella)* Iranian, *J. Vet. Med.* **2011,** *6*(4), 69–75.

Ojeda, J. L.; Icardo, J. M.; Domezain, A. Renal corpuscle of the sturgeon kidney: an ultrastructural, chemical dissection and lectin-binding study, *Anat. Record* **2003,** *272A,* 563–573.

Resende, A. D.; Lobo-da-Cunha, A.; Malhão, F.; Franquinho, F.; Monteiro, R. A. F.; Rocha, E. Histological and stereological characterization of brown trout (*Salmo trutta*) trunk kidney, *Microsc. Microanal.* **2010,** 16, 677–687.

CHAPTER 12

The Respiratory System

ABSTRACT

The gills are responsible for regulating the exchange of salt and water and play a major role in the excretion of the nitrogenous waste products. The gills of most teleosts are composed of a series of arch-like structures. Each gill arch (GA) bears rows of filaments, each row constitutes a hemibranch, while a set of hemibranchs, one on each side of the arch, constitutes a holobranch. The gills of teleost fishes are composed of four holobranchs spaced between five branchial slits. Each hemibranch bears many fine primary and secondary gill lamellae. The GA is a curved cartilaginous or osseous structure, from which the bony supports (the gill rays) of the primary lamellae radiate. The GA contains the afferent and efferent brachial arteries. The GA is covered by epidermal tissue well-endowed with mucous cells (MCs). The primary lamella has central cartilaginous support, afferent and efferent arterioles, and other anastomosing vessels. The surface epithelium (EP) of the primary lamellae is covered with cuboidal and squamous epithelial pavement cells (PVCs), pale-staining MCs, and salt-secreting chloride cells. These chloride cells are most numerous at the basal (proximal) part of the lamellae and function in ionic transport with a possible role in the detoxification. The secondary lamellae are the site of gaseous exchange. The surface of the gaseous exchange consists of overlapping or interdigitating PVCs supported and separated by pillar cells. Other cells found within the filamental interstitium include lymphocytes, macrophages, and neuroepithelial cells. The inner surfaces of the GAs carry one or more rows of stiff strainers called gill rakers (GRs). Each GR is composed of an osseous or cartilaginous core supporting the pharyngeal stratified EP and adipose connective tissue.

The gills play an important role in the oxygenation of the blood. In addition, the gills are also responsible for acid–base balance and regulating the exchange of salt and water. They also play a major role in the osmoregulation and excretion of the nitrogenous waste products, primarily ammonia. Even

slight structural damage can render a fish very vulnerable to osmoregulatory as well as respiratory difficulties. The gill epithelium (EP) is thin with a large surface area that enables a high level of exposure of gill capillaries to water. This not only allows for efficient gas exchange of oxygen absorption and carbon dioxide release but also results in the vulnerability of the gill to pathogen invasion or irritation.

The gills of most teleosts are composed of a series of arch-like structures extending from the floor to the roof of the buccal cavity. Each gill arch (GA) bears regularly spaced rows of filaments projecting posteriolaterally. Each row or stack of filaments constitutes a hemibranch, while a set of hemibranchs, one on each side of the arch, constitutes a holobranch. The gills of teleost fishes are composed of four such holobranchs spaced between five branchial slits (chambers) (Figure 12.1).

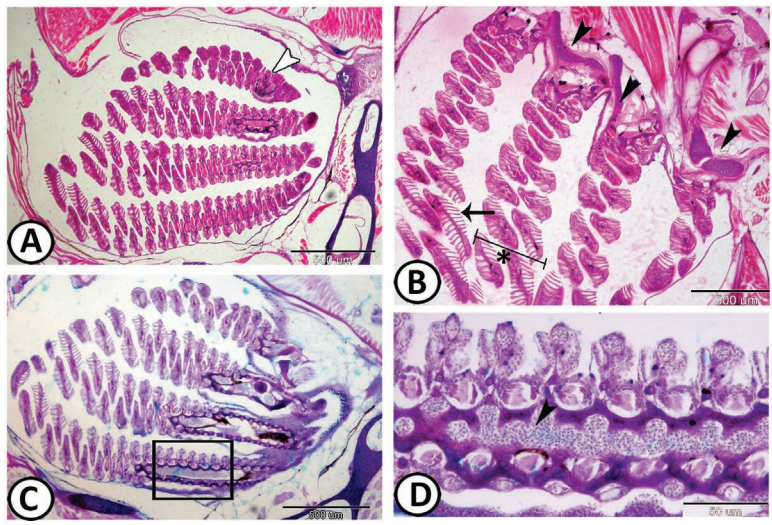

FIGURE 12.1 (A, B) Gills of guppy fish consisted of four holobranchs (white arrowhead) extend from the floor to the roof of the buccal cavity. Osseous fish have four pairs of cartilaginous or bony GAs (black arrowheads), onto which two rows of tens of GFs (asterisk) are attached. Each filament bears many plate-like secondary lamellae (arrow) (HE). (C, D) Gills of guppy stained by PAS-AB/HX showing GFs (boxed area) and afferent blood vessels (BVs) (arrowhead).

Each hemibranch bears many fine subdivisions called primary gill lamellae, which project from the arch like the teeth of a comb (Figure 12.2). The surface area of the primary lamellae is increased further by the formation of regular semilunar folds across its dorsal and ventral surface—the

secondary lamellae. The purpose of these structures is to provide a large surface area that supports respiratory and excretory functions. The efficiency of exchange, which in the case of oxygen is roughly 50%–80%, is largely a function of the countercurrent exchange between blood and water.

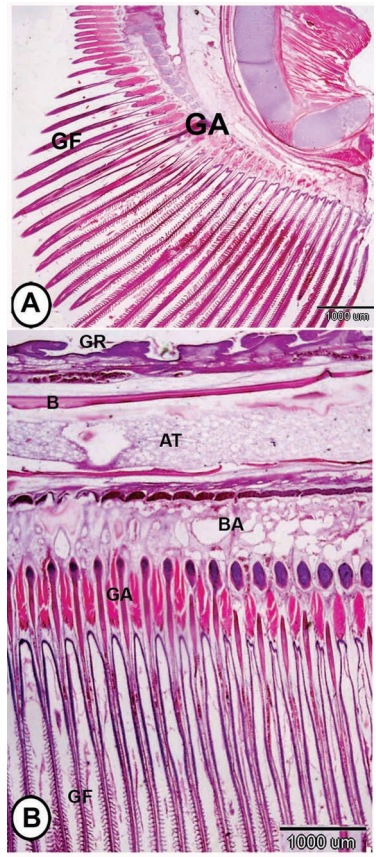

FIGURE 12.2 (A, B) Gills of Nile tilapia showing rows of gill filaments (GFs) extending from gill arch (GA) stained with HE. Note the presence of gill rakers (GRs) supported by bone (B) and followed by adipose tissue (AT) and branchial artery (BA).

12.1 THE GILL ARCH

It is a curved cartilaginous or osseous structure, from which radiate the bony supports (the gill rays) of the primary lamellae. The associated striated abductor and adductor muscles (Figure 12.3) facilitate the movement of the

gills to favorable respiratory positions. The gills are covered and protected by an operculum. Unlike the Chondrichthyes, the septa of teleosts are much reduced. The lamellae are free and this arrangement provides a larger respiratory surface.

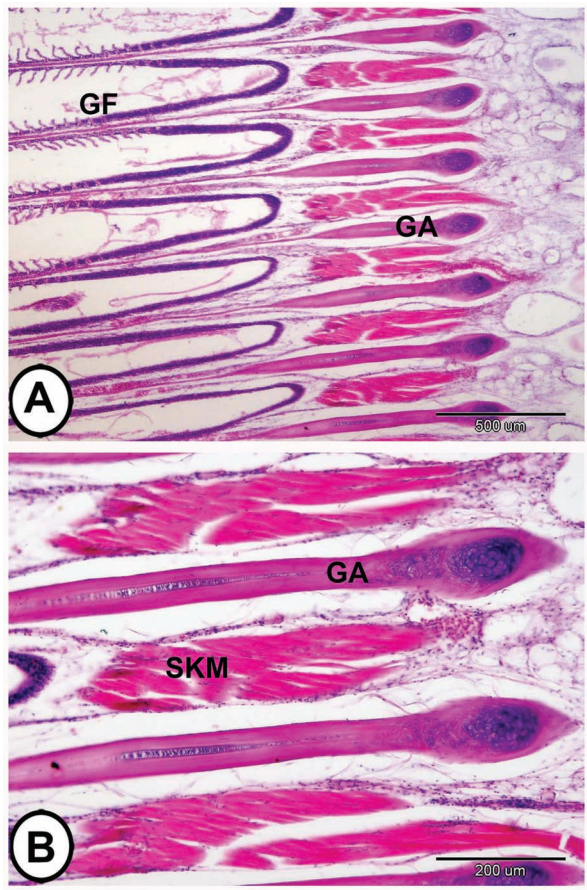

FIGURE 12.3 (A, B) The cartilaginous core of the GA extends to the GFs in Nile tilapia stained with HE. Note the presence of supported skeletal muscle fibers (SKM).

The GA contains the afferent brachial arteries (Figure 12.4) from the ventral aorta and the efferent brachial arteries serving the dorsal aorta. The ventral aorta divides into numerous fine branches as it passes up through the holobranch. Each branch runs along the opercular edge of the primary lamella to serve the secondary lamellae joining the branch of the efferent

brachial artery (BA) running down the buccal edge of the primary lamellae. Thus, the deoxygenated blood circulates through the secondary lamellae in a direction opposite to that of the water flow over the gills.

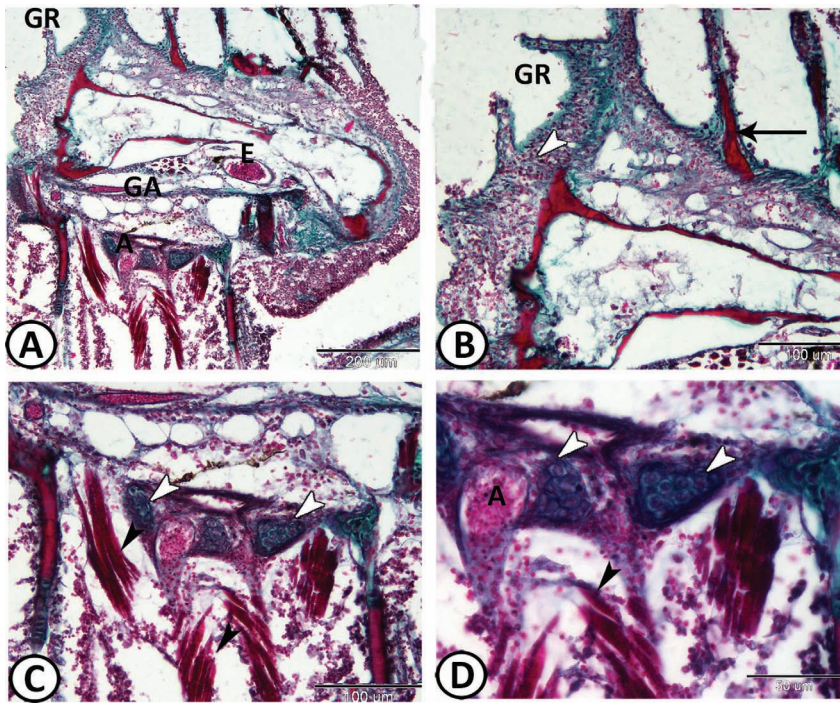

FIGURE 12.4 The GRs and GAs of molly fish stained by Crossmon's trichrome. (A) GRs are variously shaped bony or cartilaginous projections, which point forward and inward from the gill (or branchial) arch (GA). Note the afferent (A) and efferent (E) BVs. (B) The GRs are lined with the mucous pharyngeal stratified EP (arrowhead) supported by loose CT and bony pieces (arrow). (C, D) Higher magnification of the GA showing cartilaginous supports (white arrowheads) and branchial muscles (black arrowheads). Note the afferent (A) BVs.

The GA is covered by epidermal tissue (stratified EP) well-endowed with mucous cells (MCs). Below the epidermal tissue, there is usually a lymphocytic infiltration (Figure 12.5A). The scanning electron microscopy showed that the surface of the GA is composed of compactly arranged epidermal cells covered by concentrically arranged microridges (MRs). Many pores for the MCs are inserted between these epidermal cells in the form of rounded openings (Figure 12.5B).

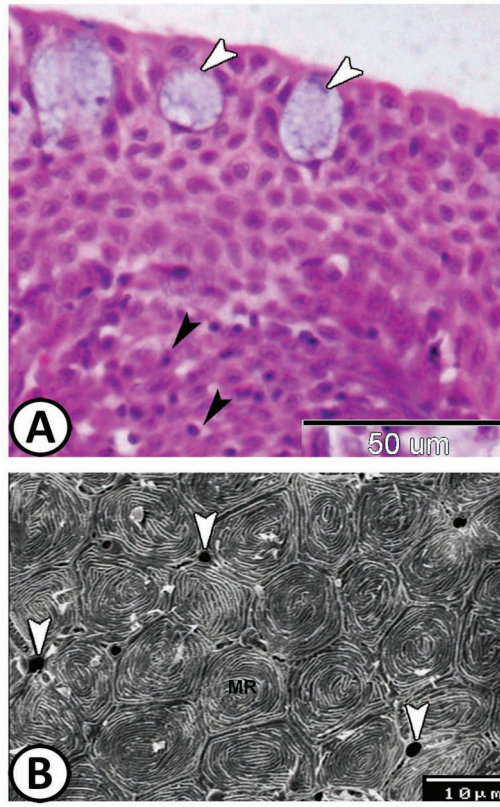

FIGURE 12.5 (A) The covering EP of the GA of grass carp stained with HE consisted of stratified epithelial cells with apical MCs (white arrowheads) and basal lymphocytes (black arrowheads). (B) Scanning electron microscopy (SEM) showing the surface EP of the GAs of guppy. Note the presence of openings for the MCs (arrowheads) and fingerprint-like MRs that cover the epithelial surface.

12.2 GILL FILAMENTS

12.2.1 THE PRIMARY LAMELLAE

The primary lamella has central cartilaginous support, afferent and efferent arterioles, and other anastomosing vessels comprising the central venous sinus (VS), which is a part of arteriovenous circulation (Figures 12.6 and 12.7).

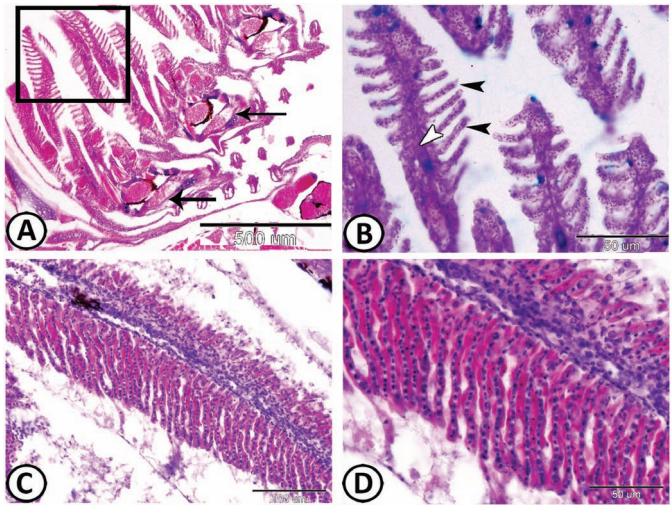

FIGURE 12.6 (A, B) Two GAs (arrows) of guppy stained by HE and AB-PAS/HX, respectively, showing the GFs (boxed area) that consist of primary (white arrowhead) and secondary (black arrowheads) gill lamellae. (C, D) Higher magnification of one primary gill lamella of guppy that bears many secondary gill lamellae (stained by HE).

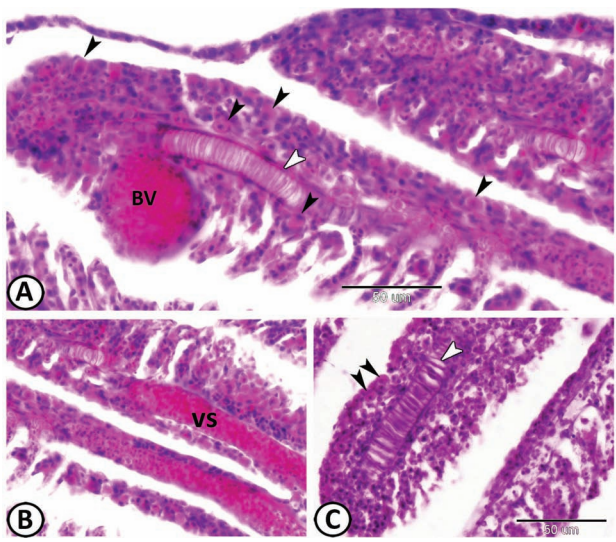

FIGURE 12.7 (A, B) Higher magnification of one primary gill lamella of guppy that has supportive cartilage plates (white arrowhead), BVs, and central venous sinus (VS). Note the presence of numerous chloride cells (black arrowheads) (HE). (C) The primary gill lamella of molly is supported by cartilage (white arrowhead) and lined by stratified EP containing chloride cells (black arrowheads) (HE).

The EP of the primary lamellae (Figure 12.7) is thicker than the EP of the secondary one, typically being composed of three or more cell layers. They are covered by epidermal tissue (stratified EP) containing MCs. The majority of the surface EP is covered with cuboidal and squamous epithelial pavement cells (PVCs), pale-staining MCs, and salt-secreting chloride cells. These chloride cells are most numerous at the basal (proximal) part of the lamellae. They function in ionic transport with a possible role in detoxification. At the origin of the primary lamellae, the epidermis is much thicker and usually contains numerous MCs (Figure 12.8B). Below the epidermis, there is a varying number of lymphocytes, eosinophils, and phagocytic cells. Blood flows via the afferent filament arteries of the primary lamellae into the blood spaces of the secondary lamellae, where CO_2 is released into the water and O_2 is taken up.

12.2.2 THE SECONDARY LAMELLAE (SITE OF GASEOUS EXCHANGE)

Each lamella is best regarded as a thin envelope of cells lying on a basement membrane (Figure 12.8). The secondary lamellae consist of one layer of epithelial cells, supported and separated by pillar cells. Spaces between pillar cells, called lacunae, connect afferent and efferent arterioles. The contractile pillar cells control the lacunar diameter thus regulating blood flow.

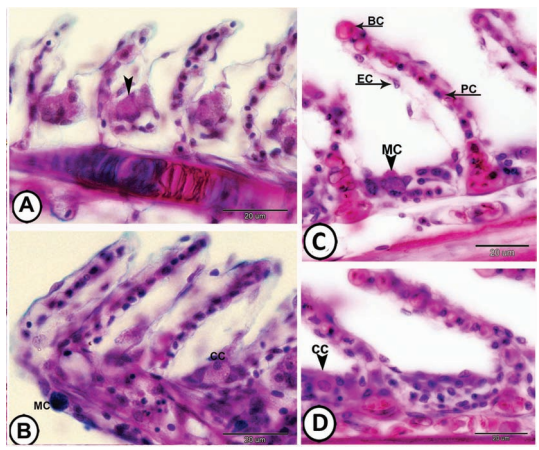

FIGURE 12.8 (A, B) GFs of molly fish stained with combined PAS-AB/HX showing positive-stained MCs and large club cells (cc, arrowhead). Note in (B), the thickness of the EP of lamellae increases at the tip. (C, D) The secondary lamella of Nile tilapia consists of pillar cells (arrow, PC), pavement epithelial cells (arrow, EC), and blood capillary (arrow, BC). Note the presence of mucous cells (arrowhead, MC) and chloride cells (cc) in the bases of interlamellar spaces.

The gaseous exchange takes place across the surface of the secondary lamellae primarily through countercurrent exchange of blood flowing in the opposite direction from the external water. The oxygenated blood leaves the secondary lamellae by efferent lamellar arteries to feed the dorsal aorta, from where it is distributed to all tissues. The surface of the secondary lamellae consists of overlapping or interdigitating squamous epithelial cells (PVC), usually one layer thick, supported and separated by pillar cells, which are arranged in rows 9–10 μm apart.

The fish gill is a highly complex organ that receives extensive nervous innervation from both afferent (sensory) and efferent (motor) fibers. Innervation from the latter source includes autonomic nerve fibers of spinal (sympathetic) and cranial (parasympathetic) origin whose primary role is to induce vasomotor changes within the respiratory or nonrespiratory pathways of the gill vasculature. The immunohistochemical analysis revealed that the GAs of molly are well endowed with nerve fibers (Figure 12.9A and B) that express glial fibrillary acidic protein (GFAP) immunoreactivity. These nerve fibers extended to gill filaments (Figure 12.9C). The EP of the primary and secondary gill lamellae contained positive-GFAP chloride cells (Figure 12.9D–F).

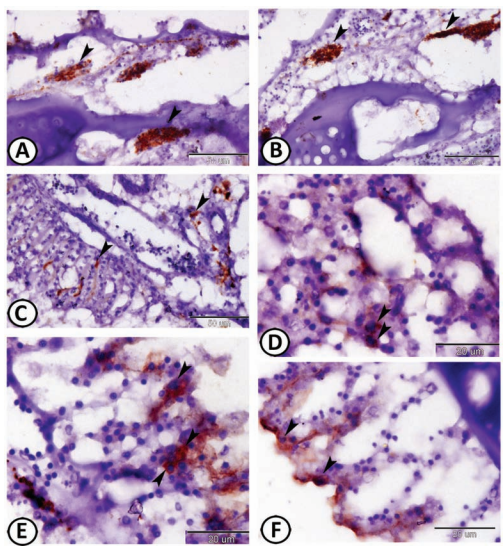

FIGURE 12.9 Immunohistochemical expression of GFAP in molly fish. (A, B) Nerve fibers (arrowheads) are distributed in the GA. (C) Nerve fibers (arrowheads) between the gill filaments. (D) Positive-immunoreactive chloride cells (arrowheads) in the EP of the GA. (E, F) Positive-immunoreactive chloride cells (arrowheads) in the secondary gill filaments.

12.2.3 CELLULAR CONSTITUENTS OF THE GILL FILAMENTS

12.2.3.1 THE PILLAR CELLS

These are modified endothelial cells with a centrally located polymorphic nucleus that support and define the lamellar blood spaces. Where the pillar cells impinge on the basement membrane, the blood capillaries spread to form flanges that coalesce with those of neighboring pillar cells to complete the lining of the lamellar blood channels, which contact the afferent and efferent lamellar arteries. They give the lamellae the appearance of a string of beads when viewed in cross section.

The pillar cells have been shown to contain columns of contractile protein similar to that found in amebae. Since the blood entering the lamellar blood spaces comes directly from the ventral aorta at high pressure. The presence of contractile elements in the supports of these spaces serves to resist their distension under normal circumstances. Also, the contraction of pillar cells can be used to control the blood flow rate through the gaseous exchange surfaces. The combined thickness of the cuticle, respiratory EP, and flanges of the pillar cells ranges from 0.5 to 4 μm. This represents the total diffusion distance for the respiratory exchange since the diameter of the lamellar blood channel is virtually the same as the diameter of the teleost erythrocyte.

12.2.3.2 CHLORIDE CELLS (MITOCHONDRIA-RICH CELLS, MRCS)

Mitochondria-rich cells (MRCs) are seen on the basement membrane of the secondary gill lamella. These cells are acidophilic and exist generally in marine fishes and rarely in freshwater fishes. The chloride cell may be elongate, ovoid, or cuboidal in shape, depending upon the species with granular cytoplasm. Chloride cells surrounded by flattened PVC can be observed at the junction between the primary and secondary lamellae. MRCs tend to be concentrated in the afferent region of the filament EP and have an intimate association with the arteriovenous circulation, notably the central VS; although in the interlamellar region, MRCs are also associated with the basal channels of the lamellar arterio-arterial circulation.

The defining feature of this cell type is a high mitochondrial density. In the apical region of MRCs is a collection of tubules and vesicles (tubulovesicular system) that are distinct from the tubular system. The apical membrane can be quite variable in appearance ranging from concave to convex, sometimes forming deep crypts.

Chloride-secreting cells are identified on the basis of their greater affinity for eosin. Since then, some more specific histological stains have been used with success to identify and enumerate MRCs. The acid fuchsin stain is used to identify MRCs in eel. The use of Champy–Maillet's fixative (ZnIOsO4) originally applied to fish MRCs has been used by a number of investigators to quantify and localize MRCs. Watrin and Mayer-Gostan stain reacts specifically with abundant membrane systems of the MRC results in its selective blackening.

The term "chloride cell" relates to the function of the MRC in chloride ions elimination. However, in general, numerous mitochondria in these cells are thought to supply the adenosine triphosphate for ion-transport proteins to drive the vectorial transport of ions as part of ion and acid–base regulation. In addition, MRCs appear in response to exposure to acid conditions, suggesting a role in acid excretion.

12.2.3.3 MUCOUS CELLS

The MCs are a prominent feature of the gill filament (GF) EP that is frequently observed in afferent and efferent edges, interlamellar space, the base of lamellae, and the outer margin of lamellae. They are large ovoid cells that are composed mostly of apical mucous secretory granules. The nucleus and cytoplasm are usually flattened and in a basal position. The biological importance of the mucus-rich interface between fish and their aqueous environment spans functions as diverse as mechanical and immunological protection in reducing the infection and abrasion and has a significant role in regulating the exchange of gas, water, and ions.

Goblet cells have been found in all fishes with the exception of the hagfishes. MCs have also been characterized by the types of mucin in their granules. The periodic acid–Schiff (PAS) method is used to detect neutral mucins, and the variations of the alcian blue method to detect acidic mucins (pH 2.5, carboxylated, and sulfated mucins; pH 0.5, sulfated mucins, and Quintarelli's acid hydrolysis sialomucins).

12.2.3.4 PAVEMENT CELLS

The most abundant cell type covering the EP (90% of the surface area) is the squamous to cuboid-shaped cell commonly referred to as the pavement

or respiratory cell. The nucleus in squamous PVC is compressed, while in cuboidal PVC it is rounded.

The apical surface of PVC is usually large and polygonal and possessed irregular microridges (MRs) that interwoven to form a web-like pattern (referred to microplicae when viewed in cross section) or microvilli (finger-like projections). A well-defined double row of MRs demarks the borders of neighboring PVC (Figure 12.10). These MRs have been suggested to enhance the mechanical flexibility and protection and to impart a firm consistency to the free surface of the epithelial cells. MRs are often interconnecting together, which may enhance their consistency or rigidity. PVCs increase the apical surface area (densities of microvilli and microplicae) in response to hypercapnia and alkaline exposure.

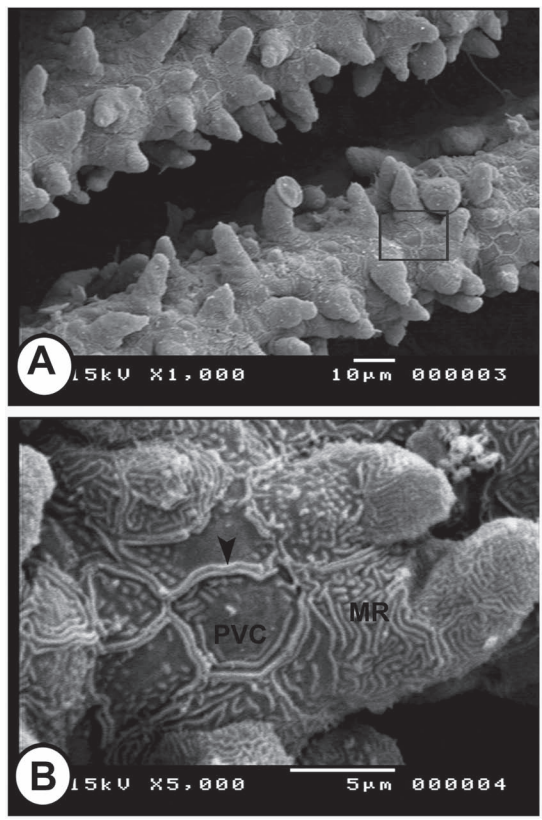

FIGURE 12.10 (A, B) SEM of the lamellar EP (square) of guppy showing the covering PVCs that covered with MRs. Note the double ridge marks the borders (arrowhead) between the neighboring cells.

12.2.3.5 OTHER CELLS

Other cells that are found within the filamental interstitium include lymphocytes, macrophages, and neuroepithelial cells. The neuroepithelial cells are found deep within the filament EP along the full length of the efferent edge although concentrated near filament tips. Neuroepithelial cells have been described in elasmobranch and teleost fishes. The fish neuroepithelial cells share common characteristics with the neuroepithelial cells that are described within the wall of the respiratory tract of mammals. These cells can be readily identified by detecting the biogenic amine fluorescence resulting from formaldehyde treatment, which has been confirmed to include 5-hydroxytryptamine by immunohistochemistry. These cells are believed to function as oxygen sensors and to be involved in the regulation of blood flow.

12.3 GILL RAKERS

The inner surfaces of the GAs carry one or more rows of stiff strainers called gill rakers (GRs). They serve to sort and aggregate particulate food material and to position larger food items before the food is passed into the esophagus and then into the stomach or intestine. The shape and number of these structures are a good indication of the diet of the fish. The rakers tend to be long, slender, and tightly packed in herbivorous fishes and particle feeders (such as anchovies, herrings, alewife, and certain scombrids) and their number can exceed 150 per arch. They are shorter, thicker, and more widely spaced in fishes that feed on larger prey. Histologically, each GR is composed of an osseous or cartilaginous supporting the pharyngeal stratified EP and adipose connective tissue (CT) (Figure 12.4).

12.4 OPERCULUM

Water is passed in, through the mouth, over the gills and out through the opercula. The water flow is driven by alternate expansion and contraction of the buccal and opercular chambers. The operculum (Figure 12.11) is located on each side of the head of the bony fishes. Some fish categories like sharks and rays do not have gill covers. This protective flap is a bony plate lined with the skin and supported by a loose CT. The operculum is composed of four bones and its morphology varies greatly between species.

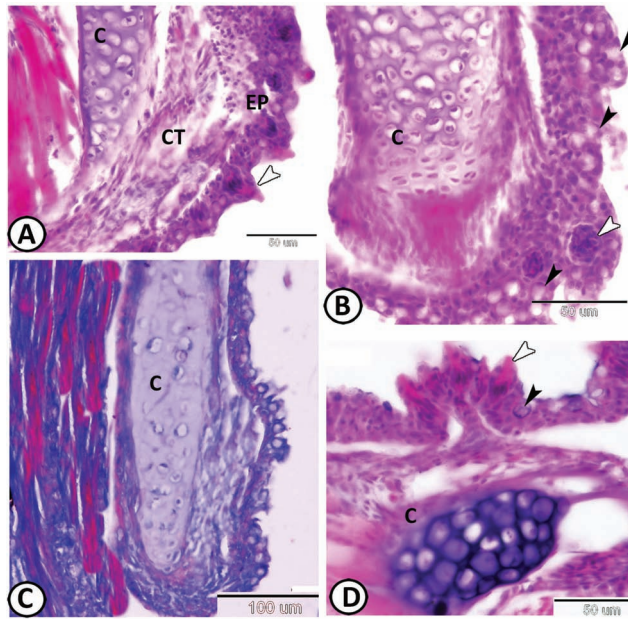

FIGURE 12.11 The operculum of guppy stained by HE (except for C is stained by Masson's trichrome). (A–D) The operculum consists of the EP, CT, and cartilage support (C). The EP contains the mucus cells (black arrowheads) and taste buds (white arrowheads).

Branchiostegals (or branchiostegal rays) are long and pointed dermal bones (or cartilages) that support the branchiostegal membrane (with some MCs and sometimes inappropriately called the gill membrane) below the operculum. Their number varies from none to up to 50. In cyprinids like the zebrafish, there are three branchiostegals. In guppy, the ventroposterior part of the operculum shows hyaline-cell cartilage containing closely packed cells separated by a scarce extracellular matrix.

KEYWORDS

- **gill epithelium**
- **gill rakers**
- **chloride cells**
- **hemibranch**
- **primary lamella**

BIBLIOGRAPHY

Elsheikh, E. H. Scanning Electron Microscopic Studies of Gill Arches and Rakers in Relation to Feeding Habits of Some Fresh Water Fishes, *J. Basic Appl. Zool*. 2013, 66(3), 121–130.

Fath-Elbab, M. R. 2nd ed.. Fundamentals of the Histology of Fish. *Part I Histology of Teleosts*, Egyptian Books House, Cairo Governorate, 2004.

Sturla, M.; Masini, M. A.; Prato, P.; Grattarola, C.; Uva, B. Mitochondria-rich cells in gills and skin of an African Lungfish, protopterus annectens, *Cell Tissue Res*. 2001, 303, 351–358.

Wendelaar Bonga, S. E.; Flik, G.; Van Der Heijden, A. J. H.; Verbost, P. M.; Eygensteyn, J.; Li, J. Mitochondria-rich cells in gills of tilapia (*Oreochromis mossambicus*) adapted to fresh water or sea water: quantification by confocal laser scanning microscopy, *J. Exp. Biol*. 1997, 200, 55–64.

Watrin, A.; Mayer-Gostan, N. Simultaneous recognition of ionocytes and mucous cells in the gill epithelium of turbot and in the rat stomach, *J. Exp. Zool*. 1996, 276, 95–101.

Wilsoni, J. M.; Laurent, P. Fish gill morphology: inside out, *J. Exp. Zool*. 2002, 293, 192–213.

Witters, H.; Berckmans, P.; Vangenechten, C. Immunolocalization of Na^+, K^+-ATPase in the gill epithelium of rainbow trout, *Oncorhynchus mykiss*, *Cell Tissue Res*. 1996, 283, 461–468.

Wright, D. E. The structure of the gills of the elasmobranch, *Scyliorhinus canicula* (L.), Z. Zellforsch. *Mikrosk. Anat*. 1973, 144, 489–509.

CHAPTER 13

Reproductive System

ABSTRACT

The female genital system consists of the ovaries and in most species a duct system communicating with the exterior. Fish ovaries may be of three types: cystovarian, gymnovarian, or secondary gymnovarian. Oogenesis involved the proliferation of oogonia by mitosis and the development of oocytes. Six stages are demonstrated: oogonia, early oocyte, late oocyte, vaculated follicles, yolk globule stage (vitellogenesis), and mature follicles. The follicular atresia is a common phenomenon of the teleost ovary and includes both oocytes and their follicular wall. Various types of cells were detected in the stroma, include telocytes, rodlet cells, mast cells, eosinophils, neutrophils, lymphocytes, fibroblasts, macrophages, melanocytes, adipocytes, dendritic cells, and endocrine (steroidogenic, interstitial) cells. Testis of teleosts is of two types: lobular and tubular. In the lobular type, a system of seminiferous tubules (STs) is arranged radially from the dorsal and lateral wall of the testis to the central lumen. The central lumen leads to efferent ducts (EDs), which are connected with each other to open into the sperm duct or vas deferens that leads to the urogenital pore. The testicular parenchyma consisted of branching tubular STs and interstitial tissue. The STs are made up of spermatocysts, where spermatogenesis occurred. In the tubular testis type, the sperms present only at the apex of the tubule, and cysts are migrating to the ED.

Ovaries and testes develop from paired masses of mesodermal tissue on either side of the dorsal mesentery in the dorsolateral lining of the peritoneal cavity. These indifferent genital ridges bulge into the developing coelom and are later invaded by primordial germ cells that will eventually give rise to oogonia or spermatogonia (SG). Covering the surface of the ovary is the so-called germinal epithelium (GE), which is continuous with the peritoneum lining the coelom.

Reproduction in most fishes is cyclic; although, the length of the cycle is extremely variable, which is correlated with photoperiod and temperature

variations. Certain salmonid and eel species spawn only once and then die, others may breed every 2 or 3 years, but most breed once or several times a year. Some teleosts and some species of oviparous skates appear to breed throughout the year.

Fishes that spawn once then die have synchronous ovaries in which all oocytes are at the same stage of development. Species that spawn once per year during short breeding season display group-synchronous ovaries which at least two populations of oocytes at different developmental stages are present; this type is common in teleosts. Ovulation at group-synchronous ovaries may occur at intervals over the breeding season so that the oocytes are released in batches. An asynchronous ovary contains oocytes at all stages of development and occurs in species that spawn many times during a long breeding season as goldfish*, Carassius auratus*.

The genital papilla is a small and fleshy tube located behind the anus that can determine the sex of the fish as this papilla is relatively smaller in females than those of males. In addition, females had three openings: the anus, the oviduct (OD) in which the eggs exit, and the urinary pore. Both the OD and the urinary pores are found in the genital papilla.

The female genital system consists of the ovaries and in most species a duct system communicating with the exterior. In addition to its cytocrine function in producing fertilizable gametes, the ovary shares with the testis the complementary endocrine function of secreting a variety of steroid hormones that regulate the development of the germ cells. ODs may be simple passageways for the eggs but often their lining is glandular and forms protective coverings for the eggs.

13.1 OVARIES

13.1.1 GROSS MORPHOLOGY

The ovaries of most fish species are paired elongated, cylindrical structure, and approximate of equal size. It is located in the posterior part of the body cavity, ventral to the swim bladder. The ovaries attach to the dorsal body wall by mesovarium and their posterior ends connect to the ODs, which open to the genital pore.

During the nonbreeding season, the ovaries are small, ribbon-like, yellowish red, occupied less than one-third of the body cavity, and the ova could not be seen. While during the breeding season, the ovaries are

extremely long and wide occupied almost entire of the body cavity and crowding the other viscera. Large numbers of spherical bright orange eggs are easily visible that gives the ovaries its granular texture. In addition, the ovaries are yellowish and vascularized. Ripped eggs are visible through a thin, distended, and transparent ovarian wall. Eggs are somewhat over a millimeter in diameter at extrusion.

Fish ovaries may be of three types: cystovarian, gymnovarian, or secondary gymnovarian. Cystovaries characterize most teleosts, where the ovarian cavity is connected directly to a short OD, an exit between the anus and the urinary pore. Gymnovaries are the primitive condition found in lungfish, sturgeon, and bowfin. In this type, the oocytes are released directly into the coelomic cavity and then enter the ostium, then through the OD are eliminated. Secondary gymnovaries shed ova into the coelom from which they go directly into the OD. The latter type is found in salmonids and a few other teleosts.

13.1.2 HISTOLOGICAL STRUCTURE

The histological examination of the ovaries shows oocytes at all stages of development and degeneration (atresia) (Figure 13.1). This occurs in cyprinids, tilapia, and other teleosts and due to multiple spawning, which is indicated by the occurrence of asynchronous oocyte development. In some fish, ovulation and spawning occur almost at the same time, whereas in others (*Salmonidae*), ovulated oocytes are retained in the peritoneal cavity, and spawning takes place later.

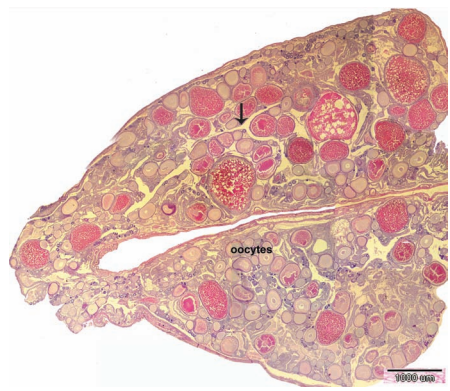

FIGURE 13.1 Oocytes of Nile tilapia at all stages of development are separated by ovocoel (arrow) (HE).

The ovocoel (ovarian cavity) is a lymph-filled space that remained in the center of the ovary as an irregular space and lined with GE (simple squamous epithelium) which is divided to give oogonia. The ovocoel continues posteriorly as the lumen of the OD (Figure 13.2).

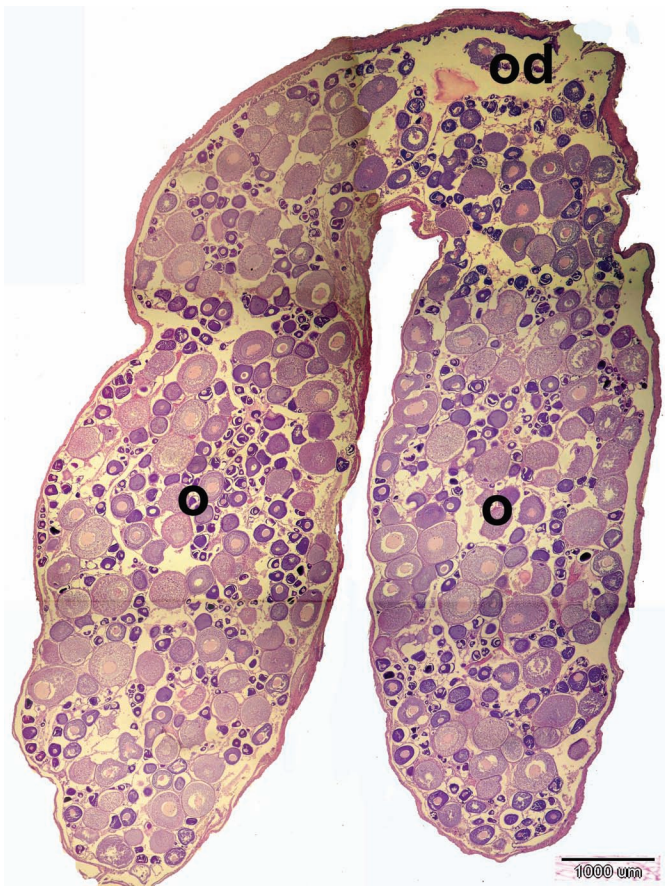

FIGURE 13.2 The two ovaries (O) of Nile tilapia by low magnification are connected to oviducts (ODs) (HE).

The ovarian wall is composed of three layers: the outermost is a thin layer of the mesothelium, the middle layer is the tunica albuginea, which is made up of collagenous, elastic fibers, and smooth muscle cells with some blood capillaries (BCs). The tunica albuginea is thin (29.18 ± 0.67 μm in thickness) and highly vascular during the breeding season, but became thick during

the nonbreeding season (its mean thickness reached 48.01 ± 4.45 μm). This may due to the expansion of the ovary by the presence of many large mature oocytes in the breeding season that pressed on the wall. The innermost layer is the GE, which projects into ovocoel in the form of finger-like ovarian lamellae that contain many oocytes at different stages of development (Figure 13.3).

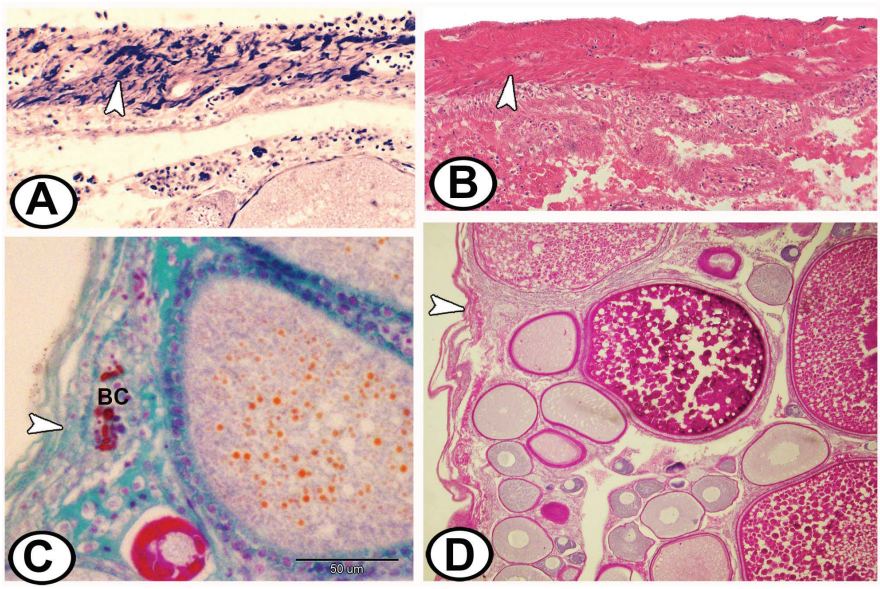

FIGURE 13.3 The ovarian wall in Nile tilapia. (A) The tunica albuginea contains elastic fibers (arrowhead) stained with Verhoeff's stain. (B) Smooth muscle fibers (arrowhead) stained by HE are scattered in tunica albuginea. (C) The tunica albuginea contains collagenous fibers (arrowhead) and blood capillary (BC) stained by Crossmon's trichrome. (D) The ovarian wall (arrowhead) is thin in the breeding season (stained by PAS-HX).

The developing ova are held together by the stroma, which consists of vascular collagenous connective tissue (CT) and few strands of smooth muscle fibers. The finger-like ovarian (ovigerous) lamellae contain ovarian follicles at different stages of oogenesis in addition to the atretic follicles (AFs). Ovigerous lamellae (OL) protruded into the ovocoel from the ovarian wall and the oogenesis occurs in these lamellae. During spawning, the stroma is extremely pressed due to the enlargement of ova (Figure 13.4).

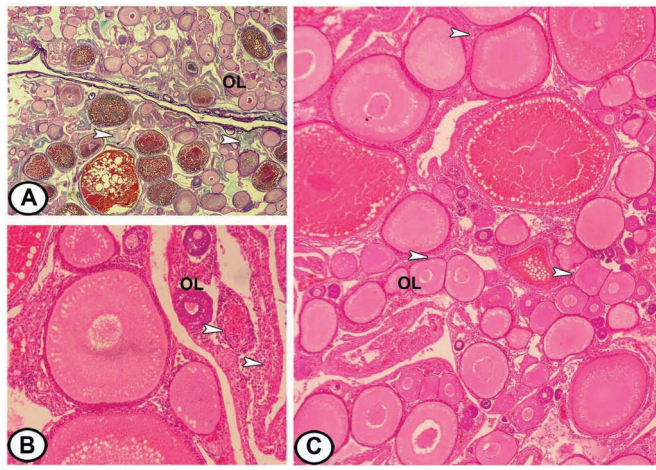

FIGURE 13.4 (A, B) The vascular collagenous stroma (arrowheads) of Nile tilapia between the ovarian lamellae (OL) stained with Crossmon's trichrome and HE, respectively. (C) The stroma (arrowheads) is reduced between distended OL during the breeding season (HE).

13.1.3 OOGENESIS

The oogenesis involves the proliferation of oogonia by mitosis and the development of oocytes. According to the changes in size, nucleus, ooplasm, and egg membranes of the developing ova, six stages are observed in *Oreochromis niloticus.*

13.1.3.1 STAGE 1—OOGONIA

Oogonia are found in groups or nests in the periphery of the OL, associated with the GE and they are the smallest cells of the germinative lineage. There are small spherical cells with large light basophilic nucleus with a single nucleolus. A thin film of faintly stained ooplasm surrounds the nucleus. All ovaries of developing and mature females have several patches of oogonia (Figure 13.5), this would be particularly important in a multiple-spawning fish, such as *O. niloticus*. Oogonia divided by mitosis to give the primary oocytes. The peak period of oogonial proliferation by mitosis occurs during the immediate postspawning period since nests of oogonia are present in the greatest abundance reaching 15 oogonia/unit area in April.

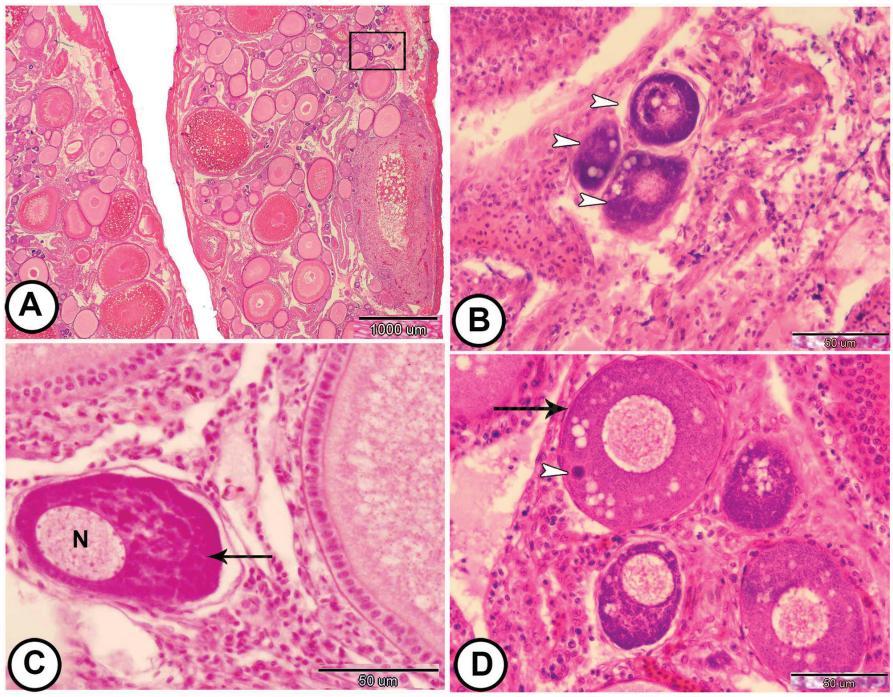

FIGURE 13.5 The stages of oogenesis in Nile tilapia stained with HE. (A) The ovary showing oocytes at all stages of maturity. The square focus in the oocytes near the tunica albuginea. (B) Groups of deep basophilic oogonia (arrowheads) with a light basophilic nucleus. (C) The chromatin nucleolus stage (arrow) contains a nucleus (N) with chromatin threads. (D) The perinucleolar oocyte stage (arrow) is surrounded by flat squamous cells. Note the presence of Balbini body (arrowhead).

During the breeding season, its mean number reaches 6.4 ± 2.1 and its mean diameter is 28 ± 0.8 µm, while during the nonbreeding season its mean number reaches 10 ± 1.5 and its mean diameter is 24.8 ± 2.0 µm. Oogonia show significant variations in the number but nonsignificant variations are found in the diameter between the breeding and nonbreeding seasons (Table 13.1). The oogonia arise from the primordial sexual cells either in or near the GE. The chromatin nucleolar stage (stage 2) originates from the oogonia and locates close to them.

TABLE 13.1 The Diameter (μm) and the Number/Unit Area of all Stages of Oocyte Development in Tilapia During Different Months of the Year

Months	Stage 1		Stage 2		Stage 3		Stage 4		Stage 5		Stage 6	
	Number	Diameter	Number	Diameter	Number	Diameter	Number	Diameter	Number	Diameter	Number	Diameter
Nonbreeding season												
October	10.0 ± 0.1	24.8	9.8 ± 0.21	40.0	9.0 ± 0.6	98.0	5.0 ± 0.2	204.0	2.0 ± 0.1	313.0	1.2 ± 0.5	509.0
November	14 ± 0.36	28.1	12 ± 0.36	42.78	10 ± 0.21	108.86	4 ± 0.47	224.01	1 ± 0.61	297.19	2 ± 0.11	521.63
December	10 ± 0.26	20.53	11 ± 0.25	35.68	7 ± 0.11	84.92	6 ± 0.16	220.01	1 ± 0.33	300.99	1 ± 1.0	505.41
January	12 ± 0.52	19.77	13 ± 0.84	33.87	18 ± 0.1	100.82	4 ± 0.15	189.39	3 ± 0.58	318.36	–	–
February	9 ± 0.54	30.4	8 ± 0.54	45.55	6 ± 0.41	95.71	6 ± 0.46	194.5	4 ± 0.91	330.5	1 ± 0.4	496.39
March	5 ±.0.33	25.41	5 ± 0.9	44.17	4 ± 0.13	100.38	5 ± 0.54	193.33	1 ± 0.28	320.6	1 ± 0.91	514.37
M ± SE	10 ± 1.5	24.8 ± 2	9.8 ± 1.4	40 ± 2.4	9 ± 2.4	98 ± 3.8	5 ± 0.4	204 ± 7.3	2 ± 0.6	313 ± 6	1.2 ± 0.2	509 ± 4
Breeding season												
April	15 ± 0.11	27.24	5 ± 0.33	45.12	4 ± 0.25	97.44	14 ± 0.33	234.73	5 ± 0.93	488.85	4 ± 0.16	671.91
May	5 ± 0.22	28.95	4 ± 0.14	36.62	2 ± 0.41	91.22	2 ± 0.51	227.48	3 ± 1.0	484.01	5 ± 0.12	1049.5
June	4 ± 0.31	29.52	2 ± 0.43	42.01	–	–	2 ± 0.32	267.8	4 ± 0.28	495.1	4 ± 0.45	874.18
July	3 ± 0.51	30.23	2 ± 0.41	51.33	–	–	3 ± 0.41	246.3	4 ± 0.54	492.6	5 ± 0.56	742.06
August	5 ± 0.24	25.3	3 ± 0.25	46.52	6 ± 0.25	111.99	6 ± 0.25	236.7	4 ± 0.28	500.24	2 ± 0.47	692.08
September	6.0 ± 0.61	28.0	4.0 ± 0.41	44.0	4.0 ± 0.2	100 ± 6	5.4 ± 2.2	242 ± 7	4 ± 0.31	492 ± 2.7	4 ± 0.5	806 ± 4
M ± SE	6.4 ± 2.1[a]	28 ± 0.8n.s.	3.2 ± 0.5[b]	44 ± 2.4n.s.	4 ± 1.1[a]	100 ± 6n.s.	5.4 ± 2.2n.s.	242 ± 7[b]	4 ± 0.3[b]	492 ± 2.7[a]	4 ± 0.5[a]	806 ± 11[b]

‘’a” indicates a significant value if $P < 0.05$;

‘’b” indicates a highly significant value if $P < 0.01$

13.1.3.2 STAGE 2—EARLY OOCYTE (CHROMATIN NUCLEOLUS STAGE)

The transformation of oogonia to oocyte includes an increase in the size of the cell and nucleus. The chromatin of the nucleus appears thread-like and distributed throughout the nucleus. The number of nucleoli increases, which is distributed throughout the nucleoplasm. The ooplasm is reduced and deeply basophilic. These oocytes have little or no affinity with dyes used (Figure 13.5C).

During the breeding season, its mean number reaches 3.2 ± 0.50 and its mean diameter is 44.0 ± 2.4 μm while during the nonbreeding season, its mean number reaches 9.8 ± 1.4 and its mean diameter is 40.0 ± 2.4 μm. Early oocytes show highly significant variations in the number but nonsignificant variations are found in the diameter between the breeding and nonbreeding seasons (Table 13.1).

13.1.3.3 STAGE 3—LATE OOCYTE (PERINUCLEOLAR STAGE)

The nucleus stains lightly and the number of nucleoli increases, and arranges themselves in the peripheral part of the nucleus. Chromosomes assemble at one side of the nucleus. Ooplasm contains the yolk nucleus (Balbini bodies), which appears as basophilic round mass, commonly close to either the nucleus or the oocyte periphery. Oocytes are surrounded by a single layer of squamous follicular epithelium (Figure 13.5D).

Also in this stage, the oocytes increase progressively in the diameter. During the breeding season, its mean number reaches 4.0 ± 1.1 and its mean diameter is 100.0 ± 6.1 μm, while during the nonbreeding season their mean number reaches 9.0 ± 2.4 and their mean diameter is 98.0 ± 3.8 μm. The late oocytes show significant variations in number but nonsignificant variations are found in the diameter between the breeding and nonbreeding seasons (Table 13.1). The ovarian lamellae are thin in nonbreeding season and are filled with previtellogenic oocytes in the perinucleolus stage. Oocytes in the oogonium and chromatin nucleolus stage are abundant (Figure 13.2).

31.1.3.4 STAGE 4—VACUOLATED FOLLICLES (YOLK VESICLE OR CORTICAL ALVEOLAR STAGE)

The nucleus increased in size to become the germinal vesicle. The nucleoplasm attains acidophilic reaction with hematoxylin and eosin (HE) and

the nuclear membrane becomes irregular. The ooplasm becomes faintly acidophilic and a large number of small yolk vesicles (Yvs) are peripherally arranged, later become cortical alveoli, and take part in the formation of perivitelline space. A few small yolk granules appear in the ooplasm around the nucleus. Zona radiata (ZR) (oolemma) begins to appear, which is an acellular thin hyaline acidophilic membrane composed of some major proteins. The follicular layer is formed of cuboidal cells. The stroma of the ovary forms flat thecal cells (thin layer of fibroblasts) that surrounded the follicular layer (Figure 13.6A).

The oocytes increase both in the number and in diameter. During the breeding season, its mean number reaches 5.4 ± 2.2 and its mean diameter is 242.0 ± 7.0 μm, while during the nonbreeding season its mean number reaches 5.0 ± 0.4 and its mean diameter is 204.0 ± 7.3 μm. The late oocytes show nonsignificant variations in number but highly significant variations are found in the diameter between the breeding and nonbreeding seasons (Table 13.1).

Perinucleolar and Yv oocytes show numerous nucleoli. This nucleoli multiplication is necessary for the formation of a population of ribosomes sufficiently large to last during the cleavage period. Also, some of these nucleoli are extruded into the surrounding ooplasm. The nucleolar extrusion may have something to do with the process of oogenesis and/or the various metabolic activities taking place in the cell. The number and the size of the nucleoli decrease in the yolk globule (YG) and mature oocytes.

13.1.3.5 STAGE 5—YG STAGE (VITELLOGENESIS)

The Yvs increase in size in this stage. The yolk granules (protein) accumulate into large YGs. Several rounded YGs (platelets) appear near the center of the oocyte and extend centrifugally until only a thin peripheral shell of cytoplasm remains. Numerous fat vacuoles occur throughout the ooplasm. It is possible that the small vesicles located close to the oocyte periphery are cortical alveoli since their size, shape, and distribution are very similar to those of the alveoli at Yv stage. ZR appears thick and the follicular epithelium (granulosa) make up of cuboidal cells. The theca folliculi divides into an outer vascular, collagenous CT thecal layer, and an inner cellular theca cells (ThCs) (Figure 13.6B).

The oocytes increase in size. During the breeding season, its mean number reaches 4.0 ± 0.31 and its mean diameter is 492.0 ± 2.7 μm, while during the

nonbreeding season its mean number reaches 2.0 ± 0.6 and its mean diameter is 313.0 ± 6.0 µm. YG oocytes show highly significant variations in number but significant variations are found in the diameter between the breeding and nonbreeding seasons (Table 13.1).

YG stage is the most important phase of the oocyte development; since during this phase, vitellogenesis occurs resulting in an extensive oocyte growth chiefly by a rapid incorporation of large amounts of exogenous hepatically derived vitellogenin. While some authors reported that the growing ovarian follicles produce steroid hormones (Estradiol). This steroid leaves the follicle via blood vessels (BVs) supplying the ThC layer and is transported to the liver where it induces the production of vitellogenin. Vitellogenin is transferred to the ovary via the circulation, where it has taken up by the oocyte and is deposited as yolk protein, which serves as building and energy material after fertilization. The oocytes reach their maximal diameter of about 500 µm.

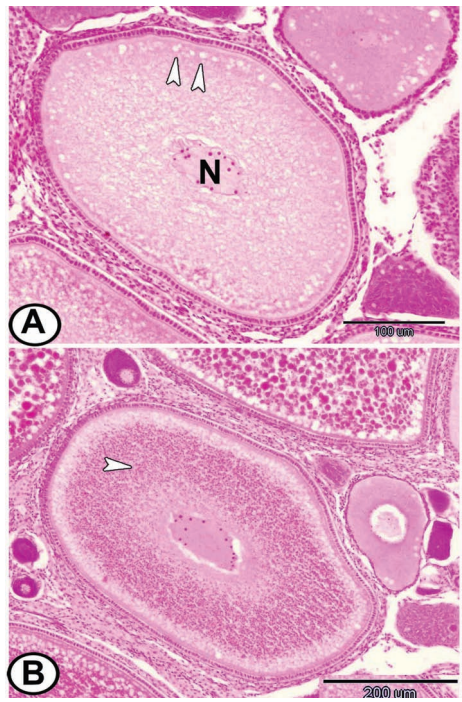

FIGURE 13.6 (A) The Yv stage in Nile tilapia contains a central nucleus (N) that had a large number of peripherally arranged nucleoli. Notice the presence of peripherally arranged yolk vesicles (arrowheads) (HE). (B) The YG stage shows a large number of yolk granules (arrowhead) distributed around the nucleus (HE).

13.1.3.6 STAGE 6—MATURE FOLLICLES

The mature follicle is characterized by the presence of many empty large vacuoles toward the oocyte periphery and the YGs increase in size. The nucleus (germinal vesicle) gradually disappears and begins to migrate to the animal pole just beneath the oocyte surface and then breakdown (germinal vesicle migration stage), which usually occurs at the end of vitellogenesis (Figure 13.7).

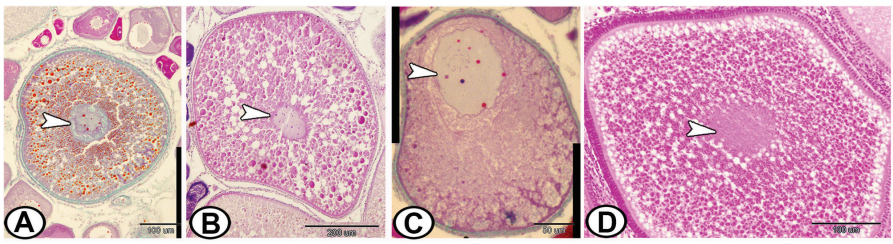

FIGURE 13.7 (A–D) The stages of migration of the nucleus (arrowheads) of mature oocytes from the central position to the animal pole in Nile tilapia. (A, C) Stained by Crossmon's trichrome. (B) Stained by PAS-HX. (D) Stained by HE.

With germinal vesicle breakdown, the protein YGs start to coalesce and the oocyte rapidly increases in its volume, then the oocyte ovulates into the ovarian lumen and becomes a mature ovum. At the end of this stage, the nucleus is not visible in the maturation stage due to the disintegration of the nuclear membrane and dispersion of its content in the cytoplasm. In addition, the follicular layers become extremely well-developed, consisted of ZR that attained its maximal thickness and surrounded by cuboidal granulosa and ThCs (Figure 13.8). This reflects the increased steroidogenic function of the granulosa and the theca during active vitellogenesis. The basal lamina (Bl) [a thin fibrous layer, periodic acid–Schiff (PAS)-positive] is found between the follicular epithelium and theca layer. On the other hand, the Yvs contain glycoprotein and exhibit a strong positive reaction to PAS stain (Figure 13.8D).

The YGs consist mainly of lipoprotein with a small proportion of carbohydrates. So, they show a weak positive reaction to PAS stain; however, strong reactivity is recorded by Crossmon's trichrome and Verhoeff's stain (Figure 13.9). Besides being the major nutritional source, YG is involved in embryogenesis. In addition, yolk proteins are useful for monitoring the environment. Moreover, the ZR reacts positively with Crossmon's trichrome

and Verhoeff's stain, because of their presence of tyrosine-encircled proteins. This is confirmed by staining with bromophenol blue (Figure 13.10). The mature follicles show positive bromophenol staining while the immature ones show a negative reaction. Also, the zona pellucida layer shows a strong affinity for this stain.

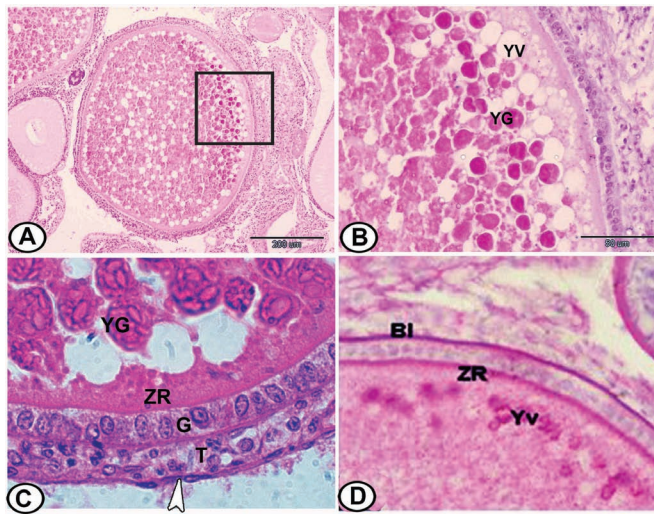

FIGURE 13.8 The mature oocytes of Nile tilapia. (A) The mature oocytes are characterized by their large size and absence of the nucleus (HE). (B) A magnified view in the boxed area of (A) showing part of the mature oocyte contained large YGs and Yv (HE). (C) The wall of the mature follicle consists of zona radiata (ZR), granulosa layer (G), and thecal layer (T). Notice the lumen of the ovary is lined with flat squamous cells (arrowhead) (HE). (D) The wall of mature oocyte showing PAS-positively reacted basal lamina (Bl), ZR, as well as a strong PAS-positive reaction in the Yvs is demonstrated.

The YGs consist mainly of lipoprotein with a small proportion of carbohydrates. So, they show a weak positive reaction to PAS stain; however, strong reactivity is recorded by Crossmon's trichrome and Verhoeff's stain (Figure 13.9). Besides being the major nutritional source, YG is involved in embryogenesis. In addition, yolk proteins are useful for monitoring the environment. Moreover, the ZR reacts positively with Crossmon's trichrome and Verhoeff's stain, because of their presence of tyrosine-encircled proteins. This is confirmed by staining with bromophenol blue (Figure 13.10). The mature follicles show positive bromophenol staining while the immature ones show a negative reaction. Also, the zona pellucida layer shows a strong affinity for this stain.

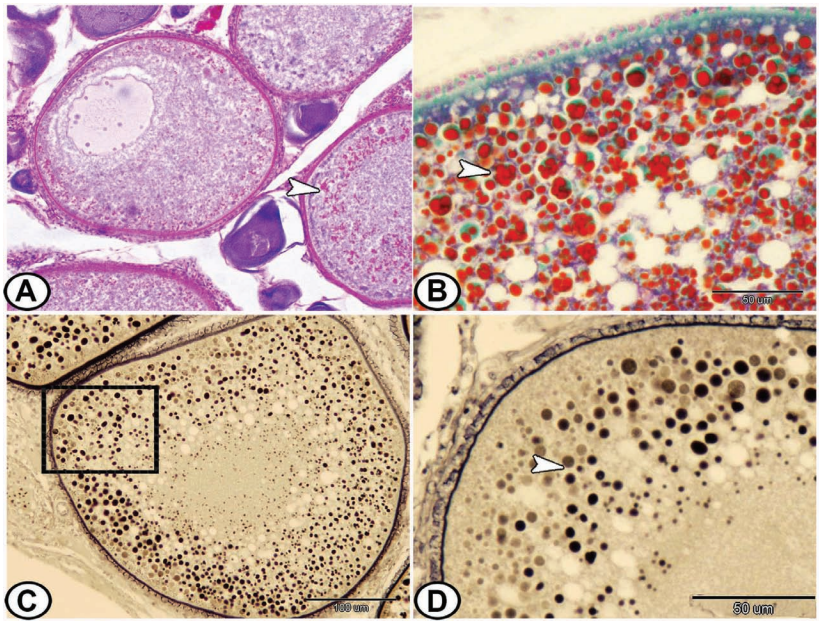

FIGURE 13.9 Histochemistry of the ovary of Nile tilapia. (A) The mature oocyte by PAS showing a positive reaction in the YGs (arrowhead). (B) A part of mature oocyte showing reddish colored coalesced YGs (arrowhead) by Crossmon's trichrome. (C, D) A mature oocyte showing a variable size of brown to blackish YGs (arrowhead) by Verhoeff's stain.

The wall of mature ovarian follicles expresses a positive immunoreaction to MMP9 (Figure 13.11D). Matrix metalloproteinases (MMPs) are a specific class of proteolytic enzymes that play critical roles in follicular development and luteinization. MMPs are the enzymes that break down the extracellular matrix and CTs to facilitate tissue remodeling.

The oocyte is large in diameter in the mature follicle, its mean diameter reaches 1049.5 µm (Table 13.1). During the breeding season, the ovarian lamellae are thick and completely obliterate the ovaries. The mean number of mature oocytes reaches 4.0 ± 0.5 and their mean diameter is 806.0 ± 15.0 µm, while during the nonbreeding season their mean number is 1.2 ± 0.2 and their mean diameter is 509.0 ± 4.0 µm. The mature oocytes show significant variations in number but highly significant variations in the diameter between the breeding and nonbreeding seasons are demonstrated.

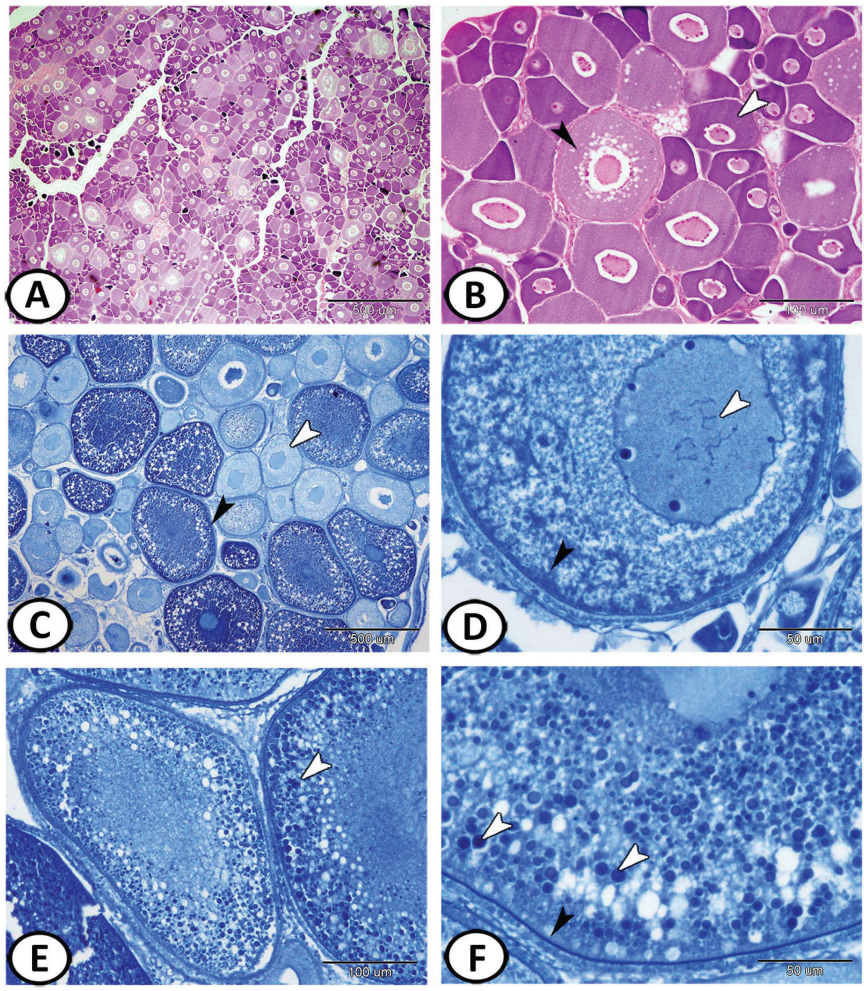

FIGURE 13.10 The ovary of Nile perch. (A, B) The ovarian lamellae are thin in non-breeding season and are filled with previtellogenic oocytes. Oocytes in the chromatin nucleolus (white arrowhead) and perinucleolus stage (black arrowhead) are abundant (HE). (C) Mature follicles at the breeding season (black arrowhead) showed a positive reaction to Bromophenol blue compared with immature ones (white arrowhead) that showed a negative reaction. (D) The stage of the nucleus migrations of the mature follicle shows dispersed chromosomes in the nucleus (white arrowhead) and positive-YGs peripherally (black arrowhead) stained by Bromophenol blue. (E, F) Mature follicles showed positive-Bromophenol blue YGs (white arrowheads) and zona pellucida (black arrowhead).

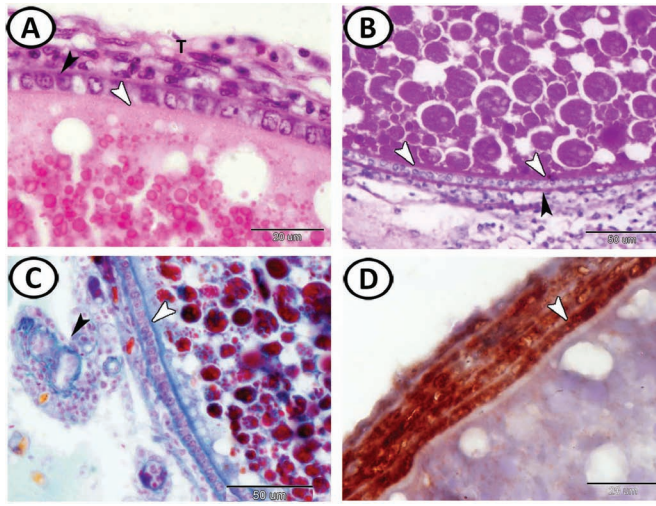

FIGURE 13.11 The wall of the mature ovarian follicles of Nile perch. (A) The wall is formed of zona pellucida (white arrowhead), zona granulosa (black arrowhead) followed by theca layer (T) (HE). (B) The zona pelluicda (white arrowhead) and the basement membrane (black arrowhead) show positive reactions to PAS. (C) The zona pelluicda (white arrowhead) stained positive to Crossmon's trichrome. Note, the neighboring blood vessels (black arrowhead). (D) The zona pelluicda expresses a positive immunoreaction to matrix metalloproteinases (MMP-9) (arrowhead).

13.1.4 ATRETIC FOLLICLES

AFs, or corpora atretica, result from the degeneration of an oocyte and its resorption by phagocytosis. The follicular atresia is a common phenomenon of the teleost ovary and includes both oocytes and their follicular wall. The atretic follicular cells enlarge and phagocytize the oocytes were not spawned and the CT surround the follicle thickened and become more vascular. The follicles contracted and folded probably as a result of the elastic properties of the theca externa. Their diameters are too variable to be measure since they are irregular structures that can be seen at any time during the oocyte maturation but they always formed at the period of post-spawning in oocytes at any stage. So, the presence of degenerated yolky oocytes indicated the occurrence of recent spawning.

Several stages of atresia are recorded in the ovary of Nile tilapia (Figures 13.12 and 13.13). Stage I: rupture of the nuclear envelope and dispersion of the chromatin in the ooplasm. Stage II: degradation and regression of yolk granules in the peripheral ooplasm with hypertrophy of follicle cells.

Stage III: the follicles display irregular shape and shrinkage, liquefaction of the YGs, disintegration, and fragmentation of the ZR. Stage IV: the yolk is almost completely phagocytosed by enzymes secreted from the follicle cells. Its ooplasm contains vacuoles and numerous small acidophilic mass of unclear nature that give a structure resemble corpora atretica or yellow-brown bodies. The theca layer is richly vascularized. Stage V: the follicle is ameboid in appearance and decreases in size and the yolk is completely reabsorbed. This stage is characterized by the accumulation of large vacuoles in the ooplasm while the ZR and follicular cells are completely digested. The CT is richly vascularized and surrounds the remaining of the follicle.

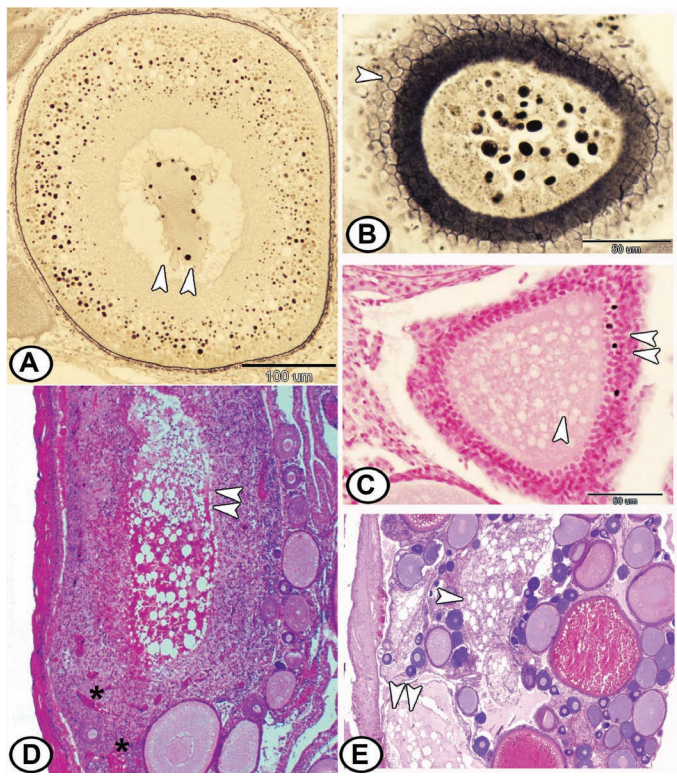

FIGURE 13.12 The stages of atretic follicles (AFs) in Nile tilapia. (A) Stage I, AF is characterized by a rupture of the nuclear envelope (arrowheads) (Verhoeff's stain). (B) Stage II, AF with hypertrophy of follicle cells (arrowhead) (Verhoeff's stain). (C) Stage III, AF with hypertrophied granulosa (double arrowheads). Note the presence of many cytoplasmic vacuoles (single arrowhead) (HE). (D) Stage IV, AF with liquefied yolk (arrowheads). Note the presence of many acidophilic masses (asterisks) (HE). (E) Stage V, shrinked and empty AFs (arrowheads) (HE).

The AFs express caspase-3 (Figure 13.13D). Caspase-3 is a protein encoded by CASP3 gene. It has a role in cell apoptosis, where it is responsible for chromatin condensation and DNA fragmentation.

Rodlet cells are observed in the follicular wall and inside the AFs (Figure 13E and F) that express α-smooth muscle actin and showed acid phosphatase activity. These results indicate that these cells have a role in atresia. The previous reports found that the rodlet cell cortex was enriched by phosphotyrosine, suggesting active protein tyrosine kinases and phosphatases are present in this structure. Tyrosine kinase and phosphatase activity have been implicated in some aspects of smooth muscle contraction. Rodlet cells contain actin cytoskeleton that may have a role in contraction to eject their contents. The rodlet cell undergoes a one-way contraction that eventually destroys the cell during the expulsion process; nuclei are either ejected or undergo structural deterioration and the rodlets along with the entire contents of the cell are expelled.

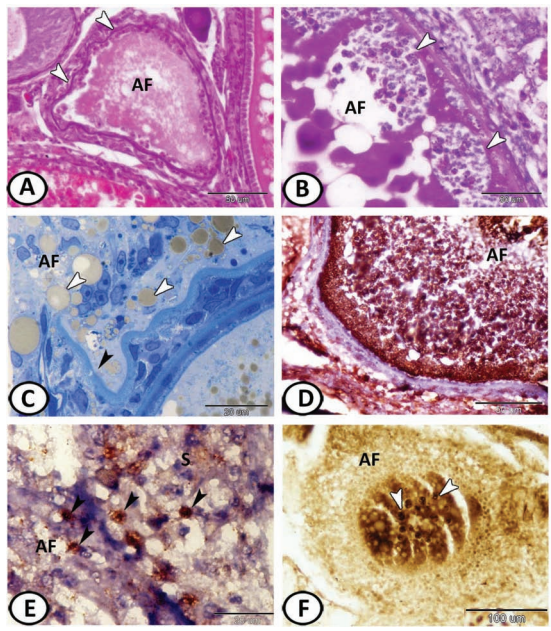

FIGURE 13.13 The AFs in the ovary of redbelly tilapia. (A) The AF showed irregular and shrinked follicular wall (arrowheads) (HE). (B) More developed AF showed invasion of the hypertrophied granulosa cells (arrowheads) into the follicles (PAS/HX). (C) A semithin section stained by Toluidine blue showing irregular wall (black arrowhead) of AF and its cytoplasm contained many fat globules (white arrowheads). (D) The AF expresses Caspase-3. (E) The rodlet cells (arrowheads) express α-SMA in the AF and stroma (S). (F) Rodlet cells (arrowheads) show acid phosphatase activity in the AF.

Acridine orange (AO) fluorescent stain revealed signs of apoptosis in the AFs (Figure 13.14) and showed the presence of rodlet cells on the follicular wall. The AO is a fluorescent versatile dye that enters the cytoplasmic acidic compartments, such as the lysosomes as well as stains DNA and RNA in living cells. Therefore, primary lysosomes, phagosomes, and apoptotic cells could be identified.

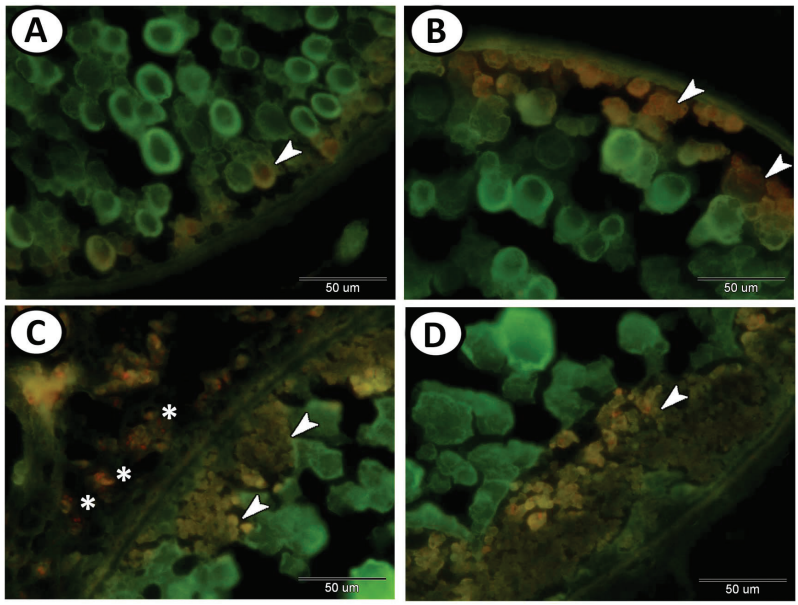

FIGURE 13.14 (A–D) Acredine orange fluorescent stain of the ovary of redbelly tilapia shows cell apoptosis (arrowheads) in the AFs. Note the presence of rodlet cells (asterisks) with their orange rodlet granules on the wall of the AFs.

Vitellogenic follicles are commonly prone to atresia more than previtellogenic ones.

On the other hand, some authors stated that some oocytes failed to reach maturation and eventually collapsed, this may be caused by environmental factors (water temperature and photoperiod) or nutritional condition. If endocrine or metabolic disorders appear during vitellogenesis, degeneration of oocytes occurred. At the onset of atresia, the ZR became convoluted and started to break up. The follicle granulosa cells and thecal cells proliferated and hypertrophied to form a compact well-vascularized structure termed the corpus atreticum. These active granulose cells invade the oocyte through the broken down ZR and digested and resorbed the yolky contents by active

phagocytosis. Corpora lutea have been detected in some fish species. In oviparous teleosts that fertilization is external, the corpora lutea are poorly developed.

13.1.5 POSTOVULATORY FOLLICLES

These follicles are commonly occurred soon after spawning and expulsion of the egg during the ovulation and show signs of degeneration with the presence of vacuoles and lysosomes. They are highly irregular structures consisted of theca and granulosa, with a large and irregular central lumen. In these follicles, the granulosa hypertrophied and theca collapsed into the follicular lumen. The follicular epithelium becomes folded and is invaded by richly vascular thecal tissue. They enlarge and form vacuoles containing proteinous materials (Figure 13.15).

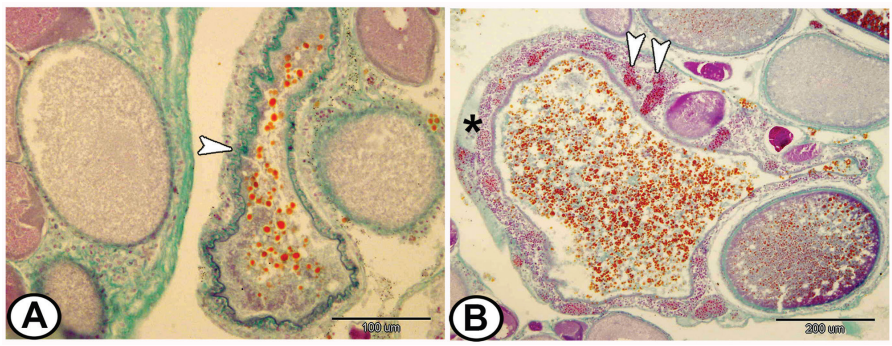

FIGURE 13.15 The postovulatory follicles (POFs) (Crossmon's trichrome) in Nile tilapia. (A) POF with an irregular folded wall (arrowhead). (B) The POF shows a hypertrophied theca (asterisk). Note the invasion of the follicular epithelium by richly vascular theca tissue (arrowheads).

The POFs remain for a short time in the ovary because they are rapidly resorbed by the follicular cells that develop a phagocytic activity. In the latest stage, it was very difficult to distinguish them from the late atretic structures. POFs are always present in partially running ovaries together with new batches of healthy growing yolked oocytes. POFs are steroidogenic, their precise role is still unclear but they may be involved in ovarian steroidogenesis.

13.1.6 THE OVARIAN STROMA

The stroma is viewed as the supportive framework of the ovary, comprising mostly of CT, BVs, and nerves. These stroma undergo changes during both the spawning and the nonspawning season, being more intense in the sex reversal species. The ovary of teleosts is supplied with blood from several arteries that branch off the dorsal aorta, entering the dorsal side of the ovary through the mesovarium. Each follicle in the ovaries is supplied by arteriole that reaches it through a stalk of stromal elements. Thick bundles of autonomic nonmyelinated nerves accompany the ovarian artery in Tilapia.

13.1.6.1 CELLULAR ELEMENTS DISTRIBUTION IN THE OVARIAN STROMA

13.1.6.1.1 Rodlet Cells

The rodlet cells are arranged in groups throughout the ovarian CT stroma with no special orientation, particularly attached to the wall of special types of BVs and constitute 10.28% of the cell of ovarian stroma in redbelly tilapia. The number of rodlet cells shows seasonal variation and the drastic changes in reproductive hormones during the spawning season might have a role in rodlet cells' abundance distribution. Rodlet cells may be associated with eosinophils or found free in the lumen of BVs. They exhibit oval to rounded-shaped cell bodies, eccentric nuclei with thick capsule enclosed cytoplasmic eosinophilic granules or rods by HE (Figure 13.16A). Rodlet cells show a wide range of staining affinity; they are green by Crossmon's trichrome (Figure 13.16B), bright red by PAS (Figure 13.16C) while retaining the blue color with bromophenol blue (Figure 13.16D) and Toluidine blue (Figure 13.16E). The positive staining of rodlet granules to bromophenol blue indicates the protein nature of these cells. Since these cells form a constituent part of the wall of the special BVs and could be traversing the endothelium, they express a strong positive reaction in the form of groups of brown structures with Grimilus silver stains (Figure 13.16F). The distribution of rodlet cells in the wall of BVs supports the proposal that the rodlet cells secrete some enzymatic and proteinous substances to the circulation. Rodlet cells expressed c-kit, S100 protein, and desmin (Figure 13.16G–I).

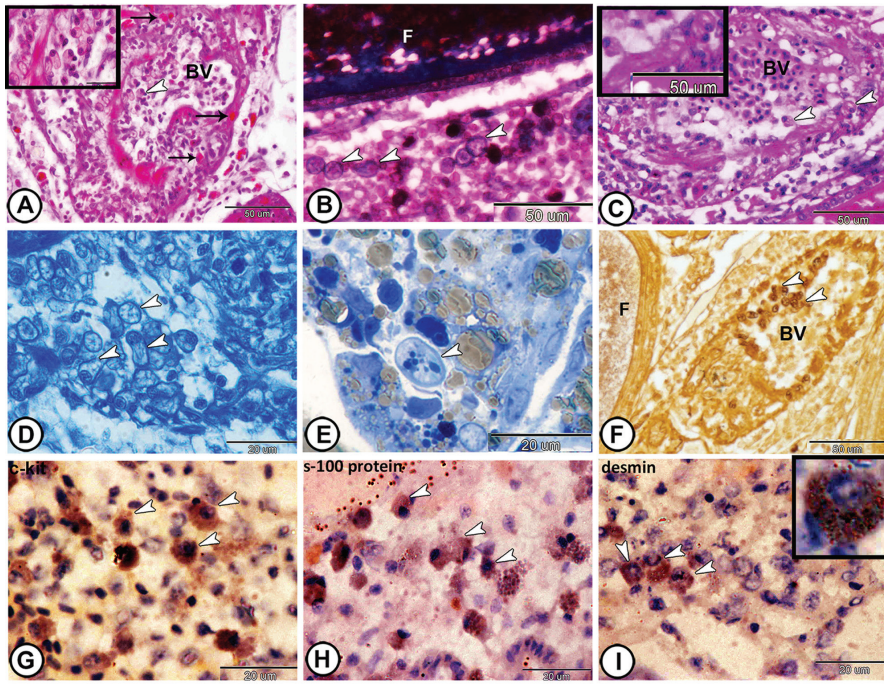

FIGURE 13.16 Histological, histochemical, and immunohistochemical identification of rodlet cells in the ovarian stroma of redbelly tilapia. (A) Rodlet cells are associated with eosinophils (arrows) or found free (arrowhead, inserted box) in the lumen of BVs. They enclosed eosinophilic granules or rods by HE. (B) Rodlet cells (arrowheads) were green structures under the follicles (F) by Crossmon's trichrome. (C) Rodlet cells (arrowheads, inserted box) attached to the wall of the BV and showed bright red color by PAS/HE. (D, E) Rodlet cells (arrowheads) stained blue with bromophenol blue and Toluidine blue, respectively. (F) These cells (arrowheads) form a part of the wall of the special BVs around the follicle (F) and expressed a strong positive reaction with Grimilus silver stains. (G–I) Rodlet cells (arrowheads) expressed c-kit, S100 protein, and desmin, respectively.

The glomus cells emit intense green fluorescence. The rodlet cells are arranged in groups around the BVs or in the intima layer of some of them or projecting to the vascular lumen and their cytoplasmic rodlet granules fluoresced brilliant orange after AO stain as they showed RNA type histochemical reaction (Figure 13.17A–D). Numerous rounded rodlet cells around the BVs and ovarian follicles show high ATPase and acid phosphatase activity (Figure 13.17E and F).

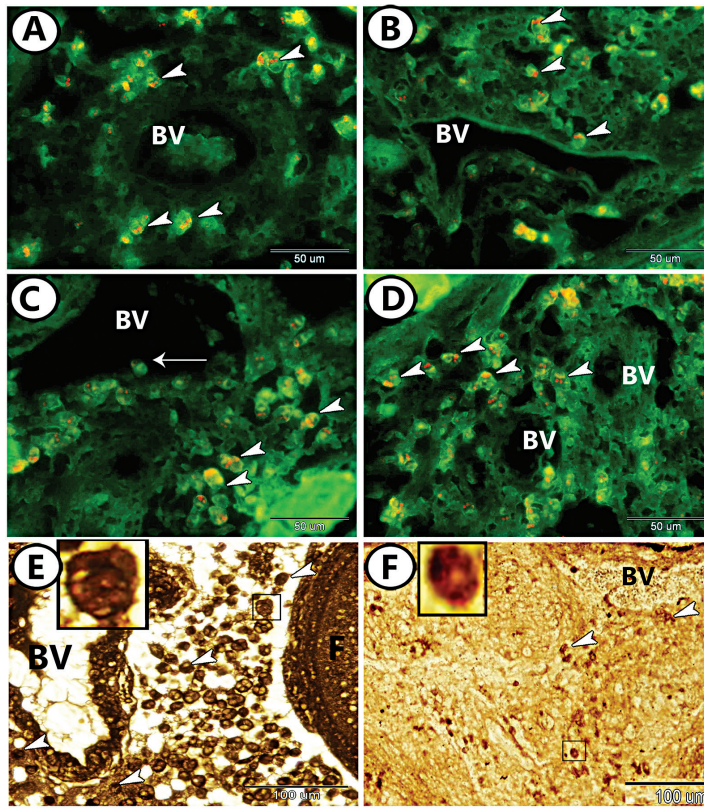

FIGURE 13.17 The fluorescence and enzyme histochemistry of the rodlet cells in the ovarian stroma of redbelly tilapia. (A) The glomus BV emits intense green fluorescence after the AO stain. The rodlet cells (arrowheads) are arranged in tunica media. (B) Rodlet cells (arrowheads) distributed around the BVs. (C, D) Some rodlet cells (arrow) projecting to the lumen of the BV, the others in tunica media and adventitia (arrowheads) and their cytoplasmic rodlet granules fluoresced brilliant orange after AO stain. (E) Numerous rodlet cells (arrowheads, inserted box) displayed around BVs, and ovarian follicles (F) showed high ATPase activity. (F) Rodlet cells (arrowheads, inserted box) in the stroma and around the BV showed acid phosphatase activity.

The distribution of rodlet cells in the ovarian stroma is probably linked to their potential role as regulatory elements and nonspecific immune cells. They are considered migratory and have been implicated in many functions, sensory function, the secretory function via holocrine mode, they are also involved in immune response and are considered as a type of the granulocytes. Rodlet cells act as ion-transporting cells and have a role in osmoregulation.

13.1.6.1.2 Mast Cells

Numerous mast cells are recorded in the ovarian stroma (10.11% of the cellular constituents), particularly in association or in the vicinity with the BVs. These cells are characterized by rounded cell bodies of various sizes with an eccentric nucleus and eosinophilic granules with HE (Figure 13.18A). The mast cells are positive with bromophenol blue (Figure 13.18B) due to the high protein contents in their granules as well as they show a metachromatic reaction with toluidine blue (Figure 13.18C). The granules of mast cells express the staining affinity for s100 protein, desmin, and c-kit (Figure 13.18D–F). Furthermore, these granules show a strong staining affinity for Safranin O (Figure 13.18G). By electron microscopy, the mast cells are characterized by a large oval euchromatic nucleus surrounded by numerous cytoplasmic electron-dense granules (Figure 13.18H). The mast cells in teleosts are like those in mammals and could generate many mediators, chemokines, and cytokines.

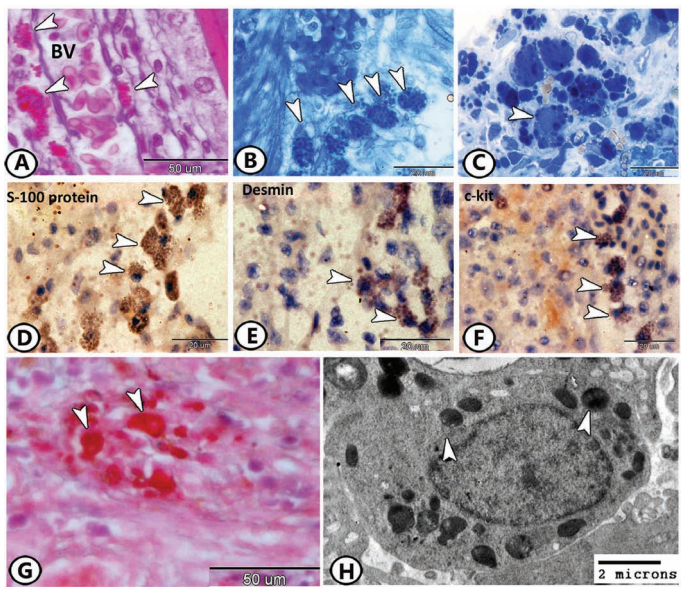

FIGURE 13.18 The mast cells in the ovarian stroma of redbelly tilapia. (A) Numerous mast cells with eosinophilic granules (arrowheads) recorded in the vicinity to BVs by HE. (B) These cells were positive to bromophenol blue (arrowheads). (C) Mast cell granules (arrowhead) showed a metachromatic reaction with toluidine blue. (D–F) Granules of mast cells (arrowheads) expressed staining affinity for s100 protein, desmin, and c-kit. (G) Mast cells (arrowheads) showed a strong positive reaction to Safranin O. (H) TEM lymphocytes (arrowheads) showed that the mast cells contained numerous electron-dense granules (arrowheads).

13.1.6.1.3 Leucocytes

Neutrophils

They are distributed around the ovarian follicles and characterized by the multilobed nucleus (Figure 13.19A and B). TEM showed that their cytoplasm contained many lysosomes, phagosomes, and specific granules (Figure 13.19C).

Eosinophils

Massive aggregations of eosinophilic granular cells are recorded in the ovarian stroma that represents 10.96% of the cellular constituents, particularly in association or in the vicinity to the endothelial tissues. These cells are characterized by rounded cell bodies of various sizes with an eccentric nucleus and eosinophilic granules with HE (Figure 13.19D). Their eosinophilic granules express S100 protein (Figure 13.19E). TEM showed the characteristic specific granules of eosinophils, lysosomes, and phagosomes (Figure 13.19F).

Lymphocytes

The lymphocytes constitute 14.87% of the cellular constituents of the ovarian stroma. They are small rounded cells with a high nucleus to cytoplasmic ratio distributed randomly in the ovarian stroma and around the BVs (Figure 13.19G and H). TEM shows that they possess heterochromatic nuclei with some indentations and their cytoplasm contains mitochondria (Figure 13.19I).

The immune system contributes to the regulation of gonadal function. Few or rare studies demonstrated a pattern of distribution of leucocytes in aquatic species. The presence of leukocytes in the ovary may represent potential in-situ modulators of ovarian function that work through local secretion of regulatory soluble factors. These factors include many cytokines that are mainly produced by the action of immune cells within the ovary. Actual follicle rupture during the ovulation may be dependent on tissue remodeling that is characteristic of an acute inflammatory reaction and includes increased leukocyte migration, the release of various mediators, and loosening of CT elements around the follicles.

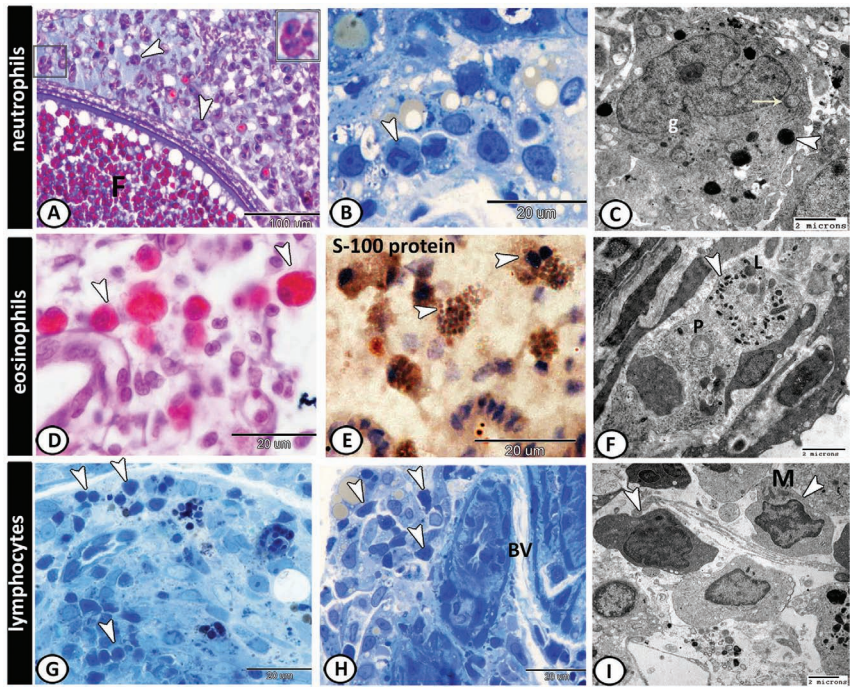

FIGURE 13.19 The leucocytes in the ovarian stroma of redbelly tilapia. (A) *Neutrophil* (arrowheads, boxed area) distributed around the ovarian follicles (F) (Crossmon's trichrome). (B) Neutrophils (arrowhead) by toluidine blue. (C) TEM showed that their cytoplasm contained many lysosomes (arrowhead), phagosomes (arrow), and specific granules (g). (D) *Eosinophils* (arrowheads) characterized by the eccentric nucleus and eosinophilic granules with HE. (E) Eosinophilic granules expressed S100 protein (arrowheads). (F) TEM showed the characteristic specific granules of eosinophils (arrowhead), lysosomes (L), and phagosomes (P). (G, H) *Lymphocytes* (arrowheads) are small rounded cells by toluidine blue distributed in the ovarian stroma and around the BVs. (I) TEM of lymphocytes (arrowheads) showed that it possessed a heterochromatic nucleus and a cytoplasm contained mitochondria (M).

13.1.6.1.4 Macrophages

Macrophages are distributed around the AFs. They are characterized by an eccentric nucleus and the presence of phagocytosed materials within their cytoplasm (Figure 13.20A and B). They show acid phosphatase activity (Figure 13.20C) and express S100 protein and desmin (Figure 13.20D and E). TEM shows that the macrophage possesses a kidney-shaped nucleus and its cytoplasm contains heterogeneous vesicles, phagosomes, electron-dense granules, and lysosomes (Figure 13.20F).

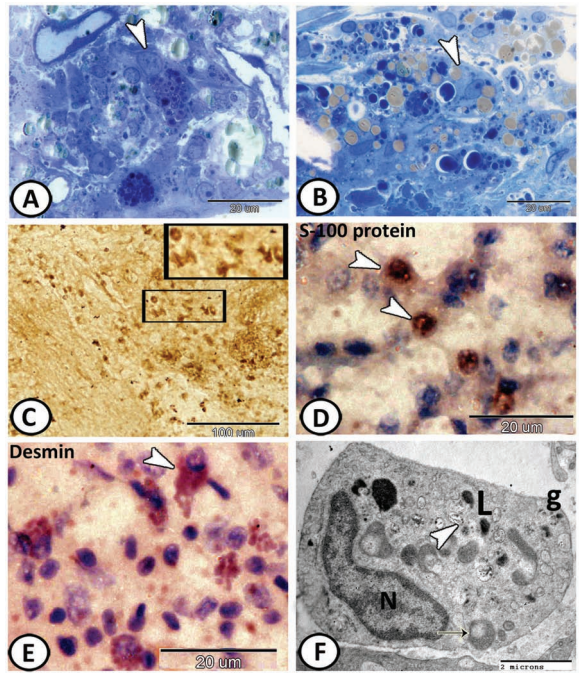

FIGURE 13.20 Macrophages in the ovarian stroma of redbelly tilapia. (A, B) Macrophages (arrowheads) characterized by the presence of phagocytosed materials within their cytoplasm by toluidine blue. (C) They showed acid phosphatase activity (boxed areas). (D) Macrophages (arrowheads) expressed S100 protein. (E) They also expressed desmin (arrowhead). (F) TEM showed that macrophage possessed kidney-shaped nucleus (N), heterogeneous vesicles (arrowhead), phagosomes (arrow), electron-dense granules (g), and lysosomes (L).

Macrophages are frequent throughout the female reproductive tissues and could be distinguished by their characteristic morphology. They are multifunctional cells that are mainly involved in the immune response including phagocytosis and degradation of foreign antigens, tissue remodeling, and production of cytokines, chemokines, and growth factors. Their specific localization and variations in the distribution in the ovary during the spawning season suggest that macrophages play diverse roles in intraovarian events including folliculogenesis and tissue restructuring after atresia.

The enzyme histochemistry revealed that macrophages and rodlet cells showed high acid phosphatase activity. It is well-known that acid phosphatase localized in the lysosomes, the main organelles in the cytoplasm of macrophages, and the acid phosphatase activity increased in the ovaries during maturation and spent stage. In addition, acid phosphatase is involved in the synthesis of essential metabolites in the ovary during the spawning season.

13.1.6.1.5 Dendritic Cells

The dendritic cells (DCs) are small dark cells with fine processes that found around the ThCs and BVs in association with macrophages and constituted 8.14% of the cellular constituents (Figure 13.21A). They express S100 protein and c-kit (Figure 13.21B and C). TEM showed that DCs were characterized by their processes, large indented heterochromatic nucleus, and rER (Figure 13.21D and E). The cytoplasm contains lysosomes and sometimes showing phagocytized materials (Figure 13.21F). They also display macropinocytotic vesicles periphery located, vacuoles of various sizes, mitochondria, and phagosomes (Figure 13.21G). The DCs are identified in some teleosts as rainbow trout, salmonids, medaka, zebrafish, and channel catfish in different tissues include kidney, spleen, and gills. They shared many functional and morphological features reported in mammals. DCs are one of the antigen-presenting cells with dendritic morphology, phagocytic ability, and strong T-cell stimulatory properties. The features of phagocytosis in Figure (13.21F and G) may signify the role of DCs in immune surveillance in the ovary.

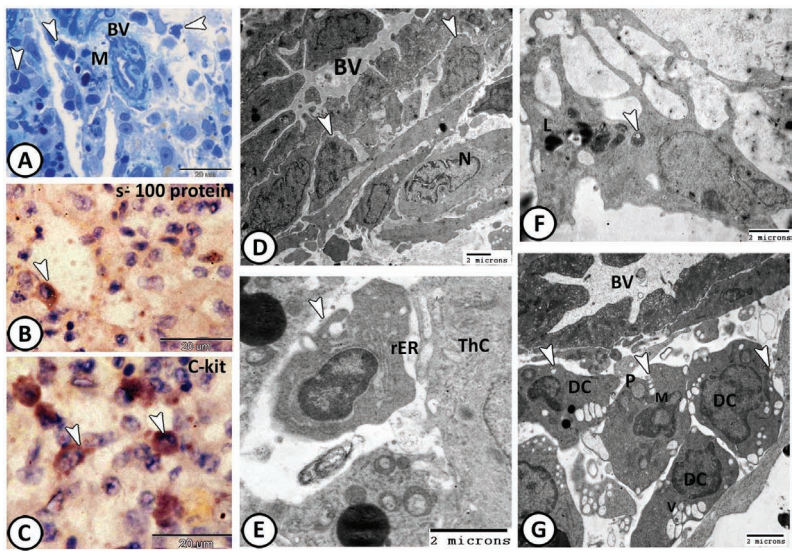

FIGURE 13.21 The dendritic cells (DCs) in the ovarian stroma of redbelly tilapia. (A) DCs (arrowheads) found around BVs in association with macrophages (M). (B) They expressed S100 protein (arrowhead). (C) They expressed c-kit (arrowheads). (D) TEM showed that DCs (arrowheads) arranged around the BVs in the vicinity to neutrophils (N) and characterized by their processes, large indented heterochromatic nucleus. (E) DC (arrowhead) found around theca cells (ThCs) and contained rER. (F) The cytoplasm contained lysosomes (L) and phagocytized materials (arrowhead). (G) The DC cytoplasm displayed macropinocytotic vesicles (arrowheads), vacuoles (V), mitochondria (M), and phagosomes (P). Note their distribution around the BVs.

13.1.6.1.6 Endocrine (Steroid Producing) Cells

They are clusters or cords of polyhedral cells observed in the stroma in close apposition to small BVs (Figure 13.22A) or at the periphery of mature vitellogenic follicles (Figure 13.22B). These cells represent 9.44% of the ovarian stroma and show positive reactions to bromophenol blue (Figure 13.22B), silver stain (Figure 13.22D), and express strong activity to S-100 protein (Figure 13.22C). TEM showed that the endocrine cells are dominated by polymorphic secretory granules, tubular mitochondrial cristae, and sER (Figure 13.22E and F). The steroid-producing cells are suggested to be originated from stromal elements. In addition, the steroids produced by steroid-producing cells play a role in the formation of the ovarian lumen and the differentiation of germ cells. It is suggested that these cells may produce estrogens during vitellogenesis. Teleosts have not typical interstitial cells like mammals.

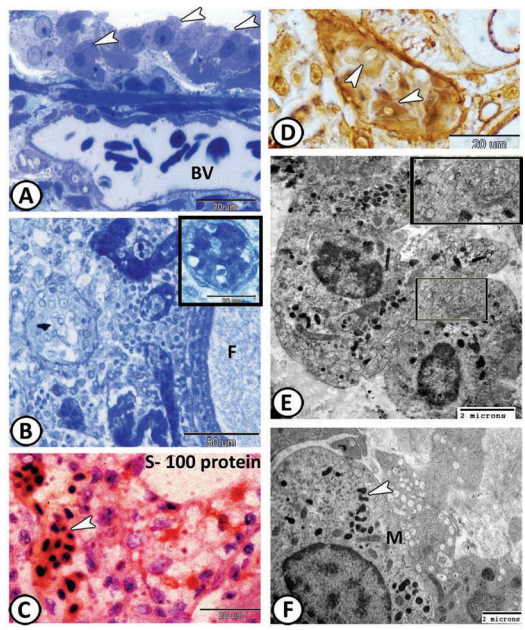

FIGURE 13.22 Endocrine (steroid-producing cell) in the ovarian stroma of redbelly tilapia. (A) Semithin section stained by toluidine blue showing endocrine cells (arrowheads) in apposition to small BVs. (B) Clusters of endocrine cells (boxed area) at the periphery of mature vitellogenic follicles (F) and showed positive reactions to bromophenol blue. (C) Endocrine cells (arrowhead) express strong activity to S100 protein. (D) Endocrine cells were positive with silver stain (arrowheads). (E, F) TEM showed that endocrine cells were dominated by polymorphic secretory granules (arrowhead), mitochondria (M), and sER (boxed areas in E).

13.1.6.1.7 Melanocytes

Melanocytes are demonstrated in the ovarian stroma around the special types of BVs and other cellular elements and constitute 5.57% of the ovarian stroma. They are characterized by their irregular-shaped cell bodies and the presence of dark brown to black melanin pigments (Figure 13.23A). They express a strong positive reaction to S100 protein and c-kit (Figure 13.23B and C). The gonadal melanin showed seasonal variations with a low level in the resting phase and the peak level in the postspawning season.

13.1.6.1.8 Adipocytes

Adipocytes or fat cells are the main components in the ovarian stroma (7.73%). They give a positive reaction to Sudan black B (Figure 13.23D). Their thin cytoplasm express S100 protein (Figure 13.23E) and their fat globules react positively to c-kit (Figure 13.23F). This fat storage may be important for vitellogenesis. Moreover, vitellogenin, a key player of reproduction, is expressed by adipocytes of teleostean ovaries.

Bundles of nonmyelinated nerves, presumably autonomic, accompanying the ovarian artery and vein were observed in the ovarian stroma. The bundles consist of nerve axons and Schwann cells (Figure 13.23G and H) and give a positive reaction to silver stain (Figure 13.23I). These bundles were previously identified in the ovaries *of O. niloticus* and suggested to have a critical role in the regulation of steroid production. Furthermore, these nerve fibers regulate ovarian muscular contraction at oviposition during the expelling of the oocytes.

13.1.6.1.9 Telocytes

TCs are small spindle-shaped cells with two or more long cell processes called telopodes (Tps). They are distributed in the ovarian stroma around the blood capillaries (BCs) (Figure 13.24A), arteriovenous anastomoses (AVAs) (Figure 13.24B), small BVs (Figure 13.24C and E), and AFs (Figure 13.24D), or scattered all over the stroma between the other CT cells (Figure 13.24F). TCs represent 7.94% of the cellular constituents. They stained positive with silver stain (Figure 13.24A) and were darkly stained with toluidine blue (Figure 13.24C–F). TCs' bodies and Tps expressed strong immunoreaction to desmin (Figure 13.24G). Moreover, the Tps expressed

positive immunoreactivity to both c-kit (Figure 13.24H), and S100 protein (Figure 13.24I).

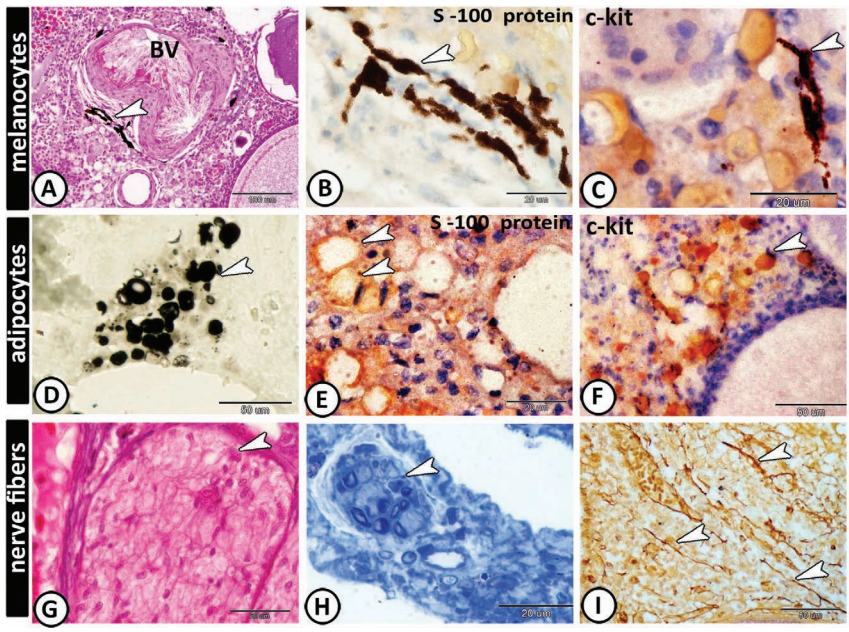

FIGURE 13.23 Melanocytes, adipocytes, and nerve fibers in the ovarian stroma of redbelly tilapia. (A) Melanocytes (arrowhead) stained by HE were demonstrated around the special type of BVs. (B) Melanocytes with characteristic melanin pigments (arrowhead) expressed a strong positive reaction to S100 protein. (C) Melanocytes expressed c-kit (arrowhead). (D) Adipocytes (arrowhead) gave a positive reaction to Sudan black B. (E) Their thin cytoplasm expressed S100 protein (arrowheads). (F) Their fat globules reacted positively to c-kit (arrowhead). (G, H) Bundles of nerve fibers (arrowheads) were observed in the ovarian stroma, stained by HE, and toluidine blue, respectively. (I) Nerve fibers (arrowheads) gave a positive reaction to silver stain.

S100 is a multigenic protein exclusively distributed in the cells of epithelial, mesodermal, and neuroectodermal origin. The differential localization of S100 protein in the ovary of the tilapia suggesting its multifunctional role mediated by its calcium modulating activity. It has been involved in the regulation of enzymatic activity, protein phosphorylation, cell proliferation angiogenesis, and vascular tone. CD117 or c-kit is a cytokine receptor expressed on the surface of hematopoietic cells as well as melanocytes, mast cells, and interstitial cells of Cajal. C-kit is involved in many functions, such as gametogenesis and hemostasis. Furthermore, signaling through CD117

plays an important role in the survival, differentiation, and proliferation of various cells. No available literature concerning the immunohistochemical studies on intermediate filaments like desmin in the teleosts' ovaries. In the ovarian stroma of redbelly tilapia, desmin was immunolocalized in rodlet cells, TCs, and mast cells. These immunoreactive cells may play a role in the contractile process of the ovaries. Furthermore, desmin is involved in tissue differentiation and provide a structural framework for the ovary.

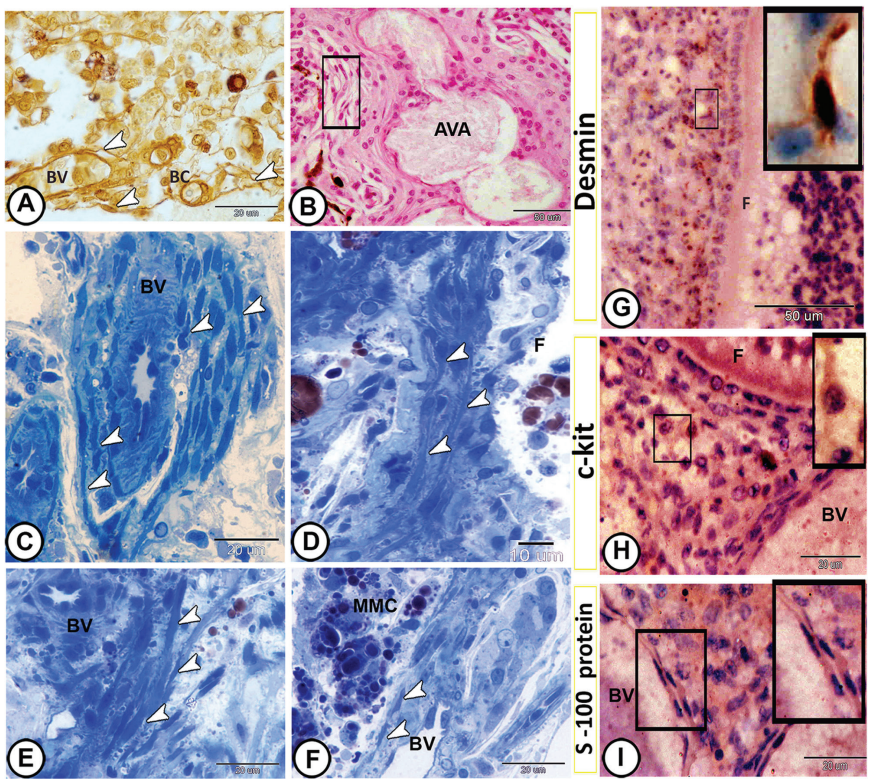

FIGURE 13.24 Histological and immunohistochemical detection of telocytes (TCs) in the ovarian stroma of redbelly tilapia. (A) TCs (arrowheads) were positive for silver stain and distributed around the blood capillaries (BCs), and small BVs. (B) TCs (boxed area) stained by HE and found in the vicinity to arteriovenous anastmoses (AVAs). (C, E) TCs (arrowheads) stained by TB and arranged around BVs. (D) TCs (arrowheads) were stained by TB and scattered around AFs (F). (F) TCs (arrowheads) were stained by TB and found near MMC. (G) TCs' bodies and Tps (boxed areas) expressed strong immunoreaction for desmin around follicle (F). (H) TCs (boxed areas) expressed positive immunoreactivity to c-kit around the follicle (F) and BVs. (I) TCs (boxed areas) expressed positive immunoreactivity to S100 protein BVs.

By EM, the TC consisted of a cell body contained euchromatic oval nucleus, and Tps displayed mitochondria and secretory vesicles (Figure 13.25A). Their Tps form a labyrinth network between the stromal cellular and vascular components. TCs established contact with each other (homocellular contact) (Figure 13.25B) and heterocellular contact with immune cells (macrophages and DCs) (Figure 13.25C), and endothelium of BVs (Figure 13.25D). Stromal telocytes (TCs) shed their secretory vesicles to the BVs (Figure 13.25C and D). They exert their effect either by direct contact or by paracrine mode.

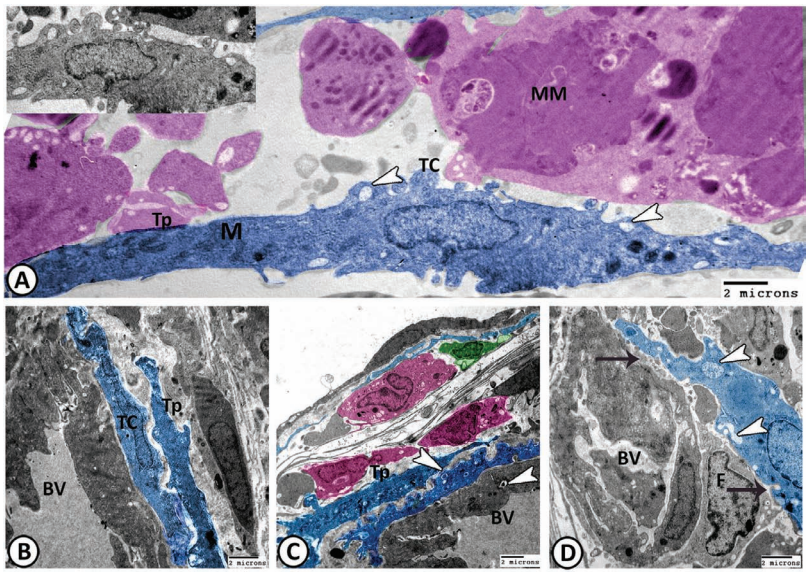

FIGURE 13.25 Digital colored TEM images of TCs (blue) in the ovarian stroma of redbelly tilapia. (A) TC (boxed area) in association with melanomacrophage (MM), telopodes (TPs) displayed mitochondria (M) and secretory vesicles (arrowheads). (B) TC's cell body established contact with Tps of another TC around BVs. (C) Heterocellular contact was observed between TCs and macrophages (pink) and DCs (green) and homocellular contact between Tp around BVs. Note, TCs shed their secretory vesicles (arrowheads) to circulating BVs. (D) TC showed heterocellular contact with the endothelium of BVs and fibroblast (F). Note, TCs shed their secretory vesicles (arrowheads) to circulating BVs and fibroblast (arrows)

13.1.6.1.10 Fibroblasts

They are characterized by triangular-shaped cell bodies with an oval large euchromatic nucleus and cytoplasmic electron-lucent vesicles of variable

shapes and sizes and rER (Figure 13.25D). In addition, occasional fibroblasts were demonstrated in the association of BVs and TCs and may be involved in the regulation of the regeneration process in the ovary during the spawning season

13.2 OVIDUCTS

ODs are convoluted posterior continuations of the ovarian tunics and the ovocoel continued posteriorly with the lumen of the OD. The ODs of right- and left-ovaries coalesce distally to open in the genital pore. The OD displays an irregular appearance. The wall of the OD is folded and well-developed; it is composed of secretory epithelium followed by a subepithelial layer of loose CT and a muscular layer made up of smooth muscle fiber and serosal layer (Figure 13.26).

FIGURE 13.26 The oviduct (OD) of Nile tilapia. (A) The connection of the ovary (O) with OD (HE). (B) The wall of the OD of tilapia in breeding season showing highly folded mucosa (MF) and well-developed smooth muscle layers (M) stained by HE. (C) The wall of the ODs stained with Crossmon's trichrome showing subepithelial collagenous CT and smooth muscle layer (M).

During the breeding season, the OD wall is highly folded made up of simple columnar ciliated epithelium that assists in the transport of eggs. Small clusters of microvillous cells found in the epithelium of OD that secret components of the ovarian fluid to the ovarian lumen to maintain its ionic gradient. The ODs have different functions such as collecting the eggs from the ovarian cavity, coating them with protective or nutrient substances, temporarily housing of eggs and have an important role in expelling of mature eggs. Moreover, viable sperms are stored for periods up to several months within the ovary and OD of the oviparous poecilid platy fish.

13.3 VIVIPARITY

Viviparity is a process in which eggs are fertilized internally and undergo development within the maternal reproductive system. Although most fishes are oviparous, 54 families of living fish have species that bear living young that include 40 families of chondrichthyans and 14 families of teleosts. Therefore, the ovary of viviparous teleosts is not only the structure where oogenesis occurs but also it receives the spermatozoa during the insemination, maintains the spermatozoa, and it allows the fertilization of oocytes and the development of offspring until birth. The sequence of these processes makes the ovary of viviparous teleosts a very complex organ, developing morpho-physiological adaptations for the insemination, the entrance and movements of spermatozoa into the ovary, the storage of spermatozoa until fertilization, the fertilization of oocytes, and the intraovarian gestation. The developing young may be housed within the ovary or in the genital ducts.

A distinctive feature of almost all viviparous teleosts occurs is the fusion of the right and left ovaries during early embryonic development. This fusion establishes a single and saccular ovary, with the GE lining the internal lumen. One of the most characteristic features of viviparous teleosts among vertebrates is that these fish species do not develop Müllerian ducts during the embryogenesis, as occurs in the rest of vertebrates; consequently, these teleosts do not have ODs. Then, the communication of the germinal zone of the ovary to the exterior occurs via the caudal zone of the ovary, which is called the gonoduct (Figure 13.27); an ovarian zone that lacks germinal cells. Therefore, the lumen of the ovarian germinal zone is continuous with that of the gonoduct, where the development of numerous folds of the mucosa forms a limit, similar to a cervix, displayed at the border of the germinal portion of the ovary and the gonoduct.

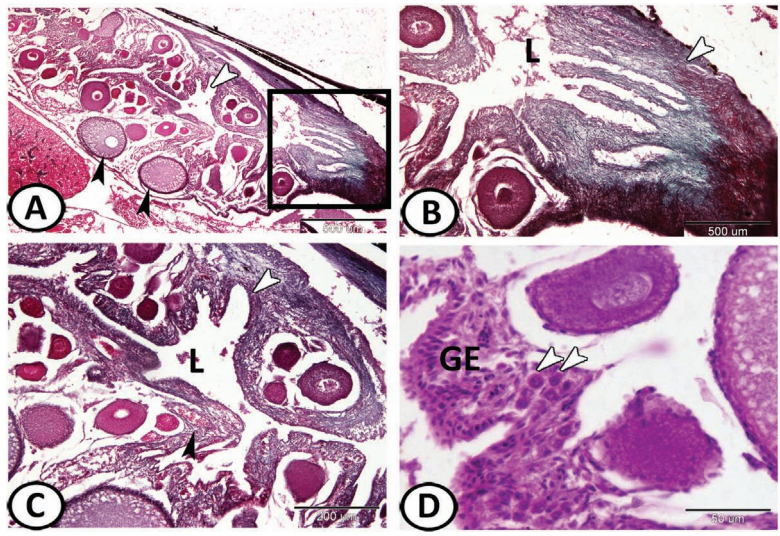

FIGURE 13.27 The ovary of molly fish. (A) The general view of the viviparous ovary stained by Crossmon's trichrome showing the central lumen lined by GE (white arrowhead) and many oocytes at various stages of oogenesis (black arrowheads). (B) Higher magnification in the boxed area in (A) showing the gonoduct (white arrowhead) that is communicated with the lumen of the ovary (L). (C) A section of the ovary stained by Crossmon's trichrome showing the lumen (L), GE (white arrowhead). Note the presence of stromal BVs (black arrowhead). (D) Higher magnification stained by HE showing oogonium formation (arrowheads) in the GE.

According to the nutrients used by the embryos during their gestation, there are two nutritional patterns in viviparous teleosts, both involving the ovarian structure and egg morphology. These patterns are lecithotrophy and matrotrophy. In lecithotrophy, the nutrients for the embryo come from the yolk and stored in the egg during the oogenesis prior to fertilization, which is similar to that occurs in oviparous fishes. In matrotrophy, the nutrients are provided not only by those stored in the egg during oogenesis but also by supply from the maternal tissues during the gestation, consequently, after fertilization.

The follicular epithelium, the maternal layer surrounding the embryo, is very active in allowing the passage of metabolites in species with matrotrophic nutrition. The follicular cells select, digest, and transport nutrients from the BVs of the maternal tissue to the embryo. The proximity of embryonic and maternal tissues also offers conditions favoring the evolution of matrotrophy. This nutrient transfer involves the association of embryonic and maternal tissues, which form the follicular placenta.

The components of the follicular placenta are the endothelium of maternal capillaries, the follicular epithelium, the embryonic surface epithelium, and the endothelium of embryonic capillaries. Consequently, a placenta allows the mother to feed the embryos during the gestation by matrotrophic nutrition, instead of the deposition of abundant nutrients into the oocyte during the oogenesis. Analysis of the structure of the placenta in several species of poeciliids allowed the identification of specialized morphological characteristics of the follicular cells that increased the active transfer of nutrients between the mother and the embryos, such as the increase in the number of microvilli and microvilli length. In the genus *Poeciliidae*, a simple kind of pseudoplacenta is found. In this case, the walls of the ovarian follicles acquire an elaborate network of capillaries that extend out as villi and make an intimate association with the external surface of the developing embryos.

The ovary of poeciliids (Figure 13.27) is of cystovarian type, as a single and saccular structure with a central lumen. Histologically, the ovarian wall consists of four tissue layers. From the interior to the exterior, these layers are (1) GE integrated by the germ cells, such as oogonia, and the oocytes scattered individually or in cell nests among the somatic epithelial cells. The GE borders the ovarian lumen and it is separated from the stroma by a basement membrane; (2) stroma, formed by loose and vascularized CT, enclosing the ovarian follicles. The follicles are integrated by oocytes in different stages of development as previtellogenesis or vitellogenesis; (3) smooth muscle layers; and (4) serosa, formed by thin CT and externally lined by mesothelium. The caudal zone of the ovary forms the gonoduct, which lacks germinal cells.

The gonoduct acquires special interest in viviparous species, where during birth the offspring goes to the exterior through the gonoduct. Consequently, the gonoduct forms a barrier between the germinal zone of the ovary and the exterior. The gonoduct of *Poecilia reticulate* and *Poeciliopsis gracilis* is a muscular tube that includes multiple longitudinal folds of the mucosa extended into the gonoductal lumen. The gonoduct is lined internally by single cuboidal or columnar epithelium with ciliated and nonciliated cells, plus a stroma of CT, smooth muscles, and serosa. Melanomacrophage centers (MMCs) are irregularly located in the CT, adjacent to the epithelium; they are round or oval aggregates of cells, such as macrophages, lymphocytes, and melanocytes. The presence of these centers suggests its involvement in the protection of the ovary and embryos by immunological functions. Macrophages and lymphocytes may be also located subjacent to the epithelium or in the lumen of the gonoduct. The presence of ciliated and

nonciliated epithelial cells may facilitate the transport of spermatozoa during the insemination and embryos during birth.

The intraovarian gestation (Figure 13.28) in poeciliids is initiated when the oocytes are fertilized in the ovarian follicle. The embryos remain in the follicle throughout all their development, until birth. That is, the fertilization and gestation in poeciliids are intrafollicular. The intrafollicular fertilization is possible by a specific structure at the periphery of each oocyte where the spermatozoa make contact with the oocyte. This structure penetrates each oocyte as a funnel-like invagination of the ovarian lining to the follicular epithelium, opening a duct from the ovarian lumen to the oocyte membrane. This invagination is called delle. Therefore, the delle is the only possible way where the spermatozoa may have access to the oocyte. When mature oocytes are fertilized by the spermatozoa into the follicle, the intrafollicular embryonic development is initiated.

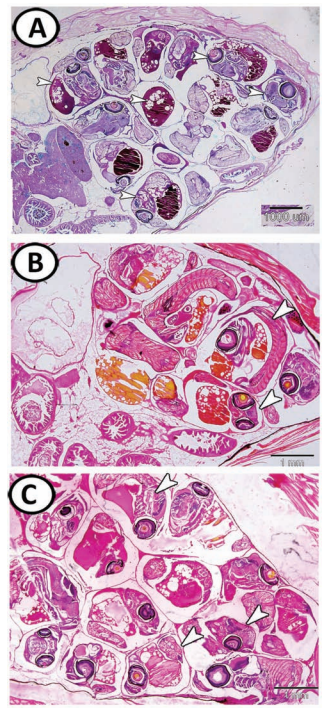

FIGURE 13.28 (A, B) The body cavity of guppy showing the developing young housed in the ovaries (arrowheads) stained with PAS-AB/HX and HE, respectively. (C) Ovary of *Poecilia reticulata* with embryos (arrowheads) during late gestation. The development of embryos is more advanced compared with that seen in the embryos in (A, B). Note the reduction of yolk.

The intrafollicular embryogenesis in poeciliids continues through the development of peripheral BVs, adjacent to the maternal tissue. These vessels permit the exchange of essential supplies for the embryos, such as the transfer of nutrients and gas for respiration, elimination of waste products of the metabolism, and fulfilling hormonal and immunological requirements. For these functions, the development of adjacent embryonic and maternal vascularization is essential. The follicular cells become squamous, simplifying the pass of metabolites between maternal and offspring BVs. In early embryogenesis, the amount of yolk is abundant, but it diminishes progressively as the embryo takes the nutrients during the advance of the gestation.

13.4 TESTIS

13.4.1 GROSS MORPHOLOGY

Testes of teleosts are the whitish-paired long, narrow structure, and approximate of equal size. It is located in the posterior part of the body cavity and attached to the dorsal body wall by mesorchium. The testes show great variation in shape, color, and length during different months of the year. During the nonbreeding season, the testes are small, flaccid, thread-like, and dull white with slight vascularization. During the breeding season, the testes are soft, creamy in texture, turgid, pinkish in color, and larger in size due to the presence of a high number of sperms in the distended seminiferous tubules (STs) and sperm duct (SD) that lead to an increase in the weight of the testis. The BVs are prominent and the milt runs with slight pressure in the breeding season.

13.4.2 HISTOLOGICAL STRUCTURE OF THE TESTES

Testis of teleosts is of two types: lobular as tilapia, catfish, sturgeon, and trout and tubular as a guppy.

13.4.2.1 LOBULAR TESTIS TYPE

Testis of tilapia is of radial lobular type, a system of STs arranged radially from the dorsal and lateral wall of the testis to the central lumen. The central lumen leads to the efferent ducts (EDs), which are connected with each other

to open into the SD or vas deferens (VD) that leads to the urogenital pore (Figures 13.29 and 13.30). The efferent ductules number a dozen, more or less, in humans.

The testis itself is organized into lobules oriented toward the central lumen. The outer part of the testis appears free from sperms while increasing the presence of sperms in the STs present in the center of the testis near the EDs (Figures 13.29 and 13.30). During the breeding season, the STs widen and elongate toward the center of the testis in which their lumen contains a high number of sperms. The sperms are free and almost neither linked nor bounded to Sertoli cells (Figure 13.29C and D).

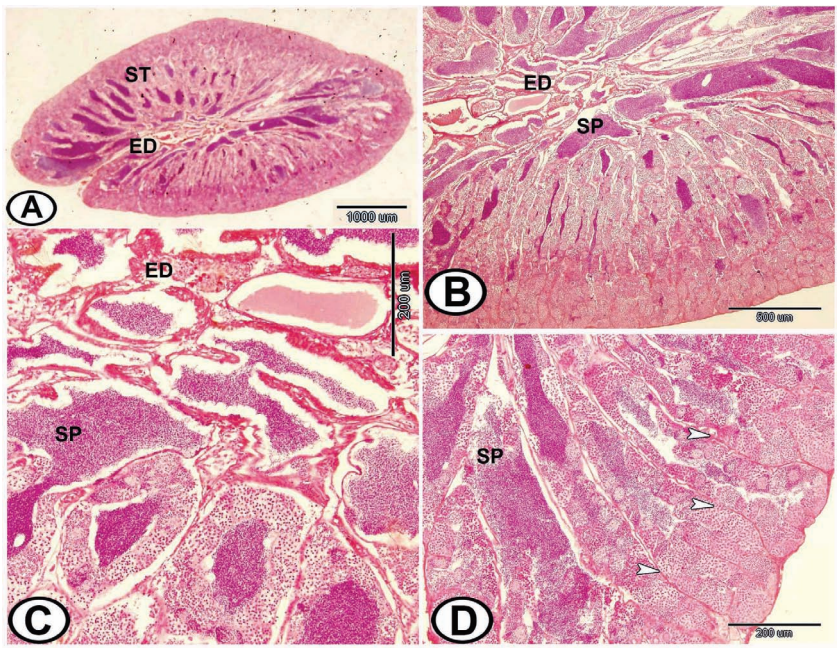

FIGURE 13.29 General histological view to the testis of *Oreochromis niloticus* stained with HE. (A) A cross section in the testis showing distended seminiferous tubules (STs) that opened in the center of the testis in the efferent ducts (EDs). (B, C) Magnified views in the center of the testis during the breeding season showing cysts of sperms (SP) opened to the ED. (D) Magnified view in the periphery of the testis showing lobules of STs (arrowheads) and cysts of sperms (SP).

The wall of the SD of Nile tilapia consists of five layers (from outside to inside): (1) a peritoneum, (2) a transverse CT layer, (3) a transverse smooth muscle layer, (4) a subepithelial loose CT network containing smooth

muscle cells, and (5) an epithelium revealing longitudinal folds that lined by secretory prismatic cells (Figure 13.30C). During the breeding season, the epithelial surface of the SD or (VD) enlarges due to the presence of numerous longitudinal folds and multilayered epithelium, as well as the lumen of the SD is distended and filled with residual spermatozoa after spermiation (sperm release), which reflects the intensive secretory activity.

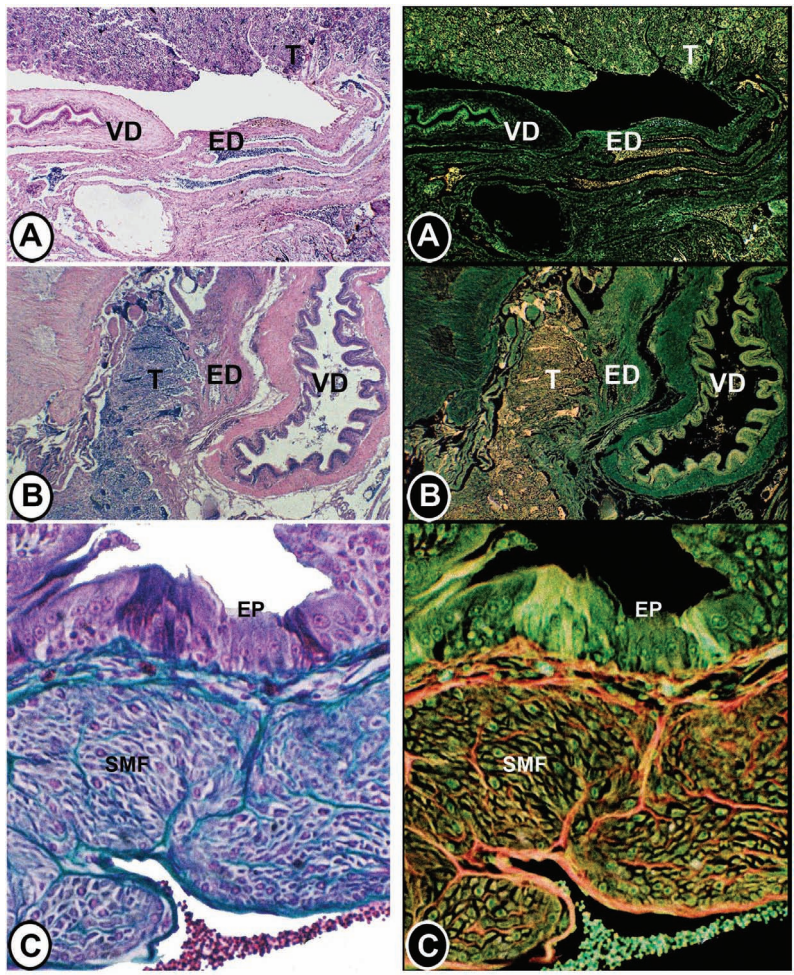

FIGURE 13.30 The duct system of the testis of Nile tilapia. (A, B) The connection between the testis (T) and EDs that filled with spermatozoa and vas deferens (VD) (HE). (C) The VD during the breeding season showing highly folded epithelium (EP) and well-developed smooth muscle layers (SMF) (Crossmon's trichrome). Note the negative images on the right side by CMEIAS color segmentation software.

The epithelium of the spermatic duct is involved in the secretion of steroids, lipids, monosaccharides, proteins, and enzymes. It, therefore, has an important function in the formation of the seminal fluid. Further, the spermatic duct is important for the storage of spermatozoa and in ionic regulation of the seminal fluid. On the other hand, a well-developed layer of smooth muscle in the spermatic duct of Nile tilapia suggests that the spermatic duct could be involved in the mechanism controlling the number of the sperm released in individual spawns; in addition, the gametic extrusion may result from the contraction of the smooth muscle walls of the SD.

The testis is enclosed completely by a tunica albuginea, which consists of a few collagenous fibers, some smooth muscle cells, and elastic fibers. The tunica albuginea is thin during the breeding season as a result of a progressive expansion of the testis by maturation. Its mean thickness reaches 21.24 ± 1.02 μm, while during the nonbreeding season, its mean thickness is 42.18 ± 2.75 μm (Table 13.2). The elastic fibers found in the wall and especially visible after spawning are responsible for the contraction of the testis and discharge of sperms. The testicular parenchyma consists of branching tubular STs and interstitial tissue (IT) (Figures 13.31 and 13.32 A, B).

TABLE 13.2 The Mean Volume Percentage of STs, IT, and Diameter of STs (μm) in Tilapia During Different Months of Year

Months	Volume Percentage of Seminiferous Tubules (%)	Volume Percentage of Interstitial Tissue (%)	Diameter of the Seminiferous Tubules (μm)
	Nonbreeding season		
October	69.3 ± 0.97	30.8 ± 0.88	106.28 ± 1.66
November	69.36 ± 1.78	30.64 ± 1.88	101.26 ± 2.0
December	70.27 ± 0.99	29.73 ± 0.97	102.37 ± 1.85
January	69.12 ± 1.08	30.88 ± 2.76	99.21 ± 1.11
February	68.23 ± 0.87	36.77 ± 1.00	96.85 ± 0.87
March	74.00 ± 2.00	26.00 ± 0.96	109.0 ± 0.95
M ± SE	70.19 ± 1.0	29.8 ± 1.72	102.94 ± 1.83
	Breeding season		
April	78.75 ± 1.23	21.25 ± 1.44	112.1 ± 0.93
May	79.11 ± 0.87	20.78 ± 2.38	119.52 ± 1.24
June	80.11 ± 0.96	19.89 ± 0.64	132.11 ± 1.98
July	78.88 ± 1.09	21.12 ± 1.04	141.51 ± 1.21
August	76.33 ± 0.95	24.67 ± 1.55	125.0 ± 1.22
September	76.0 ± 0.78	24.0 ± 0.88	118.44 ± 0.83
M ± SE	78.43 ± 0.81	21.54 ± 0.81	124.78 ± 2.32[a]

"a" indicates a significant value if $P < 0.05$.

The STs are delimited by a basal lamina (Bl) and have a central lumen surrounded by the germinal epithelium (GE) that is made up of spermatogenic cells as well as Sertoli cells. The STs are made up of spermatocysts, where the spermatogenesis occurred. The spermatocysts are formed by the cytoplasmic projections of Sertoli cells. The spermatocysts contain spermatogonium (SG), primary spermatocytes, secondary spermatocytes, and spermatids, while spermatozoa are found in the lumen of the ST. Within each spermatocyst, the germ cells are at the same stage of development, forming a clone (Figures 13.31 and 13.32C, D).

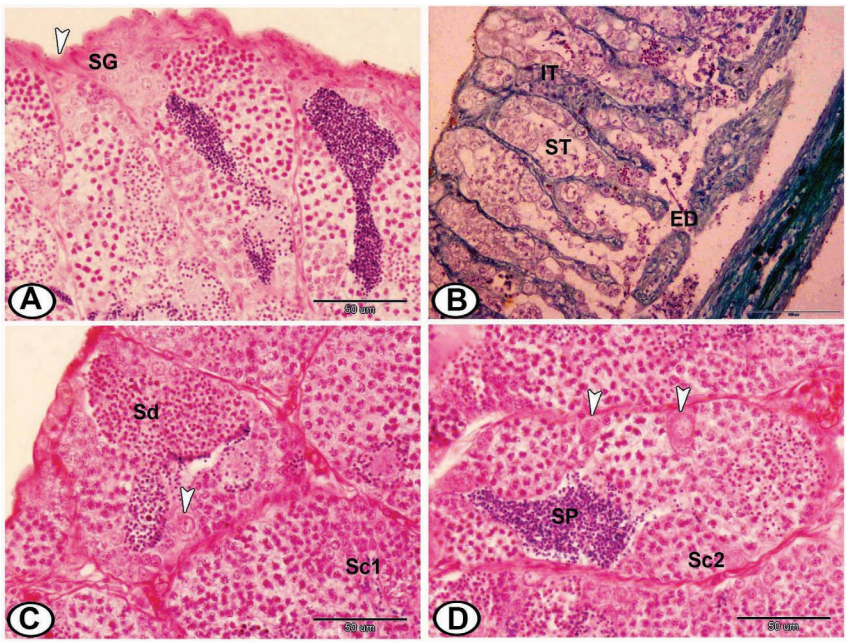

FIGURE 13.31 The histological structure of the testis of Nile tilapia. (A) The testis is covered with tunica albuginea (arrowhead). Notice the presence of cyst of spermatogonia (SG) under the tunica albuginea (HE). (B) The testis of tilapia is composed of STs that opened in the center of the testis in the EDs (Crossmon's trichrome). (C, D) The ST contained primary spermatocytes (SC1), secondary spermatocytes (SC2), spermatids (Sd), and spermatozoa (SZ). Notice the presence of Sertoli cells (arrowheads) (HE).

In the breeding season of Nile tilapia, the volume percentage of the STs increases, and its mean value reaches 78.43 ± 0.81%. The maximum mean value was 80.11 ± 0.96% in June. The diameter of the STs is significantly increased during the breeding season, and its mean diameter reaches

124.78 ± 2.32 μm. The maximum mean value was 141.51 ± 1.21 μm in July. While during the nonbreeding season, the volume percentage of STs reduces, and its mean value reaches 70.19 ± 1.0%. The minimum mean value was 68.23 ± 0.87% in February. In addition, the diameter of the STs reduces, and its mean diameter reaches 102.94 ± 1.83 μm. The minimum mean value was 96.85 ± 0.87 μm in February (Table 13.2).

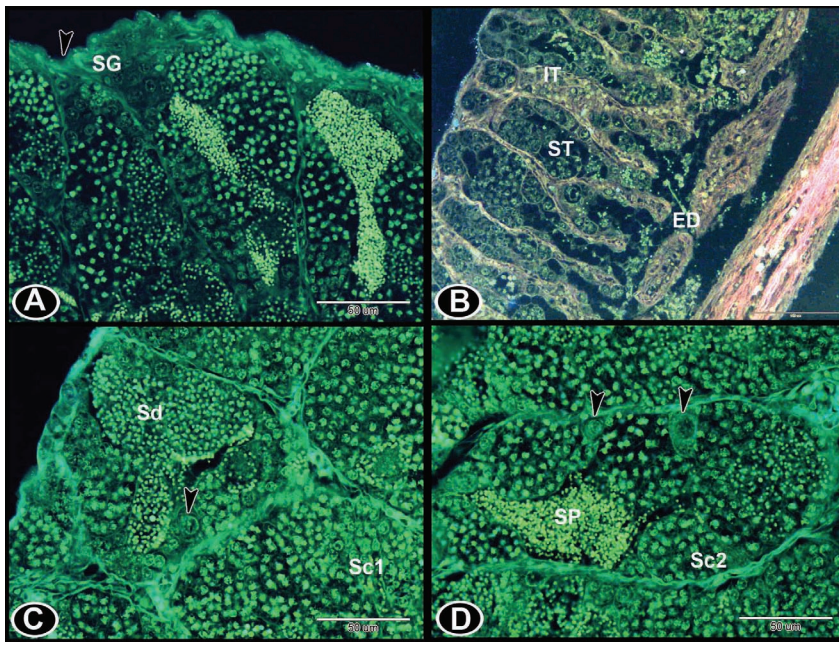

FIGURE 13.32 The negative images of Figure 13.31 by color segmentation software.

The IT usually occurs in the triangular area between the STs and composed of interstitial cells, fibroblasts, BVs, and some collagenous fibers (Figure 13.33). The mean volume percentage of the IT of Nile tilapia during the nonbreeding season was 30.8 ± 1.72%, while during the breeding season was 21.54 ± 0.81%. The volume percentage of IT decreased during the nonbreeding season, and its mean value reached 21.54 ± 0.81%. The minimum value was 19.89 ± 0.64% in June. The volume percentage of IT increased during the nonbreeding season, and its mean value reached 29.8 ± 1.72%. The maximum value is 36.77 ± 1.0% in February (Table 13.3).

TABLE 13.3 The Mean Thickness of the Tunica Albuginea, Number of Sertoli Cells/Cross Section of Seminiferous Tubules, and Spermatocyst in Tilapia during Different Months of the Year

Months	Thickness of Tunica Albuginea (μm)	Number of Sertoli Cells/Cross Section	Number of Sertoli Cells/Spermatocyst
Nonbreeding season			
October	14.35 ± 0.36	6.5 ± 0.85	1.8 ± 0.66
November	10.98 ± 0.78	7 ± 0.44	1.83 ± 0.3
December	14.02 ± o.75	6 ± 0.70	1.83 ± 0.16
January	14.38 ± 0.88	6 ± 0.70	1.66 ± 0.33
February	16.70 ± 1.76	5 ± 0.31	1.33 ± 0.21
March	15.58 ± 1.86	8 ± 0.83	2.33 ± 0.49
M ± SE	14.33 ± 0.96	6.4 ± 0.5	1.79 ± 0.16
Breeding season			
April	6.35 ± 0.69	9 ± 1.30	2.83 ± 0.30
May	6.55 ± 0.56	13 ± 1.37	3.0 ± 0.44
June	6.80 ± 1.06	10 ± 0.70	3.5 ± 0.42
July	7.48 ± 0.51	11 ± 0.44	3.1 ± 0.16
August	8.33 ± 0.71	10 ± 0.70	2.66 ± 0.33
September	7.0 ± 0.74	10.5 ± 0.33	3.2 ± 0.11
M ± SE	7.1 ± 0.36[a]	10.6 ± 0.67n.s.	3.01 ± 0.14[a]

Values are represented by mean ± standard error (SE).
[a]Means highly significant.
n.s., Means not significant.

The interstitial cells (Leydig cells, interlobular cells, and lobule boundary cells) occupy a greater part of the testis interstitium. Leydig cells are located in the fibrous supporting CT and form groups near the BCs in between the STs. They are formed of small or large clusters of polymorphous cells that contain spherical nuclei and display the ultrastructural characteristics of steroidogenic cells. Their cytoplasmic borders cannot be observed with HE stain. Furthermore, the interstitial cells undergo a maximal development (thus seeming to signal secretory activity) just before and during the breeding period; their presence may be partly obscured before spawning by the crowding and distention of the testis with sperms (Figure 13.33). Their primary function is to produce sex steroids (testosterone) needed for gametogenesis and expression of the secondary sex characteristics.

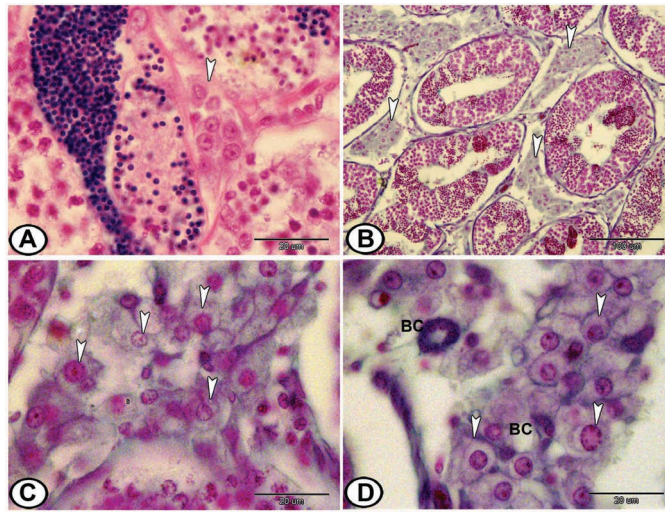

FIGURE 13.33 The interstitial tissue (IT) of Nile tilapia. (A) A reduced IT (arrowhead) of testis during the breeding season stained with HE. (B) Abundant ITs (arrowheads) of testis during the non-breeding season stained with Crossmon's trichrome. (C, D) Magnified view from (B) showing polygonal interstitial cells (arrowheads) around the BCs.

13.4.2.1.1 Spermatogenesis

The process of sperm formation occurred in the spermatocysts and pass through three major phases:

(1) renewal and mitotic proliferation (spermatogonial stem cells to differentiated SG),
(2) meiosis (spermatocytes to spermatids), and
(3) spermiogenesis (spermatids to spermatozoa).

The testis can be divided into an unrestricted spermatogonial testis type, where SG can be found all along the tubules or lobules, and a restricted spermatogonial testis type, where SG are restricted to the distal part of them. The testicular organization of *O. niloticus* corresponds to the unrestricted (cystic) type, where the spermatogenesis is completed within the spermatocysts and leads to the synchronous development of the germ cells.

The spermatogenetic process is seasonal in some fish and more or less continuous in others. For example, the testis of Perch is small from late June to late August (northern hemisphere). Then the spermatogenesis proceeds rapidly and by early November, the gonad has reached its greatest size. The

testicular volume, an indicator of spermatogenetic rate, in the top minnow, *Gambusia affinis*, is eight times as great in summer as in winter. In tilapia, the breeding season begins in April and ends in September. In males of some species of teleosts as tilapia and inshore coral trout, the spermatogenesis, spermiogenesis, and the presence of partially spent areas occurring in the same testis indicated multiple spawning.

The primary spermatogonia (sperm mother cells) are the largest cells of the germinative lineage that can occur either in isolated or in groups inside the cysts in the STs. They are large oval cells with very scarce, lightly eosinophilic cytoplasm, and large round nucleus with a single nucleolus. Primary spermatogonia were found during the breeding and nonbreeding seasons and usually present in abundance within those STs located peripherally under the tunica albuginea. Each primary spermatogonium undergoes a series of repeated mitotic divisions to produce a cluster of secondary spermatogonia encapsulated within a cyst. Clusters of cells resulting from divisions of the original germ cell maintain a consistent stage of development within the cyst. Secondary spermatogonia are rounded cells, smaller than primary spermatogonia with large lightly basophilic nuclei, and little cytoplasm. Each cluster enclosed in a cyst and divide synchronously, mitotically to form the primary spermatocytes that are smaller in size than secondary spermatogonia, the nucleus is strongly stained with hematoxylin and the cytoplasm has little affinity for dyes (Figure 13.34).

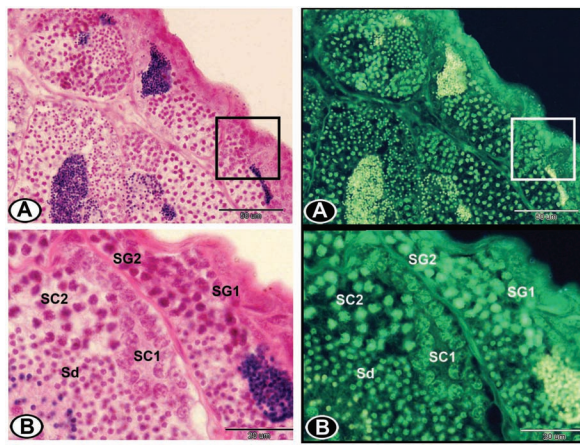

FIGURE 13.34 (A, B) Primary and secondary SG (SG1, SG2) of Nile tilapia are located in spermatocyst under the tunica albuginea (square). Note the presence of primary spermatocyte (SC1), secondary spermatocytes (SC2), and spermatids (Sd) stained with HE. Note the negative images on the right side.

The first meiotic divisions of the primary spermatocytes produce the secondary spermatocytes (haploid) that are somewhat smaller than the primary spermatocytes and show intense basophilic nuclei. The second meiotic division produces haploid spermatids, those are small with scant cytoplasm and condensed strongly basophilic nucleus. The spermatids inside the cyst increase in number toward the center of the testis. At this stage, the cyst ruptures releasing the spermatids into the testis lumen where the final maturation takes place. The metamorphosis of the spermatid to motile spermatozoa occurs in the lumen of the testis tubules after the cyst had burst and this process called spermiogenesis. The spermatozoa are smaller than spermatids with a strongly basophilic nucleus. The mature spermatocysts open to release cohorts of sperms into a central lumen, which lead to a contagious system of EDs (Figure 13.35).

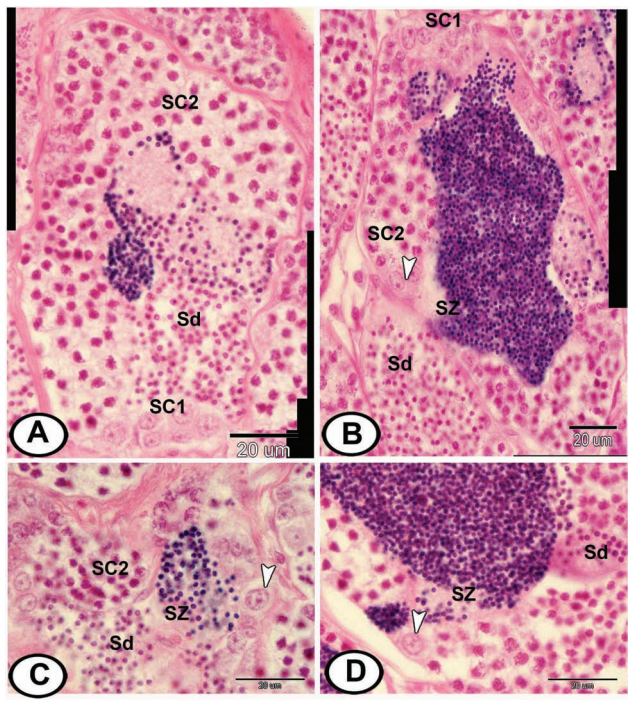

FIGURE 13.35 The stages of spermatogenesis in Nile tilapia stained by HE. (A, B) The ST contained primary spermatocytes (SC1), secondary spermatocytes (SC2), and spermatids (Sd). Note the STs in (B) in the breeding season are filled with spermatozoa (SZ) and the presence of Sertoli cells (arrowhead). (C, D) The distended STs during the breeding season showing the process of spermiogenesis. The spermatids (Sd) metamorphosed into spermatozoa (SZ). Note the presence of Sertoli cells (arrowheads) that form the spermatocysts.

During the nonbreeding season of tilapia, the STs are dominated by early stages of spermatogenesis (spermatogonia and primary spermatocytes) and have a narrow lumen free of sperms with considerably fewer spermatocysts. While during the breeding season, the STs are dominated by later stages of spermatogenesis (secondary spermatocytes and spermatids) and early stage of spermiogenesis (spermatids). The STs are strongly packed with spermatozoa in the prespawning and spawning periods (Figure 13.36).

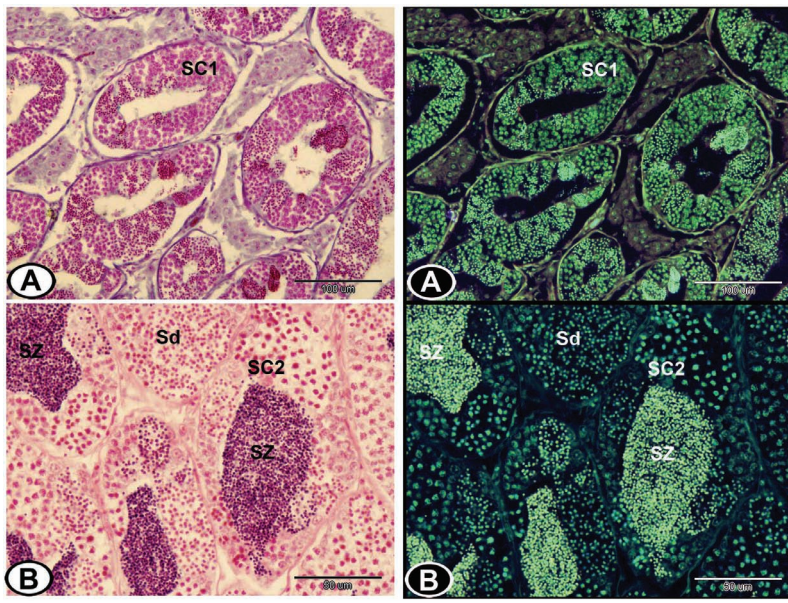

FIGURE 13.36 (A) The STs during the non-breeding season in Nile tilapia are dominated by primary spermatocyte (SC1) stained by Crossmon's trichrome. (B) The lumen of STs during the breeding season is filled with spermatozoa (SZ), the spermatocyts contain spermatids (Sd) and secondary spermatocytes (SC2) stained with HE. Note the negative images on the right side.

The growth stages of the gonads and the onset of spawning showed a correlation with the rise in water temperature and the best temperature for spawning in tilapia is between 21 and 24 °C. The reason is that the warm temperature can cause an increase of the basal gonadotropin release and of the pituitary responsiveness to the hypothalamic factor gonadotropin-releasing hormone, which in turn induced the gonadal recrudescence (high gonadosomatic index and testosterone level). On the other hand, the low temperature induces a decline in the morphological signs of sexual maturity.

Fishes are different from mammals in that they showed a cystic type of spermatogenesis in which a single clone of the germ cells enclosed by and accompanied through the different stages of spermatogenesis by a group of Sertoli cells. The Sertoli cells are pyriform cells with slightly eosinophilic cytoplasm and one basal clear nucleus exhibiting an irregular contour with one clear nucleolus. Its adluminal surface is thrown into finger-like projections, whereas its basal surface is thrown into a complex system of stubby projections. Their projections form the borders of spermatocysts. The spermatogonia and spermatocytes do not touch the Bl; they are enclosed by the cytoplasmic expansions of Sertoli cells. The spermatids and the earlier stages are associated with Sertoli cells (Figures 13.31C, D and 13.35).

Sertoli cells in fish were described by several names, as companion cells, cyst cells, sustentacular cells, intralobular cells, and follicular cells. During the nonbreeding season in tilapia, the Sertoli cells regress or severally reduced in size that could not be visible by the light microscopy; the mean number of Sertoli cells was 6.4 ± 0.5 per cross section of STs and 1.79 ± 0.16 per spermatocyst. The minimum number was 5 ± 0.31 per cross section of STs and 1.33 ± 0.21 per spermatocyst in February. On the other hand, during the spawning or breeding season, these cells flourish up, increase in size, and become well-distinct microscopically. During the breeding season, there is a significant increase in the number of Sertoli cells, its mean number reached 10.6 ± 0.67 per cross section of STs and 3.01 ± 0.14 per spermatocyst (Table 13.3).

Sertoli cell proliferation occurs primarily during spermatogonial proliferation. In Nile tilapia, the number of Sertoli cells per cyst increases from primary spermatogonia to spermatocyte cysts. Sertoli cell proliferation is strongly reduced when the germ cells have proceeded into meiosis and is stopped in postmeiotic cysts. Therefore, Sertoli cell proliferation can also be a factor responsible for increasing testicular size and sperm production.

Sertoli cells play a role in the supplying of nutrients to the germ cells, and responsible for the physical support and regulation of spermatogenesis. Moreover, Sertoli cells are involved in phagocytosis of degenerating residual sperm cells and in the spermatogonial proliferation. In addition, these cells are considered to be the main constituent of the blood testicular barrier, which developed usually before or after meiosis and it maintains features of intense protein synthesis throughout the whole spawning season.

13.4.2.2 TUBULAR TESTIS TYPE

In the male guppy and molly, the testis is a bilobed organ of tubular type, where the testis is composed of cysts-containing tubules that radiate from the two main SDs. The sperms are present only at the apex of the tubule and the cysts are migrating to the ED. At the center of the testis is a large cavity where the spermatozoa are stored. All the sperms of a number of cysts ripen at the same time. The spermatozoa of the guppy are produced in the form of unencapsulated sperm bundles called spermatozeugmata (Figure 13.37). In the later, the heads of spermatozoa point outward (attached to the Sertoli cells lining the cysts) while their tails spirally oriented in the center. In the EDs, the spermatozeugmata are surrounded by a PAS-mucoprotein complex. The spermatozoa were released into the lumen of the SDs containing secretions of seminal fluid. Then the Sertoli cells fuse with the wall of the ED, the cysts open and spermatozeugmata are released in the main SD (Figures 13.38 and 13.39).

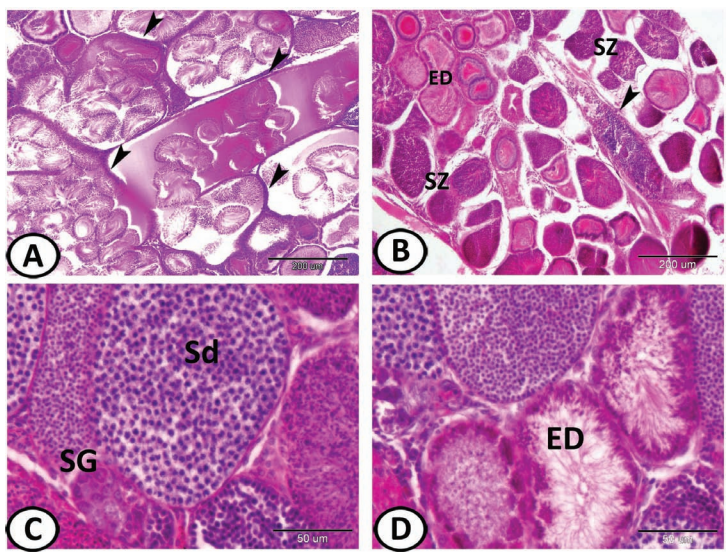

FIGURE 13.37 Testis of guppy stained with HE. (A) Sagittal section through the testis of an adult guppy. In this species, the testis is composed of cysts-containing tubules (arrowheads). When the spermatogenesis proceeds, cysts with the different spermatogenetic stages migrate from the periphery toward the sperm ducts. (B) The spermatozoa (SZ) of the guppy are produced in the form of unencapsulated sperm bundles called *spermatozeugmata* that are released in the main sperm duct (arrowhead). Note the ED. (C) Cysts of spermatids (Sd) and SG are clearly identified. (D) Higher magnification of the ED.

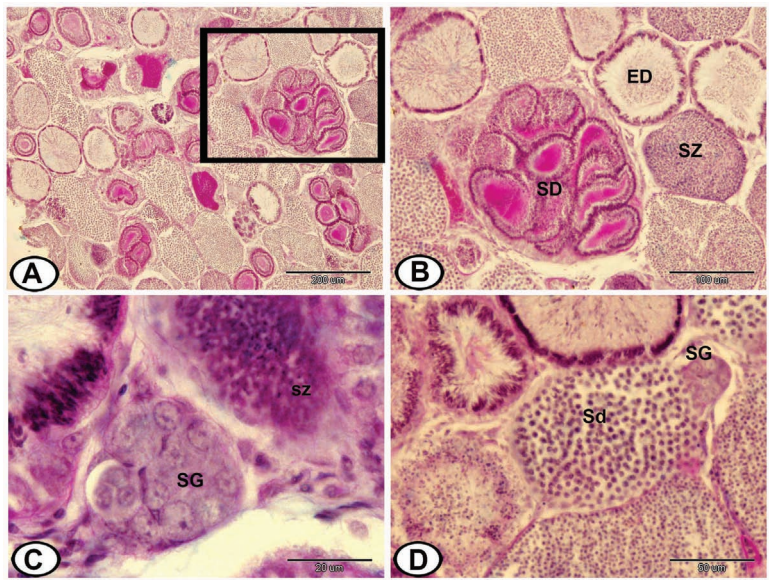

FIGURE 13.38 The distal part of the testis of molly fish stained by PAS-HX. (A, B) The spermatozoa (SZ) and final stages of spermatogenesis are present near the sperm duct (SD) and ED. (C, D) SG are found periphery. Note the presence of cysts of spermatozoa (SZ) and spermatids (Sd).

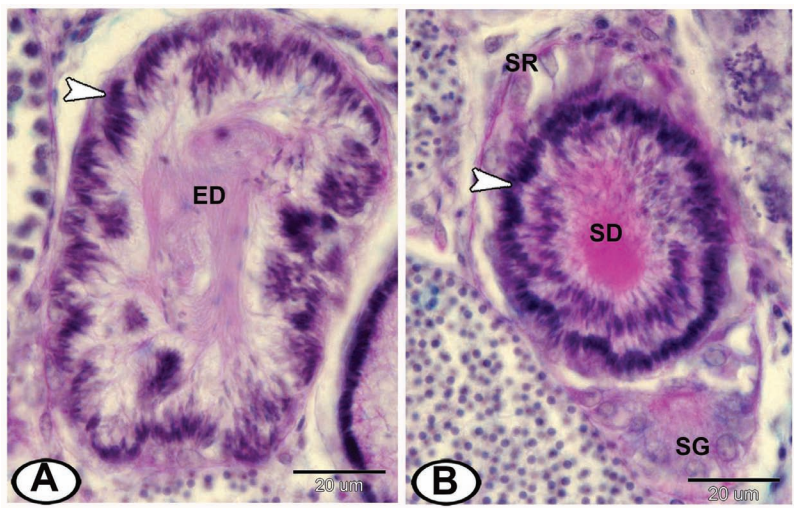

FIGURE 13.39 The duct system of molly fish stained with PAS-HX. (A) The ED showing the head of spermatozoa (arrowhead) pointed outward and the tails are oriented in the center. (B) The wall of the SD is lined with Sertoli cells (SR) and contained a large number of spermatozoa (arrowhead). Note the presence of peripheral SG.

Restricted spermatogonial testis type is found in all Atherinomorpha (Atheriniformes, Beloniformes, and Cyprinodontiformes). In this testis type, the germinal compartment extends to the periphery of the testis and terminates blindly. The lobules are formed by cysts of synchronous germinal cells and a central lumen, which contains abundant spermatozoa. Spermatogenesis in guppy seems to be continuous in the periphery of the distal part of the testis tubules in which the cysts move. The spermatogonia are associated with Sertoli cells. As spermatogenesis proceeds, cysts with the different spermatogenic stages (spermatogonia II–spermatocytes I–spermatocytes II–spermatids–spermatozoa) migrate from the periphery toward the SDs. During spermatogenesis, the later stages are progressively closer to the EDs. The spermatozoa of viviparous species are characterized by an elongated head and remain free in the SD to transform directly into the female genital tract (Figure 13.40). In *Poecilia reticulata,* the SD joins with the urethra into the urogenital sinus, which opens just behind the anus.

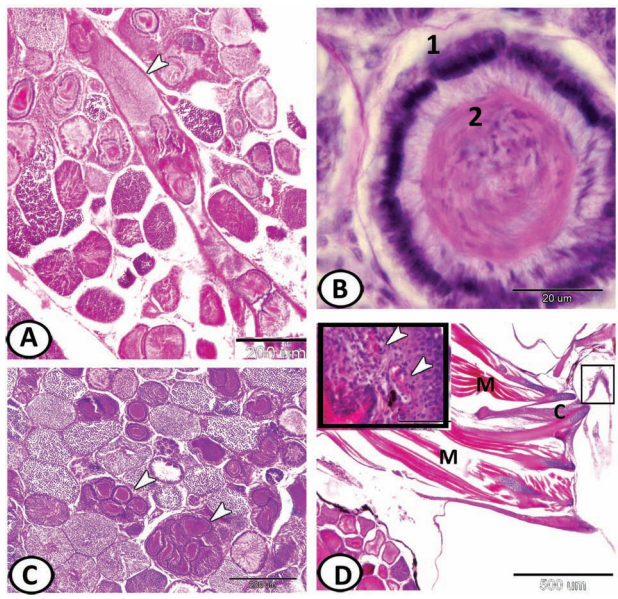

FIGURE 13.40 (A) Mature testis of a guppy shows free *spermatozeugmata* in the lumen (arrowhead) of the main duct (HE). (B) The *spermatozeugmata* are aggregations of spermatozoa in which the heads point to the periphery (1) simulating a columnar epithelium; the tails are spirally oriented to the center (2). (C) Cross section of the testis of molly fish stained with PAS showing the PAS-positive spermatic ducts (arrowheads). (D) The gonopodium of the guppy (boxed area) is supported by cartilage (C) and skeletal muscles (M). The inserted figure indicates a higher magnification of the gonopodium. Note the presence of central BVs (arrowheads).

13.4.3 THE GONOPODIUM

In a number of fish (as *Poecillidae*), fertilization is internal. Males have intromittent organs like the claspers in elasmobranchs or gonopodia in *Poecillidae.* In male Chondrichthyes, the medial portion of the pelvic fin is modified into the clasper organ. Claspers, also known as myxopterygia, are paired organs supported by fin cartilages and contain a groove along which sperm packets are conveyed into the female cloaca. The spermatozoa are ejected by this muscular organ (siphon sacs), which use seawater to propel the sperm along the groove that is lined by a stratified cuboidal epithelium supported by dense CT.

In the *Poeciliidae*, the males have a gonopodium (Figure 13.40D), which is an intromittent organ developed from modified anal fin rays and is directed posteriorly. It is a tube-like structure, through which the sperm is ejected into the female's genital tract. The epithelium covering the gonopodium is composed of stratified squamous epithelium and shows erythrocytes bathing in large central blood sinuses. The thick epithelium is supported by a basement membrane. For copulation, the gonopodium swings forward and sperm bundles (spermatozeugmata) are directly transported into the female cloaca. The gonopodium is raised, or erected, by skeletal muscle at its base. These muscular fibers (rhabdomyocytes) are supported by cartilages or bones.

KEYWORDS

- **ovaries**
- **germinal epithelium**
- **ovarian stroma**
- **viviparity**
- **testis**

BIBLIOGRAPHY

Afonso-Dias, I. P.; Hislop, J. R. G. The reproduction of anglerfish *Lophius piscatorius Linnaeus* from the North-West Coast of Scotland, *J. Fish Biol.* **1996,** *49*(A), 18–39.

Amiri, B. M.; Maebayashi, M.; Adachi, S.; Yamauchi, K. Testicular development and serum sex steroid profiles during the annual sexual cycle of the male sturgeon hybrid, the bester. *J. Fish Biol.* **1996,** *48,* 1039–1050.

Arockiaraj, A. J.; Haniffa, M. A.; Seetharaman, S.; Singh, S. Cyclic changes in gonadal maturation and histological observations of threatened freshwater catfish "Narikeliru" *Mystus montanus (*Jerdon, 1849), *J. Acta Icthyol. Piscat.* **2004,** *34*(2), 253–266.

Chmilevskii, D. A.; Kameneva, T. O. Oogenesis of *Mozambique tilapia.* IV. Yolk Formation, *J. Tsitolog.* **2003,** *45*(1), 5–13.

Cinquetti, R.; Dramis, L. Histological, histochemical, enzyme histochemical and ultra structural investigations of the testis of *Padogobius martensi* between annual breeding seasons*, J. Fish Biol.* **2003,** *63,* 1402–1428.

Coward, K.; Bromage, N. R. Histological classification of oocyte growth and the dynamics of ovarian recrudescence in *Tilapia zilli, J. Fish Biol.* **1998,** *53,* 285–302.

Ferreira, B. P. Reproduction of the inshore coral trout *Plectropomus maculates* (Perciformes: Serranidae) from the Central Great Barrier Reef, Australia, *J. Fish Biol.* **1993,** *42,* 831–844.

Francolini, M.; Lora Lamia, C.; Bonsignorio, D.; Cotelli, F. Oocyte development and egg envelope formation in *Oreochromis niloticus,* a mouth-brooding Cichlid Fish, *J. Submicrosc. Cytol. Pathol.* **2003,** *35*(1), 49–60.

Jalabert, B. Particularities of reproduction and oogenesis in Teleost fish compared to mammals, *Reprod. Nutr. Dev.* **2005,** *45,* 261–279.

Lahnsteiner, F.; Patzner, R. A.; Weismann, T. The spermatic ducts of salmonid fishes (*Salmonidae*, Teleostei). Morphology, histochemistry and composition of the secretion, *J. Fish Biol.* **1993,** *42,* 79–93.

Lopes, D. C. J. R.; Bazzoli, N.; Brito, M. F. G.; Maria, T. A. Male reproductive system in the South American Catfish *Conorhynchus conirostris*, *J. Fish Biol.* **2004,** *64,* 1419–1424.

Mokhtar, D. M. Characterization of the fish ovarian stroma during the spawning season: cytochemical, immunohistochemical and ultrastructural studies, *Fish Shellfish Immunol.* **2019,** *94,* 566–579.

Mylonas, C. C.; Woods, L. C.; Zohar, Y. Cyto-histological examination of post-vitellogenesis in captive-reared striped bass, *J. Fish Biol.* **1997,** *50,* 34–49.

Peterson, M. S.; Slack, W. T.; Brown-Peterson, N. J.; McDonald, J. L. Reproduction in nonnative environments: establishment of Nile Tilapia, *Oreochromis niloticus,* in coastal Mississippi watersheds, *Copeia* **2004,** *4,* 842–849.

Pudney, J. Spermatogenesis in nonmammalian vertebrates, *J. Microsc. Res. Tech.* **1995,** *32*(6), 459–497.

Quintana, L.; Silva, A.; Berois, N.; Macadar, O. Temperature induces gonadal maturation and affects electrophysiological sexual maturity indicators in *Brachyhypopomus pinnicaudatus* from a temperate climate, *J. Exp. Biol.* **2004,** *207,* 1843–1853.

Rasotto, M. B.; Shapiro, D. Y. Morphology of gonoducts and male genital papilla, in the bluehead wrasse: implications and correlates on the control of gamete release, *J. Fish Biol.* **1998,** *52,* 716–725.

Redding, J. M.; Patino, R. Reproductive physiology. In *The Physiology of Fishes;* Evans, D. H., ed.; CRC Press: Boca Raton, FL, 1993.

Schulz, R. W.; Menting, S.; Bogerd, J.; Franca, L. R.; Vilela, D. A.; Godinho, H. P. Sertoli Cell proliferation in the adult testis—evidence from tow fish species belonging to different orders, *J. Biol. Reprod.* **2005,** *73*(5), 891–898.

CHAPTER 14

Endocrine System

ABSTRACT

The endocrine system includes many glands that are distributed in various regions of the body. The adenohypophysis is glandular in nature while the neurohypophysis is consisting of neurosecretory nerve endings of the hypothalamo-hypophyseal tract, blood sinuses, and glial cells (pituicytes). Urophysis in most teleosts consists of an array of large neurosecretory neurons, the Dahlgren cells, which are distributed within the caudal spinal cord. Interrenal cells (ICs) represent the equivalent of the mammalian adrenal cortex. These cells line the posterior cardinal veins of the head kidney. They have a strong eosinophilic granular cytoplasm and produce corticosteroids. Chromaffin cells are homologous to the adrenal medulla of mammals. They are mixed among ICs and synthesize and secrete catecholamines. The corpuscles of Stannius, which occur uniquely in two groups of bony fishes: Holostei and Teleostei, are putative endocrine organs associated with the kidney. They produce the calcium-regulating hormone (stanniocalcin). In adult bony fishes, the thyroid gland consists of numerous diffuse follicles scattered in the posterior subpharyngeal region around the ventral aorta and afferent branchial vessels. The pancreas comprises an endocrine component of endodermal origin formed by the islets of Langerhans. These islets consist of clusters of lightly capsulated hormone-secreting cells (insulin, glucagon, somatostatin, etc.) surrounded by a capillaries network. Calcitonin is produced by the ultimobranchial cells. The pseudobranch is a gill-like structure derived from the first-gill arch and attached to the internal surface of the operculum. The choroid of the eye is composed of similar arrays of capillaries (rete mirabile) alternating with rows of fibroblast-like cells.

The endocrine system includes many glands that are distributed in various regions of the body. They control the long-term activities of organs involved in digestion, development, metabolism, growth, reproduction, etc. Animals have two types of glands, namely exocrine glands and endocrine glands.

Exocrine glands have ducts to carry off their secretion. The endocrine glands have no ducts, and their secretions, called hormones, are liberated into the bloodstream to be conveyed to other parts of the body where they produce a definite physiological effect. Hormones act specifically on target organs, which possess specific receptors.

The endocrine glands, together with the nervous system, participate in the maintenance of a steady physiologic state, called homeostasis. Their functions are intimately linked, coordinated, and sometimes even integrated as, for example, in the hypothalamo-hypophyseal complex.

14.1 PITUITARY GLAND

The pituitary gland is a complex neuroepithelial structure. As in other vertebrates, it is derived embryologically from a downward push of the floor of the hypothalamus (forming the pars nervosa) and an upgrowth of the roof of the mouth, forming the pars distalis, and pars intermedia (PI) of the adult. The pituitary gland (Figures 14.1 and 14.2) is located below the diencephalon (hypothalamus), behind the optic chiasma and anterior to the saccus vasculosus, and is attached to the diencephalon by a stalk (the pituitary stalk). The pituitary gland is completely enveloped by a delicate connective tissue capsule.

The part of epithelial origin (the stomodaeum) is known as the adenohypophysis. It is glandular in nature while the part having its origin in nervous tissue is known as the neurohypophysis, consisting of neurosecretory nerve endings of the hypothalamo-hypophyseal tract, blood sinuses, and glial cells (pituicytes). There is considerable interdigitation between the two regions.

The adenohypophysis of teleosts comprises a rostral and a proximal pars distalis and also a PI. This gland is composed of many different cell types, which secrete a variety of hormones controlling basic physiological processes, including growth, gonad development, thyroid activity, regulation of steroidogenesis by the cells of the interrenal gland, water, and electrolyte balance. Each pituitary hormone is generally associated with specific secretory cells, best identified by immunocytochemical methods, with a clear distribution within the three-adenohypophysis regions.

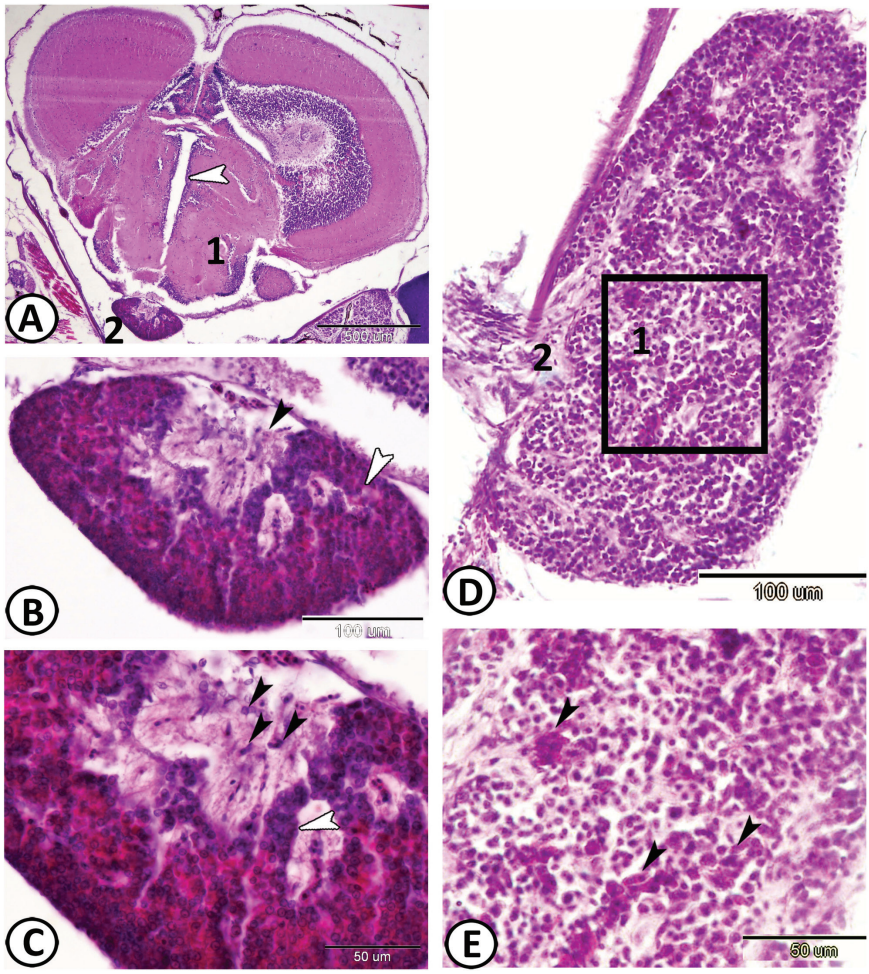

FIGURE 14.1 (A) A transverse section of the hypothalamus-hypophyseal system of molly stained by HE. This system is a neuroendocrine complex in which BVs (portal veins) and axons link the hypothalamus (1) and the pituitary gland (2) allowing endocrine communication between these two structures. The arrowhead indicates the third ventricle of the diencephalon. (B) The pituitary gland or hypophysis is divided into anterior epithelial (adenohypophysis—white arrowhead) and posterior nervous (neurohypophysis—black arrowhead) parts. (C) The neurohypophysis consists of neurosecretory nerve endings of the hypothalamo-hypophyseal tract, BCs, and glial cells (pituicytes—black arrowheads) bathing among the axons. The neurohypophysis intermingling with cords of the adenohypophysis (white arrowhead). (D, E) The pituitary gland of red-tail shark stained by PAS/HX showing the secretory cells of the adenohypophysis (1) and pars nervosa (2). The adenohypophysis contains strong PAS-positive basophils (arrowheads).

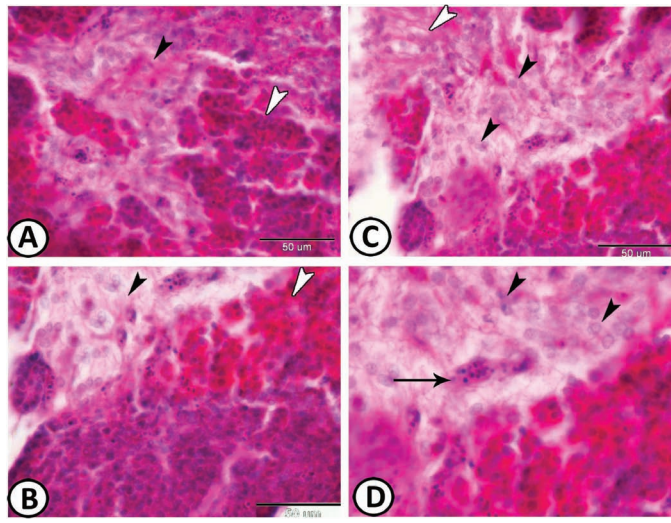

FIGURE 14.2 (A, B) The pituitary gland of guppy stained by HE showing the adenohypophysis that is composed of large cords of cells that branch and anastomose with each other (white arrowheads) and neurohypophsis (black arrowheads). (C, D) Higher magnification in the pars nervosa showing pituicytes (black arrowheads), nerve fibers (white arrowhead), and BC (arrow).

14.1.1 ROSTRAL PARS DISTALIS

It is the anterior region of the pituitary gland occupied by acidophils and basophils. The acidophils showed affinity to aniline blue and acid fuchsin and are negative to periodic acid–Schiff (PAS) orange and chromium-hematoxylin-phloxine (CHP). These cells are identified as the lactotrops or prolactin (PRL)-secreting cells. The basophils in this region are identified as the thyrotrops or thyrotropic hormone (TSH)-secreting cells. The cells form a layer in the dorsal region adjacent to the pars nervosa are identified as the corticotrops. These cells stained only faintly with PAS orange G and were negative to aldehyde fuchsin and aniline blue.

14.1.2 PROXIMAL PARS DISTALIS

There is no line of clear demarcation between the rostral pars distalis and PPD, but the regions could be distinguished by the differential staining of their cells. The basophils found in this region are identified as the gonadotrops.

These cells are strongly PAs-positive, aldehyde fuchsin-positive and aniline blue-positive. The acidophilic cells are identified as the somatotrops [growth hormone (STH)-secreting cells]. These cells are stained positively with PAS orange G, Mallory Heidenhain's, and acid fuchsin, and the granules are negative to aldehyde fuchsin and CHP.

14.1.3 PARS INTERMEDIA

This distal region surrounding the neurohypophysis is the smallest region, which is extensively innervated by the neurohypophysial tracts and is mainly constituted by the deeply stained basophils. These cells which stained positively with PAS orange G were identified as the melanotrops. The melanotrops were negative to Mallory Heidenhain's, CHP, and aldehyde fuchsin. The majority of the PI cells are melanotropic cells that synthesize the prohormone proopiomelanocortin peptide, which is converted intracellularly by peptidases into melanocyte-stimulating hormones (α-and β-MSH), β-endorphin, β-hypotrophic hormone, and β-lipotropic hormone (β-LPH). α- MSH is mainly involved in the stress response in teleost fish and may control the dispersion of melanin in melanophores in some species. A second PI cell type is present in some teleosts. These cells synthesize and secrete the hormone somatolactin, a protein molecule that belongs to the prolactin/growth hormone family.

The neurohypophysis (pars nervosa) of teleosts is composed of hypothalamic neurosecretory fibers, glial cells, and blood vessels (BVs). The nerve fibers are mainly nonmyelinated arising in the preoptic nucleus and terminate in close relationship to blood capillaries (BCs). In teleosts as in most vertebrates, the glial cells or pituicytes are regarded as support cells but also as phagocytic cells being directly involved in the functioning of the neurohypophysis. Pituicytes form synapse with neurosecretory nerve fibers. Three neurohypophysial hormones are known in teleosts: isotocin (IT), arginine vasotocin (AVT), and melanin-concentrating hormone (MCH). IT and AVT are nonapeptides whereas MCH is a heptadecapeptide (=17 amino acids). Many reports are suggesting a role for AVT in fish osmoregulation although the precise role has not yet been established. Functional receptors have been identified in the gill and kidney of teleost fishes. Very little attention has been given to the actions of oxytocin-like peptides; although, there is evidence for the presence of IT receptors in the gill and liver of trout. Several studies have reported the involvement of IT and/or AVT in spawning (oviparous fish) and parturition (viviparous fish) of some teleosts.

14.2 UROPHYSIS (CAUDAL NEUROSECRETORY SYSTEM)

A well-defined neurohemal organ (urophysis) is seen only in teleosts. In teleosts, a second neuroendocrine system and a neurohemal (in addition to the neurohypophysis) area is associated with the caudal end of the spinal cord; this is the urophysis (Figure 14.3). In most teleosts, it consists of an array of large neurosecretory neurons, the Dahlgren cells, which are distributed within the caudal spinal cord. Dahlgren cell's unmyelinated axons project posteriorly to the urophysis, which is located on the last vertebra. Apart from teleosts, Dahlgren cells are also present in elasmobranchs, condrosteans, holosteans, and dipnoans. These, however, lack a neurohemal organ.

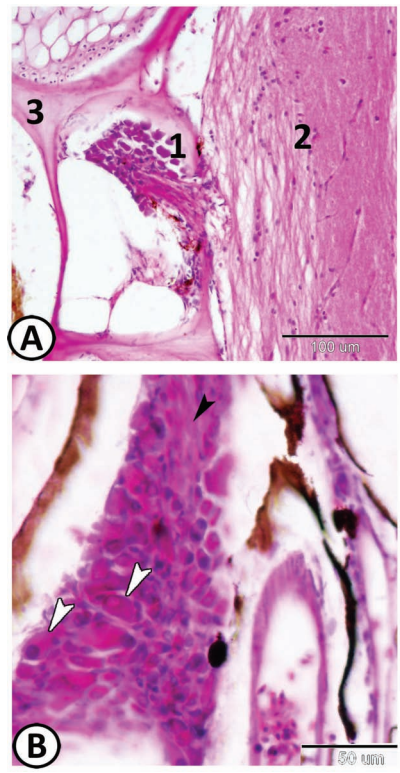

FIGURE 14.3 Urophysis of guppy stained by HE. (A) The urophysis (1) is an endocrine gland associated with the caudal end of the spinal cord (2). Note the body of the last vertebrae (3). (B) Hormones secreted by the neurosecretory cells pass down their axons through the neurosecretory tract (urophysis stalk—black arrowhead) to the urophysis. The neurosecretory cell bodies (white arrowheads) have polymorphic nuclei and basophilic cytoplasm.

The rostro-caudal extension of Dahlgren cells also varies to a large extent in the different taxa. Indeed, in elasmobranchs and condrosteans, Dahlgren cells are distributed in the spinal cord corresponding to the last 25–30 vertebrae, whereas in most teleosts, they are concentrated in the spinal cord corresponding to the last three–nine vertebrae.

In elasmobranchs, the neurosecretory cells that are called Dahlgren cells and have perikarya (cell bodies) some 20 times larger than ordinary motor neurons, extend along the terminal vertebrae region. The axons of these cells terminate at the BCs lying on the lateroventral surface of the spinal cord. In teleosts, the unmyelinated axons of the neurosecretory cells congregate with BVs to form a neurohemal complex in a manner similar to that seen in the neurohypophysis.

As with the mammalian neurohypophysis stalk, the degree of constriction of the urophysis stalk varies. In the eel (*anguilla*), there is no stalk but only a slight ventrolateral swelling of the spinal cord, while in other fish such as *Oryzias*, *Fundulus*, and *Gillichthys*, there is a well-defined stalk. The neurosecretory cell bodies lying in the spinal cord have polymorphic nuclei and basophilic cytoplasm. Urotensin I and urotensin II are two types of peptide hormones isolated from teleost urophyses. These factors secreted by this complex have been linked to various vasoactive responses, notably causing an increase in the blood pressure, and vasoconstriction in the urinary bladder, intestinal tract, and reproductive tract. An ionoregulatory response in *Anguilla* has also been reported.

14.3 INTERRENAL AND CHROMAFFIN TISSUES

There is no adrenal gland in fish but interrenal and chromaffin tissues (Figure 14.4). Interrenal cells (ICs) represent the equivalent of the mammalian adrenal cortex. These cells line the major BVs (posterior cardinal veins) of the head kidney. They have a strong eosinophilic granular cytoplasm and produce corticosteroids, including cortisol. Cortisol has a potent effect on intermediary metabolism and is an important factor in stress response. In addition, osmoregulation, protein metabolism, growth, regeneration, and anti-inflammatory reactions have also been reported as related functions of these cells.

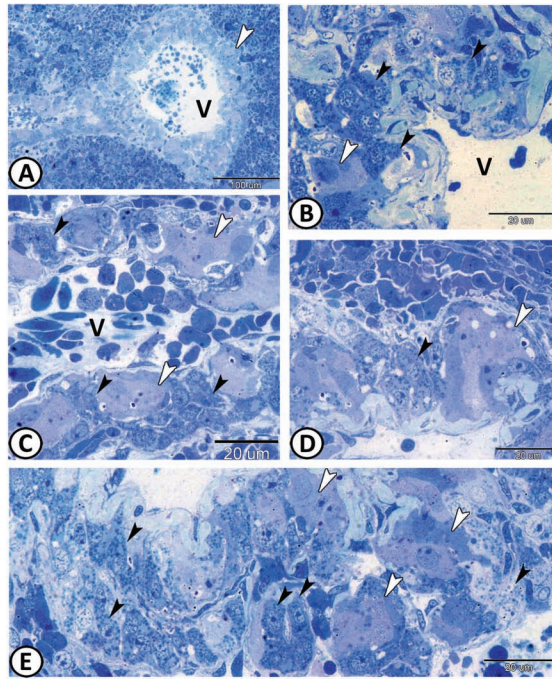

FIGURE 14.4 (A–D) Semithin sections through the head kidney of grass carp stained by toluidine blue showing the interenal cells (white arrowheads) interposed with hematopoietic tissue and chromaffin cells (black arrowheads) line the posterior postcardinal vein (V). (E) The larger ICs (white arrowheads) encloses the smaller granular chromaffin cells that form groups in the wall of the vein (black arrowheads).

Chromaffin cells are homologous to the adrenal medulla of mammals. They are mixed among the ICs and cannot be clearly distinguished with H&E staining. The chromaffin cells synthesize and secrete catecholamines, such as epinephrine and norepinephrine. Catecholamines play a role in the regulation of the rate and the force of the cardiac constriction. In addition, catecholamines have been shown to bring about systemic vasoconstriction and branchial lamellar vasodilatation in teleosts. Furthermore, they can alter the respiratory functions of blood and the activity of chloride cells in the gills.

In Chondrichthyes, the steroidogenic cells (ICs) and the catecholamine-producing cells (chromaffin tissue) form separate cell masses. The steroidogenic cells are situated along the medial edge of the kidneys; the catecholaminergic cells are located near the aorta and postcardinal veins. In

teleosts, both types of cells assemble in groups on the ventral surface of the head kidneys.

There is great variability in the interrenal morphology among teleost groups and even variability within families. The shape and size of the cells vary, sometimes being polygonal, columnar, cuboidal, or even spindle-shaped. The forms of these cells have been shown to change in response to hormones, drugs, and stress or salinity changes. The ICs formed one, two, and three layers of cells, lining the BV and were also determined to form masses enclosed by thin connective tissues. They are larger than the chromaffin cells and have round nuclei and many large vacuoles in the cytoplasm. The cytoplasm of the ICs was eosinophilic when stained with HE and acidophilic with Masson's trichrome (MT). The ICs are arranged in large anastomosing cords intermingled with numerous capillary vessels.

The interrenal gland cells were intermingled with chromaffin cells and were observed to enclose chromaffin cells lying adjacent to the BVs. The chromaffin cells were located next to the vein wall and detectable singly and in clusters among the ICs. Aside from the intermingled distribution of the chromaffin cells with the ICs, they were also situated in groups in the walls of the main veins.

Chromaffin cells are generally smaller and more uniform in appearance than ICs and their cytoplasm is granular and slightly basophilic. When stained with HE and MT, they exhibited a pale cytoplasm. The large nucleus was slightly basophilic and had a prominent nucleolus. The chromaffin cells are also arranged in groups that are surrounded by a thin connective tissue. They get their name from their staining reaction to chromic salts. They secrete sympathomimetic substances, such as adrenaline, associated with immediate stress responses. In particular, a rise in the blood levels of catecholamines causes hyperglycemia and increases the gills' functional area for gaseous and ionic exchanges. A ganglion cell in the chromaffin cell group was also observed in some cases. Neither the ICs nor the chromaffin cells showed a positive PAS staining.

The electron microscopy (Figure 14.5) showed that the chromaffin cells have many granules evenly distributed in the cytoplasm and smaller membrane-bound vesicles with an electron-dense core. According to the electron density, shape, and size of the chromaffin granules, the chromaffin cells are classified into noradrenalin cells, adrenalin cells, and small granule-containing (SGC) cells. Cells that contain vesicles with a round, electron-dense core are interpreted as noradrenaline cells, while cells with electron-lucent vesicles are identified as adrenaline cells.

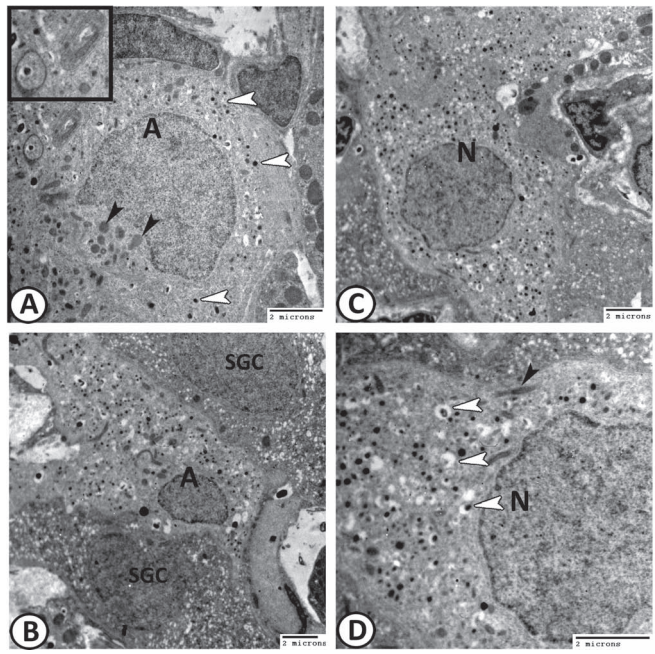

FIGURE 14.5 EM of chromaffin cells of grass carp. (A, B) Adrenalin cells (A) contain electron-dense granules (white arrowheads) and rounded mitochondria (black arrowheads). small granule containing cells (SGC) cells contain many small vesicles. The boxed area indicates the terminal nerve endings. (C, D) Nor-adrenaline cells (N) are characterized by the presence of vesicles with dense core (white arrowheads) and elongated mitochondria (black arrowhead).

Noradrenalin-cells (N-cells) have a polygonal or elongated shape with a rounded euchromatic nucleus. The nuclear membrane is indented thus revealing slightly condensed chromatin. The cytoplasm contains strongly electron-dense granules with a homogeneous matrix, bounded by a closely adherent and scarcely evident membrane. Their shape usually is round, infrequently elliptical; the average diameter is 250 nm. Small elongated mitochondria with lamellar cristae, sparse rough endoplasmic reticulum (rER) and smooth endoplasmic reticulum (sER), free ribosomes, and glycogen granules may be observed in the cytoplasm.

Adrenaline-cells (A-cells) contain chromaffin granules with a loose matrix of variable electron density, separated from the limiting membrane by a clear halo. The core of the granules is seldom eccentric. Rounded mitochondria are demonstrated in their cytoplasm. The diameter of the A-cell is average 240 nm.

SGC cells have a high nuclear to cytoplasmic ratio and contain rER, glycogen granules and free ribosomes, vesicles, and small strongly electron-dense granules resemble NA cells.

The nerve fiber endings are attached to the surface of the chromaffin cells and contain numerous synaptic vesicles, a few large dense cored vesicles and many mitochondria (Figure 14.5A). At the synaptic junctions, the plasma membranes of the nerve endings and the chromaffin cells are parallel to each other and display densities on their cytoplasmic faces.

The ultrastructural analysis of the interrenal cells (Figure 14.6) revealed that the cytoplasm contains numerous round mitochondria with tubule-vesicular cristae in an electron opaque matrix homogeneously distributed. sER, Golgi apparatus, lysosome, glycogen particles, vacuoles, and microfilaments are found in smaller numbers. Lipid droplets are not identified in these cells. The nucleus is rounded with a large nucleolus and heterochromatin adheres to the internal surface of the nuclear membranes.

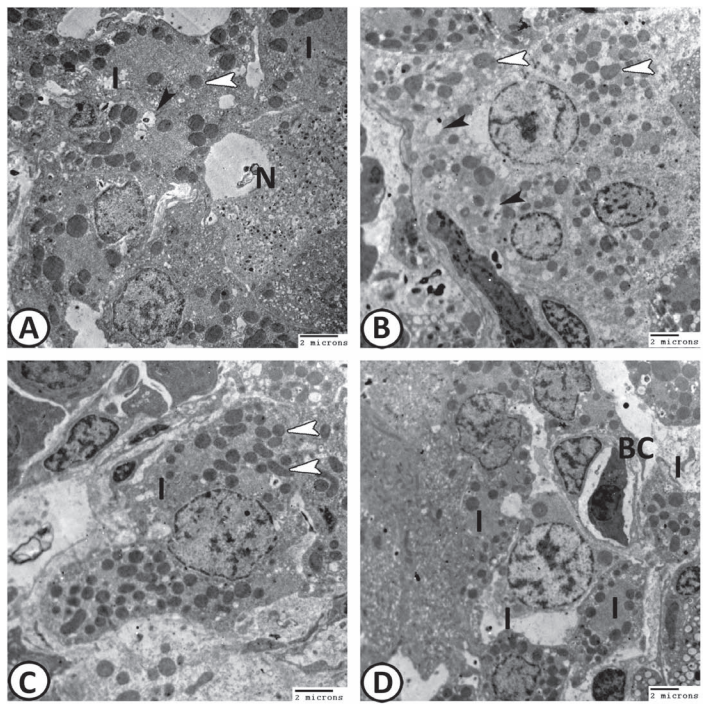

FIGURE 14.6 (A–D) TEM of ICs (I) of grass carp that associated with noradrenalin cells (N) and BCs. Note the abundance of rounded mitochondria (white arrowheads) and small vacuoles (black arrowheads).

Glial fibrillary acidic protein (GFAP) immunohistochemistry (Figure 14.7) shows the presence of the sustentacular cells, type of glial cells. The sustentacular cells are branched cells that distributed in close association with chromaffin cells and in neighboring to the blood vessels. The sustentacular cells are distinguished by their long cell processes, which express GFAP immunoreactivities. The sustentacular cells are involved in catecholamine secretion. Moreover, they modulate neuronal activity in the central nervous system.

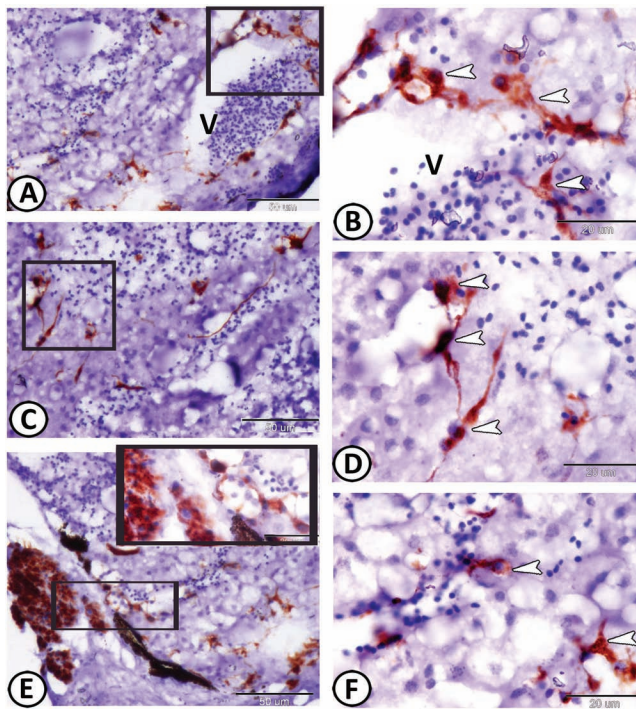

FIGURE 14.7 (A–F) GFAP expressions in sustentacular cells (arrowheads) in contact with chromaffin cells around the postcardinal vein (V) in the head kidney of molly fish.

14.4 CORPUSCLES OF STANNIUS

The corpuscles of Stannius (CS), which occur uniquely in two groups of bony fishes; Holostei and Teleostei, are putative endocrine organs associated with the kidney. They produce the calcium-regulating hormone, stanniocalcin, or called hypocalcin (a glycoprotein hormone). The secretion of this hormone is stimulated by high serum calcium. Stanniocalcin acts on the gills and small intestine to decrease calcium uptake and, therefore, serves as hypocalcemic

hormone. It inhibits excess calcium influx across the gills through inhibition of the function of branchial Ca^{2+}-activated ATPase. In addition, the organ secretes substances that elevate the arterial blood pressure and may play a role in osmoregulation.

These discrete encapsulated organs are located on the lateroventral or laterodorsal surface of the kidneys. Typically, they are paired but their number can reach 10 or more. In Nile tilapia, they are two in number, similar to the majority of Teleostei; although, the number tends to be greater in the more primitive fishes, where they are 4 or 5 in the toadfish, 3–7 in some catfishes, and 4–14 in trout and other salmonids.

Each corpuscle is surrounded by a thick connective tissue capsule separating it from the surrounding renal tissue. This capsule is highly vascular and sends septa into the gland dividing the parenchyma into lobules or cords, which are surrounded by a basal lamina (Figure 14.8). They are well-supplied with BVs and nerves. The lobules are polymorphic, closely packed, and anastomose together. The cells are columnar or polyhedral in shape with a rounded, oval, or elliptical large vesicular nucleus. Two cell types could be distinguished based on PAS staining. Type I cells are PAS-positive, which are predominated. Type II cells are PAS-negative and very rare.

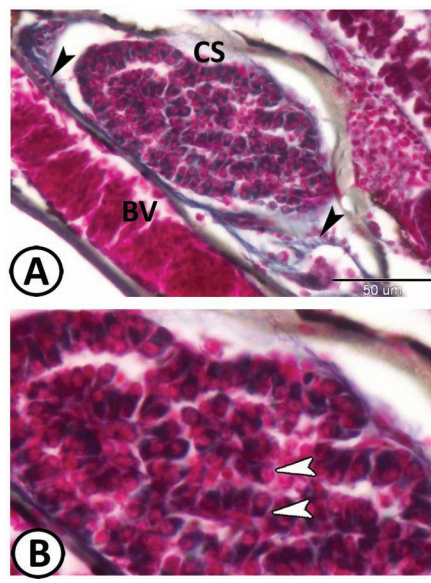

FIGURE 14.8 Corpuscles of Stannius (CS) in molly stained with Crossmon's trichrome. (A, B) The parenchymal cells (white arrowheads) of the CS are arranged in cords that are surrounded by connective tissue capsules (black arrowhead). Note the presence of BV that establishes contact with most secretory cells.

Based on ultrastructural characters, three cell types could be recognized as one type is granular while the other two types are nongranular and differentiated from each other mainly by the density of their organelles. The granular cell type is predominant. These cells are pyramidal, quadrilateral, or polyhedral in shape. The nucleus is large, euchromatic with a distinct nucleolus. The cytoplasm is electron-dense and contains rounded secretory granules distributed uniformly throughout the cytoplasm, rER, dense bodies, mitochondria, Golgi apparatus, and free ribosome. Two types of agranular cells are observed that have no secretory granules: Type I agranular cell is characterized by the presence of a large number of rER, mitochondria, and free ribosomes. The nucleus is rounded containing coarse chromatin. Type II agranular cell is characterized by a paucity of cell organelles, which give it an electron-lucent appearance. The nucleus has an irregular outline and contains very dense clumps of heterochromatin.

Removal of the glands (stanniectomy) causes a prompt rise in plasma calcium levels (hypercalcemia). Treatment of teleosts, such as eels, with extracts of corpuscles, causes a marked fall in calcium levels. Seawater is high in calcium compared to freshwater and the histological observations on the CS indicate that the glands are more active in seawater than in freshwater fish.

14.5 THYROID GLAND

In adult bony fishes, the thyroid gland (Figures 14.9 and 14.10) usually consists of numerous diffuse follicles scattered in the posterior subpharyngeal region around the ventral aorta and afferent branchial vessels. This pattern of scattered follicles can extend quite widely outside the pharyngeal region. This migration of the so-called heterotopic follicles from the pharyngeal region is probably due to the fact that the gland is not encapsulated and surrounded by connective tissue.

A few species of bony fishes (e.g., parrotfishes, *Scarus sp*.; swordfish, *Xiphias*, and tunas, *Thunnus sp.*) and all cartilaginous fishes have a thyroid contained within a connective tissue capsule. The teleostean thyroid is highly variable between and within taxa in terms of its forms and location sites. The most common site for the ectopic or heterotropic thyroid is the head kidney, although other nonpharyngeal regions (eye, spleen, and brain) have been identified in fish, usually afflicted by goiters

The histological aspect of the gland in the teleosts is essentially similar to that of tetrapods; the thyroid tissue comprises epithelial cells that vary in size depending on the degree of TSH stimulation from the hypophysis. The thyroid follicles are usually round to oval, with low cuboidal epithelium. The cells form a tight epithelium surrounding a colloid-filled lumen and have microvilli projecting into the follicular lumen. The follicles are surrounded by loose connective tissues in contact with BCs. The colloid contents are positively stained with PAS and MT, indicating the presence of rich glycoprotein.

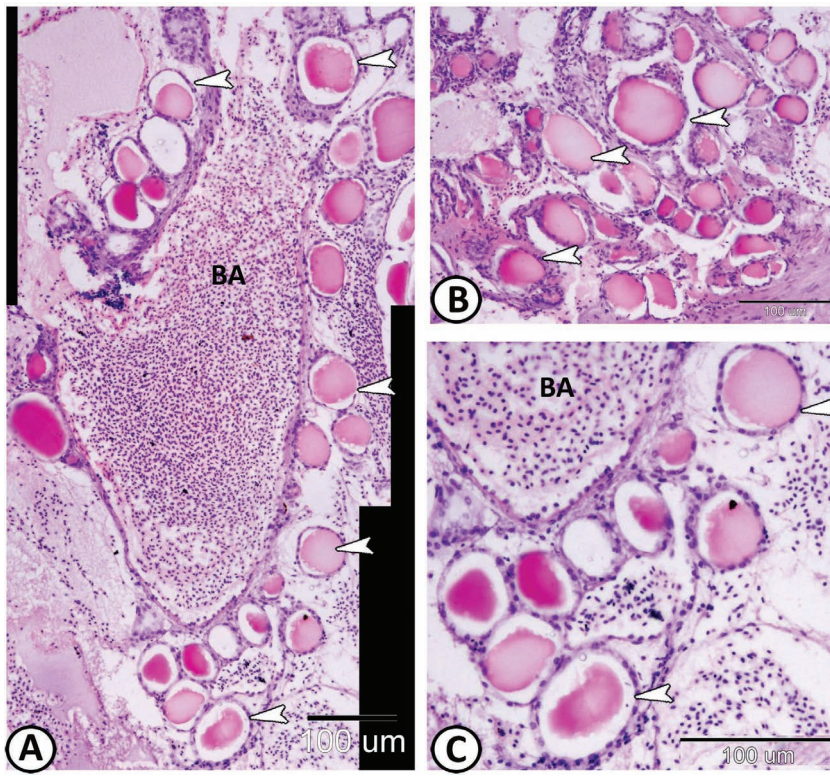

FIGURE 14.9 (A–C) Thyroid glands of grass carp stained by HE. The thyroid gland is found in the branchial region along the ventral aorta and afferent branchial arteries (BAs). The thyroid is usually not a compact gland and consists mostly of numerous scattered units called thyroid follicles (arrowheads). The lumen of the follicles are filled with thyroglobulin (brick red), a glycoprotein that stores T3 and T4.

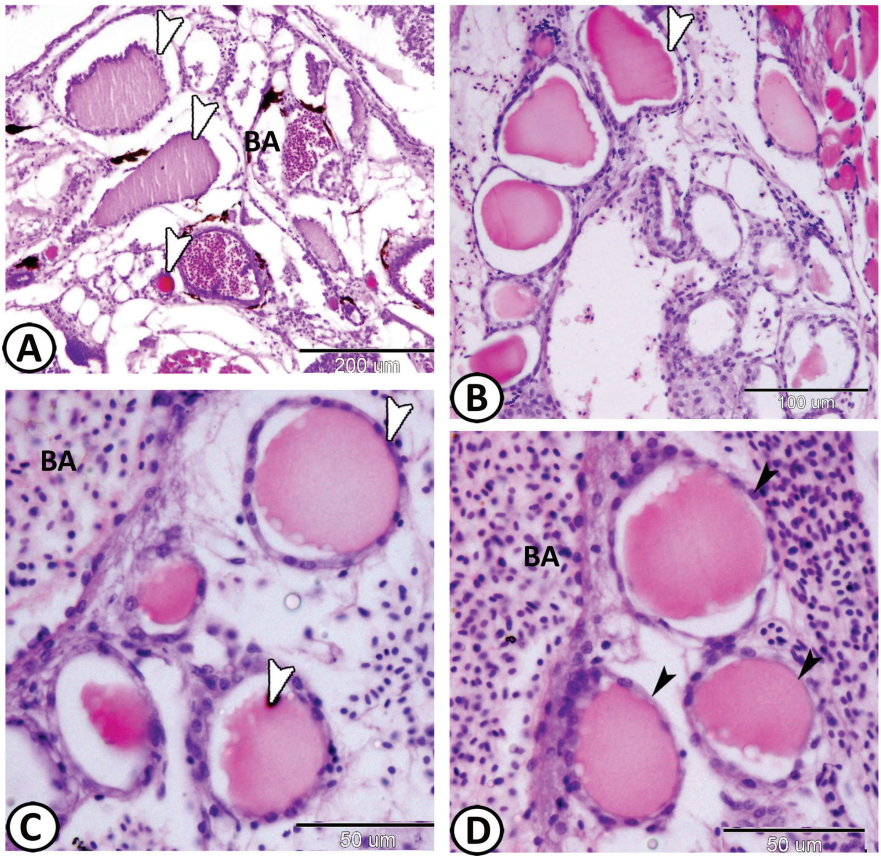

FIGURE 14.10 (A) Thyroid glands of molly fish stained with HE showing few follicles (arrowheads) surrounded the BA. (B–D) Higher magnifications of thyroid glands of grass carp stained by HE show that thyroid follicles (white arrowheads) are lined by a simple cuboidal epithelium. The follicular epithelial cells surround a lumen containing a mass of homogeneous colloid (thyroglobulin). Note in the low-active follicles (black arrowheads), the follicular cells appear flattened and the follicles are distended by a large amount of colloid. In the active glands, the follicle epithelium is much taller and the colloid is less abundant.

The thyroid hormone in fish is very similar to the thyroid hormone of higher animals and has a stimulatory effect on many metabolic processes. The distinctive feature of the gland is that the follicles are capable of trapping iodine and manufacturing the two thyroid hormones, 3,5,3′-triiodothyronine and thyroxine together with their precursors 3-monoiodotyrosine and 3,5-diiodotyrosine. Thyroid hormones play an important role in the control of physiological events, such as metamorphosis, growth, metabolism, and

reproduction. Involvement in osmoregulation and migration movements has been shown.

The thyroid gland of chondrichthyan fish is a single discrete organ located in the midline of the lower jaw. It is pear-shaped in sharks and somewhat flattened and disc-shaped in skates and rays. The thyroid follicle of elasmobranchs is similar in structure to that found in bony fish and tetrapods. The follicle cells are normally cuboidal in shape. There is variation in follicle diameter, and larger follicles are found in older fish.

14.6 ENDOCRINE PANCREAS

In addition to an exocrine component, which was described in Chapter 9, the pancreas comprises an endocrine component of endodermal origin formed by the islets of Langerhans. These islets consist of clusters of lightly capsulated hormone-secreting cells (insulin, glucagon, somatostatin, etc.) surrounded by a capillaries network. Because these cell types secrete peptide hormones, they exhibit the usual features of cells engaged in active protein synthesis. The size of islet cells may vary according to the food and season.

Endocrine parts of the pancreas of most teleosts (Figure 14.11) are organized in the liver, around the intestinal bulb, and in the mesentery of the anterior part of the intestine, as a number of lightly staining Langerhan's islets of different sizes and shapes between the exocrine acinar cells and around the pancreatic duct. Each islet is surrounded by a thin capsule of connective tissue and consists of three cell types that are arranged in the form of irregular cords and clumps. Alpha (A) cells are the most dominant cells and most common on the periphery that appeared ovoid in shape with intense acidophilic cytoplasm. Their nuclei are large oval in shape with distinct nucleoli. Beta (B) cells are large in size, polyhedral in shape with granular cytoplasm, and rounded eccentric nucleus and are grouped in small clusters. Delta (D) cells are solitary and a few in number (2–3/islet), small in size, fusiform in shape, and argyrophilic with silver stain. By Maldonado stain, the cytoplasm of A cells stained purple, and the cytoplasm of B cells stained violet-blue, while the cytoplasm of D cells stained light blue. Additional F cells are present in some species. The clumps of secretory cells are supported by delicate collagenous fibers with a rich network of fenestrated capillaries.

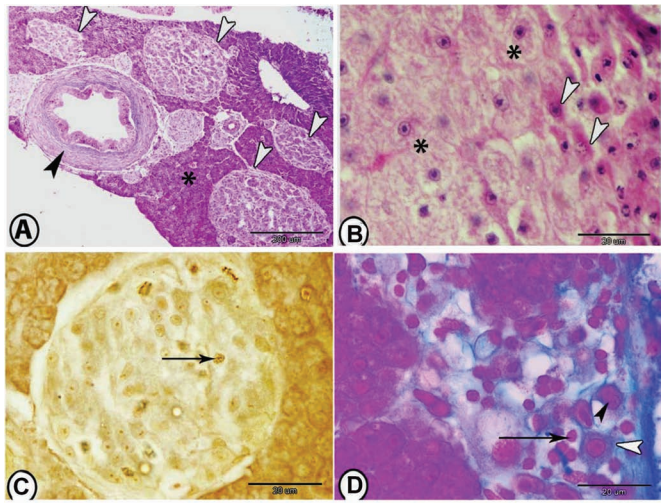

FIGURE 14.11 Distribution of endocrine portion of the pancreas of grass carp. (A) Langerhan's islets (white arrowheads) are organized between exocrine acinar cells (asterisk) and around the pancreatic duct (black arrowhead) (HE). (B) Oval-shaped alpha cells (arrowheads) and large polyhedral beta cells (asterisks) (HE). (C) Small argyrophilic delta cells (arrow) are determined (Grimelius silver stain). (D) The cytoplasm of alpha cells stain purple color (black arrowhead), beta cells stain violet-blue (white arrowhead), and delta cells stained light blue (arrow) by Maldonado's staining.

In many species, the endocrine portion of the pancreas is found as an independent organ called Brockmann bodies that are located in mesentery adjacent to the spleen. The "Brockmann body regions" from species such as tilapia (*Oreochromis niloticus*) are under investigation as a source of islet tissue for human transplants because of the compacted and pure nature of the "region."

Insulin causes hypoglycemia but fish do not exhibit the rapid blood glucose clearance response typical of mammals. Glucagon acts antagonistically to insulin in that it increases blood glucose by liver glycogenolysis. It also stimulates the incorporation of amino acids in the liver and stimulates gluconeogenesis.

14.7 ULTIMOBRANCHIAL GLAND

Just as the thyroid gland develops as a ventral outgrowth of the pharynx at the level of the first two branchial pouches, so another structure, the ultimobranchial gland, is derived from the last branchial pouch area in the

embryonic fish. This tissue migrates backward, during the development of the fish, to a position lying near the pericardium.

The gland is difficult to identify, even under the dissecting microscope. In teleosts, the ultimobranchial gland (Figure 14.12) is an unpaired structure located in the transverse septum between the abdominal cavity and the sinus venosus just ventral to the esophagus. In some cyprinids (carp, goldfish, zebrafish), the gland is composed of small follicles, whereas in the eel and the trout, it consists of two glandular units lining a central lumen. In small-sized fishes as guppy, medaka, etc., the gland shows a sheet-like structure and its observation is very limited. Colloidal substances were sometimes observed in the lumen of the follicles. The mitoses of the gland cells were very active particularly in the gland two days after spawning.

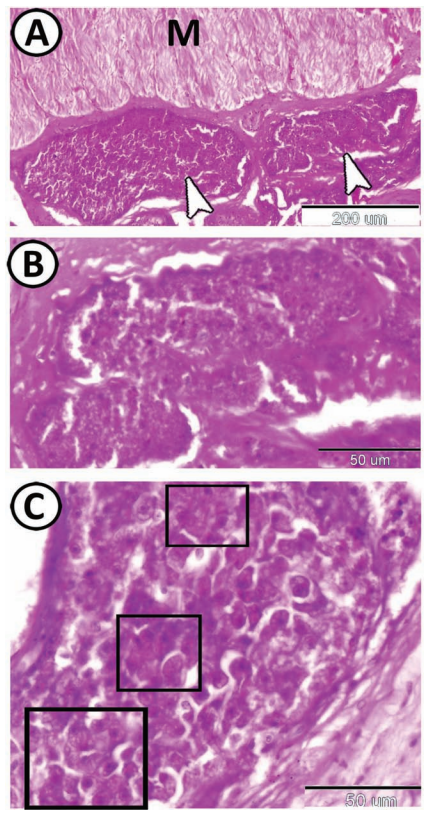

FIGURE 14.12 (A, B) In grass carp, the ultimobranchial gland consists of one or two glandular units (arrowheads) generally located in the transverse septum beneath the striated muscles (M) of the esophagus (HE). (C) In some cyprinids like the grass carp, the gland comprises small follicles surrounding a narrow lumen (boxed areas) (HE).

Electron microscopy revealed that the follicles of the ultimobranchial gland are enclosed by a thin layer of the basement membrane usually accompanied by BCs lined with the fenestrated endothelium. The follicles consisted of two types of cells, a few agranular cells and a dominant number of granular cells. The apical surface of the cells frequently shows cilia and microvilli. The agranular cells are generally small in size and showed no secretory granules. The nuclei show highly irregular contours with marginal indentations. The mitochondria tend to lie in the basal part of the cells. Glycogen particles are distributed throughout the cytoplasm. Many pinocytotic invaginations of the plasma membrane and a few pinocytotic vesicles were seen along the basal or lateral cell surface. The granular cells are characterized by an accumulation of a number of round, membrane-bound secretory granules in the supranuclear region that range from 150 to 250 nm in diameter. They had a dense or faint heterogeneous core separated from the limiting membrane by a thin electron-lucent region. Mitochondria are numerous in the basal part of the cell. The rER developed around the nucleus. Free ribosomes were sparsely scattered throughout the cytoplasm with few secondary lysosomes.

The ultimobranchial gland in fishes plays a sex-related role at least during the maturation of females. In the granular cells of mature females, the secretory granules are more abundant than in those of mature males. This increase in the number of granules is accompanied by cellular hypertrophy. An increased number of the agranular cells are observed occasionally in clusters in the female glands two days after spawning.

Calcitonin (CT) is produced by the ultimobranchial cells. Manipulation of the ultimobranchial gland helped establish roles for CT in the regulation of fluids, electrolytes, and mineral metabolism. The ultimobranchial gland also controls, apparently with more precision than the CS, the serum calcium concentration, particularly in the female during the reproduction cycle.

14.8 PSEUDOBRANCH AND CHOROID BODY

The pseudobranch (Figure 14.13) is a red, gill-like structure derived from the first-gill arch and attached to the internal surface of the operculum. It is composed of gill lamellae, connective tissue, and BVs. The lamellae consist of pseudobranchial cells on an underlying basement membrane. This latter is applied to a network of parallel BCs, which can be supported by thin cartilaginous rods. The cells of pseudobranch have clear cytoplasm with abundant acidophilic granules and a large centrally located euchromatic

nucleus with a prominent nucleolus. The cytoplasm of these cells shows a negative reaction to PAS.

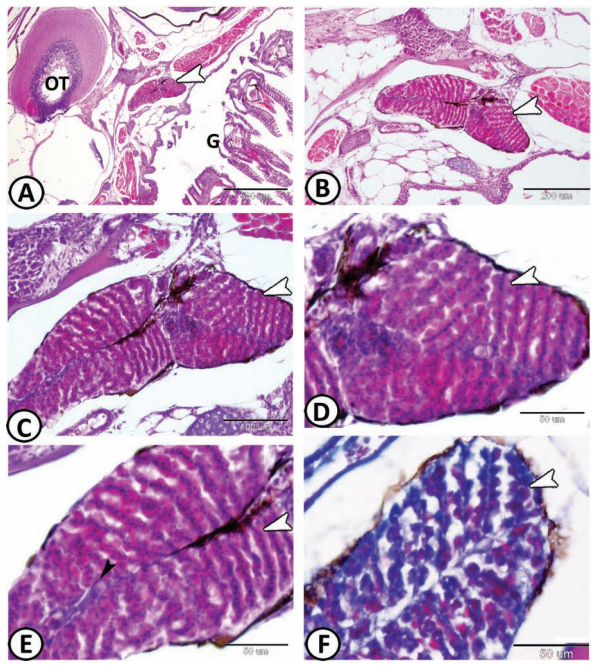

FIGURE 14.13 (A–C) Pseudobranch (arrowheads) of guppy is derived from the gill arch. OT indicates optic tegmentum and (G) indicates gills (HE). (D–F) Higher magnification shows that it consists of gill lamellae (white arrowheads), BCs (black arrowheads), and connective tissues (HE and MT, respectively).

The microscopic structure of pseudobranch varies among the species of fishes. In *Glossogobius giuris*, it is similar to the gills, while it has a glandular structure in *Notopterus chitala*. Three morphological types of pseudobranch in fishes are identified as: (1) these with distinguishable lamellae in contact with the water that the secondary lamellae are completely free. (2) Those that were covered with the opercular membrane and the connective tissue. This kind can be subcategorized into three types based on its location and its degree of isolation from the water: (A) a thin layer of connective tissue due to which lamellae cannot be separated but the filaments are free. (B) Connective tissue layer thicker than (A) due to which both the filaments and the lamellae cannot be separated. The lamellae, rays, and the vessels are well organized. (C) A thick layer of connective tissue in which the structure is so covered that

all the elements lose their identity**.** (3) Those that were completely reduced and embedded in the tissue. In this type, the pseudobranch is separated from the opercular chamber by the folds of connective tissue. This causes the sinking of the pseudobranch in the roof of the buccopharynx or the opercular cavity. The covered type of pseudobranch is demonstrated in trout, while it is embedded in Carp, free in Bass, and semifree in mullet.

The pseudobranch has a direct vascular connection with the choroid of the eye. The ophthalmic artery receives its blood from the pseudobranch and branches out in the capillaries of the choroid rete. The choroid rete is a capillary countercurrent system formed by the ophthalmic artery and vein. The choroid of the eye (Figure 14.14) is composed of similar arrays of capillaries (*rete mirabile*) alternating with rows of fibroblast-like cells.

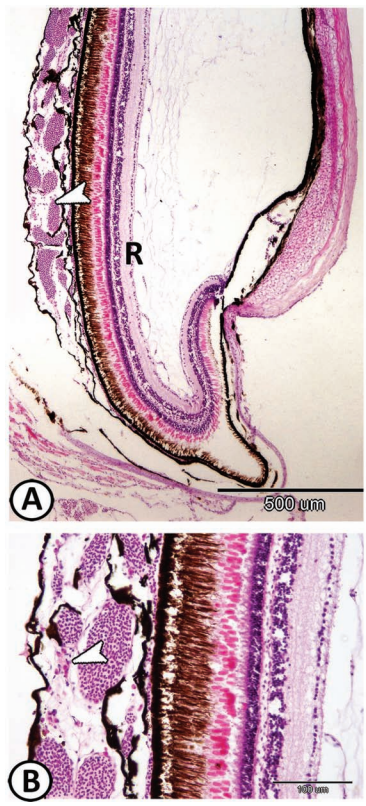

FIGURE 14.14 (A, B) The choroid of the eye of red-tail shark stained with HE. The choroid rete (rete mirabile—arrowheads) composed of arrays of capillaries alternating with rows of slender fibroblast-like cells. R indicates to the retina.

The pseudobranch is not present in all teleosts. Those fish which do not possess such structure (some *Siluridae, Ictaluridae, Notopteridae, Cobitidae, Anguillidae*, etc.) invariably also lack a choroid rete. Although it is considered to have an endocrine, neurosecretory, and regulatory function as well as it acts as an oxygen multiplier device or has hyperoxygenation function for the retinal blood supply, these are still to be defined in full.

The pseudobranch and the choroid rete appear to have a role in the maintenance of blood pressure of the eye by elevation of the arterial oxygen pressure by enzymatically acidifying the arterial blood via the action of carbonic anhydrase. In addition, the pseudobranch may have sensory properties and play a role in osmoregulation. The choroid rete may also have immune capabilities since it filters both afferent and efferent blood and contains cells that seem to be involved in antigen capture.

14.9 PINEAL GLAND

The diencephalons can be subdivided into three components: the epithalamus, the thalamus, and the hypothalamus. The epithalamus encompasses the pineal gland and the saccus dorsalis. This gland, connected to the third ventricle, is completely enclosed in a connective layer capsule and possesses an epiphyseal stalk lined by ependymocytes. The pineal gland is a light-sensitive neuroendocrine structure that projects from the roof of the telencephalon. It is now well accepted that the pineal in fish has a well-defined glandular activity and that indeed throughout the vertebrates, it is a photoneuroendocrine organ.

In bony fish, the general histological appearance of the saccular pineal closely resembles a sensory organ with photoreceptors, supporting cells, and larger cells with nerve cell characteristics (Figure 14.15). The abundant sensory cells of the organ are large and club-shaped with well-defined nuclei and mitochondria.

As in mammals, the pineal gland secretes the hormones indolamine and melatonin, as well as neurotransmitter substances. It appears to play a key role in the control of daily and seasonal rhythms such as the regulation of reproduction, growth, and seasonal migration. The gland contains the enzyme HIOMT (hydroxyindole *O*-methyltransferase) necessary for the formation of melatonin, serotonin, and a number of free amino acids, which may all act as chemical transmitters and have some physiological role.

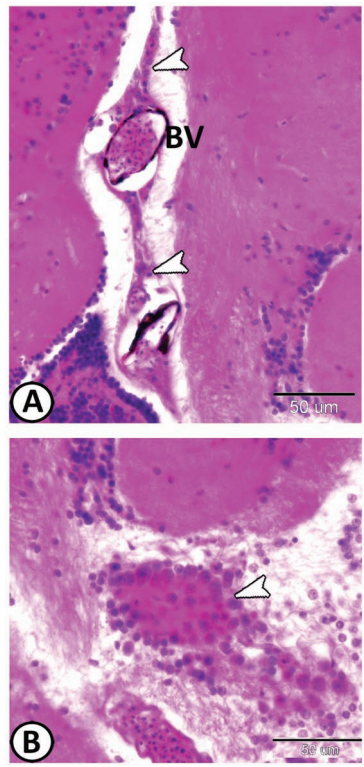

FIGURE 14.15 (A, B) Sagittal and cross section of the pineal gland of guppy stained with HE. The pineal gland (arrowheads) located in the third ventricle and usually associated with BVs.

14.10 ENDOCRINE CELLS OF THE GUT

Like in higher vertebrates, small regulatory peptides have been identified in the endocrine cells of the fish gut. Their identification was performed with immunohistochemical procedures using appropriate (specific) antibodies.

The endocrine cells of the gastrointestinal tract are located in the mucosa (Figure 14.16) and deliver their content to the bloodstream; the target organ can thus be at any distance from the endocrine cells. Ten or more subtypes of endocrine cells have been reported in teleost fishes (specific for bombesin, enkephalin, gastrin/cholecystokinin, neurotensin, substance P, somatostatin, vasoactive intestinal peptide.). The gastrointestinal hormones play important roles in the overall regulation of digestive processes, such as nutrient absorption, gut motility, and intestinal blood flow.

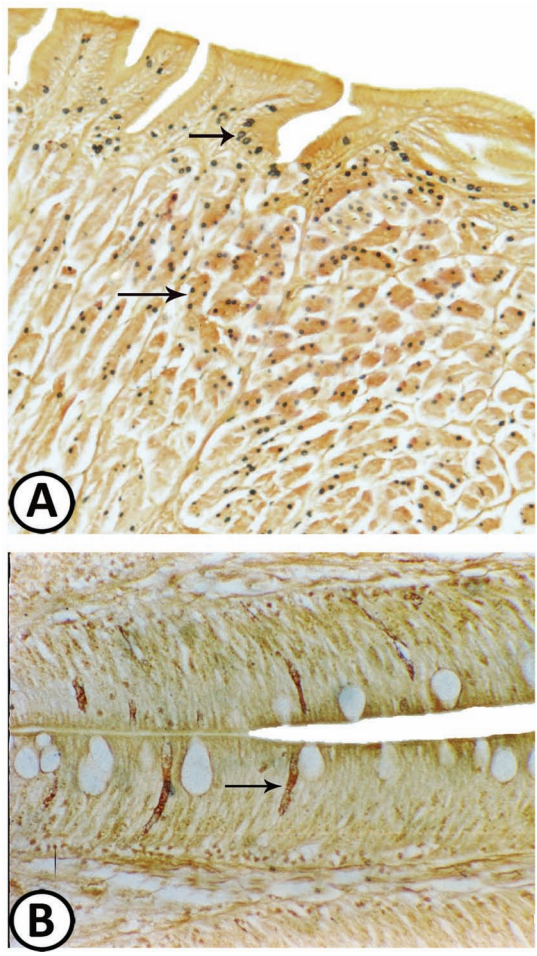

FIGURE 14.16 Endocrine cells of the gut stained by silver impregnation. (A) Endocrine cells (arrows) in the stomach of Nile catfish. (B) Endocrine cells (arrow) in the posterior intestine of Nile catfish.

14.11 GONADS

The testis interstitium contains few numbers of endocrine cells called Leydig cells (see Chapter 13). A number of steroids (androstenedione, testosterone, progesterone, etc.) have been isolated from the testes of several teleosts. The details of the interaction between the Sertoli and Leydig cells in the steroidogenic pathway in fishes are far from clear.

The thecal and granulosal cells surrounding the oocytes comprise the steroidogenic tissue of the ovary. The primary ovarian estrogen, 17β-estradiol, is one of the primary factors involved in the stimulation of the synthesis of vitellogenin, the main constituent of the yolk of the oocytes. 17β-estradiol also stimulates the hepatic synthesis of proteins that form the chorion of the oocyte. Progestagens in fish are also thought to promote ovulation. In brief, the steroids exert both local and peripheral effects.

KEYWORDS

- **pituitary gland**
- **thyroid**
- **interrenal**
- **chromaffin cells**
- **pseudobranch**

BIBLIOGRAPHY

Abdel-Aziz, El-S. H.; El-Sayed Ali, T.; Abdu, S. B. S., Fouad, H. F. Chromaffin cells and interregnal tissue in the head kidney of the grouper, *Epinephilus tauvina* (Teleostei, Serranidae): a morphological (optical and ultrastructural) study, *J. Appl. Ichthyol.* **2010,** 26, 522–527.

Civinini, A.; Padula, D.; Gallo, V. P. Ultrastructure and histochemical study on the interrenal cells of the male stickleback (*Gasterosteus aculeatus*, Teleostea), in relation to the reproductive annual cycle, *J. Anat.* **2001,** 199, 303–316.

Gaber, W.; Abdel-maksoud, F. M. Interrenal tissue, chromaffin cells and corpuscles of Stannius of Nile tilapia (*Oreochromis niloticus*), *Microscopy* **2019,** 68, 1–12.

Geven, E. J. W.; Nguyen, N. K.; van den Boogaart, M.; Spanings, F. A. T.; Flik, G., Klaren, P. H. M. Comparative thyroidology: thyroid gland location and iodothyronine dynamics in Mozambique tilapia (*Oreochromis mossambicus* Peters) and common carp (*Cyprinus carpio* L.), *J. Exp. Biol.* **2007,** 210, 4005–4015.

Kordon, A. O.; Matthew, A.; Ibrahim, I.; Abdelhamed, H.; Ahmed, H.; Baumgartner, W.; Karsi, A.; Pinchuk, L. M. Identification of Langerhans-like cells in the immunocompetent tissues of channel catfish, Ictalurus punctatus, *Fish Shellfish Immunol.* **2016,** 58, 253–258.

Machado-Santos, C.; Teixeira, M. J.; Sales, A.; Abidu-Figueiredo, M. Histological and immunohistochemical study of the thyroid gland of the broad-snouted caiman (*Caiman latirostris), Acta Scientiarum Biol. Sci.* **2013,** 35, 585–589.

Raine, J. C., Leatherland, J. F. Morphological and functional development of the thyroid tissue in rainbow trout (*Oncorhynchus mykiss*) embryos, *Cell Tissue Res.* **2000,** 301, 235–244.

Rocha, R. M.; Leme-Dos Santos, H. S.; Vicentini, C. A., Da Cruz, C. Structural and ultrastructural characteristics of interrenal gland and chromaffin cell of Matrinxã, *Brycon cephalus* Gunther 1869 (Teleostei-Characidae), *Anatom. Histol. Embryolog.* **2001,** 30, 351–355

Singh, O. N.; Ghosh, T. K.; Munshi, J. S. D. Structure of pseudobranch of two clupeoid fishes, *Hilsa ilisha* and *Gadusia chapra*, *Indian Anatomy Science, Part B*, **1986,** 52(2), 274–279.

Takahashi, A.; Kobayashi, Y.; Mizusawa, K. The pituitary-interrenal axis of fish: a review focusing on the lamprey and flounder, *Gen. Comp. Endocr.* **2013,** 188, 54e59.

CHAPTER 15

Nervous System

ABSTRACT

Five brain divisions usually observed in fish are from cranial to caudal, telencephalon or forebrain (contain two olfactory lobes and cerebrum), diencephalon (contain epithalamus, thalamus, and hypothalamus), mesencephalon or midbrain (contain two optic lobes that are connected with torus longitudinalis internally and the torus semicircularis, and optic tegmentum medially), metencephalon or hindbrain [cerebellum (CR)], and myelencephalon (medulla oblongata). The optic tectum (OT) represents the principal anatomical termination of the retinal ganglion cell axons and is considered the most obvious part of the midbrain. The development of this region reflects the importance of the visual sense in different species. Grossly, the OT is divided into two optic lobes and contains the tectal ventricle. It displays a distinctive laminar histological architecture, which is made up of six layers. The CR in teleosts is well-developed and includes three main divisions: the valvula cerebelli, the corpus cerebelli, and the vestibulolateral CR. The cerebellar cortex consists of three distinguished layers: an outer molecular, intermediate ganglionic, and inner granular layer. Notably, the gray substance in the spinal cord of teleosts displays a characteristic difference in its organization from that of higher vertebrates, in which the dorsal horns lie quite close together giving the gray substance the shape of an inverted Y. The white matter surrounds the gray matter and harbors myelinated nerve fibers. The ventricular organization is composed of the olfactory, lateral, the third, the tectal, and the fourth ventricles. The peripheral nervous system consists of nerves and ganglia.

The nervous system is the structural and functional mechanism regulating the response of an animal to environmental changes. For the nervous system to perform these responses, it is widely arranged throughout the body. The nervous system includes two major divisions: the central nervous system (CNS) and the peripheral nervous system (PNS). The CNS is consisted of the brain and spinal cord (SC), while the PNS includes the spinal and cranial

nerves with their associated roots and ganglia. The roots of the cranial and spinal nerves connect the PNS with CNS.

15.1 CENTRAL NERVOUS SYSTEM

15.1.1 THE BRAIN

In general, the brain is similar in all fishes. It is formed by the enlargement of the cephalic end of the SC. However, there are significant differences between the groups of fish regarding the development of different regions of the brain. The brain is composed of five main regions (Figure 15.1): the telencephalon contains cerebral hemispheres and two olfactory lobes, diencephalon or called "between brain," mesencephalon contains the optic lobes and tegmentum, metencephalon [cerebellum (CR)], and myelencephalon [medulla oblongata (MO)]. The MO tapers in the SC in which the narrow central canal is the posterior extension of the brain ventricular system.

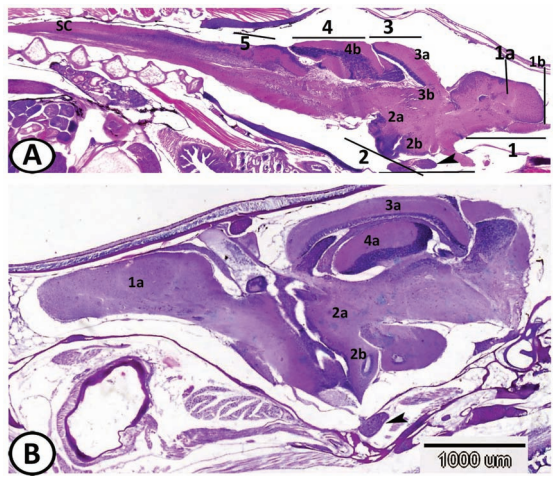

FIGURE 15.1 (A, B) Parasagittal section of the whole brain of guppy and red-tail shark (respectively) shows the five major parts of the brain: telencephalon (1), the most anterior part of the brain consisting of two cerebral hemispheres (1a) and a pair of solid olfactory lobes (1b); diencephalon (2) is divided into a dorsal epithalamus, a thalamus (2a) and a ventral hypothalamus (2b); it also consists of various appendages (pituitary body, arrowheads); mesencephalon (3) consists of the dorsally placed optic lobes (3a—OT) and the ventral tegmentum (3b); metencephalon (4) including the cerebellum, composed of the valvula cerebelli (4a) and the corpus cerebelli (4b); medulla oblongata (5) is the elongated posterior region constituting the main part of myelencephalon and continuous with the spinal cord (SC) (HE and PAS.AB/HX, respectively).

15.1.1.1 THE TELENCEPHALON

The fish telencephalon (forebrain) (Figure 15.2) is much reduced compared to that of mammals. It is composed of the olfactory lobes and right and left cerebral hemispheres (cerebrum). The expanded tip of each hemisphere is called the olfactory bulb, which possesses the cell bodies of olfactory nerve cells and acts as the primary center of the sense of smell. The olfactory lobes, a pair of structures receive and process signals from the nostrils via the two olfactory nerves. The olfactory lobes are very large in fish that hunt primarily by smell, such as hagfish, sharks, and catfish. In fish, the telencephalon is concerned mostly with olfaction. The histologic appearance of the cerebrum of teleosts is significantly different from that of mammals in that it does not have a neocortex, the characteristic six-layered structure of the mammalian cortex, and instead composes of fields of neurons interconnected by extensive neuropil (nerve endings and dendrites). In general, the forebrain is connected to the midbrain (mesencephalon) via the diencephalon.

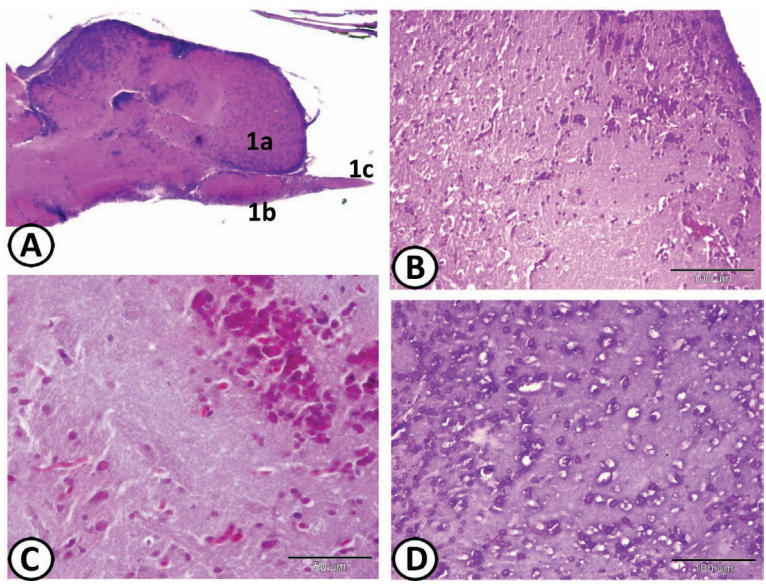

FIGURE 15.2 (A) Parasagittal section showing the anterior part of the telencephalon of guppy. One can recognize the cerebral hemisphere (1a), the olfactory lobe (1b) where sensitive nerve fibers of the olfactory nerve I end up. Fibers come from the smell receptors and join to form the olfactory tract (1c). (B) Higher magnification in cerebral hemisphere of guppy stained by HE. (C, D) Higher magnification in cerebral hemisphere of red-tail shark stained by HE and cresyl violet, respectively, showing neurons supported by neuropil.

Two main telencephalic divisions are present in teleosts, the area dorsalis telencephali displays large zones with a high degree of migration and lamination while the area ventralis telencephali is arranged into nuclei. In teleosts, the dopaminergic and substance P-immunoreactive cells have been identified in the telencephalon. In teleosts, the gustation reaches the telencephalon and diencephalon through a secondary gustatory nucleus, which is similar to the parabrachial nuclear region of mammals. In addition, there is a pattern of ascending sensory pathways to the telencephalon common to actinopterygians and tetrapods.

The forebrain in teleosts is quite aberrant and belongs to the everted type, absent in tetrapods: the dorsal and lateral parts of the hemispheres are rolled lateroventrally and thicken in two large masses containing the basal nuclei or corpus striatum and the epistriatum. The roof of the telencephalon in Osteichthyes is a very thin, composed of nonnervous vascular sheath of ependymal cells that lines the CNS. The cerebral hemispheres are in communication one with the other and form the "lateral ventricle." Unlike Osteichthyes, the roof of telencephalic (or cerebral) hemispheres in elasmobranchs are thick and constitute the pallium (complete cortex). The first and second lateral ventricles are in two separate ventricular lumens of the telencephalon and they open in the third ventricle via the foramina of MONRO.

15.1.1.2 THE DIENCEPHALON

The diencephalon (Figure 15.3) is an area that has the third ventricle and is situated between the optic lobes and the cerebral hemispheres. Sometimes called <<between brain>>. It is divided into the dorsal epithalamus, the thalamus, the hypothalamus ventrally and saccus dorsalis, or tela choroidia, which is located dorsorostraly to the diencephalon. The epithalamus is situated under the optic tectum (OT), containing the habenular ganglion and the pineal organ. It also contains the nerve endings from the telencephalon. The thalamus is present in the middle, located under the third ventricle between the hypothalamus and the tegmentum. It contains the center of autonomic functions. The hypothalamus represents the floor of the diencephalon, which is considered the main structural complex and formed from two inferior lobes and the infundibular region. The main function of the hypothalamus is to regulate the pituitary gland. The infundibular region appears as a pouch extends downward from the ventral part of the hypothalamus. The anterior portion of the hypothalamus includes the preoptic areas.

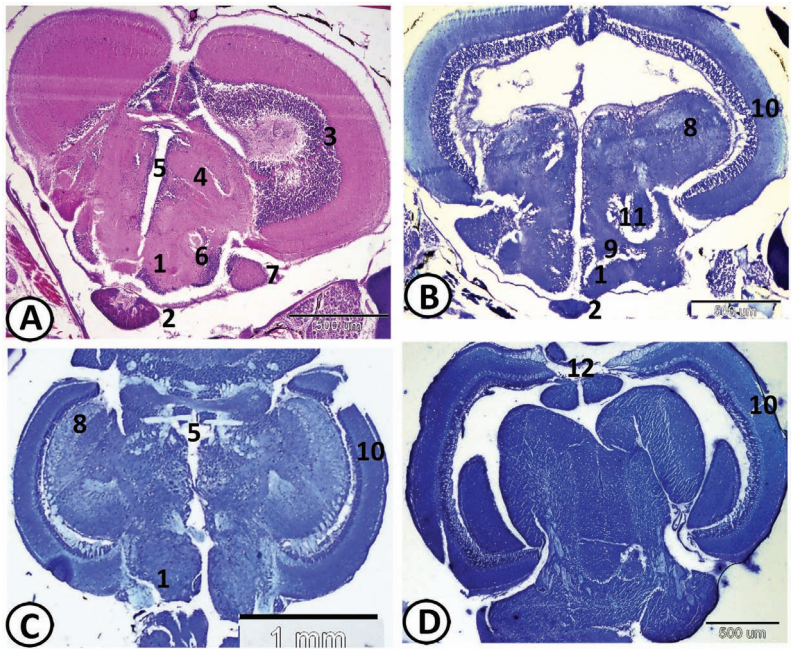

FIGURE 15.3 (A–D) Transverse section of the brain at the level of the diencephalon through the mesencephalon. The diencephalon attains its maximum development on the ventral side in the form of hypothalamus (1) and infundibulum. This latter is applied to the hypophysis [pituitary gland (2)] in the midventral line. (3) Valvula cerebelli; (4) tegmentum (with TS); (5) aquaeductus of Sylvius (ventral passage connecting the third and the fourth ventricles of the hindbrain); (6) preglomerular nucleus; (7) nucleus diffusus of the inferior lobe; (8) TS of the mesencephalon; (9) lateral recess of the inferior lobe; (10) tectum opticum; (11) nucleus glomerulosus or glomerular complex of the diencephalon; (12) torus longtudinalis. (A, B: brain section from molly stained with HE and TB, respectively; C, D: brain section from red-tail shark stained with TB).

The saccus vasculosus is situated between the two caudal parts of the inferior lobes of the hypothalamus, beneath the pituitary gland. This structure is richly vascularized, comparable to the choroid plexus of mammals. It consists of ribbons of cuboidal or columnar epithelium supported by a fibrovascular stroma with numerous capillaries (Figure 15.6). The saccus vasculosus produces the cerebrospinal fluid for the third ventricle lumen with which it is continuous. It is also suggested that it can detect water pressure.

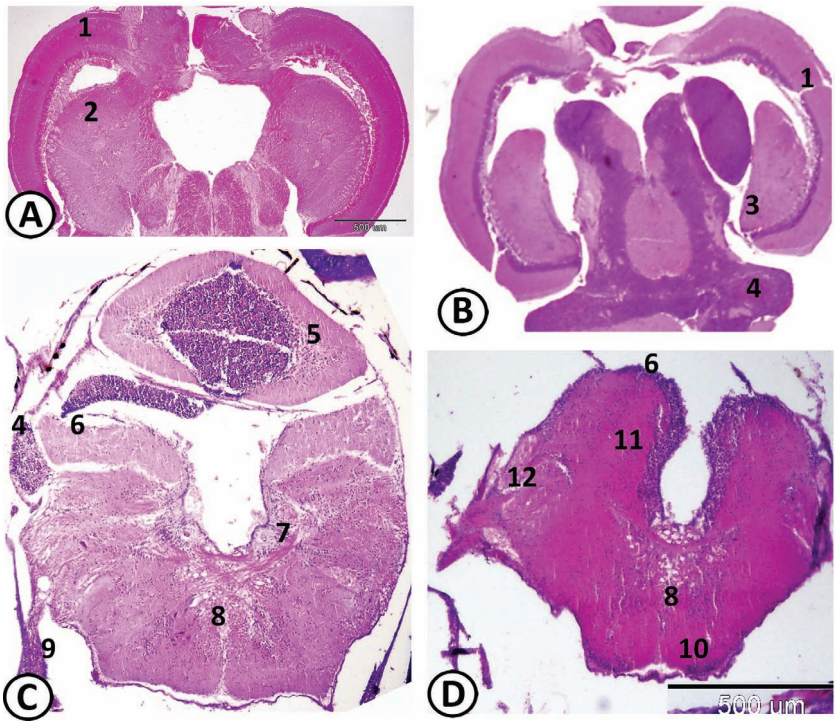

FIGURE 15.4 (A–D) Transverse section of the brain at the level of the mesoncephalon through the SC stained by HE. (1) Tectum opticum; (2) TS; (3) brachium conjunctivum; (4) eminentia granularis; (5) corpus cerebelli; (6) crista cerebellaris; (7) motor nucleus of the trigeminal nerve; (8) medial longitudinal fasciculus (MLF); (9) auditory/vestibular nerve complex; (10) reticular formation; (11) visceral sensory nucleus of the vagal nerve; (12) spinal sensory nucleus of the trigeminal nerve. (A, B: brain section from red-tail shark; C, D: brain section from molly).

15.1.1.3 THE MESENCEPHALON

In all fishes, the mesencephalon is large, comprises two optic lobes that are formed of ventral tegmentum and dorsal OT (Figures 15.3 and 15.4). In fish species that hunt by the sight such as cichlids and rainbow trout, the optic lobes are large. The bilateral lobes of the tectum are dorsally bridged by the tectal cavity (Figure 15.5). The tegmentum is dorsollaterally delimited by the tectum and the valvula cerebelli (VC), which extends into the mesencephalic ventricle dorsal to the tegmentum. The tegmentum, including the torus semicircularis (TS), lies at the caudal pole of the diencephalon and is

situated on the top of the inferior hypothalamic lobes. The TS is the main target of the octavolateral hindbrain. The octavolateral system is a collective name for three mechanosensory systems: the auditory, equilibrium, and lateral line systems that have similar receptor cells called the hair cells. It is connected to many other regions of the brain and participates in auditory and lateral line processing. The ventricle continues into the mesencephalon as a narrow cavity called the aqueductus mesencephali, or aqueduct of Sylvius.

The OT is the principal anatomical termination of the retinal ganglion cell axons. The development of this region reflects the degree of importance of the visual sense in different species. The OT is considered the most obvious part of the midbrain. It is divided grossly into two optic lobes and contains the tectal ventricle (TV). The OT has a characteristic laminar histological architecture that consists of six principal layers (Figure 15.5). These layers are unmyelinated versus myelinated axons. (1) Stratum opticum is the superficial layer that is supplied with optic nerve fibers. (2) Stratum fibrosum and stratum griseum superficiale: this layer is considered the most important center of the visual sense in the OT and contains nerve fibers and nerve cells. (3) Stratum griseum centrale contains the nerve cells of the efferent nerves. (4) Stratum album centrale contains the efferent nerve fibers and is connected with the thalamus and oculomotor nerve. (5) Stratum griseum periventriculare receives the nerve fibers of the periventricular system and composes of nerve cells. (6) Stratum fibrosum periventriculare contains numerous nerve fibers and faces the aqueductus mesencephalic. The stratum periventriculae is the most internal zone of the OT and clearly demarcated by the presence of granular cell bodies. Therefore, the cell layers of the OT can be divided into different functional layers. A periventricular ependymal layer forms the ventricular or internal boundary of the periventricular gray zone.

The OT in teleosts is a cortex exhibiting up to 15 laminae of neurons and neuropil, which receive multimodal input from many sources. These include the retina and additional visual centers such as the dorsal and ventral thalamus, the nucleus isthmi, and the pretectum, as well as nonvisual sources such as the TS or the central zone of area dorsalis of the telencephalon. The ventrolateral nucleus of the TS may act as the source of lateral line information to the tectum. In mormyrids and gymnotoids, the electrosensory information also reaches the tectum via the TS.

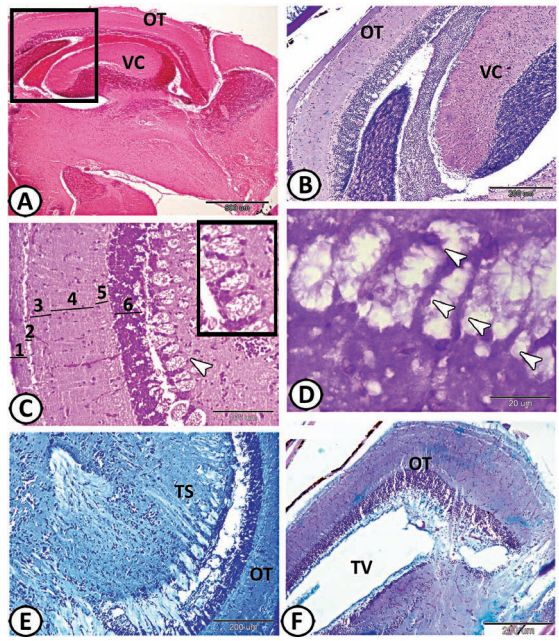

FIGURE 15.5 (A, B) Valvula cerbelli (VC) and optic tectum (OT) of red-tail shark stained by HE, PAS-AB/HX, respectively. (C) High magnification of OT of guppy stained by HE, which formed from (1) stratum opticum, (2) stratum fibrosum and stratum griseum superficiale, (3) stratum griseum centrale, (4) stratum album centrale, (5) stratum griseum periventriculare, (6) stratum fibrosum periventriculare: the arrowhead and inserted figure indicate the ependymal expansions of the diencephalon. (D) High magnification of the ependymal expansions (arrowheads) of red-tail shark stained by Cresyl violet. (E) A transverse section at the level of tegmentum with TS of red-tail shark stained with TB. Note the OT. (F) Section of the OT of guppy stained with AB/HX showing the tectal ventricle (TV).

The torus longitudinalis (TL) appears as a paired midline structure of the dorsal mesencephalon that protrudes into the ventricle in close proximity to the valvula cerebelli. It consists of two longitudinal parts that evaginate from the OT toward the mesencephalic ventricle. The TL exhibits small granular darkly stained cells (Figure 15.3D). Its cells are more diffusely distributed in the center than in the ventral and lateral periventricular zones, where they are tightly packed and adopt a laminar arrangement. Some medium-sized and lightly stained cells are also observed at the mediodorsal aspect of the TL. It has been supposed that the TL contains a center that plays a role in the integration between the sense of vision and the sense of equilibrium. Moreover, the connectivity of the TL indicates that it is the part of a multisynaptic pathway descending from the telencephalon to the brainstem.

15.1.1.4 THE METENCEPHALON (HINDBRAIN)

The metencephalon is particularly involved in swimming and balance. The CR is a single-lobed structure that is typically the biggest part of the brain. Hagfish and lampreys have relatively small cerebellae, while the mormyrid CR is massive and apparently involved in their electrical sense.

The CR is the main constituent of the dorsal metencephalon and composed of the cortex and medulla. In teleosts, it carries out the same function of sensorimotor coordination as it performs in other vertebrates through receiving the sensory inputs and transferring it toward the motor nuclei. The teleostean CR is well-developed and has three major divisions: the valvula cerebelli, the corpus cerebelli, and the vestibulolateral CR (comprising the eminentia granulares and caudal lobe). The vestibulolateral lobe and the corpus cerebelli may be homologous to the vestibular CR and corpus cerebelli, respectively, of mammals, but the valvula is present only in ray-finned fishes. Whereas the corpus cerebelli lies on top of the rostral rhombencephalon as in all vertebrates, the valvula projects forward under the tectum in the mesencephalic ventricular cavity.

In some species as goldfish, the valvula is subdivided into medial and lateral lobes. On the other hand, Mormyriformes show greatly enlarged lateral lobes of the valvula cerebelli that cover the brain laterally and dorsally. This later arrangement is named the mormyrocerebellum. Various parts of this huge CR are related to the input of the different kinds of electroreceptors. The vertebrate CR receives afferent input from two principal sources, mossy and climbing fibers. Similar to other vertebrates, the mossy fiber-like pathway in teleost fish originates from many sources such as the reticular formation (RF), the SC, and tegmentum.

The valvula and corpus cerebelli are intimately connected and may be involved in spatial orientation, proprioception, motor coordination, and eye movement. The central acoustic area forms as a granular area at the ventral cerebellar surface and varies in size with the development of the peripheral hearing apparatus.

The eminentia granulares are large and form distinct lobes lateral to the ventral 40% of the corpus CR. As the corpus CR forms a caudal lobe, it separates from the eminentia granulares (Figure 15.4). The eminentia granularis consists of the cell bodies of cerebellar granular cells that extend axons to course caudally in the crista cerebellaris, forming a type of molecular layer over the octavolateralis region. Typically, the eminentia granularis is

rostral and the crista is caudal. Inputs from the inner ear and lateral line fibers terminate at the eminentia granularis.

Superior cerebellar peduncle (brachium conjunctivum) is a paired structure of white matter that connects the CR to the midbrain. It consists mainly of efferent fibers, the cerebellothalamic tract. It also contains afferent tracts, most prominent of which is the ventral spinocerebellar tract.

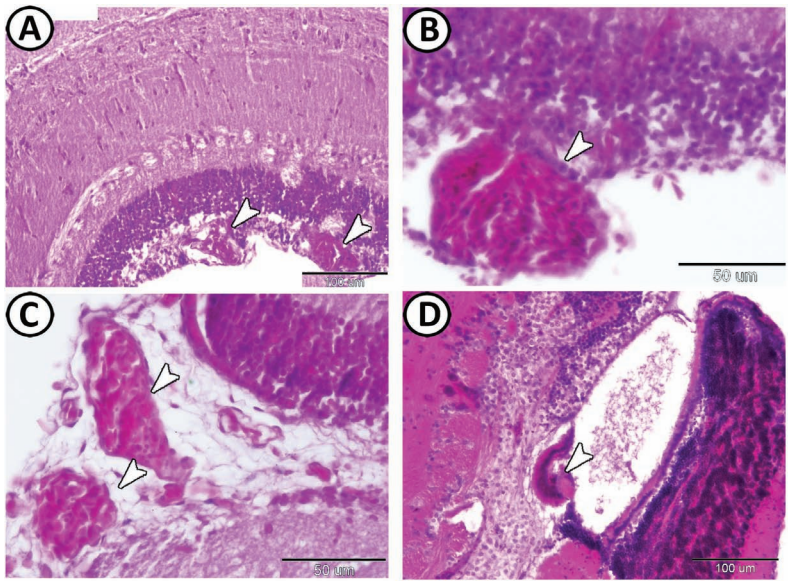

FIGURE 15.6 Saccus vasculosus. (A–C) Sacus vasculosus (arrowheads) of red-tail shark are vascular tufts located in the roof of the ventricles and extending from the tela choroidea. They consist of highly ramified vascular structures. These structures are covered by a simple or pseudostrafied columnar epithelium composed of specialized cells. (D) The saccus vasculosus lies caudal to the inferior lobes of the infundibulum and dorsal to the pituitary gland. It is an oval thin-walled folded sac with ribbons of cuboidal/columnar neural epithelium (arrowhead) supported by a highly and extensive vascular plexus bathing in connective tissue.

The cerebellar cortex consists of three layers (Figures 15.7–15.9): an outer molecular, intermediate ganglionic, and inner granular layer. The outer molecular layer possesses parallel fibers, eurydendroid cell (efferent neuron) dendrites, Purkinje cell dendrites, and stellate glia cells (small neurons). The parallel fibers run in the transverse plane, intersecting the sagitally arranged dendrites of eurydendroid and Purkinje cells. The ganglionic layer in fish is located beneath the molecular layer that similar to the mammalian Purkinje cell layer. In teleosts, this layer is named the "ganglionic" layer because

it exhibits the cell bodies of both Purkinje cells and eurydendroid cells. The somata of Purkinje cells are rounded or pear shaped. The most striking morphological feature of Purkinje cells is their characteristic palisade dendrites, which are orientated in the horizontal plane. In most cases, two thick primary dendrites arise from opposite poles of the soma and project in opposite directions. One or two additional thinner dendrites usually arise from the molecular side of the soma. The primary dendrites give off secondary branches, which are typically short, thick, and smooth. Several tertiary branchlets usually arise from each secondary branch and traverse vertically parallel to each other in the molecular layer to the apex of the ridges. The tertiary branches are typically thin and covered densely with spines. Some immunohistochemical studies using zebrin II to label Purkinje cells indicate that the zebrin II immunopositive fiber bundles and terminals project outside the CR and that these fibers originate from the Purkinje cells in the caudal corpus cerebelli and caudal lobe. Some biochemical markers have been used to label the teleost Purkinje cells: these include antibodies against parvalbumin, IP3 receptor type 1, M1, GluRδ2

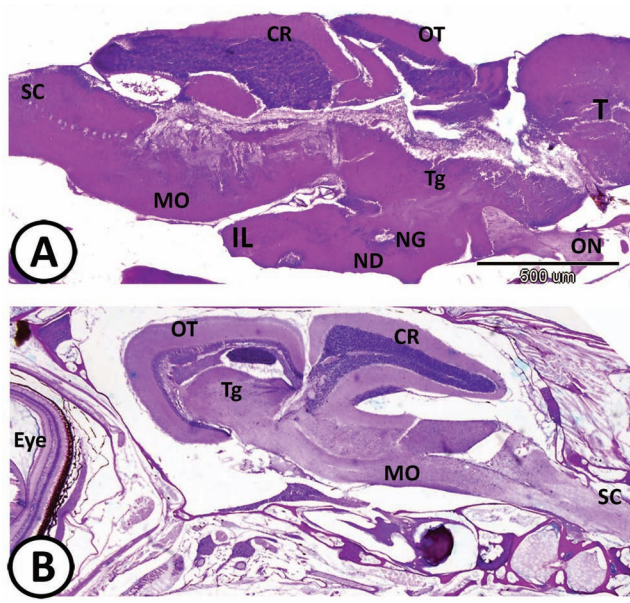

FIGURE 15.7 (A, B) Parasagittal section through the whole brain of guppy and red-tail shark, respectively, stained by HE. IL, inferior lobe of the diencephalon; ND, nucleus diffusus of the inferior lobe; NG, nucleus glomerulosus of the diencephalon; OT, tectum of the mesencephalon; Tg, tegmentum of the mesencephalon; T, telencephalon; MO, medulla oblongata; ON, optic nerve; CR, cerebellum; SC, spinal cord.

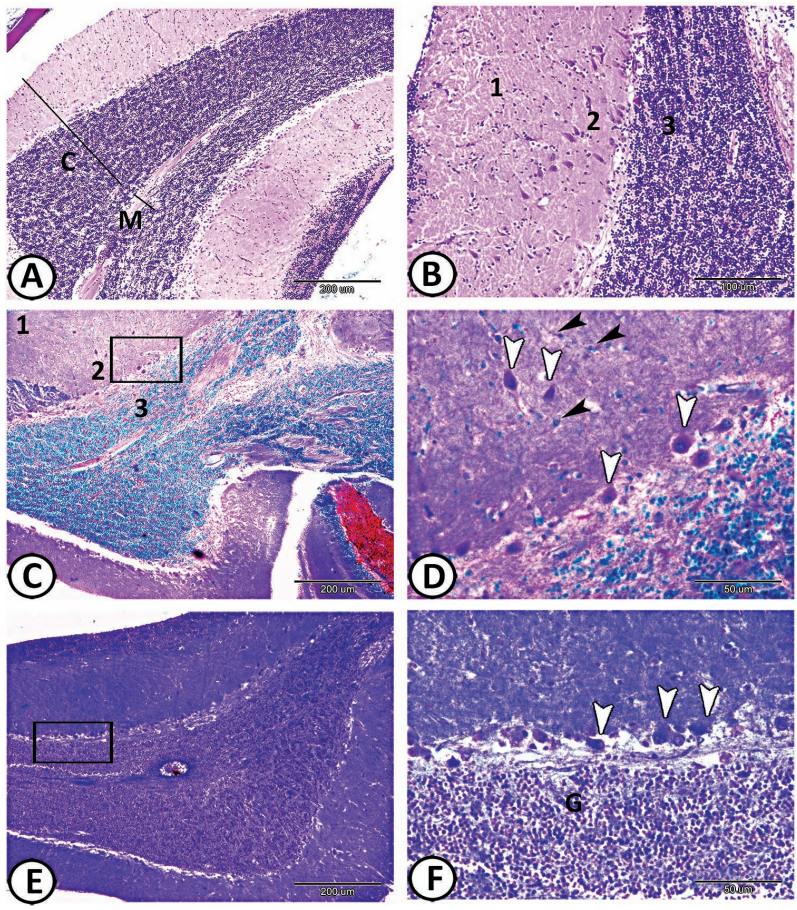

FIGURE 15.8 The CR of red-tail shark. (A, B) Section through the valvula cerebelli showing the cerebellar cortex (C) and cerebellar medulla (M). The cytoarchitectonic properties of the teleostean CR cortex are similar to other vertebrates. The valvula has a laminar organization and consists of the three characteristic layers: the molecular layer (1), the ganglionic layer (2), and the granular layer (3) (HE). (C) Section through the valvula cerebelli displays the molecular layer (1), ganglionic (2), and the granular layer (3) (Crossmon's trichrome). (D) Higher magnification in the boxed area in (C) showing the ganglionic layer contains Purkinje cells (white arrowheads) and numerous smaller cells. In contrast to the arrangement in most vertebrates, the Purkinje cells are placed less regularly between the molecular and granular layers. Purkinje cells are randomly scattered throughout the ganglionic layer and exhibit large rounded or pear-shaped cell bodies (somata). The nuclei surrounding the Purkinje cells are thought to be glial (satellite) cells (black arrowheads). (E, F) A section at the level of the ganglionic layer of the valvula cerebelli. A characteristic cell of this layer is the Purkinje cell (white arrowheads). The small rounded nuclei are those of the neurons (granular cells and Golgi cells) of the granular layer (G) (Mallory trichrome).

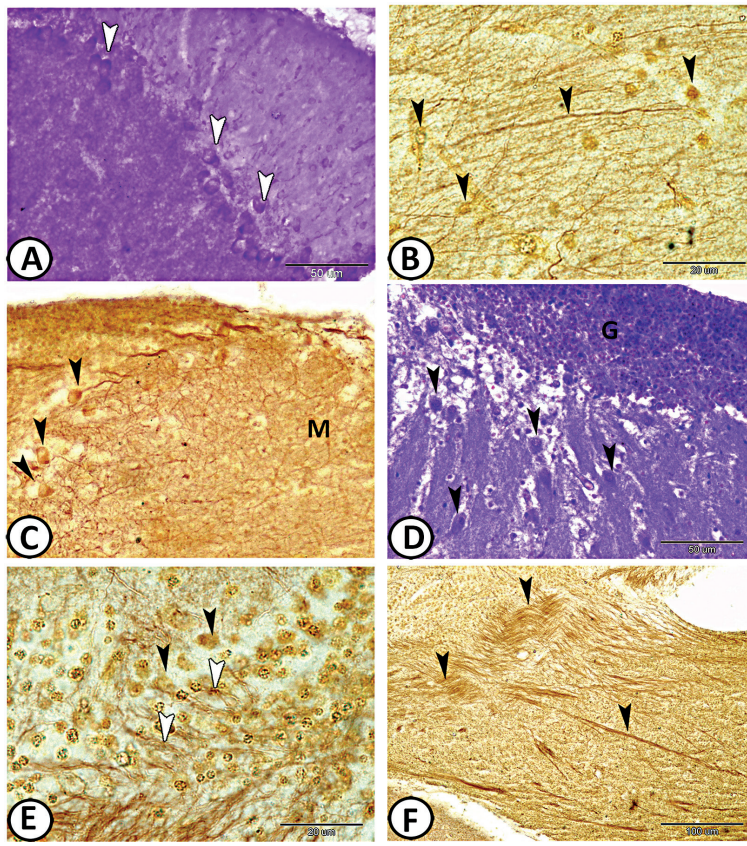

FIGURE 15.9 Cerebellum. (A) A longitudinal section of the CR of guppy stained by cresyl violet shows the positive-stained Purkinje cells (arrowheads). (B) The molecular layer of red-tail shark stained by silver stain showing the neuropil and their dendrites (arrowheads). (C) The dendrites of Purkinje fibers (arrowheads) in red-tail shark ascend through the molecular layer (M) toward the external surface (silver stain). (D) Purkinje fibers (arrowheads) at different levels in red-tail shark stained with Mallory trichrome. G indicates the granular layer. (E) Purkinje cells (black arrowheads) extend processes (white arrowheads) between the granular and molecular layers in red-tail shark (silver stain). (F) Neurofibrils and dendrites of many neurons (arrowheads) in the medulla of CR of red-tail shark stained by silver stain.

Eurydendroid cells of the ganglionic layer of the CR are efferent neurons, which are somewhat larger than the Purkinje cells. Like Purkinje cells, the eurydendroid cells have an extensive dendritic arbor along the parasagittal dimension with their spread within the molecular layer being larger than that of Purkinje cells. The cell bodies of these neurons have spindle-shaped and extend their primary dendrites broadly along the margin of the granule

cell layer and branch outward turning perpendicularly into the molecular layer. Other neurons have pyramidal, fusiform, or multipolar cell bodies. The teleost fish lack deep cerebellar nuclei. However, the eurydendroid cells directly innervate similar targets in the brain stem and SC as the deep cerebellar nuclei of other vertebrates and may thus have an equivalent function. The granular layer is situated beneath the ganglionic layer and contains densely packed small multipolar neurons called the granule cells.

Astrocytes in all cortical layers express the glial fibrillary acidic protein (GFAP) (Figure 15.10). GFAP is an intermediate filament protein that mainly expresses in astrocytes. GFAP is important for the integrity of CNS white matter architecture and maintenance of myelination.

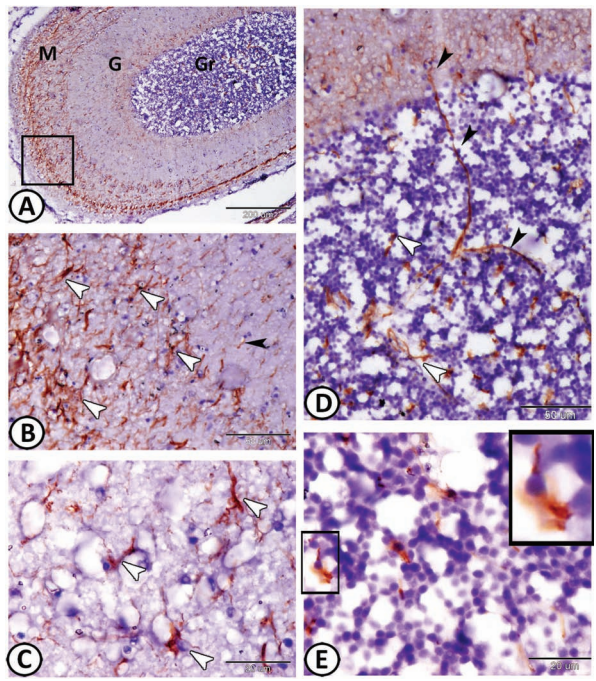

FIGURE 15.10 GFAP expression in the CR of molly. (A) GFAP express in the molecular (M), Ganglionic (G), and granular layer (Gr) of the cerebellar cortex. (B, C) Higher magnification of the boxed area in (A) shows that the molecular layer constitutes a continuous sheet of astrocytes containing a huge amount of oriented dendrites (white arrowheads). Note the array arrangement of the dendrites of astrocytes of the ganglionic cells (black arrowhead). (D) Numerous of astrocytes (white arrowheads) could be seen in the granular layer. Note the long axons of astrocytes (black arrowheads) that extend from the ganglionic layer to the granular one. (E) High magnification in the granular layer showing typical astrocytes (boxed area) with positive immunostained dendrites.

15.1.1.5 THE MYELENCEPHALON (BRAIN STEM)

The myelencephalon is the brain's posterior. The brain stem houses primary representation centers for all somatosensory faculties except olfaction and vision. As well as controlling some muscles and body organs, in bony fish at least, the brain stem governs respiration and osmoregulation.

The MO is the major part of myelencephalon that contains the fourth ventricle. The MO connects the CR to the diencephalon and continues caudally with the SC. Its major body is composed of neuropil, which contains the processes of neuroglial and other neuronal cells. The somata of Nissl's bodies are big triangular basophilic cells (Figure 15.11).

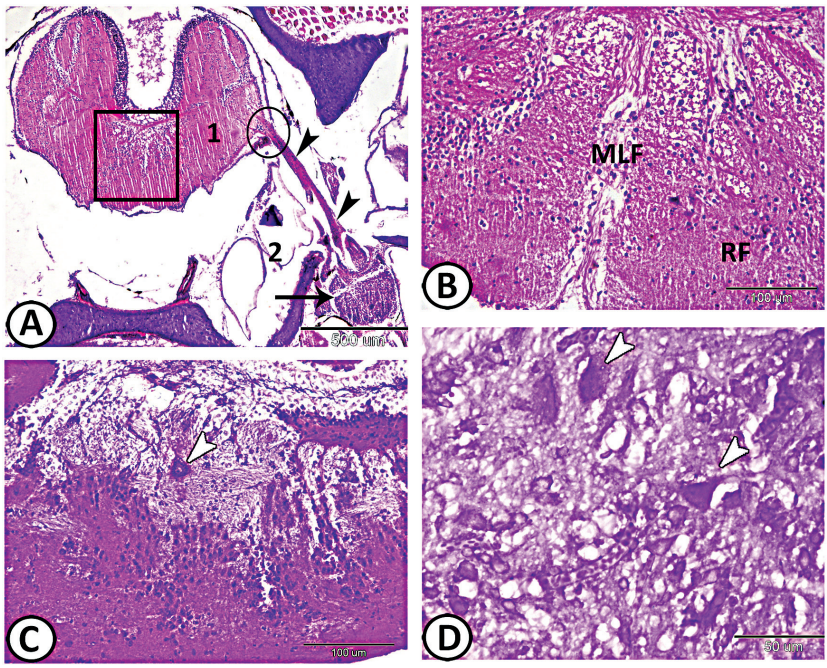

FIGURE 15.11 Medulla oblongata (MO). (A) Transverse section at the level of the MO of molly stained with HE. This micrograph illustrates the connection between the myelencephalon (1) and the inner ear (2) via the eighth cranial nerve (vestibulocochlear or statoacoustic—arrowheads). The vestibulocochlear nerve contains sensory fibers coming from various parts of the inner ear (ampullae, sacculus, utriculus). They are formed by true ganglion cells (arrow) situated close to the sensory structures and enter the MO at a dorsal position (circle). (B) Higher magnification of the boxed area in (A) showing medial longitudinal fasciculus (MLF) and reticular formation (RF). (C, D) Longitudinal section through the MO of the guppy and red-tail shark brain stained by HE and cresyl violet, respectively, showing large Mauthner neurons (arrowheads).

The MO contains the nuclei of some cranial nerves (V–X) and considered as is the site of origin of the Mauthnerian system. This system is a neuromuscular specialization, which is well-developed in teleosts. Mauthner cells have been demonstrated as command neurons. A command neuron is a special type of neuron capable of driving a specific behavior all by itself. It includes a pair of very large neuronal bodies located centrally in the medulla. Each Mauthner cell is provided by an axon that crosses over, innervating neurons at the same level of the brain and then traveling down via the SC, establishing multiple connections as it goes. Moreover, the synapses created by a Mauthner cell are so powerful that a single action potential gives rise to a great behavioral response. This response occurs within milliseconds; the fish curves its body into a C-shape, then straightens, thereby propelling itself rapidly forward. Functionally, this is a fast escape response, triggered easily by a powerful sound wave or pressure wave impinging on the lateral line organ of the fish. Moreover, the information from the lateral line system may be transmitted to the posterior part of the SC by the long axons of these cells. At the level of the brainstem junction with the SC, the spinal sensory nuclei are moderately sized. Subependymal expansions are prominent and form a septum below the central canal.

In addition to several ascending and descending fibers systems, the brain stem houses the RF, a ventrally located system for basic maintenance and life support. The RF constitutes a most complex neuronal network extending throughout the MO and into the tegmentum. The rhombencephalic RF can be divided into three longitudinal columns: a lateral, medial, and a (median) midline column. Some additional medullary structures may be considered part of the rhombencephalic RF, such as the Mauthner cell. As in all vertebrates, the locus coeruleus involves noradrenergic neurons projecting to most brain regions, including the telencephalon. Some well-defined tegmental nuclei may be considered part of the RF, such as the cerebellar-projecting perilemniscal nucleus, the spinal-projecting nucleus of the lateral lemniscus, and the nucleus ruber. The later projects to the SC and receives contralateral cerebellar input in cyprinids.

15.1.2 THE SPINAL CORD

The SC extends backward the length of the fish, from the MO, inside the neural canal of the vertebral column. In highly advanced teleosts, it ends in an endocrine gland, the urophysis.

In the SC (Figures 15.12, and 15.13), the gray substance shows a marked difference in arrangement from that of higher vertebrates in that the dorsal horns lie so close together that there is hardly any white substance between them. This gives the gray substance the shape of an inverted Y. Surrounding the gray matter is the white matter, which consists of myelinated nerve fibers. The central canal is situated in the center of the gray matter, filled with spinal fluid and lined with ciliated ependymal cells. This canal represents an extension of the ventricles. The gray matter is divided into lateral, anterior, and posterior columns, which serve as the entry or exit sites for the spinal nerve fibers. The anterior (or ventral) roots leave from the anterior columns to innervate somatic muscles or visceral organs.

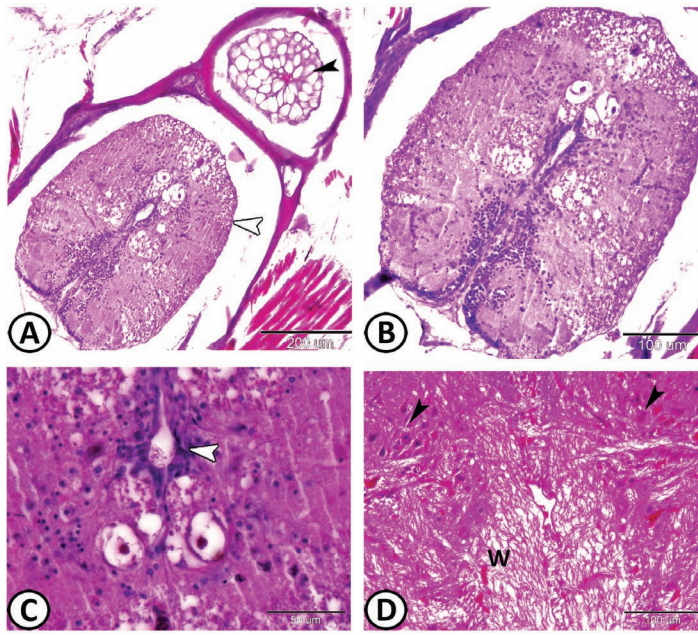

FIGURE 15.12 Transverse section of the SC. (A, B) The SC (white arrowhead) is enclosed by vertebrae that contain the notochord (black arrowhead) in molly stained by HE. (C) Higher magnification in the gray matter is mainly composed of somata of neurons, dendrites, and glial cells. The arrowhead points to the central canal. (D) Cross section through the SC of red-tail shark stained by HE, the spinal gray substance (arrowheads) shows a marked difference in arrangement from that of higher vertebrates in that the dorsal horns lie close together. This gives the gray substance the shape of an inverted Y. The white matter (W) contains numerous nerve fibers like axons, which appear as dark dots. The myelin sheath surrounding the majority of axons is composed of lipoprotein plasma membrane and is often partially dissolved by the hydrophobic solvents used during the protocol.

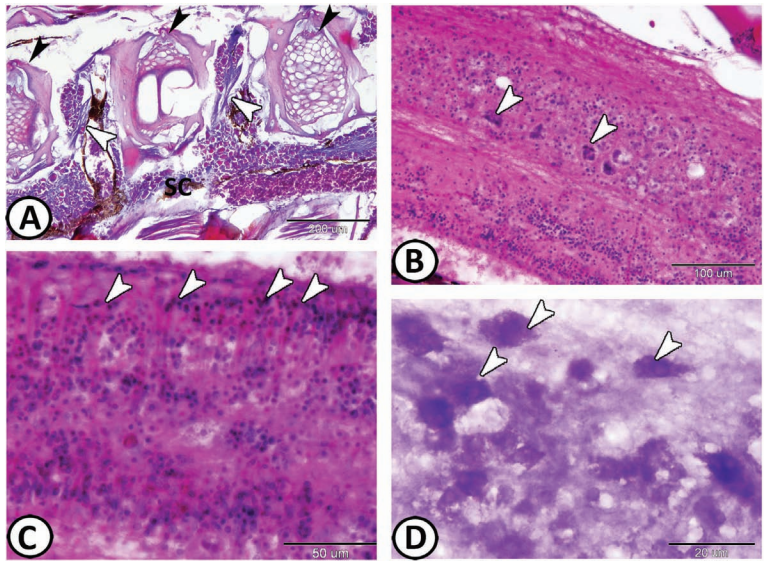

FIGURE 15.13 Longitudinal sections through the SC. (A) Two spinal ganglia (white arrowheads) lying along the vertebral column of guppy stained with Masson's trichrome. The bony vertebra (black arrowheads) bears processes (hemal arches) that protect the SC. The center of the vertebra surrounds the remains of the notochord. (B, C) The SC of molly stained by HE showing the distribution of the neurons (arrowheads). (D) High magnification of the Nissl's cells (arrowheads) of the SC of guppy stained by cresyl violet.

In fishes, two major groups of cells may be identified in the gray matter of the SC. The cells of the first group are located mostly in the dorsal region, and their function is to control the movements of the trunk musculature. The cells of the other group are situated in the ventral region of the gray matter and control the movements of fins. The spinal nerve fibers have two roots: the anterior motor root and the posterior sensory root with its ganglion.

The neurons and neuroglia are the main cellular elements of SC. The fish neurons are similar to those of mammals and possess an extensive Golgi apparatus, numerous Nissl granules (rough endoplasmic reticulum) in their cytoplasm, and a large nucleus, as well as contain dendrites and axons. The central neuroglial cells recognized in teleosts include oligodendroglia, ependymocytes, and astrocytes. Astrocytes in the SC appear like arrays and express GFAP (Figure 15.14). Teleost ependymal cells contain cilia, numerous glycogen granules, and a large number of huge mitochondria indicating a specialized metabolic activity.

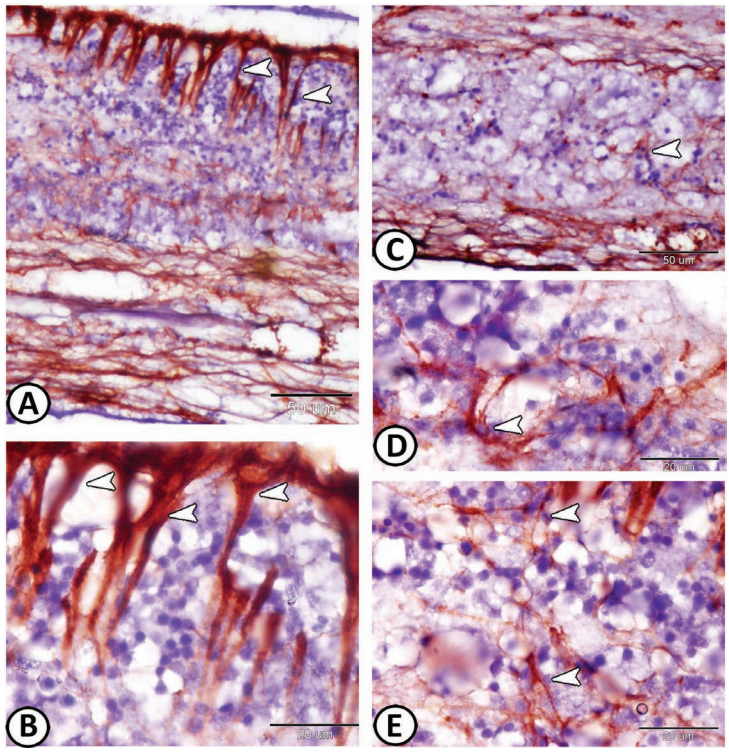

FIGURE 15.14 GFAP expression in the SC of molly (A–E) astrocytes (arrowheads) along the length of the SC express GFAP.

15.2 THE PERIPHERAL NERVOUS SYSTEM

The PNS originates from the neural crest consists of ganglia (Figures 15.15 and 15.16) and nerves (Figure 15.17). It composes mainly of groups of nerve fibers penetrating every region of the body along which the sensory impulses are brought into the SC and brain by afferent pathways, and through which causing efferent impulses to pass outwards to affect tegumental or muscular structures.

Teleosts are unique among the vertebrae in that the sympathetic ganglia occur in the cranium and the postganglionic sympathetic fibers connect with the outflow of trigeminal, facial, glossopharyngeal and vagus nerves, and innervate various effector cells in the branchial tissues, heart, and stomach. The cranial sympathetic ganglia receive the preganglionic inputs essentially from the cranial and spinal nerves.

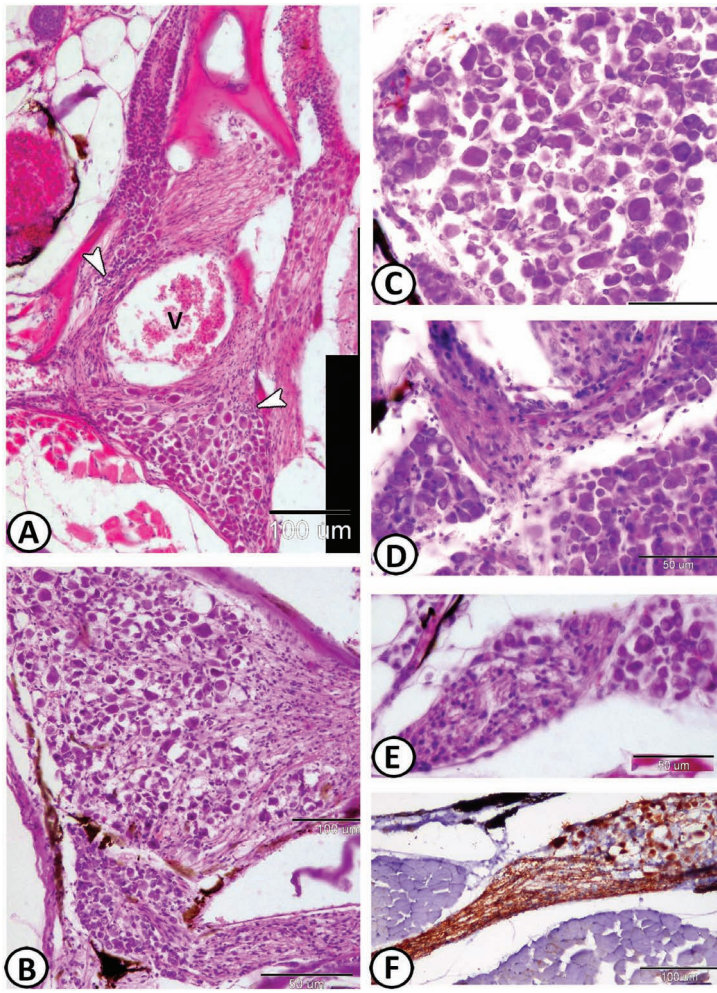

FIGURE 15.15 Sympathetic ganglia stained by HE. (A) Sympathetic ganglia in guppy near the operculum formed of large clusters of neurons (arrowheads). V indicates a vein. (B) A large cluster of neuronal cell bodies in the head of molly. Ganglia of the autonomic nervous system exhibit cell bodies more widely spaced than in spinal ganglia because of the presence of numerous neurites (axons and dendrites) in between. (C, D) Sympathetic ganglia in molly. The ganglion cells are large neurons and possess a large round euchromatic nucleus tending to be eccentrically located in the cytoplasm. They are associated with flattened glial cells (satellite cells) quite irregularly placed due to the neuronal processes. (E) Sympathetic ganglia in guppy associated with chromaffin tissue. The micrograph shows a cluster of nerve cell bodies with a large round nucleus. The ganglion cells are separated by numerous neurites. (F) The nerve cells and nerve fibers of a sympathetic ganglion between the muscles of molly express GFAP.

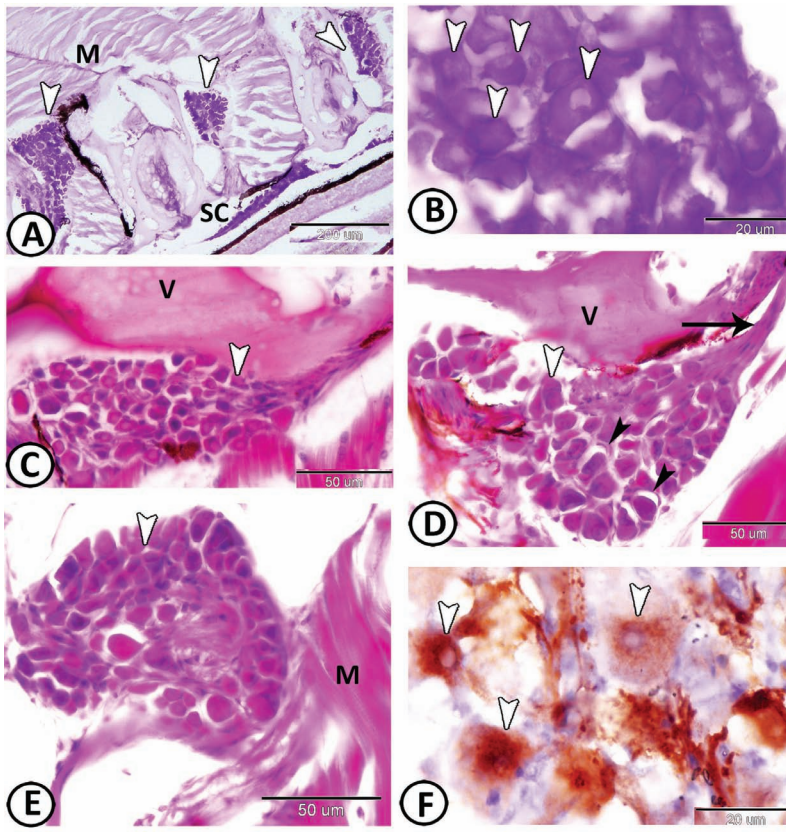

FIGURE 15.16 Spinal ganglia. (A) Spinal ganglia (arrowheads) of guppy stained with cresyl violet extending from the SC. Note the trunk skeletal muscles (M). (B) High magnification of the nerve fibers (arrowheads) in ganglia of molly stained with cresyl violet. (C–E) Spinal ganglia (arrowheads) of guppy extending between the vertebrae (V) and muscles (M) stained with HE. The cell bodies of the neurons (white arrowheads) are close together and surrounded by small nuclei (black arrowheads) of the flattened satellite cells. Some nerve fibers are cut longitudinally (arrow). (F) The nerve cells (arrowheads) of the ganglia express GFAP.

Spinal ganglia appear as swellings in the posterior nerve roots of the spinal nerves. These ganglia are situated close to the SC and compose of cell bodies of sensory neurons. The ganglion is ensheathed by a capsule of dense connective tissue that branches into trabeculae to give a framework for the neurons. Microscopically, the neurons of spinal ganglia are characterized by large sizes, as well as their cell bodies are so close together and enclosed by small nuclei of the flattened supporting satellite cells.

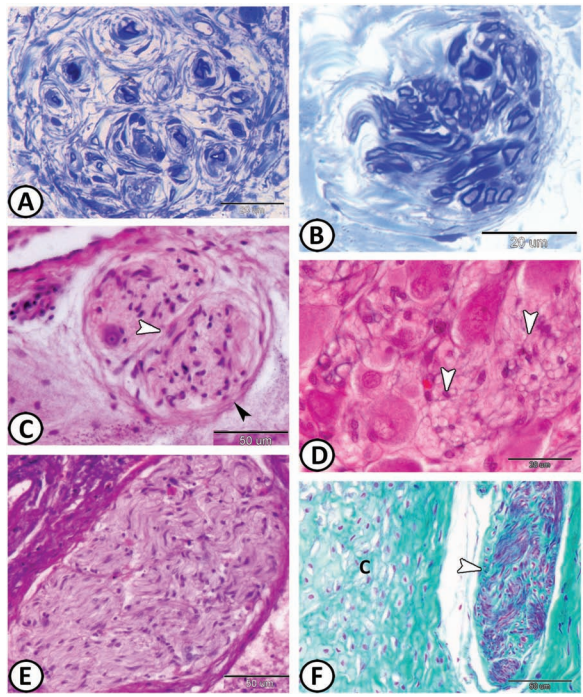

FIGURE 15.17 Nerve fibers. (A, B) Semithin transverse section through the nerve fascicles in the dermis of the lower and upper lip of silver carp, respectively, stained with TB. (C) Transverse section through the nerve fibers that ensheathed with epineurium (black arrowhead) in the lamina propria of the tongue of grass carp (stained with HE). Each bundle is surrounded by collagenous connective tissue called perineurium (white arrowhead). (D) Cross section of the nerve fibers (arrowheads) in a sympathetic ganglion in the ovary of Nile tilapia stained by HE. (E) Longitudinal section through nerve fascicles in the adventitia of oesophagus of grass carp stained by HE. Most of the dark elongated nuclei seen within the fascicles are those of Schwann cells. Note the wavy appearance of the fibers. (F) Longitudinal section through nerve fascicles (arrowhead) in neighboring to opercular cartilage (C) of silver carp stained by Crossmon's trichrome.

Myelinated axons in both longitudinal and cross and sections can be demonstrated within the ganglion. Moreover, the blood vessels are observed throughout the ganglion. Groups of parasympathetic ganglion cells (Auerbach's or myenteric plexus) are observed between the tunica muscularis of the intestine. Fluorescence histochemical techniques revealed that in teleosts, the neurons in the sympathetic ganglia are mostly aminergic and some are cholinergic.

In the head of fish, there is a special series of 10 pairs of cranial nerves. Many pairs of spinal nerves, which are all mixed, emerge from the SC

between the vertebrae. Each nerve possesses two roots (sensory neurons in the dorsal root and motor neurons in the ventral one) that emerge to form a mixed spinal nerve after leaving the SC.

A large nerve (Figure 15.18) consists of cylindrical bundles (fasciculi) of nerve fibers. The axons are enclosed by one or two satellite sheath, the Schwann cell. Each nerve is covered on the outside by a sheath of dense connective tissue, the epineurium. The perineurium is found below this layer, which constitutes a complete sleeve around a bundle of axons. The perineurial septa extend into the nerve and subdivide it into many bundles of fibers. The endoneurium is a very delicate areolar tissue that surrounds each nerve fiber. A nerve is supplied by intra- and inter-fascicular blood vessels. Generally, the nerves do not harbor the perikarya of neurons, except for certain highly specialized cranial nerves, nerves contain both motor and sensory fibers (mixed nerves).

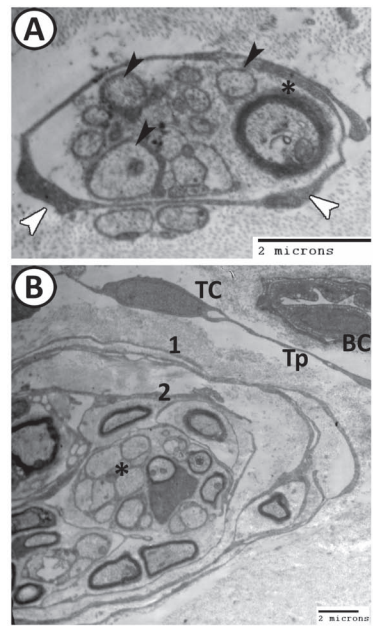

FIGURE 15.18 The fine structure of the nerve fibers in the dermis of the upper lip of silver carp. (A) Bundles of myelinated nerve fibers are observed in the dermis. The axons are enveloped by one or two satellite sheath, the Schwann cell (white arrowheads). The axons (black arrowheads) are surrounded by a multilamellar structure of myelin (asterisk). (B) Each nerve is covered on the outside by a dense sheath of connective tissue, the epineurium (1). Beneath this layer is perineurium (2). Surrounding each fiber is the endoneurium (asterisk). Note the telocyte (TC) with its telopodes (Tp) and blood capillary (BC) are associated with the nerve fibers.

Each individual axon of the peripheral nerves is either encircled by the myelin sheath formed by Schwann cells (myelinated fibers) or surrounded by the Schwann cells' cytoplasm (unmyelinated fibers). The differentiation of these nerve fibers is not always easily identified at the light microscope level. The myelin sheath appears as a multilamellar structure of multiple layers of dense lines separated by lucent zones. The myelin is formed of successive layers of the cell membrane of Schwann cells, which constitute a lipid-rich sheath around the axon. The nerve fibers appear pale pink with hematoxylin/eosin stain. In the longitudinal section, the peripheral nerves are characterized by the apparent wavy course of the axons (Figure 15.17E and F).

KEYWORDS

- **brain**
- **spinal cord**
- **GFAP**
- **cerebellum**
- **nerve fibers**

BIBLIOGRAPHY

Butler, A.B., Northcutt, R.G. The diencephalon of the pacific herring, *Clupea harengus*: cytoarchitectonic analysis. *J. Comp. Neurol.* **1993**, 328(4), 527.

Eastman, J.T., Lannoo, M.J. Anatomy and histology of the brain and sense organs of the Antarctic eel cod *Muraenolepis microps* (Gadiformes; Muraenolepididae). *J Morphol*. **2001,** 250(1), 34–50.

Eastman, J.T., Lannoo, M.J. Anatomy and histology of the brain and sense organs of the antarctic plunderfish *Dolloidraco longedorsalis* (Perciformes: Notothenioidei: Artedidraconidae), with comments on the brain morphology of other artedidraconids and closely related harpagiferids. *J. Morphol.* **2003,** 255(3), 358.

Eastman, J.T., Lannoo, M.J. Brain and sense organ anatomy and histology of the Falkland Islands mullet, *Eleginops maclovinus* (Eleginopidae), the sister group of the Antarctic notothenioid fishes (Perciformes: Notothenioidei). *J. Morphol.* **2008,** 269(1), 84.

Ikenaga, T., Yoshida, M., Uematsu, K. Cerebellar efferent neurons in teleost fish. *Cerebellum* **2006,** 5, 268–274.

Ito, H., Yamamoto, N. Non-laminar cerebral cortex in teleost fishes. *Biol. Lett.* **2009,** 5(1), 117–121.

Redzic, Z.B., Preston, J.E., Duncan, J.A., Chodobski, A., Szmydynger-Chodobska, J. The choroid plexus-cerebrospinal fluid system: from development to aging. *Curr. Top. Dev. Biol.* **2005,** 71(71), 1–52.

Rupp, B., Northcutt, R.G. The diencephalon and pretectum of the white sturgeon (*Acipenser transmontanus*): a cytoarchitectonic study. *Brain Behav. Evol.* **1998**, 51(5), 239–262.

CHAPTER 16

Sensory System

ABSTRACT

Teleosts have various sense organs like an elaborate lateral line system, olfactory organs, taste buds, eyes, and membranous labyrinth (inner ear). The inner ear of teleosts is composed of the upper labyrinth containing three semicircular canals and three otolith organs: the utriculus, the sacculus, and the lagena. Each semicircular canal bears an enlargement at one of its ends named ampulla that house sensory structure, the cristae ampullaris. A lateral line system is a group of neuromasts located superficially on the skin or just under it in fluid-filled canals in all fishes. Canals of the lateral line system are filled with fluid, which transmits vibrations to the neuromasts through the skin pores. There are two types of neuromasts; free and canal neuromasts. The olfactory rosette of most teleosts consists of several olfactory lamellae radiating from a median raphe. Each lamella consists of two layers of epithelium separated by connective tissue core. The olfactory epithelium is composed of both sensory and nonsensory areas. The sensory epithelium composed of ciliated, microvillous olfactory receptor cells (ORCs), rodlet and crypt cells. The organization of the fish eye has the same general structure found in higher vertebrates. The retinal tunic is composed of 10 distinct layers.

Teleosts possess highly developed sensory organs. Nearly all daylight fish have a color vision at least as good as normal humans. Many fish also have chemoreceptors responsible for the acute senses of taste and smell. Most fish have sensitive receptors that form the lateral line system, which detects gentle currents and vibrations and senses the motion of nearby fish and prey. Fish can sense sounds in a variety of ways, using the lateral line, the swim bladder, and in some species the Weberian apparatus.

16.1 AUDITORY SYSTEM

16.1.1 INNER EAR

The inner ear of teleosts is typical of that of other vertebrates. It is composed of the upper labyrinth (pars superior) containing three semicircular canals (oriented in one horizontal and two vertical perpendicular planes) and three otolith chambers or otolith organs: the utriculus, the sacculus, and the lagena (Figure 16.1). Each semicircular canal is lined with simple squamous epithelium and bears an enlargement at one of its ends named ampulla, which houses a sensory structure, the cristae ampullaris (Figure 16.2).

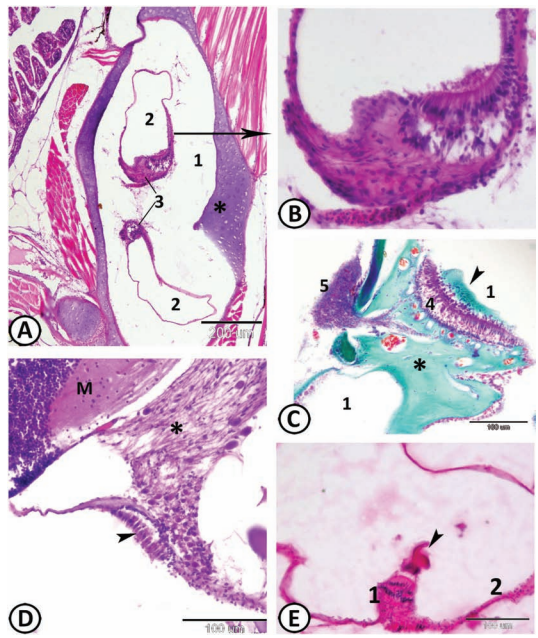

FIGURE 16.1 (A–C) Transverse sections through the ventral part of the labyrinth of guppy (A and B) and red-tail shark (C) stained with HE and Crossmon's trichrome respectively showing the lagena (1) and the sacculus (2) with their respective sensory maculae, macula sacculi (3), and the macula lagenae (4). Note the supplying auditory nerve III (5). The macula lagenae is covered by the asteriscus (arrowhead). Asterisks indicate the cartilage. **(**D**)** In nonostariophysian fishes like guppy, the sensory macula (arrowhead) attached to a ganglion (asterisk). Note the myelencephalon (M). (E) A transverse section through an otolith chamber of Molly stained with HE. The arrowhead indicates the otolith overlying the sensory epithelium (*macula*-1). The otolith chambers are lined with squamous epithelium (2) and filled with endolymph. The present otolith could be the asteriscus, which is small and shaped like a flattened hemisphere in nonostariophysan fishes.

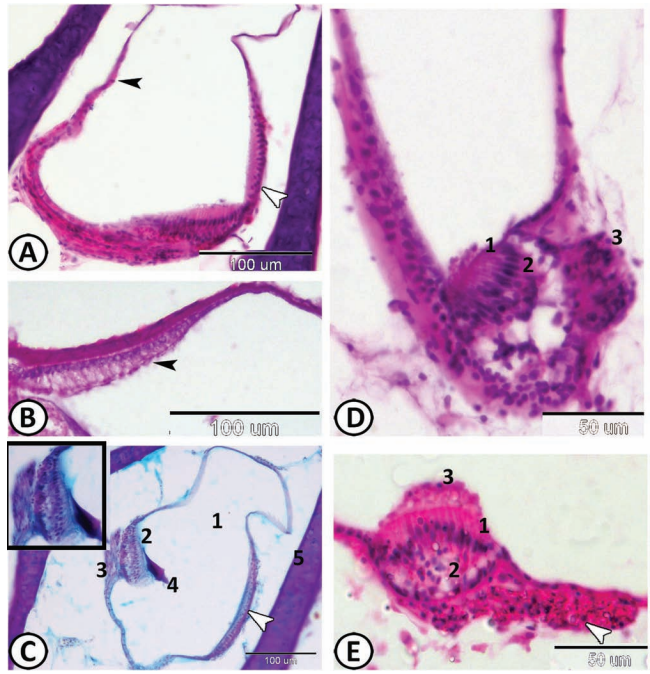

FIGURE 16.2 (A) Otolith chambers (lower labyrinth) of guppy are lined with squamous epithelium (black arrowhead). The parts of the lower labyrinth (pars inferior) each contain a sensory macula (white arrowhead) (HE). (B) Lower labyrinth wall of Molly bearing an oval sensory macula consisting of sensory hair cells and SCs. The hair bundle on the apical surface of the hair cells is indicated by an arrowhead. (C) The semicircular canal of guppy has at one end an ampullar dilatation (here the ampulla of the horizontal canal (1). Each ampulla contains a sensory area, usually elevated called the crista ampullaris (2). Each crista ampullaris is an elongated epithelium situated on a ridge of supporting tissue (3) rising from the wall of the ampulla. From this sensory organ rises a gelatinous cupula (4). The arrowhead indicates the macula of the utriculus. Hyaline cartilage (5) surrounds the semicircular canal (AB-periodic acid–Schiff [PAS]/HX). (D) Section through a semicircular canal in the inner ear of the guppy stained with HE. This photomicrograph shows the main components of the crista ampullaris. It is covered by neuroepithelium, with hair cells (1) and supporting cells (2). Fibers (3) from the eighth nerve are also seen. (E) Crista ampullaris in the ampulla of a semicircular canal of guppy stained with HE. The elongated ciliated sensory cells (neurons) are obvious (1) and are supported by sustentacular cells (2). Note the cupula (3) and the underlying connective tissue (arrowhead).

Otoliths are calcified structures of ectodermal origin and mainly composed of calcium carbonate, keratin-like proteins, and mucopolysaccharides. The center of the otolith is rather opaque and is surrounded by concentric rings (annuli). These rings are composed of alternating translucent and opaque

zones, which form thin lamellae. Otolith formation involves rhythmical variations in the deposition and size of organic matrix fibers and aragonite crystals, resulting in the formation of zonations. By measuring the thickness of individual rings, it is thus possible to obtain information on the age (daily and annual increments) of some teleost fishes by using a microscope.

Each otolith chamber has its own otolith: the lapillus (otolith of the utriculus), the sagitta (otolith of the sacculus), and the asteriscus (otolith of the lagena). These otoliths (Figure 16.1) lie close to a sensory epithelium, named the macula. Like the semicircular canals, the otolithic sacs are filled with endolymph. Maculae are large flattened areas of sensory epithelium lying on the ventral surface of the chambers. Maculae (Figure 16.2) are patch-like collections of sensory hair cells and supporting cells (SCs) and are supplied with VIII cranial nerve (acoustic nerve) terminals. Adjacent to and lying over the sensory epithelium is the tectorial membrane, which can mediate stimuli to the sensory hairs by vibration. This type of sensory apparatus of the ear is known as the organ of Corti. The maculae respond to sound, gravity, and linear accelerations of the fish body. Linear accelerations are detected by bending of the sensory hair cells, which then become depolarized and send action potentials via nerve VIII to the brain.

Fishes show an amazing diversity in hearing abilities, inner ear structures, and otolith morphology. There are many aspects of the structures of the fish ear that vary between fish groups. Among these variations are the size and shape of the semicircular canals and the otolith chambers. There is interspecific and intraspecific otolith variability (mainly the *sagitta* and the *asteriscus*) and the distribution of different types of sensory hair cells can also vary.

Fishes, in general, lack the various accessory devices by which in higher vertebrates sound waves reach the inner ear. However, the conduction of vibrations through the head skeleton to the inner ear can produce some degree of hearing (lateral line sensations are also closely allied to hearing). In most fishes, the water vibrations, to be perceived, must set up head vibrations, and these, in turn, produce endolymphatic vibrations, which can be picked up by the hair cells of the inner ear. Some bony fishes, however, have accessory structures, which parallel in a way the "hearing aids" found in tetrapods, although evolved quite independently. In these fishes, the gas bladder is utilized as a device for the reception of vibrations. In herring-like teleosts, this gas bladder sends forward a tubular extension, which comes to lie alongside part of either membranous labyrinth and thus can induce vibrations in the endolymph.

Neural processes of the four most anterior vertebrae are detached and develop independently to form the Weberian ossicles. These articulate in series to form a rigid connection between the anterior chamber of the gas bladder and the pars inferior (sacculus–lagena complex) of the statoacoustic organ. The Weberian apparatus is similar to the chain of auditory ossicles connecting the eardrum and the inner ear in the higher vertebrates, and it serves to transmit vibrations from the gas bladder to the liquids of the internal ear. Certain teleosts termed Ostariophysi includes the Siluriformes, Cypriniformes, Characiformes present Weberian ossicles.

16.2 LATERAL LINE ORGAN

Fishes, as well as larval and adult amphibians, have a very complex sensory system, very polymorphic from the anatomical point of view, which is generally known as the lateral line system (see Chapter 7).

The lateral line system plays a key role in the detection of movements, pressure changes, and vibrations in the environment. The lateral line apparatus consists of numerous sensory units (mechanoreceptors) called neuromasts arranged in a network along with the head and the body. These receptors are innervated by branches from the facial, glossopharyngeal, and vagus nerve. The lateral organs (Figures 16.3 and 16.4) communicate with the outside world via a series of openings (pores) in the skin. Canals of the lateral line system are filled with fluid (water and mucous secretion), which transmits vibrations to the neuromasts through the skin pores.

There are two types of neuromasts: those distributed on the surface of the body, the free superficial neuromasts or pit organs, and those enclosed within canals in the skin along both sides of the body, the canal organs. Many fishes possess both types of neuromasts, but the degree of development varies according to species. The neuromasts usually enclosed in canals lined by a squamous epithelium containing mucous cells (Figure 16.4A and B). Generally, the canals on the head consist of bony grooves covered or not by the skin, whereas the (usually single) trunk canal, stretching from behind the operculum to the tail, is formed by scales.

Neuromasts are composed of sensory (hair) cells and the sustentacular (supporting) cells. The sensory cells are pear-shaped cells located in the upper half of the organ and are covered by a gelatinous cupula. They possess a large centrally located nucleus. The sustentacular cells occupy the whole height of the organ and their thin apical portions extend between the hair

cells. The SCs have a basally located nucleus. The sensory cells of the neuromast have hair-like structures (stereocilia and kinocilia) that are connected to nerve cells and project into the cupula that bends in response to water currents.

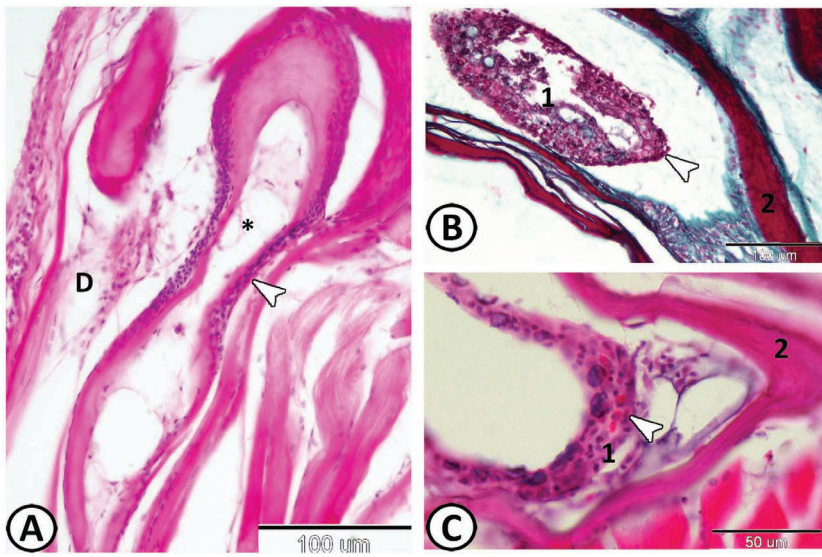

FIGURE 16.3 (A) Transverse section through the medial region of the trunk of guppy stained with HE. Teleosts usually have lateral line canals (*), embedded in the dermis (D), in which the neuromasts (arrowhead) are not directly exposed to the environment. (B and C) Lateral line organs of Molly and guppy respectively stained with Crossmon's trichrome and HE. Neuromasts of canal organs consist of a series of receptors in tunnel-like canals (arrowhead) embedded in the dermis. 1: neuromast, 2: bony tissue.

In the neuromast, movements of the cupula produced by physical stimuli from the environment (pressure, touch, vibration, water currents) strain the sensory hairs stimulating the hair cells. This stimulation is subsequently sensed by the nerve terminals of the hair cell. Lateral line neurons form somatotopic maps within the brain informing the fish of amplitude and direction of flow at different points along the body. These maps are located in the medial octavolateral nucleus of the medulla and higher areas such as the torus semicircularis. Since both the neuromasts of the lateral line system and the sensory cells of the inner ear lead from the ectoderm and perform similar functions, these two sensory systems are also collectively known as the acousticolateralis system.

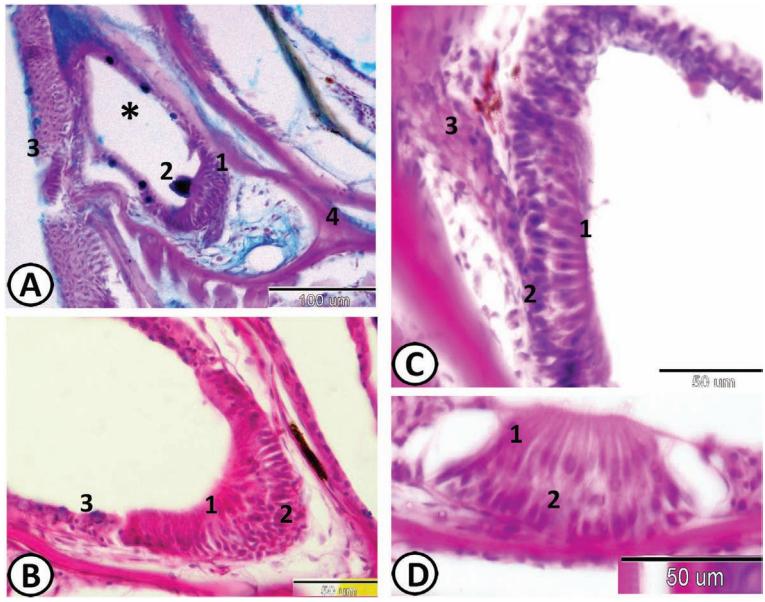

FIGURE 16.4 Neuromasts of guppy Stained with HE except for (A) stained with AB-PAS/HX. (A) A large neuromast (1) present within a groove (asterisk) located in the head region, behind the eyes. Each neuromast in the groove organs bears a jellylike cupula on its summit (2). 3: epidermis-4: bone surrounding the groove. (B) A well-defined neuromast is made up of a cluster of hair cells (1) and SCs (2). Some mucous cells (3) are often present in the adjacent simple epithelium close to the neuromast. (C and D) Transverse section through the neuromasts (sense-hillocks) of the mechanosensitive lateral line system that are typically composed of two types of cells: the sensory (hair) cells and the sustentacular (supporting) cells. The sensory cells (1) are pear-shaped cells located in the upper half of the organ. The sustentacular cells (2) occupy the whole height of the organ and their thin apical portions extend between the hair cells. The sensory cells of the neuromast are connected to nerve fibers (3).

16.3 CHEMORECEPTION

Vertebrates, including fishes, possess two principal chemoreceptive systems, termed olfaction and gustation (taste), which are adapted to respond to specific chemical substances in the environment. In all vertebrates, the chemical information that is detected and transmitted directly to the central nervous system (CNS) by bipolar neurons of cranial nerve is termed olfaction, whereas the chemical information detected by specialized epithelial cells (ECs) (i.e., taste cells) and transmitted to the CNS by neurons of cranial nerve VII (facial), IX (glossopharyngeal), or X (vagus) is termed gustation.

Receptor molecules (most probably glycoproteins) that detect and preferentially pass biologically important information have evolved and have been positioned in the membranes of the receptor cells. These receptor molecules, upon being activated by their specific stimulus or stimuli, initiate a series of cellular molecular events that can result eventually in behavioral responses, such as food search and ingestion. Because both olfactory and gustatory systems in fishes are activated by water-soluble substances, it is often difficult to determine the specific role that each system plays in a particular behavior; this difficulty adds to the confusion of taste/smell distinctions in fish.

16.3.1 TASTE BUDS

The pattern of distribution of gustatory receptors in fish shows marked interspecific variation. In general, these receptors are numerous on the surface of the head, around the mouth, on the lips, oral mucosa, and gill arches. They are also common in the barbels of carp, catfish, and loach. Taste buds in the skin or fins are sometimes also known as terminal buds.

Taste buds (Figure 16.5) are typically ovoid or pear-shaped structures and vary between 30 and 80 μm in height and between 20 and 50 μm in width, with their longitudinal axis oriented vertically to the epidermal surface. However, they can take a tubular form like those in the guppy's oral cavity. They can be found elevated on epidermal (hillocks), flush with the surrounding epidermis or sunken.

Fish taste buds consist mainly of two types of cells, sensory (receptor or gustatory) and supporting (sustentacular). The sensory cells are elongated and each of them terminates by sensitive hair-like structures, the receptor microvilli, which project to the outside or into the organ's lumen. The sustentacular cells are usually located at the periphery of the central sensory cells. The SCs are innervated by cranial nerves (VII, IX, and X). Some authors have also described two types of sensory cells and basal cells (BCs) located below the taste buds. Marginal ECs delimit the taste organ. Unlike the neuromasts, the sensory cells stretch throughout the whole height of the organ. Solitary chemosensory cells also exist.

Taste buds transmit information to enlarged lobes of the medulla oblongata via the nerves VII (facial nerve), IX (glossopharyngeal nerve), and X (vagal nerve). These three cranial nerves form a plexus at the base of the gustatory cells.

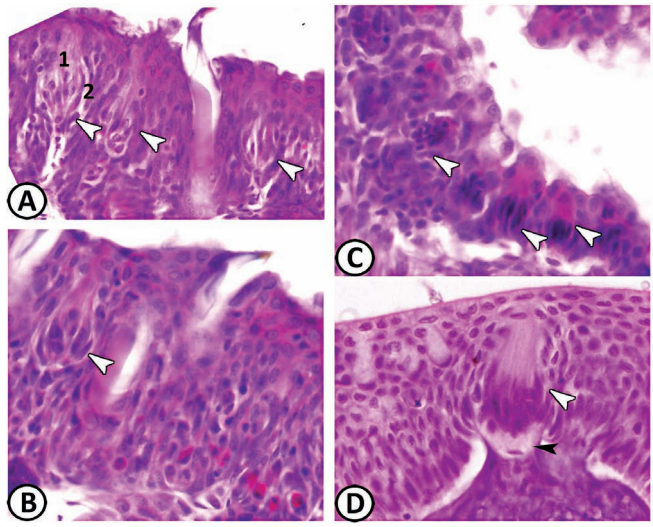

FIGURE 16.5 Taste buds stained with HE. (A and B) The pharynx of guppy showing a pear-shaped taste bud (arrowheads) within the stratified epithelium. The sensory cells (1) possess elongated nuclei and are grouped in the central zone of the bud. The SCs (2) located on the periphery of the bud. The buds can occupy the entire height of the epithelium. (C) This photomicrograph shows numerous taste buds (arrowheads) which abound within the epithelium covering the operculum of guppy. Taste buds usually consist of barrel-like or pear-shaped collections of elongated cells sunk within ectodermal epithelia. (D) The taste buds (white arrowhead) in the tongue of grass carp is supported by a connective stalk (black arrowhead). Its longitudinal axis is oriented vertically to the epidermal surface.

16.3.2 BARBELS

Barbels (Figure 16.6) are tactile, sensory structures that are classified according to location into nasal, maxillary, mandibular, or mental. Catfishes have generally a poor vision and their barbels "whiskers" serve as additional taste organs. Barbels consist of skin projections that are composed of dermis and epidermis. The dermis is composed mainly of connective tissue containing fibroblasts, some chromatophores, a large number of nerve fibers, and many blood vessels. The thick stratified epidermis contains mucous cells and many taste buds. In some species, cartilage is present in the center of the barbel. Barbels are believed to aid senses of taste and touch.

Scanning electron microscopy of the maxillary barbels of red-tail shark shows that their apical surfaces are folded separated by shallow depressions. These surfaces are formed of clusters of irregular polyhedral ECs that exhibited a honeycomb-like pattern (Figure 16.7A and B). These ECs are covered

by numerous microvilli. Rows of large and deep openings of mucous cells are organized in a parallel arrangement and their surrounding ECs are elevated and concentrically arranged in a ringlike pattern (Figure 16.7B). The mucous cells may provide the surfaces with adhesive substances. On the other hand, the surface of the mandibular barbel looks like a honeycomb and is composed of compactly arranged, well-defined polygonal ECs. These ECs are covered peripherally with microridges and centrally with microvilli. The ECs are well demarcated by double rows of microridges (Figure 16.7C and D).

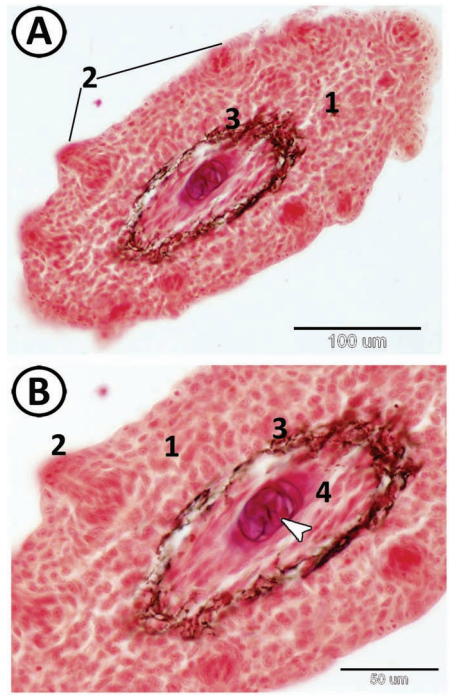

FIGURE 16.6 Transverse section of the barbel of Molly stained with Van Gieson. (A and B) The general view of the barbel shows a thick stratified epidermis (1) housing numerous taste buds (2). The dermis is made up of connective tissue containing fibroblasts, some chromatophores (3) and a large number of nerve fibers (4) surrounding cartilaginous support (arrowhead).

16.3.3 OLFACTORY ORGANS

Olfaction plays a major role in fish as the olfactory organ directly interacts with the environment and involving in various life activities include

feeding, reproduction, and social interaction. In fish, the olfactory organ possessed a considerable variation that reflecting different developmental strategies and ecological habits. In teleosts, the olfactory organ (Figures 16.8 and 16.9) can greatly differ according to the groups: it can be a simple nasal tube with no or few lamellae (*Belonidae*, *Ammoditidae*, *Scombresocidae*, *Poeciliidae*) or a highly complex epithelial tissue with multiple folds (rosettes) and cell types—catfish, minnows, carps, pikes, and salmons. It is usually paired and contains many thousands of receptor cells located in the olfactory epithelium. The sensory epithelium covering the lamella is highly folded allowing a large number of olfactory cells to be packed into the small area of the sac.

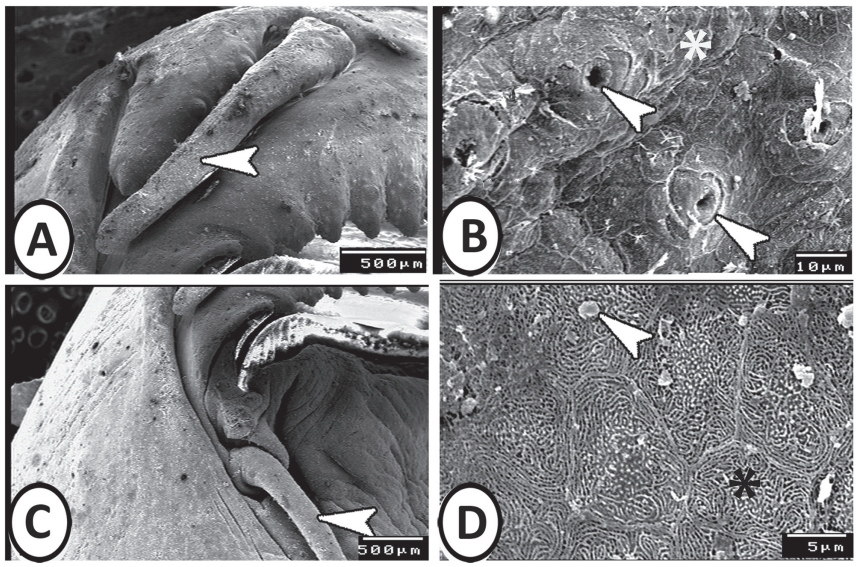

FIGURE 16.7 Scanning electron microscopy of the barbel of red-tail shark. (A) General view of the maxillary barbel (arrowhead). (B) Higher magnification of the surface of the maxillary barbel showing honeycomb pattern ECs (asterisk) and rows of deep mucous cells (arrowheads). (C) General view of the mandibular barbel (arrowhead). (D) Higher magnification of the surface of the mandibular barbel showing ECs with microridges and microvilli (asterisk). Note blobs of mucus (arrowhead).

In contrast to many other teleosteans, red-tail shark is characterized by the presence of two nasal (incurrent and excurrent) openings, which allow and regulate the passage of ventilator water flow through it and prevent the large particles from the entrance to the nasal cavity. In red-tail sharks, the

olfactory organs or olfactory rosettes (Figure 16.9) are highly developed. These organs are paired structures located in capsules on the ventral side of the snout, each covered by a simple flap of skin. They are generally spherical and composed of a series of (primary) lamellae and their secondary folds studded with numerous chemoreceptors. This arrangement greatly increases the surface area in contact with the water and thus the sensitivity.

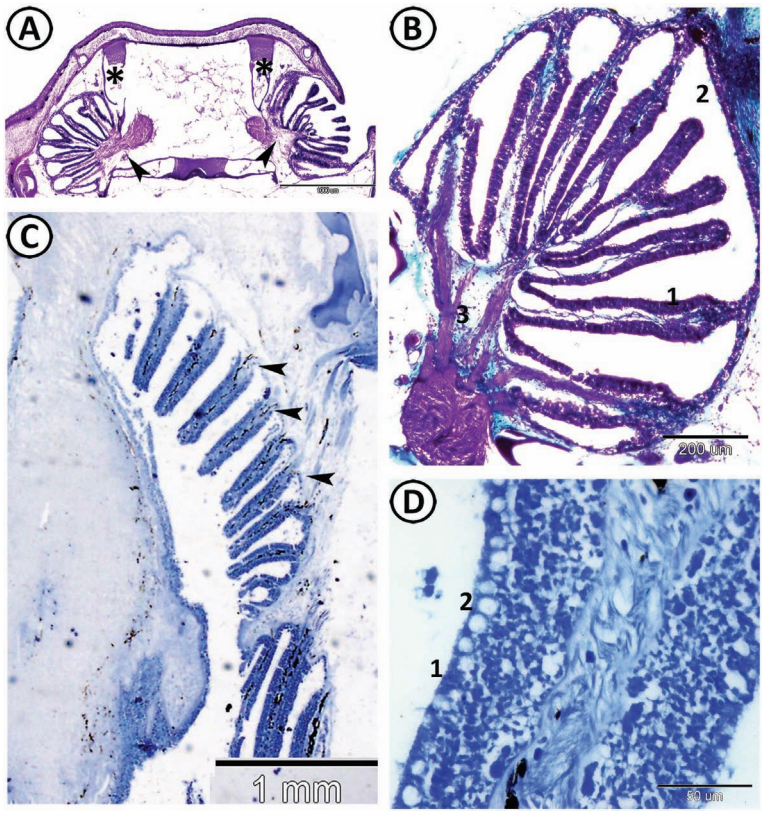

FIGURE 16.8 Olfactory organ. (A and B) Transverse section through the paired olfactory sacs (arrowheads) of Orinoco sailfin catfish stained with HE, Crossmon's trichrome respectively. The olfactory sac exhibits folds or lamellae (1), which protrude into the olfactory chambers (2). Nerve bundles (3) of nerve I (olfactory nerve) aggregate in the center of each of the sensory chambers. A fibrocartilaginous tissue (asterisks) surrounds the sacs. The olfactory epithelium lines a lamellar olfactory rosette in many teleosts. (C and D) Transverse section through the paired olfactory organs of silver carp stained by bromophenol blue showing the olfactory chambers lined with olfactory lamellae (arrowheads). The (primary) lamellae are lined by a ciliated sensory epithelium (1) containing some mucus-secreting cells (2).

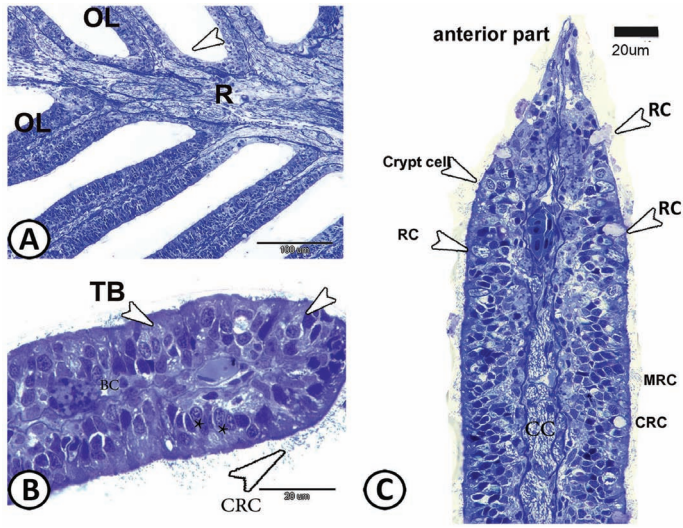

FIGURE 16.9 Semithin section of the olfactory epithelium of red-tail shark stained with Toluidine blue. (A) The olfactory rosette consisted of many olfactory lamellae (OL) radiating from a median raphe (R). Notice the distribution of the nonsensory epithelium (arrowhead) at the end of a median raphe. (B) The apical third of olfactory lamellae contain taste bud (TB, arrowhead) and ciliated receptor cells (CRC, arrowhead) and crypt cells (arrowhead). Notice the presence of supporting cells (asterisks) and basal cells (BCs). (C) The lamella consisted of two layers of epithelium above the basement membrane separated by central core (CC). The sensory epithelium comprising the major part includes microvillous receptor cells (MRC), ciliated receptor cells (CRC), crypt cells, and rodlet cells (RC, arrowheads).

The olfactory rosette in red-tail shark measuring 0.8–1.0 mm in diameter and comprises of numerous olfactory lamellae that radiate from a spindle-shaped central median raphe. Each lamella consists of two layers of epithelium separated by a connective tissue core. The central connective tissue core is separated from the olfactory epithelium by a basement membrane and filled with loose vascularized connective tissue, fibroblasts, and nerve fibers.

Fish show variation in shape, size, and lamellar arrangement as well as the arrangement of sensory and nonsensory areas. The olfactory epithelium is a complex tissue composed of sensory and nonsensory elements. The olfactory sensory epithelium possesses ORC bearing microvilli or cilia that are common in teleosts and occur in different proportions according to species. Recently, special subtypes of neurons namely crypt and rod cells were recorded in some fish species. While the nonsensory epithelium of most fish species consists of the stratified epithelium (ciliated and nonciliated cells) and mucous cells. The nonsensory ciliated cells are columnar in shape and

their motile cilia serve to ventilate the olfactory organ. The mucous cells protect the olfactory epithelium from external injuries and allow a smooth flow of water through the olfactory chamber. In addition, the mucin help in the binding of microscopic debris that enters with incoming water as well as help to decrease the friction of water in the nasal cavity. Moreover, the mucus over the olfactory lamellae forms a suitable medium for the diffusion of odorants and may trap the ions to delay the penetration of toxicants, especially the heavy metals into underlying tissues.

The sensory epithelium (Figure 16.9) is formed of ciliated, microvillous ORCs, rodlet and crypt cells. The ORCs are observed at different levels of the epithelium with a round cell body. The ciliated ORCs are provided by many cilia and their nucleus are rounded in shape. On the other hand, the microvillous ORCs exhibit broad apical ends with many microvilli and their nuclei are located more superficially in the epithelium than the ciliated ORCs. The olfactory crypt cells are oval-shaped neurons with an oval dark nucleus and light-staining cytoplasm. The SCs are located between the receptor cells and are elliptical to columnar in shape with a well-distinct centrally situated oval nucleus. The BCs are small rounded or pear-shaped with a round large central nucleus, situated at the basal part of the epithelium.

The rodlet cells (Figure 16.9C) are frequently observed along the length of the olfactory lamellae in both the sensory and nonsensory olfactory epithelium. Immature rodlet cells are found near the basement membrane of lamellae; the developing rodlet in the middle layer and mature rodlet are located at the surface. Immature rodlet cells are large polyhedral in shape with an eccentric vesicular nucleus. Mature rodlet cells consisted of pear-shaped cells with thick deeply stained capsule and oval basally located vesicular nucleus. Their cytoplasm is filled with characteristic club shape inclusions, called rodlets. Rodlet cells showing secretory activity and some cells release their content to the interlamellar space. The final or rupture stage of these cells suggested releasing their contents by holocrine mode of secretion.

The neuromast or taste bud (Figure 16.9B) is demonstrated in the apical part of the lamella. It composed of SCs surrounding a central cluster of sensory hair cells. Their position in the apical region of the lamellae allows it to react quickly with the incoming signals from the outside. The SCs are involved in the production of a gelatinous material "cupula" that helps the olfactory organ to communicate with the external environment. While the sensory cells help in the orientation of chemical stimuli and consequently in the detection of palatable food items.

Scanning electron microscopy (SEM) of the olfactory rosette of red-tail shark (Figure 16.10) reveals that it is provided with 45–48 leaf-like olfactory lamellae. Each lamella is connected to the wall of the olfactory chamber by a long connection. The epithelium of the connection between the median raphe and the olfactory lamellae consists of stratified epithelial cells (SECs) with long cilia intermingled with rodlet cells. The median raphe is covered with SECs provided by the labyrinth pattern of microridges in their apical surfaces, in addition to the presence of rodlet cells and ciliated nonsensory cells. This arrangement of microridges may protect the sensory epithelium from mechanical injuries and help in holding the mucus over the epithelium.

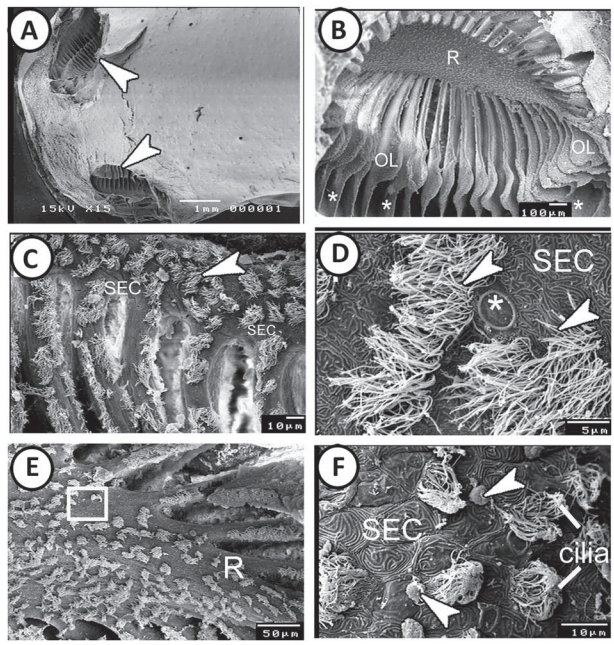

FIGURE 16.10 SEM of the general overview of the olfactory rosette and median raphe of red-tail shark. (A) General view showing a pair olfactory organ that consisted of right and left olfactory rosettes, located in olfactory chambers (arrowheads). (B) Higher magnifications of the olfactory rosette in part A showing olfactory lamellae (OL) and midline raphe (R) and connection between the raphe and the wall of the olfactory chamber (asterisks). (C and D) The epithelium of the connection between the median raphe with olfactory lamellae consists of SECs with long cilia (arrowheads) and rodlet cells (asterisk). (E) General view of the surface of the median raphe (R) showing numerous ciliated cells. (F) Higher magnification of the boxed area in part E showing the epithelium of median raphe that consisted of the stratified epithelium with fingerprint-like microridges (SEC), ciliated nonsensory ECs (cilia) and rodlet cells (RC, arrowheads).

The sensory olfactory epithelium (Figure 16.11) contains ciliated ORCs that dominant over the microvillous receptor cells. Ciliated receptor cells are provided by a tuft of long cilia. Some ciliated cells possess a long dendritic process that extended above the surface of the olfactory epithelium forming the olfactory knob (OK). These cilia appear rosette-like around the OK. The microvillous cells are provided by minute microvilli. Between these cells, rodlet cells can be identified. Taste buds were demonstrated at the anterior end of lamellae (Figure 16.11E and F). Neuromast or taste bud is a mechano-sensory organ involved in the detection of predators and the capture of prey.

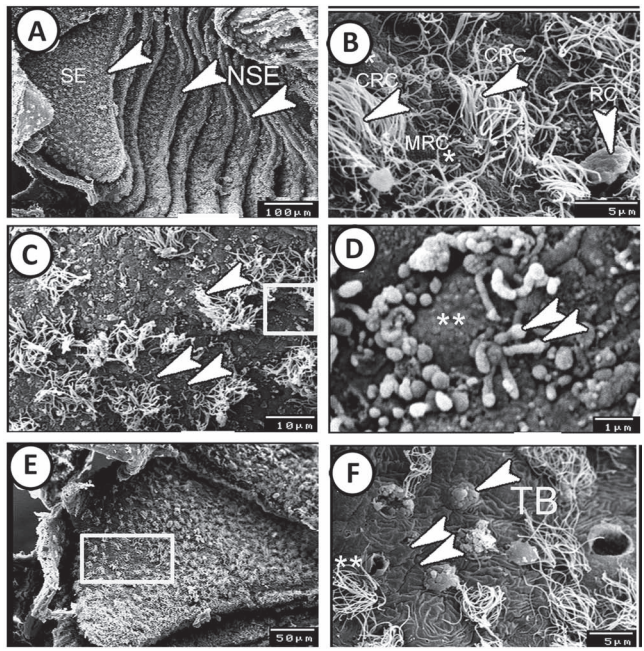

FIGURE 16.11 SEM of the distribution of the sensory region of the olfactory organ of red-tail shark. (A**)** The sensory epithelium (SE) distributed on the lateral surfaces of olfactory lamellae, while the nonsensory one (NSE, arrowheads) was distributed on the margin of the lamellae. (B) Higher magnification of sensory epithelium showing the ciliated receptor cells (CRC, arrowheads), microvillous receptor cells (MRC, asterisk) and rodlet cells (RC, arrowhead). (C) Lower magnification of sensory epithelium showing the ciliated receptor cells (two arrowheads) and the microvillous receptor cells (arrowhead). (D) Higher magnification of the boxed area in part C showing the rosette-like surface of ciliated receptor cells (two arrowheads) arranged around the olfactory knob and microvillous cells (**). (E) Lower magnification showing the anterior part of olfactory lamellae with taste buds. (F) Higher magnification of the boxed area in part E showing the taste buds (TB, arrowhead). The two arrowheads indicate the finger-print like microridges.

The nonsensory olfactory epithelium (Figure 16.12) is restricted to the margin of the lamellae and exhibited broad polygonal surface of the stratified epithelium, which divided into ciliated and nonciliated cells. The ciliated cells are provided with long cilia, whereas the nonciliated ones are free from cilia and exhibited fingerprint-like microridges. The zone of transition between the sensory and nonsensory epithelium consists of SECs with apical fingerprint-like microridges and few microvillous and ciliated receptor cells.

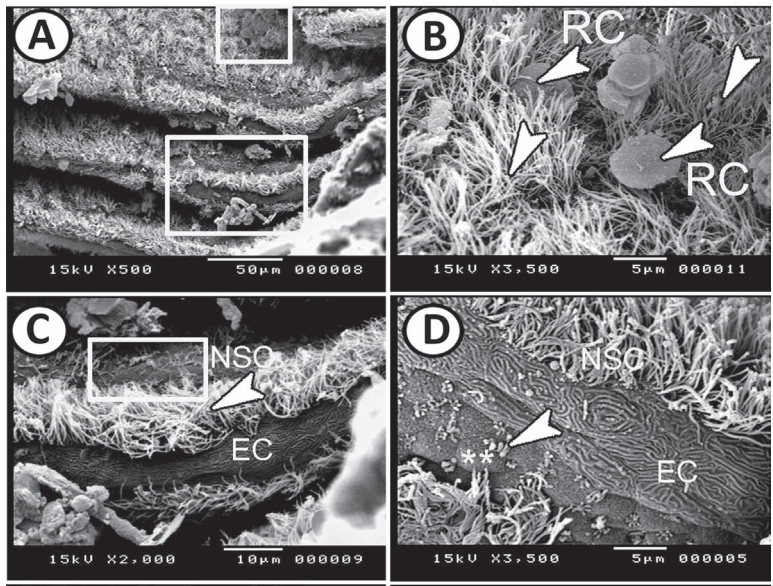

FIGURE 16.12 SEM of the nonsensory region of the olfactory organ of red-tail shark. (A) The nonsensory epithelium distributed on the margins of olfactory lamellae (large-boxed area). (B) Higher magnification of the small-boxed area in part A showing the sensory olfactory epithelium (arrowheads) and rodlet cells (RC, arrowheads). (C) Higher magnification of the large-boxed area in part A showing the nonsensory epithelium (NSC) with ciliated cells (arrowhead) and epithelial cells with fingerprint-like microridges (EC). (D) A transitional zone between the NSC with fingerprint-like microridges ECs and ciliated ORC (arrowhead) and microvillous ORC (asterisks).

The fine structure of the olfactory epithelium shows that the nuclei of the ORCs are located above the level of the neighboring nuclei of SCs. The receptor cells nuclei have a characteristics checkerboard pattern distribution of chromatin. According to the difference in staining affinity, the ciliated and microvillous receptor cells are stained darker than the surrounding SCs (Figure 16.13A). The ciliated cells have narrow apical dendrites ending in

the form of a distinct OK with several cilia arising from it (Figure 16.13B). Each cilium arises from a basal body and supported with numerous neurotubules (Figure 16.13C). The apical portions of SCs are filled with many electron-lucent vesicles and their lateral surfaces exhibit zonula adherent junctional complexes between them and the receptor cells (Figure 16.13B and C). Many ciliated ORCs are identified at the apical surface (Figure 16.13D). The microvillous receptor cells are provided with less distinct OKs. Beneath these knobs, abundant mitochondria are arranged longitudinally (Figure 16.13E).

The crypt cells (Figure 16.13F) contain electron-lucent cytoplasm with rough endoplasmic reticulum and mitochondria in the apical portion of the cell above the nucleus. Golgi apparatus can be identified in a supranuclear position and cross sections of cilia are demonstrated within these cells (Figure 16.13G). The crypt cells were detected in many fishes, including zebrafish, catfish, goldfish, and salmonids, but they are apparently absent from other species, including two types of lungfishes. The function of these cells is still unknown; however, these cells are supposed to detect sex pheromones. In addition, the crypt cells act as chemoreceptors to amino acids. The crypt cells of zebrafish expressed TrkA-like proteins and might be involved in the olfactory epithelium regeneration.

The BCs are small polyhedral cells with large nuclei contain distinct nucleoli. The differentiated or active form of these cells is characterized by a nucleus with chromatin arranged in a checkerboard pattern. They contain a few rough endoplasmic reticulum and mitochondria (Figure 16.13H and I). These cells may act as stem cells for regeneration of the olfactory epithelium, which characterized by a relatively short life span and may be replaced throughout the life by these progenitor BCs. The basement membrane of the olfactory epithelium consists of thick lamina densa and lamina reticularis layers (Figure 16.13I).

The immature form of rodlet cells appears as large polyhedral cells filled with many electron-dense and -lucent granules and eccentric basally located nucleus with a checkerboard pattern of chromatin distribution (Figure 16.13H and I). The mature rodlet cell is pear-shaped and its apex directed toward the surface while the broad basal part contains the basally located oval-shaped nucleus. The apical part of these cells is provided with short microvilli (Figure 16.13H). Some rodlet cells released their whole contents into the interlamellar space in a holocrine-like manner (Figure 16.14A).

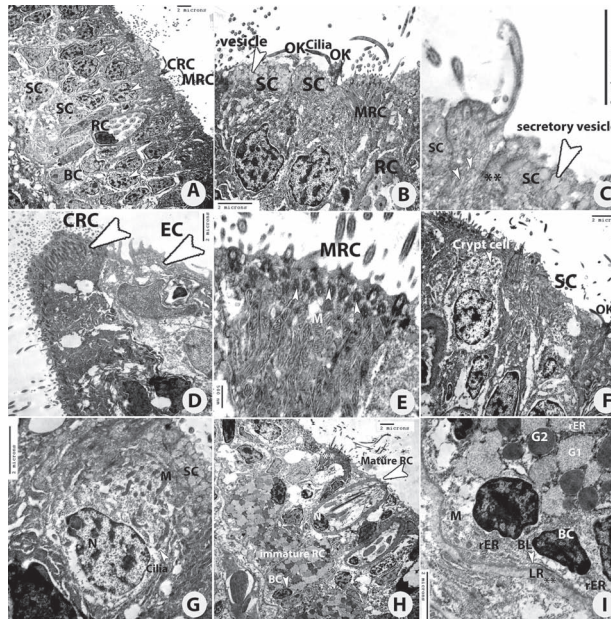

FIGURE 16.13 Transmission electron microscopy (TEM) of the sensory epithelium of the olfactory organ of red-tail shark. (A) The sensory epithelium consists of ciliated receptor cells (CRC), microvillous receptor cells (MRC), rodlet cells (RC), SCs, and BCs. (B) Ciliated receptor cells with olfactory knob (OK) and cilia, microvillous receptor cells (MRC), rodlet cells (RC), and supporting cell (SC) with apical secretory vesicles (arrowhead). (C) Higher magnification of SCs with apical secretory vesicles (arrowhead) showed zonula adherents (**) junctional complexes between it and receptor cells. Note the presence of neurotubules in the ciliated receptor cells (small arrowheads). (D) Ciliated receptor cells (CRC, arrowhead) is dominated at the tip of lamellae. Note the presence of the epithelial cells (EC, arrowhead) with microridges. (E) Microvillous receptor cells (MRC) showed well distinct basal bodies (arrowheads) with numerous microvilli and abundant mitochondria (M). (F) The crypt cell (arrowhead) was surrounded by supporting cells (SC). Note the OK of the receptor cells. (G) Higher magnification of the crypt cell showing mitochondria (M) and nucleus with heterochromatin (N). It was surrounded by SCs. Cross sections of cilia were observed within the cells (arrowhead, cilia). (H) The immature stage of rodlet cells on the basal part and the mature one (arrowhead) in the apical region. Notice the microvillous cells (**) and basal cells (arrowhead, BC). (I) Basal cells (BC) contained rER that rest on basal lamina (BL, arrowhead) with thick lamina reticularis (LR, **). The immature stage of rodlet cells contained rER, mitochondria (M), electron-lucent granules (G1), and electron-dense ones (G2).

The cilia of the nonsensory cells appeared longer than the cilia of sensory cells. Mitochondria are packed under the apical end of the cells (Figure 16.14B). Moreover, the ciliated nonsensory cells can be distinguished from the sensory ones by the absence of the OK. The epidermal cells or nonsensory epithelial cells with irregular apical end or serrated appearance are seen

in the nonsensory part (Figure 16.14C). The rodlet cell is surrounded by a thick cuticle and within their cytoplasm, rER, translucent vesicles and many club-shaped rodlet inclusion are observed. Each inclusion consisted of a high electron-dense core surrounded by a less electron-dense material. These inclusions organize as their wide part directed toward the basal nucleus and the narrow part directed toward the apex of the cells (Figure 16.14D). The macrophage is also detected in the olfactory epithelium and characterized by the kidney-shaped nucleus and its cytoplasm contained mitochondria, rER, and vesicles with apical pseudopodia (Figure 16.14E). Empty and exhausted rodlet cells are also observed in the median raphe and the connection part between the lamellae and the wall of the olfactory chamber as they released their contents into the lumen (Figure 16.14F).

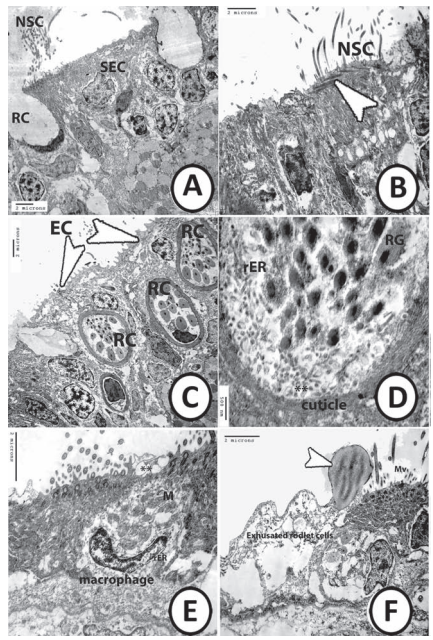

FIGURE 16.14 TEM of the nonsensory epithelium of the olfactory organ of red-tail shark. (A) The nonsensory epithelium consisted of NSC and SECs with microridges. Note the mature stage of rodlet cells (RC) releasing their contents. (B) The NEC showing broad apical surfaces provided with a high number of cilia (arrowhead). (C) The developing stages of rodlet cells (RC). Notice the presence of epithelial cells (EC, arrowheads) with microridges. (D) Developing rodlet cells is surrounded by a thick cuticle and contained rodlet granules (RG), translucent vesicles (asterisks) and rER. (E) The macrophage shows mitochondria (M), rER, apical pseudopodia, and vesicles (asterisks). (F) The connection part between the lamellae and the wall of the olfactory chamber shows microvillous cells (Mv) and some exhausted rodlet cells (arrowhead).

16.4 ELECTRIC ORGANS AND ELECTRORECEPTION

16.4.1 ELECTRIC ORGANS

Fishes are sometimes equipped with organs specifically adapted to generate an electric discharge. The vast majority of fishes are nonelectroreceptive animals: specialized receptors and electric organs are absent. Specialized electric organs and active electroreception are present in *Gymnarchidae*, *Mormyridae*, *Malapteruridae*, and *Torpedinidae*.

With the exception of the freshwater sternachids, where the electric organs are modified motor neuron terminals, fish electric organs are modified striated muscle fibers (rhabdomyocytes). The location of the electric organs varies in different animals. In *Torpedo* (marine ray), they lie on either side of the head, between the gills and the anterior part of the pectoral fin. In electric eels, the organ extends laterally along each side from the trunk to the end of the tail. In *Raja*, *Gnathonemus*, and *Gymnarchus*, they are confined to the tail region. More unusually in African catfishes (*Malapterurus*), they are situated between the skin and muscles along the whole length of the body and in *Astroscopus*, they are placed behind the eyes, in the form of patches, one on each side.

Typically, each electric organ consists of a large number of columns held together by connective tissue. Each column comprises a variable number of multinucleated, flattened, and elongated cells called electrocytes, whose cytoplasm is filled with glycogen. Electrocytes vary greatly in morphology but most are disc-like cells with a smooth innervated face and a papiliform noninnervated face. In the electric ray *Torpedo*, there are over 1000 electrocytes in a column and 500–1000 columns per organ. In the electric eel *Electrophorus*, there are about 60 columns on each side, with approximately 10,000 electrocytes per column. The electric organ of *Electrophorus* can generate a discharge of over 500 V.

16.4.2 ELECTRORECEPTOR ORGANS

Electroreceptors occur in the teleost families of gymnotids (South America) and mormyrids (Africa), which use electrical impulses for orientation. The brain of these African fishes is remarkable by the monstrous development of the *valvula cerebelli* "*mormyrocerebellum*," which extends forward and backward to cover the dorsal encephalon. To this extraordinary hypertrophy of all centers in relation with the lateral line system corresponds the existence

of remarkable sensory endings in the skin, innervated by the thickly myelinated fibers of the lateral nerves.

In adult mormyrid teleost fish, three types of electroreceptors are found in the specialized electroreceptive epithelium: the ampullary organs, the mormyromasts, and the tuberous organs (knollenorgans). With this electroreceptive system, these fish are capable of recognizing congeners, predators, and objects of varying conductivity. Ampullary organs have their role in the sensing of low-frequency signals generated by a variety of biological and nonbiological sources. Knollenorgans have their major role in electrocommunication (emission and detection of electric organ discharges of other fish and their own species), whereas mormyromasts are active in electrolocation. Afferent nerve fibers from the three electroreceptors project into different parts of the medulla.

The ampullary organ and tuberous organs or Knollenorgans are described in Chapter 7. The mormyromasts have an intraepidermal cavity filled with acid polysaccharides and possess two sensory cell classes (type A and B) distinguished by morphology and location. It is the most abundant type of electroreceptors, mainly present in the epidermis of the mouth.

The ampullae of Lorenzini are special sensitive electroreceptors on the rostral part of the head in skates, rays, and sharks. They are jelly-filled canals open to the skin surface by a pore plainly visible as a dark spot. The canals end in a cluster of small vesicles filled with special jelly enclosed in capsules of collagenous connective tissue. The deeper part of the ampullae is lined by a sensory epithelium containing thermo- and electroreceptive cells. Each ampulla is innervated by a small bundle of fibers of the facial nerve (VII). The ampullae of Lorenzini can detect electrical fields generated by moving animals (prey detection in a sandy sea-bottom) and the Earth's magnetic fields, thus helping their orientation during migrations.

16.5 VISION

The organization of the fish eye has the same general structure found in higher vertebrates. Eyes are large and round with a flattened corneal surface and no eyelids (but sharks can have elaborate eyelids; some of them can close their eyes completely and others have a third eyelid-nictitating membrane, which protects the eyes when biting prey). Some deep-water species have disproportionately large eyes to optimize the limited light available, whereas

in others, like cave fish, the development of the optic primordia is arrested and subsequently degenerates.

Each eye (Figure 16.15) is composed of three concentric layers; an external layer that consists of the sclera and the transparent cornea, a medial uveal layer, and an inner layer of nerve tissue, the retina. The additional components of the eyeball are the aqueous humor, the vitreous body, and the lens that are described as the refractive media of the eye.

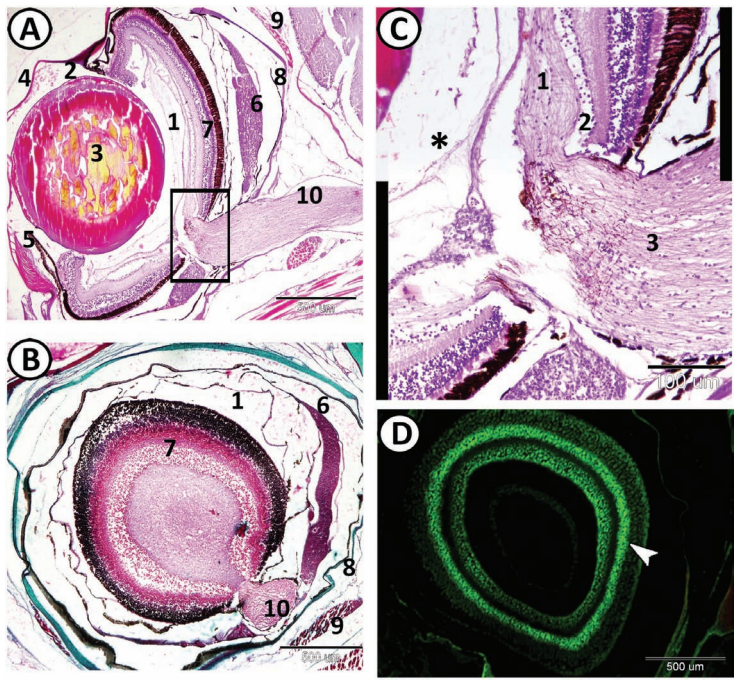

FIGURE 16.15 Eye. (A and B) Eyes of Molly are organized into the large chamber of the vitreous body (1) and aqueous cavities (anterior and posterior chambers—2) located in front of the lens (3). The anterior portion of the eye's outermost layer is modified into a transparent cornea (4) with a central hole, the pupil, surrounded by the iris (5). The middle layer of the eye is composed of a vascular tunic, the choroid rete (6). The retina (7) is the light-sensitive part internal to the choroid. Finally, the posterior part of the outermost layer constitutes the sclera (8) on which ocular muscles (9) insert. Optic nerve (10). The stains are HE and Crossmon's trichrome respectively. (C) Higher magnification of the boxed area in part A showing the optic disc. The afferent fibers (1) from the ganglion cells (2) form the optic nerve (3). The asterisk indicates the chamber of the vitreous body. The optic disc (or optic papilla) is the point where the optic nerve leaves the retina (blind spot). Note the absence of photoreceptor cells in this spot. (D) Fluorescent image stained with acridine orange showing the layers of the retina (arrowhead).

16.5.1 LENS

The teleost lens (Figure 16.15A) is a transparent disc that it is completely round and protrudes into the aqueous chamber almost to the cornea, providing a wide field of vision. The lens is an avascular tissue and is covered by a capsule consisting of carbohydrates and glycoproteins secreted by the cells contained within the lens. The lens cells are organized into two morphologically distinct cell subpopulations. The lens cells facing the anterior chamber of the eye are a monolayer of ECs while the lens cells facing the posterior chamber, bathed in the vitreous humor are extremely elongated into fibers. Crystalline protein is the major protein found in the lens cells, the latter are very elongated and separated by very little extracellular matrix.

The main function of the lens is, in combination with the cornea, to transmit and focus the incoming light onto the retina. Due to its rigidity, visual accommodation is accomplished not by deflecting the shape of the lens but by moving it forward and backward via retractor muscles and suspensory ligaments.

Aqueous humor is a transparent, gelatinous fluid similar to plasma, but it contains lower protein concentrations. It is secreted from the ciliary epithelium, a structure supporting the lens. It is located in the anterior and posterior chambers of the eye, the space between the lens and the cornea.

16.5.2 SCLEROCORNEAL LAYER

The outermost layer of the eye is divided into an external cornea and an internal sclera. The cornea (Figure 16.16C) is a transparent layer that consists of an unpigmented stratified squamous epithelium, a membranous corneal stroma, and a thin endothelium. The corneal epithelium is multilayered and contiguous with the integument of the head. The wall of the posterior portion of the eye is made up of the thick fibroblastic sclera, which is contiguous with the corneal stroma. The sclera is commonly known as the white of the eye. It consists of tough collagenous tissue that serves as the eye's protective outer coat. The sclera is nonrefractile with an external sheath of hyaline cartilage in most fishes (Figure 16.16B).

16.5.3 UVEAL TRACT

The middle layer of the eye is composed of the choroid and the iris. The choroid (Figures 16.15 and 16.16) is composed of three layers: a connective

layer adjacent to the sclera, a lamina vasculosa with large blood vessels, and a third layer, the lamina choriocapillaris rich in small vessels and adjacent to the retina. Generally, the choroid rete, surrounding the optic nerve, is a well-developed and intricate array of arterioles and capillaries forming a rete mirabile. This organ is designed to satisfy the high oxygen demands of the poorly vascularized retina. The degree of development of the choroid varies depending on the species. In carp, the plexus of blood capillaries is well developed and is known as the choroidal gland. In eel, however, the choroid is poorly supplied with blood capillaries, and no structure resembling a choroidal gland can be recognized.

The iris (Figure 16.15A), a continuation of the choroid, projects in a thin layer over the anterior surface of the lens, which often protrudes into the aqueous chamber. The iris separates aqueous and vitreous chambers with its leading edge defining the pupil. The cavity of the eyeball is filled with a transparent medium called the hyaloid body.

16.5.4 THE RETINA

The retinal tunic (Figures 16.16–16.20) is composed of 10 distinct layers: (1) the pigment epithelium, closely opposed to the choroid; (2) the elongated tips of cones and rods; (3) the external limiting membrane; (4) the outer nuclear zone containing the cell bodies and nuclei of the photoreceptors; (5) the outer plexiform layer; (6) the inner nuclear layer of

the bipolar cells, which transmit the impulses inward from the photoreceptors, and of associative glial cells; (7) the inner plexiform layer, a region of synapse formation; (8) the nuclei of the ganglion cell layer, which pick up the stimuli from the bipolar elements and transmit to fibers; (9) the nerve fiber layer contains the optic nerve that extends to the brain; and (10) the inner limiting membrane composed of the expanded processes of glial cells.

The cellular constituents of the retina include five major types:

1. Photoreceptor cells: These are the rod and cone cells. The function of the rod cells is to detect the intensity of light, and that of the cone cells is to distinguish the wavelengths, that is, color.
2. Horizontal cells: These cells are located in the outer region of the inner nuclear layer and show a slightly flattened nucleus. Some processes from these cells extend horizontally near the outer nuclear layer and serve as lines of communication between the photoreceptor cells.

3. Bipolar cells: These nerve cells are located in the innermost region of the retina and are the largest neurons observed within the retina. These neurons have spherical dense nuclei. The axons from these cells form the optic nerve.
4. Amacrine cells: These cells are located between the inner granular and inner plexiform layers and show a slightly lighter nucleus. These neurons serve as horizontal lines of communication for visual stimuli.
5. Müller cells: These cells are the major glial component of the retina. It is supported by the basal lamina that forms the inner limiting membrane and extends toward the outer limiting membrane where they make a connection through cellular junctions with the photoreceptors. Their nuclei are placed in the outer nuclear layer.

The inner limiting membrane consists of a thin membrane (0.02–0.03 pm thick), which is covered completely by Müller cell processes. The increased surface area provided by the extensive system of Müller cell end-feet and the inner limiting membrane would ensure a more effective transport mechanism for the exchange of nutritive substances throughout the retina. The oxygen supply to the inner retina mediated via the vitreal vessels, together with the choriocapillaris and choroidal body, therefore provide the entire retina with the nutrition it requires.

Ganglion cell axons are predominantly unmyelinated but rare myelinated profiles are sometimes observed. The ganglion cells are large multipolar cells with a spherical nucleus and nucleolus, and Nissl' bodies in their cytoplasm. Ganglion cell somata are of various sizes (4–10 pm in diameter) and are not confined to a single lamina but lie at various levels within aggregations between the fascicles of axons. The inner plexiform layer is approximately 38 pm in thickness and consists of a complex meshwork of ganglion, amacrine cells, and inner nuclear layer cell dendrites traversed by Müller cell processes.

The outer plexiform layer is 23-pm thick and shows a complex synaptic connection between the bipolar, horizontal, and photoreceptor terminals. The photoreceptor terminals are single synaptic ribbon, surrounded by Müller cell processes. The outer nuclear layer (20-pm thick) consists of three or four layers of darkly staining rod nuclei, which lie vitread to the cone nuclei that typically straddle the outer limiting membrane.

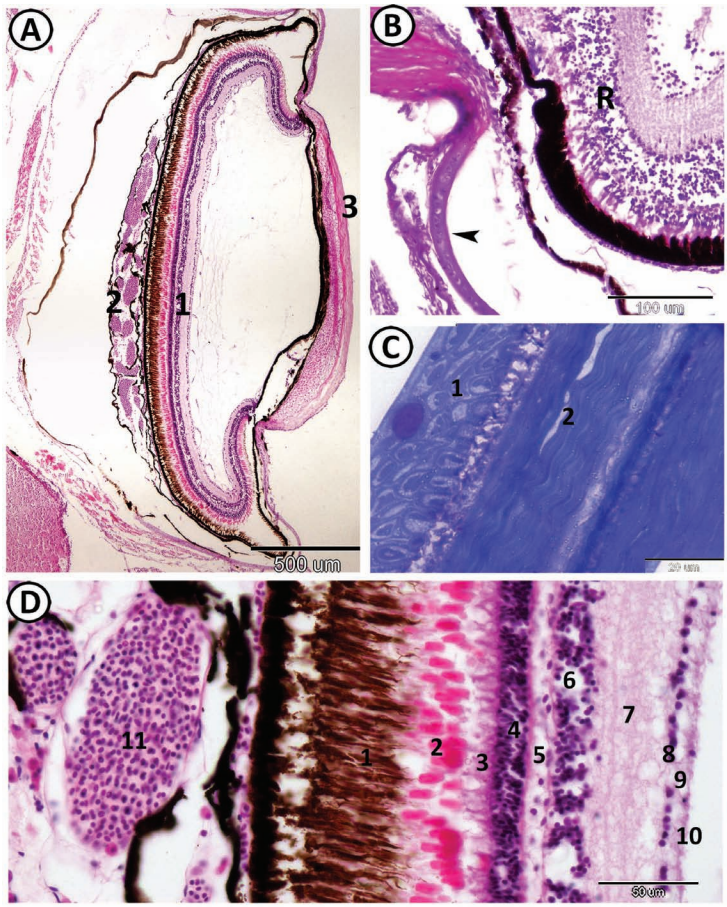

FIGURE 16.16 (A) Transverse section of the eye of red-tail shark stained with HE showing the layers of the retina (1), choroid (2), and cornea (3). (B) The posterior part of the eye of Molly shows some layers of the retina (R). The wall of the posterior portion of the eye is made up of the thick fibroelastic sclera, which is reinforced with an external sheath of hyaline cartilage (arrowhead). (C) Semithin section through the cornea (lateral side of the eye) stained with TB. In this micrograph, the layers of the cornea can be seen. 1: the squamous corneal epithelium: it is an unpigmented, transparent stratified epithelium; 2: the corneal stroma: this layer is the main constituent of the cornea and consists of tightly bound collagen fibers. (D) This photomicrograph shows the entire depth of the retina and the uveal layer. The retina is divided into ten distinct layers. 1: pigment epithelium—2: photoreceptor layer (rod and cone processes)—3: outer limiting membrane—4: outer nuclear layer consisting of the nuclei of the photoreceptors—5: outer plexiform layer—6: inner nuclear layer 7: inner plexiform layer—8: ganglion cell layer—9: layer of ganglion cell axons forming the optic nerve or nerve fibers layer—10: the inner limiting membrane. The choroid plexus (11) is a well-developed and intricate array of arterioles and capillaries forming a rete mirabile (choroid rete).

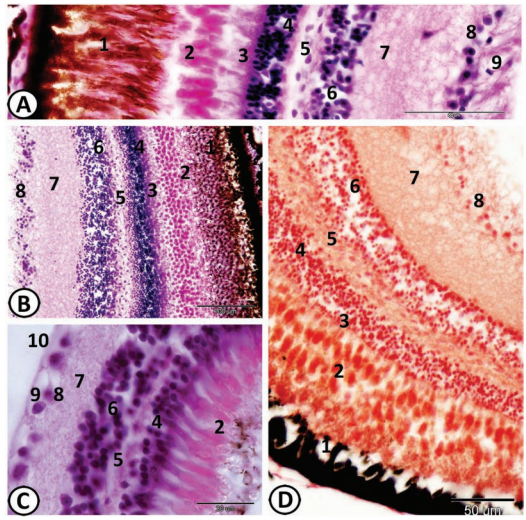

FIGURE 16.17 (A–D) Retina of red-tail shark stained with HE, PAS/HX, Van Gieson respectively showing its layers; 1: pigment epithelium—2: photoreceptor layer—3: outer limiting membrane—4: outer nuclear layer—5: outer plexiform layer—6: inner nuclear layer—7: inner plexiform layer—8: ganglion cell layer—9: the optic nerve layer—10: the inner limiting membrane. Note in part B, the outer segment of rods and cones (2) are PAS-positive.

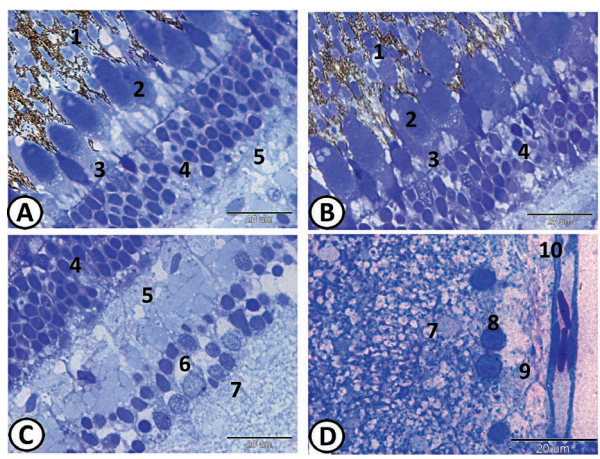

FIGURE 16.18 Semithin section through the retina of red-tail shark stained with TB. (A and B) Posterior part of the retina. The pigment epithelium (1 melanin in brown), the photoreceptor cells (the cell bodies of the cone and rod cells—2), (outer limiting membrane—3), (outer nuclear layer—4) and (outer plexiform layer—5) are clearly visible. (C and D) The anterior part of the retina—4: outer nuclear layer—5: outer plexiform layer—6: inner nuclear layer—7: inner plexiform layer—8: ganglion cell layer—9: a layer of ganglion cell axons forming the optic nerve or nerve fibers layer—10: the inner limiting membrane.

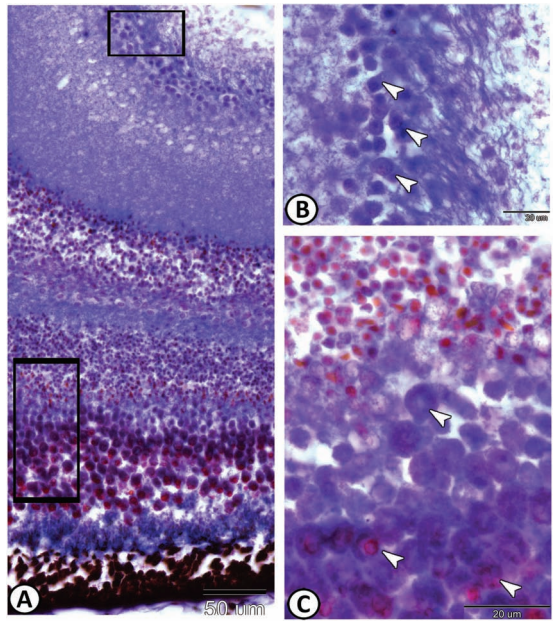

FIGURE 16.19 Eye of red-tail shark stained with Bromophenol blue. (A) The general view of the retina. (B) Higher magnification of the small boxed area in part A showing the positive-stained ganglionic layer (arrowheads). (C) Higher magnification of the large boxed area in part A showing the positive-stained neurons in the outer nuclear layer (arrowheads).

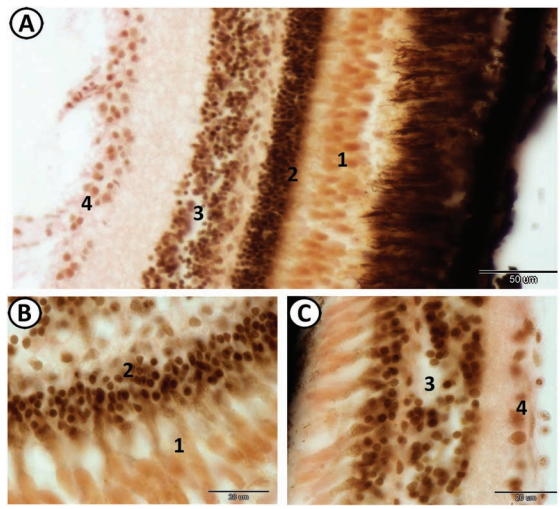

FIGURE 16.20 (A–C) Retina of red-tail shark stained with Grimilus silver stain showing the positive-stained neurons of photoreceptors (1), outer nuclear layer (2), inner nuclear layer (3), and ganglionic layer (4).

The photoreceptors are classified into four types; unequal double cones, large and small single cones, and rods. None of the photoreceptor types contains either a paraboloid or an oil droplet. Their nuclei are elongated and lie immediately under the outer limiting membrane, in the outer nuclear layer. The cell extensions reach the outer plexiform layer. Most fishes have a duplex retina, that is, one containing both rods and cones. Both these visual cells share a common plane: an outer segment containing photosensitive pigment (rhodopsin or porphyropsin), an ellipsoid packed with mitochondria, an extensive myoid, or foot piece and a nuclear region. The rods and cones are held in position by the external limiting membrane. The rod cells are particularly longer (about 100 μm) and thinner with cylindrical outer segments and ellipsoids while in cones, the outer segment is conical, and the ellipsoid rather bulbous. Rods mediate the detection of light during dim photic conditions while different populations of cones are sensitive to the red, green, or blue regions of the visible spectrum. The retina of salmonids also possesses specialized cones that are maximally sensitive to ultraviolet light, and this may also be true for other species. Twin cones are common in many bony fishes. The ratio of these photoreceptive cells varies considerably between fish species, mainly in accordance with their habitat. For instance, most deep-sea fishes have retina only with rods.

The duplex retinae of many fishes have regions of specialization. For example, an area temporalis consists of a patch of closely packed cones (with few or no rods) appropriately placed to receive light along the main axis of feeding. In pelagic feeders like herring, looking upward and forward to find food, the area is posteroventral on the retina. In horizontally feeding species such as the sailfish (*Istiophorus*), it is posterior on the retina, and in bottom feeders like the sea bream (*Sparus*), the area is posterodorsally located. The amphibious mudskipper (*Periophthalmus*) has a horizontal band of cones placed to perceive objects near the ground level where both food and predators might be present. A fovea or depression with a high density of cones (as in many vertebrates) is present in seahorses (Hippocampus) and pipefish (*Syngnathus*).

The retinal pigment epithelium is adjacent to the photoreceptors and its color is brown due to the presence of melanin. The basal region of the ECs is supported by the Bruch's membrane that is rich in collagen fibers. The ECs are cylindrical with an elongated nucleus. The apical region of the ECs presents numerous very long processes that extend toward the inner segment of cones and rods. The cytoplasm of the ECs is replenished by numerous grains of melanin of variable shapes. They seem to be synthesized in layers

resulting in concentric lamellar aspect. Melanin grains can migrate inside the cell, stimulated by light or darkness.

A fairly common special structure, the tapetum lucidum is located beneath the photoreceptors. It reflects light, thus making the "eyeshine" phenomenon common in many fishes and carnivorous mammals. Its purpose is to enhance the light sensitivity of the eye. The position and the quality of the tapetum vary considerably between different species. Some species harbor a tapetum in the choroid, whereas in others it is associated with the retinal pigment epithelium.

The glial fibrillary acidic protein (GFAP) immunohistochemistry of the retina revealed a strong localization of GFAP protein in the foot processes of Müller glia extending inward into the ganglion cells and nerve fiber layer, and in the synaptic zone (outer plexiform layer) between the photoreceptor and bipolar cells (Figure 16.21).

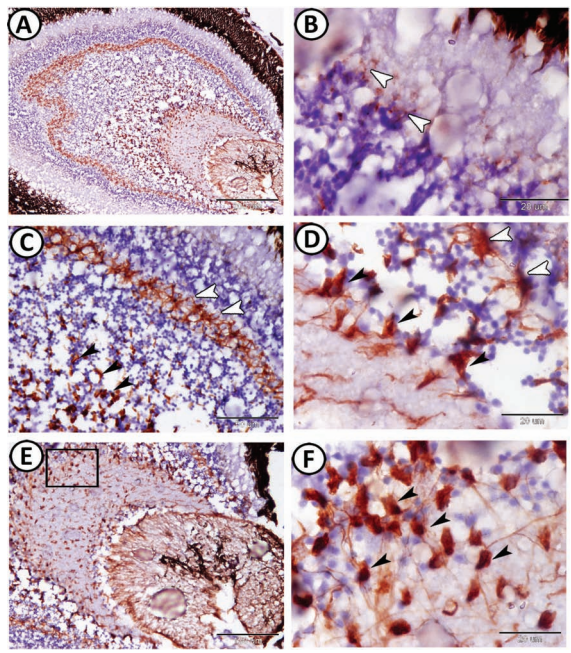

FIGURE 16.21 Glial fibrillary acidic protein (GFAP) expression in the retina of Molly. (A) The general view of GFAP expression in the retina. (B) Glia cells (arrowheads) express GFAP immunoreactivity in the outer nuclear layer. (C) Astrocytes express GFAP immunoreactivity in the outer plexiform layer (white arrowheads) and inner nuclear layer (black arrowheads). (D) Astrocytes express GFAP immunoreactivity in the inner plexiform layer (white arrowheads) and ganglionic layer (black arrowheads). (E and F) Astrocytes express GFAP immunoreactivity in the optic nerve layer (arrowheads).

KEYWORDS

- **olfactory organ**
- **neuromast**
- **lateral line**
- **inner ear**
- **eye**

BIBLIOGRAPHY

Bone, Q. and Moore, R.H. *Biology of Fishes*, 3rd ed., **2008**, Taylor & Francis, Abingdon, United Kingdom.

Carton, A.G. and Montgomery, J.C. Responses of lateral line receptors to water flow in the Antarctic notothenioid, *Trematomus bernacchii*. *Polar Biol.* **2002**, *25*, 789–793.

Fox, H., Barbels and barbel-like tentacular structures in sub-mammalian vertebrates: a review. *J. Hydrobiol.* **1999**, *403*, 153–193.

Hansen, A. and Zielinski, B.S. Diversity in the olfactory epithelium of bony fishes: development, lamellar arrangement, sensory neuron cell types and transduction components. *J. Neurocytol.* **2005**, *34*, 183–208.

Hawryshyn, C.W. Vision. In: Evans, D.H., (Eds.). *The Physiology of Fishes*, 2nd ed., **1997**, CRC Press, United States.

Hibiya, T. *An Atlas of Fish Histology—Normal and Pathological Features*, **1982**, Kondansha Ltd., Tokyo; Gustav Fischer Verlag, Stuttgart/New York.

Koke, J.R., Mosier, M.L., García, D.M. Intermediate filaments of zebrafish retinal and optic nerve astrocytes and Müller glia: differential distribution of cytokeratin and GFAP. *BMC Res. Notes* **2010**, *3*, 50.

Popper, A.N., Platt, C. Inner ear and lateral line. In: *The Physiology of Fishes*, 1st ed., **1993**, CRC Press.

Zaunretter, M., Junger, H., Kotrschal, K. Retinal structure; physiology and pharmacology. *Vis. Res*. **1991**, *31* (3), 383–394.

Index

D

E

F

G

H

I

J

K

L

M

N

O

P

R

S

T

U

V

W

X

Y

Z